

**THE DEVELOPMENT AND EVALUATION OF  
PHOTO-ANTIMICROBIAL ISOALLOXAZINE  
DYES TOWARDS INFECTION CONTROL**

**By**

**Hajira Faki**

A thesis submitted in partial fulfilment for the requirements for the degree  
of Doctor of Philosophy at the University of Central Lancashire

May 2018



I declare that while registered as a candidate for the research degree, I have not been a registered candidate or enrolled student for another award of the University or other academic or professional institution. I declare that no material contained in the thesis has been used in any other submission for an academic award and is solely my own work.

**Signature of Candidate** \_\_\_\_\_

**Date** \_\_\_\_\_

**School of physical sciences and computing**

## *Dedication*

*Dedicated to my beloved family; my parents, mother, father, sisters  
& most of all my loving brothers.*

*Mum: "For you I pushed to this day..."*

## *Acknowledgments*

I would like to start by thanking Allah for giving me the opportunity to complete this PhD research project. How little did I know it was going to be nothing but a rollercoaster ride.

My sincere gratitude and appreciation goes to my director of studies Dr Rob Smith for his continuous guidance throughout the length of this research project. I am deeply indebted to Professor Glyn Morton as words alone cannot express my gratitude for the support given by him and was an honour to be taught by such a man. My appreciation also goes to Professor Gary Bond for supporting the external conferences and Arnoux for funding me and the experience at UCLan. I would like to express my appreciation to Professor Mark Wainwright for his expertise in PDT research.

I will forever be thankful to Dr Stephen Johns for his support and guidance in the lab not to forget the continuous pessimistic outlook that was somehow positive. My thanks goes out to my friends and colleagues at UCLan: Dr. Pikey Crewe, Susan Jones, Dr. Vinod Vishwapathi, Abdullah Alakalabi, Dr. John Emmott, Dr. Sandeep Kadam, Dr. Maneea Eizadi and Dr. Temba Mudariki for their continuous distractions when needed.

A special thanks goes out to my best friend Tamar Garcia. Without Tamar the craziness and laughter would not have been. The girls from the LIS team; (Liz Green, Chrissy Woodcock, Abi) and my good mate Smiler who has always been there to help me both academically and socially. Not forgetting my special yankee friends Sherri Syfers and Peter Carlton at SciFinder for ensuring my chin stays up! I also thank Ngumi Gituro for making me smile and completing this important journey for my mum.

I would also like to thank Mansoor Ahmed for his continuous IT support given to me. I am grateful to the members of the technical department; Sal Tracey, Jim Donnelly and the staff of the whole chemistry department for always being so helpful.

Finally, my appreciation goes out foremost to all my family members for their support and prayers. Wholehearted appreciation and thanks goes out in particular to my mummy and daddy (Nasrin & Asghar) for listening to me cry and picking me up throughout the lows of this project. Without their in depth support and love I would never have reached here today.

In today's world, antimicrobial resistance is one of the biggest global health issues that mankind is facing. This most effective way to ensure a wound does not become infected is through cleanliness and continued disinfection of the wound site.

There is a lack of new antimicrobial drugs coming to the market due to economical and clinical reasons, this is evident in Lord O'Neill's 2016 report and is addressed by Professor Dame Sally Davies in Parliament, ("*We have reached a critical point and must act now on a global scale to slow down antimicrobial resistance*"<sup>2</sup>). Prescription drugs have led to this epidemic that was highlighted by O'Neill.

The latest report (2016) by O'Neill states, it is critical to improve sanitation and hygiene, refrain from overusing antibiotics in agriculture and the environment as well as introducing rapid diagnostics and vaccines<sup>3</sup>. This is leading to the need for photodynamic antimicrobial chemotherapy (PACT) that involves the use of a reactive oxygen species (ROS), photosensitiser, and light to cause microbial death. PACT is a treatment for resistant and non-resistant pathogens that is included in the treatment of multidrug resistant infections. The approach is to use novel antimicrobial drugs topically, avoiding systemic photo-toxicity, thus leading itself towards topical infection control.

Herein, we report the development of a range of novel photosensitisers based on the second generation photodynamic therapeutic dyes (PDT) that are based on the tricyclic isoalloxazine structure of riboflavin, vitamin B2. Photosensitisers were synthesised using similar strategies to the isoalloxazine for a number of reasons: e.g. photoactivity and capability of degradation. In order to investigate which photosensitisers gave the highest reactive oxygen yield, functional group changes were made on the *N*-phenyl ring by substituting a range of electron withdrawing/donating substituents at different positions (*ortho*, *meta*, *para*). The free amide moiety was used to attach the photosensitiser to a solid support that would act as proof of principal of a photosensitiser attached to a bandage.

These dyes show a phototherapeutic response via a Type I and II mechanism upon illumination by light of a selected wavelength. The mechanisms produce highly toxic oxygen-species, such as radical production via Type I pathway and singlet oxygen generation by Type II, thus causing terminal damage to microbes in a short time period. The synthesised photosensitisers are illuminated using blue light (440 - 490 nm) and white light in order to monitor and compare the singlet oxygen and radical yields generated as they absorb approximately at 440 nm, thus blue light being ideal for irradiation. The outstanding singlet oxygen result generated by compound

**12c** of 172% and a radical production by **11c** of 227% show promising generators of cytotoxic species, resulting in microbial death.

The synthesised photosensitisers have been tested against two opportunistic microbes (Gram positive and Gram negative bacteria; *Staphylococcus aureus* (*S. aureus*), and *Escherichia coli* (*E.coli*). They have proven to be problematic from its presence within the healthcare system especially when found on surgical site infections. From the statistics generated for the National Health Service (NHS) in the UK we can see that 52.4 % of *S. aureus*, and 43.1 % *E.coli* originates within the hospital environment.

Antimicrobial activity was observed for several compounds under different light regimes on and off the solid support. As a result, the best observed MIC value of 0.25 mM/mL was achieved for *S. aureus* in darkness and in blue light without the polymer support. Additionally, when these compounds were linked to a polymer support (mimicking a bandage), antimicrobial activity was retained when irradiated using blue light at 1.0 mM/mL. These results show potential towards the next generation of antimicrobial disinfection agents.

In time, these compounds could be integrated into the healthcare system for use as a new generation of self-cleaning bandages towards post-operative wound disinfection rather than employing front line antimicrobials. This is a moot subject under review in parliament and former UK prime minister has highlighted the concern. In a statement recently released, he states “*If we fail to act, we are looking at an almost unthinkable scenario where antibiotics no longer work and we are cast back into the dark ages of medicine*” – David Cameron, UK Prime Minister<sup>2</sup>.

# Table of Contents

Chapter 1	1
<b>General Introduction - Antimicrobials</b>	1
1.1 Antimicrobial resistance	1
1.2 Resistance in hospitals	5
1.2.1 <i>Staphylococcus aureus</i>	5
1.2.2 <i>Escherichia coli</i>	6
1.2.3 Hospital associated methicillin resistant <i>S.aureus</i> .	6
1.2.4 Community associated methicillin resistant <i>S.aureus</i>	7
1.3 The role of microbes in wounds	7
1.4 Cost Impact	7
1.5 Ehrlich's Magic Bullet	8
1.6 Penicillin	10
1.7 Sulphonamides	18
<b>Literature Review on PDT</b>	23
1.8 Dyes	23
1.8.1 Tyrian purple	23
1.8.2 Crystal violet	24
1.8.3 Mauve	26
1.8.4 Methylene blue-staining	27
1.8.5 Photodynamic Therapy (PDT)	28
1.8.6 Mode of action of photosensitisers	28
1.8.7 Mechanism of photodynamic therapy	29
1.9 Photosensitisers	31
1.10 Light	33
1.10.1 History	33
1.10.2 Phenothiazinium dyes	33
1.10.3 Acridines	35
1.10.4 Xanthene derivatives	38
1.10.5 Cyanine based photosensitisers	40
1.10.6 Squarine dyes	42
1.10.7 Phthalocyanine based photosensitisers	49
1.10.8 Photosensitisers designed for clinical use-cyanine	49
1.10.9 Electronic states	50
1.10.10 Jablonski	50
1.11 Applications of photosensitisers	52
1.11.1 Cancer	52
1.11.2 Applications of tumour	53
1.11.3 Port wine stain	54
1.11.4 Viral	54

1.11.5	Surface disinfection	55
1.11.6	PDT and Bacteria	56
1.12	Antimicrobial compounds, their nature, mode of action and resistance mechanisms – Biological perspective	58
1.12.1	Antimicrobial control-physical methods	58
1.12.2	Heat sterilisation	58
1.12.3	Radiation sterilisation	61
1.12.4	Filter sterilisation	61
1.13	Antimicrobial chemical control methods	61
1.13.1	Chemical antimicrobial agents	62
1.13.2	Control of growth by chemical means	62
1.13.3	Antimicrobial agents and their mode of action	62
1.14	Antimicrobial Activity	63
1.14.1	Measuring antimicrobial activity	63
1.15	Antimicrobial Agents- <i>In vivo</i>	64
1.15.1	Antimicrobial drugs	64
1.15.2	Synthetic antimicrobial drugs	64
1.15.3	Mode of action	64
1.15.4	Resistance mechanisms of bacterial cell (Figure 39-B)	67
1.16	Drug resistance	67
1.16.1	Antimicrobial drug resistance	67
1.16.2	Biocides	67
1.17	Quantitative Structure-Activity Relationship (QSAR)	68
1.18	Log P	68
1.19	Isoalloxazine analogues in literature	69
1.19.1	Synthesis of isoalloxazine analogues in literature	69
Chapter 2		78
2.1	Rationale	78
	<b><i>Results and Discussion (i)</i></b>	80
2.2	Aims/Objective	80
2.3	Introduction to flavins	81
2.3.1	Flavin background	81
2.4	Flavin redox behaviour	82
2.5	Much desired resistance antimicrobial agents-synthesised	82
2.6	Discussion on synthesis	83
	<b><i>Hypothesis</i></b>	87
2.7	Results and discussion on synthetic routes of the synthesised isoalloxazine's	88
2.7.1	Mechanism for a substituted aryl with aniline	89
2.7.2	Proposed mechanism for isoalloxazine's.	92
2.8	Discussion of the synthesised isoalloxazines	92



2.9	Synthesis of 10-phenyl isoalloxazine (R = H)	94
2.10	Amino derivatives of 10-phenylisoalloxazine (R = NH <sub>2</sub> )	98
2.11	Synthesis of the 2, 3, and 4 isomers of <i>N</i> -(aminophenyl)-2-nitroaniline ( <b>1a–3a</b> )	99
2.11.1	Synthesis of 10-(2-aminophenyl) isoalloxazine ( <b>1c</b> )	101
2.12	Hydroxy derivatives of 10-phenylisoalloxazine (R = OH)	102
2.13	Synthesis of the 2, 3, and 4 isomers of <i>N</i> -(hydroxyphenyl)-2-nitroaniline ( <b>4a–6a</b> )	102
2.13.1	Synthesis of 10-( <i>N</i> -hydroxyphenyl) isoalloxazines ( <b>4c–6c</b> )	103
2.13.2	Attempted synthesis of 10-(3-hydroxyphenyl) isoalloxazine ( <b>5c</b> )	104
2.14	Methoxy derivatives of 10-phenylisoalloxazine (R = OCH <sub>3</sub> )	105
2.14.1	Synthesis of 2, 3, and 4 isomers of <i>N</i> -(methoxyphenyl)-2-nitroaniline ( <b>7a–9a</b> )	106
2.14.2	Synthesis of 10-( <i>N</i> -methoxyphenyl) isoalloxazine ( <b>7c–9c</b> )	106
2.15	Synthesis of <i>N</i> -(3-methoxyphenyl) 2-nitroaniline ( <b>8a</b> )	108
2.15.1	Synthesis of 10-(3-methoxyphenyl) isoalloxazine ( <b>8c</b> )	108
2.16	Tolyl derivatives of 10-phenylisoalloxazine (R = CH <sub>3</sub> )	110
2.16.1	Synthesis of the 2, 3, and 4 isomers of <i>N</i> -(tolylphenyl)-2-nitroaniline ( <b>10a–12a</b> )	110
2.16.2	Synthesis of 10-( <i>N</i> -tolylphenyl) isoalloxazine ( <b>10c–12c</b> )	111
2.17	Chloro derivatives of 10-phenylisoalloxazine (R = Cl)	114
2.17.1	Synthesis of 2, 3, and 4 isomers of <i>N</i> -(chlorophenyl)-2-nitroaniline ( <b>14a–16a</b> )	114
2.17.2	Synthesis of 10-( <i>N</i> -chlorophenyl) isoalloxazines ( <b>14c–16c</b> )	116
2.18	Tosyloxy derivatives of 10-phenylisoalloxazine (R = OTs)	120
2.18.1	Synthesis of 2, 3, and 4 isomers of <i>N</i> -(tosyloxyphenyl)-2-nitroaniline ( <b>17a–19a</b> )	120
2.18.2	Synthesis of 10-( <i>N</i> -tosyloxyphenyl) isoalloxazines ( <b>17c–19c</b> )	120
2.19	Carboxy derivatives of 10-phenylisoalloxazine (R = COOH)	123
2.19.1	Synthesis of the 2, 3, and 4 isomers of ( <i>N</i> -carboxyphenyl)-2-nitroaniline ( <b>20a–22a</b> )	124
2.19.2	Synthesis of 10-( <i>N</i> -carboxyphenyl) isoalloxazines ( <b>20c &amp; 22c</b> )	126
2.20	Nitro derivatives of 10-phenylisoalloxazine (R = NO <sub>2</sub> )	128
2.20.1	Synthesis of the 2, 3 and 4 isomers of <i>N</i> -(nitrophenyl)-2-nitroaniline ( <b>23a–25a</b> )	128
2.20.2	Synthesis of 10-( <i>N</i> -nitrophenyl) isoalloxazines ( <b>23c</b> )	129
2.20.3	Attempted synthesis of 3, 4 isomers of 10-( <i>N</i> -nitrophenyl) isoalloxazine ( <b>24c and 25c</b> )	130
	<b><i>Discussion on the synthesis of polymeric isoalloxazines</i></b>	132
2.21	Synthesis of polymer bound <i>N</i> -substituted isoalloxazines	132
2.22	10-Phenylisoalloxazine-polymer bound ( <b>13d</b> )	134
2.23	<i>N</i> -Amino derivative of 10-phenylisoalloxazine-polymer bound ( <b>1d</b> )	137
2.24	<i>N</i> -Hydroxy derivatives of 10-phenylisoalloxazine-polymer bound ( <b>4d and 6d</b> )	139
2.25	<i>N</i> -Methoxy derivatives of 10-phenylisoalloxazine-polymer bound ( <b>7d–9d</b> )	141
2.26	<i>N</i> -Tolyl derivatives of 10-phenylisoalloxazine-polymer bound ( <b>10d–12d</b> )	142
2.27	<i>N</i> -Chloro derivatives of 10-phenylisoalloxazine-polymer bound ( <b>14d–16d</b> )	143
2.28	<i>N</i> -Tosyloxy derivatives of 10-phenylisoalloxazine-polymer bound ( <b>17d–19d</b> )	144
2.29	<i>N</i> -Carboxy derivative of 10-phenylisoalloxazine-polymer bound ( <b>20d</b> )	145

2.30	<i>N</i> -Nitro derivative of 10-phenylisoalloxazine-polymer bound ( <b>23d</b> )	146
Chapter 3		147
<i>Photochemistry</i>		147
3.1	Singlet oxygen and radical producers	147
3.2	Solubility studies	147
3.3	Light Source	148
3.4	Wavelength of Light	149
3.5	Selectivity of singlet oxygen markers	150
<i>General experimental-photochemistry</i>		153
3.6	Absorption spectroscopy	153
3.7	Selected markers for monitoring the generation of singlet oxygen	153
3.8	TPCPD - Singlet oxygen quencher	153
3.9	DPPH - radical quencher	154
3.10	Volume of solvents	154
3.11	Concentration of solution	154
3.12	Literature- singlet oxygen yield	154
<i>Photochemistry; Experimental</i>		156
3.13	Protocol for the <sup>1</sup> O <sub>2</sub> production of alloxazine using white light	156
3.14	Protocol for DPPH-white light	156
3.15	Protocol for DPPH-blue light	156
3.16	Protocol for TPCPD-blue light	156
<i>Discussion on photophysical studies</i>		158
3.17	Discussion of singlet oxygen data	158
3.18	Photosensitiser entries	158
	3.18.1 Measuring the singlet oxygen quantum yield spectrophotometrically	160
3.19	DPPH-radical data blue light	161
3.20	TPCPD-singlet oxygen data blue light	161
3.21	TPCPD-singlet oxygen data for <b>13c</b>	161
3.22	DPPH-Redox for <b>13c</b>	164
3.23	Photophysical studies of 10-phenyl isoalloxazine (R = H). ( <b>13c</b> )	167
3.24	Photophysical studies of amino derivatives of 10-phenylisoalloxazine (R = NH <sub>2</sub> ). ( <b>1c</b> )	168
3.25	Photophysical studies of hydroxy derivatives of 10-phenylisoalloxazine (R = OH). ( <b>4c-6c</b> )	172
3.26	Photophysical studies of methoxy derivatives of 10-phenylisoalloxazine (R = OCH <sub>3</sub> ). ( <b>7c-9c</b> )	174
3.27	Photophysical studies of tolyl derivatives of 10-phenylisoalloxazine (R = CH <sub>3</sub> ). ( <b>10c-12c</b> ).	177
3.28	Photophysical studies of chloro derivatives of 10-phenylisoalloxazine (R = Cl). ( <b>14c-16c</b> )	180

3.29	Photophysical studies of tosyloxy derivatives of 10-phenylisoalloxazine (R = OTs). ( <b>17c–19c</b> )	182
3.30	Photophysical studies of carboxy derivatives of 10-phenylisoalloxazine (R = COOH). ( <b>20c–22c</b> )	184
3.31	Photophysical studies of nitro derivatives of 10-phenylisoalloxazine (R = NO <sub>2</sub> ). <b>23c</b>	186
Chapter 4		188
<b>Results and Discussion-microbiology</b>		188
4.1	Antimicrobial & photophysical studies for the synthesised isoalloxazines	189
4.2	Comparison studies for antimicrobial results of synthesised isoalloxazines using blue light	195
4.2.1	<i>E.coli</i>	195
4.2.2	<i>S.aureus</i>	197
4.3	Antimicrobial & photophysical studies for compound <b>13c</b>	199
4.4	Antimicrobial & photophysical studies for compound <b>1c</b>	201
4.5	Antimicrobial & photophysical studies for compound <b>4c</b> and <b>6c</b>	202
4.6	Antimicrobial & photophysical studies for compound <b>7c-9c</b>	204
4.7	Antimicrobial & photophysical studies for compound <b>10c-12c</b>	206
4.8	Antimicrobial & photophysical studies for compound <b>14c-16c</b>	208
4.9	Antimicrobial & photophysical studies for compound <b>17c-19c</b>	211
4.10	Antimicrobial & photophysical studies for compound <b>20c</b> and <b>22c</b>	213
4.11	Antimicrobial & photophysical studies for compound <b>23c</b>	215
<b>Discussion on antimicrobial Studies on Polymer bound isoalloxazines</b>		216
4.12	Results and discussion of antimicrobial studies on polymer bound isoalloxazines	216
4.13	Comparison studies for antimicrobial results of synthesised isoalloxazines attached to a polymer support	221
4.13.1	<i>E.coli</i>	221
4.13.2	<i>S.aureus</i>	222
4.14	Antimicrobial studies of polymer substituted compounds	224
4.15	Antimicrobial studies for compound <b>13d</b>	224
4.16	Antimicrobial studies for compound <b>1d</b>	227
4.17	Antimicrobial studies for compound <b>4d</b>	227
4.18	Antimicrobial studies for compounds <b>7d-9d</b>	228
4.19	Antimicrobial studies for compounds <b>10d-12d</b>	229
4.20	Antimicrobial studies for compounds <b>15d</b> and <b>16d</b>	230
4.21	Antimicrobial studies for compounds <b>17d</b> and <b>19d</b>	231
4.22	Antimicrobial studies for compound <b>20d</b>	232
4.23	Antimicrobial studies for compound <b>23d</b>	233
Chapter 5		234
<b>Future work and conclusion</b>		234

5.1	Conclusion	234
5.1.1	Conclusion on library of synthesised isoalloxazines	234
5.1.2	Conclusion on antimicrobial studies for the synthesised library of isoalloxazines	237
5.1.3	Conclusive comments for antimicrobial results of synthesised isoalloxazines on polymer support	238
5.2	Future Work	240
5.2.1	Future work on the library of synthesised isoalloxazines	240
5.2.2	Future work on the antimicrobial activity of the synthesised isoalloxazines	240
Chapter 6		242
<i>Synthesis and Experimental</i>		242
6.1	Chemical Synthesis	242
6.2	Synthesis of 2-(2-nitrophenyl) aniline ( <b>1a</b> )	243
6.3	Synthesis of 10-(2-aminophenyl) isoalloxazine ( <b>1c</b> )	243
6.4	Synthesis of 2-(2-nitrophenyl amino) phenol ( <b>4a</b> )	244
6.5	Synthesis of 10-(2-hydroxyphenyl) isoalloxazine ( <b>4c</b> )	245
6.6	Synthesis of 2-(3-nitrophenyl amino) phenol ( <b>5a</b> )	246
6.7	Synthesis of 4-(2-nitrophenyl amino) phenol ( <b>6a</b> )	246
6.8	Synthesis of 10-(4-hydroxyphenyl) isoalloxazine ( <b>6c</b> )	247
6.9	Synthesis of 2-(2-nitrophenyl) 2-methoxy aniline ( <b>7a</b> )	248
6.10	Synthesis of 10-(2-methoxyphenyl) isoalloxazine ( <b>7c</b> )	248
6.11	Synthesis of 2-(2-nitrophenyl) 3-methoxy aniline ( <b>8a</b> )	249
6.12	Synthesis of 10-(3-methoxyphenyl) isoalloxazine ( <b>8c</b> )	250
6.13	Synthesis of 2-(2-nitrophenyl) 4-methoxy aniline ( <b>9a</b> )	251
6.14	Synthesis of 10-(4-methoxyphenyl) isoalloxazine ( <b>9c</b> )	251
6.15	Synthesis of 2-(2-nitrophenyl) 2-tolyl aniline ( <b>10a</b> )	252
6.16	Synthesis of 10-(2-tolylphenyl) isoalloxazine ( <b>10c</b> )	253
6.17	Synthesis of 2-(2-nitrophenyl) 3-tolyl aniline ( <b>11a</b> )	254
6.18	Synthesis of 10-(3-tolylphenyl) isoalloxazine ( <b>11c</b> )	255
6.19	Synthesis of 2-(2-nitrophenyl) 4-tolyl aniline ( <b>12a</b> )	255
6.20	Synthesis of 10-(4-tolylphenyl) isoalloxazine ( <b>12c</b> )	256
6.21	Synthesis of 2-(2-chlorophenyl) aniline ( <b>14a</b> )	257
6.22	Synthesis of 10-(2-chlorophenyl) isoalloxazine ( <b>14c</b> )	258
6.23	Synthesis of 2-(2-nitrophenyl) 3-chloro aniline ( <b>15a</b> )	258
6.24	Synthesis of 10-(3-chlorophenyl) isoalloxazine ( <b>15c</b> )	259
6.25	Synthesis of 2-(2-nitrophenyl) 4-chloro aniline ( <b>16a</b> )	260
6.26	Synthesis of 10-(4-chlorophenyl) isoalloxazine ( <b>16c</b> )	260
6.27	Synthesis of 10-(2-tosyloxyphenyl) isoalloxazine ( <b>17c</b> )	261
6.28	Synthesis of 10-(3-tosylphenyl) isoalloxazine ( <b>18c</b> )	262
6.29	Synthesis of 10-(4-tosyloxyphenyl) isoalloxazine ( <b>19c</b> )	263
6.30	Synthesis of 2-(2-nitrophenyl) 2-carboxy aniline ( <b>20a</b> )	264
6.31	Synthesis of 10-(2-carboxyphenyl) isoalloxazine ( <b>20c</b> )	265

6.32	Synthesis of 2-(2-nitrophenyl) 4-carboxy aniline ( <b>22a</b> )	266
6.33	Synthesis of 10-(4-carboxyphenyl) isoalloxazine ( <b>22c</b> )	266
6.34	Synthesis of 2-(2-nitrophenyl) benzene 1, 2-diamine ( <b>23a</b> )	267
6.35	Synthesis of 10-(2-nitrophenyl) isoalloxazine ( <b>23c</b> )	268
	<b><i>Synthesis of Polymer Support</i></b>	269
6.36	Synthesis of 10-phenyl isoalloxazine polymer bound ( <b>13d</b> )	269
6.37	Synthesis of 10-(2-aminophenyl) isoalloxazine polymer bound ( <b>1d</b> )	269
6.38	Synthesis of 10-( <i>N</i> -hydroxyphenyl) isoalloxazines polymer bound ( <b>4d-6d</b> )	270
6.39	Synthesis of 10-( <i>N</i> -methoxyphenyl) isoalloxazines polymer bound ( <b>7d-9d</b> )	271
6.40	Synthesis of 10-( <i>N</i> -tolylphenyl) isoalloxazines polymer bound ( <b>10d-12d</b> )	272
6.41	Synthesis of 10-( <i>N</i> -chlorophenyl) isoalloxazines polymer bound ( <b>14d-16d</b> )	273
6.42	Synthesis of 10-( <i>N</i> -tosyloxyphenyl) isoalloxazines polymer bound ( <b>17d-19d</b> )	274
6.43	Synthesis of 10-(2-carboxyphenyl) isoalloxazine polymer bound ( <b>20d</b> )	275
6.44	Synthesis of 10-(2-nitrophenyl) isoalloxazine polymer bound ( <b>23d</b> )	275
	<b><i>Microbiology</i></b>	276
	<b><i>Background to Biological Testing</i></b>	276
6.45	Antimicrobial testing using white light	276
6.46	Criterion for cell preparation	276
	<b><i>Methodology developed for antimicrobial testing</i></b>	277
6.47	Biological screening	277
6.48	Preparation of a washed cell suspensions in antimicrobial testing	277
6.49	MIC estimation	277
	<b><i>Protocols of Experimental – Microbiology</i></b>	278
6.50	Antimicrobial testing using blue LED light-conformational studies	278
	6.50.1 Preliminary screening over time of antimicrobial activity after 1 h exposure to blue LED light with no biocide.	278
	6.50.2 Preliminary screening of antimicrobial activity under dark conditions with no biocide	278
	6.50.3 Antimicrobial activity for the synthesised antimicrobial agents using blue LED lights	279
6.51	Antimicrobial activity for polymer bound compounds	280
	6.51.1 Antimicrobial activity for the synthesised antimicrobial agents on polymer support using blue LED lights	280
	<b><i>Appendix 1</i></b>	281
	Appendix 1 of 4.1	281
	<b><i>Appendix 2</i></b>	290
	Appendix 2 of 4.12	290
	<b><i>References</i></b>	293

# Contents of Figures

Figure 1: Timeline of bacterial resistance <sup>16</sup>	3
Figure 2: Chemical structure of methylene blue	8
Figure 3: Chemical structure of quinine	9
Figure 4: Chemical structure of chloroquine	9
Figure 5: Chemical structure of salvarsan-606	9
Figure 6: Chemical structure of neosalvarsan-914	10
Figure 7: Chemical structure of penicillin (G)	10
Figure 8: Chemical structure of methicillin	14
Figure 9: Chemical structure of a cephalosporin-ceftaroline	14
Figure 10: Derivatives of $\beta$ -lactam antibiotics <sup>92</sup>	15
Figure 11: Next generation of antibiotics/ $\beta$ -lactamase inhibitors	17
Figure 12: Derivative of sulphonamide drug	18
Figure 13: Chemical structure of trimethoprim	21
Figure 14: Chemical structure of tetrahydrofolic acid	21
Figure 15: Chemical structure of tyrian purple	23
Figure 16: Chemical structure of indigo	23
Figure 17: Chemical structure of crystal violet	25
Figure 18: Chemical structure of quinine	26
Figure 19: Chemical structure of mauveine and its derivatives	27
Figure 20: Chemical structure of methylene blue	27
Figure 21: Chemical structure of isosulfan blue	28
Figure 22: Electronic pathway of photosensitiser action -adapted from photosensitisers in biomedicine <sup>1</sup>	30
Figure 23: Electromagnetic spectrum	33
Figure 24: Squarylium equivalent dye	42
Figure 25: Croconic acid dye	48

Figure 26: Rhodizonic acid (A), Rhodizonium dye (B)	48
Figure 27: NIR fluorophore	49
Figure 28: Delocalization of cation across methine chain	50
Figure 29: Jablonski diagram <sup>169</sup>	51
Figure 30: Chemical structure of photofrin	53
Figure 31: Chemical structure of methyl aminolevulinic acid	53
Figure 32: Chemical structure of 5-aminolevulinic acid (HCl salt)	55
Figure 33: Chemical structure of proflavine	55
Figure 34: Colonisation of wound on a bandage	56
Figure 35: Chemical structure of PDT agent	56
Figure 36: Temperature effects over time on microorganism (e.g. <i>mycobacterium tuberculosis</i> ) viability <sup>263</sup> .	60
Figure 37: D for microorganisms (e.g. <i>E.coli</i> ) <sup>264</sup>	61
Figure 38: Chemical structure of salvarsan	64
Figure 39: Mode of action of antimicrobial agents(A) and mechanisms of resistance (B) <sup>290</sup>	66
Figure 40: Chemical structure of riboflavin and its degradation molecules	80
Figure 41: Chemical structure of a semi-synthetic isoalloxazine	80
Figure 42: Functionalisation of isoalloxazine	81
Figure 43: Chemical structure of flavin and riboflavin	81
Figure 44: Structural forms of quinones	82
Figure 45: <sup>1</sup> H-NMR for 10-phenyl isoalloxazine	95
Figure 46: <sup>1</sup> H- <sup>1</sup> H COSY NMR for 10-phenyl isoalloxazine	96
Figure 47: IR spectrum for 10-phenyl isoalloxazine	97
Figure 48: <sup>1</sup> H-NMR for <i>N</i> -(2-nitrophenyl)-2-nitroaniline	99
Figure 49: <sup>1</sup> H-NMR for 10-2-(aminophenyl) isoalloxazine	101
Figure 50: <sup>1</sup> H-NMR of 2-hydroxyphenyl and 2-methoxyphenyl isoalloxazines.	103
Figure 51: <sup>1</sup> H-NMR for isoalloxazines <b>9c</b> and <b>7c</b>	107
Figure 52: <sup>1</sup> H-NMR for <i>N</i> -(2-tolylphenyl)-2-nitroaniline	111

Figure 53: <sup>1</sup> H-NMR for 10-(2-tolylphenyl) isoalloxazine	112
Figure 54: IR spectrum for compound <b>11c</b>	113
Figure 55: <sup>1</sup> H-NMR for <i>N</i> -(2-chlorophenyl)-2-nitroaniline	115
Figure 56: MS of 2-(3-chlorophenyl) 2-nitroaniline	116
Figure 57: MS (ESI) for <i>N</i> -(2-chlorophenyl)-2-aminoaniline	118
Figure 58: <sup>1</sup> H NMR for 10-(4-chlorophenyl) isoalloxazine	119
Figure 59: <sup>1</sup> H Spectra for <i>p</i> -tosyloxy phenyl ( <b>19c</b> ) isoalloxazine and <i>p</i> -hydroxy isoalloxazine (6c)	121
Figure 60: <sup>1</sup> H-NMR of <i>N</i> -(2-carboxyphenyl)-2-nitroaniline	125
Figure 61: <sup>1</sup> H-NMR for 10-(4 -carboxyphenyl) isoalloxazine ( <b>22 c</b> )	126
Figure 62: MS (ESI) for compound <b>20c</b>	127
Figure 63: Mass spectrometry and msms of compound <b>23c</b>	130
Figure 64: IR spectrum for 10-phenyl isoalloxazine - identical to Figure 47	134
Figure 65: IR spectra of Wang brominated resin 4-(benzyoxy)benzyl bromide	135
Figure 66: IR spectra of compound <b>13d</b>	136
Figure 67: IR spectra of compound <b>1d</b>	137
Figure 68: IR spectra compounds <b>4d-6d</b>	140
Figure 69: Blue LED Lights	149
Figure 70: Irradiation using blue LED light at 5 cm distance	150
Figure 71: Chemical structure of indocyanine green	151
Figure 72: Chemical structure of DTTC iodide	152
Figure 73: Chemical structure of TPCPD	153
Figure 74: Chemical structure of DPPH	154
Figure 75: Chemical structure of alloxazine	158
Figure 76: Substitution position(s) for isoalloxazine	158
Figure 77: Chemical structure of (A) alloxazine and (B) <b>13c</b>	160
Figure 78: Chemical structure of TPCPD and its degradation	161
Figure 79: Singlet oxygen production of compound <b>13c</b>	162



Figure 80: Chemical structure of DPPH and its degradation	164
Figure 81: Redox production of compound <b>13c</b>	165
Figure 82: UV-Vis spectra for compound <b>13c</b>	166
Figure 83: Chemical structure of 10-phenyl isoalloxazine	167
Figure 84: Chemical structure of 10-( <i>N</i> -aminophenyl) isoalloxazines	168
Figure 85: Singlet oxygen and radical production of compound <b>1c</b> vs <b>13c</b>	170
Figure 86: Chemical structure of 10-( <i>N</i> -hydroxyphenyl) isoalloxazines	172
Figure 87: Singlet oxygen and radical production of compound <b>4c</b> and <b>6c</b> vs <b>13c</b>	173
Figure 88: Chemical structure of 10-( <i>N</i> -methoxyphenyl) isoalloxazines	174
Figure 89: Singlet oxygen and radical production of compounds <b>7c</b> and <b>9c</b> vs <b>13c</b>	175
Figure 90: Chemical structure of 10-( <i>N</i> -tolylphenyl) isoalloxazines	177
Figure 91: Singlet oxygen and redox production of compounds <b>10c-12c</b> vs <b>13c</b>	178
Figure 92: Chemical structure of 10-( <i>N</i> -chlorophenyl) isoalloxazines	180
Figure 93: Singlet oxygen and radical production of compounds <b>14c-16c</b> vs <b>13c</b>	181
Figure 94: Chemical structure of 10-( <i>N</i> -tosyloxyphenyl) isoalloxazines	182
Figure 95: Singlet oxygen and radical production of compounds <b>17c-19c</b> vs <b>13c</b>	183
Figure 96: Chemical structure of 10-( <i>N</i> -carboxyphenyl) isoalloxazines	184
Figure 97: Singlet oxygen and radical production of <b>20c</b> and <b>22c</b> vs <b>13c</b>	185
Figure 98: Chemical structure of 10-( <i>N</i> -nitrophenyl) isoalloxazines	186
Figure 99: Singlet oxygen and radical production of compound <b>23c</b> vs <b>13c</b>	187
Figure 100: Example of partial inhibition of microbes at various concentrations	189
Figure 101: Antimicrobial activity of <i>E.coli</i>	196
Figure 102: Antimicrobial activity of <i>S.aureus</i>	198
Figure 103: Antimicrobial activity of <b>13c</b> using <i>E.coli</i> and <i>S. aureus</i>	200
Figure 104: Antimicrobial activity for compounds <b>7c</b> , <b>8c</b> & <b>9c</b> -using <i>E.coli</i> and <i>S. aureus</i>	205
Figure 105: Antimicrobial activity for compounds <b>10c-12c</b> -using <i>E.coli</i> and <i>S. aureus</i>	207
Figure 106: Antimicrobial activity for compounds <b>14c-16c</b> -using <i>E.coli</i> and <i>S. aureus</i>	209
Figure 107: Antimicrobial activity of compounds on polymer support against <i>E.coli</i>	221

Figure 108: Antimicrobial activity of compounds on polymer support against <i>S.aureus</i>	222
Figure 109: Antimicrobial activity of compound <b>13d</b>	224
Figure 110: Antimicrobial activity of compound <b>13d</b> on a polymer support against gram negative and positive organisms.	226
Figure 111: Antimicrobial activity for compounds <b>10d-12d</b>	229
Figure 112: Antimicrobial activity for compounds <b>15d-16d</b>	230
Figure 113 Set-up of UV illumination on to bacterial cells and biocide	278
Figure 114: Labelled <i>E.coli</i> and <i>S. aureus</i> agar plates	279

# Contents of Schemes

Scheme 1: Mechanism for cross-linking of the bacterial cell wall <sup>1</sup>	12
Scheme 2: Mechanism of transpeptidase cross-linking	13
Scheme 3 Mechanism of action of cephalosporins	15
Scheme 4: Mode of action of clavulanic acid	18
Scheme 5: Azo reductase of prontosil to sulphanilamide	19
Scheme 6: Mechanism for the synthesis of indigo	24
Scheme 7: Berntsen synthesis	37
Scheme 8: Ullmann synthesis <sup>166</sup>	38
Scheme 9: Synthesis of xanthene derivatives – fluorescein	39
Scheme 10: Synthesis of cyanine intermediate	41
Scheme 11: Synthesis of cyanine dyes <sup>176</sup>	41
Scheme 12: Synthesis of squarylium derivatives <sup>169</sup>	44
Scheme 13: Synthesis of aminosquarylium derivatives	46
Scheme 15: Synthesis of croconium dyes	48
Scheme 16: Total synthesis of riboflavin <sup>308</sup>	69
Scheme 17: Synthesis of substituted isoalloxazines	70
Scheme 18: Microwave assisted (MW) synthesis of substituted isoalloxazine	70
Scheme 19: Synthesis of 10-aryl flavins	71
Scheme 20: Synthetic procedure for isoalloxazine	71
Scheme 21: Synthetic route for derivatives of isoalloxazine	72
Scheme 22: Hydrogenation method for the synthesis of isoalloxazine derivatives	72
Scheme 23: Hydrogenation using PtO <sub>2</sub> for the synthesis of isoalloxazine derivatives	73
Scheme 24: Hydrogenation using Pd/C for the synthesis of isoalloxazine derivatives	73
Scheme 25; Synthesis of riboflavin derivative by O. Brien et al.	74
Scheme 26: Intermediate compound of Yoneda et al <sup>319</sup>	74
Scheme 27: Ring closure to form riboflavin derivative	74
Scheme 28: Reactive intermediate species	75
Scheme 29: Vilsmeier-Haack used to synthesise flavin derivatives <sup>319</sup>	75
Scheme 30: Synthesis of 1-methylalloxazines derivatives	76
Scheme 31: Synthesis of alloxazine-5-oxide derivatives	76
Scheme 32: Synthesis of aryl dezaalloxazine derivatives	77
Scheme 33: Pathway for flavin synthesis	83

Scheme 34: Substitution mechanism of an aryl aniline	89
Scheme 35: Substitution of 2-nitrodiphenylamines	90
Scheme 36: Reduction step of substituted 2-nitrodiphenyleneamine intermediates	90
Scheme 37: Flavin formation of <i>N</i> -substituted amino aniline to <i>N</i> -substituted isoalloxazine	91
Scheme 38: Mechanism of isoalloxazine	92
Scheme 39: Substitution reaction of aniline	92
Scheme 40: Reduction of nitro aniline to amino aniline	93
Scheme 41: Cyclisation of <i>N</i> -substituted amino aniline	93
Scheme 42: Synthetic route of 10-phenyl isoalloxazine	94
Scheme 43: Synthetic route of 10-( <i>N</i> -aminophenyl) isoalloxazines	98
Scheme 44: Synthetic route of 10-( <i>N</i> -hydroxyphenyl) isoalloxazines	102
Scheme 45: Synthetic route of 10-( <i>N</i> -methoxyphenyl) isoalloxazines	105
Scheme 46: Synthetic route for additional derivatives of isoalloxazine from OMe moiety	106
Scheme 47: Synthetic route of 10-( <i>N</i> -tolylphenyl) isoalloxazines	110
Scheme 48: Synthetic route of 10-( <i>N</i> -chlorophenyl) isoalloxazines	114
Scheme 49: Zinc reduction mechanism	117
Scheme 50: Synthetic route of 10-( <i>N</i> -tosyloxyphenyl) isoalloxazines	120
Scheme 51: Synthetic route of 10-( <i>N</i> -carboxyphenyl) isoalloxazines	123
Scheme 52: Synthetic route of 10-( <i>N</i> -nitrophenyl) isoalloxazines	128
Scheme 53 : Synthetic route for polymer substitution	132
Scheme 54: Polymer synthesis of compound <b>13d</b>	134
Scheme 55: Polymer synthesis of compound <b>1d</b>	137
Scheme 56: Polymer synthesis of compounds <b>4d-6d</b>	139
Scheme 57: Polymer synthesis of compounds <b>7d-9d</b>	141
Scheme 58: Polymer synthesis of compounds <b>10d-12d</b>	142
Scheme 59: Polymer synthesis of compounds <b>14d-16d</b>	143
Scheme 60: Polymer synthesis of compounds <b>17d-19d</b>	144
Scheme 61: Polymer synthesis of compounds <b>20d-22d</b>	145
Scheme 62 Polymer synthesis of compound <b>23d</b>	146

# Contents of Table

Table 1: Aromatic structures for sulphanilamide derivatives	20
Table 2: Phenothiazinium derivatives <sup>161</sup>	34
Table 3: Acridine derivatives	35
Table 4: Xanthene derivatives	39
Table 5: Cyanine derivatives <sup>170</sup>	40
Table 6: Squarylium derivatives	43
Table 7: Heat sterilisation methods <sup>262</sup> .	59
Table 8: Table of synthesised novel isoalloxazines with different electron donating groups (EDG) electron withdrawing groups (EWG) substituted onto the <i>N</i> -10 ring.	85
Table 9: Percentage yield for 10-phenyl isoalloxazine	94
Table 10: Percentage yield for 10-( <i>N</i> -aminophenyl) isoalloxazine derivatives	98
Table 11: Percentage yields for <i>N</i> -(hydroxyphenyl)-2-nitroanilines and 10-( <i>N</i> -hydroxyphenyl) isoalloxazine derivatives	102
Table 12: Percentage yields for <i>N</i> -(methoxyphenyl)-2-nitroanilines and 10-( <i>N</i> -methoxyphenyl) isoalloxazine derivatives	105
Table 13: Percentage yields for <i>N</i> -(tolylphenyl)-2-nitroaniline and 10-( <i>N</i> -tolylphenyl) isoalloxazine derivatives	110
Table 14: Percentage yields for <i>N</i> -(chlorophenyl)-2-nitroanilines and 10-( <i>N</i> -chlorophenyl) isoalloxazine derivatives	114
Table 15: Percentage yields for 10-( <i>N</i> -tosyloxyphenyl) isoalloxazine derivatives	120
Table 16: Percentage yields for <i>N</i> -(carboxyphenyl)-2-nitroanilines and 10-( <i>N</i> -carboxyphenyl) isoalloxazine derivatives	123
Table 17: Percentage yields for <i>N</i> -(nitrophenyl)-2-nitroaniline and 10-( <i>N</i> -nitrophenyl) isoalloxazine derivatives	128
Table 18: Isoalloxazines on polymer support	133
Table 19: Polymer yield of 10-phenyl isoalloxazine	134
Table 20: Polymer yield of 10-(2-aminophenyl) isoalloxazine derivatives	137
Table 21: Polymer yields of hydroxyphenyl isoalloxazine derivatives	139
Table 22: Polymer yields of methoxyphenyl isoalloxazine derivatives	141
Table 23: Polymer yields of tolylphenyl isoalloxazine derivatives	142

Table 24: Polymer yields of chlorophenyl isoalloxazine derivatives	143
Table 25: Polymer yields of tosyloxyphenyl isoalloxazine derivatives	144
Table 26: Polymer yields of carboxyphenyl isoalloxazine	145
Table 27: Polymer yields of nitrophenyl isoalloxazine derivatives	146
Table 28: Solubility studies	148
Table 29: Singlet oxygen markers and producers	150
Table 30: Singlet oxygen yields generated by alloxazine analogues <sup>346,347</sup>	155
Table 31: Novel photosensitisers tested for singlet oxygen and radical production	159
Table 32: Singlet oxygen data for compound <b>13c</b>	163
Table 33: Redox data of compound <b>13c</b>	164
Table 34: Percentage yield for 10-phenyl isoalloxazine	167
Table 35: Photophysical data for 10-(2-aminophenyl) isoalloxazine.	168
Table 36: Singlet oxygen data for compound <b>1c</b>	169
Table 37: Redox data for compound <b>1c</b>	170
Table 38: Photophysical data for <i>N</i> -hydroxy phenyl isoalloxazine derivatives	172
Table 39: Photophysical data for <i>N</i> -methoxyphenyl isoalloxazine derivatives	174
Table 40: Photophysical data for tolylphenyl isoalloxazine derivatives	177
Table 41: Photophysical data for chlorophenyl isoalloxazine derivatives	180
Table 42: Photophysical data for tosyloxyphenyl isoalloxazine derivatives	182
Table 43: Photophysical data for carboxyphenyl isoalloxazine derivatives	184
Table 44: Photophysical data for 10-(2-nitrophenyl) isoalloxazine derivatives	186
Table 45: Compound codes (regioisomers*)	191
Table 46: Recorded MIC results against <i>E.coli</i>	193
Table 47: Recorded MIC results against <i>S.aureus</i>	194
Table 48: Antimicrobial activity & photophysical data for <b>13c</b> in blue light	199
Table 49: MIC of <b>13c</b> against <i>E.coli</i>	199
Table 50: MIC of <b>13c</b> against <i>S.aureus</i>	200
Table 51: Antimicrobial activity & photophysical data for <b>1c</b> in blue light	201

Table 52: Antimicrobial activity & photophysical data for <b>4c</b> and <b>6c</b> in blue light	202
Table 53: Antimicrobial activity & photophysical data for <b>7c</b> and <b>9c</b> in blue light	204
Table 54: Antimicrobial activity & photophysical data for <b>10c-12c</b> in blue light	206
Table 55: Antimicrobial activity & photophysical data for <b>14c-16c</b> in blue light	208
Table 56: Antimicrobial activity & photophysical data for <b>17c-19c</b> in blue light	211
Table 57: Antimicrobial activity & photophysical data for <b>20c</b> and <b>22c</b> in blue light	213
Table 58: Antimicrobial activity & photophysical data for <b>23c</b> in blue light	215
Table 59: Compound codes given to antimicrobial agents substituted onto polymer support	217
Table 60: Recorded MIC results for polymer substituted compounds against <i>E.coli</i>	219
Table 61: Recorded MIC results for polymer substituted compounds against <i>S.aureus</i>	220
Table 62: MIC of compound <b>13d</b>	224
Table 63: MIC of compound <b>1d</b>	227
Table 64: MIC of compound <b>4d</b>	227
Table 65: MIC of compounds <b>7d-9d</b>	228
Table 66: MIC of compounds <b>10d-12d</b>	229
Table 67 MIC of compounds <b>15d-16d</b>	230
Table 68: MIC of compounds <b>17d</b> and <b>19d</b>	231
Table 69: MIC of compound <b>22d</b>	232
Table 70: MIC of compound <b>23d</b>	233
Table 71: Log P values for all synthesised intermediates & final compounds, and <sup>1</sup> O <sub>2</sub> yields for <i>N</i> -substituted phenyl isoalloxazines	236
Table 72: Antimicrobial activity of <b>13c</b> : <i>E.coli</i> (+ 100% growth detected, † partial growth, - MIC)	281
Table 73: Antimicrobial activity of <b>13c</b> : <i>S.aureus</i> (+ 100% growth detected, † partial growth, - MIC)	281
Table 74: Antimicrobial activity of <b>1c</b> : <i>E.coli</i> (+ 100% growth detected)	282
Table 75: Antimicrobial activity of <b>1c</b> : <i>S.aureus</i> (+ 100% growth detected)	282
Table 76: Antimicrobial activity of <b>4c</b> and <b>6c</b> : <i>E.coli</i> (+ 100% growth detected, † partial growth)	282

Table 77: Antimicrobial activity of <b>4c</b> and <b>6c</b> : <i>S.aureus</i> (+ 100% growth detected, † partial growth)	283
Table 78: Antimicrobial activity of <b>7c-9c</b> : <i>E.coli</i> (+ 100% growth detected, † partial growth, - MIC)	283
Table 79: Antimicrobial activity of <b>7c-9c</b> : <i>S.aureus</i> (+ 100% growth detected, † partial growth, - MIC)	284
Table 80: Antimicrobial activity of <b>10c-12c</b> : <i>E.coli</i> (+100% growth detected, † partial growth, - MIC)	285
Table 81: Antimicrobial activity of <b>10c-12c</b> : <i>S.aureus</i> (+ 100% growth detected, -MIC)	286
Table 82: Antimicrobial activity of <b>14c-16c</b> : <i>E.coli</i> (+ 100% growth detected)	286
Table 83:Antimicrobial activity of <b>14c-16c</b> - <i>S.aureus</i> (+ 100% growth detected, † partial growth, - MIC)	287
Table 84: Antimicrobial activity of compounds <b>17c-19c</b> : <i>E.coli</i> (+ 100% growth detected)	287
Table 85: Antimicrobial activity of <b>17c-19c</b> : <i>S.aureus</i> (+ 100% growth detected, † partial growth)	288
Table 86: Antimicrobial activity of <b>20c</b> and <b>22c</b> : <i>E.coli</i> (+ 100% growth detected)	288
Table 87: Antimicrobial activity of <b>20c</b> and <b>22c</b> : <i>S.aureus</i> (+ 100% growth detected, † partial growth, - MIC)	289
Table 88: Antimicrobial activity of <b>23c</b> : <i>E.coli</i> (+ 100% growth detected)	289
Table 89: Antimicrobial activity of <b>23c</b> : <i>S.aureus</i> (+ 100% growth detected, † partial growth)	289
Table 90: Antimicrobial activity of compound <b>13d</b>	290
Table 91: Antimicrobial activity of compound <b>1d</b>	290
Table 92: Antimicrobial activity of compound <b>4d</b>	290
Table 93: Antimicrobial activity of compounds <b>7d-9d</b>	291
Table 94: Antimicrobial activity of compounds <b>10d-12d</b>	291
Table 95: Antimicrobial activity of compounds <b>15d</b> and <b>16d</b>	291
Table 96: Antimicrobial activity of compounds <b>17d-19d</b>	292
Table 97: Antimicrobial activity of compound <b>20d</b>	292
Table 98: Antimicrobial activity of compound <b>23d</b>	292



## Abbreviations & Acronyms

AcOH	Acetic acid
ALA	5-Aminolevulinic acid
AMR	Antimicrobial Resistance
$\beta$	Beta
CA-MRSA	Community Associated Methicillin-Resistant <i>Staphylococcus aureus</i>
CAI	Community Associated Infections
<i>C.albicans</i>	<i>Candida albicans</i>
CDCl <sub>3</sub>	Chloroform-deutarated
CHCl <sub>3</sub>	Chloroform
c. HCl	Concentrated hydrochloric acid
COSY	Correlation Spectroscopy
<sup>13</sup> C NMR	Carbon Nuclear Magnetic Resonance Spectroscopy
DAD	Diethyl azodicarboxylate
DCM	Dichloromethane
Der	Derivatives
DMF	Dimethylformamide
DMSO	Dimethylsulphoxide
DNA	Deoxyribonucleic acid
DPPH	2,2-Diphenyl-1-(2,4,6-trinitrophenyl) hydrazyl
<i>E.coli</i>	<i>Escherichia coli</i>
EtOAc	Ethyl acetate
EtOH	Ethanol
Et <sub>3</sub> N	Triethylamine
FDA	Food and drug administration
g	Grams
HA-MRSA	Hospital Associated Methicillin-Resistant <i>Staphylococcus aureus</i>
H <sub>3</sub> BO <sub>3</sub>	Boric acid
HCl	Hydrochloric acid
<sup>1</sup> H NMR	Proton Nuclear Magnetic Resonance Spectroscopy

HpD	Hematoporphyrin
HPV	Human Papilloma Virus
HRMS	High Resolution Mass Spectra
ICG	Indocyanine Green
IR	InfraRed
<i>K. pneumoniae</i>	<i>Klebsiella pneumoniae</i>
KtBuO	Potassium <i>tert</i> -butoxide
$\lambda_{\max}$	Absorption maxima
LCMS – EI	Liquid Chromatography Mass Spectrometry – Electron Ionisation
<i>m</i>	Meta
MAL	Methyl-aminolevulinic acid
MC540	Merocyanine 540
MeCN	Acetonitrile
MES	Microwave Enhanced Synthesis
MeOH	Methanol
mg	Milligrams
MHRA	The Medicines and Healthcare Products Regulatory Agency
MIC	Minimum Inhibitory Concentration
mL	Millilitres
mM/mL	Millimolar per millilitre
MRSA	Methicillin-Resistant <i>Staphylococcus aureus</i>
MW	Microwave
<i>M. tuberculosis</i>	<i>Mycobacterium tuberculosis</i>
<i>N.gonorrhoeae</i>	<i>Neisseria gonorrhoeae</i>
NIR	Near-Infrared
<i>o</i>	<i>Ortho</i>
$^1\text{O}_2$	Singlet oxygen
<i>p</i>	<i>Para</i>
<i>P.acnes</i>	<i>Propionibacterium acnes</i>
PBP	Penicillin Binding Protein

PD	Pulse dyes
PDT	Photodynamic therapy
PACT	Photodynamic antimicrobial chemotherapy
Pcs	Phthalocyanines
<i>P. aeruginosa</i>	<i>Pseudomonas aeruginosa</i>
<i>P. notatum</i>	<i>Penicillium notatum</i>
PLD	Pulse laser dye
PPA	Polyphosphoric acid
<i>p</i> -TsCl	4-Toluenesulphonyl chloride
PWS	Port wine stains
ROS	Reactive Oxygen Species
rtp	Room temperature
S <sub>0</sub>	Singlet state
<i>S. aureus</i>	<i>Staphylococcus aureus</i>
<i>S. albus</i>	<i>Staphylococcus albus</i>
T <sub>1</sub>	Triplet excited state
Sn(II)Cl	Tin (II) chloride
<i>S. pneumonia</i>	<i>Streptococcus pneumonia</i>
TPCPD	2,3,4,5-tetraphenylcyclopentadienone
TMS	Tetramethylsilane
TLC	Thin layer chromatography
UV/Vis	Ultra-violet/visible
†	Partial antimicrobial activity
+	Antimicrobial activity
-	No antimicrobial activity
Π	Pi electrons

# Chapter 1

## *General Introduction - Antimicrobials*

### 1.1 Antimicrobial resistance

Antimicrobial resistance (AMR) is becoming an symbolic feature of resistant microorganisms towards existing antimicrobial agents<sup>4</sup>. The British Society for Antimicrobial Chemotherapy is gravely concerned of the relentless rise in antimicrobial resistance, as this will have severe and harmful effects about global health and our ability to treat infections in hospitals and the community.

During the primary stages of the 1970's, clinicians were forced to abandon their beliefs that virtually all microbial infection was treatable with the range of existing antimicrobial agents<sup>5</sup>. This optimism was shattered by resistance of the bacteria to numerous antibiotics, such as *Staphylococcus aureus*, *Streptococcus pneumoniae*, *Pseudomonas aeruginosa*, and *Mycobacterium tuberculosis*<sup>6</sup>.

The rapid upsurge in the evolution of antimicrobial resistance may have been effected by several possible factors such as the prolonged and inappropriate use of antibiotics<sup>7</sup>, increased travels to both national and international countries<sup>6</sup> hence causing the spread of germs/bacterial infections. Humans have become the major driving force behind the accelerated evolution of bacterial resistance that has led to a complexity of resistance and scope, that the health care system is stretched to cope with<sup>8</sup>.

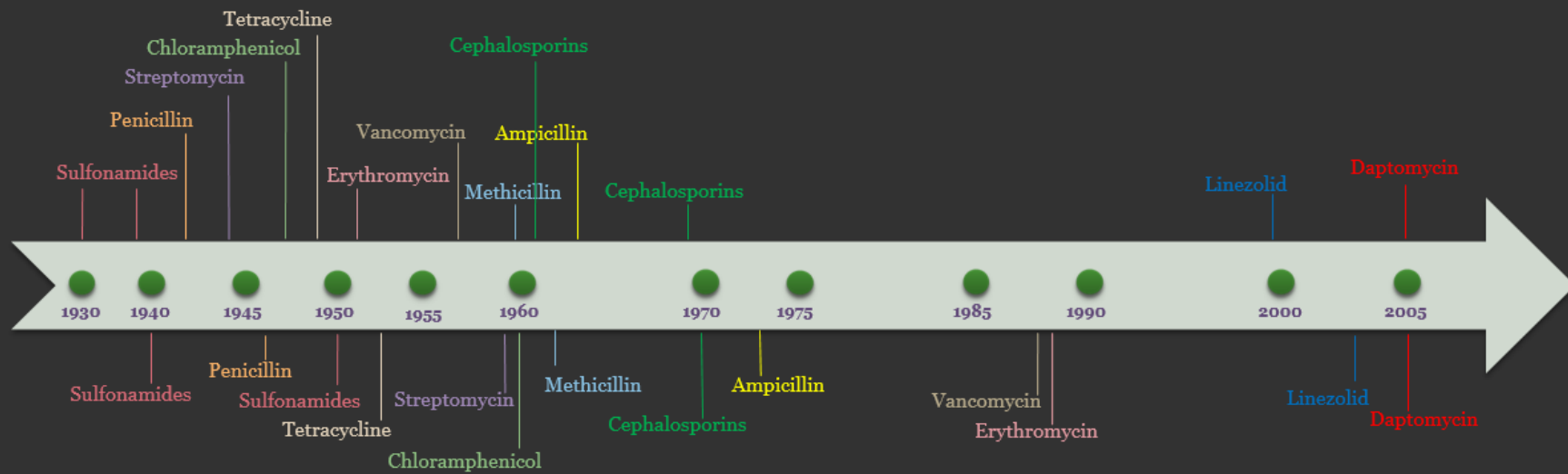
Acquired resistance to different antimicrobials has been categorised in a wide variety of bacteria<sup>9</sup>. It is known that some resistant organisms are important causes of community associated infections (CAI)<sup>10</sup>. Examples of these would be penicillin resistance *Streptococcus pneumonia* or the multi-drug resistant *Neisseria gonorrhoeae*<sup>11</sup>. Additional resistant organisms that are of crucial concern within the hospital settings are those that are responsible for “hospital acquired infections (HAI)”, otherwise known as nosocomial infections<sup>12</sup>. These are acquired either; in a hospital or a health care environment, that arise 48 hours or more after hospital admission or within 30 days post discharge following in-patient care<sup>13</sup>.

Infections with drug resistant gram negative bacteria pose a particular challenge, because of the complexities they pose that make them physically resistant, not only to drugs, but also in their spreading abilities<sup>14</sup>.

The organisms amongst the most common pathogens causing nosocomial infections are gram positive bacteria (*Staphylococcus aureus*, and *Enterococcus* species), & gram-negative- (*Pseudomonas aeruginosa*, *Klebsiella pneumoniae*, and *Enterobacter* species)<sup>15</sup>.

Over the years bacteria have rapidly developed major resistance towards existing antibacterial agents, and this is illustrated in timeline overleaf (Figure 1).

## Antibiotic Deployment



## Antibiotic Resistance Observed

Figure 1: Timeline of bacterial resistance<sup>16</sup>

The drug development of new antimicrobials to treat gram negative bacteria has been extremely challenging due to various reasons;

- I. Biologically related
- II. Clinical trials

*Biological related:* Gram negative bacteria possess an additional outer membrane, which is composed of phospholipids and lipopolysaccharides. It is located on the outer side of the peptidoglycan layer. The highly charged nature of lipopolysaccharides confer an overall negative charge to the gram negative cell wall<sup>17</sup>. The permeability of this membrane layer is controlled tightly, causing problems for many potential drugs to cross the layer<sup>18</sup>. This is one of the prime challenges faced by many researches when developing drugs for gram negative bacteria. An additional hindrance halting research of novel antimicrobial agents is the existence of numerous differing resistance mechanisms present within multi drug resistance gram negative bacteria<sup>19</sup>.

*Clinical trials:* These results from the regulatory process for antimicrobial drugs. It is crucial to show that the tests of the newly developed drugs are effective and designed adequately. For novel drugs to enter clinical trials, the regulatory approval process needs be met ethically since it is not possible to test the new drug(s) in a placebo controlled trial. This in itself becomes an obstacle as additional expenses and alternative trails must be conducted. These trials need to produce drugs that are FDA approved as well as being invested by pharmaceutical companies as they are short lived<sup>13</sup>.

In general, patients often develop drug resistant infections during their stay in hospitals<sup>20</sup>. However, these infections are caused by bacterial species that are normal elements of the human microbiota<sup>21</sup>. Gram negative bacteria is mostly resistant to antimicrobial drugs, hence the focus on these pathogens<sup>22</sup>. This is believed to be the case as majority of the antibiotic drugs are either natural products or derivatives of natural products that are produced by microbes<sup>23</sup>. Consequently majority of the naturally occurring genes have resistance to antibiotic drugs prior to the developed drugs before they have even been applied to use<sup>24</sup>. It is these resistance genes that in time become problematic once they begin to spread on clinically important bacteria<sup>25,26</sup>.

Many antimicrobial drugs have been used for agricultural purposes for example; therapeutic, prophylactic, and growth reasons<sup>27</sup>. Subsequently bacterial drug resistance are frequently being found in both meat and other foods<sup>21,28</sup>. Hence, those that are contaminated have been associated with several drug resistant enteric pathogenic outbreaks. Examples of these pathogens include *Salmonella*, *Escherichia coli (E.coli)*, and *Campylobacter*<sup>28-30</sup>. It is these drug resistant bacteria that cause resistant infections directly, or function as a pool of drug resistance genes that can be spread to other bacteria that reside in the human gut<sup>21</sup>.

## 1.2 Resistance in hospitals

The era of antibiotics began in the early 1940's. This was when hospitals were introduced to Penicillin<sup>11</sup>. Not long after (1950's) did the infamous problem of the resistance *Staphylococcus aureus* strains were isolated, as they had shown resistance towards the Penicillin drug. These antibiotic resistant organisms are biologically capable of causing life threatening infections that are proving to be challenging to manage, due to the availability of limited treatment<sup>31</sup>. Consequently, substantial problems within hospitals have evolved. In the early 1960's Methicillin and other forms of penicillin had known to be effective forms of treatment towards the resistant organism<sup>32</sup>. The proportion of infections with strains that are resistant to standard therapy is rising for several human pathogens<sup>33</sup>. The frequency of infection today is recognized as a major threat to the treatment of infectious diseases, and is of great concern to the public health<sup>34</sup>. Unfortunately, opportunistic pathogenic infections have increased resulting in the increase in frequency of hospitalisation for longer periods. This in turn has increased exposure to multidrug resistant pathogens, which are present in the healthcare settings<sup>35</sup> for example *S. aureus* is one of the major pathogens, (specifically methicillin resistant strains) that is causing enhanced morbidity, mortality, and additional costs<sup>36</sup>.

The development of a new antimicrobial drug have been followed by the evolution of resistant pathogens. Research today is primarily showing that resistant organisms to multiple antimicrobials agents have become increasingly common<sup>37</sup>, and a number of organisms have developed resistance towards the all standard antimicrobial treatments that are present today.

### 1.2.1 *Staphylococcus aureus*

*Staphylococcus aureus* (*S. aureus*) are gram positive cells that are comprised of 28 species and 7 sub species in this genus. Originally, only two species called *S. aureus* and *Staphylococcus. albus* existed. When members of the genus *Staphylococci* are observed under the microscope, they appear as spherical bacteria (*cocci*), which are between 0.5-1.5 µm in diameter. *Staphylococci* occur in various forms: individually, irregularly grouped, in pairs, or sometimes as grape like clusters<sup>38</sup>. *S. aureus* are non-motile and non-spore forming species. They have an optimum growth temperature of 37 °C.

*Staphylococcus aureus* is recognized as an important human pathogen that is currently the leading cause of infections in humans, including superficial skin infections such as boils, abscesses and other serious infections such as those infections present in the bloodstream, and pneumonia<sup>39</sup>. *S. aureus* can cause toxic shock syndrome by producing exotoxins into the bloodstream, and cause food poisoning by releasing enterotoxins into food<sup>40,41</sup>.

The major cause of nosocomial infections, (including surgical site infections and infections associated with indwelling medical services) are primarily caused by *S. aureus*<sup>42</sup>. Literature states that surgical infections have occurred as long as surgery has been performed., as an example it is



known that more than 50 % of deaths that occurred in the mid-19<sup>th</sup> century were due to post-operative surgical site infections<sup>43</sup>.

### 1.2.2 *Escherichia coli*

*E.coli* are gram negative bacteria that is a member of the *Enterobacteriaceae* family, which have a rod like shape. *Enterobacteriaceae* are a non-spore forming, facultative anaerobic bacteria. These are primarily found in the lower intestines of warm blooded organisms<sup>44</sup>. Most *E.coli* strains are motile and can ferment sugars that appear as smooth colonies, which range from 2-3 mm in diameter. Some species of the *Enterobacteriaceae* family such as Salmonella and Shigella are highly pathogenic whilst other are non-pathogenic<sup>45</sup>.

*E.coli* is one of the most prevalent aerobic gram-negative bacterial pathogen<sup>46</sup>, that causes infections such as: gastroenteritis, urinary tract infection, meningitis, peritonitis, and septicaemia<sup>47</sup>. Majority of the blood stream infections have been caused by *E.coli*<sup>48</sup>. It is also one of the most common causes of community acquired and nosocomial infections<sup>49</sup>. Research shows that enteric *E.coli* usually causes enteritis and diarrhoea<sup>50</sup>. Infections containing gram-negative bacilli, specifically in neonatals is one of the major reasons for having a high mortality rate of children<sup>51</sup>.

*E.coli* develops resistance towards fluoroquinolones, quicker than other members of the *Enterobacteriaceae*<sup>49</sup>. Fluoroquinolones are an important class of antimicrobial agents that have exceptional activity against infections caused by Gram negative bacteria, particularly *E.coli*<sup>52</sup>.

This bacteria is used frequently as an indicator to monitor faecal contamination in drinking water and in food<sup>53</sup>. It has been detected in many sources such as water, soil, and other varying environments due to faecal contamination. Studies to date show that vegetarians are most likely to contain the resistant of *E.coli* as omnivores<sup>54</sup>.

### 1.2.3 Hospital associated methicillin resistant *S.aureus*.

Over the past 20 years methicillin resistant *staphylococcus aureus* (MRSA) has become one of the most important causes of infections in both the hospital and community associated methicillin resistant infections<sup>39</sup>.

Hospital associated (HA-MRSA) and community associated (CA-MRSA) infections tend to overlap as is difficult to diagnose where they have been contracted due to the presence of strains in both environments.

HA-MRSA strains have typically been resistant to multiple antimicrobials<sup>55</sup>. There are many risk factors established due to HA-MRSA, these can be; dramatically increased length of stay in hospitals, or undergoing either multiple or prolonged antimicrobial therapy<sup>56</sup>. In many cases the patient can be present with a surgical wound, or in various cases people could be and are in contact

with MRSA patients and dialysis<sup>40</sup>.

#### 1.2.4 Community associated methicillin resistant *S.aureus*

Community acquired MRSA (CA-MRSA) describes the spread of MRSA infection, which is diagnosed outside the hospital or less than 48-72 hours of admission<sup>57</sup>.

CA-MRSA is most commonly found and associated with the skin and soft tissue infection. This however can develop into a life threatening infection<sup>58</sup>. On the contrary, this differs from HA-MRSA infections as CA-MRSA infections lack the established risk factors that HA-MRSA infection have.

Studies on CA-MRSA infections have shown different bacteriologic characteristics than those present in HA-MRSA<sup>59</sup>. The isolated pathogens of CA-MRSA are resistant to a reduced number of antimicrobial agents. These are a class of antibiotics that fall into the category of  $\beta$ -lactams, for example; penicillins and cephalosporins<sup>60</sup>, shown in Figure 10.

### 1.3 The role of microbes in wounds

The impact of microorganisms on wounds, particularly chronic wounds have been studied extensively. They have been reviewed using many types of approaches to elicit their role in the process of non-healing for example the occurrence of particular species, or groups of organisms<sup>61</sup>. A variety of bacteria and fungi has colonized the human skin. In principle, the colonization provides an effective barrier for microbial penetration and therefore aids tissue infection<sup>62</sup>. The development of a wound compromises this barrier, therefore increases the odds for invasion of what normally would be a sterile tissue and wound colonization by microorganisms. The spread of infection is majorly related to various factors including: the type of wound present, and general wound care. It is also affected by additional factors such as; underlying disease, age, nutritional and the general immune status of the patient<sup>63</sup>.

The importance of reducing microbial load in wounds is treated by the use of prophylaxis. Thus facilitating the healing process of wounds<sup>64,65</sup>. However, an infected wound prolongs the process in healing, which subsequently increases the health care costs for the patient<sup>66</sup>.

### 1.4 Cost Impact

The increase in pervasiveness of resistance is of utmost importance due to both the clinical and economic impact of infection, which is caused by the resistant organisms.

Infections on post-operative wounds have a remarkably huge impact on patients' quality of life, consequently affecting the financial cost of patient care<sup>67</sup>. Literature shows that within the US alone, in one year, approximately one million patients have had to extend their stay in hospitals due to the infection caused from an open wound, which has led to either increased pain of the

wound, sepsis and in some cases death of the patient. Thus, the cost of the stay rising to \$1.5 billion in health care costs annually within the US<sup>68</sup>.

Here in the UK, the latter part of the 1990's approximately fifty million pounds worth of antibiotics were manufactured and utilised for people both in homes and hospitals<sup>69</sup>. The financial cost in the health care system alone has estimated to have been generated more than an excess of £400 million per annum. These wounds are usually managed in the primary healthcare settings<sup>70</sup>. Nonetheless Callam et al. demonstrated that majority of the patients were managed in the community, of this 5% were inpatients in hospitals and the 12% were either by a health care team or as an outpatient<sup>71</sup>. Callam et al. suggested that 63% of areas within the UK, venous ulcers are becoming further widespread, from a more recent published article<sup>72</sup>.

### 1.5 Ehrlich's Magic Bullet

Paul Ehrlich is often seen as the father of modern day chemotherapy. His fascination within the area of dye chemistry begun during the early 1900s<sup>73</sup>. Ehrlich brought dyes into the forefront of biomedical use; the realisation that microorganisms could be selectively stained revolutionised the new and emerging areas of microbiology and molecular pathology<sup>74</sup>. From here, Ehrlich conceived the idea of selectivity toxicity (Ehrlich's magic bullet) and this was further enhanced when he used the tricyclic phenothiazine dye, methylene blue (Figure 2) to successfully treat human malaria in 1891<sup>75</sup>, causing dye therapy to become integrated into clinical medicine<sup>76</sup>. The idea behind the magic bullet was to selectively target diseased cells in the presence of healthy cells. The selectivity of methylene blue was achieved by proteins binding to invading cells, and attacking them. This detection was observed in the early 1980's when antibody experiments were tested on cancer patients<sup>77</sup>.

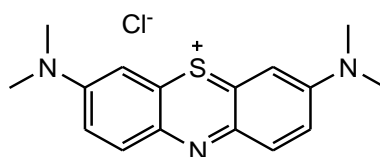


*Figure 2: Chemical structure of methylene blue*

Although methylene blue (Figure 2) showed potential as an antimalarial agent, its use was short-lived due to the emergence of quinine, (Figure 3) and quinine derivatives such as chloroquine shown in Figure 4. Methylene blue was employed to treat a whole host of alternative conditions such as treatments for psychiatric patients<sup>78</sup>.

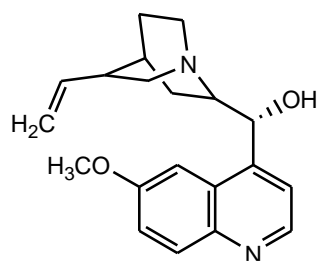


*Figure 3: Chemical structure of quinine*

Although quinine is still active today as an antimalarial, it comes with side effects such as ringing in the ears and partial deafness<sup>79</sup>. Chloroquine was seen as a good replacement for quinine for multiple reasons:

- i. Low yielding side effects
- ii. Its renowned for its efficacy
- iii. Ease of use
- iv. Reduced toxicity

Resistance to this drug is now being seen in East Africa most notably the boarder of Tanzania<sup>80</sup>.

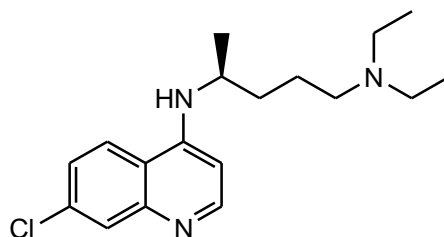


*Figure 4: Chemical structure of chloroquine*

Nonetheless, Ehrlich's quest to find better therapeutic agents to target diseases continued. His focus now changed from treating malaria, to fighting the horrific disfiguring disease Syphilis, thus leading to the infamous discovery of the arsenic containing compound Salvarsan – 606 as shown in Figure 5<sup>74</sup>. This discovery was noted as Ehrlich's magic bullet!

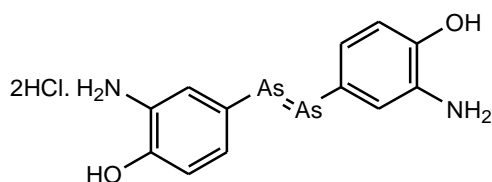


*Figure 5: Chemical structure of salvarsan-606*

Salvarsan proved effective and was introduced into clinical use at the start of 1910. Salvarsan became the world's first blockbuster drug, until in 1940's when penicillin became available. Unfortunately, Salvarsan did not respond very well with patients that suffered from the later stages of Syphilis or against other bacterial infections. However, it did responded well against the sleeping sickness disease but many physicians found it to be difficult to handle and administer.

Salvarsan was available in powder form and extremely unstable in air, thus needing to be dissolved in pure water before patient administration.

The instability and toxic effects of Salvarsan, led Ehrlich to enhance his research further on improving this drug. Upon evaluation and continuation on the research, Ehrlich discovered Neosalvarsan – 914, Figure 6. Neosalvarsan contained a lower arsenic content, had increased water solubility and appeared to be more active upon comparison with Salvarsan.

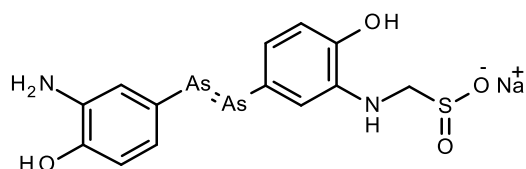
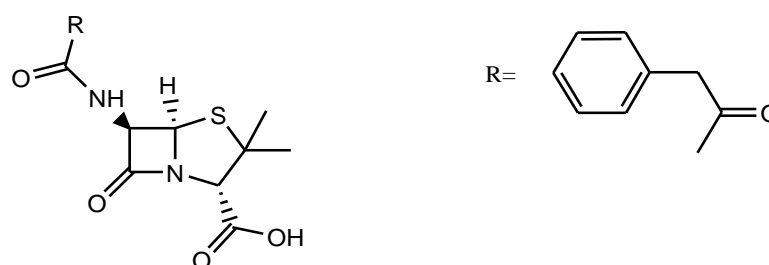


Figure 6: Chemical structure of neosalvarsan-914

By the 1920's Salvarsan became the world's most popular drug, however Ehrlich's hope that it would become the first of many magic bullets was ill-founded. However, with Europe at war, an underlying problem was now beginning to show itself, infection and how to control it. Infections caused by the most minor of injuries became uncontrollable, hospital wards were rapidly filling with the dying and desperate. With treatment wards soon turning into septic wards, doctors and nurses could do nothing but clean infected wounds and offer comfort, opposed to a curable prognosis. Thus, the need for novel active antimicrobial agents was now greater than ever!

## 1.6 Penicillin

The discovery of *penicillin*, Figure 7, in 1928 by Sir Alexander Flemming was seen as a breakthrough for antimicrobial chemotherapy and gained him the Nobel Prize. Although Sir Flemming observed that a substance produced by a fungal mould<sup>81</sup>, (*Penicillin* species) *Penicillium notatum*, had the ability to prevent growth of *Staphylococcus aureus*, he could not isolate or purify the active product, which we know today as penicillin.



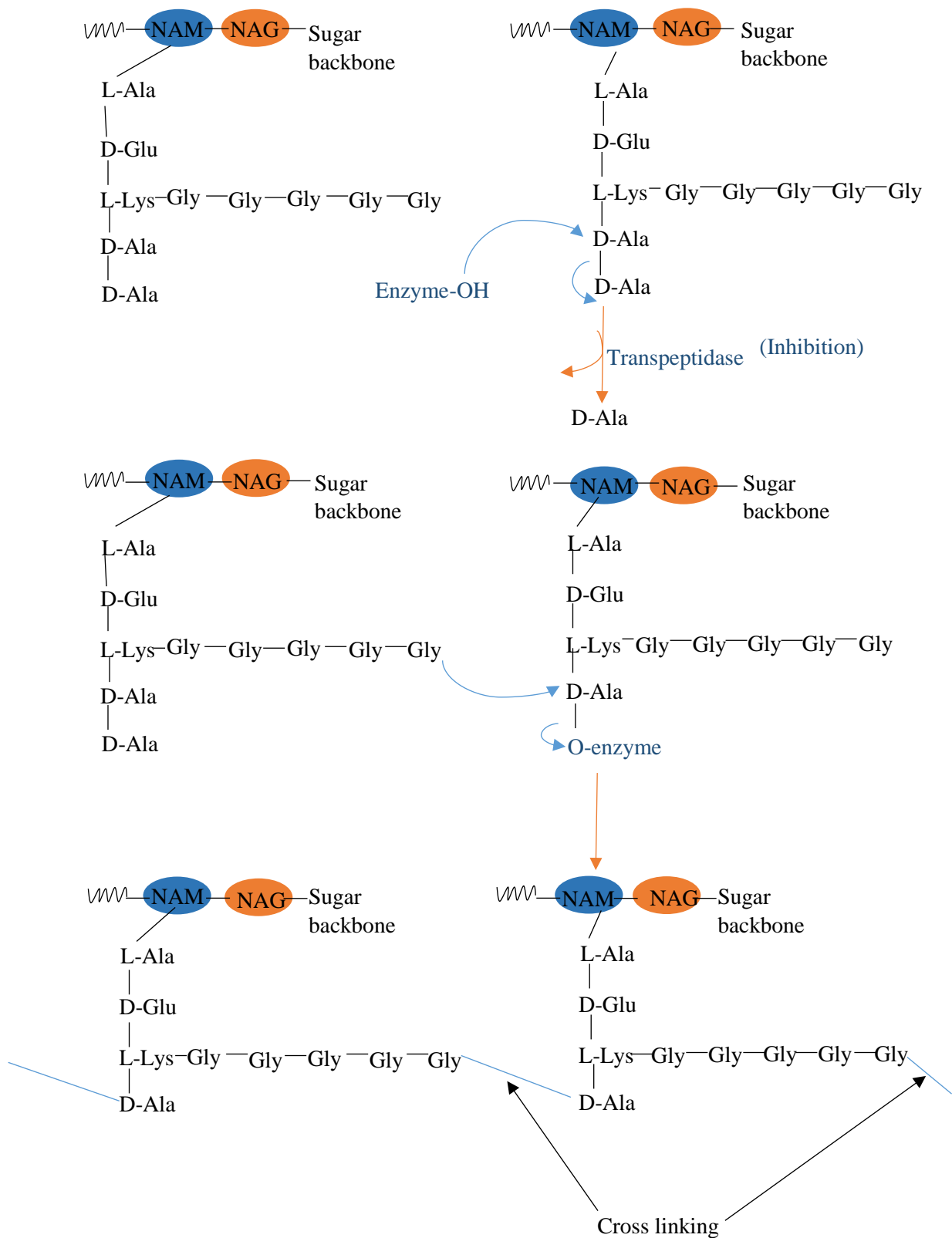
Penicillin G

Figure 7: Chemical structure of penicillin (G)

Later Sir Flemming concluded that in his opinion, the structure of penicillin was too unstable to be isolated, however Sir Flemming did note in his famous publication in 1928, that penicillin

showed great potential as an antimicrobial agent. He also noted that this molecule could one day suffer from bacterial resistance. With Europe on the verge of the Second World War, the need to push forward with the development of novel antimicrobial agent was now a priority. At this point in time, the discovery of penicillin went unnoticed for 10 years until researchers at the Dunn School of Pathology in Oxford University turned penicillin from a medical curiosity into the wonder drug. The Oxford team consisting of Howard Florey, Ernst Chain and Norman Heatley were able to grow and isolate the active ingredient penicillin and conducted successful *in-vivo* trials, with the first human to be injected with penicillin on the 27<sup>th</sup> January 1941 to test its toxicity<sup>82</sup>. For their hard work, Florey, Chain, and Fleming were awarded the Nobel Prize in 1945.

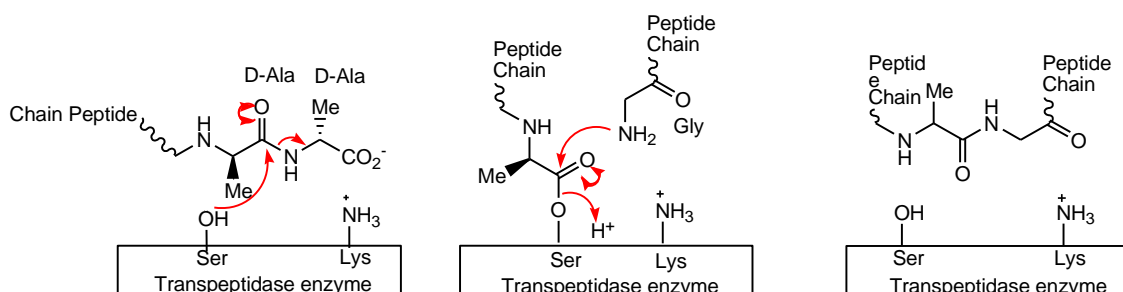
Penicillin has a unique mode of action, targeting one of the enzymes responsible for the biosynthesis of the bacterial cell wall, the transpeptidase enzyme. The transpeptidase enzyme is involved in the final cross-linking of the sugar backbones (*N*-acetylmuramic acid (NAM) and *N*-acetylglucosamine (NAG)) of the peptidoglycan cell wall of the bacteria, illustrated in Scheme 1. If this is not accomplished, it leaves the cell wall poorly constructed and susceptible to bursting, due to changes in osmotic pressures, resulting in a cell wall framework that is no longer interlinked<sup>83</sup>.



*Scheme 1: Mechanism for cross-linking of the bacterial cell wall!*

The transpeptidase enzyme is bound to the cell membranes outer surface (e.g. serine protease) this contains the serine residue in the active site and catalyse the hydrolysis of the peptide bonds. The serine, a nucleophile, splits the peptide bond between the two D-alanine units on the peptide

chain. The terminal alanine unit vacates the active site, leaving the peptide chain bound. From another peptide chain, the pentaglycyl moiety enters the active site, and the terminal glycine forms a peptide bond with the alanine unit by displacing it from the serine and linking the chains together, illustrated in Scheme 2.



*Scheme 2: Mechanism of transpeptidase cross-linking*

Although penicillin became a household name due to its life-saving ability, resistance was soon being observed in hospitals, ironically from *S. aureus*<sup>84</sup>, the bacterial culture which Fleming first noted penicillin's activity. Bacterial strains can differ in their resistance to penicillin, as noted above. *S. aureus* was initially susceptible, and can build up resistance after lengthy exposure to the drug. Although, some species such as *Streptococci* are extremely vulnerable, bacteria such as *Pseudomonas Aeruginosa* is particularly resistant. Resistance has been attributed to a number of reasons such as:

1. The presence of a  $\beta$ -lactamase enzyme.
2. Physical barriers.
3. Over production of transpeptidase enzymes caused by the bacteria.
4. Affinity of transpeptidase enzyme by penicillin.
5. Transport of penicillin- across the cell wall (efflux pumps).
6. Mutations and genetic transfers.

The most problematic resistance is caused by the presence of  $\beta$ -lactamase enzyme, and causes resistance towards many variations of the  $\beta$ -lactam antibiotics for example penicillin, cephamycin and carbapenems<sup>85</sup>. Methicillin, Figure 8 produced by Beechams in 1959, stemmed from the emergence of penicillin resistance.



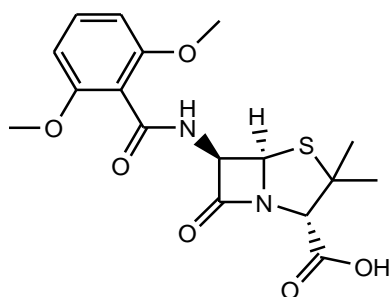


Figure 8: Chemical structure of methicillin

Not long after the introduction of methicillin into clinical trials, methicillin resistance strains of *Staphylococci* were identified, (MRSA)<sup>86</sup>. In the early 1960's, European hospitals announced the first outbreak of methicillin resistance MRSA infections<sup>87</sup>.

Prior to synthesising penicillin, the resistant strains of *staphylococci* were isolated from a surgical wound infection<sup>88</sup>. Thus, in order to combat the resistivity to penicillin's, new generations of penicillin's based on the  $\beta$ -lactams and the cephalosporin's such as Cefaroline (Figure 9) were being developed.

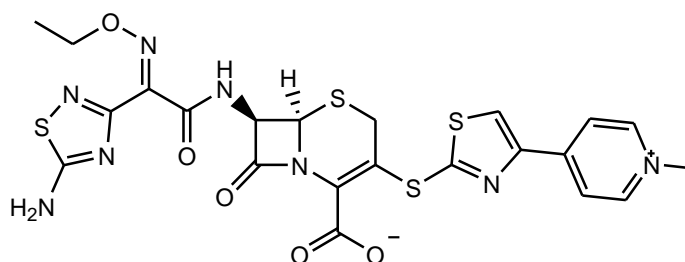
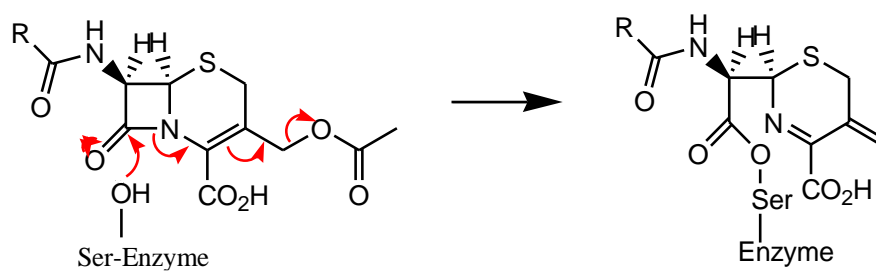


Figure 9: Chemical structure of a cephalosporin-cefaroline

Cephalosporins are a type of  $\beta$ -lactam antibiotic that is closely related to the penicillin's. They are bactericidal, and have the same mode of action as other  $\beta$ -lactams.

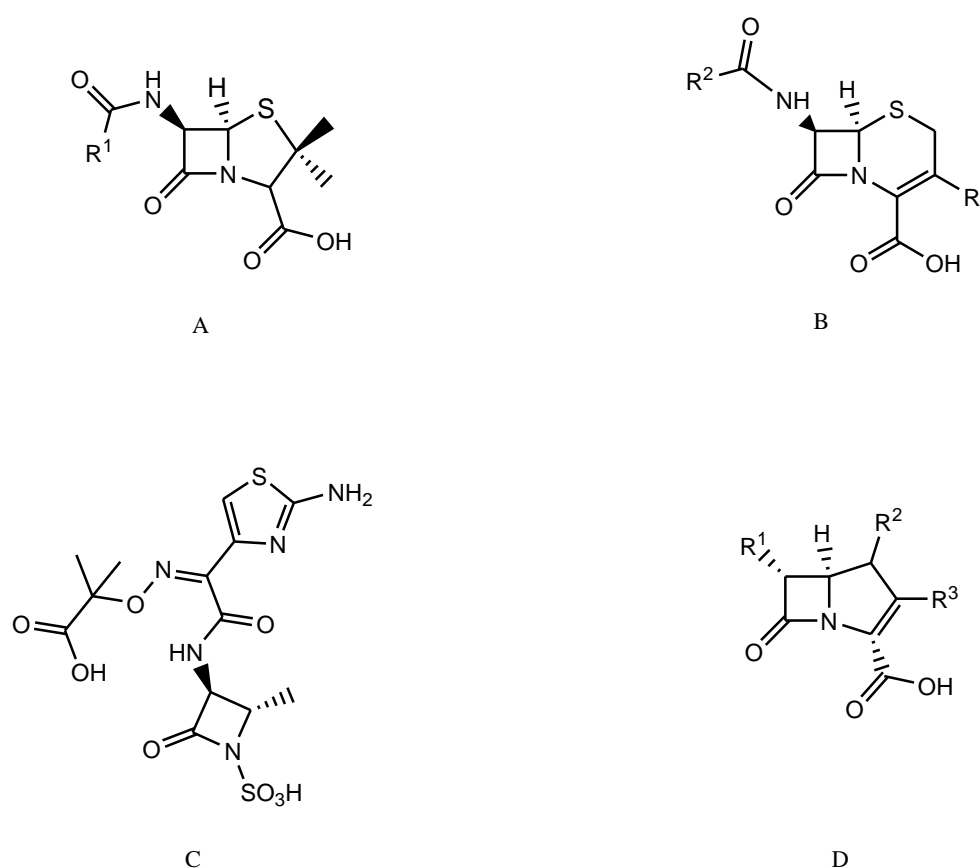
The mode of action of cephalosporins is to disrupt synthesis of the peptidoglycan layer of bacterial cell walls. Cephalosporins inhibit the synthesis of bacterial cell wall by combining with penicillin binding proteins (PBP).

As a result of over-prescribing the  $\beta$ -lactams, bacterial strains producing  $\beta$ -lactamases with different properties emerged, as well as those with other resistant mechanisms<sup>89</sup>.  $\beta$ -Lactamase breaks down  $\beta$ -lactams through a hydrolysis mechanism as shown in Scheme 3. This simply occurs by hydrolysis of the four membered  $\beta$ -lactam ring, subsequently deactivating the antibacterial properties<sup>90</sup>.



*Scheme 3 Mechanism of action of cephalosporins*

$\beta$ -Lactam antibiotics are by far the mostly used antibiotics. Derivatives of penicillin antibiotics are those containing the  $\beta$ -lactam ring (Figure 10). Most of these derivatives are known as scaffolds, which are produced by microorganisms<sup>91</sup>.



- A = Penams
- B = Cephalosporins (cephems)
- C = Monobactams
- D = Carbapenems

*Figure 10: Derivatives of  $\beta$ -lactam antibiotics<sup>92</sup>*

Carbapenems are also inhibitors of  $\beta$ -lactamases, however, they are unique types of inhibitors because they generally are resistant to hydrolysis by most  $\beta$ -lactamases, and can still target

penicillin binding proteins. Carbapenems have the greatest potency against Gram-positive and negative bacteria, and have the broadest spectrum of activity<sup>93</sup>.

For a class of  $\beta$ -lactams, the mechanism of action for carbapenams identifies that carbapenams cannot to diffuse through bacterial cell wall. However, they enter through the porins of the gram negative bacteria and acylate the PBPs. Carbapenems behave as mechanism based inhibitors for the peptidase domain of PBPs and inhibit the peptide cross-linking in parallel to other peptidase reactions<sup>94</sup>. The speciality of carbapenams is their efficacy of ability to bind to multiple different PBPs. This is illustrated in its mechanism of the cell wall formation, which is a “three-dimensional process,” with its formation and autolysis occurring at the same time. The PBPs are inhibited and autolysis continues, eventually weakening the peptidoglycan, resulting in the cell to bursts due to the osmotic pressure<sup>93,95</sup>.

$\beta$ -Lactam rings form stable adducts with the serine residue of the PBPs, which have an active site. PBPs are segregated into two forms;  $\beta$ -lactams target the class A PBP, and are crucial to cell survival.

The next generation of antibiotics, Figure 11, are highly effective in fighting infections caused by the  $\beta$ -lactamase producing organisms<sup>96</sup>. Its effectivity is increased when used in combination with  $\beta$ -lactam antibiotics e.g. amoxicillin<sup>97</sup> rather than its lone use as it will have a weak intrinsic antibacterial activity.

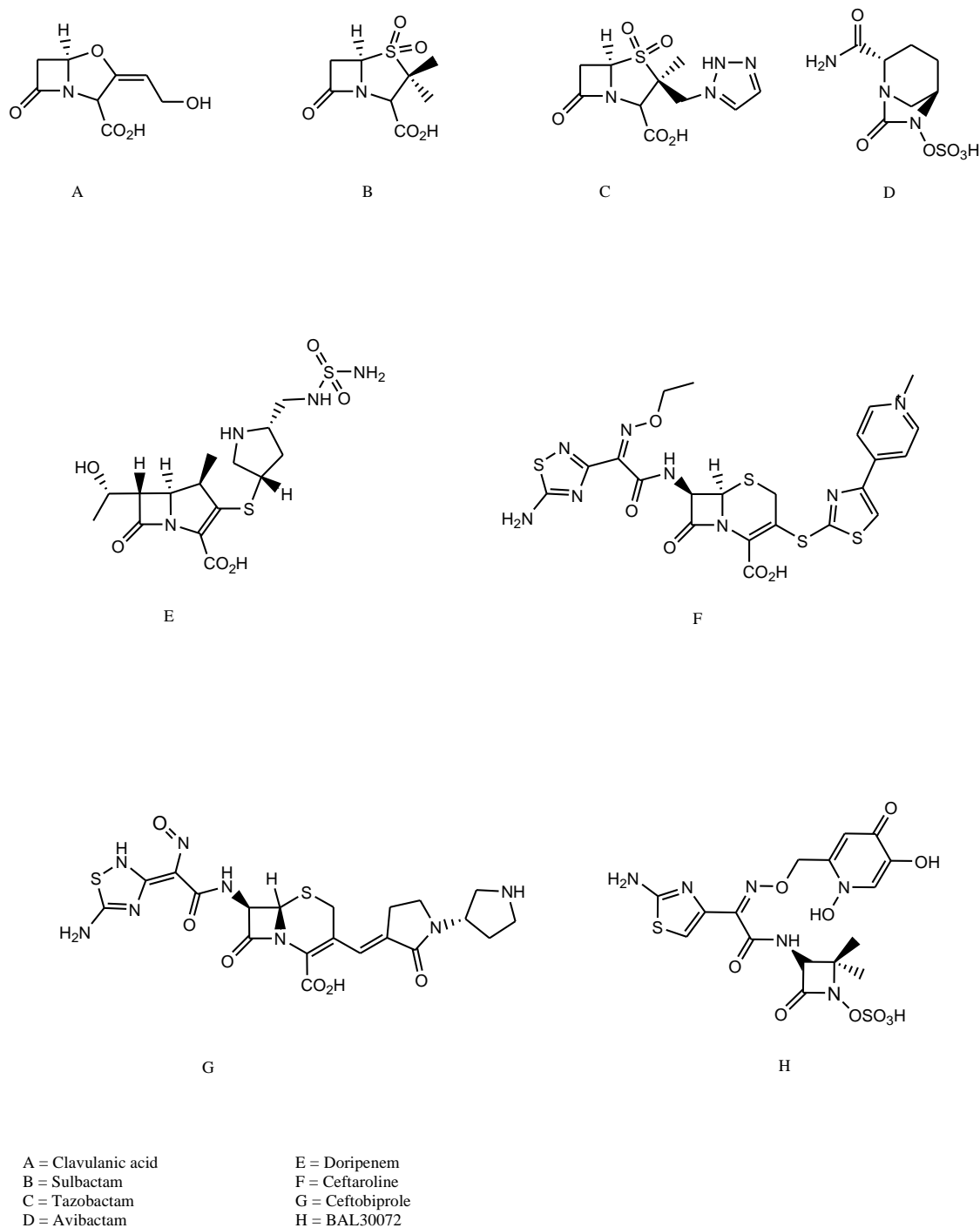
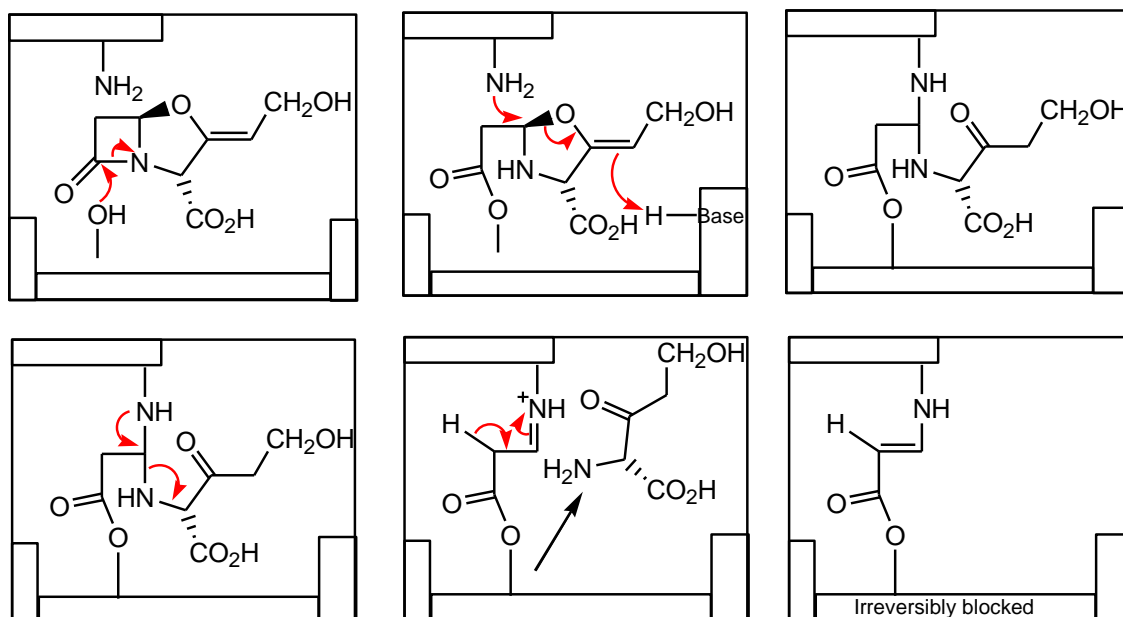


*Figure 11: Next generation of antibiotics/  $\beta$ -lactamase inhibitors*

Three of the next generation antibiotics showed great potency as  $\beta$ -lactamase inhibitors and were introduced into clinical trials. These  $\beta$ -lactamase inhibitors were: clavulanic acid-(A) (1970), sulbactam-(B) (1978) and tazobactam-(C) (1980) <sup>98</sup>.

Clavulanic acid has shown to be an active inhibitor of some class D enzymes. Although it has a  $\beta$ -lactam ring, it has either little or no inhibition activity against  $\beta$ -lactamase enzymes in class B or C but has high affinity towards the class A  $\beta$ -lactamases <sup>97</sup>. However, evidence suggests that clavulanate may influence the activity of  $\beta$ -lactam antimicrobials against pathogenic bacteria by

mechanisms other than the inhibition of  $\beta$ -lactamase. This evidence is seen in research conducted by J. Finlay *et.al.*, which identifies that  $\beta$ -lactam activity is influenced by clavulanate against *S. pneumoniae* through interaction at the cell wall and complementary binding of the clavulanate and amoxicillin to PBPs<sup>99</sup>. The mechanism of clavulanic acid is illustrated in Scheme 4.



*Scheme 4: Mode of action of clavulanic acid*

Although avibactam, Figure 11, a non  $\beta$ -lactam serine  $\beta$ -lactamase inhibitor is used in combination with cephalosporins and aztreonam, its activity becomes potent against *Klebsiella* and other gram negative infections<sup>100,101</sup>. Compound H (BAL30072) shown in Figure 11 entered clinical trials, phase one in June 2014 and is investigated for the use as an intravenous antibiotic with bactericidal properties against the multidrug resistance gram negative bacteria. It currently shows activity against *Pseudomonas aeruginosa* and metallo- $\beta$ -lactamases<sup>98</sup>.

## 1.7 Sulphonamides

In the 30 years following Ehrlich's discovery of Salvarsan-606, no significant developments had been achieved in the field of chemotherapy, then in 1939 Gerhard Domagk, a Nobel Prize winner, was the first to discover an important group of chemicals called sulphonamides or sulphur drugs, shown in Figure 12. The discovery of sulphonamides was considered to be a major advance in the chemotherapeutic industry.

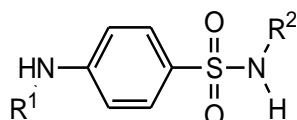
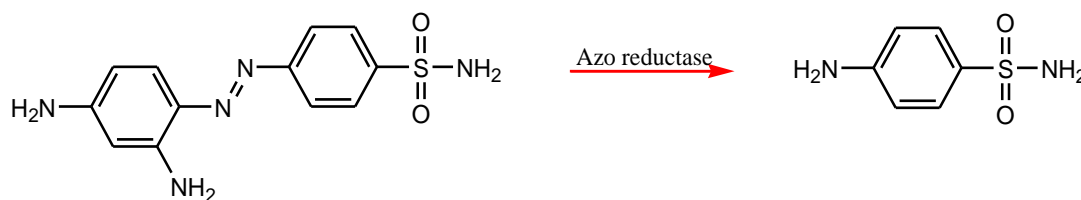


*Figure 12: Derivative of sulphonamide drug*

In 1935 Domagk unveiled sulphanilamide as a pro-drug of Prontosil. The red dye showed that it had antimicrobial properties *in vivo* but none *in vitro* thus, the discovery of sulphonamide was by mechanism of prontosil being metabolised by bacteria.

Sulphanilamides had demonstrated to be extremely effective against several bacterial infections. The affectivity of sulphanilamides proved to be so great that the fatality rate of meningococcal infections (Gram positive organisms) had dropped severely from World War I to World War II. This drug was used to treat wounded soldiers in the war. Sulphanilamide was the first commercially available antibiotic on the market<sup>102</sup>.

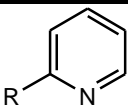
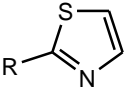
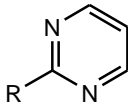
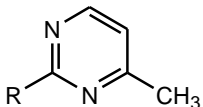
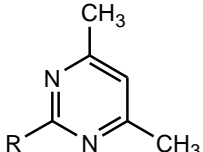
The discovery of sulphanilamide's efficacy led to researcher's to investigate further on similar types of medicinal drugs that could add to the chemotherapeutic market<sup>103</sup>. Many derivatives since have been successfully synthesised. However, the most effective derivative is the substitution of a proton on the R<sup>1</sup> group of the SO<sub>2</sub>NHR<sup>2</sup> moiety resulting in the product to be called sulphanilamide, illustrated in Scheme 5. The R<sup>1</sup> group moiety has had a range of groups that have been substituted onto this position. These groups being a library of aromatic or heterocyclic structures<sup>104</sup>.



*Scheme 5: Azo reductase of prontosil to sulphanilamide*

A number of sulphanilamide derivatives for example sulphanilamides, sulphathiazole, sulphadiazine and sulphadoxine, have been synthesised by reacting sulphanilamide with the R groups illustrated in Table 1. In all these analogues, the amino group at the *para* position must remain un-substituted or have a proton attached. An exception to this rule is the R<sup>1</sup> to be an acyl group as the amides are inactive, but have the ability to metabolise by themselves *in vivo*. These two rules are vital for drug activity<sup>104</sup>.

Table 1: Aromatic structures for sulphanilamide derivatives

R	Structure	Name
R=1		Sulphapyridine
R=2		Sulphathiazole
R=3		Sulphadiazine
R=4		Sulphamerazine
R=5		Sulphamethazine

Sulphanilamides are considered to be one of the least expensive drugs and thus accounted for the extensive use of the chemotherapeutic agent mostly in developing countries, e.g. India.

Sulphanilamides were employed to treat various types of infections systemically in humans ranging from urinary tract infections, meningitis, streptococcal pharyngitis, bacillary dysentery, trachoma, chancroid, malaria, toxoplasmosis, nocardiasis and conjunctivitis<sup>105</sup>.

Sulphapyridine and sulphamerazine have both been used to treat patients with *pneumonia*. Sulphapyridine had been the more effective analogue from the two synthetic drugs. Sulphathiazole on the other hand undergoes metabolism in the human body, resulting in an acetylated form of sulphathiazole, which is proved to be somewhat toxic due to its lack of solubility. Thus, it is poorly absorbed from the intestines. Hence the heterocyclic thiazole ring had been substituted with an aromatic pyrimidine ring, forming the sulphadiazine analogue<sup>106</sup>. The enhancement in solubility is achieved from the pyrimidine ring, which is more electron

withdrawing, hence increasing the acidity of the proton on the amino group thus stabilizing the anion (as it is protonated, and is in a salt form)<sup>104</sup>.

In the late 1950's sulphamethazine was used to treat infections in animals and promote growth in food producing animals for example in cattle, sheep and poultry. Sulphamethazine was also utilised to treat respiratory diseases. Sulphamethazine has similar properties to those of sulfamethoxazole, and is today used in a combination of drugs, for example it is used with Trimethoprim, Figure 13<sup>107</sup>.

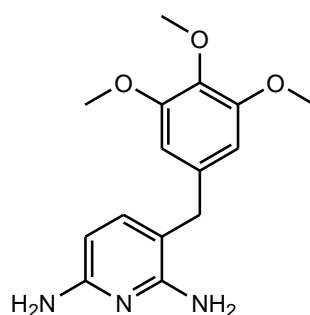


*Figure 13: Chemical structure of trimethoprim*

Trimethoprim is a synthetic antimicrobial agent and is referred to as an antifolate. It is a structural analogue of folic acid. Trimethoprim sulfonamides inhibit enzyme systems that are involved in the synthesis of tetrahydrofolic acid<sup>108</sup>.

It is important to note the core structure of all sulphonamides is the same and resembles the structure of a chemical called para-amino benzoic acid (PABA). PABA is used in the biosynthesis of a vitamin called folic acid. Sulphanilamides interfere with the biosynthesis of folic acid. Majority of the bacteria require PABA as a building block for a coenzyme called tetrahydrofolic acid, Figure 14.

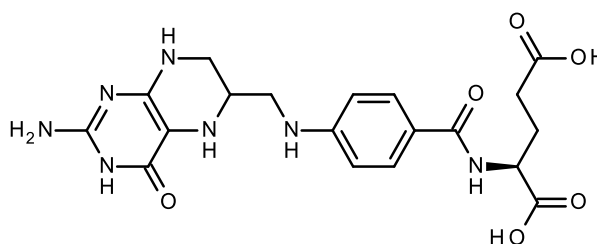


*Figure 14: Chemical structure of tetrahydrofolic acid*

Woods (1940) had demonstrated that PABA has the ability to inhibit the bacteriostatic actions of sulphonamides on various types of bacteria<sup>109</sup>. The recent report by Lord Jim O'Neill extensively discusses the overuse of antibiotics and how they constitute towards bacterial resistance globally. The report makes numerous recommendations such as; restricting the use of antibiotics, a discontinuation of antibiotics in agriculture, and monitoring the amount prescribed by GP's. In



addition to this, the search for new antimicrobial drugs is an ongoing challenge in order to combat antimicrobial resistance<sup>2</sup>.

## 1.8 Dyes

### 1.8.1 Tyrian purple

The most valuable dye in ancient history is tyrian purple, shown in Figure 15. It is a royal purple/red-ish purple dye. A minute amount of this dye is secreted by various species of snails and is said to be exceptionally expensive<sup>110</sup>. To produce 1.4 g of this pure pigment of tyrian purple 12,000 *Murex brandaris* species of snails are required, hence the cost for this dye is very high<sup>111</sup>.

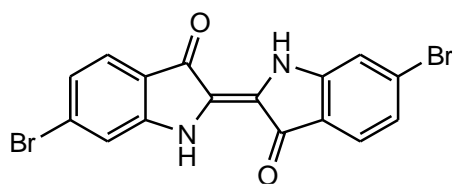


*Figure 15: Chemical structure of tyrian purple*

The ancient Phoenicians first produced tyrian purple. Tyrian purple was prized in antiquity because it became brighter and more intense with weathering and sunlight rather than fading<sup>112</sup>. Production of the dye was tightly controlled in Byzantium and subsidised by the imperial court. The use of tyrian purple was restricted for use only to colour silk for imperial use, so that a child born to a reigning emperor was porphyrogenitos, "born in the purple" <sup>113</sup>. In 1909, Paul Friedländer first identified 6,6'-dibromoindigo as the major component of tyrian purple, which is a derivative of the colour indigo,<sup>114</sup>

Figure 16. The mechanism of how tyrian purple was derived from is shown in Scheme 6.

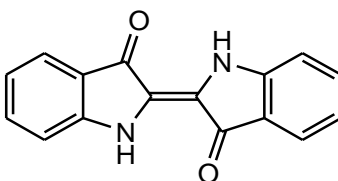
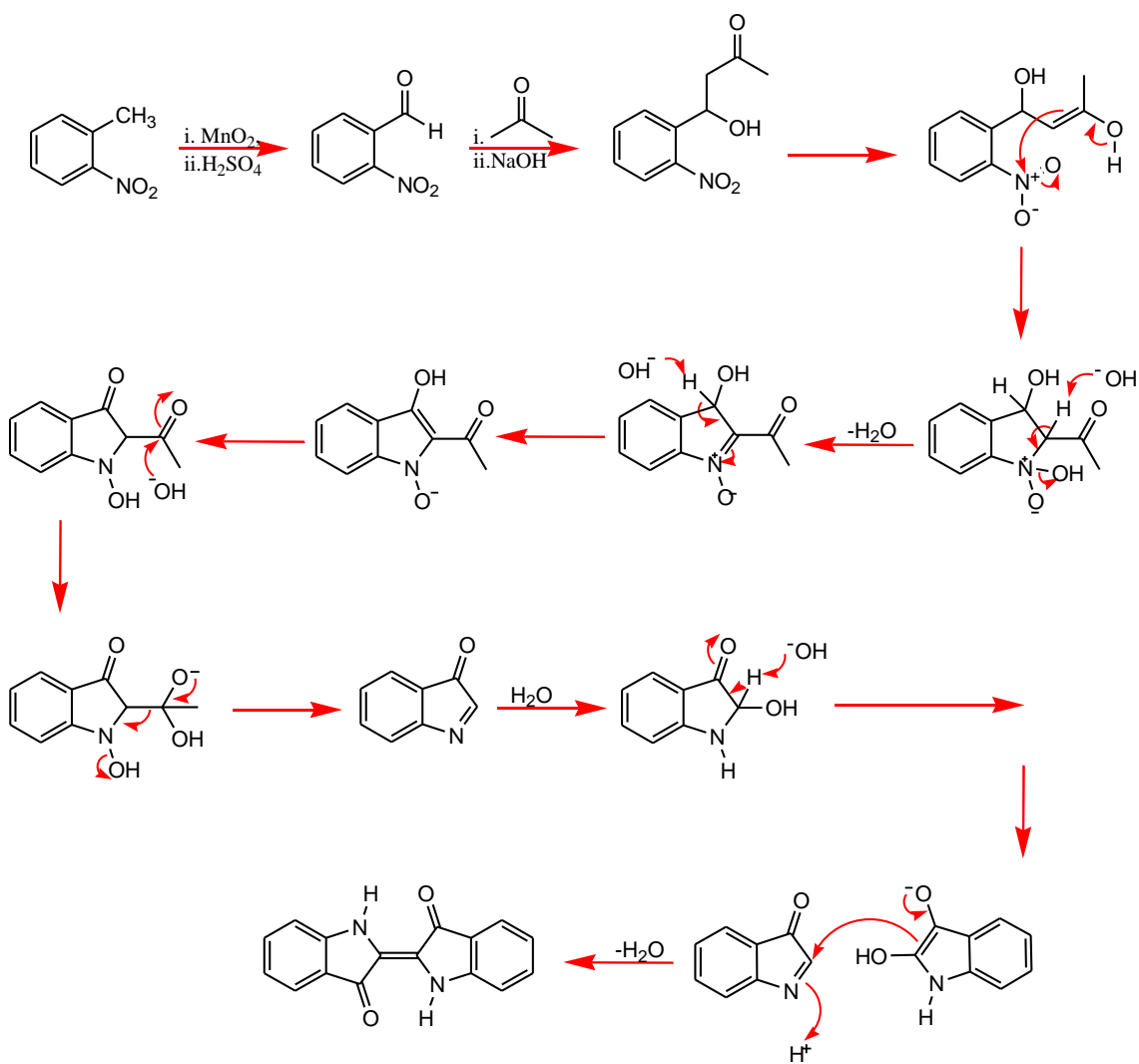


*Figure 16: Chemical structure of indigo*



*Scheme 6: Mechanism for the synthesis of indigo*

### 1.8.2 Crystal violet

A French chemist, Charles Lauth first synthesised Gentian violet/crystal violet in 1861<sup>115</sup> and was further researched in 1880 by a German pharmacist, George Grubler<sup>116</sup>. The chemical name for crystal violet (CV), Figure 17, is hexamethyl pararosaniline. It is a triarylmethane dye, which is used for histological staining.

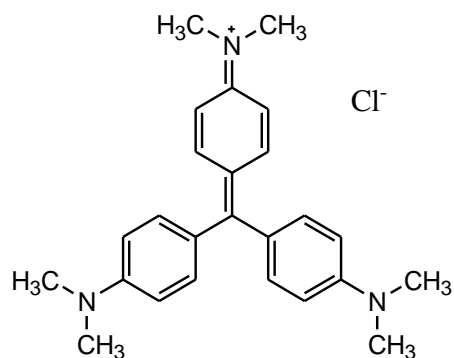


Figure 17: Chemical structure of crystal violet

Hans Christian Gram noted in 1884 the irreversible fixation of CV by Gram positive bacteria and it was this observation by Gram that became the basis of Gram staining for histological purposes<sup>117</sup>. Gram's examination of lung tissues from patients that died of pneumonia discovered that certain stains were preferentially taken up and retained by bacterial cells. In this procedure the bacterial smear was flooded with crystal violet, iodine solution (to fix the dye inside the cells), alcohol (to wash away excess dye from the bacteria) and lastly with safranin, a red dye.

Gram developed this technique to make bacteria more visible in stained sections of lung tissue and not for the purpose of distinguishing one type of bacterium from another<sup>118</sup>. However, Gram stain is employed to differentiate bacteria into either Gram positive or Gram negative. Bacteria consisting of a thick peptidoglycan layer are said to be Gram positive as they retain the stain of CV. Those that do not are classified as Gram negative bacteria<sup>119</sup>.

CV, is known to have antibacterial, and antifungal properties<sup>120</sup>. With these medicinal properties it has previously used as a topical antiseptic agent.

In 1891, Stilling introduced CV for its first use in medicinal purposes as an antiseptic. It was marketed using the name 'pyoctanin' that has various therapeutic uses particularly for wounds and infections of the eye. Literature shows that injections of pyoctanin have been given to patients and have successfully treated two cases of sarcoma<sup>121</sup>. Although this treatment had positive outcomes, further research on pyocatanin and its therapeutic uses had not been successful, thus it was abandoned.

Two decades later research carried out by Churchman in 1912 observed the effect CV had on bacteria, particularly on gram positive microorganisms both *in vivo* and *in vitro*<sup>122</sup>. In 1925, twelve patients suffering from severe sepsis were intravenously injected with CV, of these seven patients improved<sup>123</sup>. Three years later a challenging disease caused by *Staphylococcus* called Staphylococcus meningitis was cured by the use of CV<sup>117</sup>.

Crystal violet has also been used as a non-toxic dye in DNA staining<sup>124</sup> instead of using fluorescent dyes. It is important to know that CV is not used as a textile dye, but is used for paper dyeing, in addition to being used in printing, and in ball point pens. It is also used in fertilizers, antifreezes, and detergents<sup>125</sup>.

Although CV has been employed in an array of products, the discovery of sulphur drugs and penicillin in the 1940 has rapidly reduced the use of CV by physicians.

### 1.8.3 Mauve

In the event of Hoffman attempting to synthesise quinine, Figure 18, an antimalarial drug from aniline<sup>126</sup>, William Perkin learnt that aniline reacts with potassium dichromate to form a black sludge. On attempt to clean the black sludge with alcohol, Perkin noted that a purple substance was being released into the alcohol. This discovery led to further research of the purple substance by Perkin<sup>127</sup>.

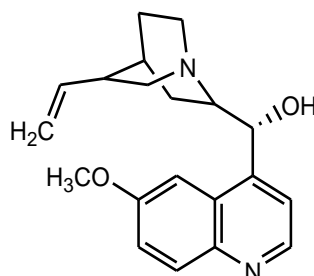


*Figure 18: Chemical structure of quinine*

Perkin, Hall and Green found the purple colour was able to dye silk. This colour did not fade when exposed to sunlight or run when washed. Thus, Perkin patented this compound, and set up an industry to manufacture the dye on a large scale. From here on this colour was named mauveine as it coloured fabrics mauve<sup>128</sup>.

Although the discovery of mauveine (A), Figure 19, a synthetic dye was obtained by William Perkin in 1856, Heinrich Caro, found an efficient way of synthesising this dye<sup>127</sup>.

Mauveine is known by two names; aniline purple and Perkins mauveine<sup>129</sup>. It is an aromatic compound, which is a mixture of other compounds derived from mauveine A. The derivatives of mauveine have varying number of methyl groups and they differ in the positions of which they are attached to the structure.

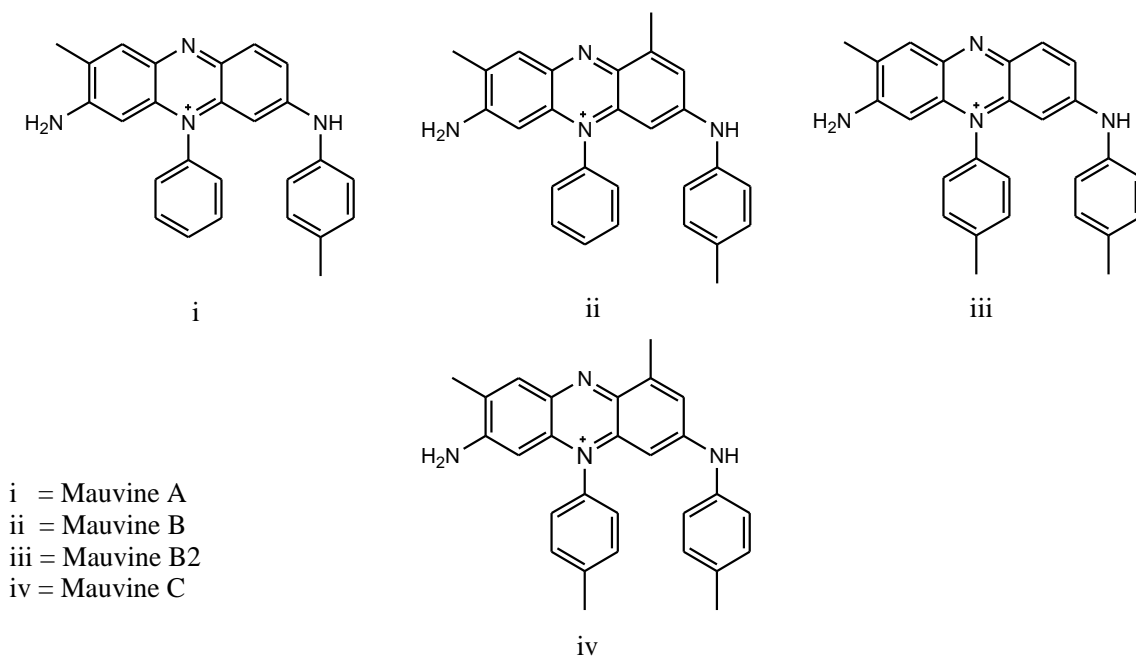


Figure 19: Chemical structure of mauveine and its derivatives

#### 1.8.4 Methylene blue-staining

Methylene Blue (MB), Figure 20, is the most common dye amongst many dyes. Methylene blue was first synthesised by Heinrich Caro, a German chemist in 1876<sup>130</sup>. For many decades, MB has been used as a redox indicator<sup>131</sup>, a photosensitiser<sup>132</sup>, a dye for cellular staining<sup>133</sup>, antiseptic and in medicine<sup>134</sup>. Within the textile industry MB is generally used for dyeing cotton and silk.

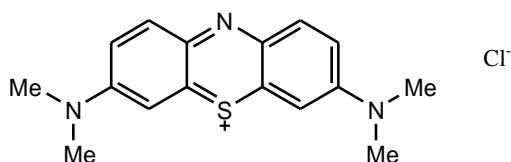


Figure 20: Chemical structure of methylene blue

Wider applications of MB include colouring paper, temporary hair colorants, and coatings for paper stock. Although methylene blue is not a very hazardous dye, it does somewhat have harmful effects for example; acute exposure to MB can cause increased heart rate, vomiting, and shock<sup>135</sup>.

The uses of MB have progressed from a simple dye used for staining to playing important roles in the medicinal field and in hygiene. MB is used to treat urinary tract infections and methemoglobinemia due to its mild antiseptic properties, which kill bacteria that is present in the urinary tract. Methylene blue is particularly used as staining agent to make certain body fluids and tissues easier to view during surgery and on an X-ray or other diagnostic examinations.

Traditionally Isosulfan blue<sup>136</sup> dye, Figure 21, was used to identify the sentinel lymph node in breast cancer, but this has now been replaced by MB as it is more cost effective<sup>137</sup>. Medicinal properties of MB have led to its use in the disinfection of blood plasma<sup>138</sup>.

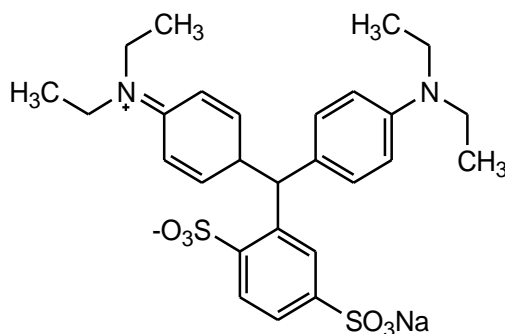


Figure 21: Chemical structure of isosulfan blue

In 1886, the medicinal talents of MB were noticed by Paul Ehrlich's curiosity during his experiments. MB turned live neurons and *plasmodium* blue. It was from here on that Ehrlich concluded the possibility of employing MB to selectively target malaria in the human body<sup>139</sup>. Years later Ehrlich tested MB to treat swamp fever as a remedy, resulting positively.

Paul Ehrlich popularized the concept of magic bullet and invented the precursor technique to Gram staining bacteria. The methods developed for staining tissue made it possible to distinguish the difference between varying types of blood cells, resulting in diagnoses of numerous blood diseases<sup>140</sup>.

### 1.8.5 Photodynamic Therapy (PDT)

Photodynamic therapy (PDT) involves the administration of a photosensitizer which can be administered systemically, locally, or topically<sup>141</sup>. Upon activation using light of an appropriate wavelength, the photosensitizer in combination with molecular oxygen produces reactive oxygen species (both singlet oxygen and redox radicals) which are both cytotoxic. These damage the target cell, consequently resulting in cellular death<sup>142,143</sup>. The use of PDT is becoming attractive and in recent years shown to be successful in treating various forms of cancer<sup>144</sup>.

### 1.8.6 Mode of action of photosensitisers

The term photodynamic action was coined near the turn of the 20<sup>th</sup> century.<sup>145</sup> Some photosensitisers used in photodynamic therapy (PDT) exhibit a degree of (tumour) selectivity. Researchers today are striving to achieve additional control over photosensitisers and their photodynamic action.

To understand the mode of action of photosensitisers, it is important to comprehend their mechanism. Thus, the movement of electrons in terms of their electronic state must be considered and is discussed further in section 1.10.9.

### 1.8.7 Mechanism of photodynamic therapy

In PDT, the mechanism of PDT involves using light of an appropriate wavelength to excite the photosensitiser into the singlet excited state<sup>146</sup>. Thus, the photosensitiser goes into a more stable but lower energy triplet state. It is here, that the interactions of the photosensitiser (excited states) with endogenous oxygen in the target cells or surrounding target tissue induces cytotoxic effects, which can lead into two pathways<sup>147</sup>. These pathways being Type I, or Type II (as shown in Figure 22).

Type I pathway involves electron-transfer reactions from the photosensitiser triplet state that result in the formation of reactive oxygen species, for example superoxide, hydroxyl radicals, and hydrogen peroxide<sup>148</sup>.

Type II pathway involves energy transfer by the photosensitiser (from the triplet state to the ground state). The cytotoxic species formed is singlet oxygen, which is produced by from the molecular oxygen<sup>149</sup>.

Bacterial damage resulting from these pathways associated with PDT has been reported to occur at both the level of nucleic acids, and on the cytoplasmic membrane<sup>150</sup>. The photosensitiser action is illustrated in Figure 22.



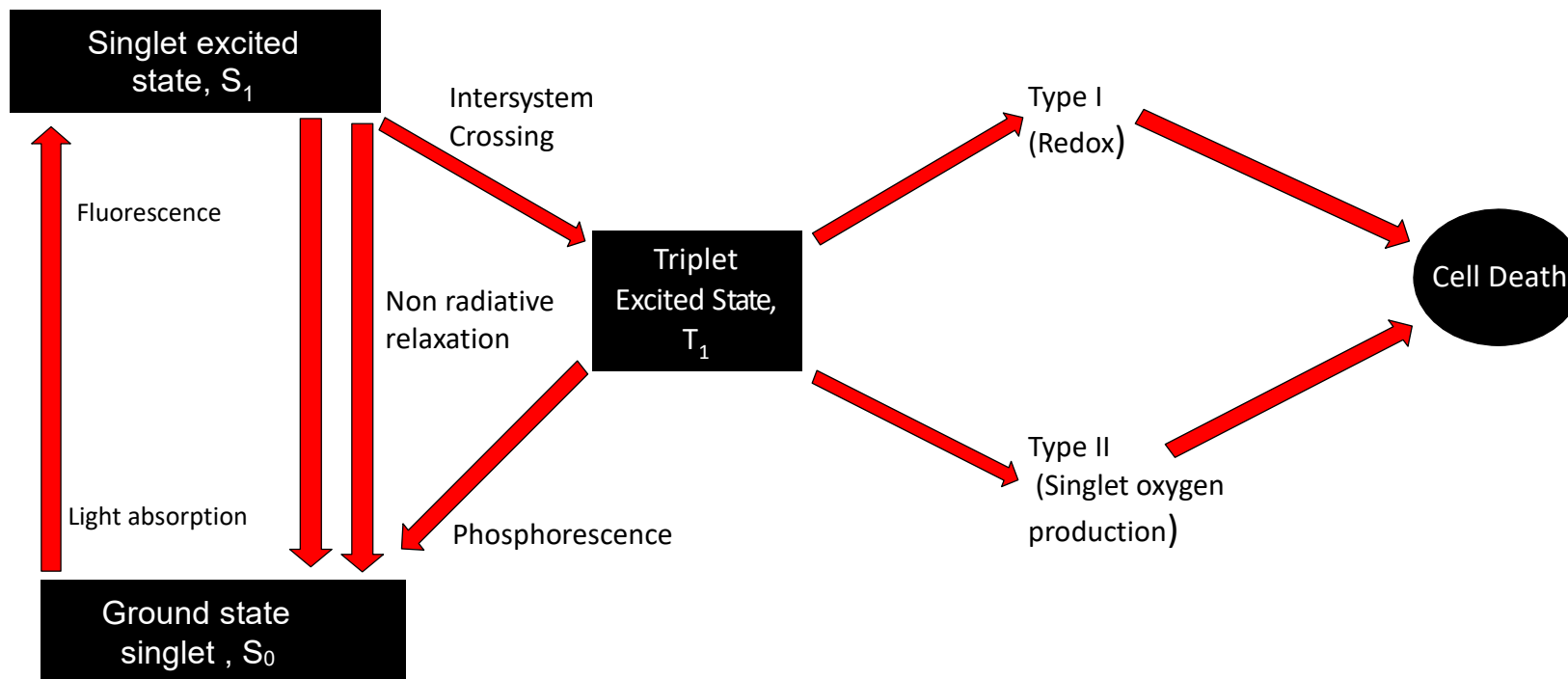
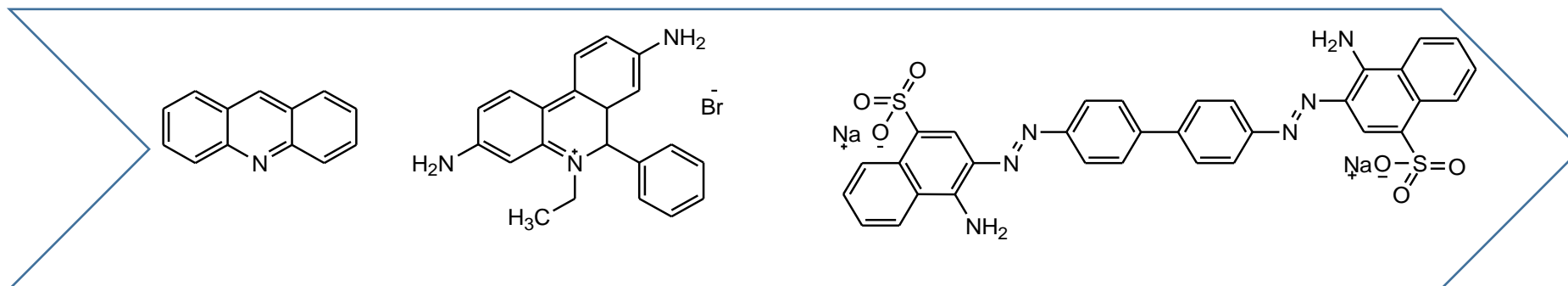


*Figure 22: Electronic pathway of photosensitiser action -adapted from photosensitisers in biomedicine<sup>1</sup>*

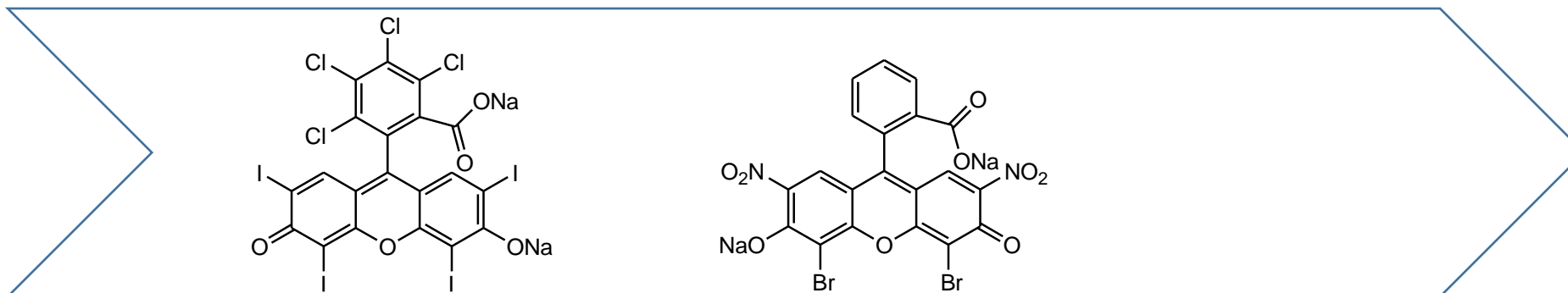
## 1.9 Photosensitisers

Shown below are a range of existing photosensitiser's with their excitation ranges from 400 nm to 900 nm.

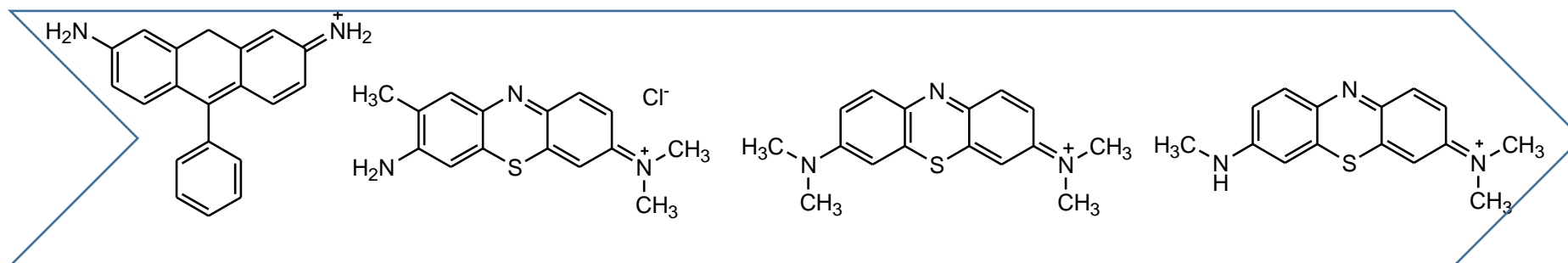
**400-500 nm**



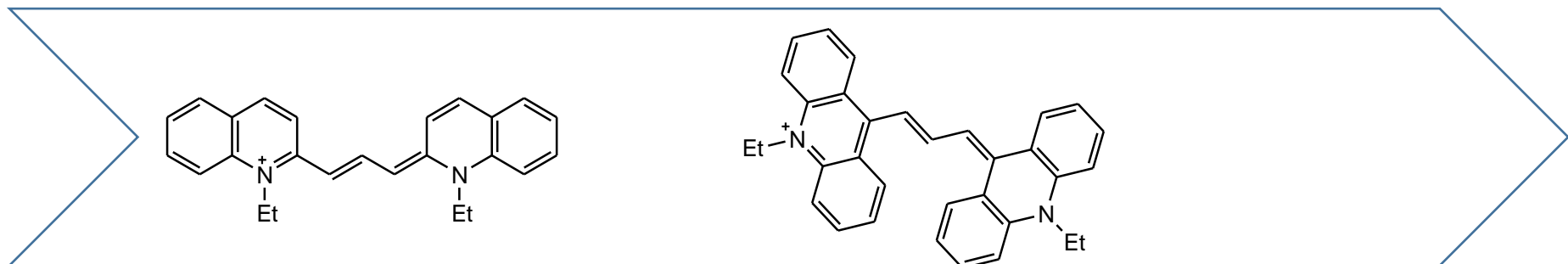
**500-600 nm**



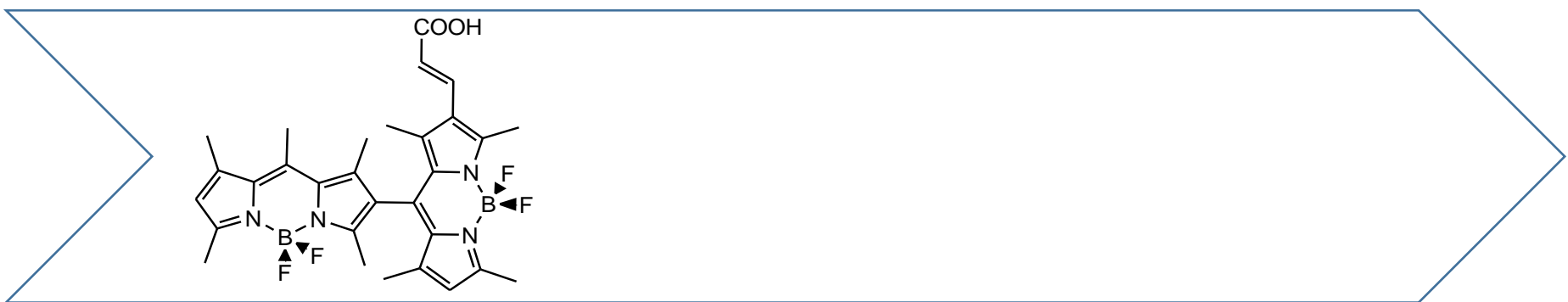
600 – 700 nm



700-800 nm



800 – 900 nm



## 1.10 Light

The value of light is underestimated as day to day life would be impossible without it. Photons are discrete bundles of electromagnetic (light) energy, which travel at the speed of light, as waves<sup>1</sup>. Applications of light in biomedical research for example molecular imaging requires the excitation of a molecule which is fluorescent (dye) and a source of light<sup>151</sup>. The excitation of the molecule results in the production of long wavelengths or lower energy of emitted light and is beneficial for use in photodynamic therapy (PDT)<sup>152</sup>. It is important to note that the absorption of light can vary in the electromagnetic spectrum (from gamma rays through to radio-waves), Figure 23.

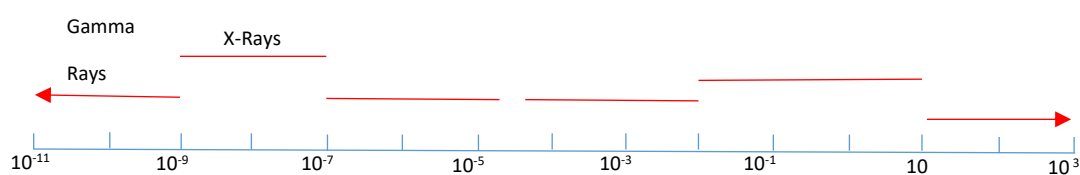


Figure 23: Electromagnetic spectrum

### 1.10.1 History

The initiation of photosensitisers stemmed from Raab's experiments of adding dyes to petri dishes containing *paramecia caudatum*<sup>153</sup>. The unexplained death of *Paramecia* during sunlight but not in the evenings led to further curiosity by Raab. He later noted a connection between light activation of the dyes and a therapeutic outcome. Further research on this showed a link between oxygen and light-dependent photodynamic reactions<sup>154</sup>. Thus, Raab successfully coined the term *photodynamic therapy*<sup>155</sup>.

### 1.10.2 Phenothiazinium dyes

Phenothiazinium dyes, such as methylene blue and toluidine blue O, have been studied for many years and are used as photosensitisers clinically<sup>156</sup>.

Some of the medical applications that phenothiazinium derivatives have been used against are: local bacterial infection such as tuberculosis<sup>157,158</sup>, trypanosomiasis, rickettsia<sup>8</sup>, fungal, viral infections<sup>159</sup> such as malaria, and cancer (bladder)<sup>160</sup>.

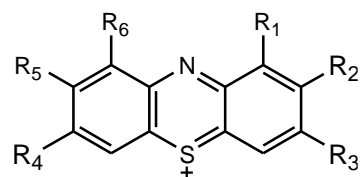


Table 2: Phenothiazinium derivatives <sup>161</sup>

Photosensitiser	R <sub>1</sub>	R <sub>2</sub>	R <sub>3</sub>	R <sub>4</sub>	R <sub>5</sub>	R <sub>6</sub>	$\lambda_{\text{max}}$	<sup>1</sup> O <sub>2</sub> yield
<b>Methylene blue (MB)</b>	H	H	NMe <sub>2</sub>	NMe <sub>2</sub>	H	H	670	1.00*
<b>Toluidine blue O</b>	H	Me	NHEt	NHEt	Me	H	630	1.35
<b>New methylene blue</b>	Me	H	NMe <sub>2</sub>	NMe <sub>2</sub>	H	Me	648	1.22
<b>Dimethyl methylene blue</b>	H	H	NMe <sub>2</sub>	NH <sub>2</sub>	Me	H	625	0.86
<b>Azure Blue</b>	H	H	NMe <sub>2</sub>	NHMe	H	H	648	0.41

\*<sup>1</sup>O<sub>2</sub> yield relative to that of MB.

### 1.10.3 Acridines

The photosensitiser acridine is not good generator of singlet oxygen and is insoluble in water<sup>162</sup>. Thus the use of acridine as a photosensitiser theoretically is not advantageous due to its toxicity levels<sup>163</sup>.

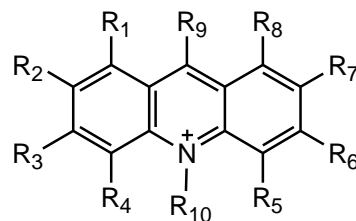


Table 3: Acridine derivatives

Photosensitiser	R <sub>1</sub>	R <sub>2</sub>	R <sub>3</sub>	R <sub>4</sub>	R <sub>5</sub>	R <sub>6</sub>	R <sub>7</sub>	R <sub>8</sub>	R <sub>9</sub>	R <sub>10</sub>	$\lambda_{\max}$
<b>Acridine</b>	H	H	H	H	H	H	H	H	H	-	450
<b>Acridine Orange</b>	H	H	N(CH <sub>3</sub> ) <sub>2</sub>	H	H	N(CH <sub>3</sub> ) <sub>2</sub>	H	H	H	-	488
<b>Proflavine</b>	H	H	NH <sub>2</sub>	H	H	NH <sub>2</sub>	H	H	H	-	445
<b>Aminacrine</b>	H	H	H	H	H	H	H	H	NH <sub>2</sub>	-	

<b>Ethacridine</b>	H	H	NH <sub>2</sub>	H	H	H	EtO	H	NH <sub>2</sub>	-
<b>Acriflavine</b>	H	H	NH <sub>2</sub>	H	H	NH <sub>2</sub>	H	H	H	CH <sub>3</sub>

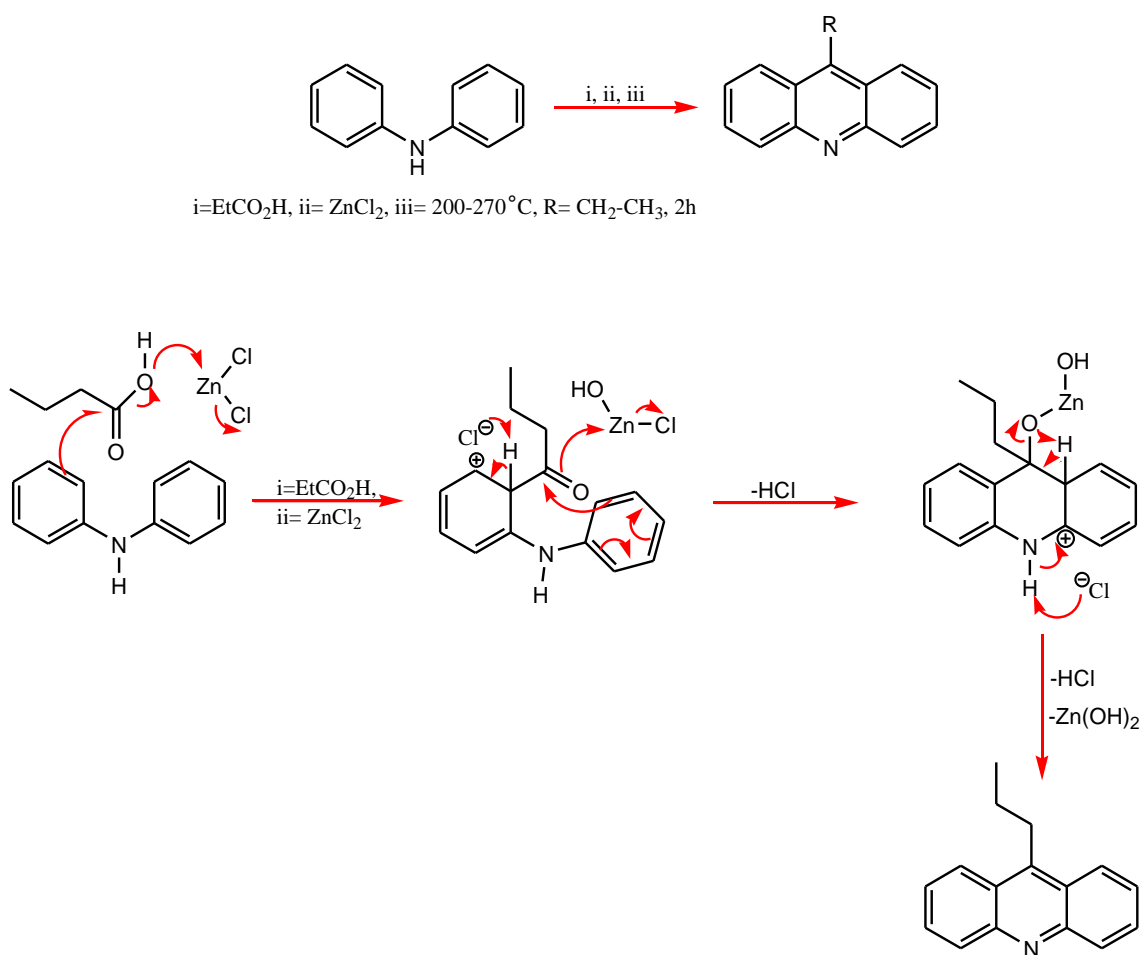
\*R<sub>10</sub> = N alkylation will generate a quaternary amine.

Research was developed further based on the acridine structure for use of these types of molecules as antimicrobial agents, (Table 3). Acridine analogues such as proflavine is of great use in both the antimicrobial application and as an anticancer treatment<sup>163</sup>.

The introduction of proflavine by Browning's into wound therapy in 1916/1917<sup>164</sup> saved many lives that would otherwise have been lost to sepsis<sup>165</sup>.

Although there are several methods reported to synthesise acridines and its analogues, the most common one used is *Bernthsen synthesis* or *Ullmann synthesis*.

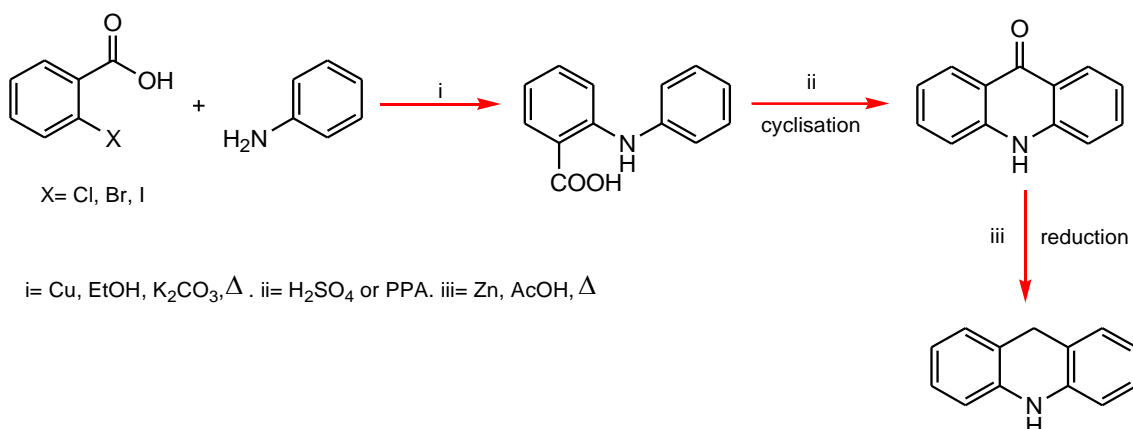
Bernthsen synthesis involves the reaction of diphenylamine with carboxylic acid in the presence of zinc chloride, resulting in the formation of acridine, Scheme 7.



*Scheme 7: Bernthsen synthesis*



The Ullmann synthesis, Scheme 8, is the condensation of a primary amine with either an aromatic aldehyde or an aromatic carboxylic acid in the presence of a strong acid for example conc. sulphuric acid or hydrochloric acid (c.H<sub>2</sub>SO<sub>4</sub>/c.HCl), followed by a dehydrogenation reaction.



*Scheme 8: Ullmann synthesis<sup>166</sup>*

#### 1.10.4 Xanthene derivatives

A search for new antimicrobial agents has necessitated due to the emergence of drug-resistant pathogens<sup>167</sup>. Thus, research has focussed on the antibacterial abilities of xanthene based photosensitisers<sup>1</sup>.

A common example of a xanthene derivative is Rose Bengal. It has four aromatic rings that differ to the way they are positioned to the phenothiazinium dyes.

Xanthene derivatives, Table 4, (particularly the fluorescein-type structures) have a positive charge delocalised around the full ring system. Fluorescein derivatives are anionic or neutral and lipophilic photosensitisers. Whereas the rhodamines are cationic or neutral<sup>1</sup>.

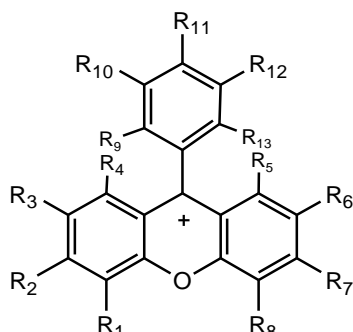
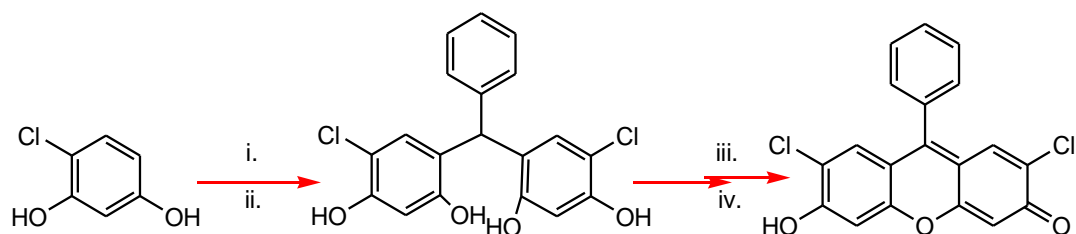


Table 4: Xanthene derivatives

Photosensitiser	R <sub>1</sub>	R <sub>2</sub>	R <sub>3</sub>	R <sub>4</sub>	R <sub>5</sub>	R <sub>6</sub>	R <sub>7</sub>	R <sub>8</sub>	R <sub>13</sub>	<sup>1</sup> O <sub>2</sub> (%) <sup>1</sup>
Rose Bengal*	I	=O	I	H	H	I	ONa	I	CO <sub>2</sub> Na	0.75
Fluorescein type*	H	OH	H	H	H	H	OH	H	CO <sub>2</sub> H	
Fluorescein	H	NaO	H	H	H	H	=O	H	CO <sub>2</sub> Na	0.03
Rhodamine type**	H	NH <sub>2</sub>	H	H	H	H	NH <sub>2</sub>	H	CO <sub>2</sub> H	0.01

\*R<sub>9</sub>-R<sub>12</sub> = Cl, \*\* R<sub>9</sub>-R<sub>12</sub> = H

Derivatives of xanthenes can be synthesised in a number of ways. One of which is by a condensation reaction of *o*-tolualdehyde and 4-chlororesorcinol in the presence of methanesulfonic acid to form the intermediate. This is reacted with *p*-toluenesulfonic acid (*p*-TsOH), purified by crystallisation and subsequently reacted with 2,3-dichloro-5,6-dicyano-1,4-benzoquinone (DDQ) to form fluorescein<sup>168</sup>, Scheme 9.



i= ArCHO. ii= H<sup>+</sup>. iii= *p*-TsOH/toluene. iv= DDQ

Scheme 9: Synthesis of xanthene derivatives – fluorescein

### 1.10.5 Cyanine based photosensitisers

In previous years cyanine based photosensitisers were used greatly in photography, particularly for its ability to transfer energy and electrons to pigments at certain wavelengths for colour film development<sup>169</sup>. It was for this purpose that cyanine based dyes were developed as photosensitisers for their potential use in the 1920's<sup>170</sup>. The development of compounds such as naphthalocyanines and cyanine bridged compounds is of great interest to scientists as the extended polymethine  $\pi$  system would alter the absorbance range to longer wavelengths, resulting in deeper tissue penetration. This of course is an ideal characteristic feature for PDT<sup>170</sup>.

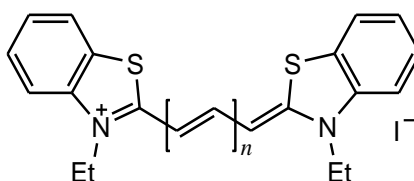


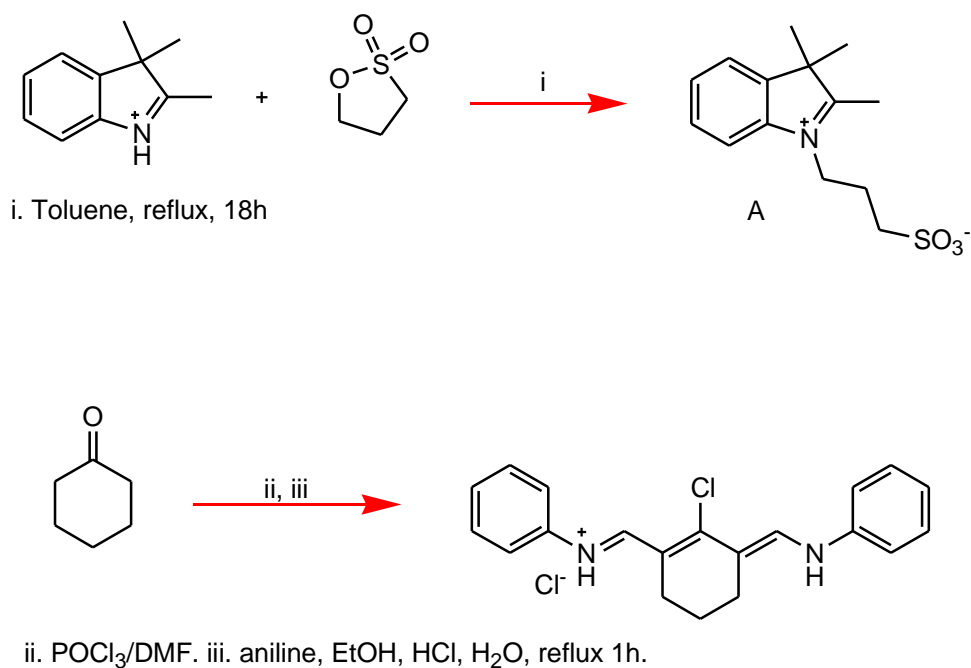
Table 5: Cyanine derivatives<sup>170</sup>

Photosensitiser	$\lambda_{\max}$	$^1\text{O}_2$ yield
<b>Indocyanine Green (ICG)</b>	780	0.01
<b>New Indocyanine Green</b>	824	0.08
<b>2-quinolinyl analogue</b>	850	1.22

Today polymethine dyes such as ICG are also used in a large range of applications, purely due to their reduced toxicity<sup>171</sup> and its excellent photo-physical properties<sup>172</sup>. The Medicines and Healthcare Products Regulatory Agency (MHRA)<sup>173</sup> and the United States Food and Drug Administration (FDA) have approved ICG dye for use in their products/industry<sup>172,174</sup>.

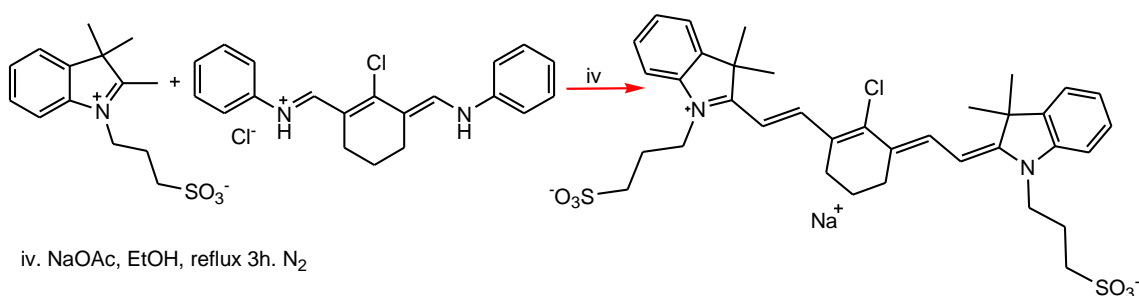
Most cyanine dyes are synthesised by a condensation reaction between a heterocyclic base that contains an activated methyl group and an unsaturated bisaldehyde or its equivalent, usually as Schiff base in the presence of a catalyst (sodium acetate)<sup>175</sup>. *Narayanan et al.* synthesised a library of cyanine derivatives replacing the catalyst with a mixture of solvents (1-butanol: benzene: 7:3 (Dean Stark conditions)). Solvents such as ethanol, acetic acid or acetic anhydride have also commonly been used for the synthesis of cyanine derivatives<sup>176</sup>.

The general synthesis of these derivatives is shown in Scheme 10 and Scheme 11.



*Scheme 10: Synthesis of cyanine intermediate*

Name of cyanine intermediate: (N-[5-Anilino-3-chloro-2,4-(propane-1,3-diyl)-2,4-pentadiene-1-ylidene]anilinium Chloride)



*Scheme 11: Synthesis of cyanine dyes<sup>176</sup>*

Additional analogues of ICG dyes have been synthesised to improve  $\lambda_{\max}$  of the dyes, resulting in a bathochromic shift, subsequently pushing the  $\lambda_{\max}$  into the NIR region. The general editions made to the ICG dyes was to the aromatic termini of the bridged polymethine chain<sup>177</sup>. Scheme 10 and Scheme 11 show the insertion of a cyclohexenyl moiety and a halogen atom (Cl) which stabilizes the molecule. Further examples of stabilized dyes with a bridge are the squaraine or squarylium type dyes, illustrated in Table 6.

### 1.10.6 Squarine dyes

Squarylium dyes have recently become a point of focus for scientists because of their special properties for example: a) high photochemical stability, b) intense absorption-in the visible NIR, making them potential candidates for photosensitisers<sup>178</sup>. It is for this reason derivatives of squarylium type dyes have become an active area of research particularly to improve their properties as PDT agents and an example of it is shown in Figure 24<sup>179</sup>.

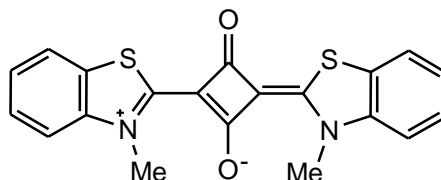


*Figure 24: Squarylium equivalent dye*

The derivatives of squarylium type dyes, with their  $\lambda_{\max}$  and singlet oxygen yields of several squarylium cyanine dyes derived from benzothiazole, benzoselenazole and quinoline presented in Table 6 were determined measuring the luminescence of the dyes in the NIR. The results obtained from their absorption and singlet oxygen generation by some of the dyes show potentiality of candidates as ideal photosensitisers for their use in PDT<sup>180</sup>.

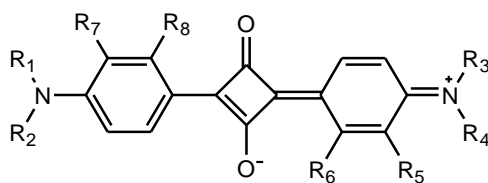
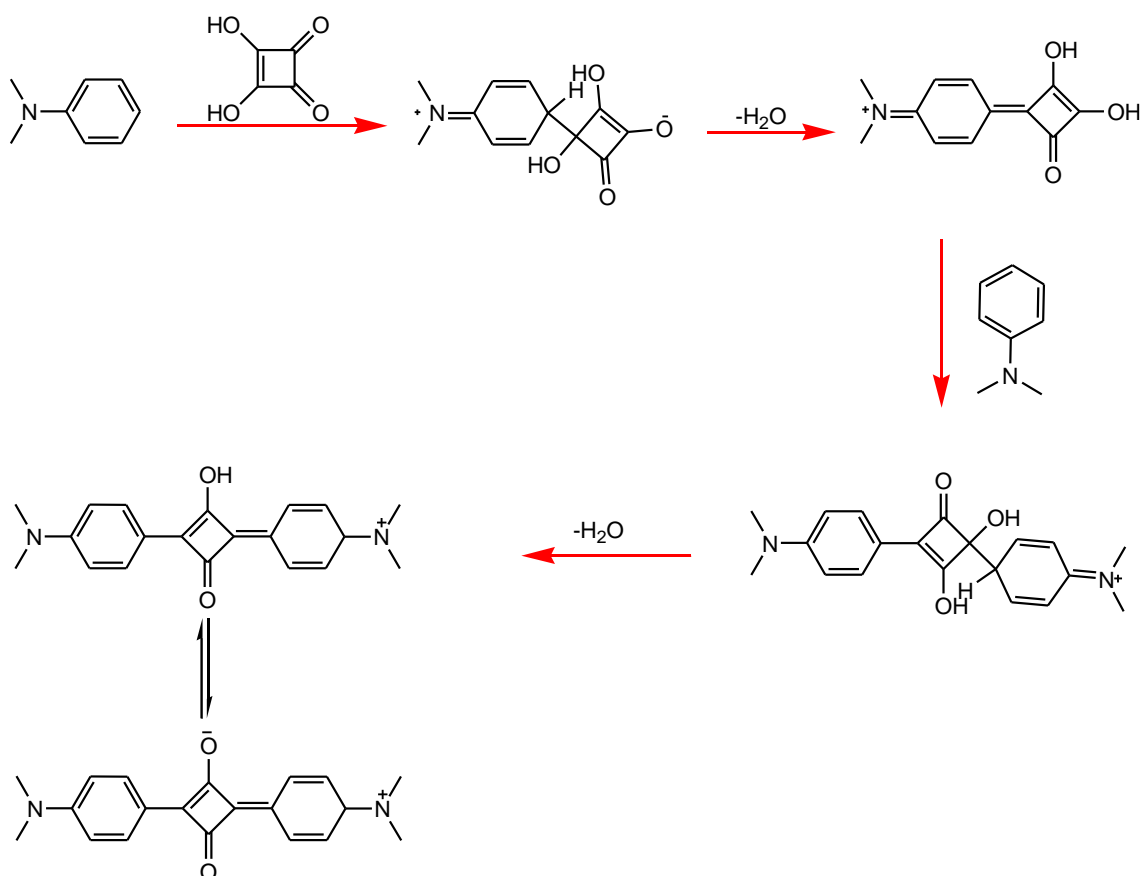


Table 6: Squarylium derivatives

Photosensitiser	$\lambda_{\max}$	$^1\text{O}_2$ yield
	591	-
	704	1.35
	786	
	647	0.17

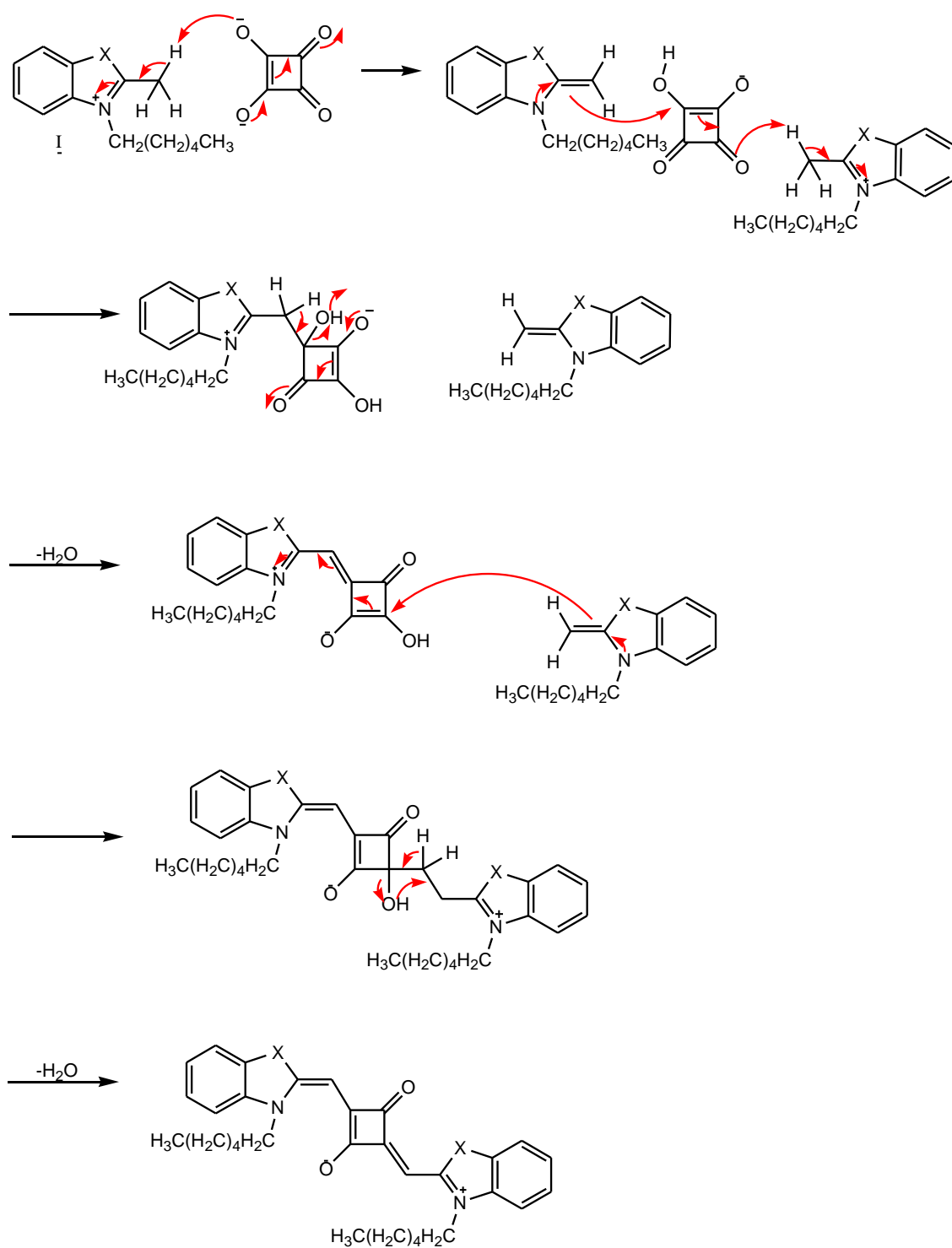
The general synthesis of squarylium derivatives is shown in Scheme 12.



*Scheme 12: Synthesis of squarylium derivatives<sup>169</sup>*

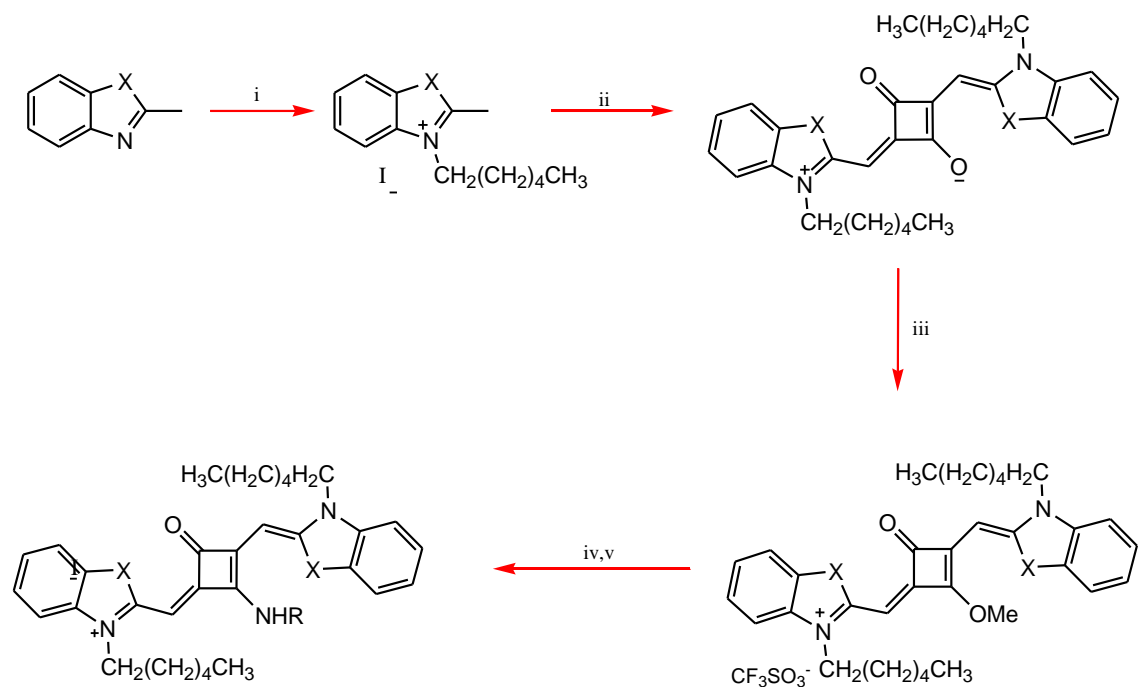
A shift in absorption further into the NIR region is observed when an amino group is added in place of the oxygen atom on the squaric acid<sup>181</sup>.

The synthesis of these derivatives (squarylium equivalent PS) differ slightly to the general synthesis of squarylium dyes themselves. The squarylium equivalent, otherwise known as ‘aminosquarylium cyanine dyes’ are synthesised from either benzothiazole, benzoselenazole and quinolone, shown in Scheme 13<sup>182</sup> and the mechanism for this is shown in



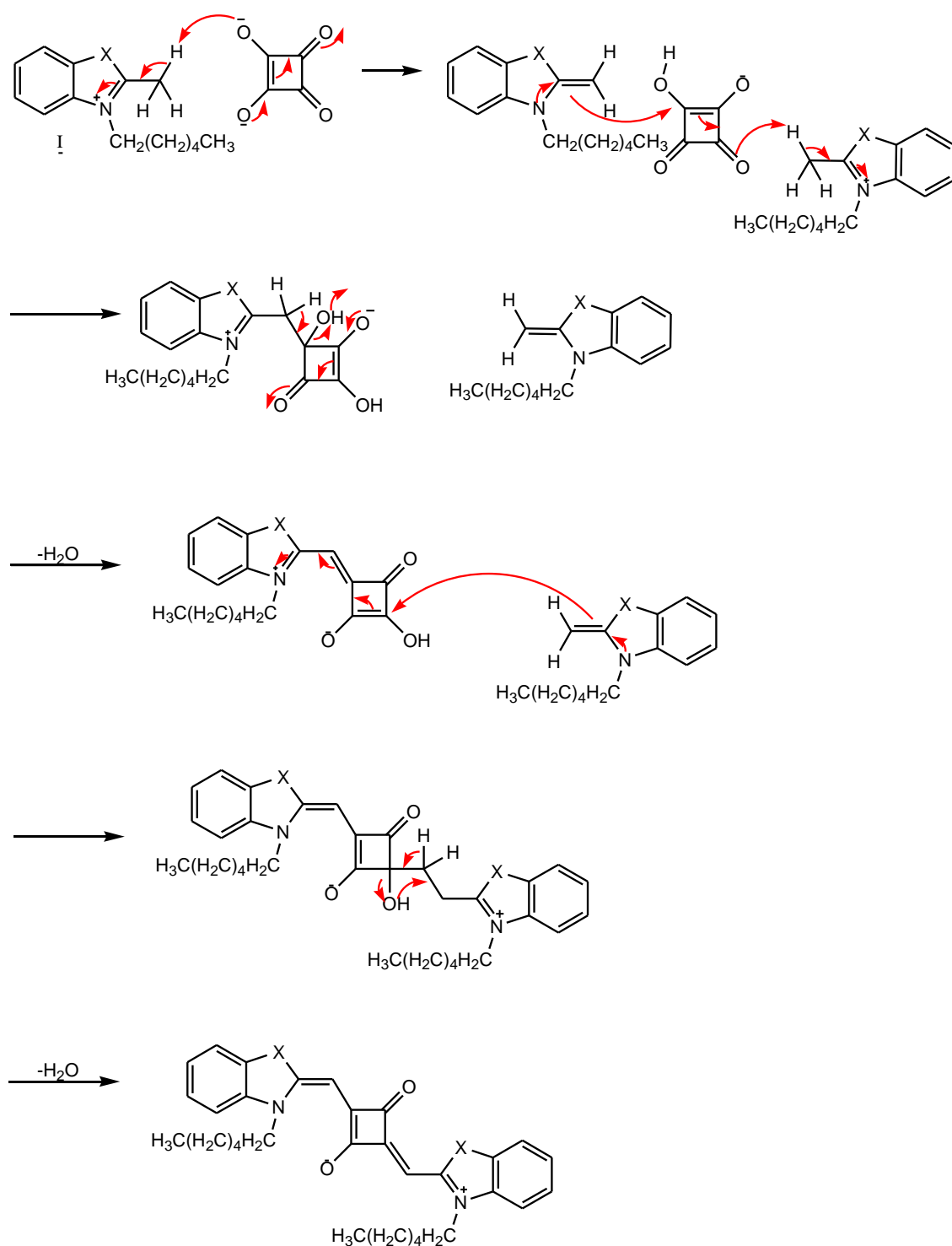
Scheme 14 .





i = ICH<sub>2</sub>(CH<sub>2</sub>)<sub>4</sub>CH<sub>3</sub>, MeCN reflux. ii = squaric acid, *n*-BuOH/pyridine, DCM, N<sub>2</sub>, reflux.  
 iii = CF<sub>3</sub>SO<sub>3</sub>CH<sub>3</sub>, DCM, N<sub>2</sub>, rt. iv=R, DCM, N<sub>2</sub>, rtp. v=R, 14% aq. KI, rt.

*Scheme 13: Synthesis of aminosquarylium derivatives*



*Scheme 14: Mechanism for the synthesis (steps ii to iii) of aminosquarylium derivative*

Croconic acid dyes, Figure 25 are similar to the squarylium dyes. The difference between these two dyes is the central ring. Croconic dyes have a five member ring present (croconic ring)<sup>183</sup>. They have been investigated and synthesised to a much lesser degree than the squarines<sup>184</sup>.

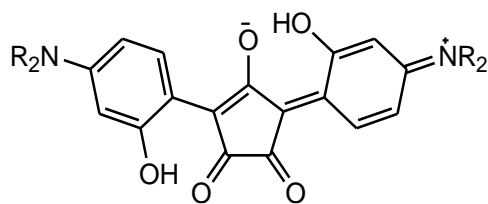
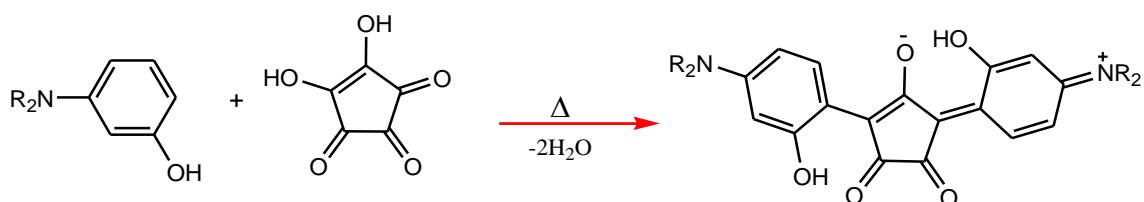


Figure 25: Croconic acid dye

Croconine dyes have strong absorption at longer wavelengths, greater photo-stability and better yields ranging in 55-70%<sup>185</sup> compared to the squarylium dyes. These characteristics make croconium dyes suitable as photosensitisers in comparison to the squaryliums<sup>186</sup>.

Synthesis of croconium dyes is similar to squarylium dyes. Instead of using squaric acid, croconic acid is used. This reaction involves a condensation reaction between aromatic or heterocyclic methylene base (2 equiv) with croconic acid (1 equiv).



Scheme 15: Synthesis of croconium dyes

Very little investigation has been done on rhodizonic acids Figure 26 (A). Rhodizonic acid is a six membered ring, which is included into the addition of xantheno derivatives. Its ring system, is very similar to the squarylium and croconium dyes, Figure 24 and Figure 25. Inclusion of the six membered ring (croconic acid) shows the derivatives absorb at longer wavelengths, approx. 800 nm<sup>1</sup>.

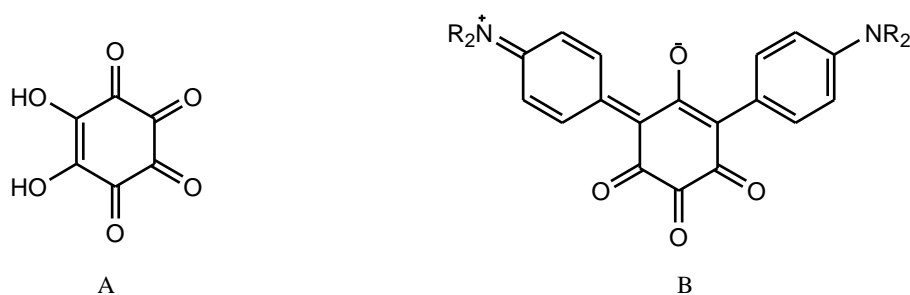


Figure 26: Rhodizonic acid (A), Rhodizonium dye (B)

The shift in absorbance makes rhodizonic acid derivatives potential candidates for use in applications such as PDT<sup>187</sup>. However, it is noted that rhodizonium dyes have a low triplet quantum yield and a small amount of experiments have been performed to prove the formation of

singlet oxygen production<sup>188</sup>. The synthesis of rhodizonic dyes is similar to the synthesis of croconium dyes.

### 1.10.7 Phthalocyanine based photosensitisers

Following the search for intense, long-wavelength absorption and a high singlet oxygen production is yet of great importance in photosensitisers. It is for this reason additional types of Photosensitisers are extensively researched. Phthalocyanines (Pcs) contain desirable photophysical properties as they absorb at longer wavelengths, bathochromic shift (red shift), thus resulting in deeper light penetration into tissues<sup>189</sup>. As Pcs can aggregate, the singlet excited state lifetime is shortened, thus decreasing the singlet oxygen quantum yield by dissipating energy through internal conversions. Hence, this problem is overcome by the addition of large substituents.

Pcs can also have metal ions in the centre that favours the photophysical properties by increasing the triplet state quantum yields, and longer lifetimes, generating singlet oxygen<sup>190</sup>. Examples of common metal containing Pcs are zinc Pcs and silicon Pcs<sup>191</sup>.

### 1.10.8 Photosensitisers designed for clinical use-cyanine

A great deal of interest recently has risen in medical imaging techniques, particularly fluorescence-based image-guided surgery<sup>192</sup>. This technique is primarily being used to detect tumours intra-operatively. NIR imaging techniques is utilised in a combinatorial manner with NIR fluorescent agents which use a wavelength range between 700–900 nm. Molecules that absorb in the NIR region (700-900 nm) are at present being used efficiently within clinical settings<sup>193</sup>. These molecules, called contrasting agents, Figure 27 (ICG-cyanine based dyes) are arguably the best known heptacyanine dyes for absorption in the long wavelength region<sup>192</sup>.

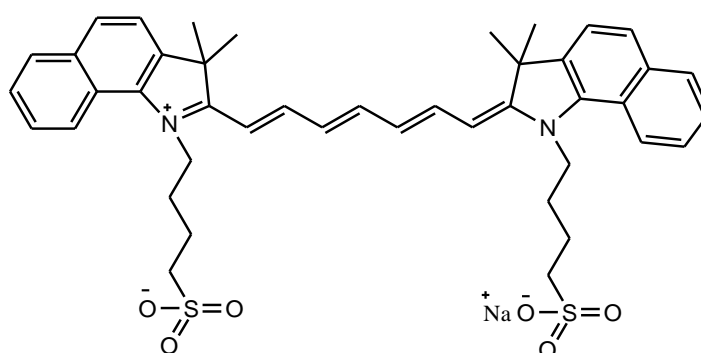


Figure 27: NIR fluorophore

The importance of these polymethine dyes, (cyanine chain) is the conjugation of the methine chain as they are composed of an odd number of carbons within their methine unit. The cationic charge from the conjugated system allows delocalization to occur over the manifold of carbon atoms<sup>194</sup>, Figure 28.

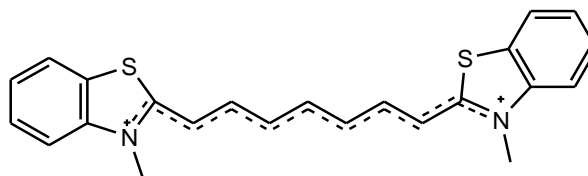


Figure 28: Delocalization of cation across methine chain

NIR imaging produces minimal photo-damage to biological samples, and negligible interference occurs from the background auto-fluorescence from the biomolecules themselves. These can be seen in the cyanine analogues Figure 27 and Figure 28 are utilised for the investigation of *in-vivo* testing to examine mammalian tissues as they produce small amounts of NIR fluorescence<sup>195</sup>. Fluorescence-based image guided surgery shows preclinical success using *in vivo* models<sup>196</sup>. It is mainly for this reason in addition to the long absorption range that porphyrin based photosensitisers in combination with polymethine chain are of great interest to scientists in the development of novel PDT agents.

#### 1.10.9 Electronic states

Electrons in molecules are restricted to particular orbits they can enter dependant on their energies. They can jump from one energy level to another, however, the orbits are forbidden to have energies other than those that are allowed in that particular energy level. Thus, electrons can be promoted to higher energy levels on absorption of the correct energy. This rule elucidates how particular radiation wavelength corresponds to excitation of electrons<sup>197</sup>.

Electrons present in orbitals exist largely in pairs, and have opposing spins to one another. This spin state is referred to as the 'singlet state'. Promotion of one singlet state electron to another energy level, (that is higher in energy) keeps the same spin state as it was prior to promotion. Thus, this electron is then in the 'singlet excited state'<sup>198</sup>.

#### 1.10.10 Jablonski

A molecule (photosensitiser) in its ground state absorbs radiation, and can produce several different electronically excited states that have different chemical and physical properties from the ground state<sup>199</sup>. The photosensitiser has a higher amount of energy in the excited state that can be utilised in several ways e.g.; chemical reactions, emission of radiation of long wavelengths or by heat loss.

Photosensitisers in the ground state are said to be in the singlet state ( $S_0$ ) as they have no unpaired electrons. Upon absorption of light from the lowest electronic level, the molecule gets promoted to one of the many populated vibrational levels in the excited state ( $S_1$ )<sup>200</sup>.

The lifetime of these species in the singlet excited state is extremely short lived (approximately: singlet:  $10^{-9}$  s, triplet:  $10^{-3}$  s) because further internal conversions of the molecule occur to other higher vibrational levels within the ground state, resulting in the possibility to fluoresce by returning to the ground state<sup>201</sup>.

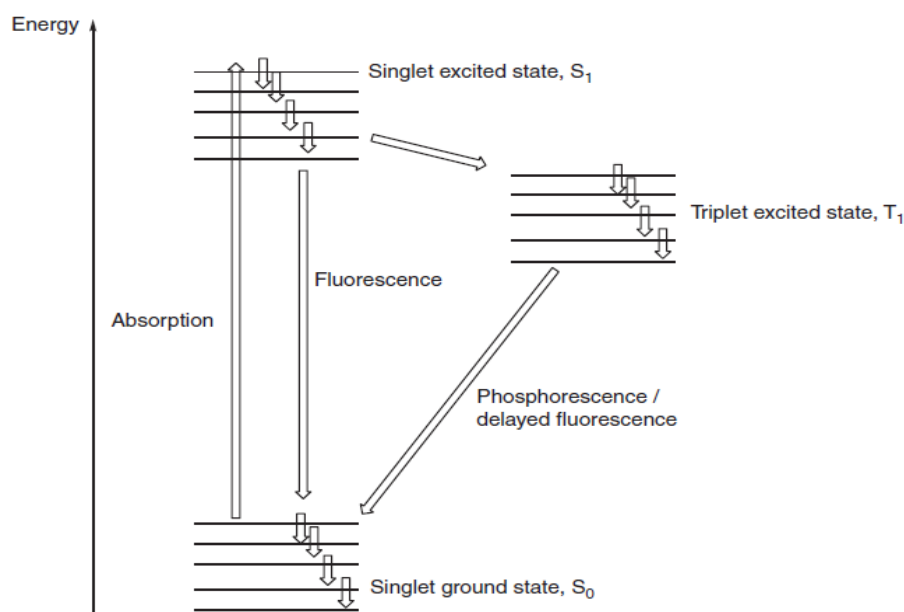


Figure 1.5 Absorption, fluorescence and phosphorescence.

Figure 29: Jablonski diagram<sup>169</sup>

Jablonski diagram (Figure 29) show changes in the spin state of a molecule that occurs via an intersystem crossing, from the lowest vibrational level of the  $S_1$  state into a vibrational state of the  $T_n$ , triplet electronic state. Vibrational relaxation occurs incredibly rapidly in the  $T_n$  state, as in the singlet excited state<sup>147</sup>. However, here additional processes also occur from their lowest vibrational states. This is due to the spin forbidden nature between the singlet to triplet transition. The singlet excited state tends to have a shorter life span than that of a triplet excited state<sup>198</sup>. The overall mechanisms of deactivation involve a net reduction in energy. These include: vibrational relaxation into the  $S_0$  state of the lowest vibrational level, intersystem crossing, and radiative decay again back to the  $S_0$  state resulting in phosphorescence.

A long-lived triplet excited state photosensitiser can be achieved by two key features:

- i. Attachment of halogens atoms to the photosensitiser.
- ii. Chromophoric atoms could be replaced with sulphur or oxygen atoms-(atoms from a low period).

These would increase the spin-orbit coupling, resulting in enhanced antimicrobial action<sup>1</sup>.

### 1.11 Applications of photosensitisers

Today the applications of photosensitisers is of great importance<sup>202</sup>. Dermatological diseases are amongst the first to be studied using photosensitisers and a light source<sup>203</sup>. The application of photodynamic therapy (PDT) *in vivo* is growing significantly. However, there remains a large gap for the use of photosensitisers in areas of medical applications<sup>1</sup>. Currently the main application of PDT is in the treatment of cancer and ophthalmology<sup>204</sup>.

Photodynamic antimicrobial chemotherapy (PACT) follows principles to PDT, and its application is not fully exploited<sup>205</sup>. The applications of PACT are currently limited because of its dependency towards exposure of a directed light source, consequently affecting the treatment that can be carried out and therefore PACT can only be used as a local treatment source<sup>206</sup>.

An example of local photosensitiser use, is to treat the microbial organism called *propionibacterium acnes* (*P. acnes*) (acne) by clearing the skin of these microorganisms<sup>207</sup>. Fungal infections particularly toe nails are becoming increasingly common in humans. PACT is being used successfully to treat this infection, in addition to this PACT has been approved for its use in treatment of dental infections<sup>206,208</sup>.

#### 1.11.1 Cancer

PDT is employed to treat a range of cancers for example esophageal cancer, and lung cancer<sup>209</sup>. Photofrin™, Figure 30, is a porphyrin based photosensitiser also known as porfimer sodium is used for treatment in cancer<sup>210</sup>. In 1993 hematoporphyrin derivative (HpD) was the first photosensitiser to receive regulatory approval<sup>209</sup>. Since then HpD has been approved for its use in USA, Europe, and Japan particularly to treat cervical, endobronchial, bladder, and gastric cancers<sup>211</sup>.

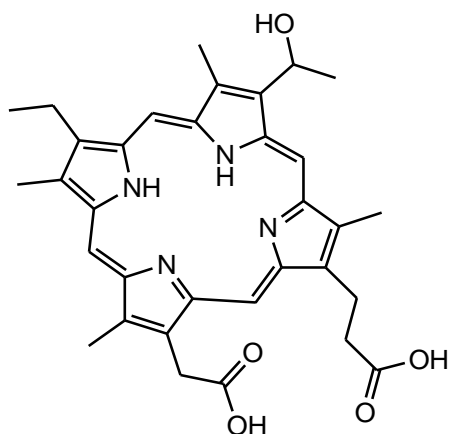


Figure 30: Chemical structure of photofrin

### 1.11.2 Applications of tumour

Tumours are an abnormal mass growth of tissue that can be classified as benign or malignant<sup>212</sup>. Benign tumours grow slower than malignant and do not invade other nearby tissue or spread to other parts of the body unlike cancer<sup>213,214</sup>.

Tumours are usually named from their cell origin, for example; sarcomas, carcinomas, and lymphomas<sup>215</sup>. Cutaneous T-cell lymphoma is a lymphoma which affects the skin, and caused by uncontrolled multiplication and growth of the T-cell lymphocytes<sup>214</sup>.

PDT has emerged due to its safety and efficacy. Methyl-aminolevulinic acid (MAL), Figure 31, is a methyl-ester derivative of ALA<sup>216</sup>, Figure 32 and is used for the treatment of mycosis fungoides (cutaneous lymphoma).

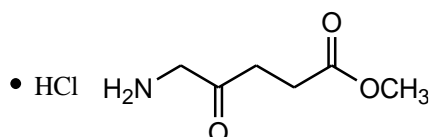


Figure 31: Chemical structure of methyl aminolevulinic acid

5-Aminolevulinic acid (ALA), Figure 32 and MAL are both known photosensitizer prodrugs. ALA is a precursor in the heme biosynthetic pathway. MAL has proven to be more effective and produces fewer side effects than ALA when used for treatment of actinic keratoses and basal cell carcinomas<sup>217</sup>.

The administration of exogenous ALA induces the build-up of the natural endogenous photosensitizer protoporphyrin IX (PpIX).<sup>218</sup> The accumulation of PpIX in tissues is achieved by exogenous administration of its natural precursor 5-aminolevulinic acid (ALA). The haem biosynthesis cycle tightly regulates the endogenous levels of ALA. ALA administered



exogenously bypasses the feedback control and consequently free PpIX accumulates in the cells<sup>219</sup>. MAL is selectively absorbed into cancer cells. The drug is converted into photoactive porphyrins, naturally occurring intracellular photosensitising chemicals that bind with iron to make haemoglobin. When cancer cells full of porphyrins are exposed to a specific wavelength of light (570-670 nm), a molecular reaction occurs that results in destruction of the cancer cells<sup>220</sup>. MAL is more lipophilic than ALA and selective towards tumour cells. It is this property that enables the PDT agent to penetrate better through the epidermis and deeper into tumour than ALA<sup>221</sup>.

Other types of tumours PDT has been reported for treatment purposes are Kaposi's sarcoma<sup>222</sup>, extra mammary paget's disease<sup>223</sup>, and cutaneous B cell lymphoma<sup>224</sup>.

### 1.11.3 Port wine stain

Port wine stains (PWS) is a vascular birthmark, caused by abnormal development of blood vessels in the skin<sup>225</sup>. The complete fading of PWS has proven to be difficult to achieve using laser systems. This technique generally involves using a pulse dye system and a laser to undergo selective photothermolysis<sup>226</sup>.

During the 1980's lasers and pulse dyes (PD) revolutionized clinically for the treatment of PWS. PD lasers produce pulses of visible light at a particular wavelength. The first PD laser therapy used a wavelength of 577 nm<sup>227</sup>. This treatment proved to be unsuccessful as penetration of light was not deep enough to enter into the tissue to enable maximum clearance of the lesion<sup>228</sup>.

The lack of effectivity of laser treatment for complete removal of port wine stains is forcing researchers to seek alternative means for this therapy. Thus PDT has been introduced as a new means for its effectivity to treat PWS<sup>229</sup>.

In PDT the absorption of light triggers a photochemical- biological reaction which leads to the generation of cytotoxic species such as singlet oxygen, resulting in cell death<sup>230</sup>. Using PDT as a technique to remove PWS, has proven to be an effective treatment as the pulse dye lasers<sup>225</sup>, particularly for purple flat lesions rather than the pink flat lesions<sup>231</sup>.

### 1.11.4 Viral

The discovery of PDT using photosensitisers to kill organisms was over 100's of years ago<sup>232</sup>. PDT has also been used for applications of viral infections too, examples of this are infections caused by herpes and papilloma viruses<sup>204</sup>. During the 1970's, initial studies of PDT involved clinical trials of viral lesions<sup>233</sup>. However, this treatment ceased in 1975<sup>234</sup> due to new findings that the treatment were infective and the cause of cancer<sup>235</sup>.

Viral warts have also reported to have been treated using PDT without causing any side effects<sup>236</sup>. An example of the virus being treated with PDT is photosensitiser; 5-aminolevulinic acid (ALA), Figure 32.

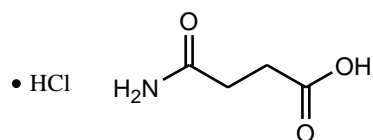


*Figure 32: Chemical structure of 5-aminolevulinic acid (HCl salt)*

The treatment of warts with PDT showed a therapeutic strategy for successive reduction of the virus<sup>237</sup>. Herpes keratitis, is also a viral infection, that was known to heal using PDT and proflavine, Figure 33, as the photosensitiser<sup>238</sup>.

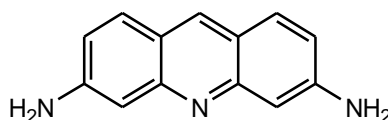


*Figure 33: Chemical structure of proflavine*

Other viral infections for example genital herpes utilized PDT as a treatment. Eradication of the infection was possible; however, prevention for reoccurrence was unsuccessful<sup>239</sup>.

Human papilloma virus (HPV), is a virus which affects the skin and spreads between people through skin to skin contact<sup>240</sup>. PDT is used against HPV both systemically and topically. Numerous clinical trials of PDT have been conducted against viral infections including the HPV<sup>241</sup>. Statistical studies show a decrease of the virus by approximately 50%, thus proving to be a promising treatment for HPV<sup>242</sup>.

Alternative applications of PDT have also been utilized for the sterilization of blood plasma in order to remove blood borne viruses<sup>243</sup>, agricultural uses which include insecticides and herbicides<sup>244</sup>.

### 1.11.5 Surface disinfection

The food industry has also utilized PDT with regular white light as a source of disinfectant for surface cleaning and sanitation<sup>245</sup>. The purpose of surface disinfection has risen from medical fields, as photosensitisers are employed as antimicrobial agents. The ability of PDT agents to kill bacterial and viral pathogens in addition to yeasts and protozoa, (which can be readily found in the food industry) is favourable for hygienic purposes<sup>246</sup>.

Other areas of integrating PDT for surface disinfectants for either eradication of microorganisms or the control of disease(s) can be disinfectants in surface coatings and bedside tables (the PDT agent would behave as a biocide)<sup>232</sup>.

PDT agents can ideally work in textiles that are used in the medicinal field, for example wound dressings<sup>247</sup>. This principle for PDT agents on wound dressing is represented diagrammatically in Figure 34

Principle: PDT agents would be attached to the wound dressing (bandage) that would be illuminated with light of certain wavelength to eradicate the microorganisms, consequently reducing infections.

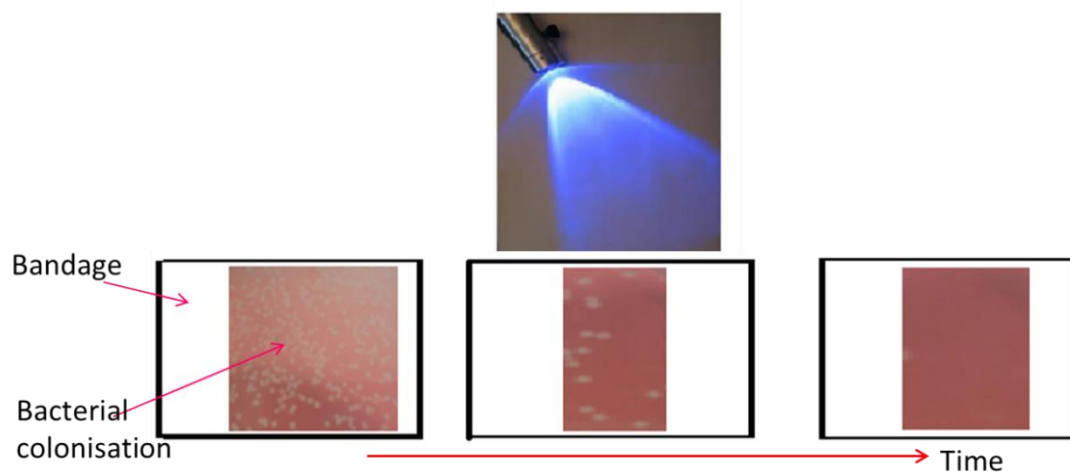
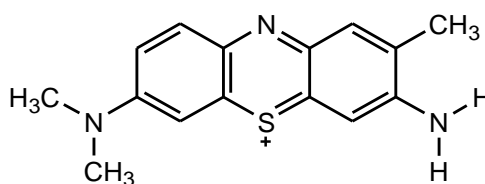


Figure 34: Colonisation of wound on a bandage

### 1.11.6 PDT and Bacteria

The search for new approaches to eradicate bacteria and not induce the appearance of undesired drug-resistant strains suggests that PDT has advantages over the traditional therapeutic use of antibiotics<sup>248</sup>. Antimicrobial photodynamic therapy is beginning to be considered as a promising alternative approach to resistant infections<sup>249</sup> as we are fast approaching the post antibiotic era<sup>206</sup>. Today an increasing amount of photosensitisers are being used in PDT to eradicate pathogenic microorganisms, such as *S. aureus*<sup>250</sup>. Research using PDT for elimination of pathogenic bacteria have demonstrated effective bactericidal effects *in vitro* against microbial resistance by employing the photosensitiser's; methylene blue and toluidine blue O<sup>251</sup>, Figure 35.



Toluidine blue O

Figure 35: Chemical structure of PDT agent

Photodynamic action on the eradication of pathogenic microorganisms (from infections) were studied using methylene blue (Figure 20) and toluidine blue O<sup>252</sup>. Bacterial species such as *S. aureus*<sup>253</sup> is one of the most significant causes of skin infections that have been known to develop into serious or even fatal systemic diseases<sup>204</sup>. Other species such as *P. aeruginosa*, and *C.*

*albicans*, (fungi) are still being investigated using PDT for eradication of pathogenic organisms<sup>249</sup>. Antifungal photodynamic therapy is a developing area of research in PDT<sup>254</sup>, particularly as resistance of yeast (*Candida*)<sup>255</sup> to antifungal agents are increasingly being reported<sup>256</sup>.

## 1.12 Antimicrobial compounds, their nature, mode of action and resistance mechanisms – Biological perspective

### 1.12.1 Antimicrobial control-physical methods

“Antimicrobial resistance is a crisis that must be managed with the extreme urgency” as it is becoming a symbolic acknowledged feature of microorganisms to be resistant towards antimicrobial agents<sup>257</sup>.

It is very important to understand the basic principles of antimicrobial mechanisms, therefore, this section will briefly give a broad overview of antimicrobials with respect to their microbiology.

The control of microorganisms in medicine, industry, and in our homes includes the use of physical methods to achieve microbial decontamination<sup>258</sup>. Examples of physical methods to control, prevent, remove or destroy microbial growth, are the use of heat, radiation and filtration<sup>259</sup>.

### 1.12.2 Heat sterilisation

Heat sterilisation is one of the most widespread methods used to control microbial growth. The susceptibility of microorganisms to heat is affected by temperature, type of heat (dry/moist), and the duration of heat treatment<sup>260</sup>.

At high temperatures microorganisms lose viability because denaturing of the macromolecules occurs, thus causing loss of structure and function, (Figure 36)<sup>261</sup>. Hence, in many laboratories and industries, autoclaves are frequently used for decontamination/sterilisation of materials harbouring microorganisms. Heat resistant endospores can effectively be killed off at temperatures above boiling point of water (approximately 120 °C steam), which is achieved by applying pressure in an autoclave at 100 k Pa (15 psi)<sup>262</sup> for 15 minutes<sup>263</sup>. Examples of sterilization methods and conditions used are explained in Table 7.

Table 7: Heat sterilisation methods<sup>262</sup>.

Method	Sterilizing conditions	Advantages	Precautions	Spore testing
Steam	15-20 mins at 250 °C	Time efficient	Corrosion of non stainless steel items.	<i>Bacillus</i>
Autoclave	3.5-10 mins at 270 °C	Good penetration	Items are wet after cycle. Can't use close containers, may leave deposits.	<i>B. stearothermophilus</i> strips or vented vials
Unsaturated chemical vapour	20 mins at 270 °C	Time efficient, no corrosion.	May damage plastic & rubber items. Must use special solution.	<i>B. stearothermophilus</i>
Dry heat (oven type)	60-120 mins at 320 °C	No corrosion, closed containers can be used.	May damage plastic & rubber items. Long cycle times.	<i>B. stearothermophilus</i>
Dry heat (rapid transfer)	12 mins at 375 °C	Time efficient, no corrosion.	May damage plastic & rubber items.	<i>B. stearothermophilus</i>

The “decimal reduction time”,  $D$ , (time required for a 10-fold reduction) in the viability of microbial population which is used to calculate the effectivity of heat sterilization at a given temperature (70 °C, 60 °C, and 50 °C). An example of this is shown in Figure 36.

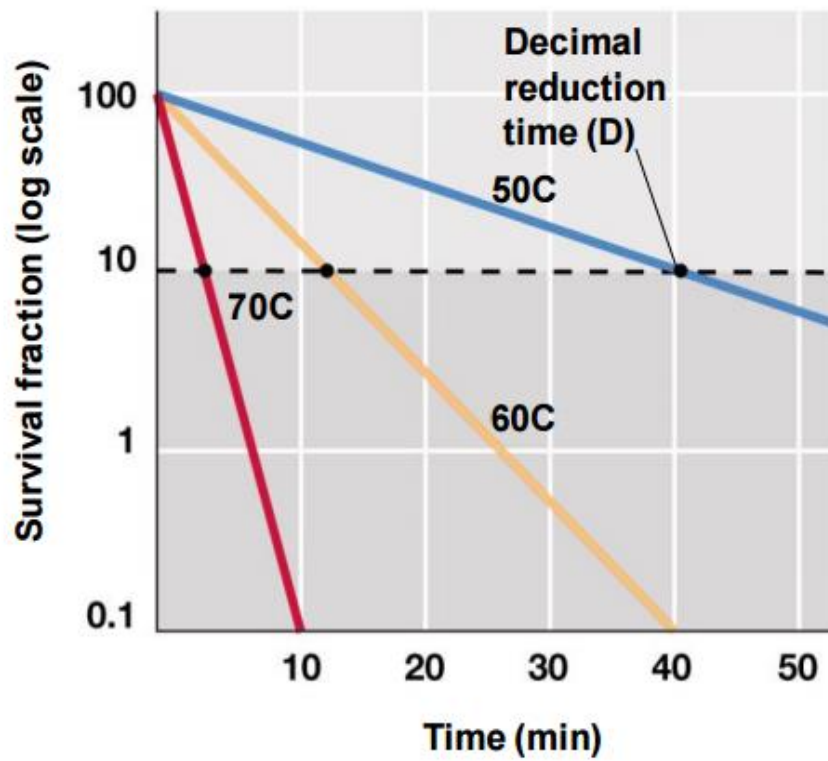
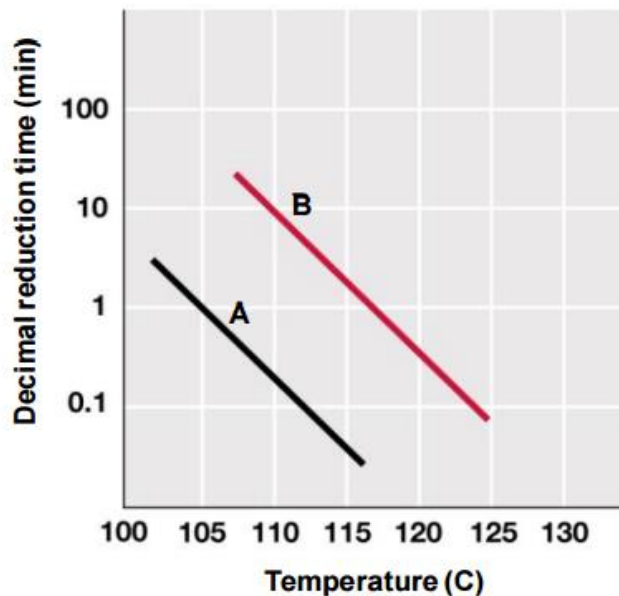


Figure 36: Temperature effects over time on microorganism (e.g. *mycobacterium tuberculosis*) viability<sup>263</sup>.

At lower temperatures, sterilisation of microorganisms takes longer than at higher temperatures and is dependent on the type of heat used (moist/dry).

The relationship between temperature and the rate of death of microorganisms is generally of first order. The rate increases rapidly as temperature rises. However, this differs for mesophiles and thermophiles, which is shown in Figure 37<sup>264</sup>.



Data were obtained for decimal reduction times, D, at several different temperatures. For organism A, a typical mesophile, exposure to 110°C for less than 20 sec resulted in a decimal reduction, while for organism B, a thermophile, 10 min was required to achieve a decimal reduction.

Figure 37: D for microorganisms (e.g. *E.coli*)<sup>264</sup>

### 1.12.3 Radiation sterilisation

Radiation in the form of microwaves, ultraviolet, x-rays, and gamma rays, are also effective methods to remove or reduce unwanted microbial growth<sup>265</sup>. Antimicrobial effects from microwave radiation occur by thermal effects. Microorganisms can also be killed or inactivated using other forms of radiation.

### 1.12.4 Filter sterilisation

Filter sterilization is based upon the size of contaminants to be removed. It is utilised for removal of decontaminants in liquids and gasses.

There are three types of filters that exist: depth, membrane and nucleopore filters. Membrane filtration technique is commonly employed in sterilization of liquids in microbiology laboratories.

## 1.13 Antimicrobial chemical control methods

Many types of chemical technologies are used to control the growth of microbes in particular environments<sup>266</sup>. To this end, a range of chemical antimicrobial agents are employed to kill microorganisms. Chemical antimicrobial agents include antiseptics, disinfectants and sanitizers all of which are used on a daily basis to either kill or control these pathogenic microorganisms<sup>267</sup>.

An antimicrobial agent, including chemical agents, should be:

- effective against a wide range of microbes,
- remain effective in the presence of organic material



- toxic to microbes but non-toxic to living tissue and non-corrosive to surfaces<sup>268</sup>

If all three of these properties were present in one antimicrobial agent, the problem of resistant pathogenic organisms would not occur. However, this is not the case as yet, and therefore, a range of antimicrobial agents have been developed that can be used individually for specific targets. Hence, the importance of carefully selecting the correct chemical agent<sup>269</sup>.

### 1.13.1 Chemical antimicrobial agents

Antimicrobial chemical agents are used in the home and in the workplace. Commercial laboratories use chemicals routinely to control microbial growth<sup>258</sup>. Natural or synthetic chemicals which either inhibit microbial growth or kill microorganisms are referred to as 'antimicrobial agents'. Antimicrobial agents that kill bacteria, fungi, viruses, or algae are called bacteriocidal<sup>270</sup>, fungicidal<sup>271</sup>, viricidal agents<sup>272</sup>, and algicide respectively.

### 1.13.2 Control of growth by chemical means

The toxicity of antimicrobial agents can differ from agent to agent. It is important to note that 'selective agents' are more toxic to microorganisms than they are to animal tissues<sup>273</sup>. Antimicrobial agents which have selective toxicity are useful for treating infectious diseases because they can kill selected microorganisms *in vivo*, usually without damaging the host cells<sup>274</sup>.

### 1.13.3 Antimicrobial agents and their mode of action

Observing the effects of antimicrobial agents on bacterial cultures can help to determine their classification i.e. whether they are bacteriostatic, bactericidal or bacteriolytic<sup>275</sup>.

Bacteriostatic agents inhibit protein synthesis, usually by binding to ribosomes. Some antibiotics work in a similar fashion as they use a comparable mechanism to that used by the bacteriostatic agents<sup>276</sup>. Bactericidal antimicrobial agents work by binding very tightly to their cellular targets and thus killing the cell. Antibiotics, such as the penicillin's and certain detergents such as alcohol, and cationic detergents for example, lysol, are considered as bacteriolytic agents which work by inhibiting cell wall synthesis and/or by rupturing the cytoplasmic membrane of the cell<sup>277</sup>. Chemical agents can be categorized into two broad classes;

1. Antiseptics
2. Sterilants/ disinfectants/ sanitizers.

Various types of antiseptic agents are: alcohol (60-85% ethanol-cleaning), Isopropyl alcohol (IPA) in water (topical antiseptics), phenol containing compounds (soaps, lotion), and cationic detergents (topical disinfectants, soaps)<sup>278</sup>. Antiseptics are non-toxic enough to kill the microorganism, however can still be applied for use on living tissue. For example, topical agents can be used for treatments of surface wounds, and hand washing.

Sanitizers are generally used in industry to disinfect surfaces and production areas, and in hospitals to disinfect medical equipment<sup>279</sup>. Some common sanitizers, disinfectants, include:

- ❖ chlorine gas- for the purification of water supplies
- ❖ chlorine related compounds- cleaning agents in food industry e.g. equipment,
- ❖ copper sulphate – used in water storage and in pools
- ❖ ethylene oxide - sterilizing plastic and lensed instruments
- ❖ 60-85% ethanol and isopropyl alcohol (IPA) for use in water as topical antiseptics
- ❖ phenolic compounds - used in the formulation of soaps and lotions<sup>280</sup>.

## 1.14 Antimicrobial Activity

Antimicrobial activity against pathogenic microorganisms is of importance as it helps to identify whether the antimicrobial agent used is successful in killing the microorganism(s), or simply damaging the cell<sup>264</sup>. The site of action and the mode of action of any potential antimicrobial agent, against its target organism (s) is important information to have. Antimicrobial activity can also be used to understand how toxic the agent is towards the pathogenic microorganisms by carrying out simple biological techniques such as ‘minimal inhibitory concentration’, MIC<sup>281</sup>.

### 1.14.1 Measuring antimicrobial activity

Antimicrobial activity can be measured in numerous ways. One of the frequently used methods is by measuring the MIC<sup>282</sup>. MIC involves determining the minimal amount of an antimicrobial agent required to inhibit growth of the organism(s).

In this investigation the MIC of selected compounds was tested against the Gram negative and Gram positive organisms *Escherichia coli*, and *Staphylococcus aureus* respectively.

The standard method for testing the MIC of a compound is called ‘tube dilution’<sup>283</sup>. This involves using tubes of broth containing an increasing concentration of the antimicrobial agent to be tested, which are all inoculated with the same level of microorganism to be tested. After a period of incubation these tubes are checked for the turbidity of the cultures. The tube with the lowest concentration showing no growth (no turbidity) is this concentration that is then referred to as the MIC<sup>284</sup>.

An alternative method of measuring MIC is via a technique called the ‘disc diffusion technique’<sup>285</sup>. This involves using filter paper discs, which contain a known concentration of antimicrobial agent that are placed onto the surface of agar in a petri dish, which has been seeded with the organism to be tested. The antimicrobial agent diffuses from the disc into the agar, which establishes the gradient<sup>281</sup>. The further the antimicrobial agent diffuses from the filter paper discs, the lower is its concentration in the agar, thus the MIC is measured from establishing the diffusion gradient<sup>286</sup>, these are usually referred to as a zones of inhibition.

## 1.15 Antimicrobial Agents-*In vivo*

Chemical antimicrobial agents, such as the mild antiseptics (as discussed above in section 1.13.3), are used as topical agents for control of infection. However, these agents cannot be administered internally due to their toxic effects<sup>287</sup>. Hence, the purpose of research into the development of antimicrobial drugs for their potential use as systemic agents usage which in due course would help reduce and/or control the spread of infection.

### 1.15.1 Antimicrobial drugs

The development of new antimicrobial drugs in the 1960's presented an array of treatment options for antimicrobial resistance and life threatening diseases<sup>288</sup>. The discovery of antimicrobial drugs has played a major role within the fields of medicine and agriculture. Antimicrobial drugs are classified in two broad categories: 'synthetic agents', and 'naturally occurring antimicrobial drugs' (antibiotics). These are sub classified into their molecular structure and on their mechanism of action.

### 1.15.2 Synthetic antimicrobial drugs

The infamous Paul Ehrlich made the initial discovery of precursor staining for bacteria. From this time onwards, the development of synthetic drugs, such as, Salvarsan, (Figure 38), began. Salvarsan, an arsenic containing compound was used to treat syphilis<sup>289</sup>.

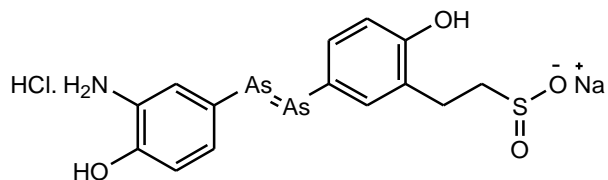


Figure 38: Chemical structure of salvarsan

Paul Ehrlich was the pioneer of the modern day chemotherapeutic drugs and was awarded as a Nobel prize in 1908 for his concept of the 'magic bullet theory'<sup>275</sup>. The magic bullet concept is the ability of the chemical compound (antimicrobial agent) to kill off or inhibit the microorganism(s) selectively, without damaging the host cells<sup>287</sup>.

### 1.15.3 Mode of action

The mode of action of antimicrobial compounds is classified according to their site of action i.e. the target structures in the bacterial cell. This is shown in Figure 39<sup>290</sup>.

Antimicrobial agents generally affect a limited and well defined group of microorganisms<sup>275</sup>. There are a number of antimicrobial agents that are very specific and affect the growth of only a single genus. For example penicillins are affective against both gram positive and negative bacteria<sup>69</sup>. The  $\beta$ -lactam antibiotics are known to be inhibitors of cell wall synthesis. The

transpeptidase enzymes bind to the penicillin or other  $\beta$ -lactam antibiotics (referred to as 'penicillin binding proteins' (PBPs) <sup>291</sup>. Once the PBPs are bound to penicillin they lose the ability to catalyse the transpeptidase reaction, however, cell wall synthesis continues. Consequently, the newly synthesised cell wall is not cross linked and is unable to maintain its strength resulting in a weak, and a self-degrading cell wall. Thus, the cell wall can be digested by the enzyme autolysin, whose release is stimulated by the antibiotic-PBP complex. Thus, the difference in osmotic pressure between the inner and outer cell cause a lysis<sup>292</sup>.  $\beta$ -lactam antibiotics are selective and not toxic to their host cells because they do not have cell walls<sup>291</sup>.

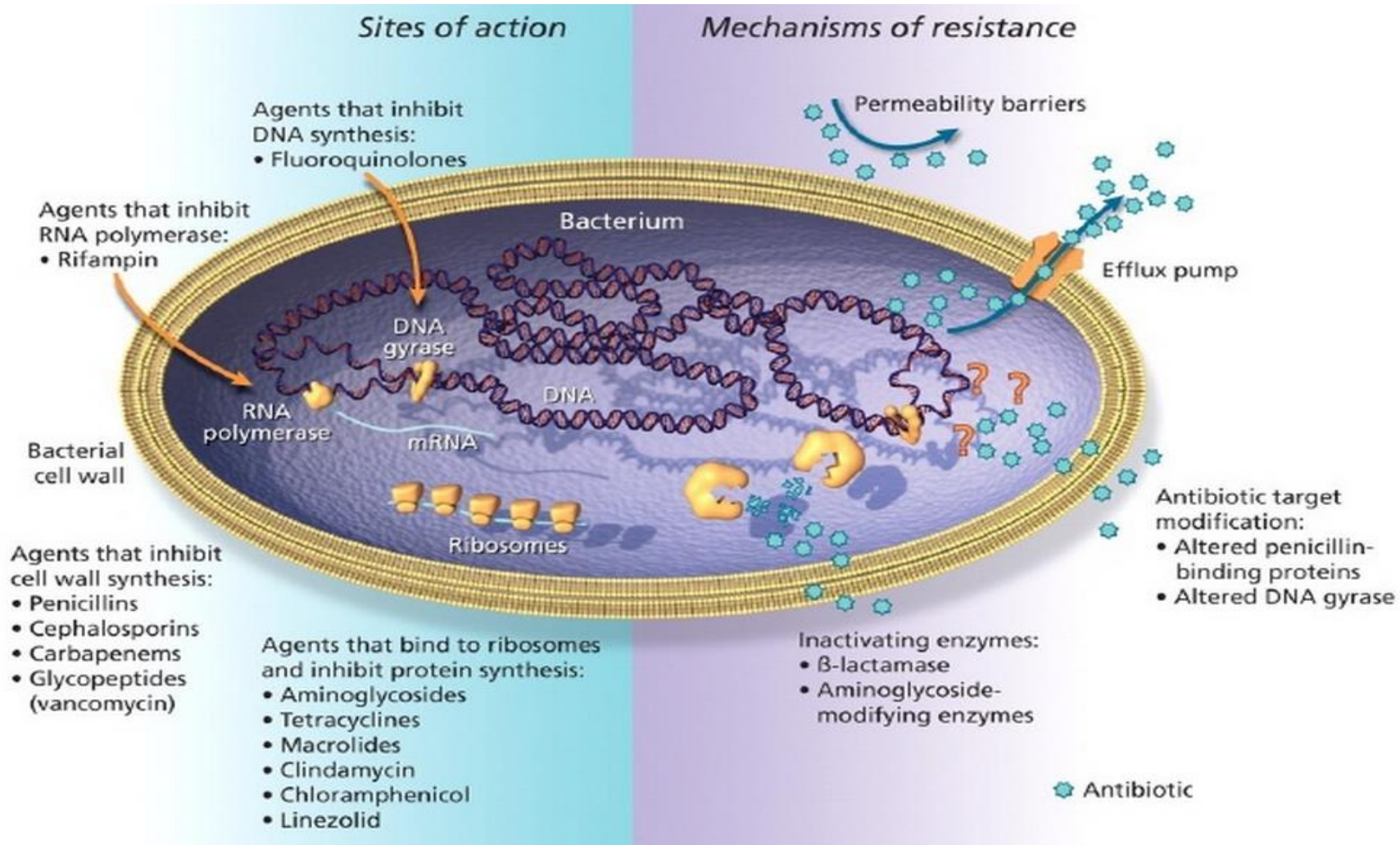


Figure 39: Mode of action of antimicrobial agents(A) and mechanisms of resistance (B) <sup>290</sup>

#### 1.15.4 Resistance mechanisms of bacterial cell (Figure 39-B)

- pathway which modifies the bacterial cell wall so that it does not contain the binding site of the antimicrobial agent.
- The bacterial genome can contain mutations that limit access of antimicrobial agents to its intracellular target site<sup>293</sup>.
- The organism can develop resistance to drugs, particularly sulphur containing compounds that are inhibitors of folic acid.
- The bacteria may have efflux pumps that extrude the antibacterial agent from the cell before it reaches its target site <sup>294</sup>.

#### 1.16 Drug resistance

Drug resistance is the ability of microorganisms to resist the effects of the antimicrobial agents to which they are normally susceptible to<sup>295</sup>. There is no single antimicrobial agent that is able to inhibit all microorganisms<sup>296</sup>. For antimicrobial drug resistance to occur the microorganism producing the antibiotic must be able to neutralize and destroy its own antibiotic<sup>297</sup>. Hence, the importance of gene encoding in organisms that allows, antimicrobial drug resistance to occur by the transfer of resistance genes between microorganisms<sup>298</sup>.

##### 1.16.1 Antimicrobial drug resistance

In healthcare antimicrobial drug resistance is of great concern, as it is a major problem to deal with in countless pathogenic microorganisms<sup>299</sup>. Resistant bacteria spreads rapidly and is therefore causing problems not only in general healthcare settings, but also in community associated settings<sup>300</sup>. The increasing spread of bacterial resistance within the community poses obvious difficulties for infection control in environments, such as, long-term care facilities, military recruitment centres, and day care centres. Thus, there is a real need to be aware of the problem and to develop new antimicrobial drugs to fight and control the spread of the unwanted microbial resistance.<sup>301</sup>

##### 1.16.2 Biocides

Biocides are antimicrobial molecules that are used for killing microorganisms or their harmful effects by either chemical or biological means<sup>302</sup>. Examples of biocides in common use include disinfectants, preservatives<sup>303</sup>, antiseptics, pesticides, herbicides<sup>304</sup>, fungicides and insecticides<sup>305</sup>. The use of biocides is generally unpopular because of their toxic nature and potential danger to the environment<sup>296</sup>. However, importance of using biocides is socially recognised by organisations such as COST 511 and the European Biocide Directives, as they have a role in combating the rapid increase of microbial resistance, predominantly within the healthcare settings<sup>306</sup>.

### 1.17 Quantitative Structure-Activity Relationship (QSAR)

The relationship between chemical structure and the activity of chemical compounds helps in understanding the mechanism of bioactivity and provides a tool to predict the activity of new compounds based on knowledge of the structural parameters. Quantitative structure-activity relationship (QSAR) methods have been utilized for estimating a potential toxicity of organic compounds and development of drugs<sup>307</sup>. Hansch and Fujita in 1964 proposed a method for correlating biological activity with the chemical structure. A general model for biological QSAR was derived from a linear free energy-related approach, later called Hansch analysis. All parameters used by Hansch were linear free energy-related values derived from rates or equilibrium constants.

### 1.18 Log P

Log P is the logarithm of the *n* octanol/water partition coefficient as a measure of the hydrophobicity. The goal of this study is to understand the relationship between the structural parameters (in terms of electron withdrawing and donating substituents attached to the molecule) and the antimicrobial activity ultimately providing a tool to predict the biocidal properties of new compounds.

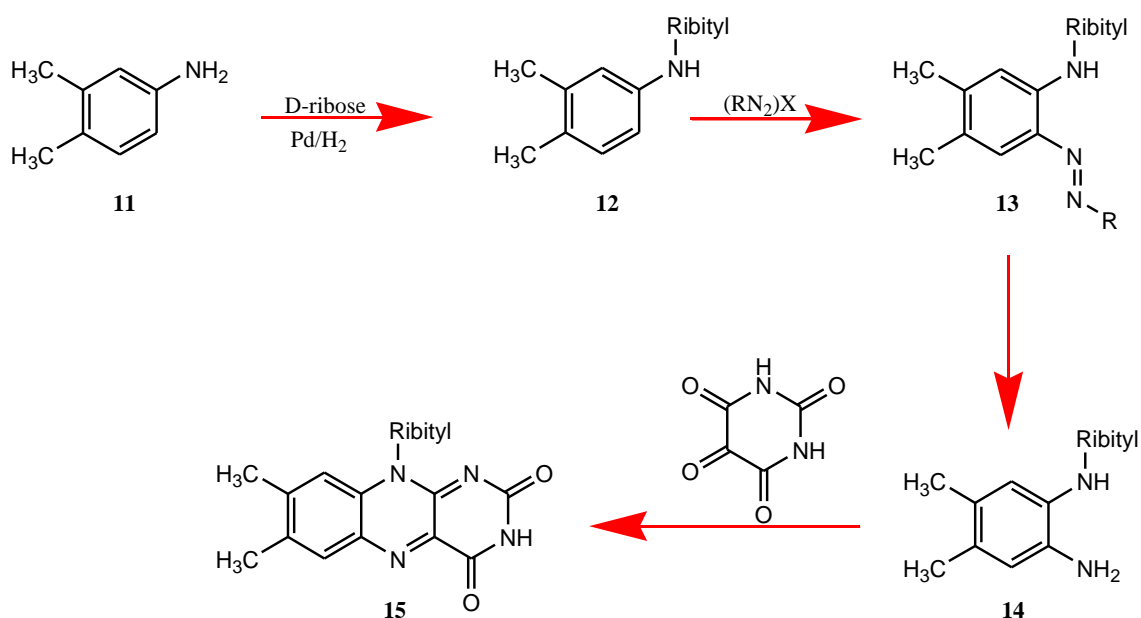
## 1.19 Isoalloxazine analogues in literature

The crucial search for the ideal photosensitisers are persistently being developed by scientists. For the purpose of this research the synthesis of alloxazine analogues in literature is studied in order to find a synthetic pathway to achieve this aim.

### 1.19.1 Synthesis of isoalloxazine analogues in literature

The total success in synthesis of riboflavin was accomplished by Paul Karrer in 1935<sup>308</sup>. He received the Nobel Prize for this work in 1937. It was this work that provided a platform for the synthesis of further riboflavin analogues.

The original method devised by Karrer describes the reductive amination of 3,4-dimethylaniline with D-ribose (**13**), followed by the addition of an amine group by using a diazonium species, with the nitrogen becoming position N5 of the flavin (Figure 43). Alloxan was then reacted with the intermediate species (**14**), resulting in formation of a riboflavin (**15**), Scheme 16.



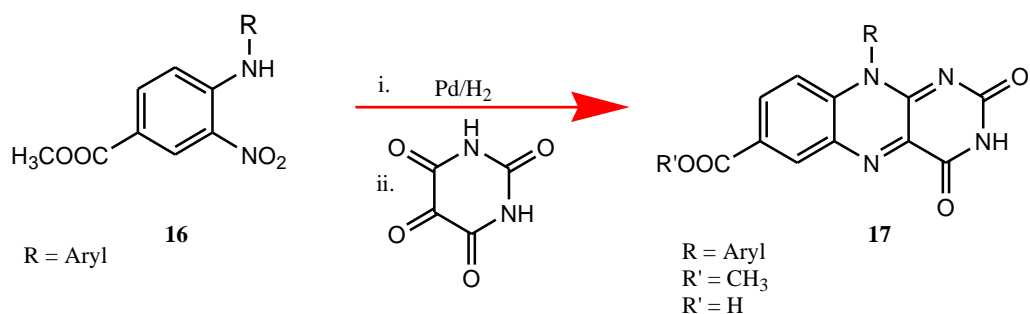
(RN<sub>2</sub>)X = one of many diazonium salts used by Karrer

*Scheme 16: Total synthesis of riboflavin<sup>308</sup>*

Although this synthesis, (Scheme 16) has been developed by Karrer, other researchers have continued on enhancements of this reaction. Improvements to individual reactions and/or alternative routes have been developed largely due to the advancement knowledge of organic chemistry. Examples of these can be seen from Scheme 17 to Scheme 32.

One of the routes used to synthesise the substituted isoalloxazines by Ram Singh and Geetanjali involved cyclo-condensation of the *N*-substituted 2-aminophenyl aniline with alloxan monohydrate in aqueous or organic solvents, Scheme 17.

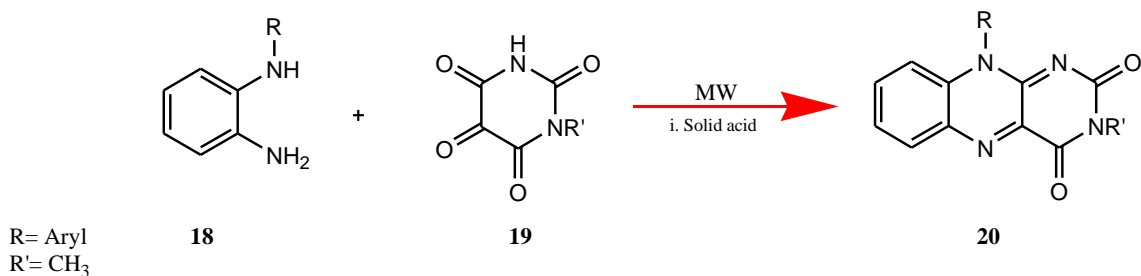




*Scheme 17: Synthesis of substituted isoalloxazines*

This method was utilised for the synthesis of a library of isoalloxazines that were used as chemical models for flavin monooxygenase and tested as potential anti-malarial agents<sup>309</sup>.

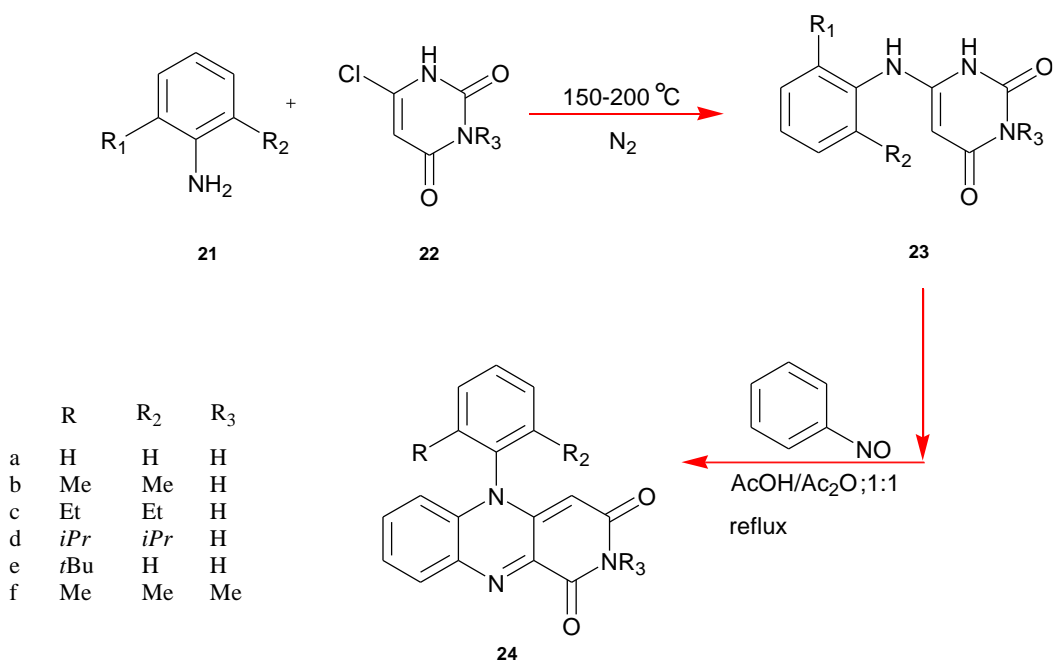
The same authors (Ram Singh and Geetanjali) used an alternative route to synthesise 10-substituted isoalloxazine (**20**). This route involved using microwave assisted reactions in the presence of solid acids<sup>310</sup> (Scheme 18).



*Scheme 18: Microwave assisted (MW) synthesis of substituted isoalloxazine*

These researchers observed that an increased yield was obtainable if the reaction was carried out using microwave irradiation. The addition of a catalyst or mineral based reagents for example alumina, clays, silica, and zeolites showed further enhancement on the overall yield of the product. It is the catalysts/mineral based reagents that are referred to as the “solid acid”. The yield was enhanced from 18-40% to 74-84% respectively<sup>311</sup>.

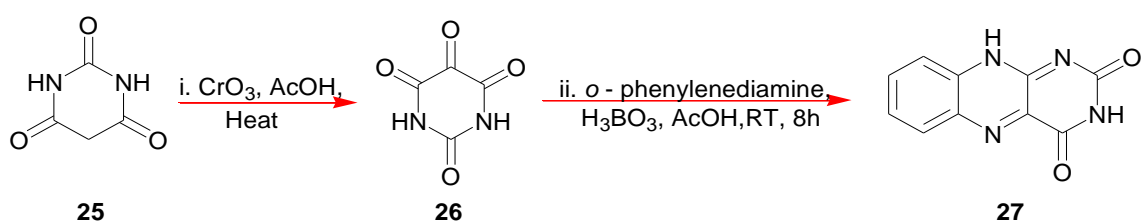
Researchers Dadova et al<sup>312</sup> synthesised isoalloxazines using an additional method, which is shown in Scheme 19.



*Scheme 19: Synthesis of 10-aryl flavins*

The 10-aryl isoalloxazines (**24**) were synthesised by converting the substituted anilines (**21**) with 6-chlorouracil (**22**) into 6-arylaminoouracil (**23**). It was noted that there was an overall decrease in the yields of the 10-aryl isoalloxazines, which was caused by steric hindrance on positions C2 and C6 of the phenyl ring. However, the non-substituted isoalloxazine derivatives- phenyl isoalloxazine, could only be isolated in moderate yields upon elongated reaction times. Changing conditions within this reaction scheme showed no enhancements in the yields of the synthesised isoalloxazines. The observed yields for this method were between 13-25%.<sup>312</sup>

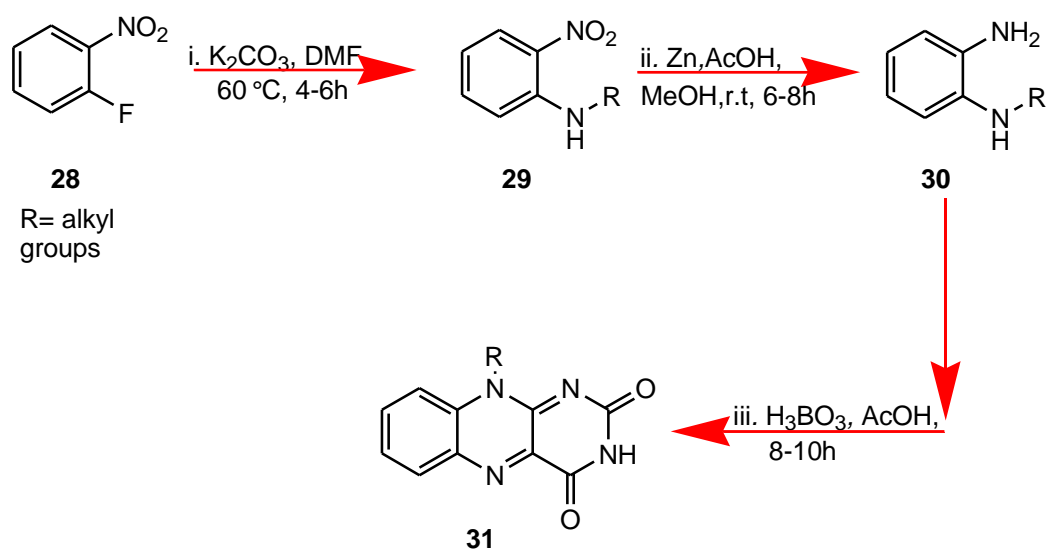
A.M. Kanhed *et al.* initially synthesised alloxan monohydrate and continued synthesis to form isoalloxazine, shown in Scheme 20.



*Scheme 20: Synthetic procedure for isoalloxazine*

The oxidation of barbituric acid (**25**) was used to prepare alloxan monohydrate (**26**)<sup>313</sup>. This in turn was utilised to synthesise the isoalloxazine derivatives (**27**) by cyclisation with *o*-phenylenediamine in presence of boric acid and acetic acid at room temperature, Scheme 21.

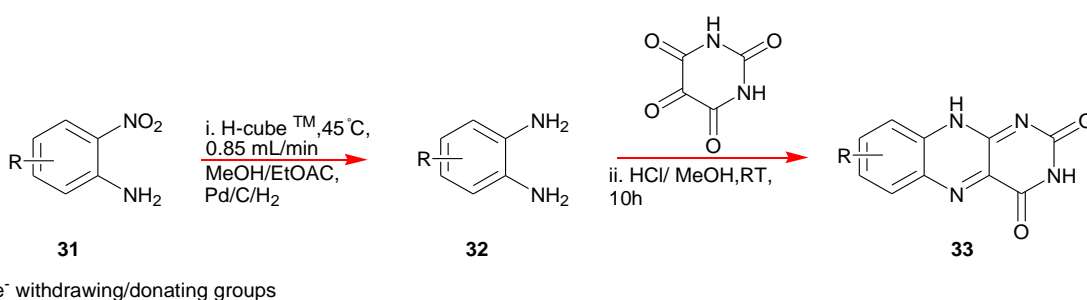
An additional route used by the same research group is shown in Scheme 22.



*Scheme 21: Synthetic route for derivatives of isoalloxazine*

The second route shows alkylation of the synthesised isoalloxazines at the 10 position using a range of alkyl reagents. The starting material, 1-fluoro-2-nitrobenzene (**28**) was reacted with the required alkyl or aryl amine in the presence of a  $K_2CO_3$ , with DMF as the solvent to yield the substituted intermediate (**29**). The intermediate product was subsequently reduced using zinc in acetic acid and methanol to form the substituted amino aniline (**30**). This was consequently cyclised to form the final product (**31**) using boric acid in acetic acid<sup>314</sup>.

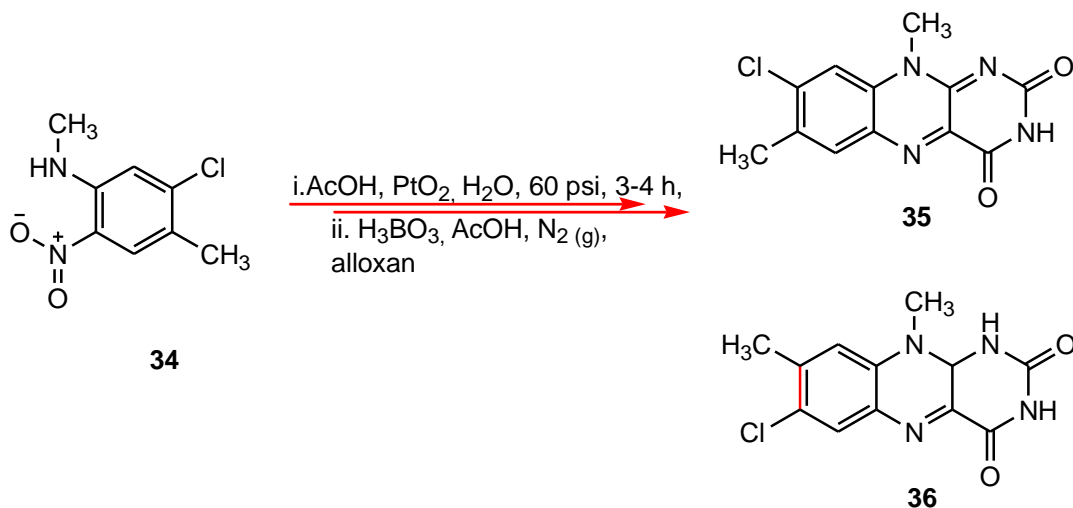
M. Baumann *et al.* also synthesised a range of isoalloxazine derivatives in 2014. The difference in this synthesis (Scheme 22 to Scheme 21) is the method used for reduction of the nitro moiety to the amine, and not the final cyclisation step to form the isoalloxazine derivative. This method involved hydrogenation using an H-cube<sup>TM</sup>. The H-cube<sup>TM</sup> flow hydrogenation system was used to prepare 1, 2-diaminobenzene intermediates (**32**) using 2-nitroaniline (**31**) as the starting material in methanol/ethyl acetate (1:1).



*Scheme 22: Hydrogenation method for the synthesis of isoalloxazine derivatives*

This research group, did not isolate the substituted 1,2-diaminobenzene intermediates (**32**) instead they simply transferred the intermediate in a stirred vial containing alloxan in methanol and HCl to afford the desired isoalloxazine (**33**), Scheme 22. The best purification and yield was observed when the reaction was performed at room temperature<sup>315</sup>.

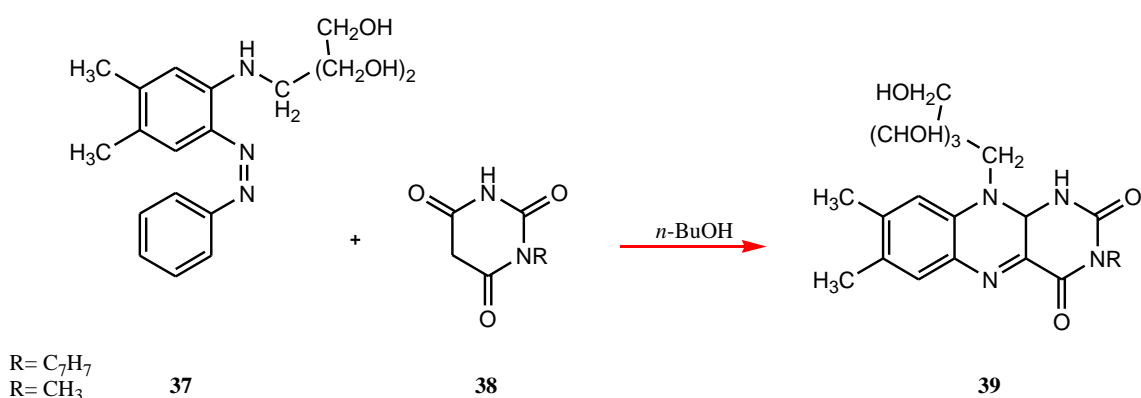
V. Kumar *et al.* in 1986 synthesised a range of isoalloxazine derivatives, which were functionalised at the 8-position. During the synthesis of a particular flavin, 8-chlorolumiflavin (**35**), it was noted that an additional compound (**36**) was formed with the desired product and is shown in Scheme 23<sup>316</sup>.



*Scheme 23: Hydrogenation using PtO<sub>2</sub> for the synthesis of isoalloxazine derivatives*

The synthetic route involved the reactants to be hydrogenated using platinum oxide using pressure. This suspension was subsequently suspended into alloxan monohydrate and boric acid. The resulting material formed a mixture of 2 products; compounds **35** and **36**. The products were isolated and purified by crystallisation, The yields of these isoalloxazines were reported to be 54% and 39% respectively<sup>316</sup>, Scheme 24.

Another research team from Geneve (Muller and Dudley) also synthesised derivatives of isoalloxazines shown in Scheme 25.

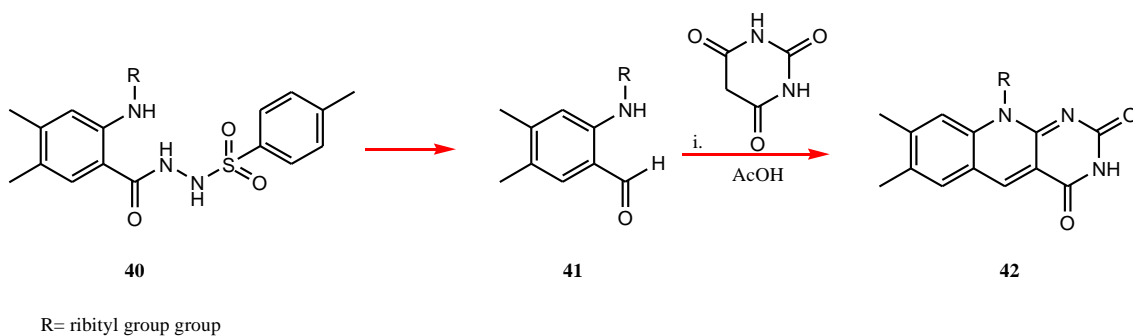


*Scheme 24: Hydrogenation using Pd/C for the synthesis of isoalloxazine derivatives*

This synthesis involved a condensation reaction with the starting material **37** and **38**. This synthesis seemed straight forward, however four addition steps, which proved to be a lengthy procedure were required for the removal of the chain to form a flavin with the methyl group

attached to the *N*-10 position. For this reason this method was not used a classical route to synthesise isoalloxazine derivatives<sup>317</sup>.

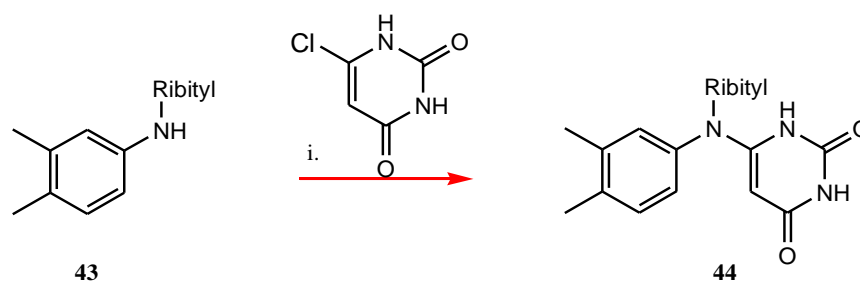
O'Brien *et al* reported difficulties between the starting materials 4,5-dimethyl-*N*-ribitylanthranilaldehyde and barbituric acid in the synthesis of a riboflavin derivative, Scheme 25. Nonetheless, a similar method was reported by Weinstock *et al.* using 2,4,6-piperidinetrione instead of barbituric acid.



*Scheme 25; Synthesis of riboflavin derivative by O. Brien et al.*

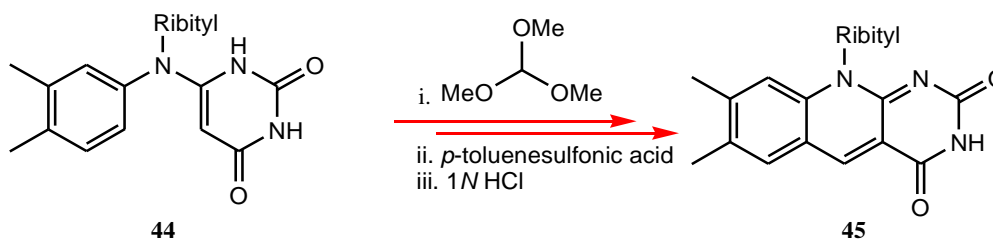
Although the reaction proved to be successful, several undesired by-products were also identified, consequently resulting in lower yields of the desired product<sup>318</sup>.

A synthetic breakthrough for the synthesis of riboflavin analogues was achieved by Yoneda *et al* in 1976. Whilst synthesising riboflavin and riboflavin *N*5-oxide, the intermediate compound (**44**) (Scheme 26) during this synthesis was identified to be a remarkable compound and was employed as the starting reagent in further synthesis of flavin analogues, Scheme 27<sup>319</sup>.



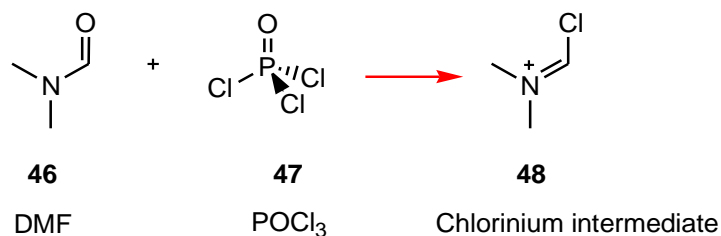
*Scheme 26: Intermediate compound of Yoneda et al*<sup>319</sup>

Ring closure of this intermediate (**44**) material was achieved using trimethyl orthoformate and *p*-toluenesulfonic acid, which was obtained in a 46 % yield, Scheme 27.



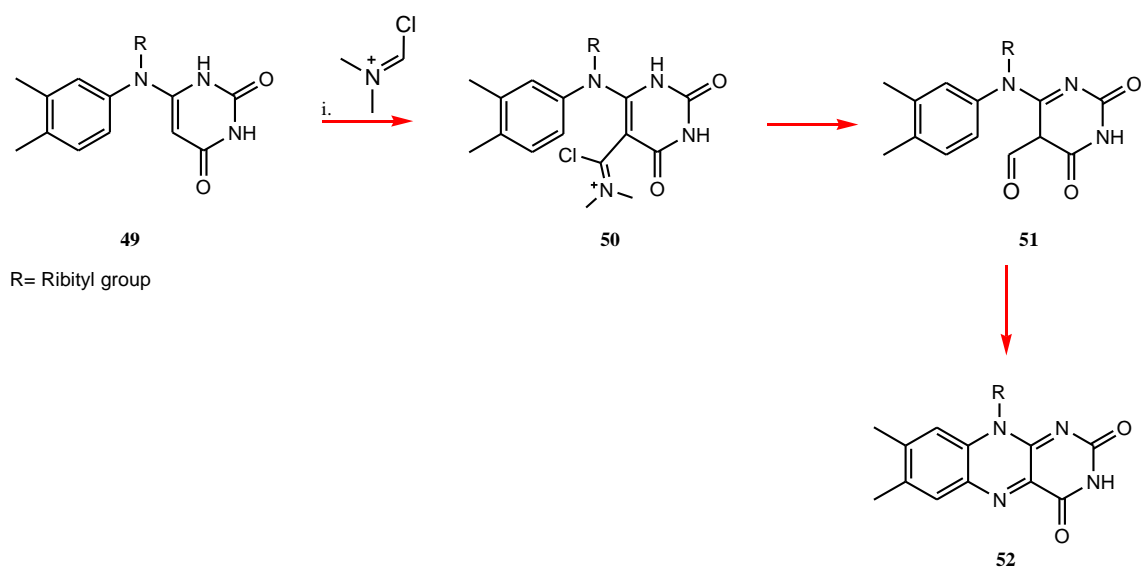
*Scheme 27: Ring closure to form riboflavin derivative*

An alternative route for the synthesis of flavin derivatives is also reported by Yoneda *et al*, who used Vilsmeier-Haack reagents, phosphorus oxychloride (POCl<sub>3</sub>) and dimethylformamide (DMF) to primarily introduce a reactive intermediate species, which would be susceptible to nucleophilic attack<sup>320</sup> which can be seen in Scheme 28



*Scheme 28: Reactive intermediate species*

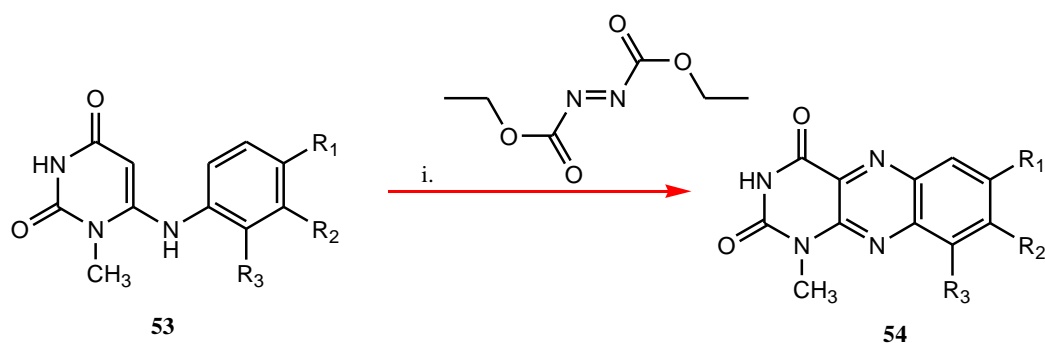
This reactive species (**48**) was then reacted with a bicyclic intermediate (**49**) to form an iminium species (**50**), which could undergo an intramolecular reaction resulting in the desired isoalloxazine (**52**), Scheme 29<sup>319</sup>.



*Scheme 29: Vilsmeier-Haack used to synthesise flavin derivatives<sup>319</sup>*

Shaker Youssif devised a one pot route to synthesise a library of alloxazine derivatives. The synthesis involved intramolecular cyclization of a substituted 6-anilinouracils via Vilsmeier reagent<sup>321</sup>.

6-Anilino-1-methyluracils (**53**) were reacted with diethyl azodiformate (DAD) to undergo a cyclization reaction to form 1-methylalloxazines derivatives (**54**), Scheme 30.

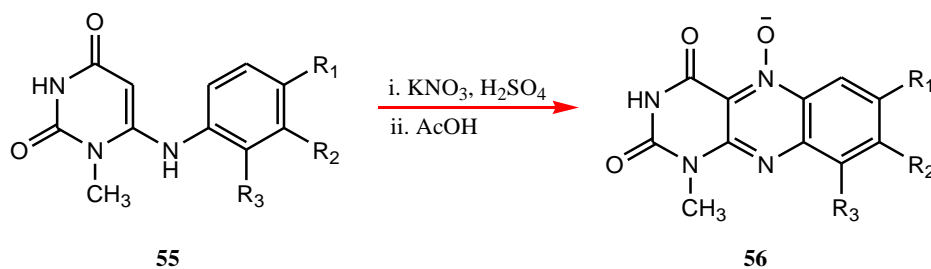


- a= R<sub>1</sub>= H, R<sub>2</sub> = H, R<sub>3</sub>= H  
 b= R<sub>1</sub>= Br, R<sub>2</sub> = H, R<sub>3</sub>= H  
 c= R<sub>1</sub>= OCH<sub>3</sub>, R<sub>2</sub> = H, R<sub>3</sub>= H  
 d= R<sub>1</sub>= F, R<sub>2</sub> = Cl, R<sub>3</sub>= H  
 e= R<sub>1</sub>= Cl, R<sub>2</sub> = H, R<sub>3</sub>= CH<sub>3</sub>

*Scheme 30: Synthesis of 1-methylalloxazines derivatives*

The isoalloxazine derivative in this reaction was synthesised over a broad yield, ranging from 35 to 83%.

The same author treated 6-anilino-1-methyluracils (55) with potassium nitrate and acetic acid in the presence of sulfuric acid to result in alloxazine-5-oxide derivatives (56).

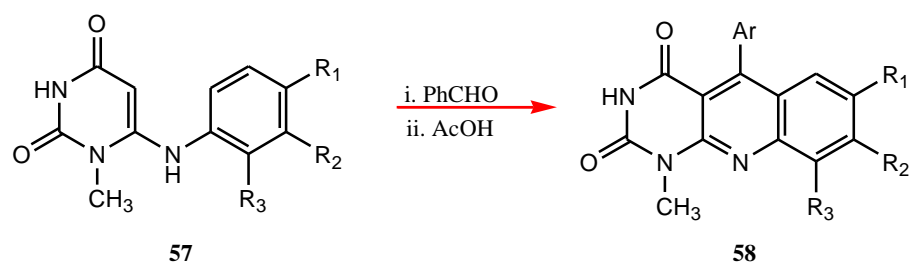


- a= R<sub>1</sub>= H, R<sub>2</sub> = H, R<sub>3</sub>= H  
 b= R<sub>1</sub>= Br, R<sub>2</sub> = H, R<sub>3</sub>= H  
 c= R<sub>1</sub>= OCH<sub>3</sub>, R<sub>2</sub> = H, R<sub>3</sub>= H  
 d= R<sub>1</sub>= F, R<sub>2</sub> = Cl, R<sub>3</sub>= H  
 e= R<sub>1</sub>= Cl, R<sub>2</sub> = H, R<sub>3</sub>= CH<sub>3</sub>

*Scheme 31: Synthesis of alloxazine-5-oxide derivatives*

These derivatives were synthesised in a yield ranging from 40 to 85%. By analysis this clearly shows that using potassium nitrate, acetic acid in the presence of sulfuric acid was a better method to use as there was a light enhancement in the overall yield<sup>321</sup>.

Derivatives of aryl-5-deazaalloxazines (58) were synthesised by Youssif by reacting 6-anilino-1-methyluracils (57) with a variation of aryl aldehydes e.g. benzaldehyde, anisaldehyde in the presence of glacial acetic acid.



- a= R<sub>1</sub>= H, R<sub>2</sub>= H, R<sub>3</sub>= H, Ar= Ph  
 b= R<sub>1</sub>= Br, R<sub>2</sub>= H, R<sub>3</sub>= H, Ar= Ph  
 c= R<sub>1</sub>= OCH<sub>3</sub>, R<sub>2</sub>= H, R<sub>3</sub>= H, Ar= Ph  
 d= R<sub>1</sub>= H, R<sub>2</sub>= H, R<sub>3</sub>= H, Ar= Ph  
 e= R<sub>1</sub>= OCH<sub>3</sub>, R<sub>2</sub>= H, R<sub>3</sub>= H, Ar= P.OCH<sub>3</sub>C<sub>6</sub>H<sub>4</sub>

*Scheme 32: Synthesis of aryl deazaalloxazine derivatives*

Derivatives of deazaalloxazine, (**58**) were synthesised in a range yielding between 49 to 71%. This synthesis of dezaalloxazine showed its yields to be somewhat less than both the yields obtained from synthesising methylalloxazines, and alloxazine-5-oxide derivatives as shown in Scheme 31 and Scheme 32.

Literature has shown a number of methods to synthesise flavins. Based on the methods analysed, the isoalloxazines in this project shall be synthesised using the pathway described in Scheme 33.



## Chapter 2

### 2.1 Rationale

In 2013, Professor Dame Sally Davies addressed the UK parliament and informed its members that “Antimicrobial resistance poses a catastrophic threat. If we don’t act now, any one of us could go into hospital in 20 years for minor surgery and die because of an ordinary infection that can’t be treated by antibiotics”. In 2014, the World Health Organisation (WHO) published a report highlighting the significant rise in antimicrobial resistance around the globe. The WHO worryingly predicted a situation where common infections and small injuries will once again bring death in a post-antibiotic era (The Alliance to Save Our Antibiotics, 2014). In 2015 the O’Neill Report (commissioned by the UK government) made similar predictions (O’Neill, 2015). The recently published O’Neill Review (O’Neill, 2016) made final suggestions on “methods to globally tackle drug resistant infections”. The council of European Union published a report (June 2016) to adopt a One Health approach to combat antimicrobial resistance. It’s clear that there are numerous issues around creating new antimicrobial agents to fight our pathogenic foes and these have been highlighted by the British Society for Antimicrobial Chemotherapy (BSAC) Working Party within the Journal of Antimicrobial Chemotherapy. To expand these issues cover:

1. The economics of antibacterial resistance and its control – The magnitude of this threat has and is being recognised to the point that WHO have estimated that 10 million lives a year and more that 100 trillion USD of economic outputs are at risk.
2. Discovery research: the scientific challenge of finding new antibiotics.
3. Regulatory opportunities to encourage technology solutions to antibacterial drug resistance
4. The urgent need for new antibacterial agents

It is clear that we must now save our life saving wonder drugs whilst focusing on infection control. This project seeks to generate a wound care technology which would generate a non-invasive self-cleaning bandage capable of keeping a wound clean and infection free. The concept behind this technique is to generate novel range of photoactive dyes that will provide doctors to treat bacterial colonisation promptly and efficiently, thus allowing early treatment of potential infections. Subsequently reducing the need for systemic antibiotics and provide a cheap and quick form of post-operative wound care.

With the above criterion in mind this project seeks to:

1. Develop a range of semi-synthetic molecules based on the tricyclic isoalloxazine structure of Riboflavin (Vitamin B2), which is known to generate singlet oxygen upon the application of blue light. Indeed, Riboflavin has been shown to be active against the Human Immunodeficiency Virus (HIV 1 and HIV 2).
2. Quantify the amount of singlet oxygen and redox radicals upon illumination with blue light using a non-direct spectrophometric measurement.
3. Test the new developed photoantimicrobials against two different pathogenic species of Gram positive- (*S.aureus*) and Gram negative (*E. coli*) bacteria. The rational for using these species is because they are responsible for 25% of HAI. *S.aureus* are particularly responsible for infections around the skin and tissue.
4. Add the synthesised antimicrobial agents to a solid support- as proof of principal testing, towards self-cleaning bandages.

## 2.2 Aims/Objective

The rationale behind using the riboflavin structure is as follows:

- i. Riboflavin is recognised to be photoactive due to its isoalloxazine structure.
- ii. Riboflavin's are known to degrade to form two further isoalloxazines, which are both known to be photoactive and are shown in Figure 40.

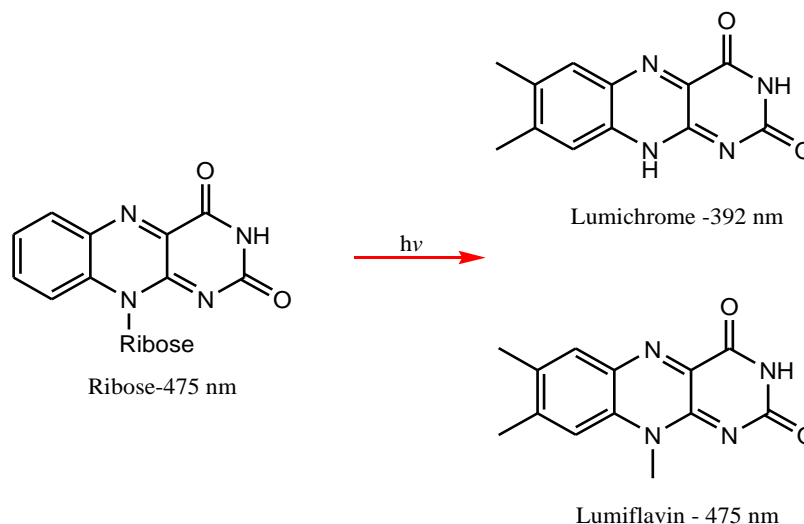


*Figure 40: Chemical structure of riboflavin and its degradation molecules*

- iii. Semi-synthetic isoalloxazine (Figure 41) is cost effective to synthesise and this is explained in section 1.4.

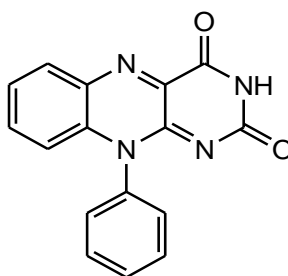


*Figure 41: Chemical structure of a semi-synthetic isoalloxazine*

- iv. There is the ability to functionalise (via a variety of electron withdrawing/donating substituents) the phenyl ring (Figure 42). This should effect the enhancement of yield production for singlet oxygen and redox radicals, due to differing electronic effects.
- v. Free amide allows further attachment of a solid support as shown in Figure 42.

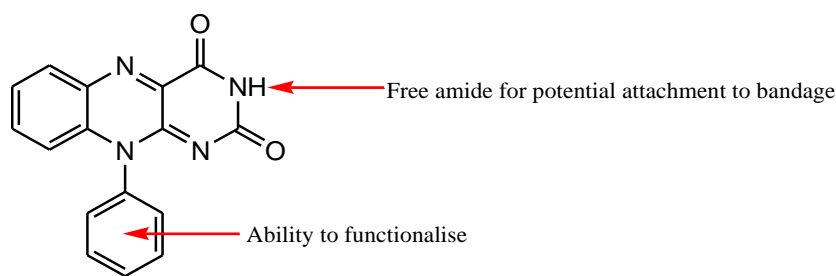


Figure 42: Functionalisation of isoalloxazine

The need for developing new antimicrobial agents for mankind with unmet medical needs is essential in the fight against superbugs. The emergence of resistance has accelerated and is threatening our ability to control infection by not responding to the existing drugs.

## 2.3 Introduction to flavins

### 2.3.1 Flavin background

The term “flavin” is derived from the Latin ‘flavus’, meaning yellow. Flavus describes a biological molecule containing a tricyclic isoalloxazine structure, depicted in Figure 43. Its unique structure permits flavin to be used in a diverse range of functions for example; they may act as a redox cofactor<sup>322</sup>, a light accepting chromophore in the detoxification and removal of free-radicals and peroxides within the cell, or as a signal transducer during programmed cell death<sup>323</sup>.

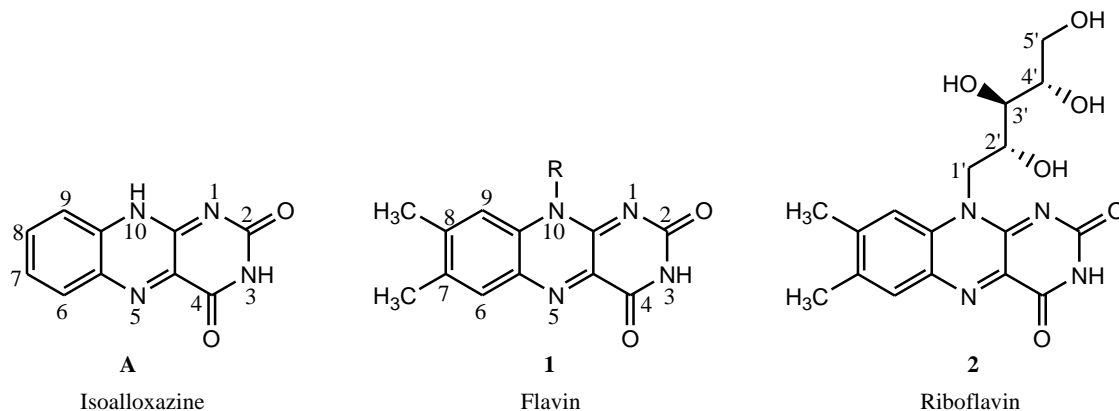


Figure 43: Chemical structure of flavin and riboflavin

Riboflavin (**2**), also known as vitamin B<sub>2</sub>, Figure 43, is the simplest form of flavin (**1**) (isoalloxazine-A) formed by nature<sup>324</sup>. The name indicates it is a combination of a ribose sugar and isoalloxazine, which are linked together by the nitrogen in the 10<sup>th</sup> position (N10) of the flavin, Figure 43. The D-ribityl group (attached to the flavin) is originally derived from the sugar ribose, which in nature is only present as the D-enantiomer. Its original stereochemistry is retained throughout all biological forms of flavin. Riboflavin is a cofactor enzyme in many flavoprotein enzyme reactions.

## 2.4 Flavin redox behaviour

Flavins generally have good chromophores because of the extended delocalisation of electrons throughout the structure<sup>325</sup>. They have a planar,  $sp^2$  hybridised structure and (flavins) commonly appear as yellow in colour because they are able to accept photons of visible wavelength, 445 nm to 450 nm<sup>325</sup>.

Flavins can be easily reduced at positions N1 and N5, to yield a “hydroquinone” form, by accepting 2 electrons and 2 protons, forming Flavin Mono Nucleotide (FMNH<sub>2</sub>) or Flavin Adenine Dinucleotide (FADH<sub>2</sub>) these are referred to as Fl<sub>ox</sub> and Fl<sub>red</sub>, Figure 44.

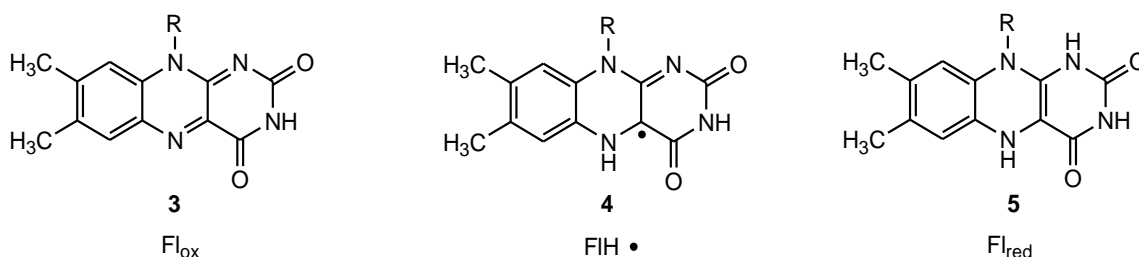


Figure 44: Structural forms of quinones

Upon reduction of the flavin, a loss of aromaticity occurs. The loss of conjugation leads to a reduction in extinction coefficient and therefore a shift in the absorbance of Fl<sub>ox</sub> (3) from 445 nm to 395 nm. As a result of this, both electron transfer and energy transfer is feasible by flavins as the loss of aromaticity is energetically unfavourable.

Flavins can form stable radical intermediate states<sup>326</sup>, known as the flavin semiquinone (FlH•) (4). The stability of this intermediate allows the transfer of single electrons in the electron transport chain.

## 2.5 Much desired resistance antimicrobial agents-synthesised

From the address of Professor Dame Sally Davies to the UK parliament with regards to the increase in the fast approaching catastrophic effects of antimicrobial resistance around the globe, there is a vital need to develop a new generation of photo-antimicrobials to save public health from this serious threat.

In order to control this threat The British Society for Antimicrobial Chemotherapy (BSAC) have reported global measures to curtail inappropriate use of antibiotics<sup>32</sup>. The control for overuse of antibiotics is urgently required as it contributes heavily to the cause of drug resistant bacteria<sup>327</sup>. Although Lord Jim O'Neill suggested (in the 2016, annual report) improving the use of existing treatments as discovery of novel drugs can take a long time, research must prevail<sup>328</sup>.

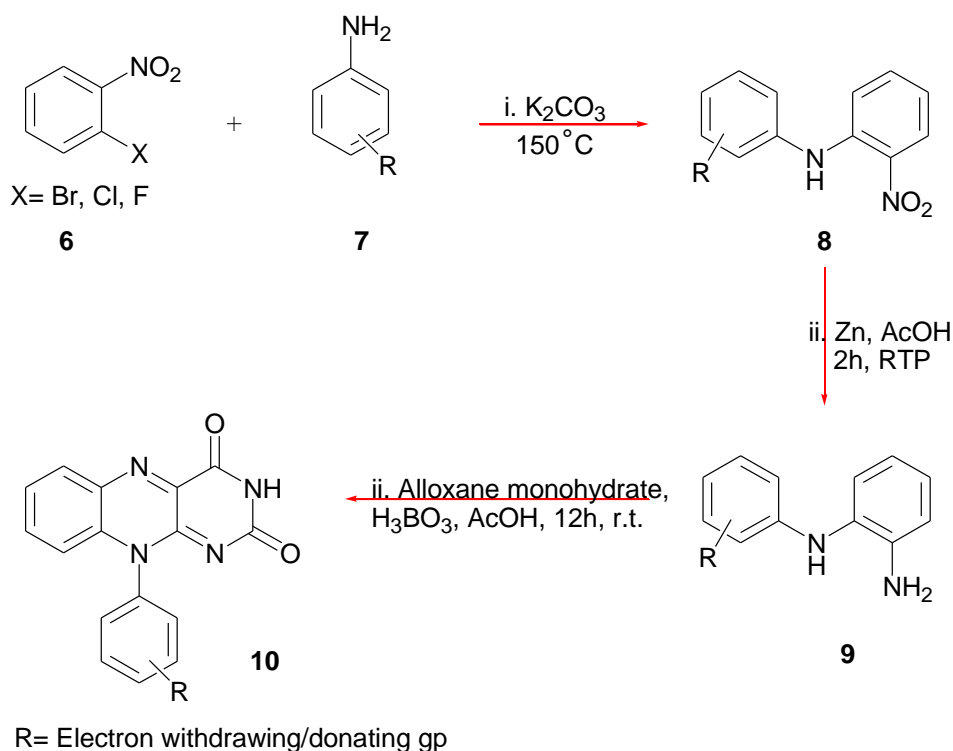
The question arises; how do we prevent this threat to global public health? How can we achieve this in today's environment and make it viable to ensure this catastrophe does not happen?

One of the many approaches to help tackle this ongoing challenge of emergence of resistance, is to develop novel antimicrobials agents. A second approach would be to monitor the

photophysical properties under different wavelengths of light. An additional strategy would be to observe the cytotoxic species generated by these antimicrobial agents in different wavelengths of light. Further approaches to help with this crucial microbial resistance challenge is to substitute the antimicrobial agents onto a polymer support in order to mimic a bandage that is commonly used in hospitals. The antimicrobial activity of these agents both with and without the polymer support could be tested under different wavelength of light.

## 2.6 Discussion on synthesis

Based on the rationale in section 2.1, this challenge was achieved by synthesising a range of novel photodynamic therapeutic dyes. The synthetic portion of this research demonstrates the development of experimental conditions for the synthesis of isoalloxazines. A library of novel fluorescent chemotherapeutic dyes, are synthesised via a number of routes. Varied methodologies were involved in the overall synthesis. Scheme 33 shows a general synthetic route used as the main pathway to synthesise novel isoalloxazines.



*Scheme 33: Pathway for flavin synthesis*

A halogenated nitrophenyl (**6**) is reacted with a substituted aniline (**7**) via microwave irradiation in the presence of a base ( $\text{K}_2\text{CO}_3$ ) to form a substituted nitrophenyl phenyl aniline (**8**). The nitro moiety is reduced using a reducing agent (zinc powder) under acidic conditions to form aminophenyl phenyl aniline (**9**). This subsequently will be cyclised upon reacting with alloxane monohydrate and boric acid in acetic acid, resulting in the formation of a cyclised product, isoalloxazine (**10**). The resulting isoalloxazine would be a synthetic structure that is based on the tricyclic isoalloxazine riboflavin. The mechanism for this is shown in Scheme 38.

For this project a range of flavins based on the structure of riboflavin, were synthesised to test their photophysical ability using blue and white light in order to generate (cytotoxic species) singlet oxygen and/or radicals to incur cell death.

Table 8: Table of synthesised novel isoalloxazines with different electron donating groups (EDG) electron withdrawing groups (EWG) substituted onto the *N*-10 ring.



*o* = ortho, *m* = meta, *p* = para

<i>Compound Code</i>	<i>o</i>	<i>m</i>	<i>p</i>
<b>1c</b>	NH <sub>2</sub>	H	H
<b>2c*</b>	H	NH <sub>2</sub>	H
<b>3c*</b>	H	H	NH <sub>2</sub>
<b>4c</b>	OH	H	H
<b>5c*</b>	H	OH	H
<b>6c</b>	H	H	OH
<b>7c</b>	OMe	H	H
<b>8c</b>	H	OMe	H
<b>9c</b>	H	H	OMe
<b>10c</b>	CH <sub>3</sub>	H	H
<b>11c</b>	H	CH <sub>3</sub>	H
<b>12c</b>	H	H	CH <sub>3</sub>
<b>13c</b>	<i>H</i>	<i>H</i>	<i>H</i>
<b>14c</b>	Cl	H	H
<b>15c</b>	H	Cl	H
<b>16c</b>	H	H	Cl
<b>17c</b>	OTs	H	H
<b>18c</b>	H	OTs	H
<b>19c</b>	H	H	OTs
<b>20c</b>	COOH	H	H
<b>21c*</b>	H	COOH	H
<b>22c</b>	H	H	COOH
<b>23c</b>	NO <sub>2</sub>	H	H
<b>24c*</b>	H	NO <sub>2</sub>	H
<b>25c*</b>	H	H	NO <sub>2</sub>

\* = Denotes compounds unable to synthesise



All the substituents shown in Table 8 below 10-phenylisoalloxazine (**13c**) are in order of weakest electron withdrawing groups going down to the strongest electron withdrawing group. For this research 10-phenylisoalloxazine (**13c**) has no substituents attached, and thus is said to be a neutral compound, which is used as a control. The positional isomer (*o,m,p*) of each substituent was analysed to determine if the Quantitative Structure Activity Relationship (QSARs) affected the toxicity of the overall antimicrobial activity. The antimicrobial activity of these newly synthesised photodynamic therapeutic dyes (antimicrobial agents) was achieved by monitoring their toxicity towards the commonly found bacteria within hospital associated environments, for example Gram negative and positive bacteria (*E.coli* and *S.aureus*).

In 1937 Louis Plack Hammett developed the Hammett equation<sup>329</sup> in order to monitor qualitative observations in a 1935 publication. The Hammett equation (Equation 1) describes a linear free-energy relationship, between a series of reactions with substituted aromatics and the hydrolysis of benzoic esters with the same substituents. This is linked by two parameters; a substituent constant and a reaction constant<sup>330</sup>.

$$\log_{10} \frac{K}{K_0} = \sigma\rho$$

Or *Equation 1*

$$\log_{10} \frac{k}{k_0} = \sigma\rho$$

Where:  $K$  or  $k_0$  = Log of either the reaction rate/equilibrium constant

$\rho$  = reaction constant- proportionality constant between log of  $k$  (or  $K$ ) values and  $\sigma$ .

$\sigma$  = substituent constant - A measure of the total polar effect exerted by substituent X (relative to no substituent) on the reaction centre.

It is important to note that electron donating substituents will have a negative effect on the  $\sigma$  value, whereby electron withdrawing will have a positive effect on the  $\sigma$  value. The values achieved by Hammett substitution constant are dependent on whether the substituents are *meta* or *para* directors.

With Hammett's theory in mind, for this study the isoalloxazines were synthesised with varying electron withdrawing and donating groups (shown in Table 8) in order to investigate the effects caused by the change in electron density on the photophysical properties in the production of the cytotoxic species (singlet oxygen/radicals), with respect to compound **13c** (10-phenylisoalloxazine, substituted with hydrogens). Using Hammett's theory it is hoped that the biological activity is greatly affected by the substituted moieties due to their electronic properties. Thus, compounds ranging from **1c** to **12c** are hypothesised to have an abundant effect on the photophysical properties, consequently an increase in the production of cytotoxic species, resulting in microbial death caused by the effects of substituted electron donating group(s) because of their electronic properties. An additional hypothesis to this is also that the chlorine substituent may too generate a high quantity of singlet oxygen and/or radical yields because of its heavy atom effect<sup>331</sup>. Atoms of relatively high atomic number (e.g. chlorine, bromine, iodine) attached to the chromophore cause enhanced rates of singlet-triplet or triplet-singlet intersystem crossing (ISC)<sup>332</sup>. Thus, the dependence on a long-lived triplet excited state has encouraged synthesis to promote this by the addition of a heavy atom<sup>169</sup>.

Analysis of the results achieved from the chloro substituents due to the heavy atom are of interest to evaluate and compare with alternative substituents in order to determine if resonance or inductive effects also affect the production of the ROS and microbial death.

## 2.7 Results and discussion on synthetic routes of the synthesised isoalloxazine's

One of the major problems continuously arising from synthesising the isoalloxazines, was the purity of the intermediate step of the synthesised compounds. A number of purification techniques were employed to obtain pure compounds. These ranged from gravity based column chromatography, using an array of varying eluting solvents, over alumina based silica gel. Flash column chromatography, was not used as the compounds to be separated were very close one another in respects of their R<sub>f</sub> values. The eluting solvents for column chromatography were used both as pure solvents and as a mixture from polar to non-polar solvents. In addition to this purification technique, crystallization using minimal hot solvent(s), and filtration using activated charcoal dissolved in several selected solvents(s) were also used to identify the best method to solve this reoccurring issue of purity.

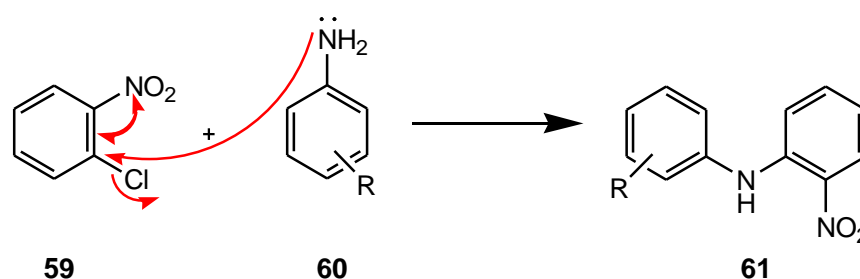
By analysis it was noted that gravity column chromatography achieved the best result in the level of purity of the final compound. However, column chromatography had a detrimental impact on the overall yield, as poor yields were continuously achieved due to the impure material remaining on the silica and largely minute amount of the compound was synthesised. Consequently, on numerous occasions insufficient amount of material was obtained, resulting in a halt to continue research on these compounds. Evidently, either other purification methods were required to be used or conditions with the synthetic steps had to be changed to solve this reoccurring difficulty.

A potential solution to rectify the purity issue was to use a green method. This involved investigating the route of using microwave enhanced synthesis in the hope to obtain purer products by purity, and an increase the yield productivity.

Microwave technology has become very important in synthesis and is considered greatly to be a green methodology. The principles of green chemistry are used in the application of chemical products and processes that reduce or eliminate the use and generation of hazardous substances<sup>333</sup>. Microwave synthesis is advantageous as it is commonly recognised that many chemical reactions require high heating temperatures and/or pressures for reactions to simply proceed more rapidly or for the reaction to actually occur. Thus, microwave technology, employs a different type of heat in comparison to conventional heating. This type of heat, known as microwave dielectric heating has a bulk effect, thus the heating is a consequence of dielectric loss. However, if one or more species in the reaction mixture has a permanent dipole then dielectric heating by irradiation with microwave energy, at 2.45 GHz, will be possible<sup>334</sup>. Hence, solvents such as methanol, DMF, acetonitrile, ethyl acetate and water are commonly employed in microwave enhanced synthesis. Solvents, which contain no dipoles for example hexane, are not able to couple with the energy from the microwave<sup>335</sup>.

The reactions shown in Scheme 34 and Scheme 35, use either 1-chloro or bromo-nitrobenzene (50 mmol) in a stoichiometric ratio of substituted anilines was irradiated for 3 h. at 150° C, under solvent free conditions in the presence of a base (K<sub>2</sub>CO<sub>3</sub>, 70 mmol) under neat conditions. No solvent was used as 1-bromo-2-nitrobenzene melts between 40-42° C. A red precipitate was produced within the reaction vessel upon removal from the microwave reactor; this colour is well documented for these types of compounds. The reaction was allowed to cool, neutralised with c. HCl<sub>(aq)</sub>, extracted with DCM, dried over anhydrous Na<sub>2</sub>SO<sub>4</sub>, and concentrated under vacuum. Although no other side products were present, a very minute amount of impurity was showing in the analysis of thin layer chromatography and <sup>1</sup>H-NMR. For this reason, gravity column chromatography; using silica gel was carried out and all impurities were removed quickly and efficiently. In addition to this, a significant improvement was made not only in the overall yield but also the amount of impurity had reduced to what was seen in the previous wet synthetic routes. The purity of these intermediate isolates were confirmed by <sup>1</sup>H-NMR, <sup>13</sup>C-NMR, and LC-*mz*. For this particular reaction, the structure was confirmed by the appearance of a broad singlet at ~9.5 ppm attributed to the NH moiety, in the <sup>1</sup>H-NMR. A mechanism for this reaction is shown in Scheme 34. The mechanism shows that it is a standard S<sub>N</sub>r reaction, which occurs as a standard electron sync.

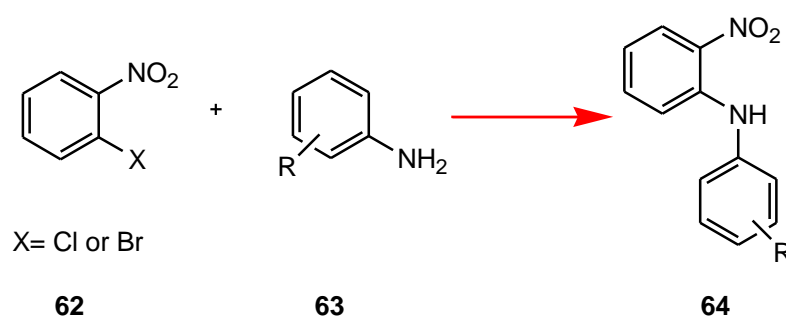
### 2.7.1 Mechanism for a substituted aryl with aniline



*Scheme 34: Substitution mechanism of an aryl aniline*

For the synthetic methodology of isoalloxazines with EWG moiety, the reduction of intermediate compounds (62) was necessary in order to complete cyclisation for the final step to synthesise the substituted isoalloxazine.

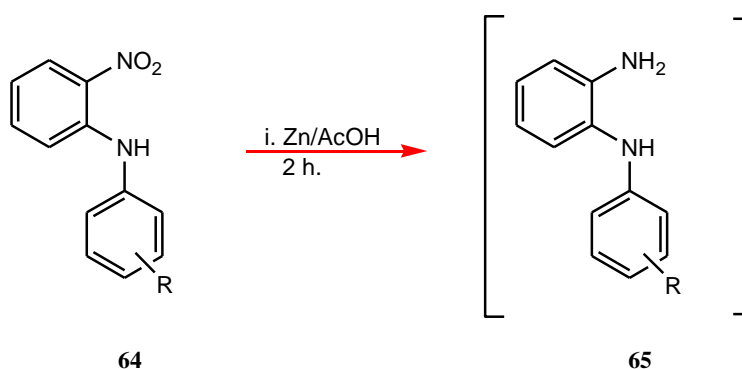
### 2.7.1.1 The synthesis of substituted 2-nitrodiphenylamine intermediates



*Scheme 35: Substitution of 2-nitrodiphenylamines*

The pathway shown in Scheme 35 utilises a range of substituted anilines (**63**) by setting to reflux for a period of 6 h with varied solvents, (e.g. methanol, water). This type of reaction has provided established research groups with somewhat difficulties in obtaining good yields, consequently numerous methodologies have been put in place to overcome this issue. Such examples involve using solvent free conditions<sup>336</sup> refluxing in DMF<sup>337</sup> or methanol<sup>338</sup> and even altering the base in the reaction e.g. using DBU, and tBuO-K. Although each method has its advantages, huge limitations were noted such as purity, cost and/or yield. Thus, the decision made was to carry out this reaction in amyl alcohol in the presence of potassium carbonate and copper powder. Although, isolation of the product was not achieved, it was apparent that higher yields of the final isoalloxazines were produced.

### 2.7.1.2 Reduction of the substituted 2-nitrodiphenylamine intermediates



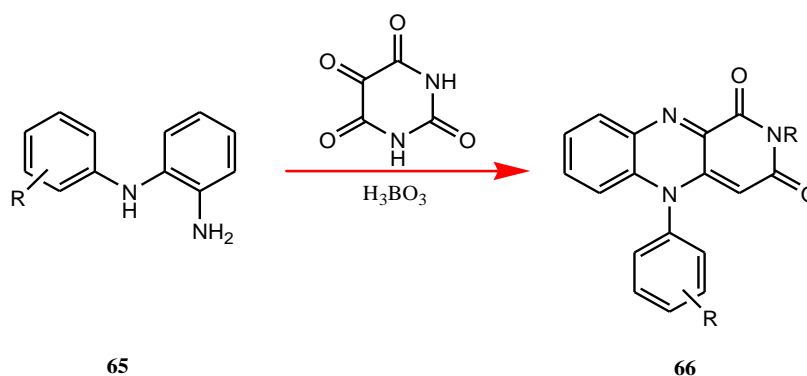
*Scheme 36: Reduction step of substituted 2-nitrodiphenylamine intermediates*

Reduction of the substituted 2-nitrodiphenylamine intermediates (**64**) is required to form the free 1° amine, Scheme 36.

The reaction takes place under acidic conditions using glacial acetic acid in the presence of a reducing agent, zinc dust. The reaction mixture was cooled in ice, (due to the exothermic nature of the reaction) followed by the gradual addition of zinc dust. Upon completion, the reaction was removed from the ice bath and allowed to stir at room temperature for 2 h. A colour change was observed from dark brown to light greenish brown over a two hour period. It was also noted that

the compound had fully dissolved in the acidic solution after the two hour reaction. The reaction was filtered over celite™ to remove the zinc. The product was isolated and analysed using mass spectrometry (electrospray ionisation-ESI) to observe a loss in the mass of 30 g/mol<sup>-1</sup>, a change in the molecular ion (*m/z*) from the NO<sub>2</sub> to 184 NH<sub>2</sub>.

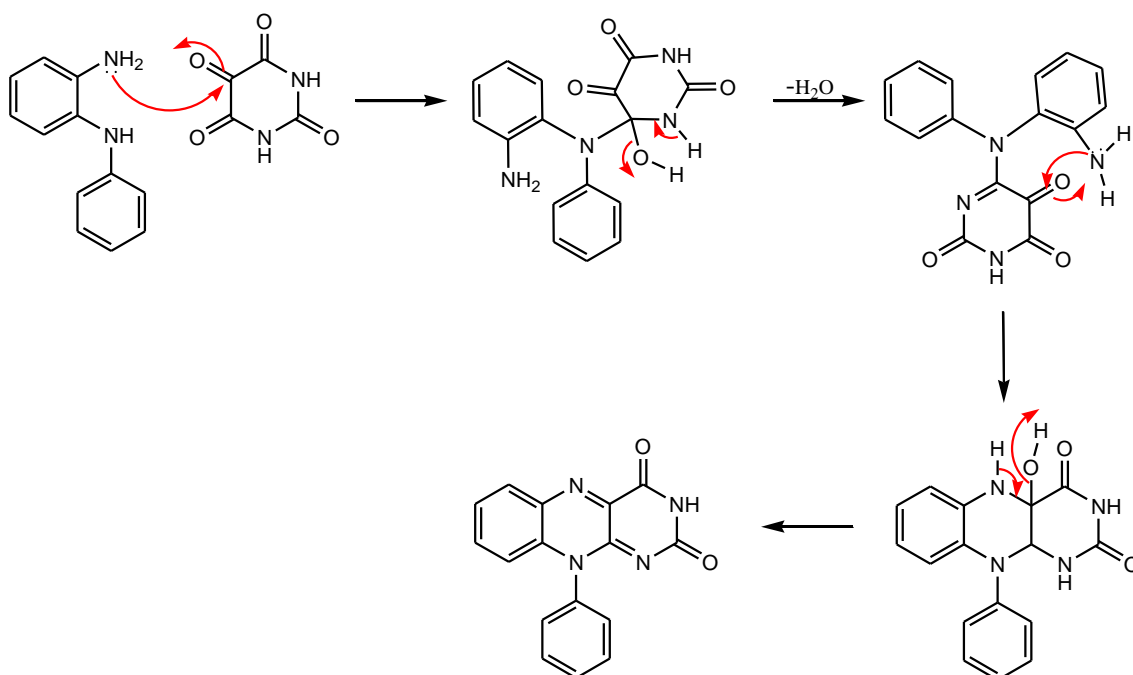
### 2.7.1.3 Formation of the Flavin



*Scheme 37: Flavin formation of N-substituted amino aniline to N-substituted isoalloxazine*

Upon generating the free primary amine (**65**), a stoichiometric amount of alloxan monohydrate and boric acid was added to undergo a cyclocondensation reaction to form the flavin (**66**). The reaction was monitored using TLC, with the silica plate being illuminated at 365 nm to observe the formation of the flavin. Due to the enhanced conjugation of the product, a large amount of fluorescence was observed, enabling the reaction completion to be monitored easily and in some cases purification by column chromatography was required even after the compound was synthesised. However, on numerous occasions <sup>1</sup>H-NMR showed a pure compound was synthesised. Scheme 38 shows the proposed mechanism for the synthesis of isoalloxazine's.

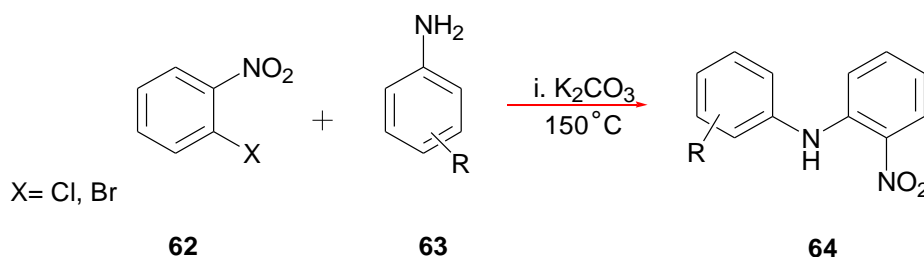
### 2.7.2 Proposed mechanism for isoalloxazine's.



*Scheme 38: Mechanism of isoalloxazine*

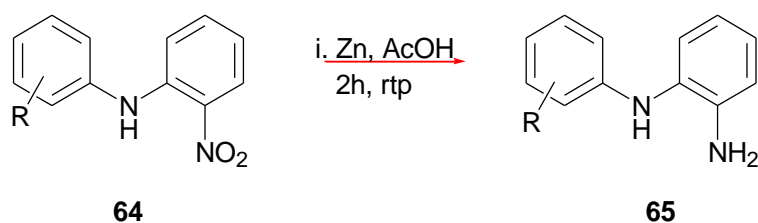
## 2.8 Discussion of the synthesised isoalloxazines

The synthesis of isoalloxazine derivatives was straight forward after fine tuning the conditions. No harsh methods were required for these compounds. The flavin derivatives were prepared in three stages using a substituted aniline as its starting material, Scheme 39.



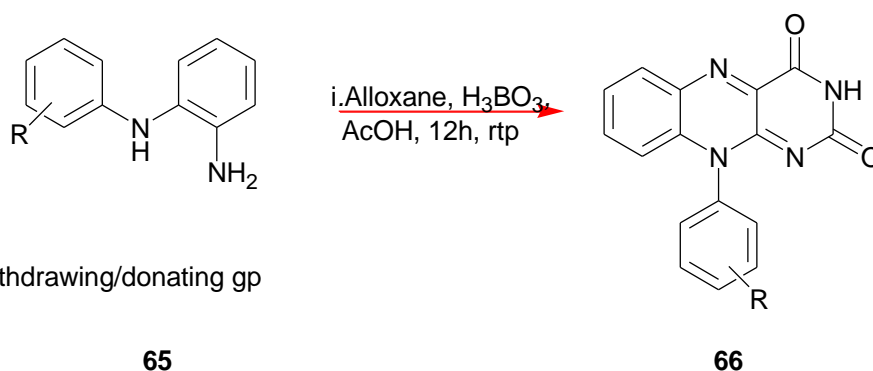
*Scheme 39: Substitution reaction of aniline*

The substituted (2-nitrophenyl) phenyl aniline (**64**) from Scheme 39 was reduced using zinc powder in a ten-fold excess with acetic acid as its solvent, Scheme 40, resulting in the successive formation of the substituted (2-aminophenyl) phenyl aniline amino aniline (**65**). The reduction step required the temperature to be kept below 0 °C to control the exothermic reaction.



*Scheme 40: Reduction of nitro aniline to amino aniline*

The solution of substituted amino aniline (**65**) was subsequently cyclised using alloxan monohydrate and boric acid in acetic acid, resulting in the formation of a yellow precipitate, isoalloxazine (**66**). This yellow powder was isolated and washed well with cold hexane.

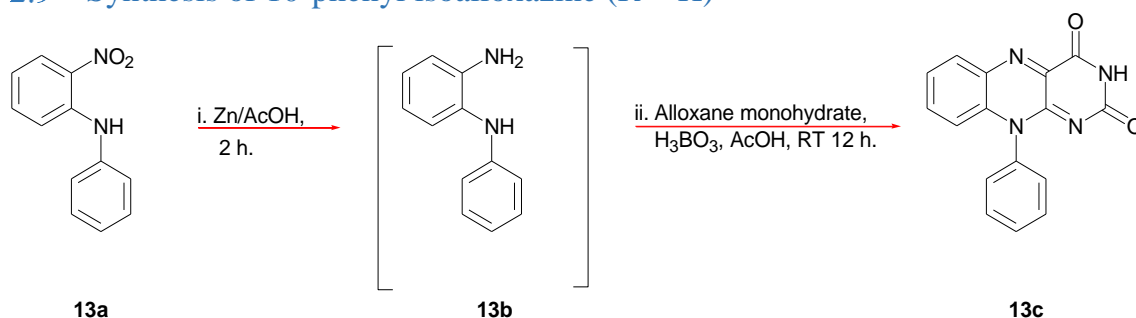


*Scheme 41: Cyclisation of N-substituted amino aniline*

The analogues for the substituted anilines were purified by column chromatography, mainly eluting with ethyl acetate



2.9 Synthesis of 10-phenyl isoalloxazine (R = H)



Scheme 42: Synthetic route of 10-phenyl isoalloxazine

Table 9: Percentage yield for 10-phenyl isoalloxazine

Compound	<i>o</i> (R <sub>1</sub> )	<i>m</i> (R <sub>2</sub> )	<i>p</i> (R <sub>3</sub> )	Yield (%)
<b>13c</b>	H	H	H	98

10-Phenylisoalloxazine (**13c**) was seen as an important isoalloxazine to prepare, due to the lack of functional substituents on the phenyl ring in the *N*-10 position. This compound can therefore be considered electronically as a “neutral/standard compound” when making comparisons against singlet oxygen yields generated by other isoalloxazine’s containing both electron donating and withdrawing substituents. Compound **13c** was synthesised using a standard literature method with minor alterations<sup>336</sup> (e.g. extended reaction time between **13b** and alloxan) and the synthetic route is shown in Scheme 42. The crude product 2-aminodiphenylamine (**13b**) was impregnated onto silica and was purified by column chromatography using ethyl acetate (EtOAc) as eluent. Subsequently, compound **13b** was dissolved in glacial acetic acid and with constant stirring, alloxan monohydrate and boric acid (both in 1;1.2 mole excess) was added to the acidic solution. A yellow solid precipitated after 12 hours, which was isolated at the pump, to yield 10-phenylisoalloxazine, **13c** as a bright yellow powder Figure 44 shows the <sup>1</sup>H NMR for **13c**. The broad singlet at 11.45 ppm is attributed to the acidic CO(NH)CO amide with an integration of 1H. The aromatic region (9 – 6 ppm) also shows the correct number of protons for this molecule. To expand, three broad doublets are seen at 8.19 ppm (1H), 7.44 ppm (2H) and 6.75 ppm (1H) respectively. A broad multiplet is observed between 7.77–7.59 ppm, indicating non-distinguishable coupling from the aromatic protons from the *meta* and *para* positions on the phenyl ring, attached to the nitrogen on the 10<sup>th</sup> position, in addition to the two aromatic protons in the 7<sup>th</sup> and 8<sup>th</sup> position of the main tricyclic isoalloxazine structure. This is confirmed by the COSY NMR shown in Figure 46 (and illustrated on the structure as well as a connecting square drawn in Figure 46). Two signals are also seen up-field at 3.30 ppm and 2.50 ppm respectively;

this can be attributed to a water saturation in the deuterated solvent (3.30 ppm) and d<sub>6</sub>-DMSO solvent residue signal (2.50 ppm).

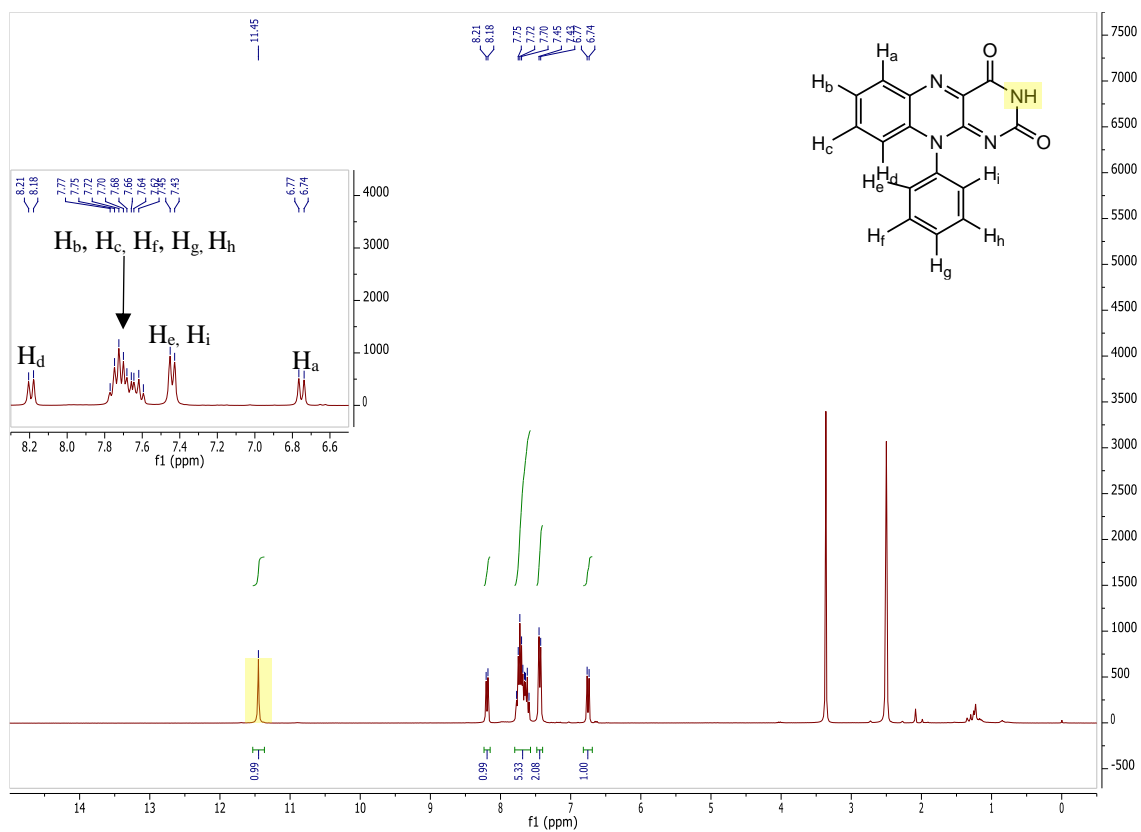


Figure 45: <sup>1</sup>H-NMR for 10-phenyl isoalloxazine

This molecule was also analysed by  $^{13}\text{C}$ , HMQC, and  $^{135}\text{DEPT}$  NMR. The compound also gave the correct molecular formulae by HR-MS (ESI)  $m/z$  calcd for  $[\text{C}_{16}\text{H}_{10}\text{N}_4\text{O}_2]^+$  290.280  $\text{g mol}^{-1}$ , and found 291.087  $\text{g mol}^{-1}$  as  $[\text{M}^+]$ .<sup>1</sup>

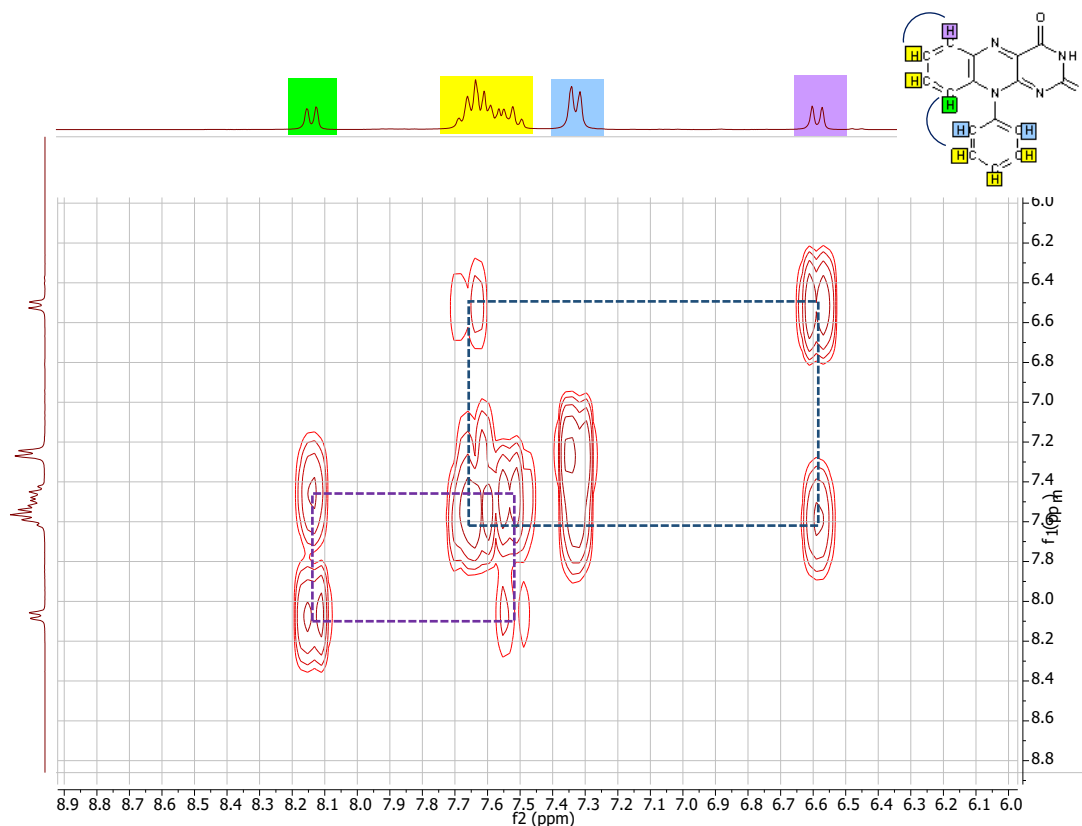


Figure 46:  $^1\text{H}$ - $^1\text{H}$  COSY NMR for 10-phenyl isoalloxazine

An IR spectrum was also taken for this molecule to identify which functional groups were present in order to confirm the structure of this compound, (**13c**).

The IR spectrum shown in Figure 47, revealed the main functional groups corresponding to **13c**. The peak present at  $\nu$ : 3068.72  $\text{cm}^{-1}$  indicates the presence of C-H groups. The band at 2822  $\text{cm}^{-1}$  specifies the presence of C-H aromatic bonds. The sharp peaks at 1689  $\text{cm}^{-1}$  and 1640  $\text{cm}^{-1}$  are attributed to the carbonyl (C=O) group belonging to the amide moiety. The peaks seen at 1540  $\text{cm}^{-1}$ , 1490  $\text{cm}^{-1}$ , and 1437  $\text{cm}^{-1}$  correlate to the aromatic C=C bonds from the aromatic rings. The sharp peak present at positions 1288  $\text{cm}^{-1}$  and 1207  $\text{cm}^{-1}$  are attributed to the C-N bonds. Lastly, the C-H bonds from the aromatic rings are confirmed by the peaks in the fingerprint region; 915  $\text{cm}^{-1}$ , 806  $\text{cm}^{-1}$ , 767  $\text{cm}^{-1}$ , 713  $\text{cm}^{-1}$ , 691  $\text{cm}^{-1}$ .

<sup>1</sup> HR-MS was obtained from the EPSRC National Mass Spectrometry Centre in Swansea, Wales.

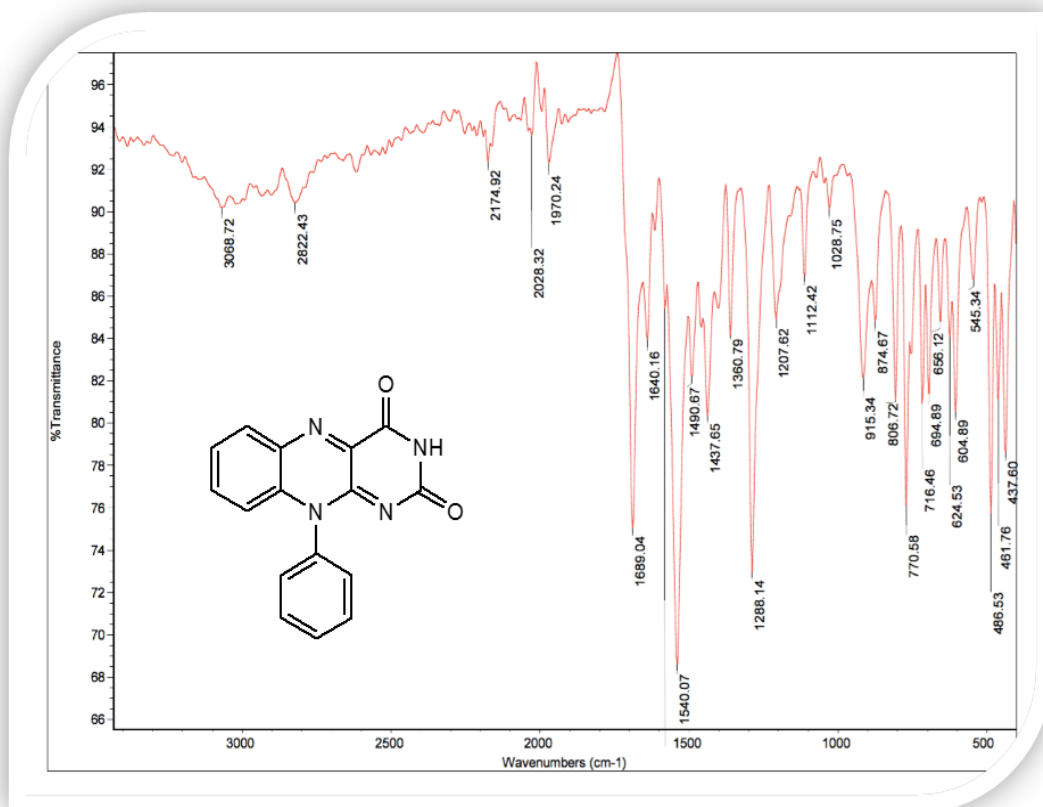
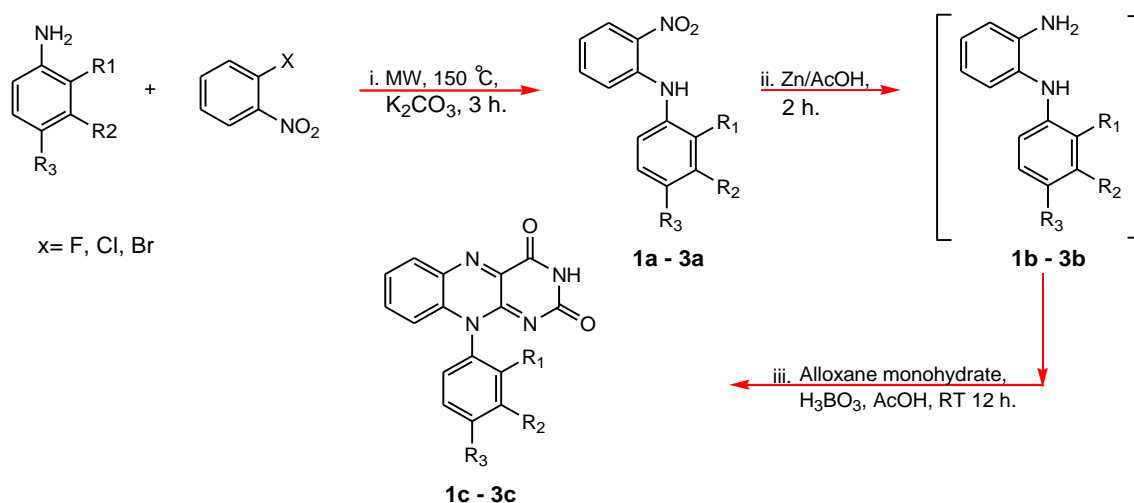


Figure 47: IR spectrum for 10-phenyl isoalloxazine

## 2.10 Amino derivatives of 10-phenylisoalloxazine (R = NH<sub>2</sub>)



Scheme 43: Synthetic route of 10-(*N*-aminophenyl) isoalloxazines

Table 10: Percentage yield for 10-(*N*-aminophenyl) isoalloxazine derivatives

Compound	<i>o</i> (R <sub>1</sub> )	<i>m</i> (R <sub>2</sub> )	<i>p</i> (R <sub>3</sub> )	Yield (%)
<b>1a</b>	NH <sub>2</sub>	H	H	46
<b>2a</b>	H	NH <sub>2</sub>	H	N/A <sup>2</sup>
<b>3a</b>	H	H	NH <sub>2</sub>	N/A
<b>1c</b>	NH <sub>2</sub>	H	H	69
<b>2c</b>	H	NH <sub>2</sub>	H	N/A <sup>2</sup>
<b>3c</b>	H	H	NH <sub>2</sub>	

\*, singlet oxygen and radical yields were not measured for all *N*-substituted phenyl 2-nitroanilines throughout the project.

The synthesis of the amino derivatives of 10-phenyl isoalloxazine is shown in Scheme 43. It should be noted that only the *o*-isomer could be synthesised due to issues in the synthesis of the *m* and *p* isomers. Both these isomers were unsuccessful in their synthesis. Each attempt in synthesis showed large quantities of starting material which was identified frequently in TLC and <sup>1</sup>H-NMR even though reactions times and conditions were elongated and changed. This potentially indicates solubility issues with the starting materials. The lack of success in synthesis of the *m* and *p* isomers could also be a result of having two competing nucleophilic sites as two amines present in the starting material that are able to react, resulting in the lack of formation of these compounds.

<sup>2</sup> Synthesis unsuccessful.

Lone pairs associated with the nitrogen atom in anilines are conjugated strongly with the  $\pi$  electron cloud from the benzene ring. Thus, the effect of the electron withdrawing substituents is a net reduction in the electron density at the nitrogen atom.

## 2.11 Synthesis of the 2, 3, and 4 isomers of *N*-(aminophenyl)-2-nitroaniline (**1a–3a**)

The synthesis of each of the *N*-(aminophenyl)-2-nitroaniline derivatives (**1a–3a**) was synthesised using microwave enhanced synthesis. The reaction proceeded by adding *N*-phenylenediamine derivative and 1-fluoro-2-nitrobenzene in a microwave reaction vessel with  $K_2CO_3$ . The reaction proceeded for 3 hours at 150 °C at a pressure of 200 psi. This reaction was monitored at regular intervals ( $t = 30, 60, 120$  and 180 minutes) throughout heating. Compound **1a** eluted first and was observed as an orange compound. Upon completion, the reaction was poured over a small amount of ice and the aqueous solution was adjusted to pH=6 to neutralise the  $K_2CO_3$  and this was followed by an extraction into chloroform to isolate the crude product which was subsequently concentrated under reduced pressure, resulting in a red solid. The red solid was purified by flash column chromatography over silica gel eluting with PE:  $CHCl_3$  (1:1) to afford the pure product, *N*-(2-nitrophenyl)-2-nitroaniline (**1a**), Figure 48, as dark red crystals.

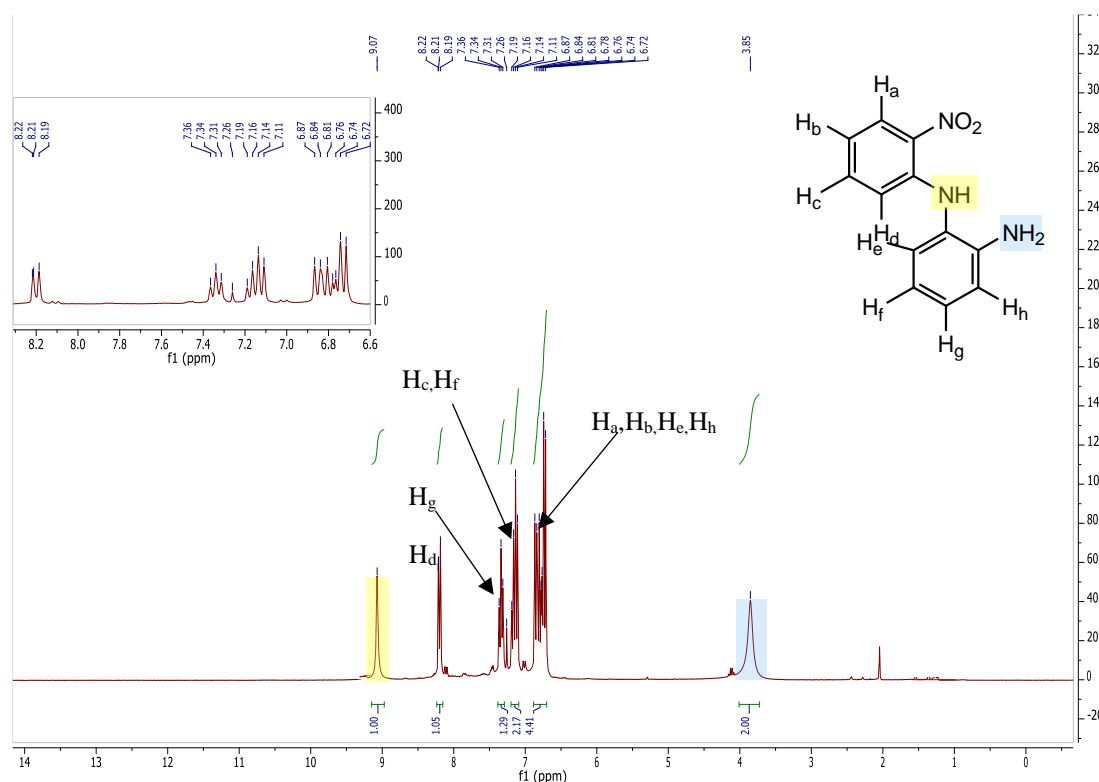


Figure 48:  $^1H$ -NMR for *N*-(2-nitrophenyl)-2-nitroaniline

Figure 48 shows  $^1H$ -NMR for **1a**. The singlet peak shown at 9.07 ppm corresponds to secondary amine (NH) with an integration of 1H. The correct integration of 8H, on peaks showing at 8.22ppm – 6.72 ppm can be seen in the aromatic region. A broad singlet peak at 3.85 ppm with

an integration of 2 is attributed to the primary amine NH<sub>2</sub>. This confirms the correct compound was synthesised.

The synthesis of compounds 10-(3-aminophenyl)-2-nitroaniline (**2a**) and 10-(4-aminophenyl)-2-nitroaniline (**3a**) were attempted using the method described above for compound **1a**. Upon monitoring the reaction by TLC and <sup>1</sup>H-NMR, the presence of both starting materials; *m*-phenylenediamine and 2-fluoronitrobenzene were seen. As this synthesis did not prove successful, alterations to the synthetic procedure was made by changing the ratios of the starting materials. The stoichiometric ratio of reagents *m*-phenylenediamine to 1-fluoro-2-nitrobenzene ratio was changed to 0.5:1 respectively. Again, upon analysis of TLC and <sup>1</sup>H-NMR, the results showed the presence of both starting materials with additional impurities. The reaction time was also elongated from 3 to 6 hours since the starting materials were still present in TLC and <sup>1</sup>H-NMR. Despite lengthening the reaction times combined with the changes of the stoichiometric ratios of starting materials, using standard spectroscopic techniques no change of the reaction was observed. On further testing, the reaction the temperature was increased to 200 °C for a further 3 hours. Analysis of the spectroscopic data for this reaction, the compound was unsuccessful using microwave enhanced synthesis. Therefore another method for the synthesis of compound **2a** had to be pursued.

Compound **2a** was subsequently attempted to be synthesised in a round bottom flask. The starting materials used in this reaction were *m*-phenylenediamine, 1-fluoro-2-nitrobenzene, and K<sub>2</sub>CO<sub>3</sub>. This was heated to 150 °C for 5 hours. The reaction was monitored at 60 minute intervals using silica TLC plates, eluting with a mixture of 40-60: P.E: CH<sub>3</sub>Cl (1:1). No change was observed during the reaction, and therefore concluded unsuccessful synthesis of this compound, (**2a**). As a result of this, 10-(3-aminophenyl) isoalloxazine (**2c**) was not possible to synthesise.

Compound **3a** was attempted to be accomplished using *o*-phenylenediamine and 1-fluoro-4-nitrobenzene respectively, via microwave enhanced synthesis. Compound **3a** was unsuccessful in synthesis as analysis of the standard spectroscopic techniques showed the presence of a substantial amount of impurity and a negligible amount of product formed. The purification of the crude material, **3a**, was proving to be incredibly difficult. To obtain a pure compound the crude material was purified using a number of purification techniques for example; crystallisation using a range of solvents, column chromatography eluting with a variety of solvent mixtures e.g: 40-60 P.E: CH<sub>3</sub>Cl (1:1), and the impure compound was also boiled in activated charcoal. Regrettably, a pure product of compound **3a** was not isolated successfully as it was impossible to remove all the impurities and therefore the reaction could not proceed to the final step.

### 2.11.1 Synthesis of 10-(2-aminophenyl) isoalloxazine (**1c**)

The synthesis of 10-(2-aminophenyl) isoalloxazine (**1c**) was accomplished using the same synthetic route as highlighted in section 2.11. 2-Aminophenyl isoalloxazine, **1c** precipitated from the acidic reaction mixture and was isolated at the pump as a bright yellow powder with the yield 69% as shown in Figure 49. The spectroscopic data obtained clearly shows the correct compound.

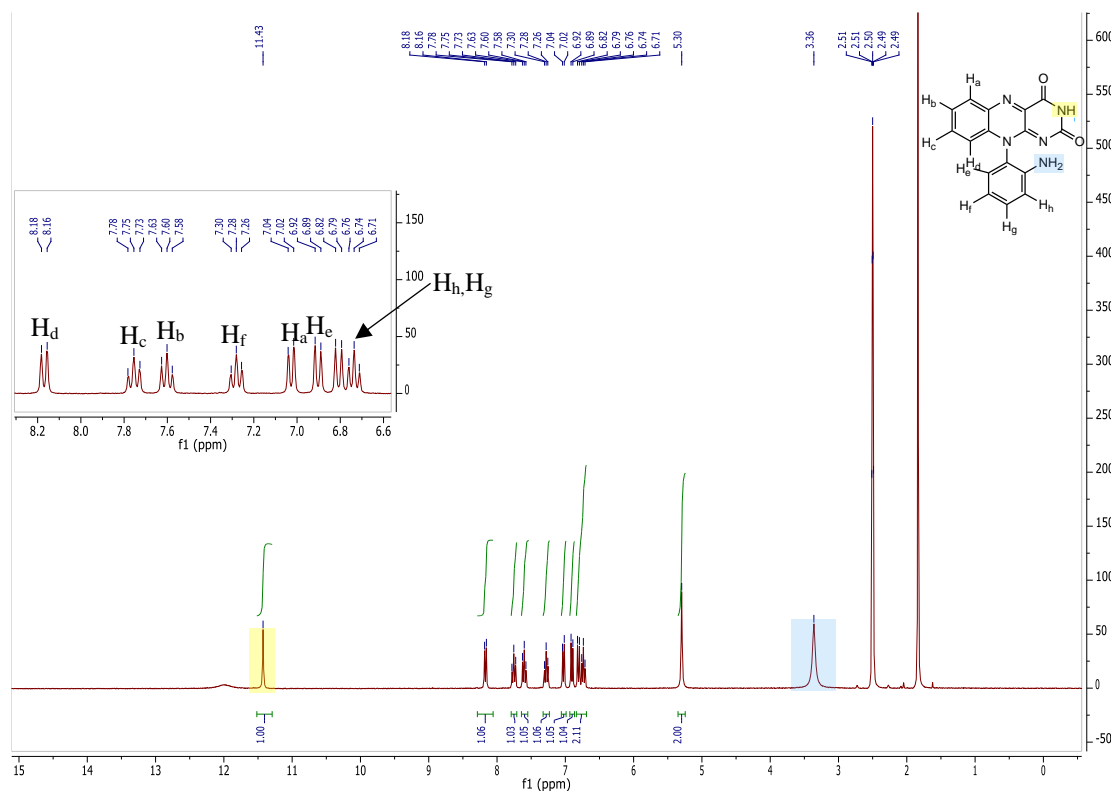
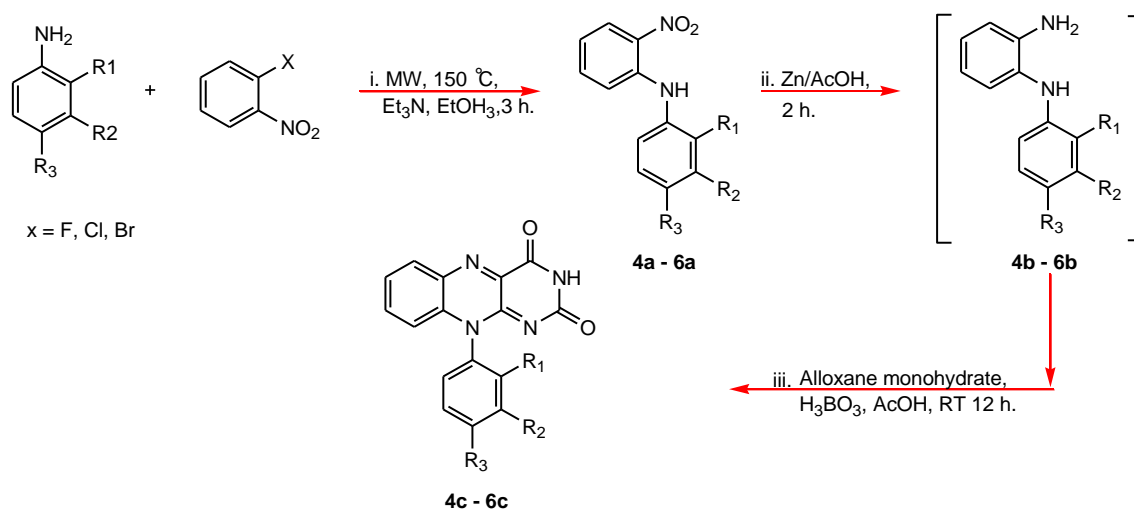


Figure 49:  $^1\text{H-NMR}$  for 10-2-(aminophenyl) isoalloxazine

$^1\text{H-NMR}$  for **1c** is shown in Figure 49. The singlet peak shown at 11.43 ppm is attributed to the acidic  $\text{CO}(\text{NH})\text{CO}$  amide with an integration of 1H. The aromatic region (9 – 6 ppm) also shows the correct number of protons (8H) for this molecule. To expand, one doublet and three triplets are seen at 8.18 ppm (1H), 7.75 ppm (1H) 7.60 ppm (1H) and 7.28 ppm (1H) respectively are correctly attributed to the aromatic protons with an integration of one proton each. A broad singlet peak seen at 5.30 ppm with an integration of 2H, is attributed to the primary amine  $\text{NH}_2$ . This confirms the correct compound was synthesised.



## 2.12 Hydroxy derivatives of 10-phenylisoalloxazine (R = OH)



*Scheme 44: Synthetic route of 10-(N-hydroxyphenyl) isoalloxazines*

Table 11: Percentage yields for *N*-(hydroxyphenyl)-2-nitroanilines and 10-(*N*-hydroxyphenyl) isoalloxazine derivatives

Compound	<i>o</i> (R <sub>1</sub> )	<i>m</i> (R <sub>2</sub> )	<i>p</i> (R <sub>3</sub> )	Yield (%)
<b>4a</b>	OH	H	H	39
<b>5a</b>	H	OH	H	28
<b>6a</b>	H	H	OH	43
<b>4c</b>	OH	H	H	63
<b>5c</b>	H	OH	H	N/A <sup>3</sup>
<b>6c</b>	H	H	OH	59

Due to issues in the synthesis the *meta* isomer (**5c**) could not be synthesised

Two methods were used to prepare the materials:

1. Demethylation using boron tribromide, and
2. Synthesis from the starting amine via microwave enhanced synthesis.

## 2.13 Synthesis of the 2, 3, and 4 isomers of *N*-(hydroxyphenyl)-2-nitroaniline (**4a-6a**)

Synthesis of the substituted hydroxyphenyl isoalloxazine derivatives was initially attempted via demethylation of the methoxy moiety to an OH. Although this pathway achieved the desired compound (**4c**), an extremely poor yield was obtained. Consequently, it was decided to synthesise each of these compounds (**4a-6a**) using microwave enhanced synthesis as shown in Scheme 44.

<sup>3</sup> Intermediate was synthesised however cyclising with alloxan monohydrate proved unsuccessful.

To expand, *N*-(2-hydroxyphenyl)-2-nitroaniline was synthesised from the starting amine 2-aminophenol and 1-fluoro-2-nitrobenzene in ethanol and trimethylamine. The change in base ( $K_2CO_3$  to  $Et_3N$ ) is attributed to side reactions that are possible with the free phenol, particularly as the pKa of phenol is 10.0, thus being acidic enough to react with  $K_2CO_3$ . The pure products were isolated using column chromatography over silica gel eluting with EtOAc: PE (1:2) to afford a red solid. Upon analysis via  $^1H$  NMR, slight impurities were present therefore these compounds were recrystallized from hot toluene and dried in *vacuo* to afford the pure products, in yields (**4c** = 26.79% and **6c** = 8.11%) shown in Table 11 as dark red crystals.

### 2.13.1 Synthesis of 10-(*N*-hydroxyphenyl) isoalloxazines (**4c-6c**)

As highlighted above (below Table 11) compound **4c** was synthesised via a demethylation of compound **7a** in a solution of dry DCM with a slow addition of boron tribromide ( $BBr_3$ ). The temperature of the reaction was initially kept at  $-78$  °C using dry ice and acetone and kept to stir for 4 hours, under argon gas at r.t.

Although this reaction was successful, the yield obtained was only 21% after purification. The reaction was monitored via TLC and  $^1H$ -NMR confirmed the demethylation reaction had taken place by the disappearance of the  $OCH_3$  moiety at 3.71 ppm and the appearance of a broad phenol peak at 9.95 ppm as shown in Figure 50.

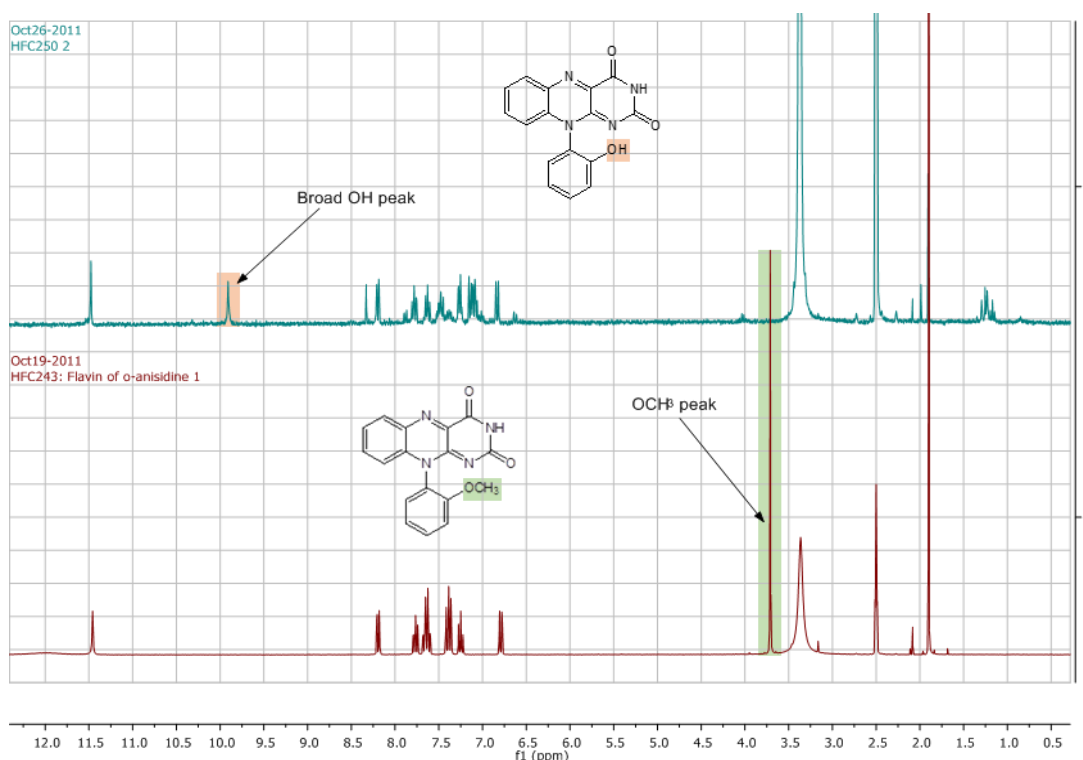


Figure 50:  $^1H$ -NMR of 2-hydroxyphenyl and 2-methoxyphenyl isoalloxazines.

Upon successful synthesis of each of the compounds of this series (**4a-6a**) via microwave enhanced synthesis, the reduction of these compounds was achieved using the reducing agent zinc powder

in glacial acetic acid as shown in Scheme 44 resulting in the intermediate compounds (**4b** and **6b**) which were not isolated. Subsequently, these compounds were reacted with alloxan monohydrate and boric acid in glacial acetic acid to afford the pure compounds. As before the target compounds **4c** and **6c** precipitated out of the reaction mixture and isolated by filtration at the pump and were washed well with cold hexane to isolate the product in the yields (**4c** = 63% and **6c** = 59%) shown in Table 11. It was encouraging to observe that both of these compounds were able to generate singlet oxygen and radicals. Compound **4c** yielded singlet oxygen in 26.79% and a poor radical yield of 2.11% was generated. In comparison to this, compound **6c** generated extremely poor yields of both singlet oxygen and radical (8.11% and 0.08%).

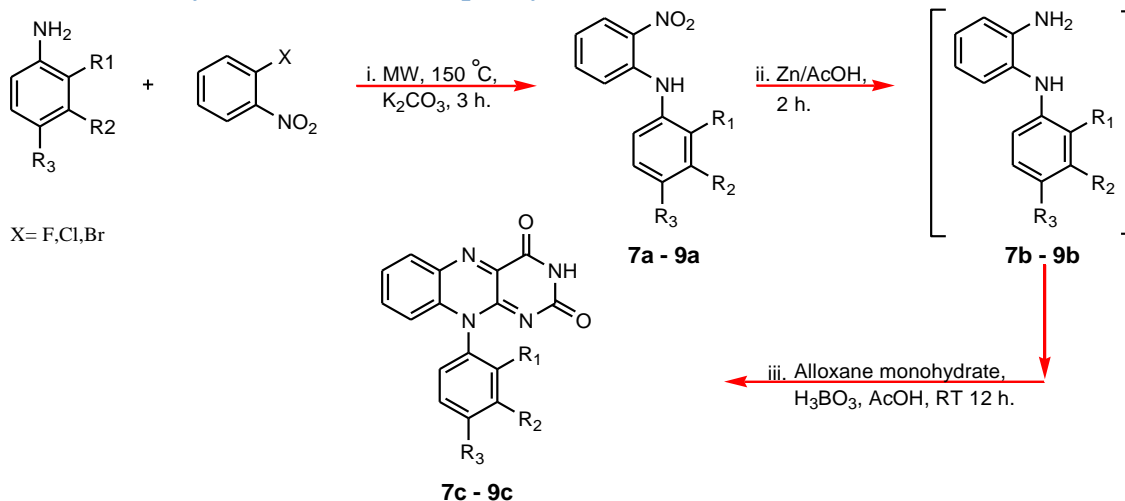
### 2.13.2 Attempted synthesis of 10-(3-hydroxyphenyl) isoalloxazine (**5c**)

10-(3-Hydroxyphenyl) isoalloxazine (**5c**) was not successfully synthesised even though all other analogues of this series were accomplished. The intermediate, **5a** was effectively purified and isolated in a 28% yield using microwave enhanced synthesis. The amine (**5b**), from the subsequent reduction reaction proved problematic, often resulting in mixtures of impurities and/or lack of a reduction occurring. In order to investigate this further, the reduction time was varied from 30 minutes to 12 hours and this again did not yield the free amine. Each reduction attempted was monitored by TLC, <sup>1</sup>H NMR and LCMS and on all occasions the analytical data showed only the starting material (**5a**) present. As a result of no success in the reduction of **5a** to form compound **5b**, this isoalloxazine derivative could not be synthesised.

Phenol derivatives are highly susceptible to electrophilic aromatic substitution. Lone pair electrons from the oxygen are involved in resonance with aromatic systems, thus making the phenol ring strongly activated. Hydroxyl moiety have electron withdrawing effects by induction, and also have very strong mesomeric electron donating effects, thus, the overall effect on aromatic system is electron donating.

By analysis of the yields obtained for the two isomers of the hydroxyphenyl isoalloxazines, it can clearly be seen the *ortho* and *para* positions of the benzene ring with hydroxyl substituents are the most activated positions on the ring. The presence of the hydroxyl group at the *para* position reacted better than the hydroxyl on the *ortho* position, and this is evident from the yields obtained.

## 2.14 Methoxy derivatives of 10-phenylisoalloxazine (R = OCH<sub>3</sub>)



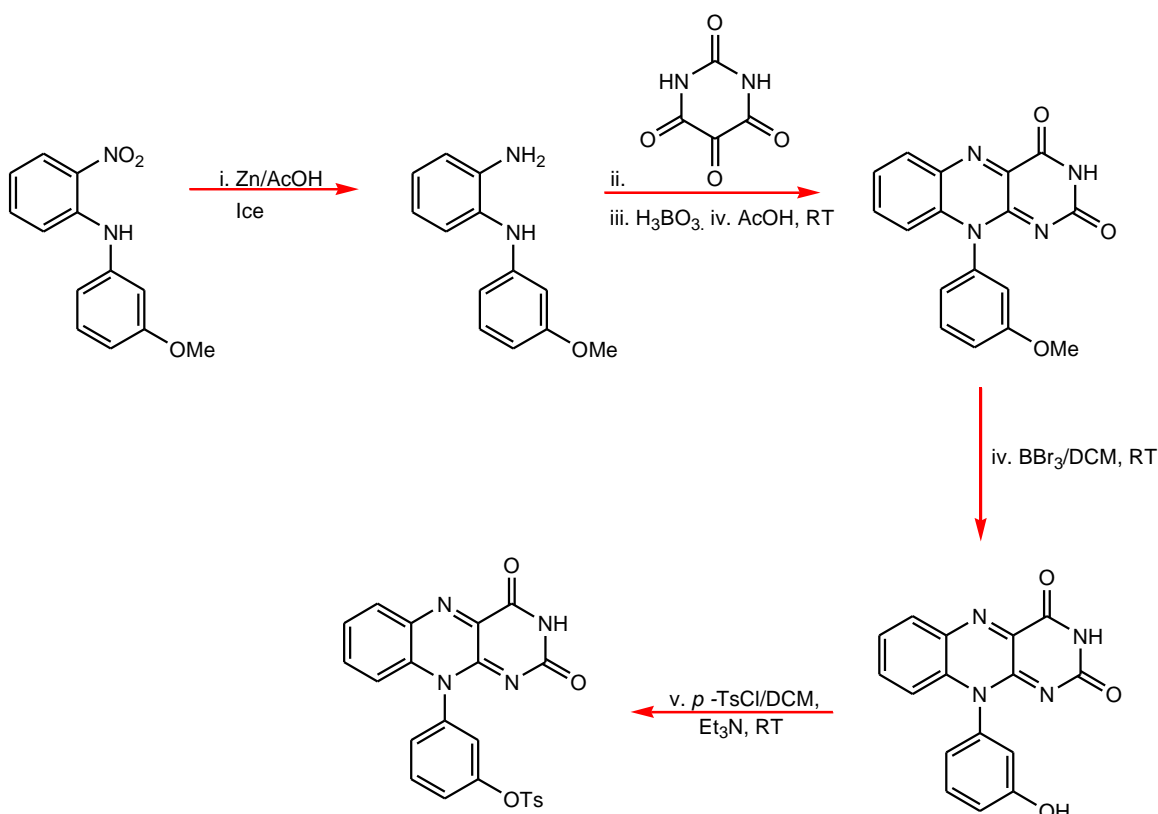
Scheme 45: Synthetic route of 10-(*N*-methoxyphenyl) isoalloxazines

Table 12: Percentage yields for *N*-(methoxyphenyl)-2-nitroanilines and 10-(*N*-methoxyphenyl) isoalloxazine derivatives

Compound	<i>o</i> (R <sub>1</sub> )	<i>m</i> (R <sub>2</sub> )	<i>p</i> (R <sub>3</sub> )	Yield (%)
7a	OMe	H	H	38
8a	H	OMe	H	20
9a	H	H	OMe	50
7c	OMe	H	H	53
8c	H	OMe	H	96
9c	H	H	OMe	82

At this junction it is important to discuss structural variations in respect to the isoalloxazines that were prepared. Table 8, shows each of the different electronic substituents that were added to 10-phenylisoalloxazine.

The versatility of *N*-methoxyphenyl derivatives is of immense importance as the OMe provides an electron donating substituent to the phenyl ring whilst also providing another synthetic route to additional isoalloxazine derivatives (i.e. OH, OTs) as shown in Scheme 46 with the synthesis of the *meta* derivatives.



Scheme 46: Synthetic route for additional derivatives of isoalloxazine from OMe moiety

### 2.14.1 Synthesis of 2, 3, and 4 isomers of *N*-(methoxyphenyl)-2-nitroaniline (**7a-9a**)

The synthesis of **7a-9a** was accomplished using the methodology discussed in section 2.11. Different isomers of anisidine and 2-nitro-haloaromatic were used as the starting materials in order to prepare each of the substituted (*N*-methoxyphenyl)-2-nitroanilines. To expand, the intermediates were prepared using the base; potassium carbonate in a 10-fold excess, whilst the starting materials were used in equal stoichiometric ratios (1:1).

The reaction was monitored throughout heating using TLC with silica plates and eluting with a mixture of 40-60: PE:EtOAc (1:2). Upon neutralizing the reaction mixture to pH=6 with c. HCl the crude compounds were each filtered at the pump, purified by flash column chromatography over silica gel eluting with PE: EtOAc (1:2) to afford the pure products **7a-9a** in the yields shown in Table 12.

### 2.14.2 Synthesis of 10-(*N*-methoxyphenyl) isoalloxazine (**7c-9c**)

The synthetic route for 10-(*N*-methoxyphenyl) isoalloxazines (**7c-9c**) was accomplished by the route depicted in Scheme 45, with the yields shown in Table 12. The <sup>1</sup>H-NMR for 10-(2-methoxyphenyl) isoalloxazine (**7c**) is shown in Figure 51. The aromatic region (9 – 6 ppm) also shows the correct number of protons for this molecule. To expand, one doublet and one triplet

can be seen at 8.19 ppm (1H), and 7.77 ppm (1H) respectively, which are correctly attributed to the aromatic protons with an integration of one proton each. Two multiplet's seen at 7.70-7.58 ppm (2H) and 7.44 – 7.34 ppm (2H), correspond correctly to the aromatic protons with an integration of two protons each. Two sets of signals with a splitting of a triplet and a doublet at 7.25 ppm (1H) and 6.79 ppm (1H) respectively can be seen with an integration of one proton each and are attributed to the aromatic protons. A sharp singlet peak can be seen at 3.71 ppm, which is attributed to the protons off the methoxy moiety, with an integration of 3H, confirming the synthesis of the correct compound.

Figure 51 also shows the <sup>1</sup>H-NMR for 10-(4-methoxyphenyl) isoalloxazine with the correct number of protons and splitting pattern for the *para* isomer of the methoxy moiety on the phenyl ring.

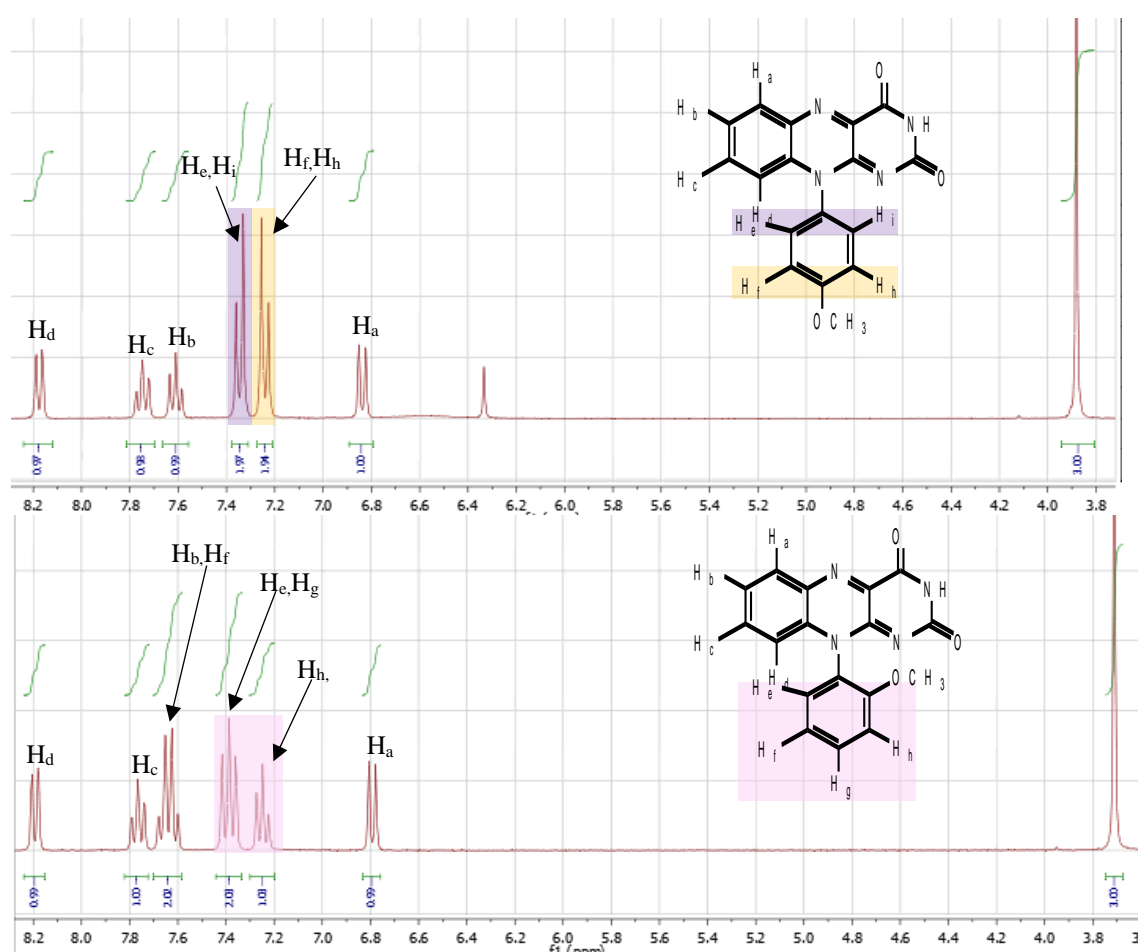


Figure 51: <sup>1</sup>H-NMR for isoalloxazines 9c and 7c

Figure 51 shows the <sup>1</sup>H-NMR as an overlay to clearly see the splitting pattern observed for an *ortho* and *para* substituted isoalloxazine. By analysing Figure 51 closely, a slight shift in the sharp singlet signals of the methoxy moiety from the *o* and *p* isomers can be seen. This <sup>1</sup>H-NMR highlights (in colours) the main differences in splitting patterns between the synthesised molecules 7c and 9c. The correct number of protons for this molecule are shown in the aromatic region (9 – 6 ppm). To expand, one set of doublet (shown in purple and yellow colour for ease of identity), and two signals for triplets (shown in pink colour) can be seen at 8.18 ppm (1H), 7.75

ppm (1H) and 7.61 ppm (1H) respectively, which are correctly attributed to the aromatic protons with an integration of one. Two sets of  $J_{A-B}$  doublets appear at 7.35 ppm (2H) and 7.24 ppm (2H) with a coupling constant of 8.9 Hz and 8.9 Hz with an integration of two protons each, are attributed to the phenyl ring attached to the *N*-10 position. These two doublets also show the correct splitting pattern for a *p*-isomer molecule. A clear doublet can be seen at 6.84 ppm (1H) with an integration of one is attributed to the aromatic proton. A sharp singlet signal appears at 3.88 ppm (3H) attributed to the OCH<sub>3</sub> with a correct integration of three protons. This <sup>1</sup>H-NMR confirms the correct compound, **9c** was synthesised. It is clearly noted from the singlet signal at 3.88 ppm attributed to the OCH<sub>3</sub> moiety appears further down field compared to the *o*-isomer at ~ 3.7 ppm (**7c**). The slight shift in the signals having the correct intergration confirms th formation of different isomers of the methoxyphenyl isoalloxazine..

Although the methoxy substituents are overall electron donating, they are electron withdrawing by inductive effects from the oxygen atom. Methoxy moiety strongly activates the *ortho* and *para* positions of the benzene ring and are *ortho/para* directors.

Evaluation of yields obtained for the three methoxyphenyl isoalloxazine isomers (*ortho*, *meta* and *para*) show enhanced yields for the *ortho* and *para* substituted isomers and this can be correlated to electronic effects produced by the methoxy moiety. This indicates that electronic properties of the substiuent have ability to interact with the main alloxazine ring system, resulting in a good production of singlet oxygen and radicals. Although 38% yield was achieved by the *meta* isomer, this was still an average yield production for an electron donating moiety<sup>339</sup>.

## 2.15 Synthesis of *N*-(3-methoxyphenyl) 2-nitroaniline (**8a**)

The synthesis of compound **8a** was accomplished using the method described in section 2.11. However, a slight modification was made to this synthesis as the starting materials used had to be changed for the required compound. For this synthesis 3-anisidine, and 1-fluoro-2-nitrobenzene were used as the starting reagents. The reaction was monitored at regular intervals (t = 60, 120 and 180 minutes) throughout heating using TLC with silica plates and eluting with a mixture of 40-60 PE:EtOAc (1:2). Compound **8a** eluted second and was observed as an orange compound. The crude black solid was purified by flash column chromatography over silica gel eluting with PE: EtOAc (1:2) to afford the pure product, *N*-(3-metoxyphenyl)-2-nitroaniline (**8a**), as dark red crystals in a 38% yield. Isolation of the correct compound, **8a**, was confirmed by the standard spectroscopic techniques of <sup>1</sup>H-NMR, <sup>13</sup>C NMR and LC-MS.

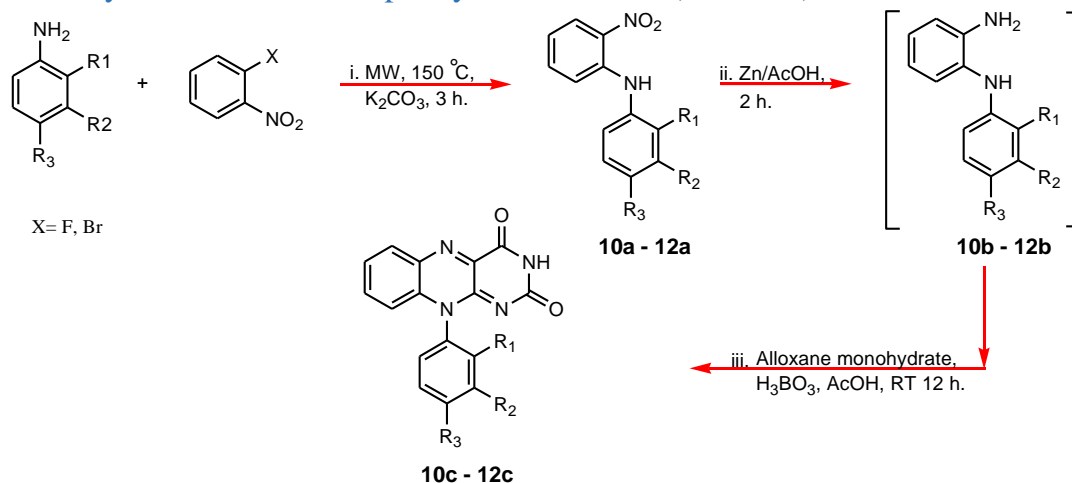
### 2.15.1 Synthesis of 10-(3-methoxyphenyl) isoalloxazine (**8c**)

10-(3-Methoxyphenyl) isoalloxazine (**8c**) was synthesised by heating the starting materials in a round bottom flask. Column chromatography eluting in ethyl acetate yielded the pure product in 20% yield.

Compound **8c** was re-synthesised using the microwave enhanced synthesis to compare both the purity and yield achieved from the two different synthetic routes. Microwave irradiation showed a yield enhancement of the final compound, **8c** (38%) and improvement in the purity of the desired material.



## 2.16 Toly derivatives of 10-phenylisoalloxazine (R = CH<sub>3</sub>)



Scheme 47: Synthetic route of 10-(N-tolylphenyl) isoalloxazines

Table 13: Percentage yields for *N*-(tolylphenyl)-2-nitroaniline and 10-(*N*-tolylphenyl) isoalloxazine derivatives

Compound	<i>o</i> (R <sub>1</sub> )	<i>m</i> (R <sub>2</sub> )	<i>p</i> (R <sub>3</sub> )	Yield (%)
<b>10a</b>	CH <sub>3</sub>	H	H	60
<b>11a</b>	H	CH <sub>3</sub>	H	73
<b>12a</b>	H	H	CH <sub>3</sub>	58
<b>10c</b>	CH <sub>3</sub>	H	H	53
<b>11c</b>	H	CH <sub>3</sub>	H	37
<b>12c</b>	H	H	CH <sub>3</sub>	82

The methyl substituents on 10-(*N*-tolylphenyl) isoalloxazine are weakly donating. All isomers of the tolyl derivatives gave an above average yield for the synthesised products. Unsurprisingly, the *ortho* and *para* isoalloxazines resulted in better yields that could result of the activated ring positions of the phenyl ring.

### 2.16.1 Synthesis of the 2, 3, and 4 isomers of *N*-(tolylphenyl)-2-nitroaniline (10a–12a)

The synthesis of the intermediates **10a–12a** was accomplished using the method described in section 2.11. For each of these intermediates, different derivatives of the 2-nitrohaloarene starting materials were used along with the different isomers of tolylamine. To expand, for **10a**: 2-tolidine was reacted with 1-fluoro-2-nitrobenzene, for **11a**: 3-tolidine was reacted with 1-bromo-2-nitrobenzene and for **12a**, 4-tolidine was reacted with 1-fluoro-2-nitrobenzene. Each of the intermediates were prepared using equal stoichiometric ratios, whilst the base, potassium carbonate, was in excess. The formation of each of the intermediates was monitored at regular

intervals ( $t = 30, 60, 120$  and  $180$  minutes) throughout heating, using TLC with silica plates and eluting with a mixture of 40-60 PE: EtOAc (1:2). After three hours of heating within the microwave, each of the crude intermediates **10a–12a** were isolated by pouring over ice and neutralizing to  $\text{pH}=6$  using c. HCl. Upon filtration at the pump, each compound was purified using column chromatography to yield intermediates **10a–12a** as pure compounds (according to  $^1\text{H-NMR}$  &  $^{13}\text{C-NMR}$ ) in the yields (**10a** = 60%, **11a** = 73%, **12a** = 58%) shown in Table 13. Two key indications of the formation of the intermediates were; 1. the characteristic colour of the nitro substituted intermediate(s) that were bright orange to red along with; 2. the disappearance of the broad singlet around 3 - 4 ppm indicating the aromatic amine, and appearance of a broad singlet at approximately 9.5 ppm indicating the  $2^\circ$  aromatic amine. Its appearance downfield can be attributed to the electron withdrawing effects from the nitro group. The  $^1\text{H-NMR}$  of *N*-(2-tolylphenyl)-2-nitroaniline is shown in Figure 52.

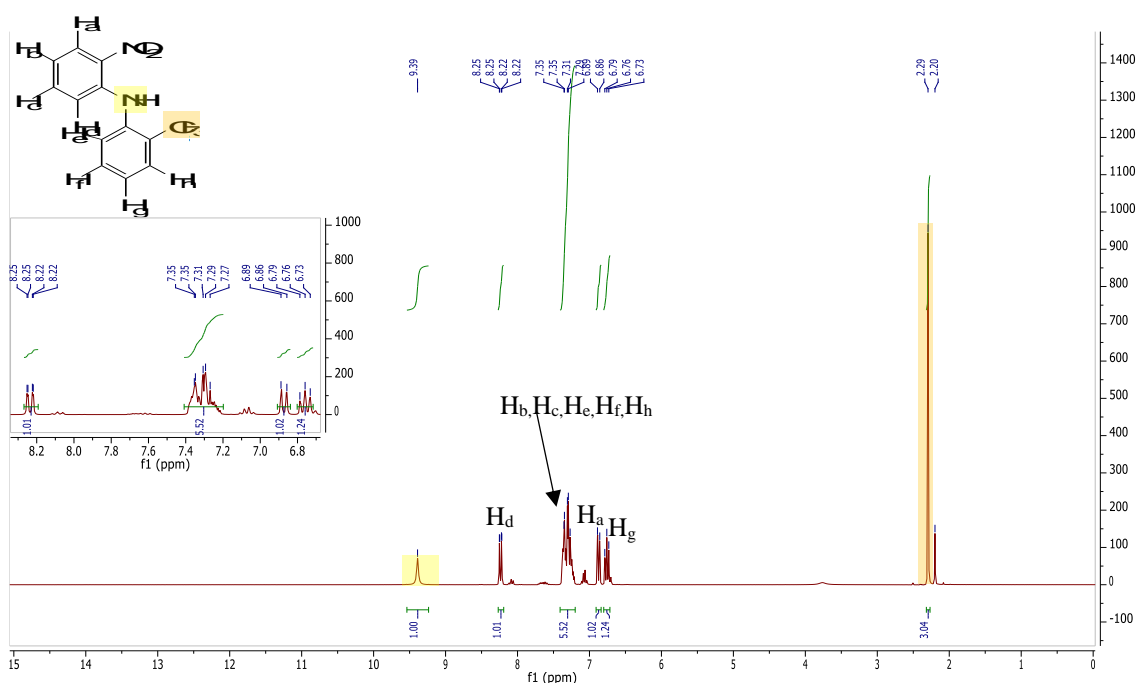


Figure 52:  $^1\text{H-NMR}$  for *N*-(2-tolylphenyl)-2-nitroaniline

### 2.16.2 Synthesis of 10-(*N*-tolylphenyl) isoalloxazine (**10c–12c**)

Each of the intermediates **10a–12a** were reduced in the presence of zinc and glacial acetic acid to yield compounds **10b–12b** as the primary aromatic amines. Although the compounds were not isolated, two key observations were noted during the reduction. The first was the disappearance of the bright orange colour upon filtration, which is characteristic of the nitro functional group to a paler green upon filtration through celite™. The second and most conclusive observation, was the change in the mass spectrum from the nitro to the amine (loss of  $30 \text{ g/mol}^{-1}$ ). Upon filtration through celite™, the acidic solution was subsequently added to a round-bottom flask with a 1:1.2

stoichiometric molar excess of boric acid and alloxane monohydrate. The reaction proceeded for 12 hours at room temperature, which resulted in the precipitation of a bright yellow solid. This reaction could be followed using mass spectrometry (ESI), with appearance of the parent ion at  $m/z = 321 M^+$ , although, a key indication that the isoalloxazine has formed is a green fluorescence colour from the reaction flask upon illumination of light at 365 nm. Each of the final compounds for this series were isolated at the pump and washed well with cold hexane. These were then dried under *vacuo* to give a bright yellow powder in the yields (**10c** = 53%, **11c** = 37% and **12c** = 82%) shown in Table 13.

Looking at the  $^1\text{H-NMR}$  for the 10-(2-tolylphenyl) isoalloxazine (**10c**) Figure 53, its clear to see that the acetic acid signal is still present at 11.88 ppm and a small bump around 12 ppm is shown that can be attributed potentially to the starting material alloxan monohydrate. The acetic acid can be removed by stirring the solid in diethyl ether, followed by filtration and washed further with cold diethyl ether. However, a clear indication of the formation of the isoalloxazine in the  $^1\text{H-NMR}$  is the characteristic amide signal at 11.43 ppm as a broad singlet.

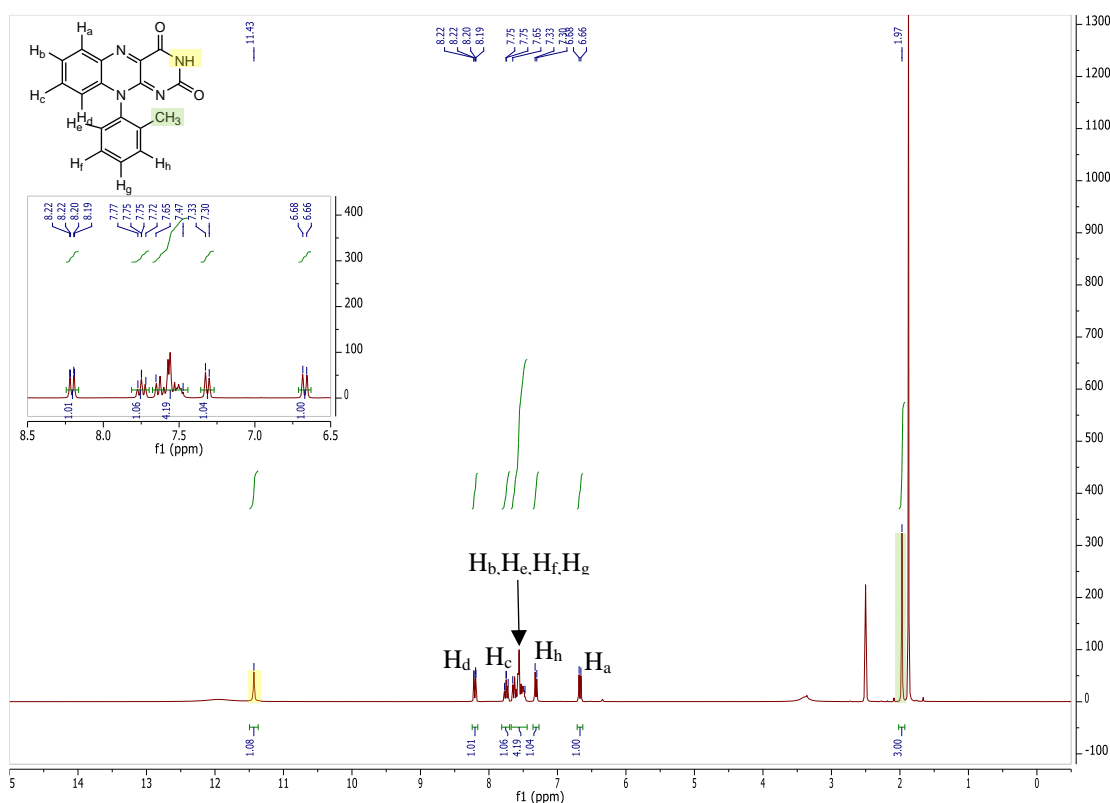


Figure 53:  $^1\text{H-NMR}$  for 10-(2-tolylphenyl) isoalloxazine

The tolyl substituents are *ortho/para* directors. They have affinity to push electron density into the  $\pi$  system of the benzene ring making them high in electron density, consequently making the ring more reactive.

By analysis of all the electron donating substituents, *para* isomers overall are more reactive than *ortho* substituents, and *ortho* are more reactive than the *meta*. This observation correlates well to the order of reactivity series for electron donating groups on aryl ring given in literature<sup>340</sup>.

For each of the compounds in the tolyl series (**10c** - **12c**) an IR spectrum was taken in order to identify the functional groups present in the synthesised novel compounds and this was done for all the synthesised analogues of isalloxazines within this study. Figure 54 shows the IR spectrum for the *meta* tolyl substituted isoalloxazine (**11c**). This was

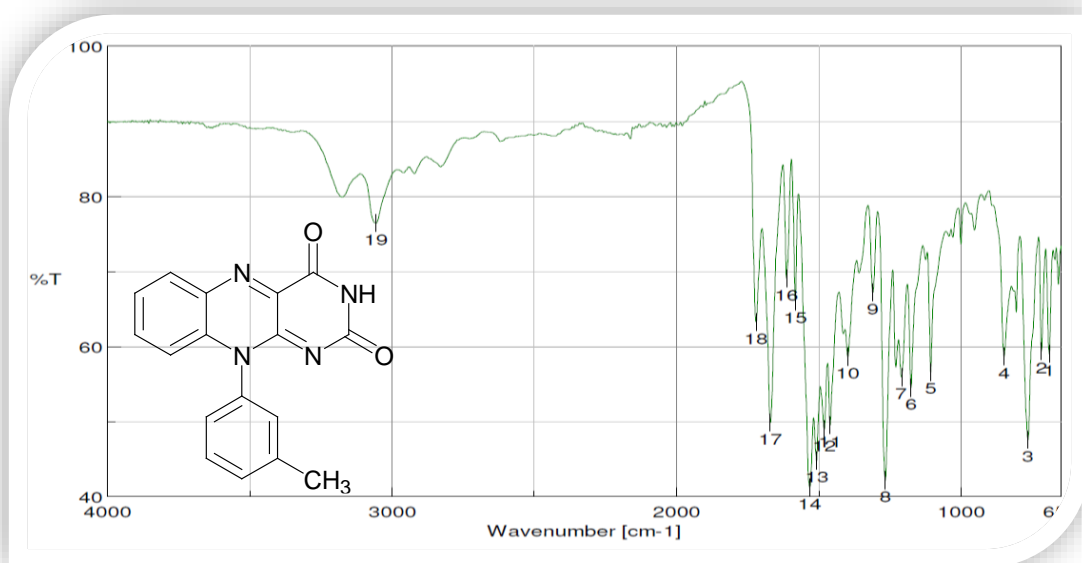
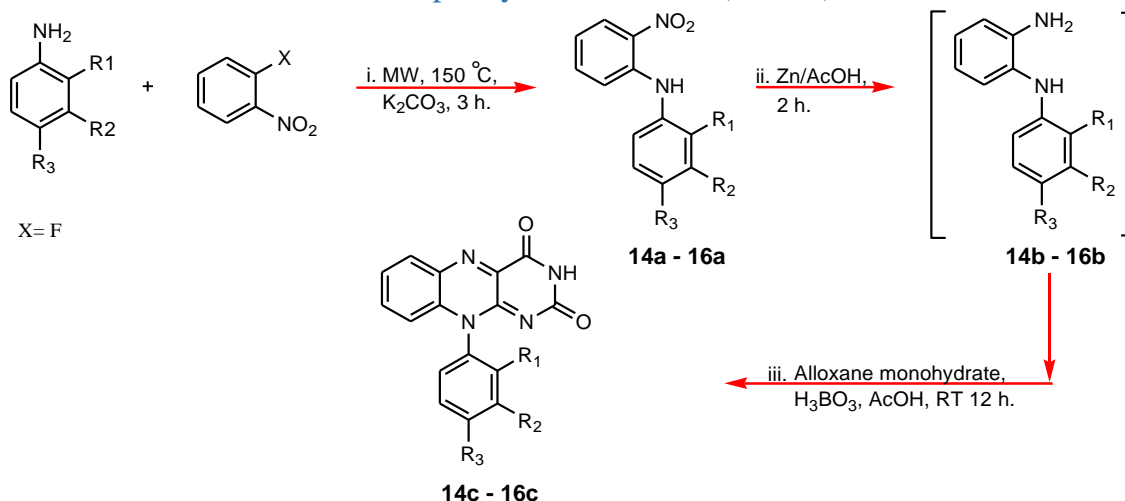


Figure 54: IR spectrum for compound **11c**

The key functional groups attributed to compound **11c** present in the spectrum above Figure 54. The peak present at  $\nu$  (number 19)  $3055.66\text{ cm}^{-1}$  indicates the presence of aromatic C-H groups. The band at  $1721\text{ cm}^{-1}$  specifies the presence of C=O aromatic bonds. Sharp peaks observed at  $1671\text{ cm}^{-1}$  and  $1613\text{ cm}^{-1}$  are attributed to carbonyl (C=O) group belonging to the amide (3° amide) moiety. The bands seen at  $1583\text{ cm}^{-1}$ ,  $1532\text{ cm}^{-1}$  and  $1508\text{ cm}^{-1}$  correspond to aromatic C=C stretch. The peaks present at positions  $1481\text{ cm}^{-1}$ ,  $1460\text{ cm}^{-1}$  and  $1398\text{ cm}^{-1}$  are attributed to aromatic C-C=C. The bands at  $1310\text{ cm}^{-1}$ ,  $1267\text{ cm}^{-1}$ ,  $1210\text{ cm}^{-1}$ ,  $1176\text{ cm}^{-1}$  and  $1106\text{ cm}^{-1}$  indicates the presence of C-N bonds.

## 2.17 Chloro derivatives of 10-phenylisoalloxazine (R = Cl)



*Scheme 48: Synthetic route of 10-(N-chlorophenyl) isoalloxazines*

Table 14: Percentage yields for *N*-(chlorophenyl)-2-nitroanilines and 10-(*N*-chlorophenyl) isoalloxazine derivatives

Compound	<i>o</i> (R <sub>1</sub> )	<i>m</i> (R <sub>2</sub> )	<i>p</i> (R <sub>3</sub> )	Yield (%)
<b>14a</b>	Cl	H	H	98
<b>15a</b>	H	Cl	H	5
<b>16a</b>	H	H	Cl	21
<b>14c</b>	Cl	H	H	26
<b>15c</b>	H	Cl	H	34
<b>16c</b>	H	H	Cl	71

The synthesis of the chloro substituted isoalloxazines is of importance as it allows the electron withdrawing properties of chlorine, (as a substituent) can be studied by monitoring the singlet oxygen and radical generated. Substituted chlorine's have electron withdrawing effects inductively; however, the substituent behaves as an electron donating group through resonance.

### 2.17.1 Synthesis of 2, 3, and 4 isomers of *N*-(chlorophenyl)-2-nitroaniline (**14a–16a**)

Compounds **14a-16a** were synthesised using the methodology described in section 2.11. Microwave irradiation was used to react each of the starting materials in the presence of K<sub>2</sub>CO<sub>3</sub>. 1-Fluoro-2-nitrobenzene and derivatives of *N*-chloroaniline were used as the starting materials in stoichiometric ratios to prepare the compounds **14a-16a**. For each derivative of chloroaniline, microwave irradiation was used to heat the reaction. The formation of each of the intermediates (**14a-16a**) was monitored regularly using TLC with silica plates. Upon purification of each of the compounds by flash column chromatography over silica gel eluting with PE: EtOAc (1:2), the

pure products, *N*-chlorophenyl)-2-nitroaniline (**14a-16a**) were isolated as dark red crystals in yields shown in Table 14. The isolation of each of the intermediates was identified using spectroscopic techniques. Figure 55, shows  $^1\text{H-NMR}$  for *N*-(2-chlorophenyl)-2-nitroaniline, confirming the synthesis of the substituted chloroaniline.

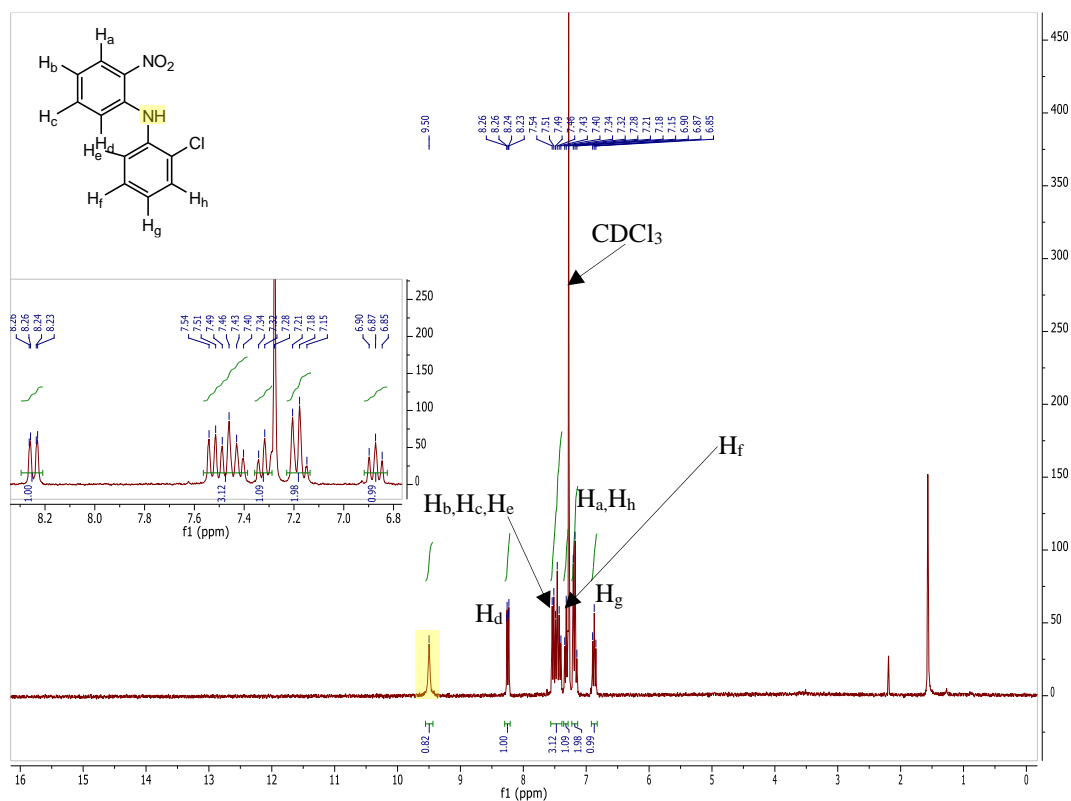


Figure 55:  $^1\text{H-NMR}$  for *N*-(2-chlorophenyl)-2-nitroaniline

The appearance of a broad singlet peak at 9.50 ppm (1H) indicates the formation of the 2° amine. The dd seen at 8.23 ppm with an integration of 1, can be attributed to the proton on the aromatic ring *ortho* to the nitro functional group, due to the electron withdrawing effects of the nitro moiety. A multiplet seen at 7.54 – 7.40 ppm (3H), with an integration of three looks like a doublet and triplet merging together resulting as a multiplet. These protons are attributed to the phenyl ring with the chloro substituent attached. A multiplet seen at 7.32 ppm (1H), which is overlaying the solvent peak of  $\text{CDCl}_3$  at 7.26 ppm looks to be a triplet peak attributed to the aromatic ring and has an integration of one proton. A multiplet and triplet showing at 7.18 ppm (2H) and 6.87 ppm (1H) respectively are attributed to the aromatic rings. From analysing the  $^1\text{H-NMR}$ , it can clearly be noted; that, the signals are not very well defined for this molecule as there are three different functional groups attached to the aromatic rings (Cl,  $\text{NO}_2$  and 2° NH) that affect the splitting pattern due to their electron donating and withdrawing nature. Hence many multiplet's for this  $^1\text{H-NMR}$  are observed.

A full mass spectrometry (MS) (electrospray ionization-(ESI)) for each of these molecules **14a** - **16a** was found to be  $m/z$  248  $M^+$ . This confirms a successful synthesis of the substituted *N*-chloroanilines and is illustrated in Figure 56.

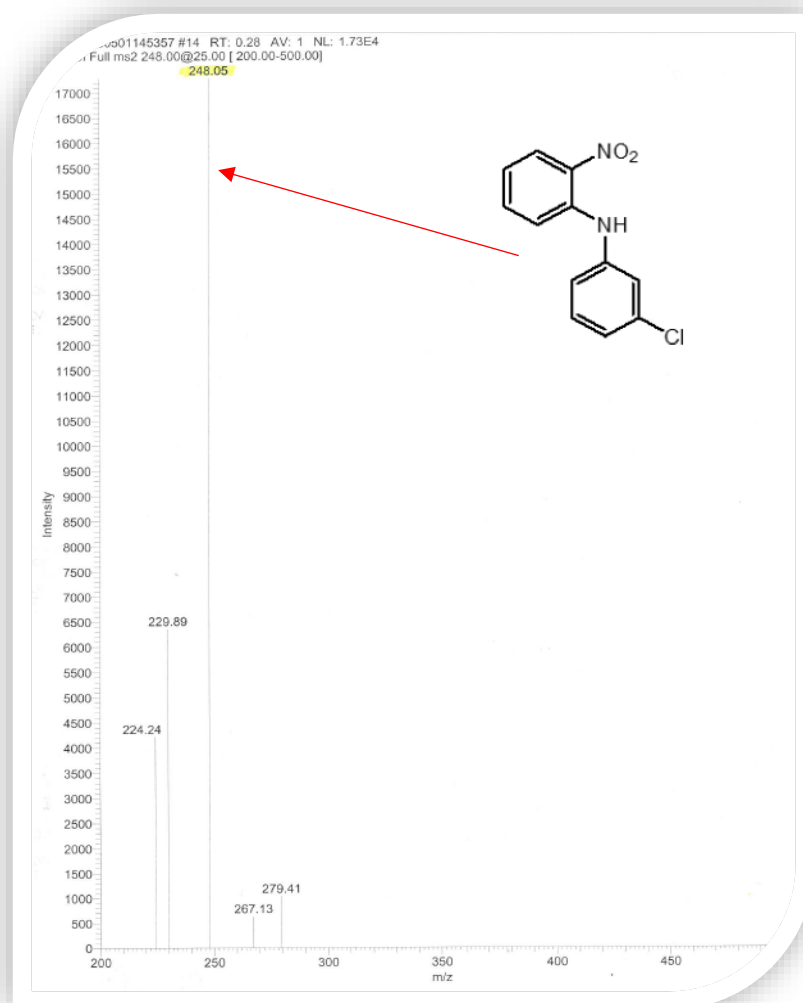
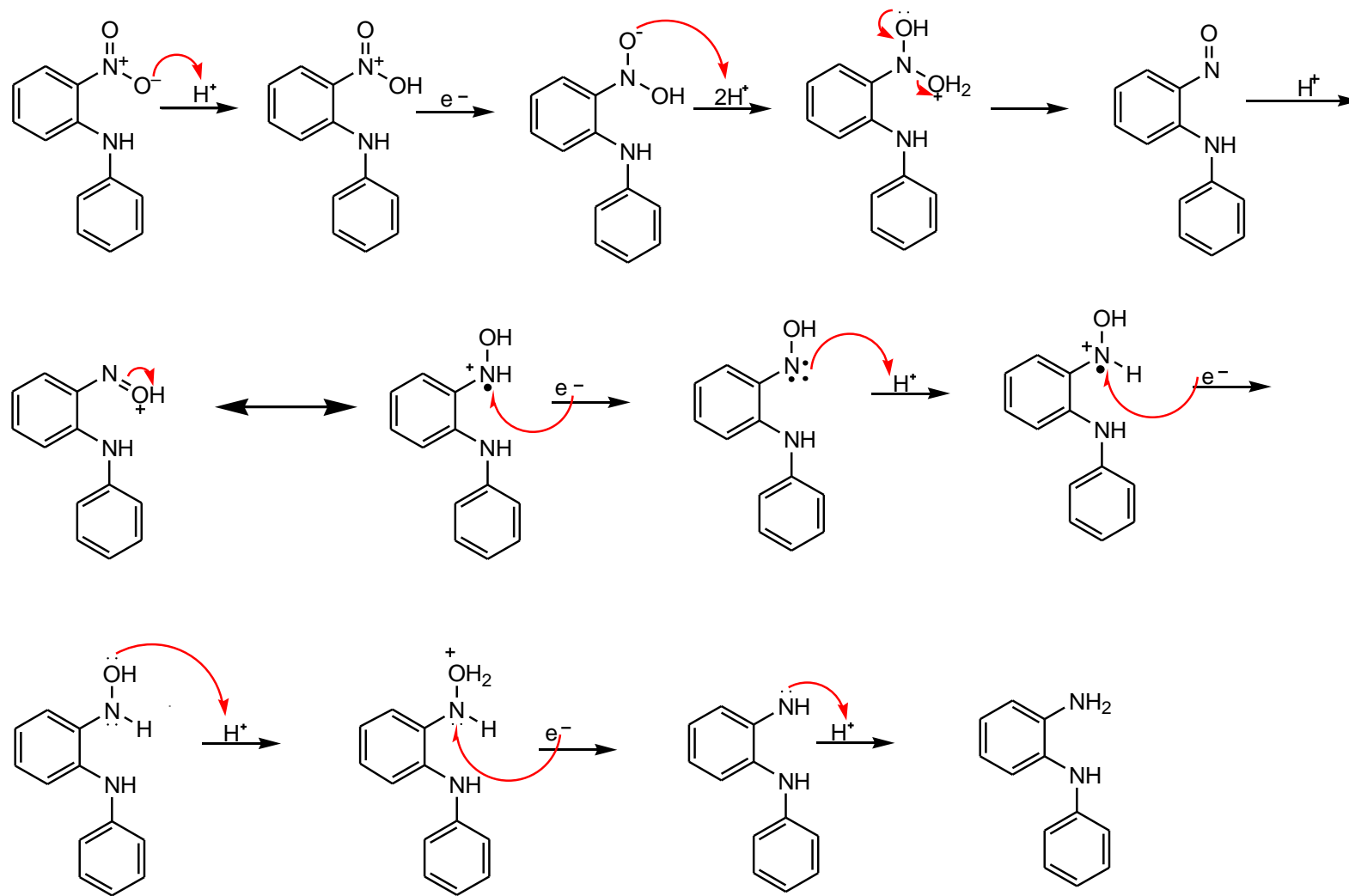


Figure 56: MS of 2-(3-chlorophenyl) 2-nitroaniline

### 2.17.2 Synthesis of 10-(*N*-chlorophenyl) isoalloxazines (**14c-16c**)

The intermediates **14a-16a** were reduced in the presence of zinc powder and acetic acid using a 10-fold stoichiometric excess of zinc. The reaction was monitored carefully, and the mechanism for zinc reduction is shown in Scheme 49.



Scheme 49: Zinc reduction mechanism



The newly synthesised amines (**14b–16b**) was confirmed by mass spectrometry (ESI-MS) shown in Figure 57 as a loss of  $30 \text{ g mol}^{-1}$  was detected by the reduced compounds from a nitro group to an amine. The freshly reduced amines were dissolved in acetic acid and isolated by filtration through celite™.

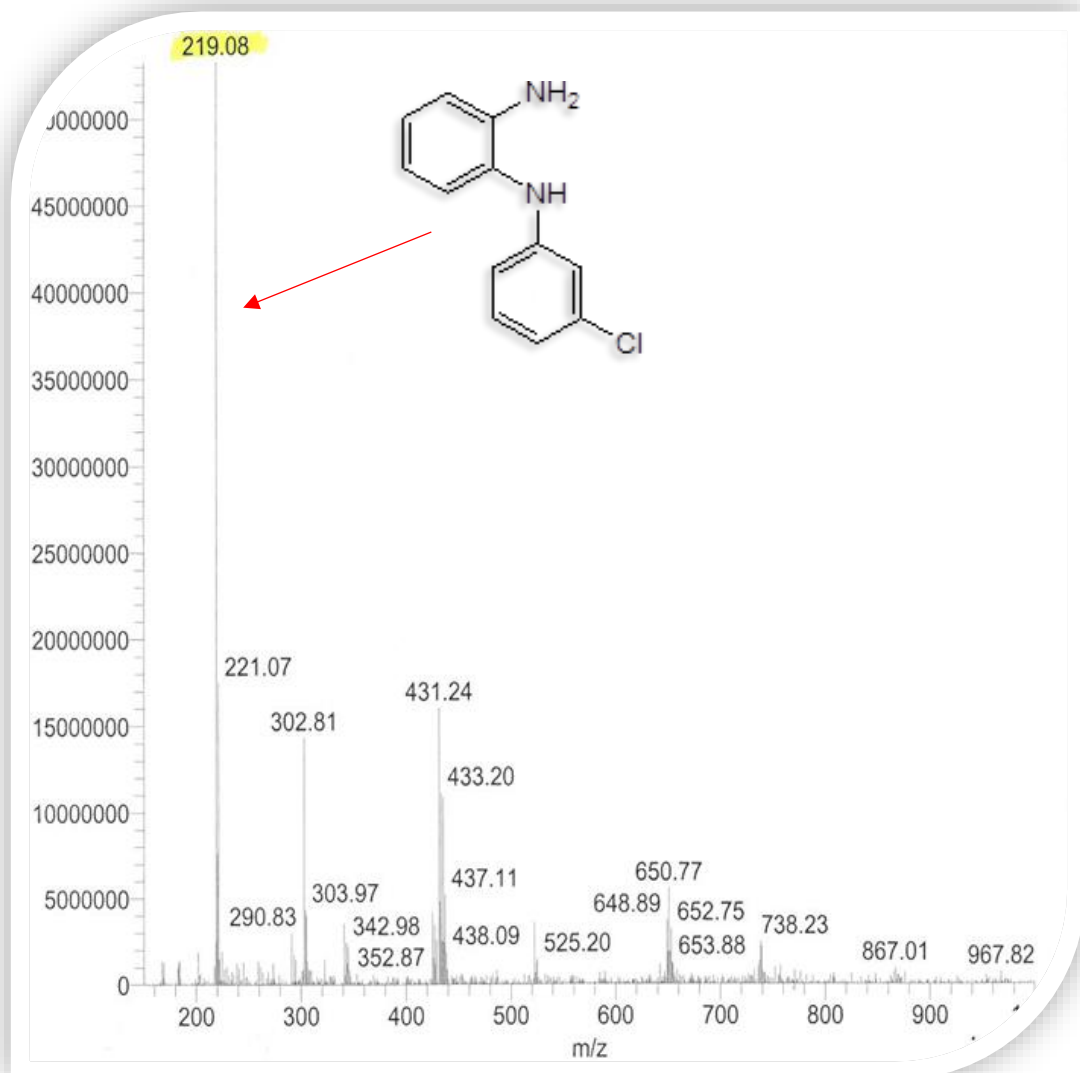


*Figure 57: MS (ESI) for N-(2-chlorophenyl)-2-aminoaniline*

To the acidic solution was added alloxan monohydrate and boric acid in a 0.02 molar excess and this was left to stir at room temperature for 12 hours. After 12 hours the formation of a yellow precipitate was observed and the acidic mixture was filtered at the pump to isolate each of the 10-(*N*-chlorophenyl) isalloxazine (**14c–16c**) compounds. Each of these products were washed well with cold hexane and dried under vacuo to give a bright yellow powder in the yields (14c = 29% 15c = 77% and 16c = 47%) shown in Table 14.

Figure 58 shows the  $^1\text{H-NMR}$  for the compound; 10-(4-chlorophenyl) isoalloxazine, **16c**.

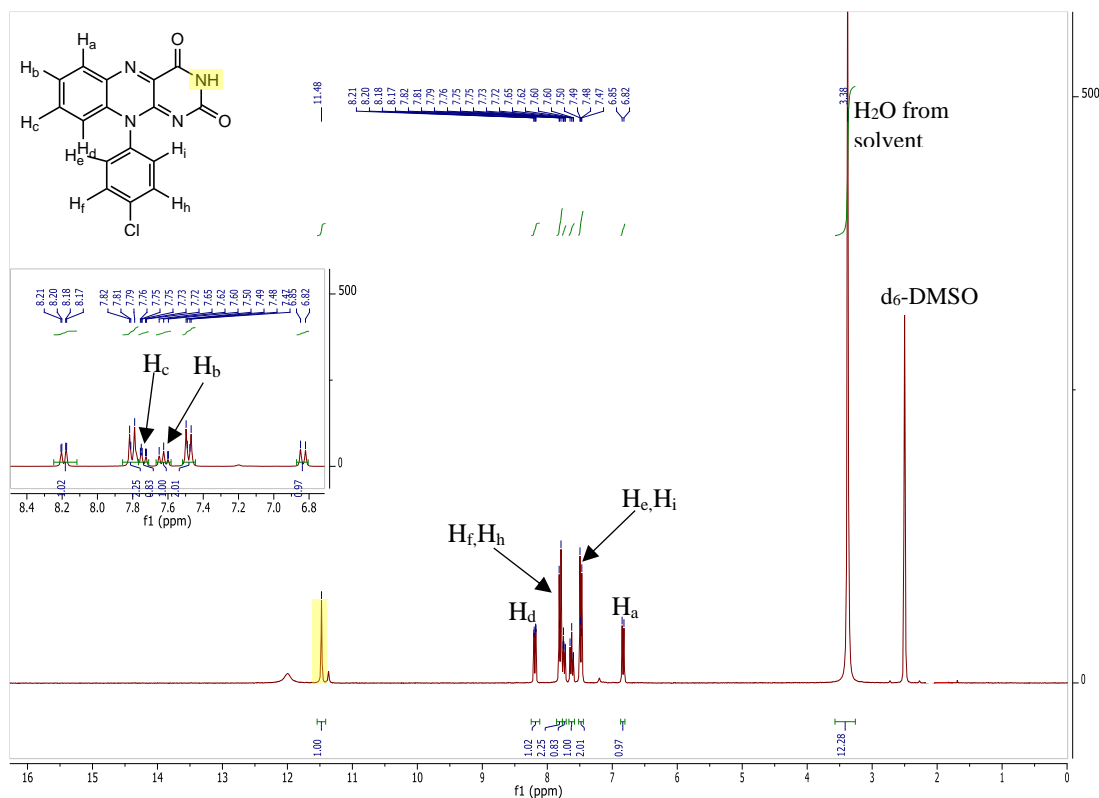
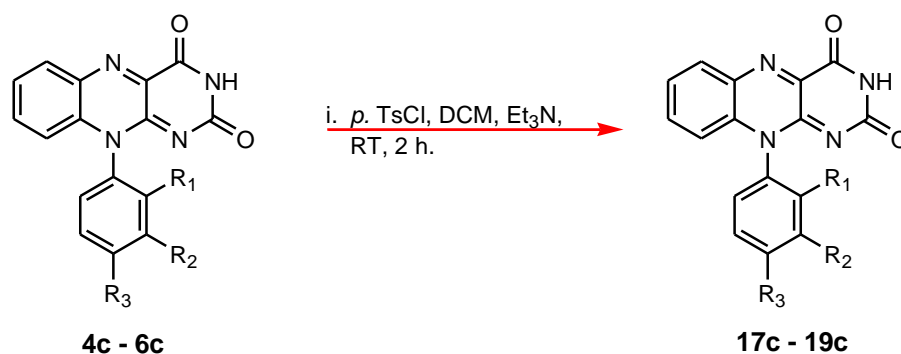


Figure 58:  $^1\text{H-NMR}$  for 10-(4-chlorophenyl) isoalloxazine

A sharp singlet signal detected at 1.90 ppm shows the presence of acetic acid and a small peak at 12 ppm can be attributed to the starting material alloxan monohydrate, which was removed by stirring the compound in diethyl ether. By removing the two signals as well as the solvent residue signal and water saturation formation of isoalloxazine **16c** is confirmed. The signal at 11.47 ppm is attributed to the acidic  $\text{CO}(\text{NH})\text{CO}$  amide and is shown as a broad singlet signal with an integration of 1H. This signal is a characteristic peak for all the synthesised isoalloxazines containing an acidic  $\text{CO}(\text{NH})\text{CO}$  amide. The aromatic region (9 – 6 ppm) illustrates the correct number of protons for this molecule. with one doublet, a doublet of doublet and a triplet are seen at 8.19 ppm (1H), 7.78 ppm (3H) and 7.62 ppm (1H) respectively.

## 2.18 Tosyloxy derivatives of 10-phenylisoalloxazine (R = OTs)



*Scheme 50: Synthetic route of 10-(N-tosyloxyphenyl) isoalloxazines*

Table 15: Percentage yields for 10-(N-tosyloxyphenyl) isoalloxazine derivatives

Compound	<i>o</i> (R <sub>1</sub> )	<i>m</i> (R <sub>2</sub> )	<i>p</i> (R <sub>3</sub> )	Yield (%)
<b>17c</b>	OTs	H	H	62
<b>18c</b>	H	OTs	H	22
<b>19c</b>	H	H	OTs	13

The tosylate group (OTs) is used commonly in synthetic chemistry as a protecting group. Tosylates also behave as very good leaving groups. However, for the purpose of this research OTs group was employed to alter the electron density of the aromatic rings. Thus, allowing the study of the difference in singlet oxygen generated to be monitored by having the OTs substituent attached at different positions on the phenyl ring.

It should be noted that although compound **5c** was synthesised as an impure material, it was still proceeded further to react with *para*-toluene sulphonyl chloride to form the desired isoalloxazine (**18c**), in the hope to achieve a pure compound. Surprisingly, compound **19c** was successfully synthesised as a pure yellow powder.

### 2.18.1 Synthesis of 2, 3, and 4 isomers of *N*-(tosyloxyphenyl)-2-nitroaniline (**17a–19a**)

Compounds **17a–19a** were not synthesised, as the starting materials used for the synthesis of *N*-tosyloxyphenyl isoalloxazines (**17c–19c**) were compounds **4c–6c**.

### 2.18.2 Synthesis of 10-(*N*-tosyloxyphenyl) isoalloxazines (**17c–19c**)

The synthesis of the tosyloxy substituents, **17c–19c** was accomplished through reacting compounds **4c–6c** with *para*-toluene sulphonyl chloride in basic conditions. These analogues were synthesised in order to study the singlet oxygen and radical yields when a weak electron withdrawing substituent (OTs) is attached to the phenyl substituent on the isoalloxazine *N*-10 ring.

Although the synthesis for 10-(3-tosyloxy-phenyl) isoalloxazine (**18c**) required 10-(3-hydroxyphenyl) isoalloxazine (**5c**) as the starting material, this impure material was nonetheless used to synthesise compound **18c** in order to investigate the possibility of success in synthesis. Fortunately, the reaction proved to be successful and compound **18c** was isolated as a pure product in a yield of 22%. This molecule was obtained in an average yield, particularly as aforementioned, 10-(3-hydroxyphenyl) isoalloxazine (**5c**) was not isolated. Spectroscopic data;  $^1\text{H-NMR}$ ,  $^{13}\text{C-NMR}$  and HRMS confirmed the correct product was isolated as a pure product.

Compound **19c** was isolated in a very poor yield of 13%. The surprisingly low yield presumably resulted from various reasons; such as, the reaction time set was 2 hours, which is considerably less for a typical substitution reaction to occur for a tosyloxy group and therefore reaction may not have gone to a total completion even though the product was formed. An alternative possibility of resulting in a very low yield could be that the product was lost during the work up procedure. An additional reason for achieving a poor yield could possibly be due to the electronic effects attributed from the tosylate moiety. The yield comparison from the three isomers peculiarly show that the *meta* derivative has a better yield production than the *para* substituent. Figure 59 shows the  $^1\text{H-NMR}$  for compounds **19c** and **6c** that are employed to compare synthesis of the two molecules by analysing their splitting pattern and integration.

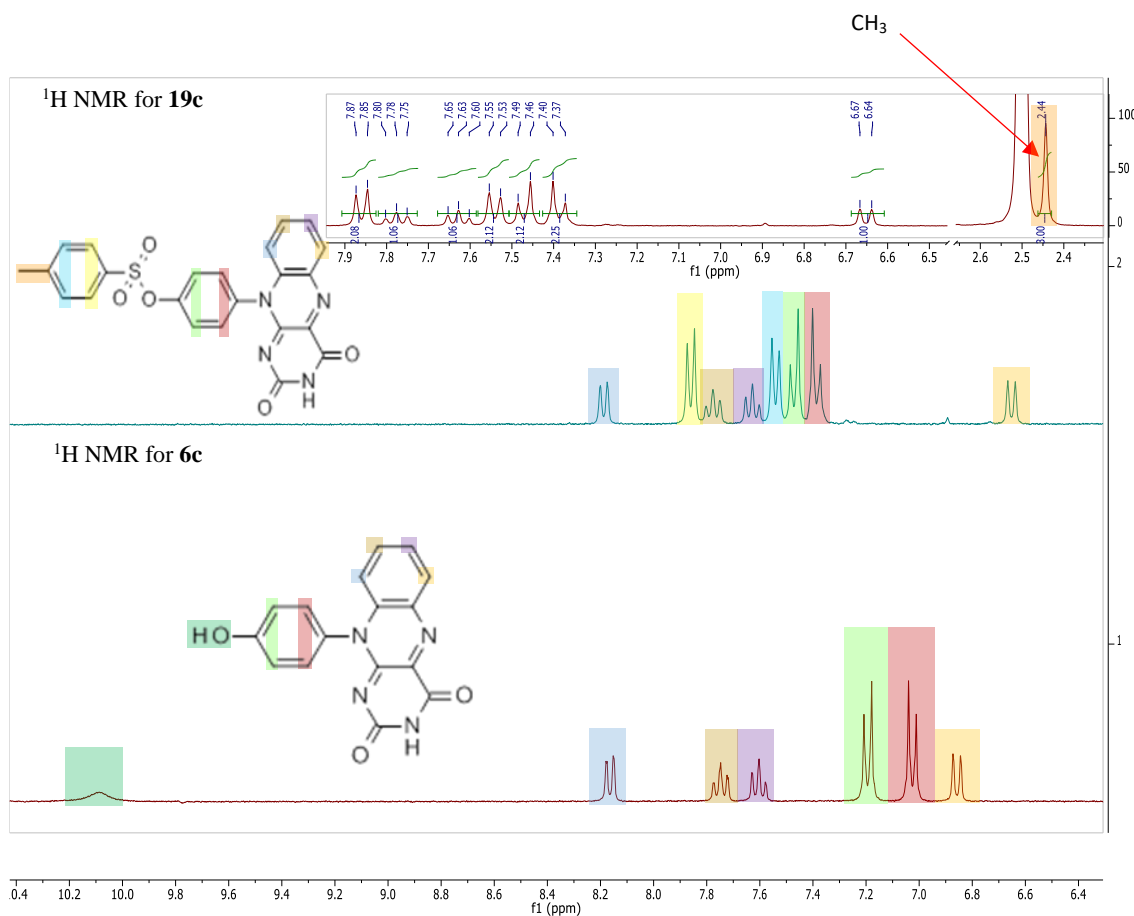
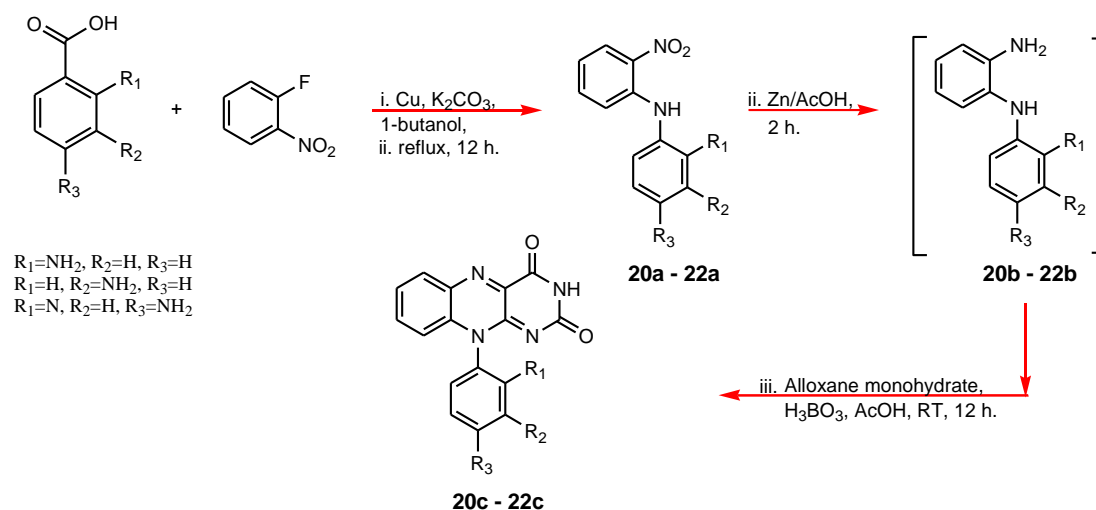


Figure 59:  $^1\text{H}$  Spectra for *p*-tosyloxy phenyl (**19c**) isoalloxazine and *p*-hydroxy isoalloxazine (**6c**)

The peaks in Figure 59 are highlighted in different colours in order to identify which peaks belong to what protons in the molecule. For the molecule **19c**, a broad singlet at 11.46 ppm is attributed to the acidic CO(NH)CO amide with an integration of 1H (not shown in spectra). The aromatic region (9 – 6 ppm) shows the correct number of protons for this molecule (16H) as well as a correct splitting pattern. To summarise, two sets of doublets can be seen at 7.86 ppm (2H) and 7.54 ppm (2H), (highlighted in yellow and blue) with an integration of two protons are attributed to the aromatic ring protons from the OTs ring. A sharp singlet peak correlating to the CH<sub>3</sub> moiety from the tosylate group with an integration of three protons was also present on the <sup>1</sup>H-NMR in the correct high-field region (illustrated in the full <sup>1</sup>H-NMR of OTs, within Figure 59) confirming the syntheses of the desired compound **16c**. By close observation of the <sup>1</sup>H-NMR shown in Figure 59 (compound **6c**) a broad singlet peak seen at 10.09 ppm (1H), is attributed to the hydroxyl moiety of compound **6c**. In addition to this, the disappearance of the two sets of doublets which appeared at 7.86 ppm and 7.54 ppm with an integration of two protons each attributed to the tosyloxy ring confirm that the tosyloxy moiety was substituted correctly onto the phenyl ring attached to the *N*-10 position of the main tricyclic isoalloxazine ring.

## 2.19 Carboxy derivatives of 10-phenylisoalloxazine (R = COOH)



*Scheme 51: Synthetic route of 10-(N-carboxyphenyl) isoalloxazines*

Table 16: Percentage yields for *N*-(carboxyphenyl)-2-nitroanilines and 10-(*N*-carboxyphenyl) isoalloxazine derivatives

Compound	<i>o</i> (R <sub>1</sub> )	<i>m</i> (R <sub>2</sub> )	<i>p</i> (R <sub>3</sub> )	Yield (%)
<b>20a</b>	COOH	H	H	71
<b>21a</b>	H	COOH	H	N/A <sup>4</sup>
<b>22a</b>	H	H	COOH	77
<b>20c</b>	COOH	H	H	40
<b>21c</b>	H	COOH	H	N/A <sup>5</sup>
<b>22c</b>	H	H	COOH	66

The carboxy moiety is an electron withdrawing group that moderately deactivates the aryl ring. Thus, making the  $\pi$  ring system less reactive to nucleophilic attacks. The change in electron density around the tricyclic ring structure is of interest to monitor the effects in the production of both singlet oxygen and radicals.

The synthesis of the 10-*N*-carboxyphenyl isoalloxazines was changed from using microwave enhanced synthesis particularly for the first step of the synthesis (**20a–22a**) as discussed in section 2.11 because the reaction was not going to completion, although minute yields were synthesised. Thus, an alternative pathway was therefore used to achieve higher yields of these compounds.

<sup>4</sup> Synthesis proved unsuccessful.

<sup>5</sup> Not synthesised as intermediate was unsuccessful. Therefore photophysical studies was not conducted.

Literature search showed a number of methods to synthesise compounds similar to **20a-22a**, however, most routes showed low yield production. Research conducted by Hunziker *et al* to synthesise 2-(4-chloro-2-nitrophenylamino)benzoic acid used the Ullmann coupling conditions, yet low yield, 22% of the product was formed<sup>341</sup>. Thus further search in literature was conducted to find other means of synthesis for compounds similar to **20a-22a**. A similar reaction was carried out by Hermkens Pedro whom utilised 2-fluoro-5-chloronitrobenzene with anthranilic acid, K<sub>2</sub>CO<sub>3</sub> as the base with copper as a catalyst in pentanol at 140°C, which yielded the compound in 43%. As an improvement in yield was observed in this method, compounds **20c-22c** were synthesised following this route with slight variations of the reagents and solvent<sup>342</sup>.

The synthesis for the 10-*N*-carboxyphenyl derivatives is described in the method shown in section 2.19.1. It should be noted that the *meta* isomer could not be synthesised due to issues in the synthesis.

### 2.19.1 Synthesis of the 2, 3, and 4 isomers of (*N*-carboxyphenyl)-2-nitroaniline (**20a-22a**)

Each of the (*N*-carboxyphenyl)-2-nitroaniline (**20a-22a**) was synthesised using the Ullman reaction. The starting materials were heated in a round bottom flask. The reaction proceeded by adding K<sub>2</sub>CO<sub>3</sub>, copper powder, 4-aminobenzoic acid, and 1-bromo-2-nitrobenzene in 1-butanol. The reaction resulted in an orange precipitate after 12 hours of stirring at 150 °C. The precipitate was crushed with diethyl ether and collected by suction filtration and transferred into a conical flask and distilled water was added. The aqueous solution was adjusted to pH 9 using c. NH<sub>4</sub>OH<sub>(aq)</sub>, and set to reflux. Upon cooling, the solution was filtered through celite™. This solution was then adjusted to pH 5, using c. HCl<sub>(aq)</sub> forming a bright orange solid which was filtered from the mixture and dried under *vacuo* to yield the substituted (*N*-carboxyphenyl)-2-nitroaniline (**20a** and **22a**) as an orange powder in yields shown in Table 16.

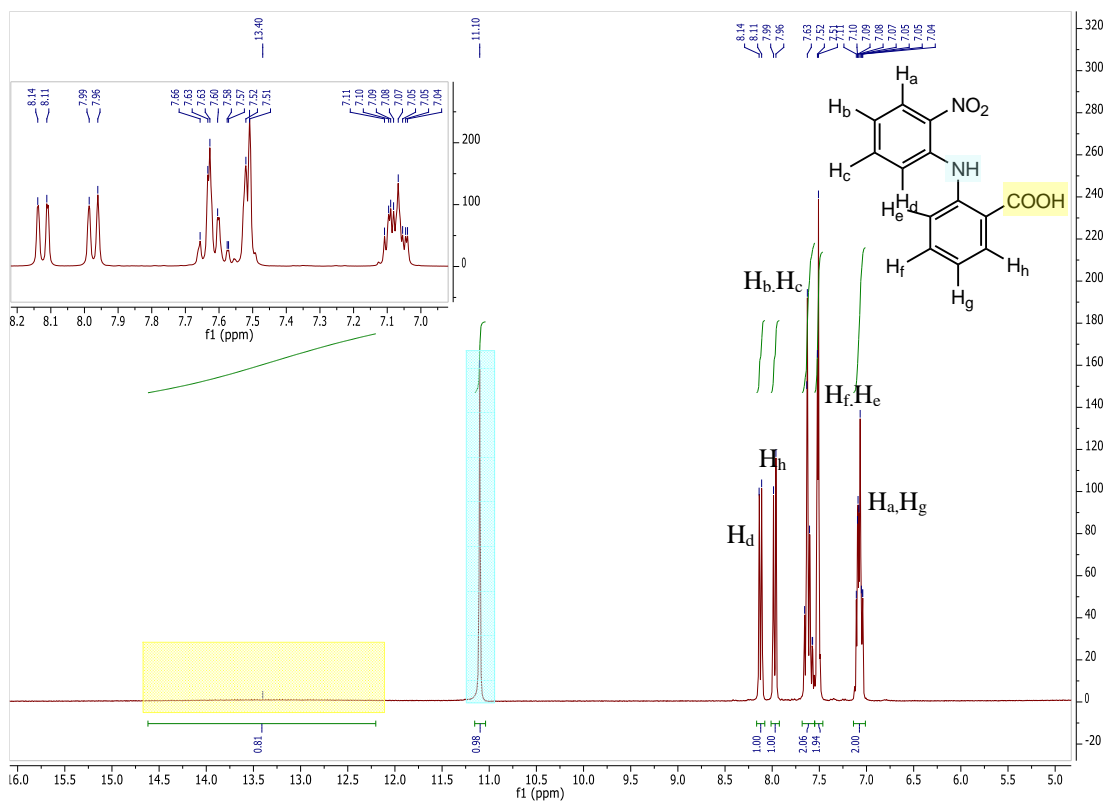


Figure 60: <sup>1</sup>H-NMR of N-(2-carboxyphenyl)-2-nitroaniline

Figure 60 shows the <sup>1</sup>H-NMR for 10-(2-carboxyphenyl)-2-nitroniline (**20a**). The broad peak shown at 13.40 ppm (1H) (highlighted in yellow) is attributed to the proton on from the carboxylic acid on the phenyl ring substituted on the *N*-10 position. The singlet peak shown at 11.10 ppm (1H) (highlighted in blue) corresponds to secondary amine (NH) with an integration of 1. This peak is appearing at a higher region for an amine due to the presence of the COOH group causing a downfield shift. The peaks shown between 8.14 ppm and 7.04 ppm, in the aromatic region show the right number of integrations (10H) for the molecule.

Compound **21a** was attempted to be synthesised following the same procedure as described in section 2.19.1. However, this compound was not successfully achieved. The unsuccessful synthesis of compound **21a** was surprising as carboxy substituents are *meta* directors and therefore (presumably) be easier to form than other isomers. The TLC on silica plates for compound **21a** was eluted in different solvents. One TLC plate was eluted in toluene (100%) and the second TLC plate was eluted in CHCl<sub>3</sub> (100%). The two TLC plates showed the presence of starting materials with additional impurities. No appearance of the desired compound (**21a**) could visually be seen on these plates or in the <sup>1</sup>H-NMR. Thus, it was decided that the synthesis of this compound was unsuccessful.



## 2.19.2 Synthesis of 10-(*N*-carboxyphenyl) isoalloxazines (**20c** & **22c**)

The *N*-carboxyphenyl isoalloxazine derivatives (**20c** and **22c**) were synthesised using the method described above (section 2.19.1), following Scheme 51. Although the carboxy substituent is a *meta* director and has strong electron withdrawing properties, a very good yield was obtained for both an *ortho* and *para* substituted molecules. Spectroscopic analysis by <sup>1</sup>H-NMR and <sup>13</sup>C-NMR identify the correct compound was synthesised and can be seen in Figure 61. HRMS also confirmed isolation of the correct product.

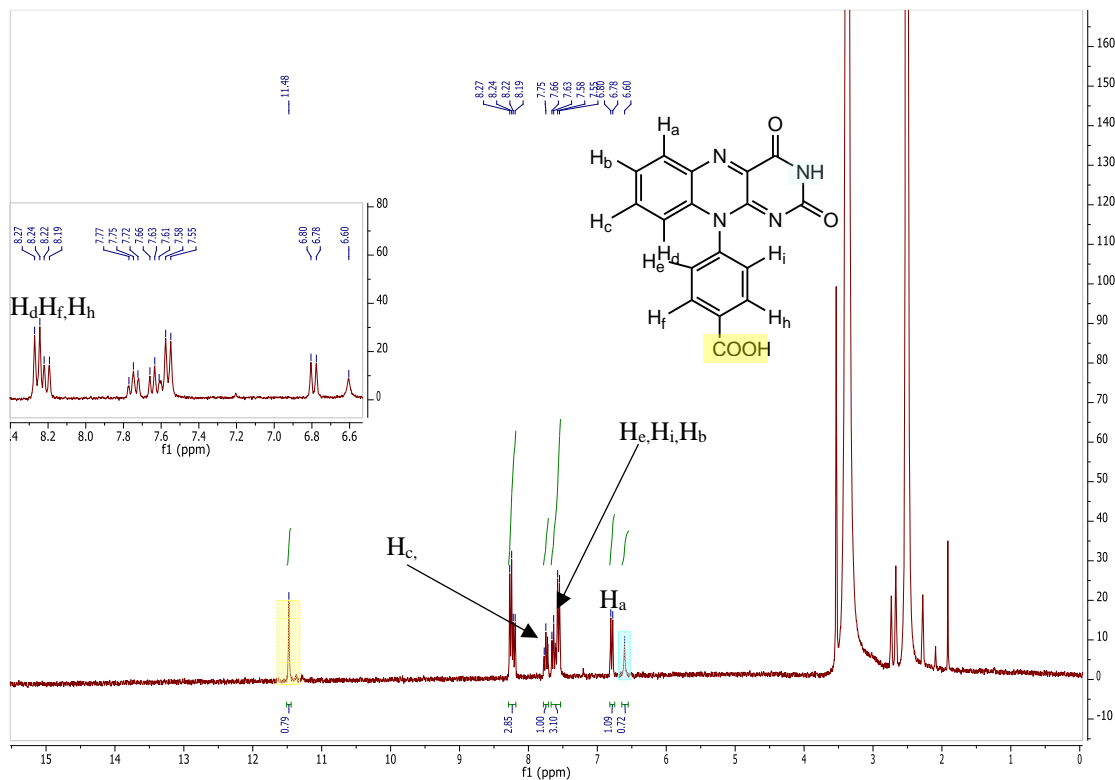


Figure 61: <sup>1</sup>H-NMR for 10-(4-carboxyphenyl) isoalloxazine (**22c**)

Figure 61 shows the <sup>1</sup>H-NMR for **22c**. The singlet peak shown at 11.48 ppm is attributed to the acidic CO(NH)CO amide with an integration of 1H, (highlighted in yellow for ease of observation). The aromatic region (9-6 ppm) show the correct number of protons corresponding to this molecule (9H). A broad singlet at 6.60 ppm (1H) (highlighted in blue) can be seen with an integration of one proton, attributed to the carboxylic acid moiety, confirming the synthesis of the correct compound.

Mass spectrometry (ESI) for these molecules (**20c** and **22c**) was found to be  $m/z$  335 M<sup>+</sup> confirming a successful synthesis of the 10-(*N*-carboxyphenyl) isoalloxazine, and is shown in Figure 62 for compound **20c**.

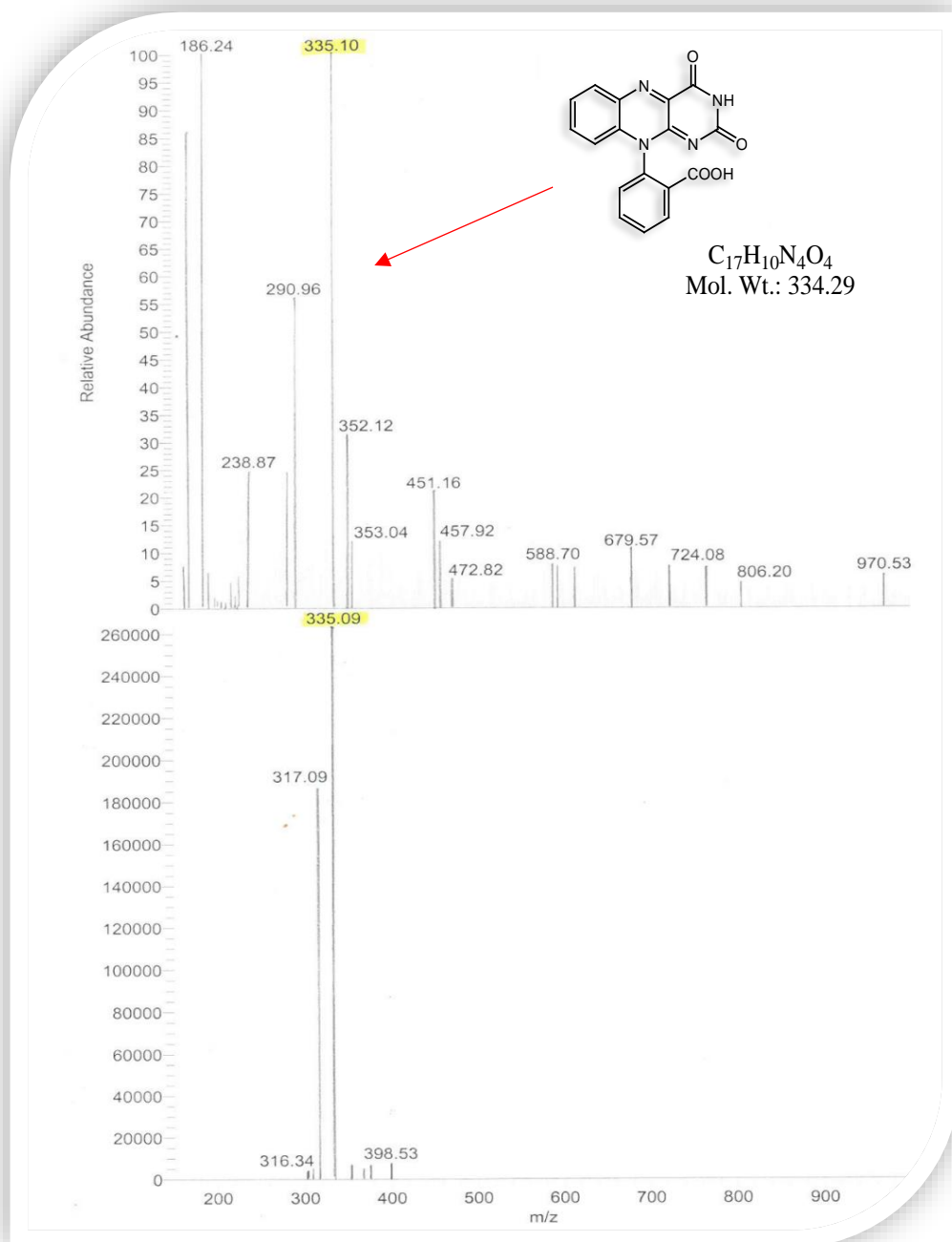


Figure 62: MS (ESI) for compound 20c

As a result of the unsuccessful achievement of compound **21a**, the isoalloxazine 10-(3-carboxyphenyl) **21c** could not be synthesised.



nitroaniline (**23a** - **25a**) as a black solid. Upon monitoring this reaction using TLC plates with silica plates and eluting with EtOAc, significant amount of impurities and starting material were observed. No visual evidence was seen to confirm the presence of the desired compound. This was further confirmed using standard spectroscopic techniques.

As neither of the compounds were synthesised successfully via this route, the reaction was repeated using microwave irradiation with the required derivatives of phenylenediamine as starting materials. However, 1-bromo-2-nitrobenzene was replaced by 1-fluoro -2-nitrobenzene due to the difference in electronegativity.

2-Phenyleneamine and 1-fluoro -2-nitrobenzene were irradiated for 3 h at 150 C in a CEM microwave at full power. The substituted (*N*-nitrophenyl)2-nitroaniline was achieved as a black solid (**13a**). The compound, 2-(nitrophenyl)-2-nitroaniline eluted second on TLC plate and was observed as an orange compound. The crude solid was purified by flash column chromatography over silica gel eluting with EtOAc to afford the pure product as dark red crystals. Isolation of the correct compound was confirmed by the standard spectroscopic techniques.

Compounds **24a** and **25a** were not successfully synthesised due to the continuous presence of both impurities and starting materials constantly observed in the <sup>1</sup>H-NMR, <sup>13</sup>C-NMR and TLC. Frequent monitoring of this reaction presented no evidence of final product at all, indicating that the reaction was not forming the required product or going to completion. The lack of formation of this product is somewhat ambiguous as nitro substituents are electron withdrawing and *meta* directors, thus the *N*-(nitrophenyl)-2-nitroaniline was expected to form easily.

### 2.20.2 Synthesis of 10-(*N*-nitrophenyl) isoalloxazines (**23c**)

10-(2-Nitrophenyl) isoalloxazine (**23c**) was accomplished using compound **23a** that was dissolved in glacial acetic acid and with constant stirring at room temperature, alloxan monohydrate and boric acid (1:1.2 mole excess) were added to the acidic solution. A yellow solid precipitated after 12 h and was isolated at the pump, to yield 10-(2-nitrophenyl) isoalloxazine, (**23c**) as a bright yellow powder, in the yield (25%) shown in Table 17.

Figure 63 shows a full mass spectrometry (MS) for compound **23c**. The *m/z* was found to be 336 M<sup>+</sup>. This confirms a successful synthesis of the substituted 10 (2-nitrophenyl) isoalloxazine.

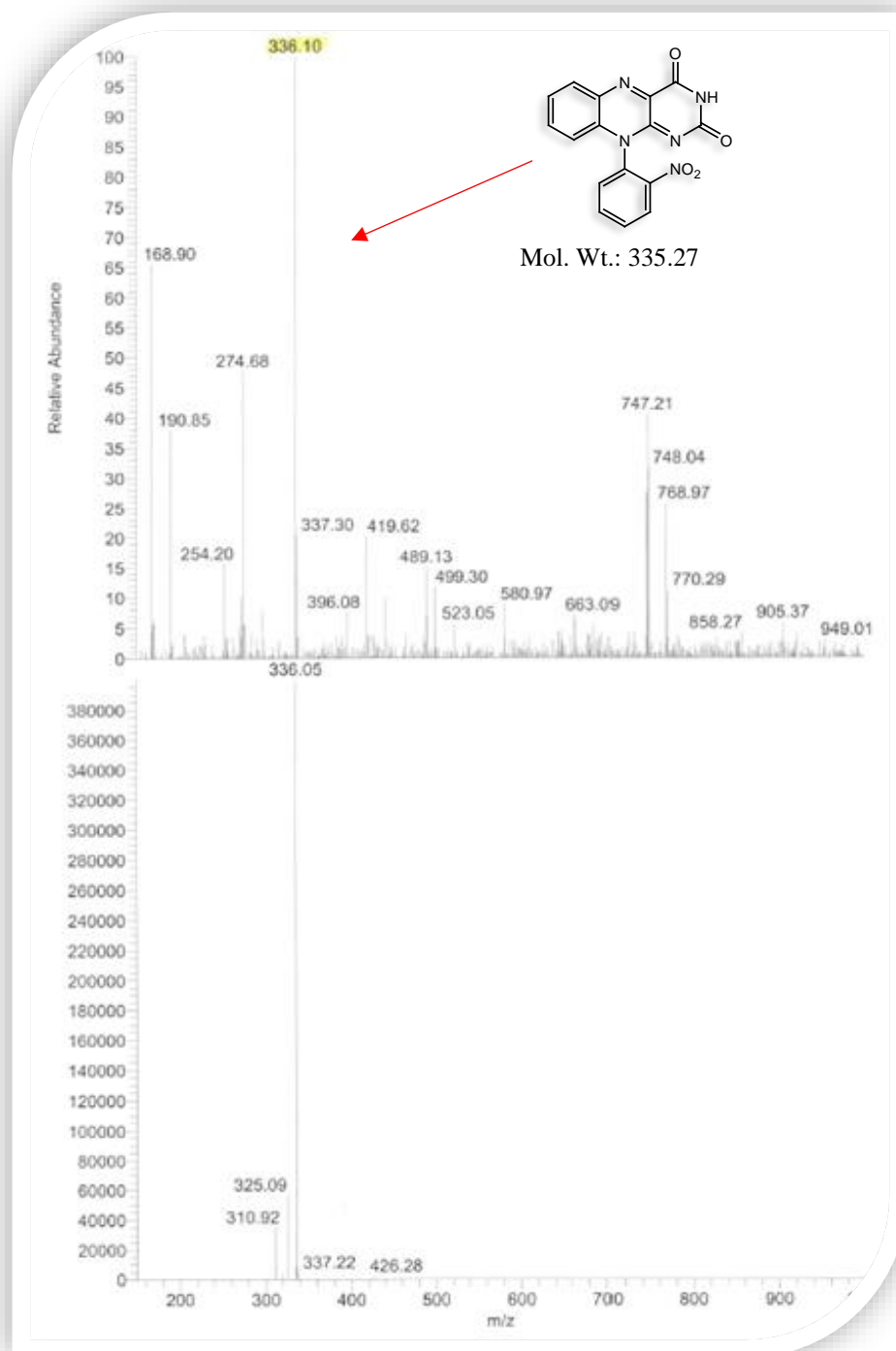


Figure 63: Mass spectrometry and msms of compound 23c

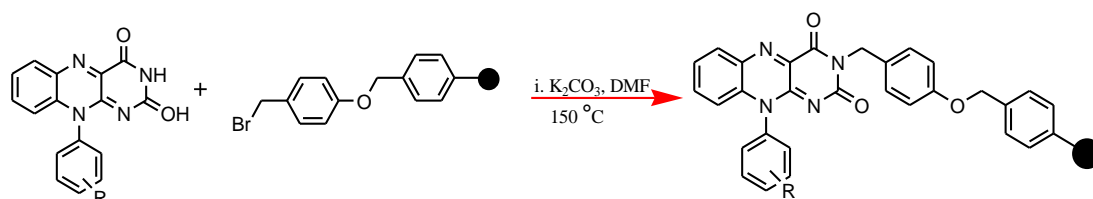
### 2.20.3 Attempted synthesis of 3, 4 isomers of 10-(N-nitrophenyl) isoalloxazine (24c and 25c)

The isoalloxazine for compound **24c** and **25c** was unfortunately not synthesised successfully for two reasons; both starting materials were seen prominently in the spectroscopy analysis indicating no change during the 2 h reaction period. The reaction was elongated by a further 3

hours, and monitored closely using TLC with silica plates eluting with EtOAc. TLC endlessly showed the presence predominantly of the starting materials. This was not surprising as nitro substituents have strong electron withdrawing properties, and therefore deactivate the benzene ring. This ultimately would not drive the reaction forward, resulting in a lack of formation in the *meta* substituted isomer. The problematic synthesis of these two isomers could be reasoned with the strong electronic effects of the nitro group. The secondary amine (NH) group is strongly electron donating, whereby the NO<sub>2</sub> moiety is strongly electron withdrawing, subsequently, both strong electronic groups are competing against one another.

## Discussion on the synthesis of polymeric isoalloxazines

The ethos of the project was to test the feasibility of generating a bandage or a material capable of destroying any microbial colonisation that appears during the healing process. In order to test this hypothesis, a Wang brominated resin was used to test this proof of principal.



Scheme 53 : Synthetic route for polymer substitution


The synthesised derivatives of *N*-substituted isoalloxazines were attached to a Wang brominated resin called 4-(benzyloxy)benzyl bromide. The *N*-substituted isoalloxazines was used in an excess ratio of 1.9:1 mmol to the Wang brominated resin.

### 2.21 Synthesis of polymer bound *N*-substituted isoalloxazines

The polymeric supports were attached to isoalloxazines derivatives by reacting the *N*-substituted isoalloxazines and dissolving in anhydrous DMF (3 mL). To this was added base,  $K_2CO_3$  in excess, and 4-(benzyloxy)benzyl bromide (0.10 g). The reaction mixture was heated at  $150\text{ }^\circ\text{C}$  overnight to afford the polymer bound product. The reaction mixture was cooled to room temperature and filtered under suction. The polymer beads were washed well with a range of polar solvents ranging from cold DMF, distilled water, ethyl acetate, methanol, acetone and finally distilled water until the washings ran clear. Subsequently, the product was dried *in vacuo* to give the weight as yellow polymeric beads.

The synthesised isoalloxazines that were attached to the polymeric support are shown in Table 18 with the weights obtained after thorough washings and drying.

Table 18: Isoalloxazines on polymer support



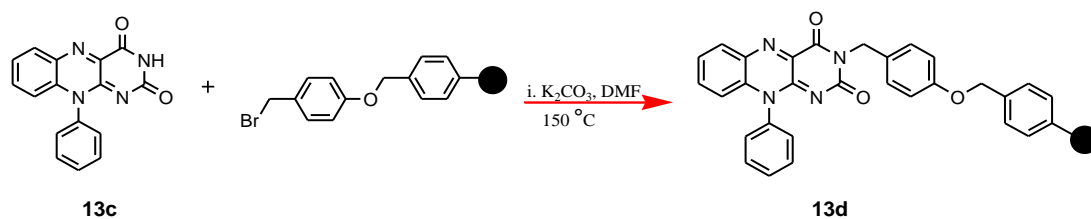
*o* = ortho, *m* = meta, *p* = para

Compound Code	<i>o</i>	<i>m</i>	<i>p</i>	Yield (g)
<b>1d</b>	NH <sub>2</sub>	H	H	0.21
<b>4d</b>	OH	H	H	0.06
<b>6d</b>	H	H	OH	0.05
<b>7d</b>	OCH <sub>3</sub>	H	H	0.14
<b>8d</b>	H	OCH <sub>3</sub>	H	0.10
<b>9d</b>	H	H	OCH <sub>3</sub>	0.16
<b>10d</b>	CH <sub>3</sub>	H	H	0.25
<b>11d</b>	H	CH <sub>3</sub>	H	0.22
<b>12d</b>	H	H	CH <sub>3</sub>	0.27
<b>13d</b>	H	H	H	0.23
<b>14d</b>	Cl	H	H	0.06
<b>15d</b>	H	Cl	H	0.03
<b>16d</b>	H	H	Cl	0.03
<b>17d</b>	OTS	H	H	0.04
<b>18d</b>	H	OTS	H	0.03
<b>19d</b>	H	H	OTS	0.02
<b>20d</b>	COOH	H	H	0.06
<b>23d</b>	NO <sub>2</sub>	H	H	0.02

In order to confirm the substitution of the polymer support onto the amide moiety of each of the isoalloxazines, infrared spectroscopy was used to determine the presence of the functional groups from both the *N*-substituted isoalloxazine and the Wang brominated resin. Thus, IR spectra of each of the starting material was taken in order to compare the appearance/disappearance of additional peaks from the polymer bound isoalloxazine.



## 2.22 10-Phenylisoalloxazine-polymer bound (**13d**)



Scheme 54: Polymer synthesis of compound **13d**

Table 19: Polymer yield of 10-phenyl isoalloxazine

Compound	<i>o</i> (R <sub>1</sub> )	<i>m</i> (R <sub>2</sub> )	<i>p</i> (R <sub>3</sub> )	Yield (g)
<b>13d</b>	H	H	H	0.23

Compound **13d** was synthesised in a yield of 0.23 g as yellow polymeric beads via the method described in section 2.21.

Figure 64 and Figure 65 show IR spectra for compounds **13c** and the Wang brominated resin, 4-(benzyloxy)benzyl bromide respectively, which were used as the starting materials for the substitution reaction of the polymer onto the isoalloxazine.

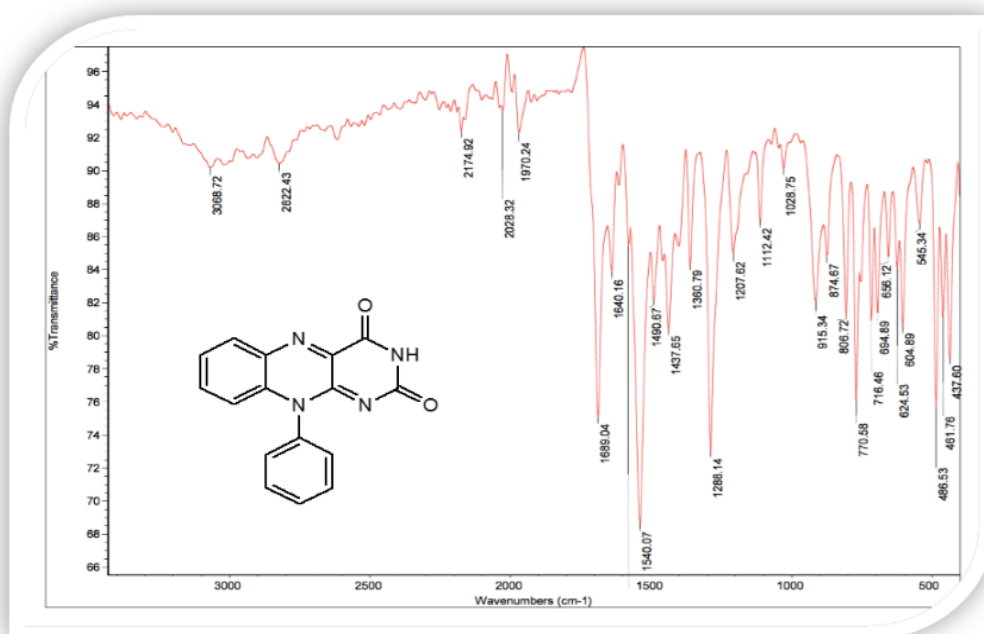
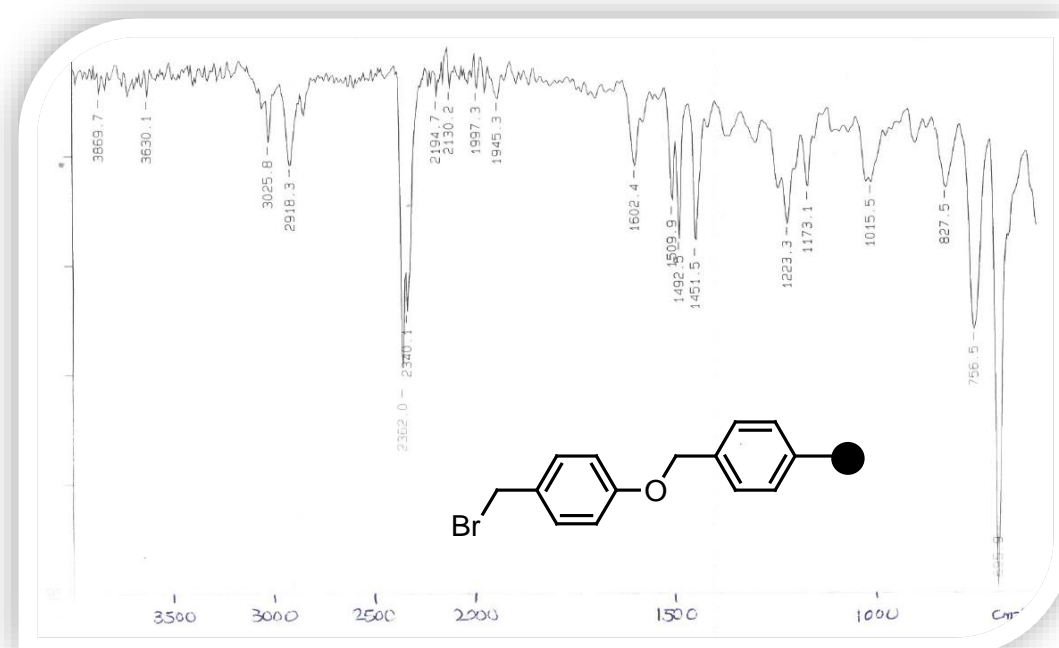


Figure 64: IR spectrum for 10-phenyl isoalloxazine - identical to Figure 47

The functional groups present in compound **13c** (Figure 64) have been discussed previously in section 2.9. Figure 64 is shown again in order to compare the additional peaks attributed to 4-(benzyloxy)benzyl bromide.

Figure 65 illustrates the IR spectra for the polymer; 4-(benzyloxy)benzyl bromide. The bands appearing at  $3025\text{ cm}^{-1}$  and  $2918\text{ cm}^{-1}$  are attributed to the C-H bonds from the aromatic ring. The sharp peaks seen at  $2362\text{ cm}^{-1}$  and  $2340\text{ cm}^{-1}$  indicates the presence of an asymmetric stretch of C-O. The peak at  $1602\text{ cm}^{-1}$  is attributed to the C-C bonds from the aromatic rings. The bands seen at  $1509\text{ cm}^{-1}$ ,  $1492\text{ cm}^{-1}$  and  $1451\text{ cm}^{-1}$  correspond to the aromatic C=C bonds. The peaks showing at  $1223\text{ cm}^{-1}$  and  $1173\text{ cm}^{-1}$  are attributed to the alkyl halide,  $(\text{CH}_2\text{X})$  stretch of  $\text{CH}_2\text{O}$ . The peak seen at  $1015\text{ cm}^{-1}$  corresponds to the C-O stretch and the bands at  $827\text{ cm}^{-1}$  and  $756\text{ cm}^{-1}$  are characteristic of the C-H aromatic out of plane stretch bands. The sharp peak at  $695\text{ cm}^{-1}$  indicates the presence of an alkyl halide (C-Br).



*Figure 65: IR spectra of Wang brominated resin 4-(benzyloxy)benzyl bromide*

The newly synthesised isoalloxazine compound 10-phenyl isoalloxazine on a polymer support, (**13d**) is illustrated in the IR spectra labelled Figure 66. This confirms the correct function groups are present for the synthesised molecule.

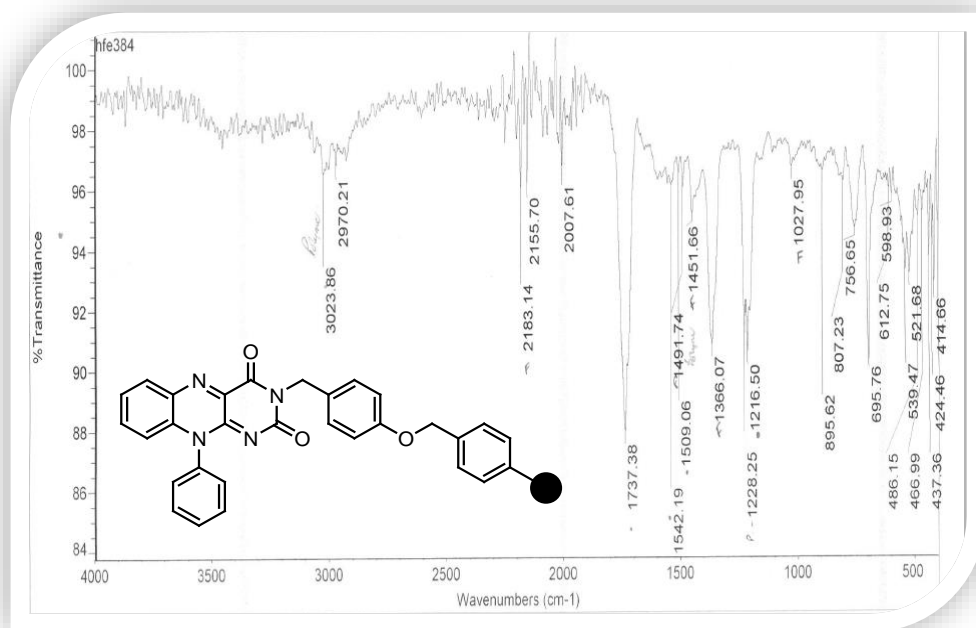
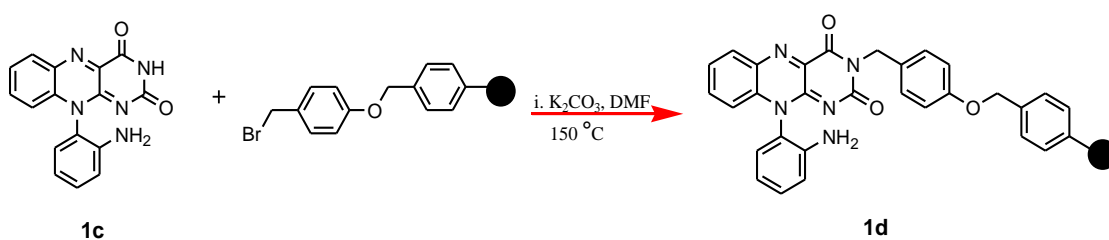


Figure 66: IR spectra of compound 13d

This IR reveals the main functional groups corresponding to compound **13d**. The peak present at  $\gamma$ : 3023 cm<sup>-1</sup> and 2970 cm<sup>-1</sup> indicates the presence of C-H groups and is present in both compound **13c** and the Wang brominated resin. The bands at 2183 cm<sup>-1</sup> and 2155 cm<sup>-1</sup> and 2007 cm<sup>-1</sup> are weak overtones that correlate to aromatic C-H bonds. The sharp peak at 1737 cm<sup>-1</sup> is attributed to the carbonyl (C=O) group belonging to the amide moiety and was not present in either of the IR's of the starting materials. The peaks seen at 1542 cm<sup>-1</sup>, 1509 cm<sup>-1</sup>, 1491 cm<sup>-1</sup>, and 1437 cm<sup>-1</sup> correlate to the aromatic C=C bonds from the aromatic rings. The C-C stretch (in ring) from aromatic rings is seen at 1451 cm<sup>-1</sup>. The sharp peak arising at 1366 cm<sup>-1</sup> corresponds to the C-N as an aryl stretch. The bands appearing at 1228 cm<sup>-1</sup>, 1216 cm<sup>-1</sup>, and 1027 cm<sup>-1</sup> are due to C-H in-plane bending of the aromatic rings. The out of plane bending bands appearing intensely in the fingerprint region at 823 cm<sup>-1</sup>, 755 cm<sup>-1</sup>, and 695 cm<sup>-1</sup> are attributed to the C-H stretch.

A key feature to note in the IR spectra of each of the polymer bound isoalloxazines is the disappearance of a significant sharp peak (Figure 66) in the region of 1680-1630 cm<sup>-1</sup>, however in this Figure 66, it is evident that a reduction in the peak has occurred, yet a small peak is visible, which is a result of the excess polymer used during the synthesis of the polymer to the isoalloxazine. Nonetheless, the disappearance or a vast reduction of this sharp peak typically indicates the disappearance of the amide functional group proving substitution of the polymer was successful.

## 2.23 *N*-Amino derivative of 10-phenylisalloxazine-polymer bound (**1d**)



*Scheme 55: Polymer synthesis of compound 1d*

Table 20: Polymer yield of 10-(2-aminophenyl) isoalloxazine derivatives

Compound	<i>o</i> (R <sub>1</sub> )	<i>m</i> (R <sub>2</sub> )	<i>p</i> (R <sub>3</sub> )	Yield (g)
<b>1d</b>	NH <sub>2</sub>	H	H	0.21

Compound **1d** was synthesised via the method described in 2.21. The starting material used for this synthesis was compound **1c** and Wang brominated resin. Compound **1d** was synthesised in 0.21 g as yellow polymeric beads. The IR spectra for compound **1d** is shown in Figure 67.

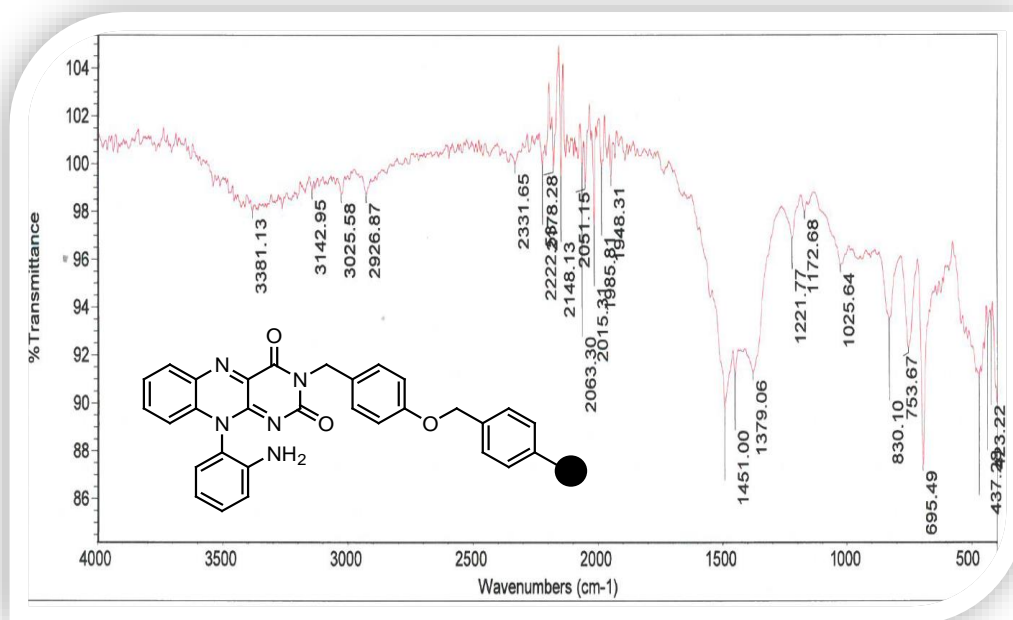
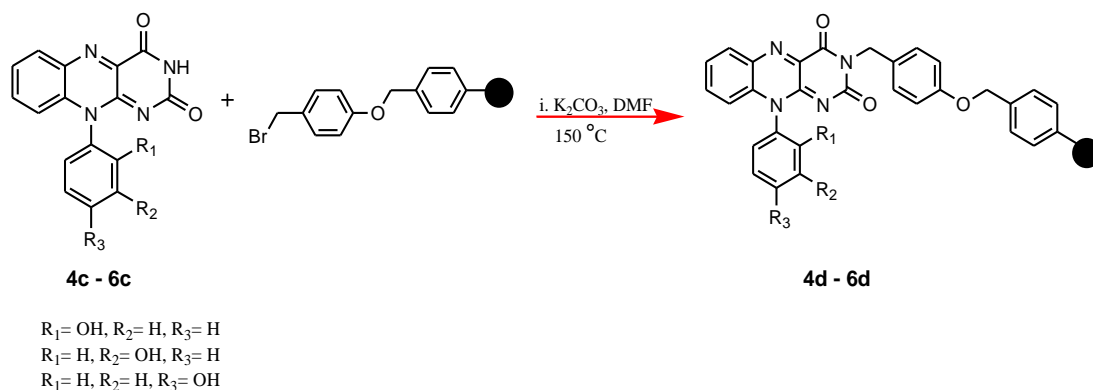


*Figure 67: IR spectra of compound 1d*

The broad band in Figure 67 seen at  $\gamma$ : 3381  $\text{cm}^{-1}$  corresponds to 1° amine stretch. The bands appearing at 1221  $\text{cm}^{-1}$ , 1172  $\text{cm}^{-1}$  correspond to the CH<sub>2</sub>O group from the polymer. The

disappearance of the sharp peak at  $\sim 1680\text{-}1630\text{ cm}^{-1}$  (amide functional group) proves successful substitution of the polymer onto the *o*-amino isoalloxazine resulting in compound **1d**.

## 2.24 *N*-Hydroxy derivatives of 10-phenylisoalloxazine-polymer bound (**4d** and **6d**)



*Scheme 56: Polymer synthesis of compounds 4d-6d*

Table 21: Polymer yields of hydroxyphenyl isoalloxazine derivatives

Compound	<i>o</i> ( $R_1$ )	<i>m</i> ( $R_2$ )	<i>p</i> ( $R_3$ )	Yield (g)
<b>4d</b>	OH	H	H	0.06
<b>6d</b>	H	H	OH	0.05

Compounds **4d** and **6d** were accomplished via the method described in 2.21. The starting materials used for the synthesis of each compound were **4c** and **6c** and the Wang brominated resin. These compounds (**4d** and **6d**) were synthesized as yellow polymeric beads in yields shown in Table 21.

The IR spectra for compounds **4d** is shown in Figure 68. The peaks shown for compound **4d** at  $\gamma$ :  $3025 \text{ cm}^{-1}$  corresponds to the alkene ( $=\text{C-H}$ ) stretches. The peak at  $1673 \text{ cm}^{-1}$  indicates the presence of alkane  $\text{C}=\text{C}$  stretch. The bands seen at  $1601 \text{ cm}^{-1}$ , and  $1554 \text{ cm}^{-1}$  correspond to the amide functional groups as well as a peak at  $1511 \text{ cm}^{-1}$  corresponding to the presence of  $1^\circ$  amine stretch. The bands at  $1223 \text{ cm}^{-1}$  and  $1090 \text{ cm}^{-1}$  identify the presence of a  $\text{C-N}$  stretch. Strangely no typical characteristic peak for the hydroxyl functional group is seen in the range of  $3600 \text{ cm}^{-1} - 3300 \text{ cm}^{-1}$ . The disappearance of the peak at  $\sim 1680\text{-}1630 \text{ cm}^{-1}$  (amide functional group) confirms substitution of the polymer to the isoalloxazine (**4d**).

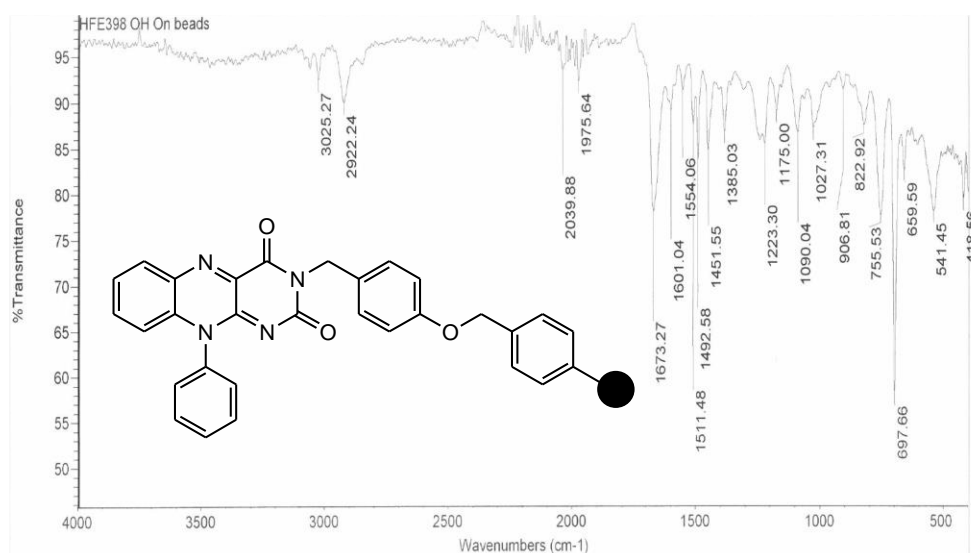
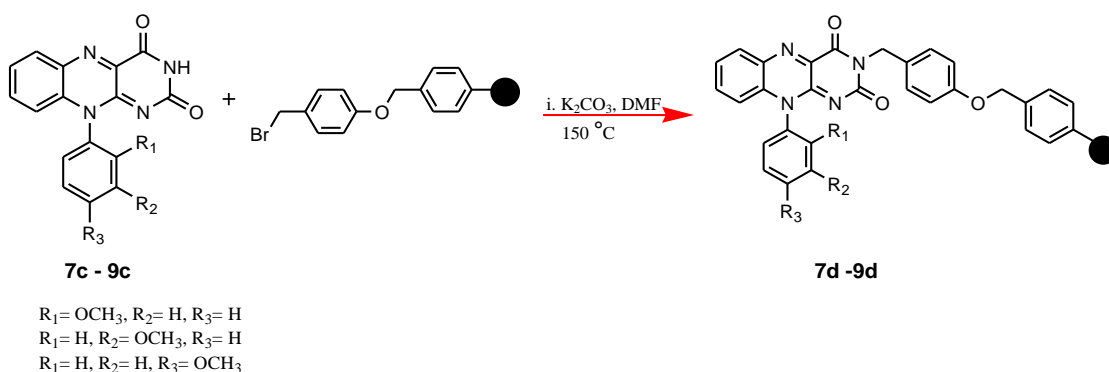


Figure 68: IR spectra compounds 4d-6d

IR spectrum for compound **6d** was accomplished in a yield of 0.05 g as yellow polymeric beads. Similar peaks as **4d** are observed in the spectrum. The correct peaks attributing to the functional groups present in **6d** were identified (see experimental section 6.38). This spectrum also showed the disappearance of a peak at ~1680-1630 cm<sup>-1</sup> indicating the successive substitution of the polymer to the *p*-hydroxyphenyl isoalloxazine (**6d**).

## 2.25 *N*-Methoxy derivatives of 10-phenylisoalloxazine-polymer bound (**7d–9d**)



*Scheme 57: Polymer synthesis of compounds 7d-9d*

Table 22: Polymer yields of methoxyphenyl isoalloxazine derivatives

Compound	<i>o</i> ( $R_1$ )	<i>m</i> ( $R_2$ )	<i>p</i> ( $R_3$ )	Yield (g)
<b>7d</b>	OCH <sub>3</sub>	H	H	0.14
<b>8d</b>	H	OCH <sub>3</sub>	H	0.10
<b>9d</b>	H	H	OCH <sub>3</sub>	0.16

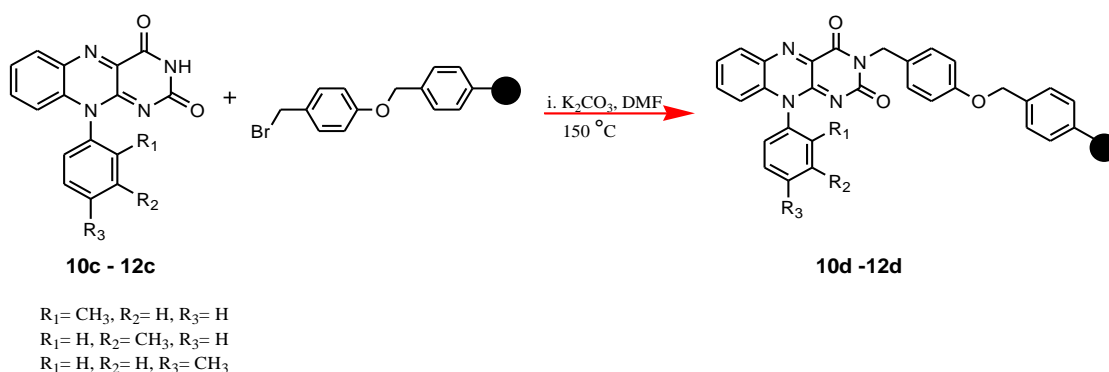
The synthesis of compounds **7d** and **9d** was accomplished via the method described in 2.21. The starting materials used for the synthesis were compounds **7c** and **9c**, which was reacted with the Wang brominated resin. These compounds (**7d** and **9d**) were synthesised as yellow polymeric beads in yields shown in Table 22.

To confirm substitution of the Wang brominated resin onto the isoalloxazine an IR spectra was used to identify the functional groups present. The disappearance of the most important at  $\sim 1680\text{-}1630\text{ cm}^{-1}$  attributed to the amide functional group indicated the polymer was substituted onto the *N*-methoxyphenyl isoalloxazines (**7d** and **9d**).

For both these compounds the IR spectra showed a band at  $1736\text{ cm}^{-1}$  which was attributed to the C=O stretch. An intense peak seen at  $1673\text{ cm}^{-1}$  corresponds to an amide C=O stretch. Compound **7d** identifies a peak at  $1384\text{ cm}^{-1}$  indicating the presence of N-O stretch. Both compounds recorded a peak at  $1225\text{ cm}^{-1}$ ,  $1174\text{ cm}^{-1}$  identifying the presence of a CH<sub>2</sub>O functional group. The bands at  $\sim 1216\text{ cm}^{-1}$  and  $1092\text{ cm}^{-1}$  identifies the presence of a C-N stretch. The spectra for these compounds can be seen in the experimental section 6.39.



## 2.26 *N*-Tolyl derivatives of 10-phenylisoalloxazine-polymer bound (**10d–12d**)



*Scheme 58: Polymer synthesis of compounds 10d-12d*

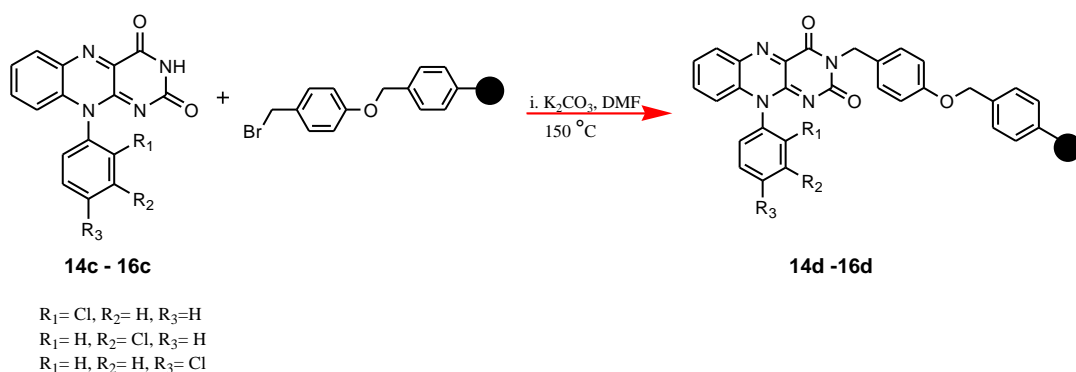
Table 23: Polymer yields of tolylphenyl isoalloxazine derivatives

Compound	<i>o</i> ( $R_1$ )	<i>m</i> ( $R_2$ )	<i>p</i> ( $R_3$ )	Yield (g)
<b>10d</b>	CH <sub>3</sub>	H	H	0.25
<b>11d</b>	H	CH <sub>3</sub>	H	0.22
<b>12d</b>	H	H	CH <sub>3</sub>	0.27

The synthesis of compounds **10d-12d** was accomplished via the method described in 2.21. The starting materials used for the synthesis were compounds **10c-12c** and the Wang brominated resin. These compounds (**10d-12d**) were synthesised as yellow polymeric beads in yields shown in Table 23.

The IR spectra of compounds **10d-12d** show the correct peaks present for the functional groups of the synthesised molecules on the polymer support. A peak at 1669 cm<sup>-1</sup> corresponds to an amide C=O stretch. The band at 1220 cm<sup>-1</sup> indicates the presence of C-N stretch of an aromatic amine. For compound **11d** presented peaks at  $\nu$ : 3559 cm<sup>-1</sup>, 3449 cm<sup>-1</sup>, and 3291 cm<sup>-1</sup> attributing to an amide (N-H) stretch. For the tolyl series, bands were seen at ~1491 cm<sup>-1</sup> is attributing to aromatics (in ring) C-C stretch and the presence of a weak band at 1450 cm<sup>-1</sup> corresponded to the aromatic C=C stretch. Peaks were also seen in the range of 1228 cm<sup>-1</sup>, 1216 cm<sup>-1</sup>, and 1018 cm<sup>-1</sup> identifying the presence of a C-N stretches for these molecules. For each of the polymer substituted *N*-tolyl derivatives no presence of peaks at ~1680-1630 cm<sup>-1</sup> were evident, thus concluding the polymer support was substituted onto the *N*-tolylphenyl isoalloxazine's (**10d-12d**).

## 2.27 *N*-Chloro derivatives of 10-phenylisoalloxazine-polymer bound (**14d-16d**)



*Scheme 59: Polymer synthesis of compounds 14d-16d*

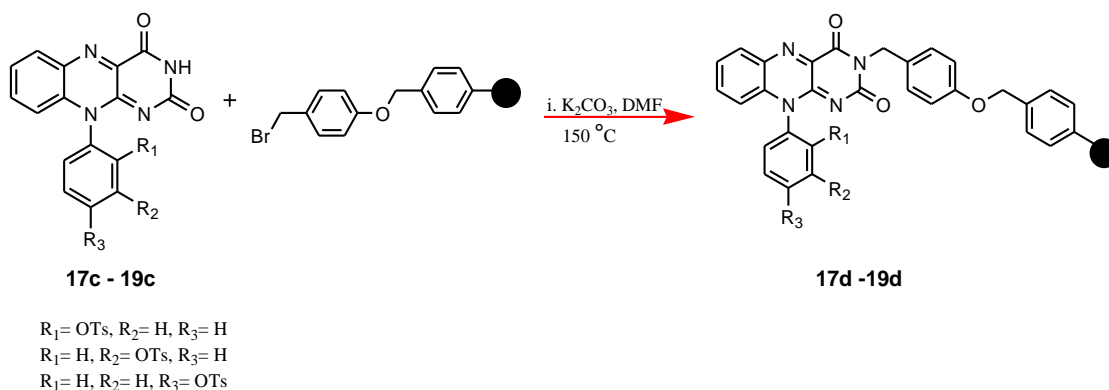
Table 24: Polymer yields of chlorophenyl isoalloxazine derivatives

Compound	<i>o</i> ( $R_1$ )	<i>m</i> ( $R_2$ )	<i>p</i> ( $R_3$ )	Yield (g)
<b>14d</b>	Cl	H	H	0.06
<b>15d</b>	H	Cl	H	0.03
<b>16d</b>	H	H	Cl	0.03

The synthesis of compounds **14d-16d** was accomplished via the method described in 2.21. The starting materials used for the synthesis were compounds **14c-16c** and the Wang brominated resin. These compounds (**14d-16d**) were synthesised as yellow polymeric beads in yields shown in Table 24.

The substitution of polymer support to the each of the substituted *N*-chlorophenyl isoalloxazines (**14d-16d**) was confirmed by IR spectroscopy. The absence of a peak appearing at  $\sim 1680\text{-}1630\text{ cm}^{-1}$  attributed to the amide functional group confirmed substitution of the polymer support onto each of the isoalloxazine. The IR spectra showed a band at  $2358\text{ cm}^{-1}$  indicating the presence of an asymmetric stretch of a C-O. Peaks observed at  $\sim 1223\text{ cm}^{-1}$  are attributed to the presence of a  $\text{CH}_2\text{O}$  functional group. For each of the synthesised compounds (**14d-16d**) the IR spectra showed functional groups corresponding to the synthesised compounds and can be seen in section 6.41.

## 2.28 *N*-Tosyloxy derivatives of 10-phenylisoalloxazine-polymer bound (**17d**–**19d**)



*Scheme 60: Polymer synthesis of compounds 17d-19d*

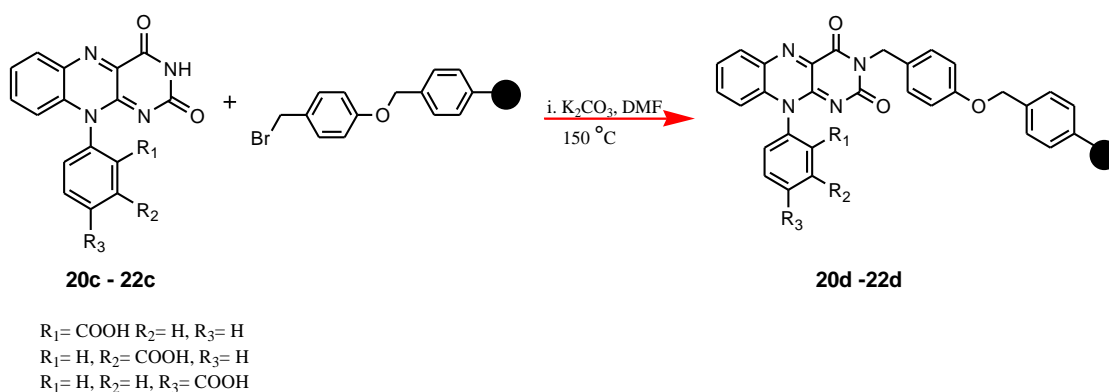
Table 25: Polymer yields of tosyloxyphenyl isoalloxazine derivatives

Compound	<i>o</i> ( $R_1$ )	<i>m</i> ( $R_2$ )	<i>p</i> ( $R_3$ )	Yield (g)
<b>17d</b>	OTs	H	H	0.04
<b>18d</b>	H	OTs	H	0.03
<b>19d</b>	H	H	OTs	0.02

Compounds **17d-19d** was achieved using the synthetic method discussed in section 2.21. Compounds **17c-19c** were used as the starting materials for the synthesis were and reacted with the Wang brominated resin. These compounds (**17d-19d**) were synthesised as yellow polymeric beads in yields shown in Table 25.

The IR spectra of compounds **17d-19d** show the correct peaks present for the functional groups of the synthesised molecules on the polymer support. The presence of an amide C=O stretch is observed by a peak appearing at  $1669\text{ cm}^{-1}$  and at  $1220\text{ cm}^{-1}$  indicates the presence of C-N stretch of an aromatic amine. For the tolyloxy series, bands were seen at  $\sim 1491\text{ cm}^{-1}$  is attributing to aromatics (in ring) C-C stretch and the presence of weak bands at  $1450\text{ cm}^{-1}$  corresponded to the aromatic C=C stretch. For each of the polymer substituted *N*-tosyloxyphenyl derivatives no presence of peaks at  $\sim 1680\text{-}1630\text{ cm}^{-1}$  presenting evidence of successful substitution of the polymer support onto the *N*-tosyloxyphenyl isoalloxazine's (**17d-19d**).

## 2.29 N-Carboxy derivative of 10-phenylisoalloxazine-polymer bound (**20d**)



*Scheme 61: Polymer synthesis of compounds 20d-22d*

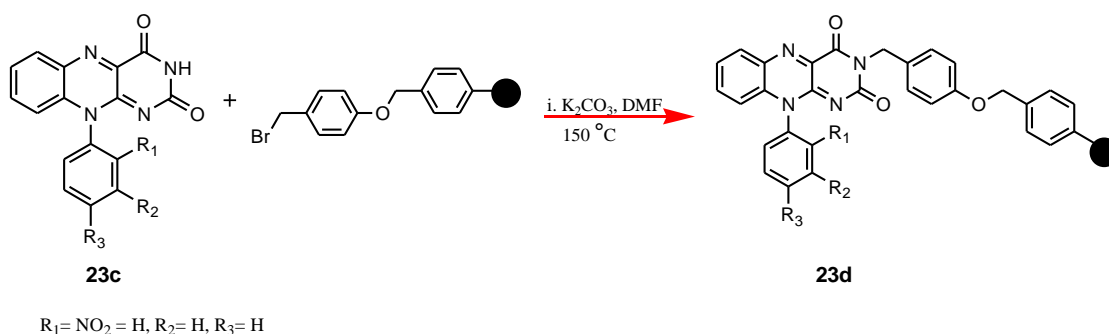
Table 26: Polymer yields of carboxyphenyl isoalloxazine

Compound	<i>o</i> ( $R_1$ )	<i>m</i> ( $R_2$ )	<i>p</i> ( $R_3$ )	Yield (g)
<b>20d</b>	COOH	H	H	0.06

The synthetic pathway used to accomplish compound **20d** was the method described in 2.21. The starting materials used for the synthesis of **20d** were compounds **20c** and the Wang brominated resin. This compound (**20d**) was synthesised as yellow polymeric beads in (0.06 g) yield shown in Table 26.

IR spectroscopy was used to determine the successful synthesis of compound **20d**. The peaks shown for compound **20d** presented peaks for the functional groups present in this molecule. The disappearance of the peak at  $\sim 1680\text{-}1630\text{ cm}^{-1}$  corresponding to the amide functional group confirms substitution of the polymer to the isoalloxazine (**20d**). The IR data for this compound can be in section 6.43.

### 2.30 *N*-Nitro derivative of 10-phenylisoalloxazine-polymer bound (**23d**)



*Scheme 62 Polymer synthesis of compound 23d*

Table 27: Polymer yields of nitrophenyl isoalloxazine derivatives

Compound	<i>o</i> ( $R_1$ )	<i>m</i> ( $R_2$ )	<i>p</i> ( $R_3$ )	Yield (g)
<b>23d</b>	NO <sub>2</sub>	H	H	0.02

The synthesis of compound **23d** was accomplished via the method described in 2.21. The starting materials used for the synthesis were compounds **23c** and the Wang brominated resin. This compound (**20d**) was synthesised in as yellow polymeric beads in yield shown in Table 27.

The substitution of polymer support to the 2-nitrophenyl isoalloxazines was confirmed by IR spectroscopy. The absence of a peak appearing between ~1680-1630 cm<sup>-1</sup> attributed to the amide functional group confirmed substitution of the polymer support onto the isoalloxazine. The IR spectrum of **23d** showed a band appearing at 2360 and 2339 cm<sup>-1</sup> identifies the presence of an asymmetric stretch of C-O, a band seen at 1342 cm<sup>-1</sup> corresponds to the C-N aryl stretch. All other peaks confirmed the correct functional groups were present for compound **23d**.

The antimicrobial activity of compound **23d** presents encouraging results as partial antimicrobial activity was recorded. It was promising to observe a reduction in microbial growth for the gram negative organism. This compound also presented complete cellular death towards *S.aureus* and an MIC was recorded at 1 mM/mL. Knowing this compound can present biocidal effects whilst attached to the polymer support is extremely encouraging as this will help achieve new successful antimicrobial agents to be used potentially in hospital environments.

### 3.1 Singlet oxygen and radical producers

The absorbance window of the synthesised isoalloxazine is between 432-437 nm. Thus, suited markers for detection of singlet oxygen/radicals was selected by insuring the absorbance was not within this region. For this research the designated absorbance range for singlet oxygen markers was between 410 and 500 nm (Table 29). This assured avoidance of markers overlapping the absorbance of the synthesised isoalloxazine and would aid determination of the singlet oxygen being generated by the investigative isoalloxazines.

### 3.2 Solubility studies

Solubility studies showed that each of the synthesised isoalloxazines dissolved readily in numerous solvents. However, a number of difficulties arose with the solubility of alloxazine. Alloxazine was insoluble in all solvents in which the synthesised isoalloxazines were soluble in. Numerous solvent studies identified that alloxazine completely dissolved in DMSO. Subsequently, all experiments monitoring the singlet oxygen/radical production was conducted in DMSO.

### Table of solvents testing solubility on isoalloxazines and alloxazine

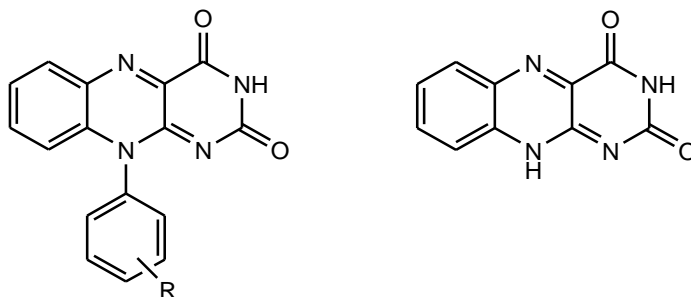


Table 28: Solubility studies

Solvent	Isoalloxazines dissolved or not	Alloxazine dissolved or not
Water	√	X
Dimethylsulfoxide (DMSO)	√	√
Dimethylformamide (DMF)	√	Partially
Acetonitrile	√	X
Methanol	√	X
Ethanol	√	X
Acetone	√	X
Ethyl acetate	√	X
Chloroform	√	X
Dichloromethane	√	X
Diethyl ether	Partially	X
Toluene	X	X
Petroleum ether	X	X
Hexane	X	X

### 3.3 Light Source

Three types of light sources were initially used to irradiate the photosensitisers. These being a white strip light (fluorescence tube - 40W), a desk lamp (filament lamp – 40W) and a blue light with LED's (10 X 9 LED, with a power output of 19 lumens). Evaluating use of the white fluorescent light, it was noticed that majority of illuminated light was not possible to be absorbed by the cuvette (with the photosensitiser solution) due to the width of the cuvette and thus wasted. Although these white fluorescent lights contain a diffuser, the actual intensity of light absorbed by the solution was impossible to be determined. As the exact amount of light absorbed by both the isoalloxazines and singlet oxygen marker was unknown, the use of the white strip fluorescent light was eliminated.

An additional reason for the removal of the white fluorescent light is the range at which white light absorbs at. For the purpose of this project, the focus of these novel synthesised photosensitizers was to ideally achieve activation in the absorbance range of 440 nm to 490 nm, thus blue light being ideal to illuminate the photosensitizers with, particularly as new photosensitizers are attractive in the modern era of PDT<sup>343</sup>.

In replacement of the fluorescent strip light, a desk lamp was used. This designated a neat set up to use a black box to cover the lamp and allow all light intensity to be absorbed by the isoalloxazines and the singlet oxygen and radical marker.

Blue LED light was used to ensure irradiation of isoalloxazines at a different wavelength than the white light. This facilitated a comparison study of singlet oxygen production in blue and white light.



*Figure 69: Blue LED Lights*

### 3.4 Wavelength of Light

The distance of light positioning was important and monitored using preliminary tests. This was investigated by testing the singlet oxygen generated at a range of distances. Additional factors considered for this study were the type and power of the light used. The combination of these together aided evaporation of the solvent (from the cuvette) used for monitoring the singlet oxygen production. Monitoring the light distance was vital as evaporation of the solvent affected the results achieved. Subsequently, inconclusive results were obtained within the preliminary studies due to this finding. As a result of this, it was important to keep the cuvette covered with the lid and parafilm to ensure no evaporation or leakages occurred during the illumination period of the experiment.



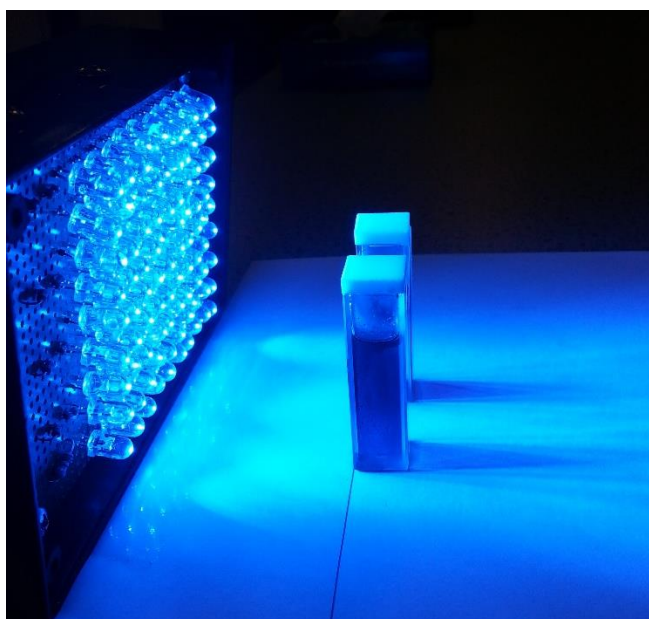


Figure 70: Irradiation using blue LED light at 5 cm distance

### 3.5 Selectivity of singlet oxygen markers

The selection of a correct singlet oxygen marker was important as this research was predominantly based on the study of singlet oxygen generation by the synthesised isoalloxazines (within the therapeutic window). Table 29 shows a range of known markers used as detectors of singlet oxygen.

Table 29: Singlet oxygen markers and producers

Marker	Wavelength (nm)	Emission (nm)
Alloxazine	355 in acetonitrile	432
Dibenzofuran	320	
Indocyanine green (ICG)	600-900	830
1,3-Diphenylisobenzofuran (DPIBF)	420	455/477
<i>p</i> -Nitrosodimethylaniline ( <i>p</i> -RNO)	440	
Riboflavin	445 in phosphate buffer 443 in CH <sub>3</sub> OD/ CH <sub>3</sub> OH	514
3-Ethyl-2-[7-(3-ethyl-2-benzothiazolinylidene)-1,3,5-heptatrienyl]benzothiazolium iodide, DTTC iodide, DTTCI (DiSC <sub>2</sub> (7)	765 in phosphate buffer 347 in CH <sub>3</sub> OD	800
2,3,4,5-tetraphenylcyclopentadienone (TPCPD)	506	

Although alloxazine is a singlet oxygen marker, it is difficult to determine whether the synthesised isoalloxazines also behave as singlet oxygen markers especially as these compounds are synthesised as ‘novel isoalloxazines’ for this project. This hypothesis is made, as there are similarities in the chemical structure between alloxazine and isoalloxazines. For the purpose of this project, alloxazine was not selected as the singlet oxygen marker because its absorption window is very close to the synthesised isoalloxazines, which could possibly show an overlap in the actual absorbance of isoalloxazines.

Dibenzofuran and DPIBF are known common markers. Both of which could not be used as dibenzofuran has a low absorbance, and DPIBF would pose a risk of overlap as its absorbance is very close to the synthesised isoalloxazines.

ICG (Figure 71) is commonly used as an angiographic agent and has interesting photochemical properties such as strong absorption, between 600 – 900 nm<sup>344</sup>. This absorption range is beneficial for this research (melanine does not absorb in this region), as deep penetration into tissues is possible<sup>345</sup>. Absorbance of ICG indicates that it operates in near infrared (NIR), in which tissues are much more translucent than in visual wavelengths.

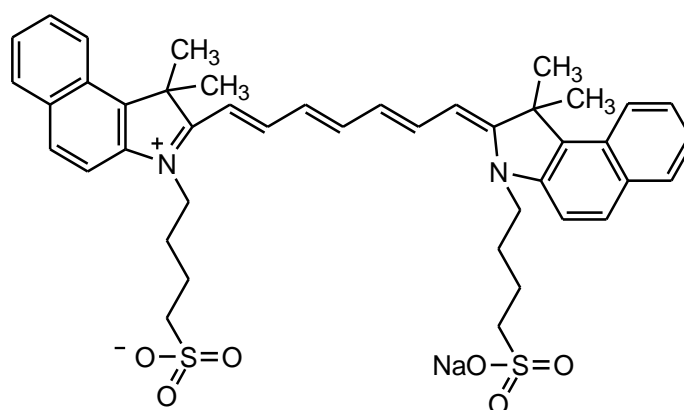


Figure 71: Chemical structure of indocyanine green

Initially, ICG was used to run preliminary tests against the isoalloxazines to monitor singlet oxygen production. However, upon analysis, it was noted that ICG could not be used, as it is a singlet oxygen generator itself. Thus, a new marker had to be selected to continue these studies.

*p*-RNO, was also not the selected marker for use, because an overlap in absorbance between *p*-RNO and the investigative isoalloxazine would occur, as *p*-RNO absorbs at 440 nm.

Alloxazine in this research was used as a standard against other singlet oxygen generators. It was represented as a 100% singlet oxygen producer to aid comparison between the synthesised flavins.

Flavins are derived from the tricyclic heterocyclic rings called isoalloxazine. The biochemical source of isoalloxazine is vitamin B2, known as riboflavin. Riboflavin is found in the body and it exists as co-enzymes. The co-enzyme behaves as the electron shuttle. Riboflavin can be synthesised in bacteria, fungi, plants and in some animals. Mammals have lost the ability to make it. Instead, for humans riboflavin is usually obtained from food.

Riboflavin (Figure 40) and DTTC iodide, a size 7 dye (Figure 72) were not selected for use as they both generate singlet oxygen, instead of quenching.

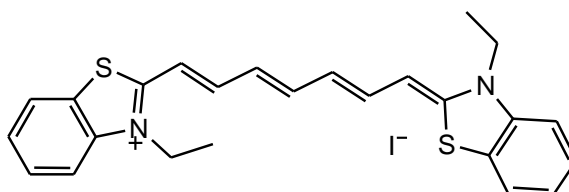


*Figure 72: Chemical structure of DTTC iodide*

The nominated marker to monitor singlet oxygen generated by the synthesised isoalloxazines is 2,3,4,5-tetraphenylcyclopentadienone (TPCPD), illustrated in Figure 73, and 2,2-diphenyl-1-(2,4,6-trinitrophenyl) hydrazyl (DPPH) is the selected marker to monitor the radical formation. Both of these markers absorb in ranges where no overlap can occur with the synthesised isoalloxazine.

### 3.6 Absorption spectroscopy

Double beam Shimadzu UV-2450 Scan UV-Visible spectrophotometer was used to record the absorption spectra over a wavelength range 200–800 nm using quartz 1 cm<sup>3</sup> by 1 cm<sup>3</sup> cuvettes for measurements in solution. Blue LED light (10 X 9 (In built)) with a power output of 19 lumens.

### 3.7 Selected markers for monitoring the generation of singlet oxygen

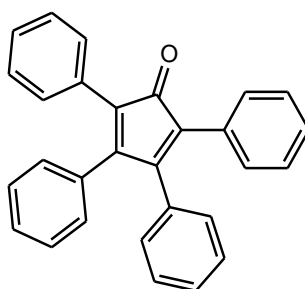


Figure 73: Chemical structure of TPCPD

2,3,4,5-Tetraphenylcyclopentadienone (TPCPD), illustrated in Figure 73 is the nominated marker to monitor singlet oxygen generation for the purpose of this study as it absorbs in the range (506 nm) where no overlap in absorbance is possible with the synthesised isoalloxazines.

The singlet oxygen yield for all derivatives was calculated using Equation 2. The efficiency of photosensitisation is calculated by the time taken for a 50% decrease in absorption of all the derivatives under the same experimental conditions, ( $t_{1/2 \text{ Der}}$ ). Thus, for these calculations the photosensitisation of alloxazine ( $t_{1/2 \text{ ALL}}$ ) was taken to be at 1.0, or 100% for the DPPH or TPCPD absorption to decrease by 50%.

$$\Phi_{\Delta \text{ Der}} = \Phi_{\Delta \text{ ALL}} \cdot \frac{(t_{1/2 \text{ ALL}})}{(t_{1/2 \text{ Der}})} \quad \text{Equation 2}$$

### 3.8 TPCPD - Singlet oxygen quencher

The decolourisation of a photosensitiser called 2,3,4,5-tetraphenylcyclopentadienone (TPCPD, Figure 73) in DMSO, was assayed to measure the singlet oxygen production using blue light. This was done by monitoring the reduction of absorption spectrophotometrically at 506 nm, using the Cincotta *et al* method<sup>147</sup>.

### 3.9 DPPH - radical quencher

2,2-Diphenyl-1-(2,4,6-trinitrophenyl) hydrazyl, (DPPH), Figure 74, is known commonly as a radical scavenger. DPPH is a stable free radical trap for other radicals and is an effective quencher of singlet oxygen. It strongly absorbs at 520 nm. DPPH radical exists as a deep violet colour when in solution, when the radical quencher is neutralised the solution becomes colourless or pale yellow. Typically, DPPH uses this character to show free radical scavenging activity.

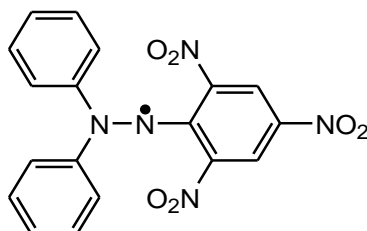


Figure 74: Chemical structure of DPPH

The decolourisation of this radical scavenger DPPH in dimethyl sulphoxide (DMSO) was assayed to measure the singlet oxygen production using white light.

The reduction absorption for the purpose of this project was monitored spectrophotometrically at 520 nm using the Cincotta *et al* method<sup>147</sup> and the decomposition of DPPH was observed to be relatively equal to the radicals produced by the synthesised isoalloxazines.

### 3.10 Volume of solvents

Total concentration of the stock solution was initially prepared as 50 mg in 100 mL volumetric flask. The stock solution was scaled down to a 10 mL volume at the same concentration as a 4 cm<sup>3</sup> quartz cuvette was used in the spectrophotometer.

### 3.11 Concentration of solution

The used concentration of 2,3,4,5-tetraphenylcyclopentadienone (TPCPD) was 50 mg in 100 mL. This was the optimum concentration of the TPCPD solution that could be used. Concentration solutions above this were unable to be measured on the spectrophotometer as no absorbance could be recorded. Thus, using the best determined concentration of the solution (50 mg in 100 mL), the singlet oxygen production was monitored without any inaccuracy in measurements of the signal to noise ratio.

### 3.12 Literature- singlet oxygen yield

The photochemistry of alloxazine has been of great interest particularly for their interaction with light in the presence of oxygen, as they are efficient photosensitisers and producers of singlet oxygen. Table 30 shows a number of literature yields generated by analogues of alloxazine in water and acetonitrile.

Table 30: Singlet oxygen yields generated by alloxazine analogues<sup>346,347</sup>

Compound	Singlet oxygen yield, $\phi_{\Delta}$	Solvent
Alloxazine	0.36	Acetonitrile
Lumichrome	0.73	Acetonitrile
6-Methylalloxazine	0.45	Water
7-Methylalloxazine	0.42	Water
8-Methylalloxazine	0.37	Water
9-Methylalloxazine	0.39	Water

Experimental carried out by M. Sikorski *et al* (Table 30) showed the production of singlet oxygen by alloxazine and lumichrome in acetonitrile. The results demonstrate that these photosensitisers are generators of singlet oxygen. The quantum yield of singlet oxygen produced by alloxazine (36%) indicates it is not a very good generator, however lumichrome proves otherwise (as 78% of singlet oxygen is generated)<sup>347</sup>.

No radical data for the analogues of alloxazine could be found in literature.

### 3.13 Protocol for the $^1\text{O}_2$ production of alloxazine using white light

Alloxazine, a known photosensitiser is used as a standard to measure the singlet oxygen production. A solution of alloxazine with a concentration of 50 mg in DMSO in 100 mL volumetric flask was prepared.

Alloxazine was placed in a 4 cm<sup>3</sup> quartz cuvette and irradiated using the white light source for one min (for a period of ten minutes, and continued to be illuminated at every five minutes intervals for a total period of 1 hour) at a distance of 5 cm. The singlet oxygen production was monitored using the spectrophotometer at 420 nm.

### 3.14 Protocol for DPPH-white light

A solution of DPPH with a concentration of 50 mg in DMSO in 100 mL volumetric flask was prepared. A second solution of the substituted isoalloxazine of concentration 10 mg in DMSO in 10 mL volumetric flask was also prepared.

In one 4cm<sup>3</sup> quartz cuvette, a volume of 3.5 mL of the prepared DPPH solution alone was filled. In a second 4cm<sup>3</sup> quartz cuvette, a 1:1 volume of DPPH isoalloxazine derivative mixture was placed in a 4cm<sup>3</sup> quartz cuvette and mixed well.

The absorbance was measured spectrophotometrically of both these solutions individually at time = 0, (T=0). The cuvettes with their solutions were irradiated using the white light source for one min (for a period of ten minutes, and continued to be illuminated every five minutes for a period of 1 hour) at a distance of 5 cm. The singlet oxygen production was monitored using the spectrophotometer at 520 nm, from T=0 to T=60.

### 3.15 Protocol for DPPH-blue light

The same procedure as DPPH using white light (section 3.14) was followed. However, for this experiment blue light was used to illuminate the prepared solutions in order to insure the synthesised isoalloxazines are activated using a different wavelength (440 nm – 490 nm) to monitor and compare the generated singlet oxygen.

### 3.16 Protocol for TPCPD-blue light

A solution of TPCPD with a concentration of 50 mg in DMSO in 100 mL volumetric flask was prepared. A second solution of the substituted isoalloxazine of concentration 10 mg in DMSO in 10 mL volumetric flask was prepared.

In one 4cm<sup>3</sup> quartz cuvette, a volume of 3.5 mL of the prepared TPCPD solution alone was filled. In a second 4cm<sup>3</sup> quartz cuvette, a 1:1 volume of TPCPD: isoalloxazine derivative mixture was placed in a 4cm<sup>3</sup> quartz cuvette and mixed well. The cuvette with its reaction mixture was irradiated using the blue light source for one min (for a period of ten minutes, and

continued to be illuminated every five minutes for a period of 1 hour) at a distance of 5 cm. The singlet oxygen production was monitored using the spectrophotometer at 506 nm.



### 3.17 Discussion of singlet oxygen data

The ongoing search for novel photosensitisers for use as photo-antimicrobial agents (particularly in this research) is based on the riboflavin structure. Based on this, alloxazine (illustrated in Figure 75) is used as the standard compound in order to compare the generation of singlet oxygen (initially) against riboflavin (Figure 43).

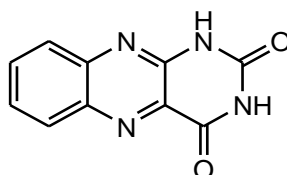
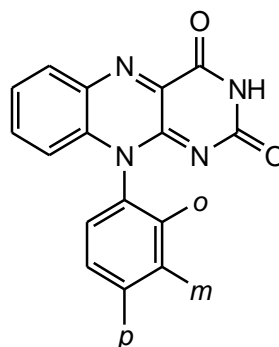


Figure 75: Chemical structure of alloxazine

### 3.18 Photosensitiser entries

The synthesised photosensitisers library were investigated for their production of singlet oxygen under different wavelengths of light. Table 31 shows the library of compounds with substituents attached on different positions (*o*, *m*, *p*) to the phenyl ring, Figure 76.



*o* = ortho, *m* = meta, *p* = para


Figure 76: Substitution position(s) for isoalloxazine

The singlet oxygen generated by the family of substituent(s) attached were compared against the standard phenyl isoalloxazine (**13c**). This comparison allowed determination of selecting which substituents (electron withdrawing or donating) would be beneficial to use in order to design ideal candidate(s) as potential photo-antimicrobial agent(s).

The success of any novel photosensitizer for PDT critically depends on its photophysical and photochemical properties. These being strong absorptions where photosensitisers are able to absorb within the therapeutic window (600–1000 nm)<sup>180</sup>. The tissue light scattering range is low, hence the depth of light penetration in tissues increases. In addition to this, a high quantum yield of the photosensitisers triplet state formation, combined with high triplet lifetime can be

achieved. This results as photochemical reactions predominantly occur in the excited state and a good efficiency of the conversion of triplet oxygen to cytotoxic singlet oxygen is crucial<sup>348</sup>.

Table 31: Novel photosensitisers tested for singlet oxygen and radical production



*o* = ortho, *m* = meta, *p* = para

Photosensitiser	<i>o</i>	<i>m</i>	<i>p</i>
<b>1c</b>	NH <sub>2</sub>	H	H
<b>4c</b>	OH	H	H
<b>6c</b>	H	H	OH
<b>7c</b>	OMe	H	H
<b>8c</b>	H	OMe	H
<b>9c</b>	H	H	OMe
<b>10c</b>	CH <sub>3</sub>	H	H
<b>11c</b>	H	CH <sub>3</sub>	H
<b>12c</b>	H	H	OCH <sub>3</sub>
<b>13c</b>	H	H	H
<b>14c</b>	Cl	H	H
<b>15c</b>	H	Cl	H
<b>16c</b>	H	H	Cl
<b>17c</b>	OTs	H	H
<b>18c</b>	H	OTs	H
<b>19c</b>	H	H	OTS
<b>20c</b>	COOH	H	H
<b>22c</b>	H	H	COOH
<b>23c</b>	NO <sub>2</sub>	H	H
	alloxazine		
	polymer*		
*4-(Benzyloxy)benzyl bromide polymer-bound			

Alloxazine and the polymer called 4-(benzyloxy)benzyl bromide polymer, which are covalently bound to the isoalloxazine were also tested for their singlet oxygen and radical production, in order to compare the yield generated both on and off the support.

### 3.18.1 Measuring the singlet oxygen quantum yield spectrophotometrically

The sub-unit structure of 10-phenyl isoalloxazine (**13c**, (B)) is based on the structure of alloxazine (A), Figure 77. The synthesised compounds are semi synthetics based on the alloxazine structure, which is a natural product.

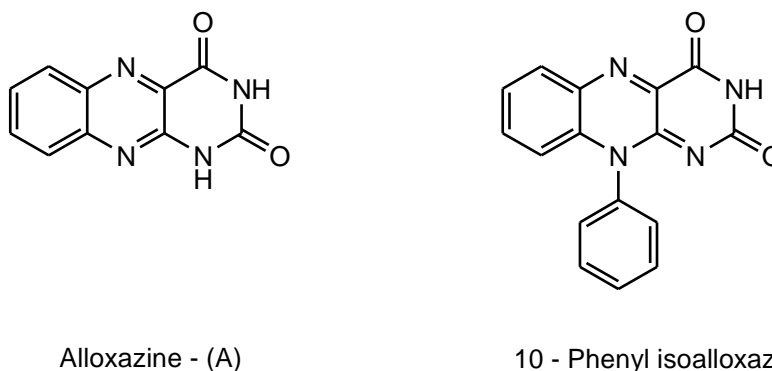


*Figure 77: Chemical structure of (A) alloxazine and (B) 13c*

The singlet oxygen and radical yields for alloxazine was calculated using Equation 3. A decrease in absorption of 2,3,4,5-tetraphenylcyclopentadienone (TPCPD) at 506 nm was monitored over time using alloxazine (Figure 77-(A)) as the standard photosensitiser for control purposes. The absorption decrease of TCPD to 50% was directly proportional to its reaction with singlet oxygen due to alloxazine photosensitisation ( $t_{1/2}$  **Allox**).

$$\text{Reactive } ^1\text{O}_2 \text{ Yield} = \frac{(t_{1/2} \text{ Allox})}{(t_{1/2} \text{ Der})} \quad \text{Equation 3}$$

The calculations deduced the production of singlet oxygen yield for the standard photosensitiser, alloxazine is 0.4825 ( $\Phi_{\Delta \text{ALL}}$ ). Thus, the lower the  $t_{1/2}$  value for the derivative, the greater its  $^1\text{O}_2$  yield is.

Using the formula highlighted in Equation 4 the singlet oxygen/radical yields can be determined for each of the synthesised substituted isoalloxazine dyes, with the standard being the unsubstituted phenyl isoalloxazine, **13c**.<sup>349</sup>

$$\Phi_{\Delta \text{Der}} = \Phi_{\Delta \text{13c}} * \frac{(t_{1/2} \text{ 13c})}{(t_{1/2} \text{ Der})} \times 100 \quad \text{Equation 4}$$

The time it takes for a 50% decrease in absorption results from each of the derivatives under identical conditions ( $t_{1/2}\text{Der}$ ) gives a measure of its photosensitising efficiency. For these

calculations the photosensitisation of **13c** ( $t_{1/2}$  **13c**) was taken to be at 1.0, or 100% (both mean the same) for DPPH (radical scavenger) and TPCPD (singlet oxygen quenching agent) absorption to decrease by 50%.

### 3.19 DPPH-radical data blue light

The radical yield for alloxazine, a known photosensitiser in the solvent DMSO is determined using the method discussed in section 3.22 and is known to be previously quantified<sup>350</sup>.

As mentioned in section 3.18.1 the yield of radical for alloxazine ( $\Phi\Delta_{ALL}$ ) was 0.4825 at ( $t_{1/2}$   $ALL$ ) 60.97, and was taken to be 100%. Thus, singlet oxygen generated by unsubstituted isoalloxazine was compared relative to alloxazine.

### 3.20 TPCPD-singlet oxygen data blue light

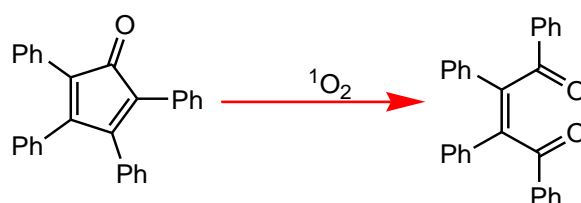


Figure 78: Chemical structure of TPCPD and its degradation

The singlet oxygen yield ( $\Phi\Delta$ ) for the novel standard photosensitiser, phenyl isoalloxazine ( $\Phi\Delta_{13c}$ ) was 0.4893 at ( $t_{1/2}$  **13c**) 40.45, and was taken to be 100%. Thus, singlet oxygen generated by other analogues was compared relative to compound **13c**. The method of these achieved calculations is discussed in section 3.21.

The value for the fluorescence quantum yield for isoalloxazines are obtained by comparing them initially against the standard alloxazine. Comparison of the generated singlet oxygen and radicals were made against the standard alloxazine initially, because the sub unit structure of the synthesised isoalloxazines are similar to alloxazine. However, alloxazine was used only as a control for calculation purposes of of the cytotoxic species. Subsequently, the synthesised phenyl isoalloxazine (**13c**) with no substituents attached to the *N*-10 phenyl ring was used as the standard compound, and thus all generated data of singlet oxygen/radical was compared against compound **13c**.

### 3.21 TPCPD-singlet oxygen data for **13c**

The synthesised compounds were dissolved in the solvent DMSO in order to record the singlet oxygen yields. DMSO was the chosen solvent for two reasons: firstly, it solubilises both isoalloxazine and TPCPD, and secondly no side reactions are noticed during the experiments. For the purpose of this study, the isoalloxazine was illuminated with a blue light (10 X 9 LED,

with a power output of 19 lumens) at a distance of 5 cm. This distance was identified as the optimum distance for illumination when compared to other tested distances, 10, 15 and 20 cm. A straight-line equation is represented by Equation 5. Using the data obtained (Table 32) from Equation 5 of Figure 79, it was possible to determine the half-life, and the relative singlet oxygen yields (RSOY).

$$y = mx + c$$

Equation 5

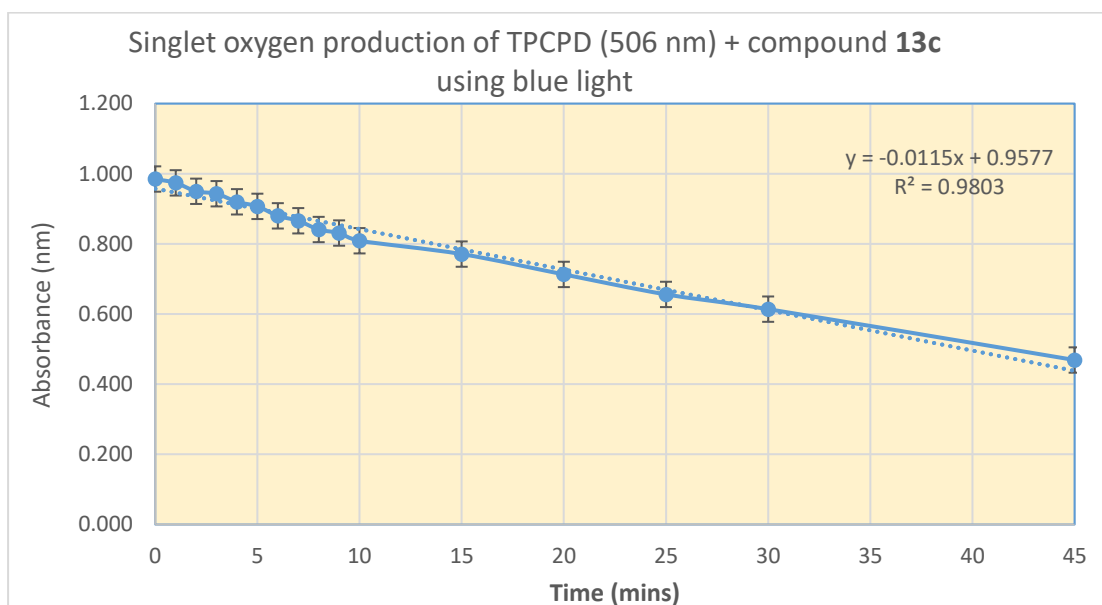


Figure 79: Singlet oxygen production of compound 13c

Table 32 shows the degradation of TPCPD (through its loss of absorption) when **13c** was illuminated with blue light.

Table 32: Singlet oxygen data for compound **13c**

Time (mins)	TPCPD (Abs-nm)	<b>13c</b> +TPCPD (Abs-nm)	Actual (Abs-nm)
0	1.560	0.985	0.985
1	1.555	0.974	0.974
2	1.555	0.950	0.950
3	1.555	0.941	0.943
4	1.553	0.920	0.920
5	1.553	0.906	0.907
6	1.552	0.880	0.880
7	1.552	0.864	0.866
8	1.550	0.840	0.841
9	1.549	0.831	0.831
10	1.549	0.808	0.809
15	1.548	0.768	0.771
20	1.545	0.711	0.713
25	1.543	0.654	0.656
30	1.541	0.606	0.614
45	1.533	0.466	0.469

Prior to illumination of **13c**, the absorbance at  $t = 0$  was measured to be 0.985 (Table 32). Thus, its absorbance upon reaching  $t = \frac{1}{2}$  would be 0.493. This was subtracted from the “c” value (0.9577) of the straight-line equation, to give -0.4647. This value was subsequently divided by the “m” value (-0.011) to give its  $t \frac{1}{2}$  at 40.45 min. Thus, the value taken for  $t \frac{1}{2}$  **13c** = 40.45 and this value will be used when calculating the subsequent yields for the other substituted isoalloxazines.

By comparing the singlet oxygen production of the two compounds (alloxazine and 10-phenyl isoalloxazine, Figure 77), it was noted that the addition of the extra phenyl ring at the *N*-10 position produced +1.50 times the amount of singlet oxygen in comparison to the alloxazine. Based on this result, it was decided that substitution across the *N*-phenyl ring system; an increase relative production of singlet oxygen could be achieved than the natural product alloxazine. Thus, phenyl isoalloxazine was used as the standard for further calculations, due to the substitution on the phenyl ring.

### 3.22 DPPH–Redox for **13c**

The radical production of the synthesised isoalloxazines were monitored using a radical scavenger called 2,2-diphenyl-1-(2,4,6-trinitrophenyl)hydrazyl, (DPPH), Figure 80, using the same method as for measuring the singlet oxygen production.

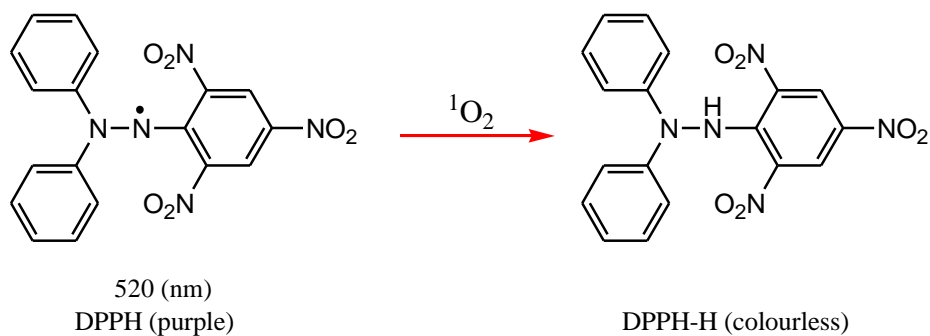


*Figure 80: Chemical structure of DPPH and its degradation*

The library of compounds were individually dissolved in DMSO and illuminated with blue LED light for one minute at a distance of 5 cm. The absorbance of the radical scavenger and the compound was measured spectrophotometrically at 520 nm. The radical data collected for compound **13c** is shown in Table 33, and in Figure 81 below.

Table 33: Redox data of compound **13c**

Time (mins)	13c + DPPH (Abs-nm)	Actual Absorbance (nm)
0	2.102	2.102
1	1.456	1.458
2	0.988	0.989

Using the data obtained from Equation 5 in Figure 81, the half-life, and the radical production was calculated using the same method as discussed above for the RSOY.

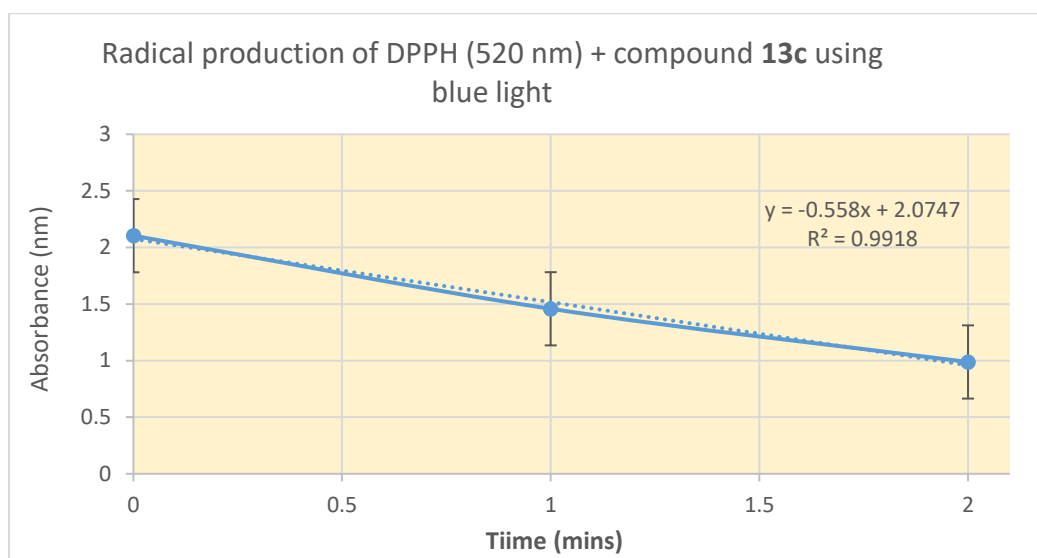


*Figure 81: Redox production of compound 13c*

The absorbance at  $t = 0$  was measured for **13c** to be (Table 33) 2.102. The absorbance upon reaching  $t = \frac{1}{2}$  would be 1.051. This was subtracted from the “c” value (2.0728) of the straight line equation, to give -1.0218. Subsequently, this value was divided by the “m” value (-0.5565) to give its  $t_{\frac{1}{2}}$  at 3.114 min. Thus, the value taken for (radical production)  $t_{\frac{1}{2}}$  **13c** = 3.11, and it is this value that will be used when calculating the radical production yields for the other substituted isoalloxazines.



For each of the synthesised isoalloxazines, the absorbance was also measured. The  $\lambda_{\text{max}}$  (nm) at 433.5 nm for compound **13c**. The absorbance in Figure 82 at 1.40 with a  $\lambda_{\text{max}}$  of 266 nm can be attributed to DMSO, as this was the solvent used to conduct the spectrometry experiments.

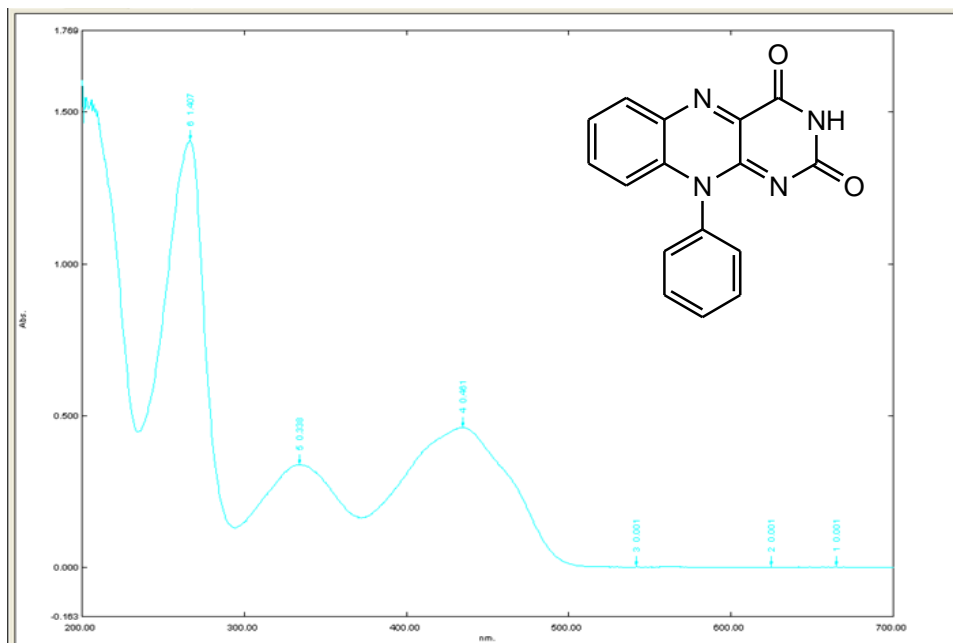
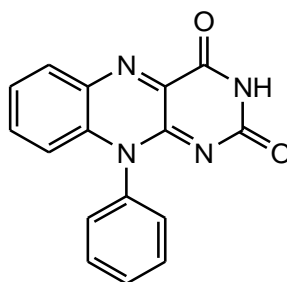


Figure 82: UV-Vis spectra for compound **13c**

It is also noted that phenyl isoalloxazine (**13c**) shows two maxima in its absorption spectra (Figure 82), between 300 nm and 500 nm. It can be predicted that these two long wavelength bands arise from the  $\pi$ - $\pi^*$  transitions.

Upon evaluating all the novel synthesised isoalloxazines, it was noted that there was no fundamental difference in the shift of the UV/Vis absorption for any of the isoalloxazines. Although these molecules have an auxochromic effect resulting from the different substituents attached to the *N*-10 ring, neither of the synthesised isoalloxazines shifted further than 435 nm. Hence, the reason for selecting markers that absorb above this range (TPCPD - 506 nm and DPPH - 520 nm). Analysis of absorbance for each of the synthesised isoalloxazines showed no overlap of the isoalloxazines and the markers, which resulted from the auxochromic shift.

### 3.23 Photophysical studies of 10-phenyl isoalloxazine (R = H). (**13c**)



**13c**

*Figure 83: Chemical structure of 10-phenyl isoalloxazine*

Table 34: Percentage yield for 10-phenyl isoalloxazine

Compound	<i>o</i> (R <sub>1</sub> )	<i>m</i> (R <sub>2</sub> )	<i>p</i> (R <sub>3</sub> )	Yield (%)	S/O yield (%)	Radical yield (%)
<b>13c</b>	H	H	H	98	150	294

The photophysical data for the un-substituted compound (**13c**) shows a brilliant production for both the cytotoxic species. The singlet oxygen yield was detected in 150% and radical was generated in a yield of 294%. Comparing the singlet oxygen yield generated against alloxazine and its analogues (Table 30) clearly demonstrates that the novel synthesised isoalloxazine (compound **13c**) is a much better generator of singlet oxygen. Neither of the alloxazine analogues in any of the solvents showed a singlet oxygen production above 73%<sup>338</sup>. Achieving these results seems exceptionally promising as the results indicate novel analogues of **13c** can be potential photosensitisers that are good generators of cytotoxic species.

### 3.24 Photophysical studies of amino derivatives of 10-phenylisoalloxazine (R = NH<sub>2</sub>). (**1c**)

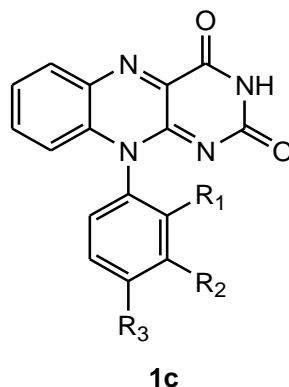
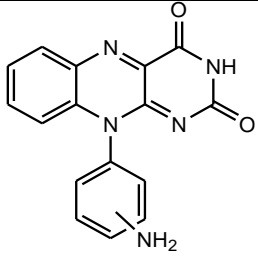


Figure 84: Chemical structure of 10-(N-aminophenyl) isoalloxazines

Table 35: Photophysical data for 10-(2-aminophenyl) isoalloxazine.

	Type II (S/O)		Type I (Rad)	
	<b>t<sub>1/2</sub> (mins)</b>	<b>Yield (%)</b>	<b>t<sub>1/2</sub> (mins)</b>	<b>Yield (%)</b>
<b>1c/o</b>	96.82	41.77	370.52	0.84
<b>13c</b>	40.45	100	3.14	100

The singlet oxygen studies was calculated for compound **1c** using the method described in section 3.21 by the data generated through degradation of TPCPD with compound **1c**, and is illustrated in Table 35. The absorbance at  $t = 0$  was measured at 1.237 (Table 35), thus the absorbance at  $t = 1/2$  would be 0.618. Upon further calculations using Equation 5 the calculated value of  $t_{1/2}$  **1c** = 96.82 mins.

Table 36: Singlet oxygen data for compound **1c**

Time (mins)	<b>1c</b> +TPCPD (Abs-nm)	Actual (Abs-nm)
0	1.237	1.237
1	1.230	1.232
2	1.295	1.299
3	1.294	1.297
4	1.292	1.293
5	1.290	1.291
6	1.289	1.291
7	1.282	1.285
8	1.210	1.282
9	1.278	1.278
10	1.275	1.277
15	1.272	1.273
20	1.270	1.271
25	1.269	1.270
30	1.268	1.270
45	1.265	1.268
60	1.262	1.262

Compound **1c** generated a singlet oxygen yield of 41.77%. Evidently, a lower yield of both singlet oxygen and radical was produced than **13c**, being 1.00 (100%). From this, it is deduced that having an amino moiety substituted onto phenyl ring at the *ortho* position does not enhance the production of singlet oxygen.

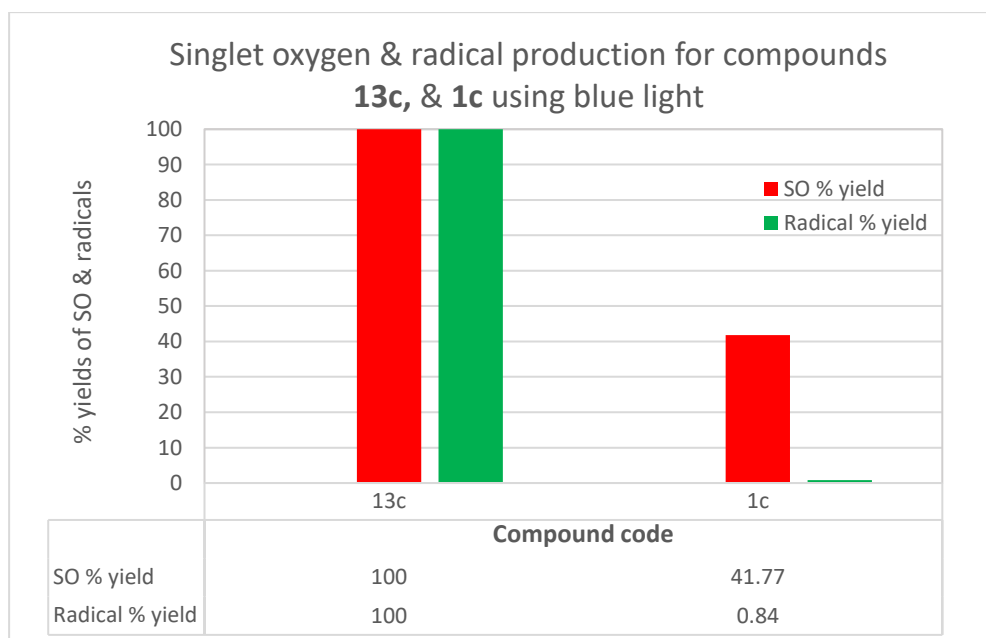
In contrast to this, the redox production of compound **1c** with the radical scavenger DPPH in DMSO was monitored as described in section 3.22. Prior to illumination the absorbance at  $t = 0$  was measured to be 1.934 (

Table 36), therefore the absorbance at  $t = t_{1/2}$  would be 0.967. From the generated data Equation 5 was used to calculate the value of  $t_{1/2}$  **1c** = 370.50 mins.

Table 37: Redox data for compound **1c**

Time (mins)	1c +DPPH (Abs-nm)	Actual (Abs-nm)
0	1.934	1.934
1	1.928	1.924
2	1.927	1.923
3	1.924	1.923
4	1.922	1.920
5	1.919	1.916
6	1.919	1.917
7	1.918	1.914
8	1.915	1.914
9	1.907	1.904
10	1.902	1.898
15	1.894	1.892
20	1.878	1.878

The radical production of **1c** was compared against compound **13c** in Table 37, and illustrated in Figure 90. The generated yield was calculated using both Equation 4 and Equation 5. Compound **1c** produced a radical yield of 0.84%. It is deduced from the result that **1c** is not a radical producer since it generates very low yield of radicals. Thus, the conclusion made from comparison of these two compounds (**1c** and **13c**), is that compound **13c** is a better molecule at producing radicals having no substituents attached to the phenyl ring at the *N*-10 position.



*Figure 85: Singlet oxygen and radical production of compound 1c versus 13c*

Research conducted by Wenbin *et al.* also presented results concluding that although amino substituent, a strong electron donating moiety on the *N*-10 phenyl ring are generators of singlet oxygen medium electron donating substituents for example methoxy substituents are

nonetheless better producers<sup>339</sup>. This is clearly evident for results obtained within this study as the methoxy substituents have generated higher singlet oxygen yields, and this can be seen in section 3.26.

### 3.25 Photophysical studies of hydroxy derivatives of 10-phenylisoalloxazine (R = OH). (**4c-6c**)

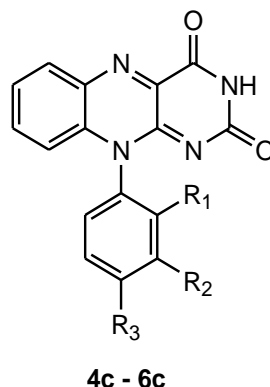


Figure 86: Chemical structure of 10-(N-hydroxyphenyl) isoalloxazines

Table 38: Photophysical data for N-hydroxy phenyl isoalloxazine derivatives

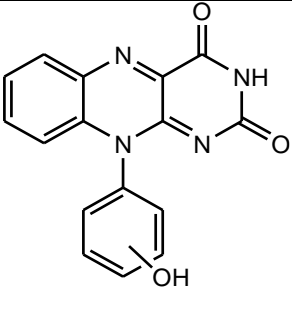
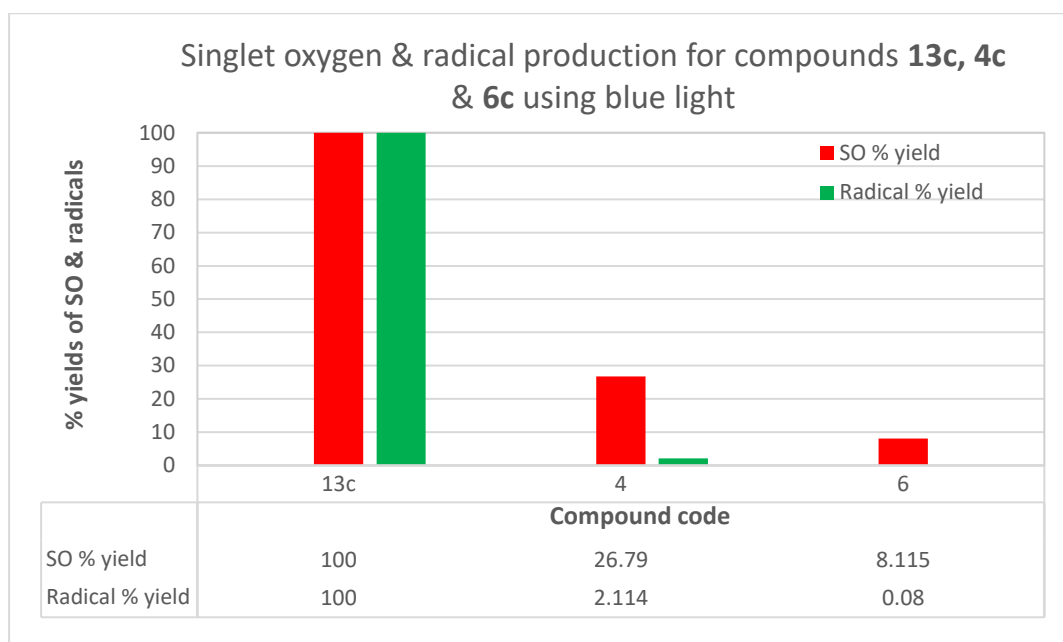
	Type II (S/O)		Type I (Rad)	
	$t_{1/2}$ (mins)	Yield (%)	$t_{1/2}$ (mins)	Yield (%)
<b>4c/o</b>	150.97	26.79	147.254	2.11
<b>6c/p</b>	498.45	8.12	3178	0.08
<b>13c</b>	40.45	100	3.114	100

Table 38 highlights the photophysical data (S/O and radical) obtained from compounds **4c** and **6c** respectively, whilst comparing against **13c** as the non-substituted standard. This data was determined using Equation 4 and Equation 5 from the data sets collected and calculated via the non-direct spectrophotometry method as discussed in section 3.21.

The singlet oxygen yield generated by **4c**, upon illumination with blue light, is 26.79% in comparison to that of **6c** which shows a threefold decrease in the amount of singlet oxygen 8.11% produced.

It is interesting to note that the radical yields produced by both **4c** and **6c** are miniscule when compared to **13c**. To expand, **4c** was calculated to be 2.11% whilst **6c** was 0.08%, indicating their microbial action is due to Type II photosensitisation. Figure 87 shows a graphical representation of this with comparison against **13c**.



*Figure 87: Singlet oxygen and radical production of compound 4c and 6c vs 13c*

Comparing the singlet oxygen productions for compounds **4c** and **6c** against **13c** highlighted in Figure 87, it can be determined that the *ortho* substituted isomer is a better producer of singlet oxygen than the *para* substituted isoalloxazine. The yield of singlet oxygen generated by both isomers show a low production that is primarily seen when the hydroxyl substituent is attached to the phenyl ring on the *para* position. It was assumed that having a hydroxyl moiety as a substituent, the singlet oxygen production in comparison to the standard phenyl isoalloxazines would increase significantly because of the electronic effects of the OH group. The OH moiety being an electron donator would activate the *N*-10 ring, making the ring more reactive thus increasing the production of singlet oxygen/radical<sup>351</sup>. However, the results disproved this assumption as both isomers (**4c** and **6c**) barely produced any singlet oxygen. Fundamentally, the radical production between compounds **4c** and **6c** on evaluation deduced that the hydroxyl moiety in the *ortho* position (**4c**) has a much shorter half-life and produces more radicals than in the *para* position (**6c**). Upon further evaluation of the radical production based on compound **13c**, which is taken to be 1 (100%) demonstrates no enhancement on production of cytotoxic species was observed compared to the standard isoalloxazine, **13c**. Thus, overall the hydroxy series are singlet oxygen generators rather than radical producers. They are not however better producers than phenyl isoalloxazine.



### 3.26 Photophysical studies of methoxy derivatives of 10-phenylisoalloxazine (R = OCH<sub>3</sub>). (**7c-9c**)

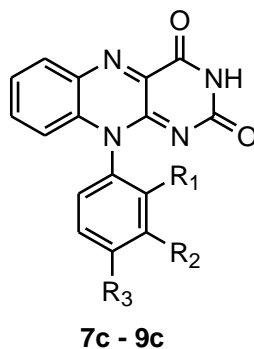
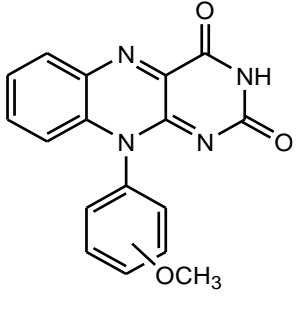


Figure 88: Chemical structure of 10-(N-methoxyphenyl) isoalloxazines

Table 39: Photophysical data for N-methoxyphenyl isoalloxazine derivatives

	Type II (S/O)		Type I (Rad)	
	$t_{1/2}$ (mins)	Yield (%)	$t_{1/2}$ (mins)	Yield (%)
<b>7c/o</b>	41.14	98.32	106.79	2.91
<b>8c/m</b>	234.5	17.25	139.59	1.71
<b>9c/p</b>	102.56	39.44	81.08	3.84
<b>13c</b>	40.45	100	3.11	100

The singlet oxygen yields for the substituted methoxy isoalloxazine derivatives generated were calculated using the method discussed previously in section 3.21 and are expanded further below.

The absorbance for compound **7c** prior to illumination was measured at 0.896 and its absorbance at  $t_{1/2} = 0.448$ . The singlet oxygen yields were determined using Equation 4 and Equation 5 from the data generated via the degradation of the TPCPD. The  $t_{1/2}$  calculated for compound **7c** was;  $t_{1/2} = 41.14$  mins and a singlet oxygen yield of 98.3%. Comparing this value of singlet oxygen production with **13c** being 1.00 (100%), it is evident that compound **7c** produces singlet oxygen at greater quantity than the standard phenyl isoalloxazine.

The same principle for determining the singlet oxygen yield of compound **9c** was used as **7c**. The absorbance measured at  $t = 0$  was 0.982 for compound **9c**. Upon reaching its  $t_{1/2}$  the absorbance was 0.491. The straight line equation determined the  $t_{1/2}$  **9c** = 102.56 mins. Further calculations using Equation 4 determined the singlet oxygen yield of 39.4%.

The synthesised methoxy derivatives of 10-phenyl isoalloxazines were monitored for their radical production. Thus, the degradation of DPPH was monitored for compounds **7c** and **9c**. The radical yields were calculated for these compounds using the methods discussed previously in section 3.22. Figure 89 shows the redox and singlet oxygen production for the 10-(*N*-methoxyphenyl) isoalloxazines and for **13c**.

The calculated  $t_{1/2}$  for compound **7c** was;  $t_{1/2} = 106.79$  mins with a radical yield of 2.91%. Upon comparison of this value against the radical production of compound **13c** shows that compound **7c** generates a radical production lower than the standard phenyl isoalloxazine.

Radical production for compound **9c** was also calculated using the method described using Equation 4 and Equation 5. Compound **9c** prior to illumination had a  $t = 0$  of 1.643 and its absorbance at  $t_{1/2}$  was measured to be 0.822. Thus, its  $t_{1/2}$  was 81.08 mins and the radical yield was calculated to be 3.84%. The photophysical data for these compounds are shown in Table 39 compared against phenyl isoalloxazines.

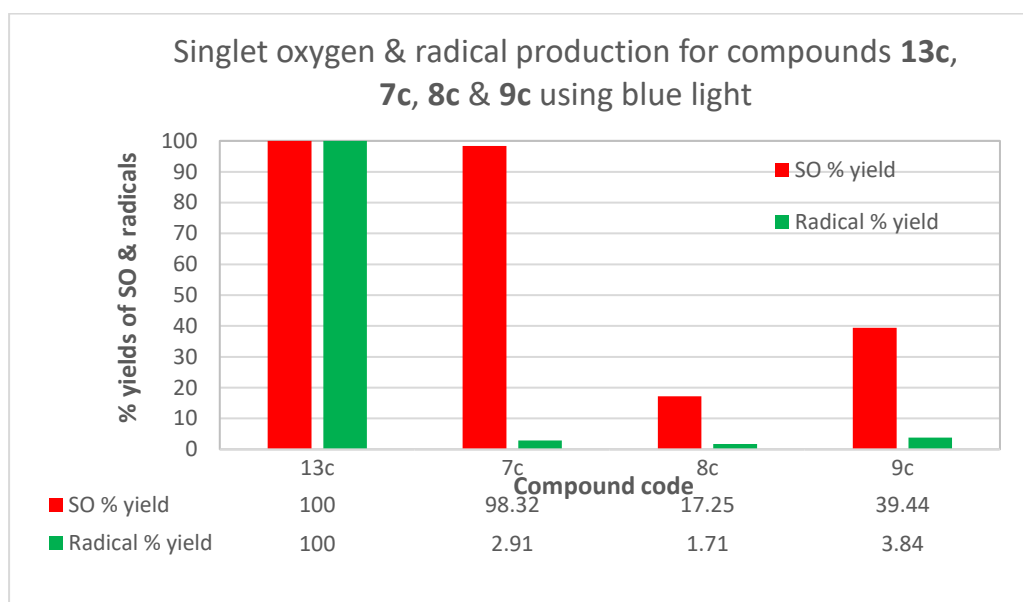


*Figure 89: Singlet oxygen and radical production of compounds 7c and 9c vs 13c*

Upon evaluating the singlet oxygen yields for compounds **7c-9c**, the *ortho* isomer (**7c**) produced a singlet oxygen yield of 98.3%. Compound **8c** and **9c** produced a yield of 17.2% and 39.4%, and these yields elucidated compound **7c** to be a good generator of singlet oxygen but does not produce more than the standard phenyl isoalloxazine, **13c**.

In terms of radical comparison between the derivatives, the *para* isomer (**9c**) is a slightly better radical producer as it generates a yield of 3.84%. Whereby the *meta* substituted isomer (**8c**) produced the lowest radical yield (1.71%) within the series. A minute difference between the two derivatives is observed in the yields produced. Nonetheless, it is evident that methoxy

substituents are not great radical generators in comparison to the standard isoalloxazine structure, as they do not show an improvement in the production of radical yields against compound **13c**.

These compounds were tested as antimicrobial agents against gram positive and gram negative bacteria. Compounds (**7c-9c**) have proven to be successful candidates in producing cytotoxic effects particularly towards gram negative (*E.coli*) pathogens. Although compound **7c** demonstrated to be a better singlet oxygen generator than **9c**, both compounds presented antimicrobial activity in blue light and in darkness at 1 mM/mL concentration. However, no antimicrobial activity was observed towards against gram positive bacteria (*S. aureus*).

Some differences are seen in terms of productivity of ROS when comparing the substituent position on the *N*-10 ring. However, evaluating the results achieved for majority of the electron donating substituents show the substituent effects are very small; indicating that the substituents on the *N*-10 phenyl substituents may not be able to interact on the alloxazine ring system due to the steric effects of the substituents or the *N*-10 ring may be perpendicular to the main ring, and this is similarly highlighted in research conducted by F.Bosca *et al*<sup>352</sup>.

### 3.27 Photophysical studies of tolyl derivatives of 10-phenylisoalloxazine (R = CH<sub>3</sub>). (**10c–12c**).

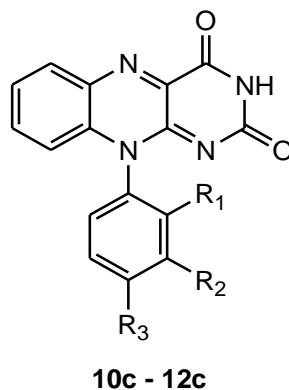
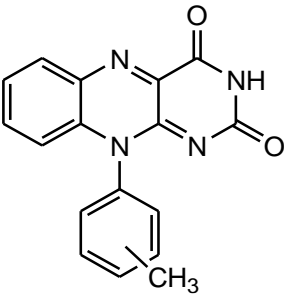


Figure 90: Chemical structure of 10-(N-tolylphenyl) isoalloxazines

Table 40: Photophysical data for tolylphenyl isoalloxazine derivatives

	Type II (S/O)		Type I (Rad)	
	<i>t</i> <sub>1/2</sub> (mins)	Yield (%)	<i>t</i> <sub>1/2</sub> (mins)	Yield (%)
<b>10c/o</b>	48.19	83.99	4304.5	0.01
<b>11c/m</b>	97.24	41.58	1.369	227
<b>12c/p</b>	22.23	172.17	88.02	3.53
<b>13c</b>	40.45	100	3.114	100

As tolyl substituents are electron donating by inductive effects, it was interesting to compare both the singlet oxygen and the radical yields produced by each of these isoalloxazines (**10c–12c**).

The singlet oxygen yields were calculated using Equation 4 from the data sets obtained by each of the tolyl isoalloxazine derivatives and highlighted in Table 40. The singlet oxygen data were generated through loss of absorbance of TPCPD.

Calculations determined the singlet oxygen yield for compound **10c** to be 83.99%. Comparing this yield with the yield produced by **13c**, it is concluded that compound **10c** generates a lower quantity of singlet oxygen. The singlet oxygen were calculated for compound **11c** using Equation 4 and Equation 5. Compound **11c** produced a value of 41.58% and **12c** generated an

enhanced singlet oxygen yield of 172.17%, proving this compound a better singlet oxygen generator than **13c**.

Monitoring each of tolyl derivative produced the following radical yields: compounds **10c** produced 0.0072%, **11c** produced 227% and compound **12c** produced 3.53%. This photophysical data sets achieved for compounds **10c-12c** as well as **13c** and are shown in Figure 91 and illustrated graphically in Table 40.

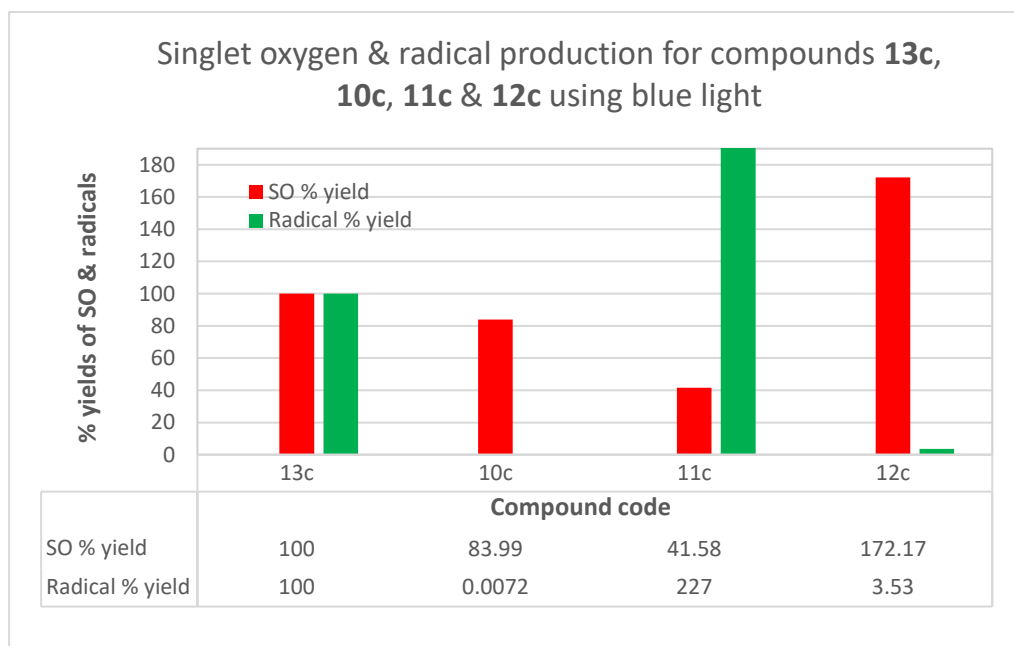


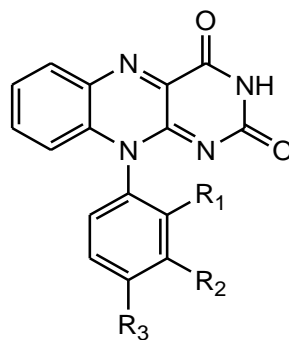
*Figure 91: Singlet oxygen and redox production of compounds 10c-12c vs 13c*

By observing the singlet oxygen yields generated and comparing against the oxygen yield produced by **13c**, taken to be 1.00 (100%) at  $t_{1/2} = 0.493$ , it can be concluded that compound **12c** approximately generates a two-fold increase in the singlet oxygen yield. Thus, having a tolyl group substituted at the *para* position of the phenyl ring makes it a better compound in terms of the singlet oxygen generation than the standard isoalloxazine when having no substituents attached across the phenyl ring system. It was interesting to note that although this compound (**12c**) is a good generator of singlet oxygen it is not effective in terms of its antimicrobial activity against neither gram positive or negative organisms as no antimicrobial activity was observed at all for compound **12c** post irradiation of microorganisms using blue light.

Having evaluated the results achieved from the radical data sets, it is deduced that compound **11c** is a very good producer of radicals. These results indicate that a tolyl substituent in the *meta* position of the phenyl ring shows that radicals are generated at a much improved rate than the standard phenyl isoalloxazine, **13c**. Compound **11c** has a 1.74 times greater radical production when compared to compound **13c** and (**11c**) proved to show toxic effects towards both *E.coli* and *S. aureus* at different concentrations. The microbial activity for compound **11c** against the gram positive bacteria *S.aureus* was observed at 0.25 mM/mL.

From the results achieved by the tolyl derivatives, it is deduced that the electronic effects of the CH<sub>3</sub> moiety as electron donating substituents unquestionably have an effect on both the singlet oxygen and radical production<sup>353</sup>. As a radical producer, the tolyl moiety substituted on the *meta* position gave the best result and as a singlet oxygen generator the *para* substituted isomer produced enhanced amounts of singlet oxygen. In conclusion to this series the tolyl moiety have proved to be good substituents as radical/singlet oxygen generators compared to alternative electron withdrawing / donating groups.

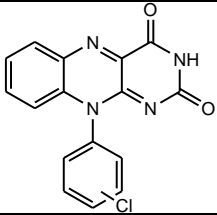
### 3.28 Photophysical studies of chloro derivatives of 10-phenylisoalloxazine (R = Cl). (**14c–16c**)



**14c - 16c**

Figure 92: Chemical structure of 10-(N-chlorophenyl) isoalloxazines

Table 41: Photophysical data for chlorophenyl isoalloxazine derivatives

	Type II (S/O)		Type I (Rad)	
	$t_{1/2}$ (mins)	Yield (%)	$t_{1/2}$ (mins)	Yield (%)
<b>14c/o</b>	139	29.08	36.00	8.64
<b>15c/m</b>	52.2	77.49	3.13	99.47
<b>16c/p</b>	85.5	47.3	11.49	27.09
<b>13c</b>	40.45	100	3.114	100

Chloro, an electron withdrawing moiety substituted to the phenyl ring affects the electron density of the tricyclic ring system. Thus, it was fascinating to evaluate the photophysical results obtained with the electron withdrawing substituent attached to the ring and comparing the results with **13c**.

The singlet oxygen yields were calculated using Equation 4 from the data obtained by each of the chlorophenyl isoalloxazine derivatives (**14c–16c**) and presented in Table 41 with compound **13c**. Compounds **14c** produced 29.08%, **15c** produced 77.49% and compound **16c** generated a yield 47.30%. Upon evaluation of these results, it can be concluded that a *meta* substituted isomer produced a higher quantity of singlet oxygen yield compared to other isoalloxazine isomers. The interesting observation made with this molecule (**15c**) was that it did not pose any antimicrobial effects against *E.coli* at the tested concentrations from 1.0 mM/mL–0.063 mM/mL. However, antimicrobial activity was observed against the gram-positive bacteria (*S.aureus*) at a concentration of 0.125 mM/mL.

The comparison of radical yields for chlorophenyl substituted isoalloxazine was monitored using the methods discussed as before. The radical yields were for compounds **14c–16c** were calculated using Equation 5. Compound **14c** produced a radical yield of 8.64%, **15c** produced 99.47% and **16c** generated a yield 27.09%. The photophysical data achieved are tabulated in Table 41 and illustrated graphically in Figure 93 with the data set of compound **13c**.

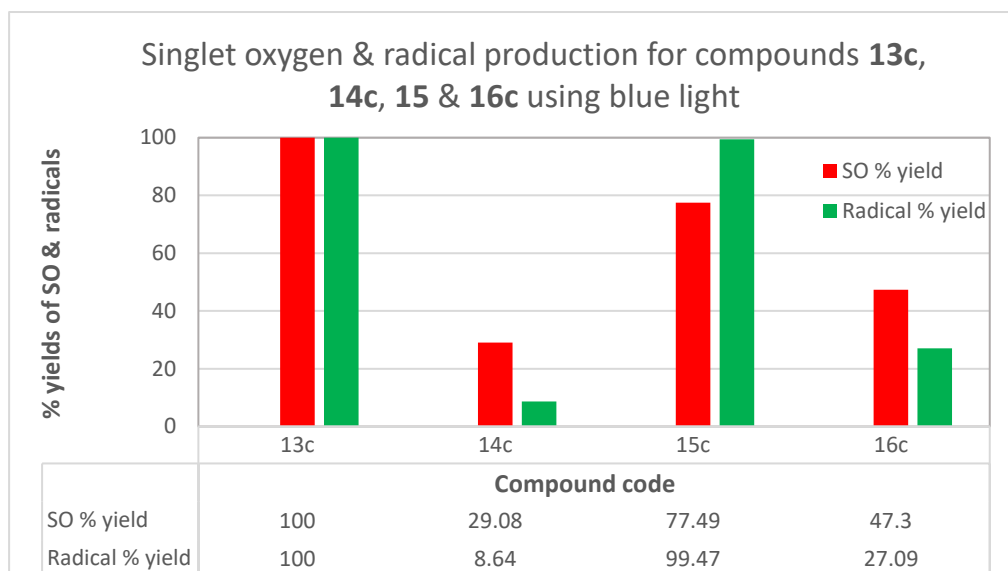


Figure 93: Singlet oxygen and radical production of compounds **14c–16c** vs **13c**

The results achieved from calculations of the radical yield production show that although chloro substituents can generate radicals, they are not better producers than **13c** as enhanced yields than the standard phenyl isoalloxazine were not produced. However, it is encouraging to observe the *meta* isomer (**15c**) produced a very close radical yield to **13c**.

Upon observation of the singlet oxygen yields generated and comparing against phenyl isoalloxazine, **13c**, it is deduced that neither derivatives of the chloro series (**14c–16c**) are better generators of singlet oxygen, as no isomer produced a yield greater than **13c**.

It was of great interest to note that having electron withdrawing groups that are *ortho/para* directors and weakly deactivate the phenyl ring, have no effect on the production of singlet oxygen. This evidently shows that the ring system is definitely being deactivated due to the electronic effects of the chlorine substituents.



### 3.29 Photophysical studies of tosyloxy derivatives of 10-phenylisoalloxazine (R = OTs). (**17c–19c**)

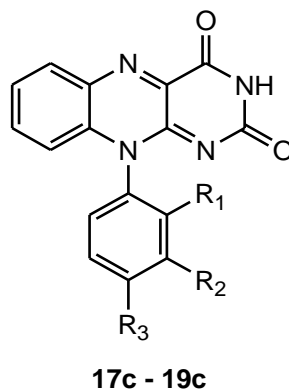
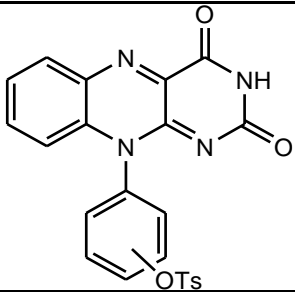


Figure 94: Chemical structure of 10-(N-tosyloxyphenyl) isoalloxazines

Table 42: Photophysical data for tosyloxyphenyl isoalloxazine derivatives

	Type II (S/O)		Type I (Rad)	
	$t_{1/2}$ (mins)	Yield (%)	$t_{1/2}$ (mins)	Yield (%)
<b>17c<sub>o</sub></b>	53.34	75.78	69.7	4.46
<b>18c<sub>m</sub></b>	59.41	68.08	2032	0.12
<b>19c<sub>p</sub></b>	41.72	96.94	17.86	13.41
<b>13c</b>	40.45	100	3.11	100

Photophysical studies of the 10-(N-tosyloxyphenyl) isoalloxazines are of interest because tosylate substituents are weakly electron withdrawing, and are *ortho/para* directors. The OTs moiety would change the electron density of the ring system and it is for this reason the comparison of both radical and singlet oxygen yields generated by each (**17c–19c**) of the derivative is of great interest.

The singlet oxygen yields for each of the tosyloxyphenyl derivatives, were calculated using Equation 4 from the half-life and absorbance data obtained experimentally.

Compound **17c** produced singlet oxygen yields of 75.75%, **18c** generated 68.08% and compound **19c** produced 96.94%.

The radical production for the tosyloxyphenyl series were calculated using the method discussed for all other library of isoalloxazines and highlighted in Table 42, and represented graphically in Figure 95. The radical yields achieved for each of the OTs isoalloxazine derivatives reveals

that compounds **17c** produced 4.46%, **18c** produced 0.12% and compound **19c** produced 13.41%.

By analysis it is observed that each of the 10-(*N*- tosyloxyphenyl) isoalloxazine isomers are not great radicals producers as neither of the derivatives generated radicals at an enhanced amount than the standard phenyl isoalloxazine.

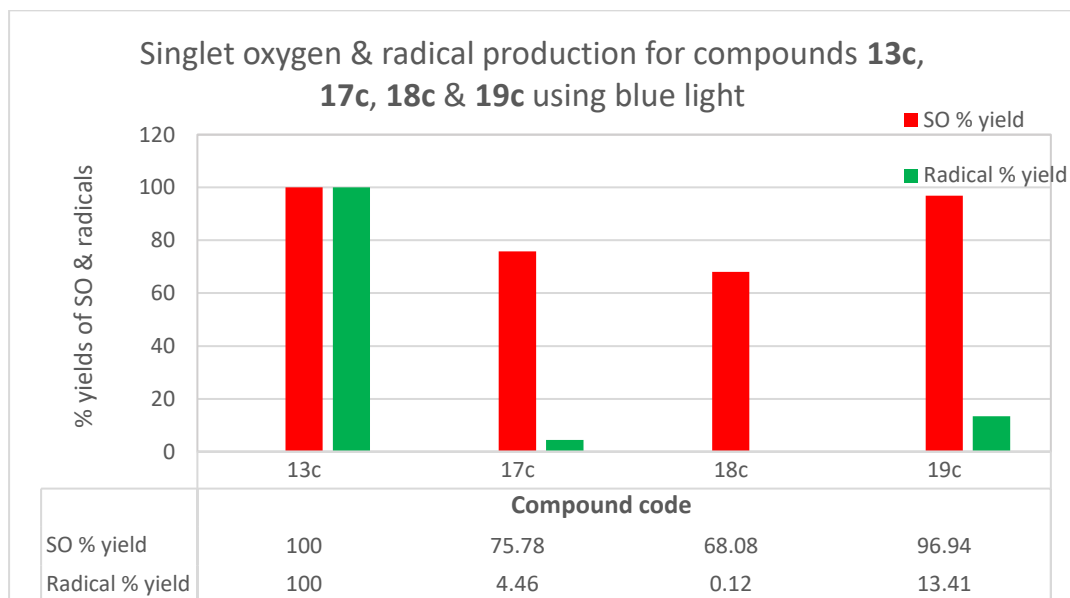
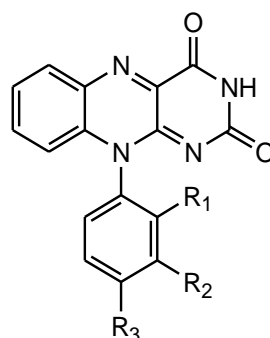


*Figure 95: Singlet oxygen and radical production of compounds 17c-19c vs 13c*

Evaluation of the singlet oxygen yields show that compound **19c**, *para* substituted OTs on the phenyl ring produces singlet oxygen yield very close to **13c**. Figure 95 clearly shows that having these weak electron withdrawing groups (OTs) substituted to the phenyl ring system not alter the electron density significantly. Although compounds **17c-19c** predominantly produce more singlet oxygen than radicals, neither isomer was able to generate an enhanced yield than **13c**. Whilst comparing the efficiency of cytotoxicity for this series of isoalloxazines it was also determined that no antimicrobial effect was observed against the gram negative bacteria. However, there is evidence to show that antimicrobial activity was present towards *S.aureus*, gram positive organism at an improved rate than the standard phenyl isoalloxazine and is discussed in sections 4.9 and 4.21.

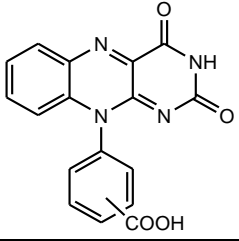
### 3.30 Photophysical studies of carboxy derivatives of 10-phenylisoalloxazine (R = COOH). (**20c–22c**)



**20c - 22c**

Figure 96: Chemical structure of 10-(N-carboxyphenyl) isoalloxazines

Table 43: Photophysical data for carboxyphenyl isoalloxazine derivatives

	Type II (S/O)		Type I (Rad)	
	$t_{1/2}$ (mins)	Yield (%)	$t_{1/2}$ (mins)	Yield (%)
<b>20c/o</b>	286.46	14.12	1065.62	0.29
<b>22c/p</b>	319.11	12.67	351.64	0.88
<b>13c</b>	40.45	100	3.11	100

The photophysical data accumulated for these electron withdrawing substituents attached to the isoalloxazines are highlighted in Table 43.

The singlet oxygen yields for compounds **20c** and **22c** were calculated using the same method as used for the library of isoalloxazines. Compound **20c** generated a singlet oxygen yield of 14.12% and **22c** was determined to be 12.67%. Evaluation of the yields achieved by the electron withdrawing isoalloxazines demonstrate that having a carboxylic acid moiety does not induce the generation of singlet oxygen production at higher yields than that of the isoalloxazine with no substituents attached, (**13c**).

The radical production for compounds **20c** and **22c** was calculated from the data set obtained. Each on these compounds produced negligible radical yields, **20c** produced 0.29% & **22c** generated a yield of 0.88%. Upon evaluation of the yields achieved, it is noted that not only is the radical production lower than the standard phenyl isoalloxazine but also of singlet oxygen, which is evident in Figure 97.

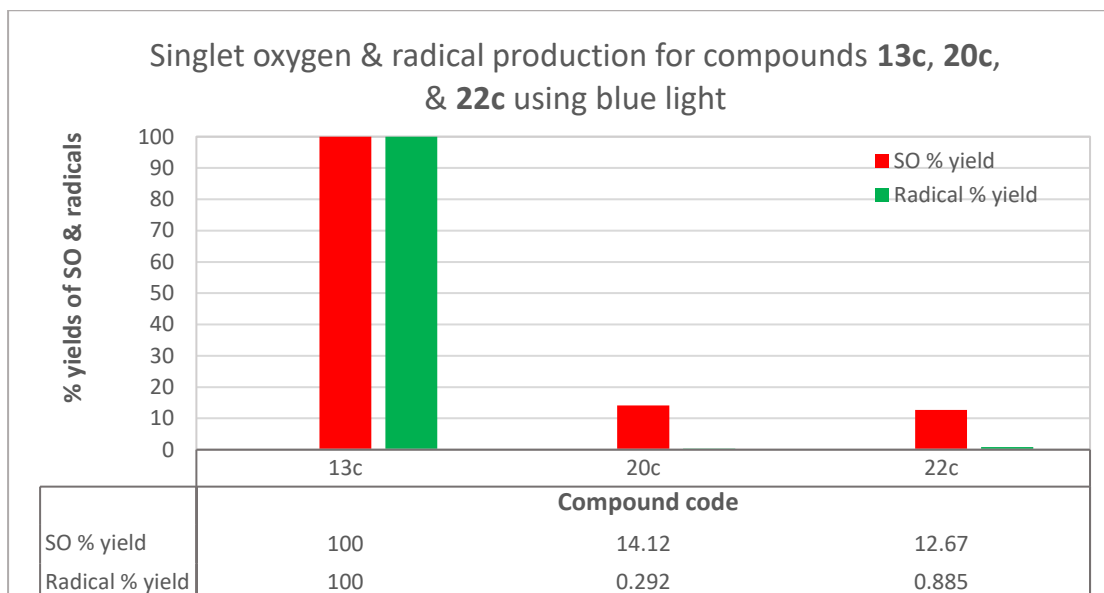


*Figure 97: Singlet oxygen and radical production of 20c and 22c vs 13c*

### 3.31 Photophysical studies of nitro derivatives of 10-phenylisoalloxazine (R = NO<sub>2</sub>). **23c**

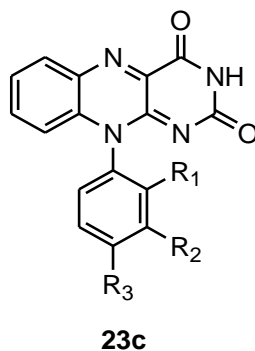
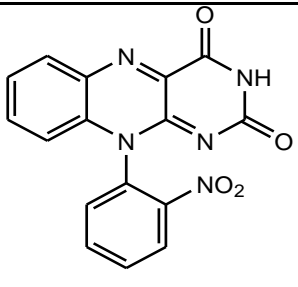


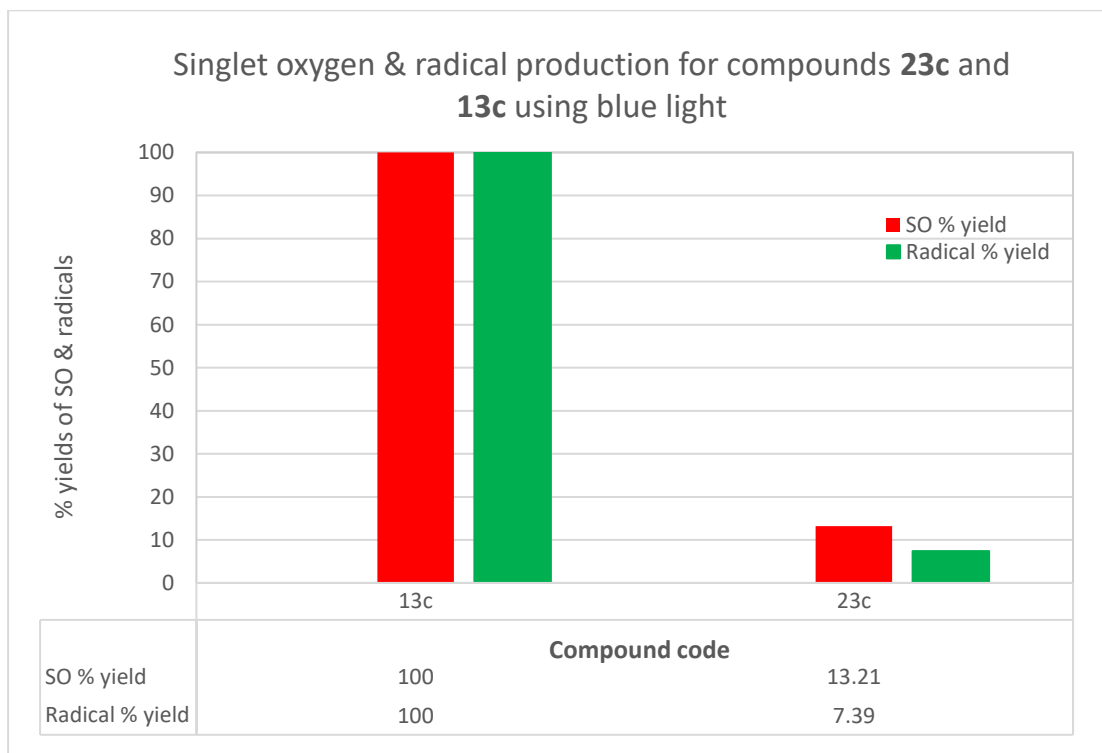
Figure 98: Chemical structure of 10-(N-nitrophenyl) isoalloxazines

Table 44: Photophysical data for 10-(2-nitrophenyl) isoalloxazine derivatives

	Type II (S/O)		Type I (Rad)	
	t <sub>1/2</sub> (mins)	Yield (%)	t <sub>1/2</sub> (mins)	Yield (%)
<b>23oc</b>	306.09	13.21	42.12	7.39
<b>13c</b>	4.45	100	3.11	100

The singlet oxygen yield for compound **23c** was calculated using Equation 4 and Equation 5. Compound **23c** generated a yield production of 13.21%. Whilst comparing this yield with phenyl isoalloxazine, **13c**, it is deduced that a lower yield was generated, consequently making **13c** a better generator of singlet oxygen having no substituents attached to the phenyl ring.

The radical production was determined for compound **23c** via the same principle as singlet oxygen production and generated a radical yield of 7.39%. Comparison of this yield with **13c** clearly illustrates that compound **23c** is not a radical producer and these results are highlighted in Figure 99.



*Figure 99: Singlet oxygen and radical production of compound 23c vs 13c*

## Chapter 4

### *Results and Discussion-microbiology*

In the present study, the antimicrobial activity of a library of synthesised isoalloxazines, alleged to have cytotoxic effects were evaluated for their potential antimicrobial activity against the medically important bacteria *Staphylococcus aureus* and *Escherichia coli*.

In microbiology, the Minimum Inhibitory Concentration (MIC) is the lowest concentration of an antimicrobial that will inhibit the visible growth of a microorganism after overnight incubation. Minimum inhibitory concentrations are important in diagnostic laboratories to confirm resistance of microorganisms to an antimicrobial agent and also to determine the potency of new antimicrobial agents. An MIC is generally regarded as the most basic laboratory measurement of the activity of an antimicrobial agent against an organism.

In the present work it was noticed that reduced growth of colonies was observed at certain concentrations, and this was designated 'partial inhibition' and given the symbol †. Figure 100 illustrates an example of reduced growth of the microbes. This is not numerically verified, as it is intended to be a screening process only and not as a definitive assay which shows the presence of antimicrobial activity.

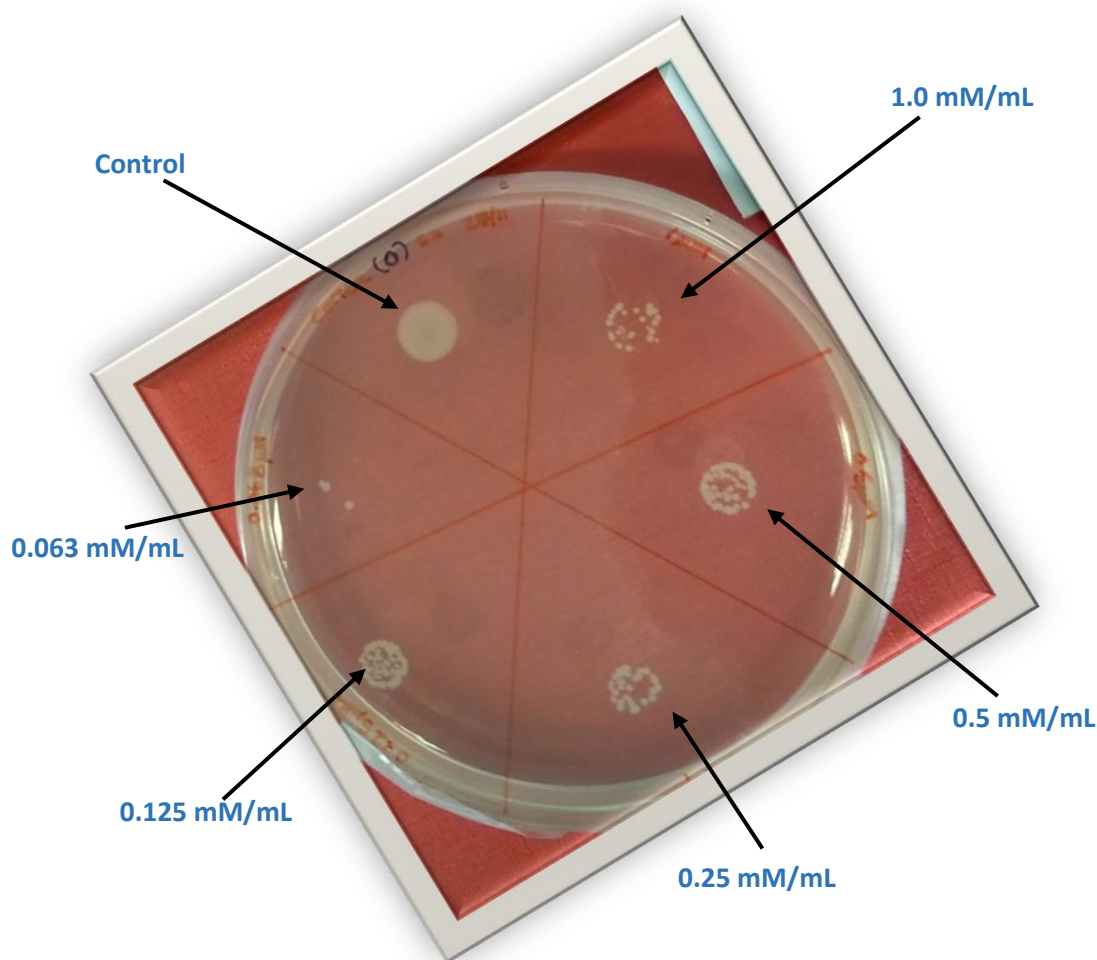


*Figure 100: Example of partial inhibition of microbes at various concentrations*

Figure 100 shows how a typical MIC was recorded of both the gram negative and gram positive microbes at the said concentrations (ranging from 1.0 mM/mL to 0.063 mM/mL). It can be seen that no antimicrobial activity has occurred in the control, whereas all other concentrations including 0.063 mM/mL show ‘partial inhibition’ of growth. Although partial inhibition is detected, it is important to note that it is not considered as an MIC value, but evidence of antimicrobial activity. Concentrations lower than 0.063 mM/mL were not tested as preparation of this concentration was proving to be difficult in terms of accuracy. To avoid such errors, testing of lower concentrations was not undertaken.

#### 4.1 Antimicrobial & photophysical studies for the synthesised isoalloxazines

The antimicrobial activity of the synthesised library of isoalloxazines was monitored in the dark and in blue light in order to investigate whether the wavelength (450-495 nm) of blue light effected the antibacterial activity in terms of the MIC.

In order to follow the compound codes through the text, Table 45 designates each of the molecules with a given code that can be used as reference.



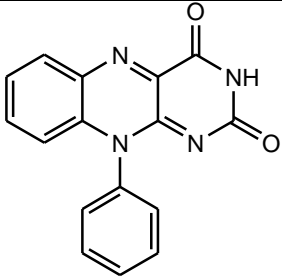
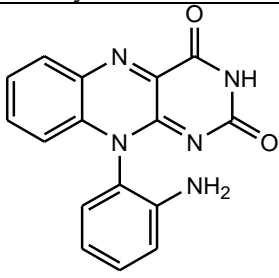
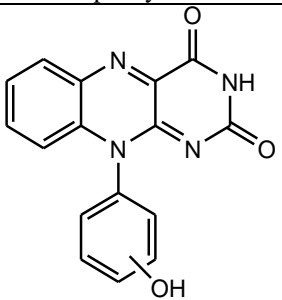
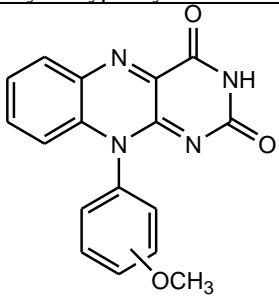
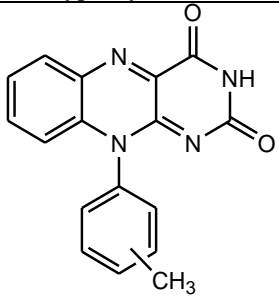
Table 46 and Table 47 present the antimicrobial activity of the compounds tested in terms of values considered as MIC's

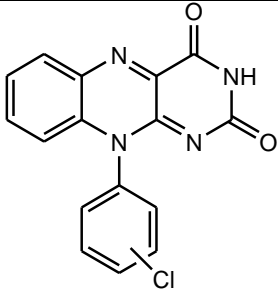
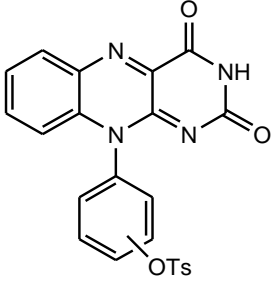
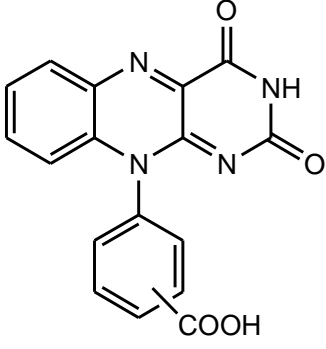
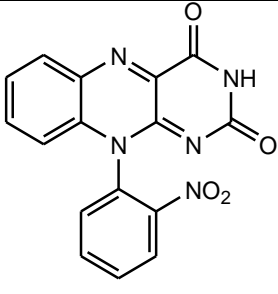
Figure 101 and Figure 102 present the antimicrobial activity of the compounds tested in terms of MIC values and partial inhibition values recorded. The figures presented are intended as an aid to the results and discussion, in that they highlight partial or reduced (compared to the growth in the dark) microbial growth where it was recorded, and may point to antimicrobial activity.

Table 48 to Table 58, present antimicrobial activity in terms of actual MIC values obtained, where Table 48, Table 53, Table 54, Table 55, Table 56, Table 57 and Table 58 present antimicrobial activity in terms of MIC values together with photophysical data.

Where anomalous results were obtained, they can be referred to in Table 72 to Table 89 in Appendix 1.

Table 45: Compound codes (regioisomers\*)

Antibacterial Agent/Biocide	Compound Code
 <p data-bbox="472 555 730 584">10-Phenyl isoalloxazine</p>	<p data-bbox="1106 398 1150 427"><b>13c</b></p>
 <p data-bbox="453 882 782 911">10-Aminophenyl isoalloxazine</p>	<p data-bbox="1086 719 1169 781"><b>1c</b> <i>o</i>-NH<sub>2</sub></p>
 <p data-bbox="443 1229 791 1258">10-Hydroxyphenyl isoalloxazine</p>	<p data-bbox="1046 1055 1209 1117"><b>4c/6c</b> <i>o</i>-OH/ <i>p</i>-OH</p>
 <p data-bbox="443 1574 791 1603">10-Methoxyphenyl isoalloxazine</p>	<p data-bbox="956 1402 1302 1464"><b>7c/8c/9c</b> <i>o</i>-OCH<sub>3</sub>/ <i>m</i>-OCH<sub>3</sub>/ <i>p</i>-OCH<sub>3</sub></p>
 <p data-bbox="461 1921 772 1951">10-Tolylphenyl isoalloxazine</p>	<p data-bbox="991 1749 1267 1812"><b>10c/11c/12c</b> <i>o</i>-CH<sub>3</sub>/ <i>m</i>-CH<sub>3</sub>/ <i>p</i>-CH<sub>3</sub></p>

 <p>10-Chlorophenyl isoalloxazine</p>	<p><b>14c/15c/16c</b> <i>o</i>-Cl/ <i>m</i>-Cl/ <i>p</i>-Cl</p>
 <p>10-Tosyloxyphenyl isoalloxazine</p>	<p><b>17c/18c/19c</b> <i>o</i>-OTs/ <i>m</i>-OTs/ <i>p</i>-OTs</p>
 <p>10-Carboxyphenyl isoalloxazine</p>	<p><b>20c/22c</b> <i>o</i>-COOH/ <i>p</i>-COOH</p>
 <p>10-Nitrophenyl isoalloxazine</p>	<p><b>23c</b> <i>o</i>-NO<sub>2</sub></p>

\*Compounds with more than one code are regioisomer.

Table 46 and Table 47 present an overview of the MIC results obtained for the tested isoalloxazines with varying functional groups attached to each of the phenyl ring, against the gram negative and positive bacteria.

Table 46: Recorded MIC results against *E.coli*

Compound Code	<i>Gram negative organism: E.coli</i>	
	MIC concentration (mM/mL) in Dark	MIC concentration (mM/mL) in Blue light
<b>13c*</b>	MIC > 1.0	MIC > 1.0
<b>1c</b>	MIC > 1.0	MIC > 1.0
<b>4c*</b>	MIC 0.5	MIC > 1.0
<b>6c</b>	MIC > 1.0	MIC > 1.0
<b>7c</b>	MIC 1.0	MIC > 1.0
<b>8c</b>	MIC > 1.0	MIC > 1.0
<b>9c</b>	MIC 1.0	MIC 1.0
<b>10c*</b>	MIC > 1.0	MIC 1.0
<b>11c</b>	MIC 1.0	MIC > 1.0
<b>12c</b>	MIC > 1.0	MIC > 1.0
<b>14c</b>	MIC > 1.0	MIC > 1.0
<b>15c</b>	MIC > 1.0	MIC > 1.0
<b>16c</b>	MIC > 1.0	MIC > 1.0
<b>17c</b>	MIC > 1.0	MIC > 1.0
<b>18c</b>	MIC > 1.0	MIC > 1.0
<b>19c</b>	MIC > 1.0	MIC > 1.0
<b>20c</b>	MIC > 1.0	MIC > 1.0
<b>22c</b>	MIC > 1.0	MIC > 1.0
<b>23c</b>	MIC > 1.0	MIC > 1.0

Table 47: Recorded MIC results against *S.aureus*

<i>Gram positive organism: S.aureus</i>		
<b>Compound Code</b>	<b>MIC concentration (mM/mL)in Dark</b>	<b>MIC concentration (mM/mL) in Blue light</b>
<b>13c*</b>	MIC > 1.0	MIC > 1.0
<b>1c</b>	MIC > 1.0	MIC > 1.0
<b>4c*</b>	MIC 0.5	MIC > 1.0
<b>6c</b>	MIC > 1.0	MIC > 1.0
<b>7c*</b>	MIC > 1.0	MIC > 1.0
<b>8c</b>	MIC > 1.0	MIC 0.25
<b>9c*</b>	MIC > 1.0	MIC > 1.0
<b>10c*</b>	MIC > 1.0	MIC > 1.0
<b>11c*</b>	MIC > 1.0	MIC 0.25
<b>12c*</b>	MIC > 1.0	MIC > 1.0
<b>14c</b>	MIC > 1.0	MIC > 1.0
<b>15c</b>	MIC 1.0	MIC 0.25
<b>16c*</b>	MIC 1.0	MIC > 1.0
<b>17c</b>	MIC > 1.0	MIC > 1.0
<b>18c</b>	MIC > 1.0	MIC > 1.0
<b>19c</b>	MIC > 1.0	MIC > 1.0
<b>20c</b>	MIC > 1.0	MIC > 1.0
<b>22c</b>	MIC 1.0	MIC 1.0
<b>23c</b>	MIC > 1.0	MIC > 1.0

Asterisks (\*) in Table 46 and Table 47 denote partial inhibition values recorded

## 4.2 Comparison studies for antimicrobial results of synthesised isoalloxazines using blue light

### 4.2.1 *E.coli*

The antimicrobial results achieved for the full library of synthesised isoalloxazines are collated and illustrated in Figure 101.

It is evident that little antimicrobial activity is observed in the majority of the synthesised isoalloxazines against the gram negative organism- *E.coli*. It was interesting to note the standard phenyl isoalloxazine (compound **13c**) did not record an MIC against *E.coli*. Thus, a comparison of antimicrobial activity for all other synthesised isoalloxazines was important to see whether having additional substituents could affect the microbial action in terms of its toxicity towards the gram negative organism.

The results achieved for the compounds in the library, showed that compounds with electron donating properties- i.e. compounds **9c** and **10c**, were able to exert toxic effects on the gram negative microorganism when illuminated with blue light. The two compounds (**9c** and **10c**) recorded antimicrobial activity at 1 mM/mL. Although compound **10c** recorded an MIC for *E.coli*, it was also the only compound to inhibit growth of this organism, as partial activity was detected for the additional tested concentrations (Table 80, Appendix 1). No other isoalloxazine produced a total biocidal effect against *E.coli*. Compound **10** also produced partial toxic effects at lower concentrations. It was interesting yet disappointing to note that four other antimicrobial agents (**4c**, **7c**, **8c**, **11c**) presented partial microbial activity against *E.coli* at 1.0 mM/mL concentration (Table 76, Table 78, and Table 80).

### Antimicrobial activity of all antimicrobial agents against *E.coli* in blue light.

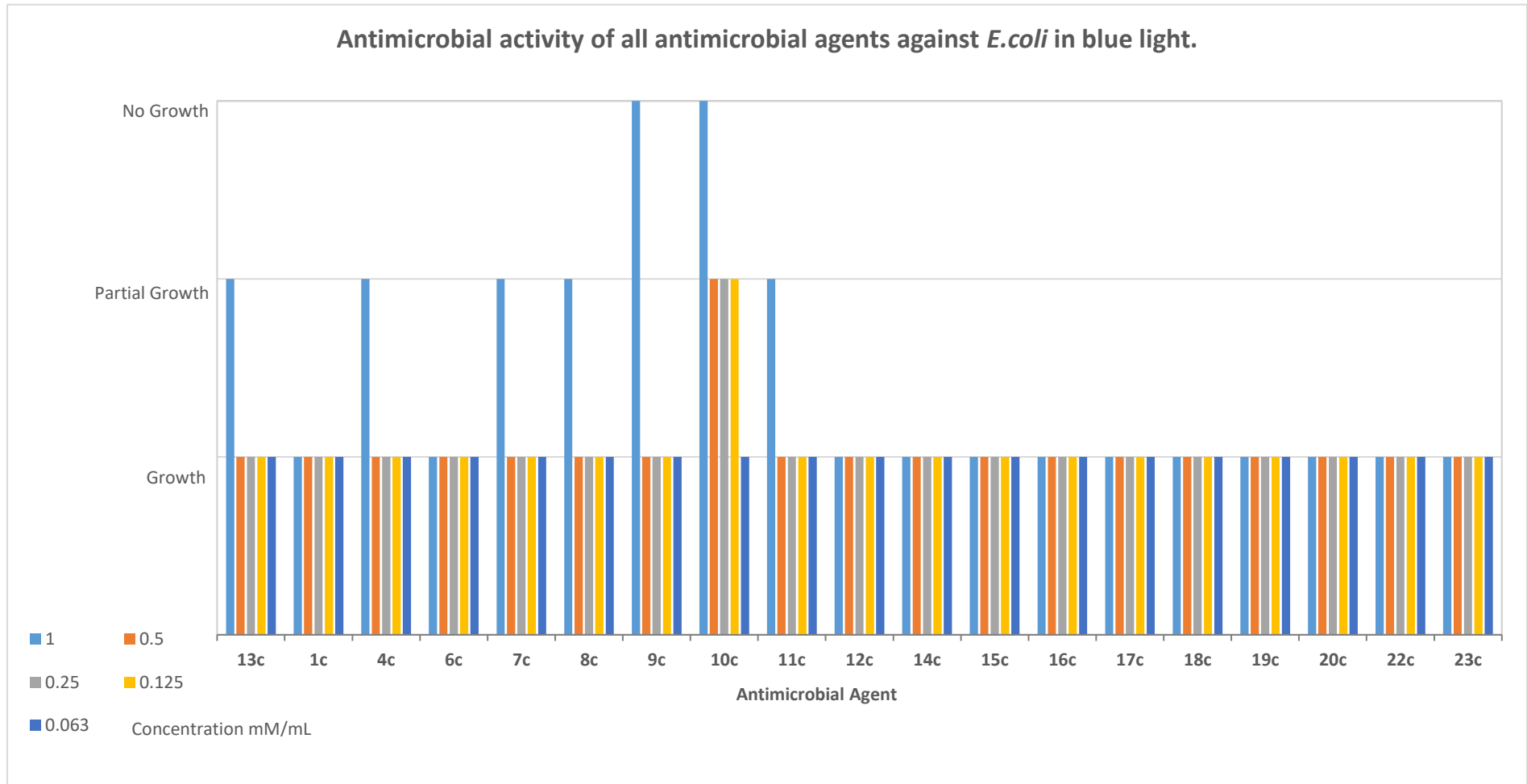


Figure 101: Antimicrobial activity of *E.coli*

#### 4.2.2 *S.aureus*

The complete synthesised library of isoalloxazines was tested for their antimicrobial activity against *S.aureus*. The results of antimicrobial activity is illustrated in Figure 102.

Figure 102 shows an increase in antimicrobial activity towards *S.aureus* compared to *E.coli*. Having tested the synthesised library of isoalloxazines for their antimicrobial activity it is seen that four isoalloxazines produced antimicrobial activity for the tested microorganisms. Total antimicrobial activity was observed for compounds **8c**, **11c**, **15c**, and **22c**. Of these compounds **8c-11c** have electron donating substituents attached. Compound **13c** is taken to be a neutral/standard isoalloxazine as no substituents are attached to the phenyl ring and antimicrobial activity of all other synthesised isoalloxazines are compared against the standard. Compound **13c** presents an MIC at 0.5 mM/mL and its partial activity is observed at 1 mM/mL (Table 73) Compounds **15c**, **16c**, and **22c** (Appendix 1, Table 83 and Table 86) have electron withdrawing substituents attached to the phenyl ring system. It is interesting to note that majority (ten) isoalloxazines presented partial antimicrobial activity (Figure 102). Of these compounds the partial activity is observed for isoalloxazines that have electron withdrawing substituents attached. Only two compounds (**4c** and **6c**) have electron donating substituents. Although only partial activity is observed for these isoalloxazines, further moderation of the isoalloxazine structure may indicate the possibility of achieving greater microbial activity, resulting in a biocidal effect on the pathogenic bacteria. It was dissapointing to observe that many of the number six (**1c**, **7c**, **9c**, **10c**, **12c**,and **14c**) isoalloxazines had no antimicrobial activity at all. Of these compounds **1c**, **7c**, **9c**, **10c**, and **12c** have electron-donating properties and **14c** has an electron withdrawing effect from the substituent attached to the phenyl ring.



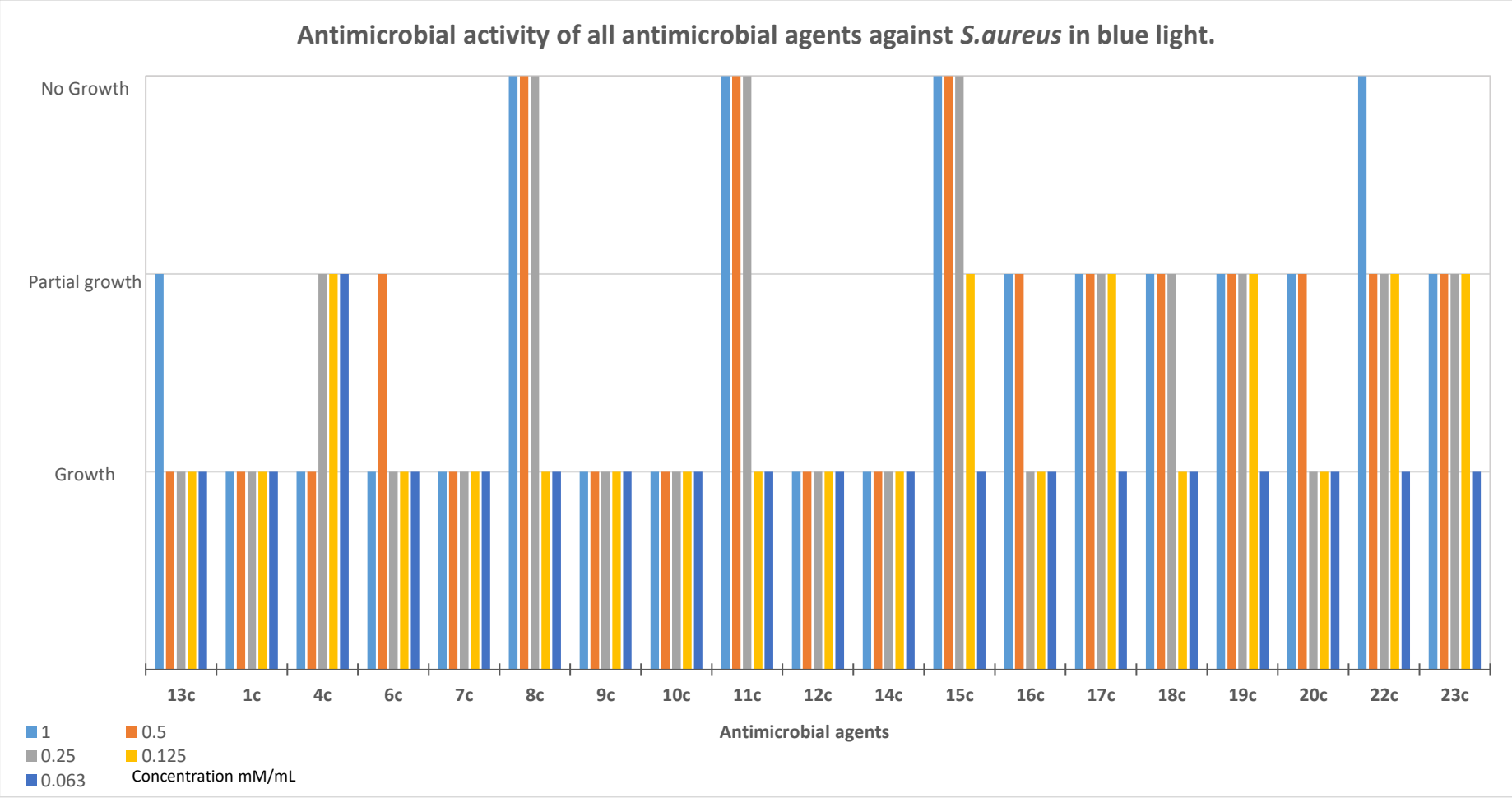


Figure 102: Antimicrobial activity of *S.aureus*

### 4.3 Antimicrobial & photophysical studies for compound 13c

Table 48 shows an overview of the antimicrobial and photophysical data obtained from the standard phenyl isoalloxazine, **13c**

Table 48: Antimicrobial activity & photophysical data for **13c** in blue light

Compound	MIC(mM/mL)	MIC(mM/mL)	<sup>1</sup> O <sub>2</sub> Yield (%)	Radical yield (%)
	<i>E.coli</i>	<i>S. aureus</i>		
<b>13c</b>	>1.0	>1.0	100	100

Compound **13c** was dissolved in methanol and ringers solution, to prepare a stock solution of 1.0 mg/mL<sup>-1</sup>. This solution was diluted to give 1 mM/mL, 0.5 mM/ mL, 0.25 mM/ mL, 0.125 mM/ mL, and 0.063 mM/ mL). To each of these dilutions, the freshly prepared bacteria (*E.coli* and *S.aureus*) were individually added. The varying concentrations containing the bacterial suspensions were illuminated for 12 hrs in blue LED light. Each of the concentrations was then inoculated onto an agar plate and incubated for a further 12 hours at 37 °C in order to show the minimum antimicrobial activity of each concentration.

Table 49 and Table 50 show the antimicrobial activity results achieved for compound **13c** against both *E. coli* and *S.aureus*.

Table 49: MIC of **13c** against *E.coli*

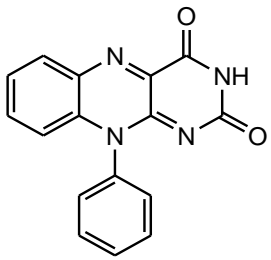
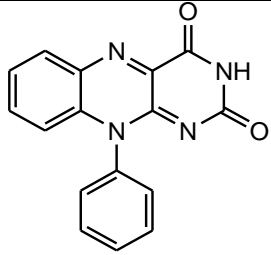
Antibacterial Agent/Biocide	Compound Code	Gram negative organism: <i>E.coli</i>					
		Light	Concentration in mM/mL/MIC				
 10 - Phenyl isoalloxazine			1	0.5	0.25	0.125	0.063
	<b>13c</b>	Dark	MIC >1.0				
	<b>13c*</b>	Blue Light	MIC >1.0				

Table 49 shows that an MIC value was not obtained for this compound against *E. coli* in the dark, as it was greater than 1.0 mM/mL. This indicates the compound was not a potential inhibitor, as the MIC value is predicted to be above the maximum tested concentration. Illumination of this compound with blue light also gave an MIC value to be greater than 1.0 mM/mL. Partial inhibition was recorded at 1mM/mL (Table 72, Appendix 1, Figure 103)

The antimicrobial activity for *S. aureus* was determined and shown in Table 50.

Table 50: MIC of **13c** against *S.aureus*

Antibacterial Agent/Biocide	Compound Code	Gram positive organism: <i>S.aureus</i>					
 10 - Phenyl isoalloxazine		Light	Concentration in mM/mL/MIC				
			1	0.5	0.25	0.125	0.063
	<b>13c</b>	Dark	MIC >1.0				
	<b>13c*</b>	Blue Light	MIC >1.0				

The MIC for this compound (**13c**) was above the concentration range tested under both light regimes. However, partial inhibition was observed at 1 mM/mL after illumination with blue light (Table 73, Appendix 1 and Figure 103).

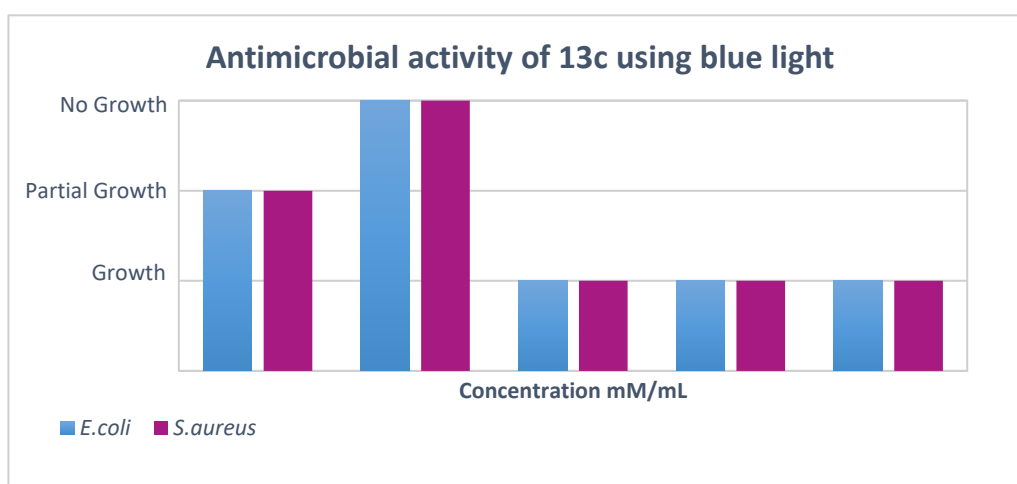


Figure 103: Antimicrobial activity of 13c using *E.coli* and *S. aureus*

This result was interesting as the two organisms have a different cell wall structure and yet the same toxic effects were recorded for both the organisms. The bacteria cell envelope is a complex multi-layered structure that protect the organisms from the hostile environment. The gram positive bacteria lacks an outer membrane layer but has a thick peptidoglycan layer. However, this differs from the gram negative organisms as they have a chemically complex layer, which contains a thin peptidoglycan cell wall that is surrounded by an outer membrane consisting of lipopolysaccharides<sup>354</sup>. With this in mind, it was not surprising to observe for this project, less antimicrobial activity overall was detected on the gram negative (*E.coli*) organism than the gram positive (*S.aureus*).

#### 4.4 Antimicrobial & photophysical studies for compound **1c**

The antimicrobial activity was monitored for compound **1c**. After incubating the microbes with compound **1c** at 37 °C for 12 hours, its antimicrobial activity was determined and compared to the photophysical data obtained (Table 51) for compound **1c**.

Table 51: Antimicrobial activity & photophysical data for **1c** in blue light

Compound	MIC(mM/mL) <i>E.coli</i>	MIC(mM/mL) <i>S.</i> <i>aureus</i>	<sup>1</sup> O <sub>2</sub> Yield (%)	Radical yield (%)
<b>1c</b>	>1.0	>1.0	41.44	0.84

Analysis of the results obtained from both the gram negative and positive organisms showed that no antimicrobial activity was seen in either blue light or in darkness. Although the amino (NH<sub>2</sub>) substituent a strong electron donator attached to the phenyl ring is a singlet oxygen generator, no biocidal activity was observed towards either organisms.

As no antimicrobial activity in terms of MIC against *E.coli* was noted at any of the concentrations tested under the light regimes, suggests that the MIC value is greater than 1mM/mL.

Compound **1c** again showed no antimicrobial activity against *S.aureus* being observed under either of the light regimes at all tested concentrations, indicating the MIC value for this compound is above 1 mM/mL.

Having a strong electron donating substituent (NH<sub>2</sub>) attached to the phenyl ring; no toxic effects were seen at the tested concentrations or as a result of illumination with blue light. These results were surprising, as ‘some’ antimicrobial activity could potentially be expected as singlet yield (41.44%) was achieved in a good yield.

## 4.5 Antimicrobial & photophysical studies for compound **4c** and **6c**

The photophysical data was obtained for compounds **4c** and **6c**, with a hydroxyl moiety substituted in the *ortho* and *para* position of the phenyl ring. The antimicrobial activity for these newly synthesised molecules was tested and compared against the photophysical data obtained, as shown in Table 52.

Table 52: Antimicrobial activity & photophysical data for **4c** and **6c** in blue light

Compound	MIC(mM/mL) <i>E.coli</i>	MIC(mM/mL) <i>S. aureus</i>	<sup>1</sup> O <sub>2</sub> Yield (%)	Radical yield (%)
<b>4c</b>	>1.0	>1.0	26.79	2.11
<b>6c</b>	>1.0	>1.0	8.11	0.08

No antimicrobial activity was seen for compound **6c** at the tested concentrations of 1-0.063 mM/mL in the dark. Compound **4c** after illumination with blue light presented partial growth of the microorganism at 1 mM/mL and no microbial activity was recorded for compound **6c**. For both these compounds, an MIC greater than 1 mM/mL was recorded for *E.coli*.

These compounds (**4c** and **6c**) were also tested against the gram positive organism, *S. aureus* and all MIC values for the hydroxyphenyl series were above tested range. The MIC for compound **4c** was above 1.0 mM/mL, an anomalous results was recorded at a concentration of 0.5 mM/mL in the dark where no growth was detected (Table 76, Appendix 1). When compound **4c** was illuminated with blue light, the MIC was also recorded to be greater than 1.0 mM/mL. A partial growth was seen at lower concentrations, this being between 0.25-0.125 mM/mL. Compound **6c** at 0.5 mM/mL was seen to give partial growth inhibition for both the tested regimes and this result of partial inhibition is still recorded as microbial growth.

When considering the photophysical results for these compounds, it can be seen that although an average yield (26.79%) of singlet oxygen was produced by compound **4c**, partial microbial growth at 0.25-0.125 mM/mL was observed as a result of illuminating with blue light, but no MIC was detected.

Compound **6c** shows extremely low productions of cytotoxic species (singlet oxygen and radicals). When comparing the production of singlet oxygen and radicals generated by the isoalloxazine with electron donating substituent (OH) attached to the phenyl ring, with the antimicrobial activity for compound **6c**, it could be considered that either none or very little microbial growth would occur as a result of low levels of toxic species.

The results show that no toxic effects were recorded for *E.coli* at all. However, the antimicrobial activity by *S. aureus* shows partial growth under both blue light and darkness. No direct relationship can be seen in the antimicrobial results obtained for the two hydroxyphenyl isomers after illumination with blue light. For compound **4c** at the concentration of 1 mM/mL, partial microbial growth against *E.coli* can be associated with the singlet oxygen generated (26.79%). Although low yields of singlet oxygen and/or radical was produced, partial inhibition of compound **4c** against *S. aureus* was detected at the lower concentrations (0.25 – 0.063) mM/mL, yet, this is not considered to be the official MIC value.

Extremely low yields of the cytotoxic species were obtained for compound **6c** and no MIC or reduction in growth was observed for *E. coli* at any of the concentrations tested. This can be associated to the low production of cytotoxic species. Although very low yields of singlet oxygen and radicals were produced for this compound (**6c**), surprisingly reduced growth was observed at 0.5 mM/mL against *S.aureus*.

## 4.6 Antimicrobial & photophysical studies for compound 7c-9c

Table 53 shows an overview of the antimicrobial and photophysical data obtained from the methoxy substituted isoalloxazines for compounds 7c–9c.

Table 53: Antimicrobial activity & photophysical data for 7c and 9c in blue light

Compound	MIC (mM/mL) ( <i>E. coli</i> )	MIC (mM/mL) ( <i>S. aureus</i> )	<sup>1</sup> O <sub>2</sub> yield (%)	Radical yield (%)
7c	>1.0	> 1.0	98.32	2.91
8c	>1.0	0.25	17.25	1.71
9c	1.0	0.5	39.44	3.84

For each of the synthesised isoalloxazines the antimicrobial activity was tested on freshly prepared bacteria and compared against the photophysical data obtained.

Under dark conditions the MIC of compound 7c was achieved at concentration 1 mM/mL. Using blue light illumination, compound 7c shows a partial reduction in growth (Table 78, Appendix 1 and Figure 104) at the same concentration, suggesting the MIC value to be greater than 1.0 mM/mL. No further activity was observed at any of the tested concentrations in either light regimes.

The *meta* substituted methoxyphenyl isoalloxazine (compound 8c) shows no evidence of antimicrobial activity in the dark, however partial reduction in microorganism growth is seen after illuminating with blue light at 1 mM/mL, and no further antimicrobial activity was observed at all other tested concentrations for this compound. The MIC for compound 9c was recorded at 1 mM/mL under both light regimes. Analysis of the photophysical data shows that singlet oxygen was achieved at 39.44%, indicating that this quantity of the cytotoxic species was enough to kill 100% of the gram negative organism (*E.coli*).

The antimicrobial activity for the methoxy series of isoalloxazines were tested against the gram positive, *S.aureus* microorganism. The MIC was determined using the standard protocol by monitoring the antimicrobial activity using blue light illumination and in darkness.

Compound 7c showed no growth at the concentration 0.5 mM/mL under darkness, this is an anomalous result as growth is observed at 1 mM/mL. Upon re-testing this compound, the same result was achieved on all three occasions. Knowing that methoxy substituent is an electron donating moiety and activates the *N*-10 phenyl ring making it reactive; could suggest the reason for antimicrobial activity to be detected at this concentration (0.5 mM/mL)). No additional activity is observed after illuminating this compound with blue light. The *meta* substituted isoalloxazine (8c) in the dark shows no antimicrobial activity. However, when illuminating with

blue light no growth is detected from 1 mM/mL to 0.25 mM/mL resulting in the MIC value as 0.25mM/mL. The last compound in this series (compound **9c**) also gave an anomalous result at 0.5 mM/mL under both light regimes, (Table 79, Appendix 1 and Figure 104) even after being re-tested on multiple occasions. The results achieved by this compound seems somewhat anomalous particularly having an extremely poor yield for the radical production (3.84%).

Figure 104 illustrates the antimicrobial activity for all three isomers of the methoxyphenyl isoalloxazines when illuminated from a 5 cm height using blue light.

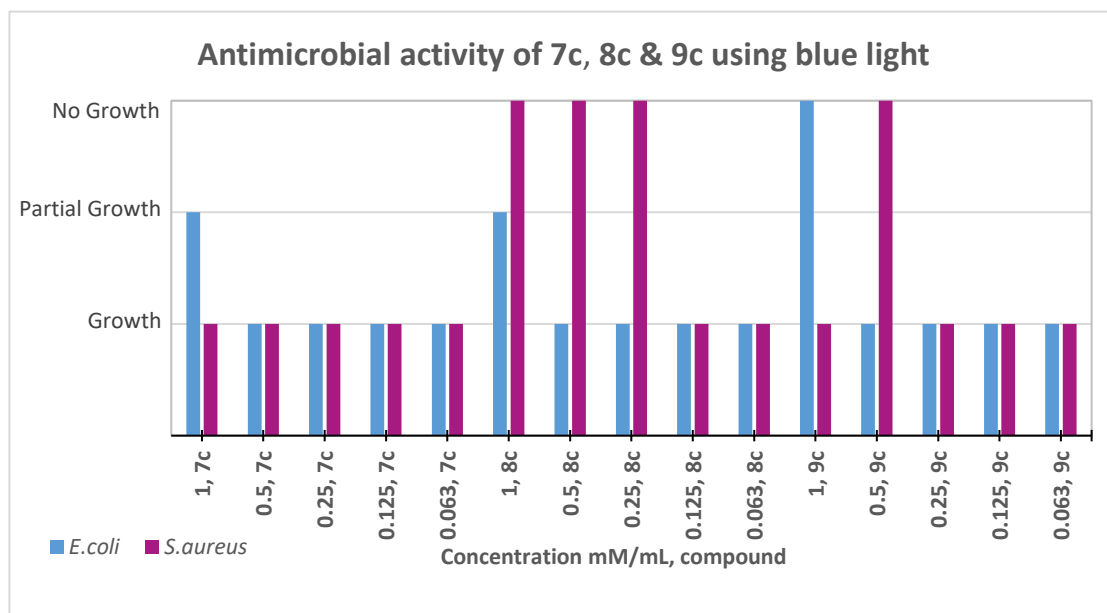


Figure 104: Antimicrobial activity for compounds 7c, 8c & 9c-using *E.coli* and *S. aureus*

The results show no immediate similarities in antimicrobial activity. It can be seen that compound **7c** showed partial microbial growth at 1 mM/mL for *E.coli* and no antimicrobial activity was observed for *S. aureus*. This result was surprising as the singlet oxygen yield produced by **7c** was extremely high (98%, Table 53) yet minimal toxic effects were recorded for both microorganisms. In contrast to this, an interesting result was achieved by compound **8c** as partial antimicrobial activity was observed at 1 mM/mL for *E.coli*. However, it is seen to be the most potent isomer in killing the *S.aureus* microorganism, as compound **8c** showed 100% inhibition of growth at concentration range from 1 mM/mL to 0.25 mM/mL.

A comparison of the substituted methoxyphenyl isomers, (Figure 104) illustrates that a reduction in antimicrobial action is predominantly produced by compound **8c**. This result is interesting as the photophysical data shows that **8c** generated the least quantity of cytotoxic species-singlet oxygen and radicals. Whereby, the *para* substituted compound (**9c**), shows 100% inhibition of microbial growth at 1 mM/mL for *E.coli*, and at 0.5 mM/mL for *S.aureus* (although this is not recorded as the official MIC value). The singlet oxygen produced by **9c** was 39%, signifying that this yield was sufficient to inhibit the bacteria at these concentrations.



The methoxy substituted isalloxazines were attached to a polymer support as discussed in section 4.18 and tested against microbial activity. Compound **7d** presented no antimicrobial activity against either of the tested organisms. However, **9d** recorded an MIC value of 1.0 mM/mL against the gram positive organism. Achieving this result was promising as this confirmed that the synthesised isoalloxazine substituted to a polymer support is able to retain its antimicrobial activity.

#### 4.7 Antimicrobial & photophysical studies for compound **10c-12c**

An overview of the antimicrobial and photophysical data obtained for the substituted tolyl isoalloxazines compounds **10c-12c** are illustrated in Table 54.

Table 54: Antimicrobial activity & photophysical data for **10c-12c** in blue light

Compound	MIC (mM/mL) ( <i>E. coli</i> )	MIC (mM/mL) ( <i>S. aureus</i> )	<sup>1</sup> O <sub>2</sub> yield (%)	Radical yield (%)
<b>10c</b>	1.0	>1.0	83.99	0.01
<b>11c</b>	>1.0	0.25	41.58	227
<b>12c</b>	>1.0	>1.0	172.17	3.53

The antimicrobial activity was monitored for each of the synthesised compounds in the dark and in blue light.

For the whole series of substituted tolylphenyl isoalloxazines, interesting results against both microbes were observed, particularly with the *ortho* substituted compound (**10c**) under darkness. It was noted that compound **10c** proved to be an inhibitor of microbial growth at the same concentration (0.25 mM/mL) under darkness. This result clearly indicates that the singlet oxygen generated in an excellent yield (84%) was able to cause a total biocidal effect towards the microbes without the use of additional help, in this case blue light. However, against the gram negative organism (*E. coli*), compound **10c** after illumination with blue light recorded the MIC at 1.0 mM/mL and a partial growth is seen from 0.5 to 0.125 mM/mL. Compound **11c** shows an MIC at 1 mM/mL and complete growth was observed for the lower tested concentrations in the dark. It was promising to observe microbial death at this concentration in the dark, particularly as illumination with blue light of this compound only presented partial antimicrobial activity at 1 mM/mL and no further activity for other concentrations, (Table 80, Appendix 1 and Figure 105). The *para* substituted isomer, **12c**, showed partial antimicrobial activity at 0.25 mM/mL in the dark, and no inhibition was observed at all when illuminated using blue light.

The substituted tolylphenyl isoalloxazines were tested for their antimicrobial activity using *S. aureus* as the tested microorganism both in the dark and with blue light.

Compound **10c** gave an anomalous result for antimicrobial activity against *S. aureus* in the dark at the concentration 0.25 mM/mL. Upon re-testing this compound, the same result was achieved,

nonetheless, this value is not considered as the MIC value as growth in higher concentrations is detected (Table 80, Appendix 1, and Figure 105). After illumination with blue light, this compound presented no antimicrobial activity within the range of concentrations tested. The *meta* tolylphenyl isoalloxazine, **11c**, showed no growth at 0.25 mM/mL in the dark, which again could not be recorded as the MIC value. However, under blue light illumination an MIC of 0.25 mM/mL was recorded. The results obtained for the tolyl series are presented in Figure 105.

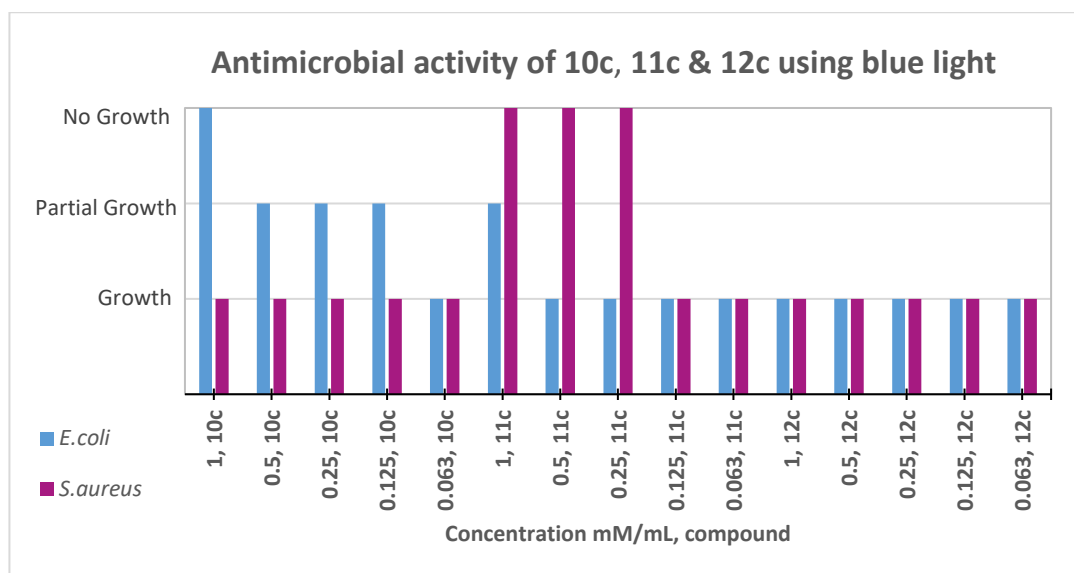


Figure 105: Antimicrobial activity for compounds 10c-12c-using *E. coli* and *S. aureus*

The antimicrobial activity achieved under blue light illumination was used to see whether there was any relationship with the photophysical data, (Table 54). When compound **10c** was illuminated with blue light, the MIC for *E. coli* was seen at 1 mM/mL. The reduction in growth was seen to occur from concentrations 0.5 mM/mL to 0.125 mM/mL. This result was not surprising as the cytotoxic species, singlet oxygen yield was generated in 84%. It could be hypothesised that-if a higher production of singlet oxygen was achievable the partial antimicrobial activity observed could possibly show a total (100%) kill, resulting in a lower MIC value. Although this was not achievable, the MIC for the *ortho* substituted isomer (**10c**) was recorded at 1 mM/mL for *E. coli*. Interesting results were seen for the activity against *S. aureus* as no antimicrobial activity was observed even though high singlet oxygen yield (84%) was obtained. In addition to this, for compound **11c** the photophysical data shows that singlet oxygen was generated at a yield of 41% and radicals at a brilliant rate of 227% yield. Partial antimicrobial activity was observed at 1 mM/mL for *E. coli* and *S. aureus* showed 100% antimicrobial inhibition in the concentration range of 1 mM/mL to 0.25 mM/mL after illumination with blue light. These results could be because of the high generation of the cytotoxic species, resulting in death of microorganisms. Compound **12c** shows results that are difficult to explain, in that no antimicrobial activity was observed against either organisms even though singlet oxygen was

generated at a yield of 172%. Complete inhibition of microbial growth was expected as a high generation of cytotoxic species, either singlet oxygen or radicals would result in cellular death, however, these results unfortunately still show microbial growth.

Tolyl substituted isoalloxazines were also attached to the polymer support (**10d-12d**) as discussed in section 4.19 in order to test their activity against microbes. The antimicrobial activity results recorded by each of the tolyl isoalloxazine derivatives presented interesting microbial activity. It was noted that having the tolyl isoalloxazine's onto a polymer support enhanced antimicrobial activity. This was interesting to observe, as the presence of any antimicrobial activity monitored by these compounds indicates the molecules to be promising antimicrobial agents. It was pleasing to record a reduction in microbial growth particularly towards the gram negative organism (*E.coli*). Thus, signifying the possibility of achieving better antimicrobial results after moderating either the functional groups present on the isoalloxazines or the experiments themselves. Compound **12d** presented antimicrobial activity against the gram positive organism (*S.aureus*) resulting in an achievable MIC value of 1mM/mL.

#### 4.8 Antimicrobial & photophysical studies for compound **14c-16c**

Antimicrobial activity was monitored for compounds **14c-16c**. Having incubated the microbes with each of the isoalloxazines (**14c-16c**) at 37 °C for 12 hours, the MIC was determined and compared with the photophysical data obtained (Table 55) for these compounds.

Table 55: Antimicrobial activity & photophysical data for **14c-16c** in blue light

Compound	MIC (mM/mL) ( <i>E. coli</i> )	MIC (mM/mL) ( <i>S. aureus</i> )	<sup>1</sup> O <sub>2</sub> yield (%)	Radical yield (%)
<b>14c</b>	>1.0	>1.0	29.08	8.64
<b>15c</b>	>1.0	0.25	77.49	99.47
<b>16c</b>	>1.0	> 1.0	47.30	27.09

The antimicrobial activity for compounds **14c-16c** investigated in the dark and in blue light presented no MIC or partial activity throughout the series for the chlorophenyl isoalloxazines against *E.coli*. The results achieved are somewhat unexpected yet interesting as having an electron withdrawing substituent (Cl) attached to the molecule was expected to effect the microbial growth, particularly when illuminating with blue light. It was predicted that blue light would activate the chlorine in order to damage the cellular structure resulting in cell death.

These compounds (**14c-16c**) were also tested for their antimicrobial activity against the gram positive organism, *S. aureus* under both (dark/blue) light regimes.

No antimicrobial activity is observed for compound **14c** under either light condition against *S.aureus*. Compound **15c** shows an MIC in the dark at 1 mM/mL.

When **15c** was illuminated with blue light, an MIC of 0.25 mM/mL and a reduction in growth is observed at 0.125 mM/mL (Table 83). This shows that having a chloro substituent in the *meta* position helps to achieve microbial death at lower concentrations with the aid of blue light. Compound **16c** showed an MIC at 1.0 mM/mL in darkness yet after illumination with blue light, the MIC was observed to be greater than 1.0 mM/mL. Partial antimicrobial activity was seen at 1.0 mM/mL and 0.5 mM/mL, Table 83, Appendix 1, and Figure 106) but no MIC was detected for this isomer.

The antimicrobial results obtained for the substituted chlorophenyl isoalloxazines are illustrated in Figure 106 in order to detect similarities between each isomer and from the photophysical data obtained for these antibacterial agents.

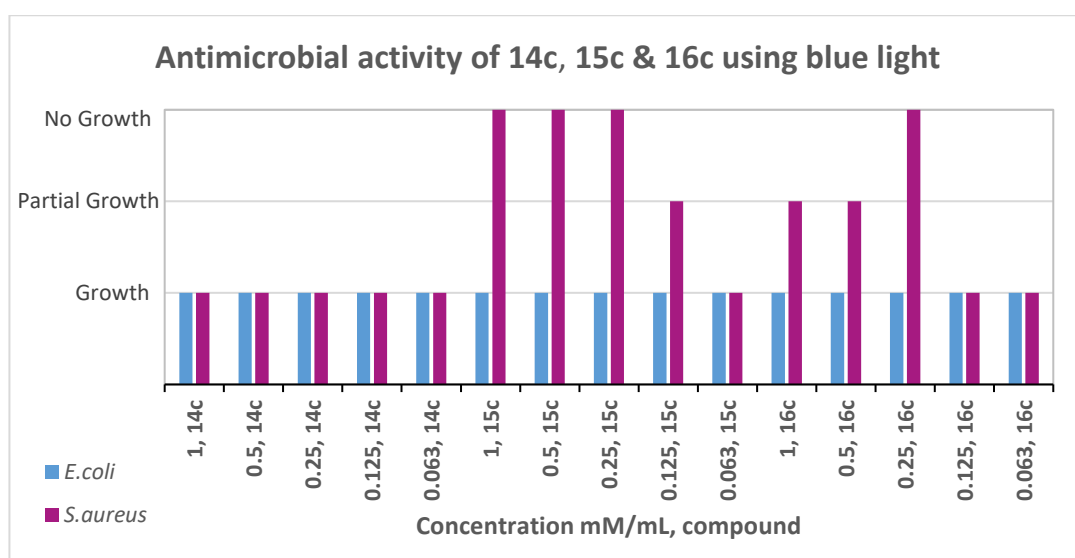


Figure 106: Antimicrobial activity for compounds 14c-16c-using *E.coli* and *S. aureus*

Having considered the antimicrobial results obtained with the singlet oxygen (29%) and radical (9%) yields generated by compound **14c**, the absence of antimicrobial activity observed for both microorganisms can be explained by the very low yields of cytotoxic species generated. The photophysical data obtained by the *meta* chlorophenyl isoalloxazine (**15c**) generated a high singlet oxygen yield of 77% and an excellent radical production of 99%. The high yields generated by this compound explains the achieved MIC values for both the microorganisms, *E.coli* and *S. aureus*. However, the obtained antimicrobial activity results for *E.coli* are not as expected as no inhibition of microbial growth was observed. This most certainly was unexpected, considering the generation of high yields of cytotoxic species would incur cellular death. Thus, it can be concluded that the chloro substituent does not affect the complex *E.coli* cell wall as no damage to the microorganism is recorded. However, the results achieved for *S. aureus* shows the isoalloxazine, **15c** to be effective antimicrobial activity was detected at a concentration range (1-

0.25 mM/mL) giving an MIC value of 0.25 mM/mL and partial antimicrobial activity is observed at 0.125 mM/mL (Table 83). Subsequently, the relationship between the antimicrobial activity and production of high yields of singlet oxygen and/or radicals at this point can be made that a high generation of cytotoxic species led to the cell death, for the gram positive species. The singlet oxygen for compound **16c** was produced in a 47% and radical was generated in a 27% yield. By comparing the antimicrobial activity obtained for the other chlorophenyl isoalloxazine isomers, it was not surprising to see that no antimicrobial activity was observed for compound **16c** against *E.coli*. However, partial antimicrobial activity observed for *S. aureus* with **16c** at concentrations 1 mM/mL and 0.5 mM/mL with an anomalous result detected at 0.25 mM/mL (Table 87, Appendix 1 and Figure 106). The reduction in growth can be reasoned with the generated photophysical data for the gram positive organism, *S. aureus* in addition to the blue light affecting the microbial growth.

The chlorophenyl isoalloxazines were also attached to a polymer support as mentioned in section 4.20 and tested for their antimicrobial activity. Although compound **15d** disappointingly recorded no antimicrobial activity against *E.coli*, a reduction in microbial growth was observed against *S.aureus* for both **15d** and **16d**. It was inspiring to observe an MIC value achieved against *S.aureus* by compound **16c**. Evaluation of the polymer substituted *N*-chlorophenyl isoalloxazines clearly indicates antimicrobial activity is retained whilst the isoalloxazine is attached to the polymer support, resulting in these compounds to be potential antimicrobial agents.

## 4.9 Antimicrobial & photophysical studies for compound 17c-19c

Table 56 shows the photophysical data obtained for compounds **17c-19c**, with the tosyloxy moiety as its substituent on the phenyl ring. The antimicrobial activity for these newly synthesised molecules was tested and compared against the photophysical data obtained.

Table 56: Antimicrobial activity & photophysical data for **17c-19c** in blue light

Compound	MIC (mM/mL) ( <i>E. coli</i> )	MIC (mM/mL) ( <i>S. aureus</i> )	<sup>1</sup> O <sub>2</sub> yield (%)	Radical yield (%)
<b>17c</b>	>1.0	>1.0	75.78	4.46
<b>18c</b>	>1.0	>1.0	68.08	0.12
<b>19c</b>	>1.0	>1.0	96.94	13.41

The electron withdrawing nature of the tosyloxy substituent was employed to monitor the antimicrobial activity of compounds **17c-19c** in the dark and in blue light illumination.

It is surprising to note that no antimicrobial activity is detected in the range of tested concentrations for the complete series of tosyloxyphenyl isoalloxazines, especially as the singlet oxygen production for each of the compounds was above 65%. The antimicrobial results are unexpected as the tosyloxyphenyl substituent is presumed to affect the electron density of the molecular structure due to the electron withdrawing properties of the OTs group resulting in damage to the cellular structure in order to destroy the microbes. Dissappointingly no microbial inhibition was observed for the gram negative organism, *E.coli* both in the dark and after illumination with blue light for any isomers of the tosyloxyphenyl isoalloxazines.

The antimicrobial activity for *S.aureus* was also monitored for compounds **17c-19c**. Compound **17c** in the dark showed no antimicrobial activity towards the gram positive microorganism. After illumination with blue light, a reduction in microbial growth was observed at concentration range from 1 mM/mL to 0.125 mM/mL (Table 85), suggesting the MIC value to be greater than 1.0 mM/mL for this compound. Observing partial reduction in microbial growth suggests that having an electron withdrawing substituent attached (OTs) at the *ortho* position shows this compound could be an effective compound in microbial killing, especially as compound **18c** presented an MIC greater than 1.0 mM/mL as no antimicrobial action in the dark was recorded against *S.aureus*. However, after illumination of blue light, partial antimicrobial activity is observed from 1.0 mM/mL to 0.125 mM/mL and no further activity is detected for the lower concentrations. The partial activity observed at the higher concentrations indicate that the MIC for this compound to be greater than 1.0 mM/mL. The *para* substituted isomer (**19c**) tested under the dark illustrates no antimicrobial activity, and under blue light illumination, partial microbial

activity is observed from concentrations 1 mM/mL to 0.125 mM/mL, indicating the MIC value to be greater than 1.0 mM/mL.

No antimicrobial activity for compound **17c** against *E.coli* under any of the tested concentrations, although the singlet oxygen production for **17c** was generated in a good yield (76%). Unfortunately, the antimicrobial results for **17c** are disappointing because the generation of cytotoxic species is hypothesised to kill microbes and yet no antimicrobial activity is recorded. The same results were achieved after repeating the experiments three times concluding no microbial inhibition for this isoalloxazine. *S.aureus* on the other hand presented partial microbial activity at concentration ranges from 1 mM/mL to 0.125 mM/mL after illuminating with blue light. The fact that partial activity occurs, seems encouraging, yet disappointing as no MIC was recorded in the tested concentration range. The occurrence of any antimicrobial activity at all is promising. The photophysical data obtained for compound **18c** shows a singlet oxygen yield of 68% and an extremely poor radical yield of 0.1%. The antimicrobial activity of the *meta* substituted tosyloxyphenyl isoalloxazine (**18c**) against *E.coli* disappointingly shows no toxic effects at all. *S.aureus* shows no total (100%) inhibition for compound **18c**, however, a partial reduction in microbial growth is observed. Compound **19c** produced photophysical data (Table 56) of singlet oxygen production; 97% and radical yield of 13%. For this compound, no microbial activity was seen against *E.coli* but *S.aureus* showed partial microbial activity from 1 mM/mL to 0.125 mM/mL even though an excellent production of singlet oxygen was achieved. It can be suggested that the gram negative organism presents total resistance (Table 85) towards all isomers of the tosyloxyphenyl isoalloxazine, as no biocidal affects are observed. In contrast to this, *S.aureus* presents partial microbial activity for majority of the series of tosyloxyphenyl isoalloxazines, proving the cell structure of the gram positive organism being less complex than the gram negative organism.

The tosyloxy derivatives were substituted to the polymer support highlighted in section 4.9 to test their killing ability against microbes. Unfortunately, this series of isoalloxazines did not present positive results in terms of their antimicrobial activity. Compound **18d** was the only derivative from this family to present reduction in microbial growth against *S.aureus*. All other derivatives presented total microbial growth against both microorganisms, resulting in no achievable MIC value.

#### 4.10 Antimicrobial & photophysical studies for compound **20c** and **22c**

The antimicrobial action of compounds **20c** and **22c** was interesting to observe against the photophysical data obtained and is shown in Table 57.

Table 57: Antimicrobial activity & photophysical data for **20c** and **22c** in blue light

Compound	MIC (mM/mL) ( <i>E. coli</i> )	MIC (mM/mL) ( <i>S. aureus</i> )	<sup>1</sup> O <sub>2</sub> yield (%)	Radical yield (%)
<b>20c</b>	>1.0	>1.0	14.12	0.29
<b>22c</b>	>1.0	1.0	12.67	0.88

Both the compounds show results of the antimicrobial activity for the substituted carboxyphenyl isoalloxazines (**20c** and **22c**) against the gram negative organism (*E.coli*) under darkness and in blue light did. Unfortunately neither of these compounds presented any potency in terms of their killing ability. These results were not unexpected as the the photophysical data obtained by these compounds was not generated in a great yield, hence it would have been surprising to expect to have observed any antimicrobial activity against *E.coli* under any of the investigated conditions. The carboxyphenyl isoalloxazines (**20c** and **22c**) were investigated for their activity against *S. aureus* for both these compounds under the tested light regimes.

Compound **20c** in the dark presented no antimicrobial activity in the tested range, therefore it is suggested that the MIC for compound **20c** greater than 1.0 mM/mL. Blue light illumination presented partial growth inhibition at 1 mM/mL and 0.5 mM/mL (Table 87). This suggests that the MIC to be above 1mM/mL. Compound **22c** recorded an MIC at 1 mM/mL in the dark. After illumination of compound **22c** total antimicrobial activity is observed at 1.0 mM/mL and partial activity in growth can be seen at concentrations 0.5 mM/mL - 0.125 mM/mL.

The photophysical data recorded for compounds **20c** and **22c** show a very low yield production of cytotoxic species generated (Table 57). Compound **20c** generated a singlet oxygen yield of 14% and a radical production of 0.27%. The absence of antimicrobial activity observed for *E.coli* can be explained by an insufficient yield of cytotoxic species generated thus resulting in no cellular damage. Although no total inhibition was detected for *S. aureus* partial microbial growth at 1 mM/mL and 0.5 mM/mL was observed. Compound **22c** generated singlet oxygen in 13% and a radical yield of 0.9%. Having a low production of cytotoxic species may account for the lack of antimicrobial activity against *E.coli* by compound **22c**. However, this theory does not prove conclusive for the gram positive organism an MIC of 1.0 mM/mL is recorded for *S.aureus* at 1 mM/mL. It is encouraging to observe partial microbial activity is present for concentrations 0.5 mM/mL to 0.125 mM/mL even though extremely low yields of cytotoxic species were generated (Table 87).



Compound **20c** was substituted onto a polymer support resulting in compound **20d** as shown in section 6.43. Compound **20d** was used to test the antimicrobial activity against *E.coli* and *S.aureus*. An interesting result was achieved even though no MIC value was achieved by this compound. It was encouraging to notice that a reduction in microbial growth was observed against both pathogenic microorganisms (*E.coli* and *S.aureus*). This indicates that **20d** could potentially be used as an antimicrobial agent if a complete kill of this pathogen (*E.coli*) is observed, regrettably majority of the synthesised isoalloxazines did exert toxic effects to the gram negative organism.

#### 4.11 Antimicrobial & photophysical studies for compound **23c**

The antimicrobial activity of compound **23c** was monitored and Table 58 shows an overview of the photophysical data obtained by this compound (**23c**).

Table 58: Antimicrobial activity & photophysical data for **23c** in blue light

Compound	MIC (mM/mL) ( <i>E. coli</i> )	MIC (mM/mL) ( <i>S. aureus</i> )	<sup>1</sup> O <sub>2</sub> yield (%)	Radical yield (%)
<b>23c</b>	>1.0	>1.0	13.21	7.39

This compound **23c** was tested for its antimicrobial activity in darkness and in blue light. No antimicrobial activity under either of the tested conditions and concentrations against *E.coli* was observed indicating the MIC to be above 1.0 mM/mL.

The microbial growth was monitored for compound **23c** against the gram positive organism, *S.aureus*. Under darkness no antimicrobial activity is observed for either of the tested concentrations possibly indicating the MIC value to be above 1.0 mM/mL. After illumination with blue light, compound **23c** recorded partial growth inhibition from 1 mM/mL to 0.125 mM/mL, but no MIC was recorded for *S.aureus*, also indicating the MIC is at a value greater than 1.0 mM/mL. Although it was disappointing to observe no cellular death incurred under either of the light regimes and concentrations, it was still promising to see that a strong electron withdrawing moiety affects the microbial growth. However, it was nonetheless disappointing to observe total microbial kill was not observed.

## *Discussion on antimicrobial Studies on Polymer bound isoalloxazines*

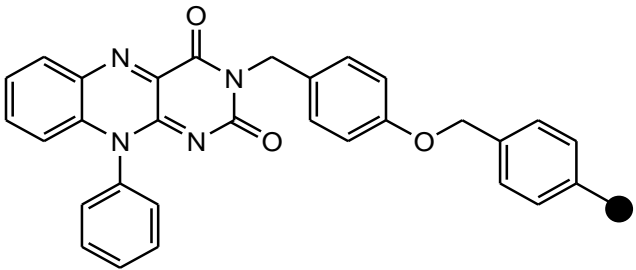
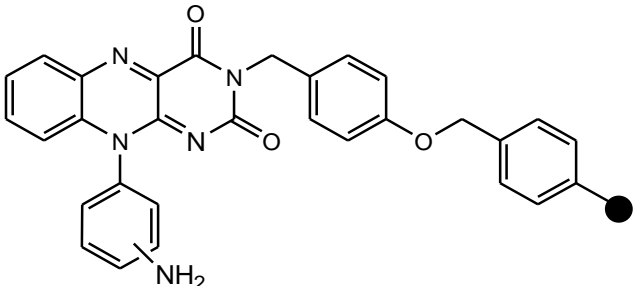
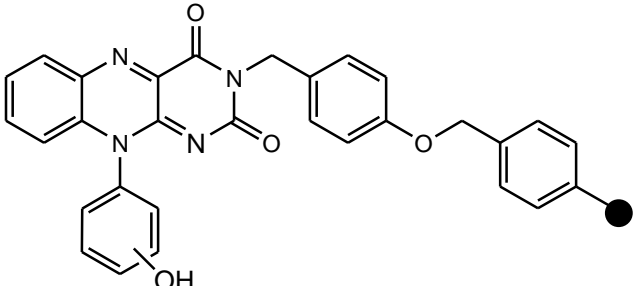
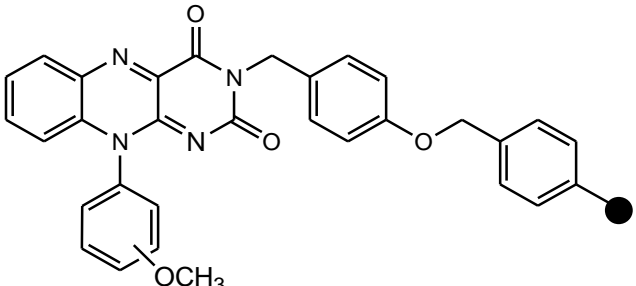
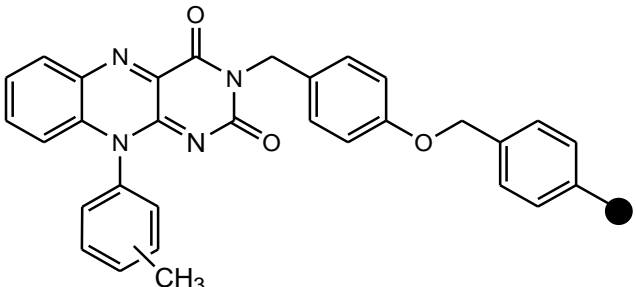
### 4.12 Results and discussion of antimicrobial studies on polymer bound isoalloxazines

A Wang brominated resin called 4-(benzyloxy)benzyl bromide, polymer-bound (which is referred to as 'polymer support') was used to simulate the bandage material that is commonly used in hospitals. Each of the synthesised antimicrobial agents was substituted (chemically attached) onto this resin in order to investigate how it would behave in a polymer support situation i.e as a bandage.

The antimicrobial agents substituted onto the polymer support were tested for their antimicrobial activity in terms of their MIC values against the hospital associated infections (HAI) caused by the gram negative and positive bacteria, (*Escherichia coli* and *Staphylococcus aureus*) respectively

The activity of these antimicrobial agents on the polymer support was tested against the bacteria using blue light. The importance of these agents is to recognise that the wounds themselves will receive the blue light, as the light will be shone onto polymer support (bandage) and thus hit the wound. However, as the photoantimicrobial agent is attached to the bandage, the bandage should remain free of pathogenic microbes. Hence, during this healing process as light will be applied to the bandage the photoantimicrobial agent becomes activated upon shining of blue light, which consequently generates cytotoxic species in order to combat the pathogenic microbes. It is vital to note that it is not possible for leaching of the antimicrobial agent to occur as it is covalently bound to the polymer support. This study was specifically undertaken in order to determine the proof of principle of this research.

Table 59: Compound codes given to antimicrobial agents substituted onto polymer support

Antibacterial Agent/Biocide	Compound Code
	<p style="text-align: center;"><b>13d</b></p>
	<p style="text-align: center;"><b>1d</b></p>
	<p style="text-align: center;"><b>4d/6d</b></p>
	<p style="text-align: center;"><b>7d/8d/9d</b></p>
	<p style="text-align: center;"><b>10d/11dc/12d</b></p>

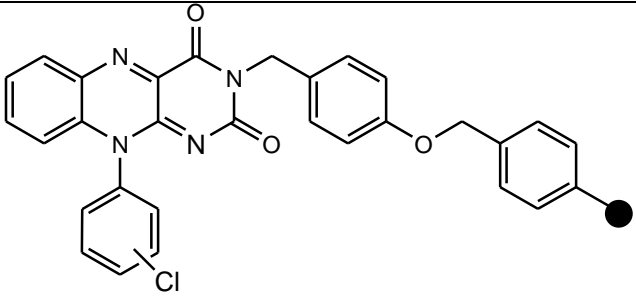
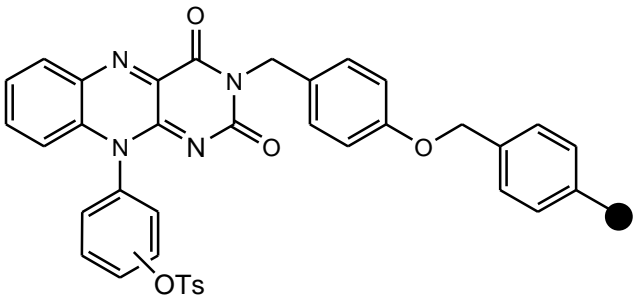
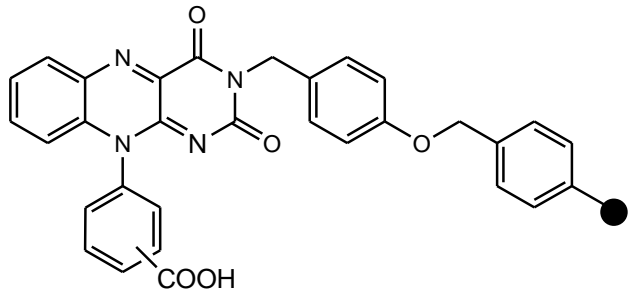
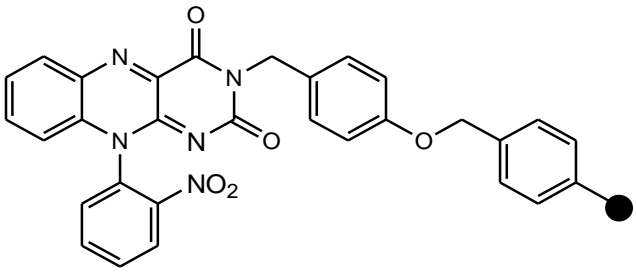
	<p><b>14d/15d/16d</b></p>
	<p><b>17d/18d/19d</b></p>
	<p><b>20d/22d</b></p>
	<p><b>23d</b></p>

Table 60 and Table 61 presents an overview of the MIC results obtained for the tested isoalloxazines with varying functional groups attached to each of the phenyl ring, against the gram negative and positive bacteria.

Table 60: Recorded MIC results for polymer substituted compounds against *E.coli*

<b>Compound Code</b>	<b>MIC at 1.0 mM/mL concentration in blue light</b>
<b>13d</b>	MIC > 1.0
<b>1d</b>	MIC > 1.0
<b>4d</b>	MIC > 1.0
<b>6d</b>	**
<b>7d</b>	MIC > 1.0
<b>8d</b>	MIC > 1.0
<b>9d</b>	MIC > 1.0
<b>10d</b>	MIC > 1.0
<b>11d</b>	MIC > 1.0
<b>12d</b>	MIC > 1.0
<b>14d</b>	**
<b>15d</b>	MIC > 1.0
<b>16d</b>	MIC > 1.0
<b>17d</b>	MIC > 1.0
<b>18d</b>	MIC > 1.0
<b>19d</b>	MIC > 1.0
<b>20d</b>	MIC > 1.0
<b>22d</b>	**
<b>23d</b>	MIC > 1.0

\*\* = Insufficient quantity of material to carry out investigation

Table 61: Recorded MIC results for polymer substituted compounds against *S.aureus*

<b>Compound Code</b>	<b>MIC at 1.0 mM/mL concentration in blue light</b>
<b>13d</b>	MIC 1.0
<b>1d</b>	MIC > 1.0
<b>4d*</b>	MIC > 1.0
<b>6d</b>	**
<b>7d</b>	MIC > 1.0
<b>8d</b>	MIC > 1.0
<b>9d</b>	MIC 1.0
<b>10d</b>	MIC > 1.0
<b>11d</b>	MIC > 1.0
<b>12d</b>	MIC 1.0
<b>14d</b>	**
<b>15d</b>	MIC > 1.0
<b>16d</b>	MIC 1.0
<b>17d</b>	MIC > 1.0
<b>18d</b>	MIC > 1.0
<b>19d</b>	MIC > 1.0
<b>20d</b>	MIC > 1.0
<b>22d</b>	**
<b>23d</b>	MIC 1.0

\*\* = Insufficient quantity of material to carry out investigation

## 4.13 Comparison studies for antimicrobial results of synthesised isoalloxazines attached to a polymer support

### 4.13.1 *E.coli*

The results achieved for antimicrobial activity of the complete library of isoalloxazines substituted onto a polymer support, against the gram negative organism is illustrated Figure 107.

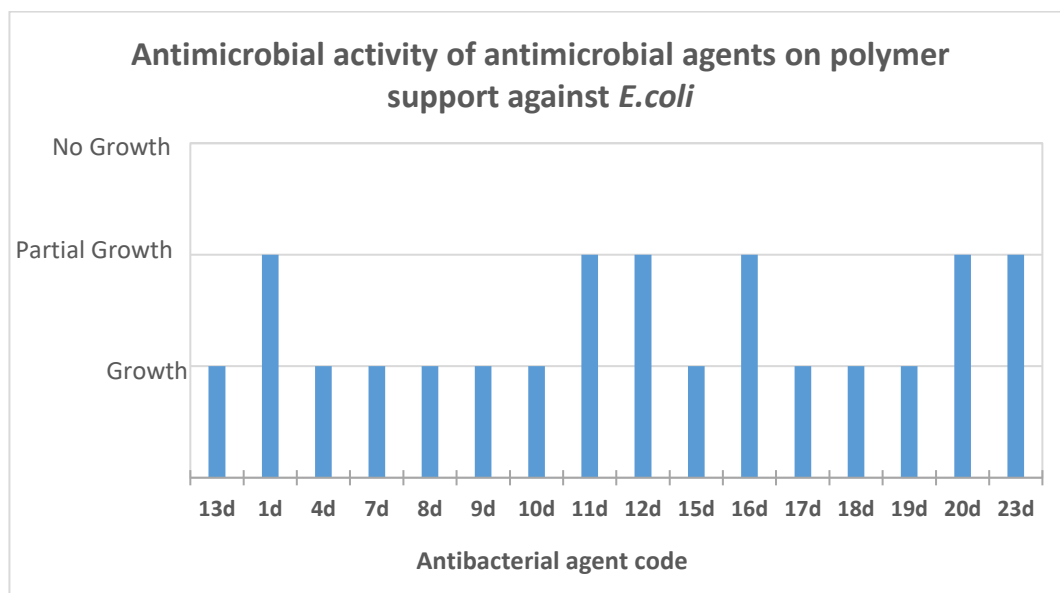


Figure 107: Antimicrobial activity of compounds on polymer support against *E.coli*

Figure 107 shows that no MIC values were obtained for *E.coli*. Most of the synthesised compounds substituted onto the polymer support illustrate complete growth of the pathogenic organism. However, a reduction in microbial growth is observed in a number of these compounds pointing to evidence of total antimicrobial activity, (after moderation of these experiments to achieve MIC values it could be possible to enhance antimicrobial activity. see section 5.2.2).

An interesting observation was seen for the standard phenyl isoalloxazine, compound **13d**. This compound did not record an MIC against *E.coli*, however, **13d** presented microbial death against the gram positive microorganism *S. aureus*. This successful result against *S. aureus* signifies the standard phenyl isoalloxazine (**13d**) which is covalently bound to a polymer support can potentially be used as an ideal photosensitiser to eradicate pathogenic species. Analysis of Figure 107 presents negligible bactericidal effects were caused on *E. coli* whilst irradiated to blue light. It is disappointing to see that results obtained did not produce any change in terms of microbial toxicity.

The antimicrobial activity of compound **13d** was compared with all other synthesised isoalloxazines in order to investigate microbial effects (if any) caused by different moieties attached to the standard phenyl isoalloxazine structure.



Having considered the results obtained from the synthesised library of compounds, it was interesting to note that although no MIC was achieved, compounds **1d**, **11d** and **12d**, contain electron donating substituents, which can produce damaging effects towards *E.coli*, since a reduction in microbial growth was observed (Appendix 2; Table 91 and Table 94). Three compounds (**15d**, **20d** and **23d**) containing electron withdrawing moieties were able to exert partial biocidal effects towards *E.coli* as reduced growth was observed for these compounds<sup>355</sup> (Appendix 2, Table 95, Table 97 and Table 98). After reviewing these results, it was disappointing to note that no MIC was achievable for these compounds whilst on the polymer support.

#### 4.13.2 *S.aureus*

The antimicrobial activity for the complete library of synthesised isoalloxazines was monitored against the gram positive organism using blue light. The antimicrobial results achieved, are illustrated in Figure 108

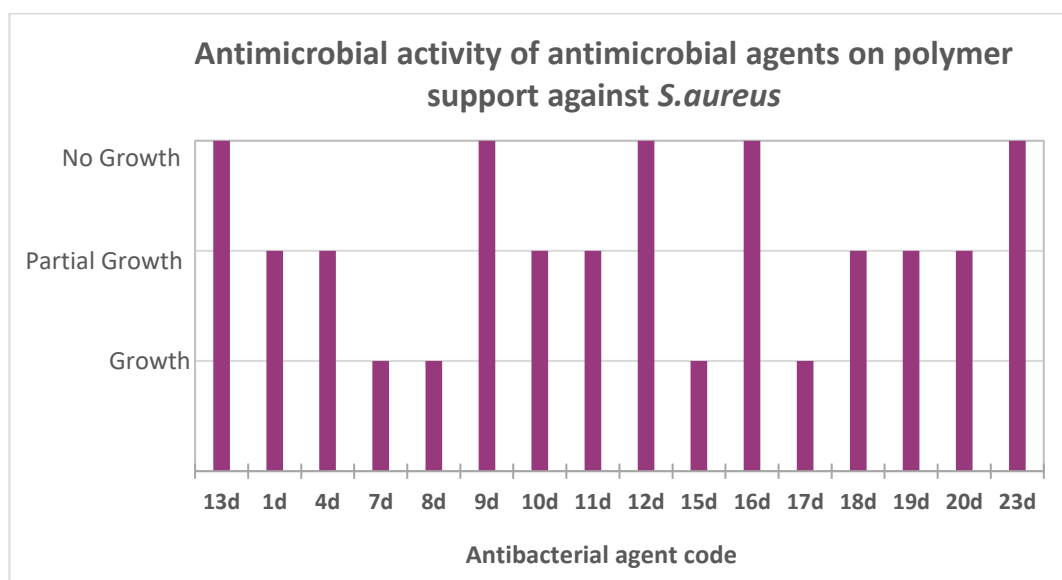


Figure 108: Antimicrobial activity of compounds on polymer support against *S.aureus*

These results clearly illustrate (Figure 108) that numerous isoalloxazines presented total inhibition of microbial growth, resulting in MIC values. It was interesting to note the antimicrobial activity of the standard phenyl isoalloxazine (**13d**) produced toxic effects towards the gram positive pathogenic organism (*S.aureus*). This result was compared with the antimicrobial results achieved against each of the synthesised isoalloxazines with varying substituents attached to the *N*-10 position of the phenyl ring.

Four additional compounds (**9d**, **12d**, **16d** and **23d**) (Figure 108, Appendix 2, Table 79, Table 81, Table 83 and Table 89) presented complete inhibitory effects towards *S.aureus*. Of these compounds, **9d** and **12d** contain moieties with electron donating properties, compounds **16d** and **23d** have electron withdrawing substituents that also presented total antimicrobial activity.

It is interesting to note that (seven) isoalloxazines presented partial antimicrobial activity (Figure 108). Of these compounds the partial activity was observed for four isoalloxazines (**1d**, **4d**, **10d** and **11d**) (Appendix 2, Table 91, Table 92 and Table 94) have electron withdrawing substituents attached. Observation of partial activity is encouraging as moderation of the experiment and/or structure of the isoalloxazines may possibly achieve better antimicrobial activity, causing toxic effect on the pathogenic microorganisms. No antimicrobial activity in terms of MIC was observed in five isoalloxazines (**7d**, **8d**, **15d**, **16d**, and **17d**). It was surprising to note that none of these isoalloxazines produced any biocidal effects, as it was assumed these substituents (OMe, Cl and OTs) in particular would potentially help increase the inhibitory growth effects due to their electronic properties resulting in these isoalloxazines having greater antimicrobial activity. Evaluating the results achieved in Figure 108 identify that significant bactericidal effects were caused on the pathogenic organism *S. aureus*. These results indicate that exposure of *S. aureus* to blue light reduces microbial growth especially whilst linked to the polymer support.

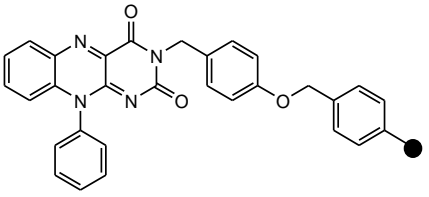
#### 4.14 Antimicrobial studies of polymer substituted compounds

#### 4.15 Antimicrobial studies for compound 13d

Compound **13c** was dissolved in methanol and ringers solution, to prepare a solution of 1.0 mM/mL. To the solution, the freshly prepared bacteria (*E.coli* and *S.aureus*) was added. The solution containing the bacterial suspension was illuminated for 12 hrs in blue LED light. The 1mM solution was then inoculated onto an agar plate and incubated for a further 12 hours at 37 °C in order to show the minimum antimicrobial activity of each concentration.

The results achieved for compound **13d** following illumination with blue light show that compound **13d** did not exhibit antimicrobial activity against the gram negative organism *E. coli*. However, the compound presented complete toxification effects towards *S.aureus*. Table 62 shows the MIC for compound **13d** and is represented in Figure 109.

Table 62: MIC of compound 13d

Antibacterial Agent/Biocide	Concentration: 1 mM/mL		
	Compound Code	<i>E.coli</i>	<i>S.aureus</i>
 10-Phenyl isoalloxazine polymer bound	<b>13d</b>	MIC > 1.0	MIC 1.0

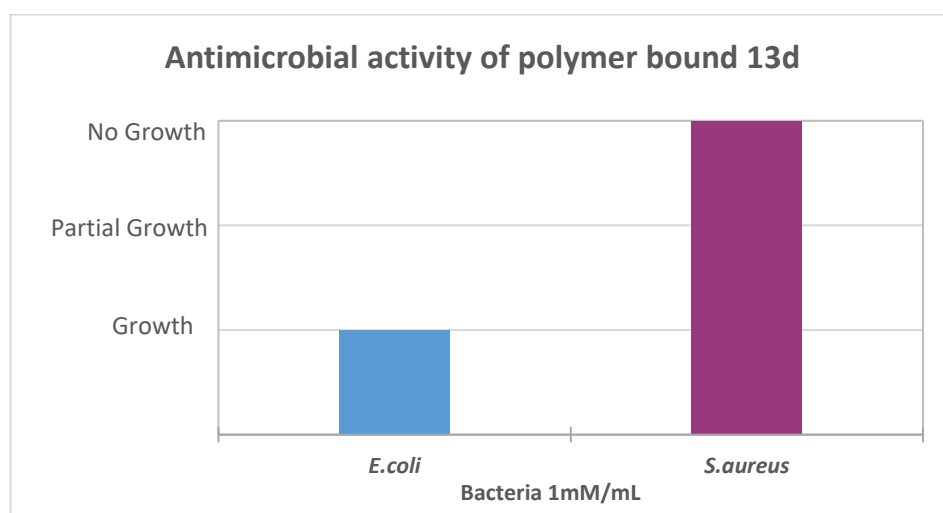


Figure 109: Antimicrobial activity of compound 13d

Figure 109 illustrates that no antimicrobial activity was observed against *E.coli*, and total inhibition was detected for the gram positive organism using the standard isoalloxazine, **13d**. The achieved result against *S.aureus* is extremely positive to observe, especially as the unsubstituted

phenyl ring at the *N*-10 position was specifically attached (to molecule) in order to distinguish if the addition of an electron withdrawing/donating substituents affects the antimicrobial activity particularly when the molecule is covalently bound to the polymer support (which typically would mimic a bandage). As the sub-unit structure of compound **13d** is based on alloxazine (Figure 75), it is interesting to note that evidentially antimicrobial activity occurs for the standard phenyl isoalloxazine (**13d**) yet no results are observed in literature for the microbial activity against alloxazine.

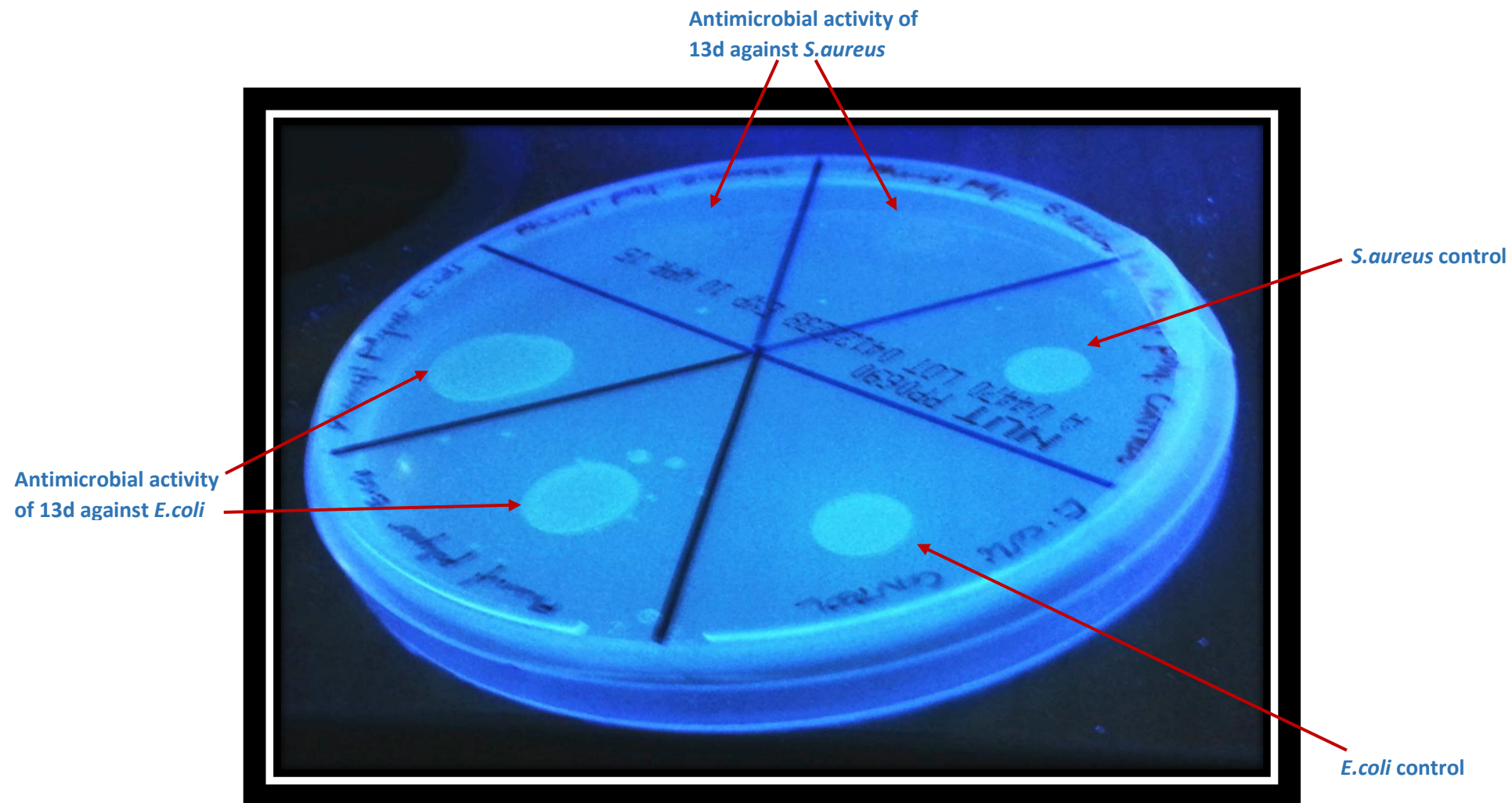
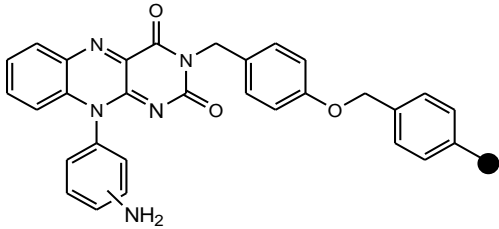


Figure 110: Antimicrobial activity of compound 13d on a polymer support against gram negative and positive organisms.

#### 4.16 Antimicrobial studies for compound 1d

The results achieved for compound **1d** shows that it did not present antimicrobial activity against either *E. coli* or *S.aureus*. This indicates the MIC value is greater than the tested concentration (1mM/mL) and is shown in Table 63.

Table 63: MIC of compound 1d

Antibacterial Agent/Biocide	Concentration: 1 mM/mL		
	Compound Code	<i>E.coli</i>	<i>S.aureus</i>
 <p>10-Aminophenyl isoalloxazine polymer bound</p>	<b>1d</b>	MIC > 1.0	MIC > 1.0

Evaluation of compound **1d** presented partial antimicrobial activity against both the gram negative and positive microorganisms. A reduction in growth was recorded under blue light illumination.

#### 4.17 Antimicrobial studies for compound 4d

The antimicrobial activity for compound **4d** was tested against the gram negative organism, *E.coli*, and gram positive organism *S.aureus* that were illuminated with blue light.

Table 64: MIC of compound 4d

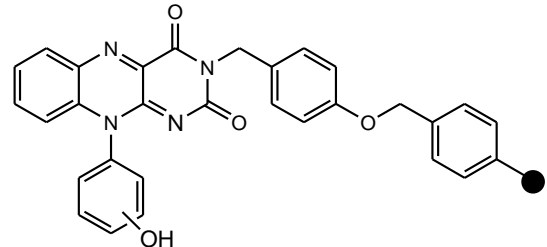
Antibacterial Agent/Biocide	Concentration: 1 mM/mL		
	Compound Code	<i>E.coli</i>	<i>S.aureus</i>
 <p>10-Hydroxyphenyl isoalloxazine polymer bound</p>	<b>4d</b>	MIC > 1.0	MIC > 1.0

Table 64 shows the antimicrobial results achieved by both organisms. Unfortunately no antimicrobial activity was observed against *E.coli* at all. However, it was encouraging to observe some antimicrobial activity present for compound **4d** as partial inhibition of microbial growth against the gram positive organism *S.aureus* was observed. Although only partial inhibition was

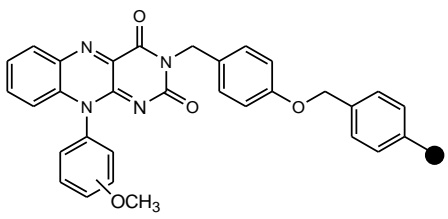
observed with the hydroxyl moiety attached to the *N*-10 phenyl ring at the *ortho* position, this still proves to be an encouraging result.

It is evident from the antimicrobial results that the synthesized compound (**4d**) possessed moderate potency against *Staphylococcus aureus* and nothing against *Escherichia coli*<sup>356</sup>.

#### 4.18 Antimicrobial studies for compounds **7d-9d**

Table 65 shows the antimicrobial results achieved for compounds **7d-9d** after illumination with blue light.

Table 65: MIC of compounds **7d-9d**

Antibacterial Agent/Biocide	Concentration: 1 mM/mL		
	Compound Code	<i>E.coli</i>	<i>S.aureus</i>
 10-Methoxyphenyl isoalloxazine polymer bound	<b>7d</b>	MIC > 1.0	MIC > 1.0
	<b>8d</b>	MIC > 1.0	MIC > 1.0
	<b>9d</b>	MIC > 1.0	MIC 1.0

Compound **7d** and **8d** did not produce evidence of antimicrobial activity for either gram negative or positive microorganisms at the tested concentration range and these results are presented in Table 65.

From the hypothesis made in section 2.6 with reference to electron donating substituents would increase the production of cytotoxic species resulting in an increase of cellular death, here proves somewhat unfortunate as all three isomers (**7d-9d**) yielded no cellular death against *E.coli* despite having generated a brilliant production of singlet oxygen (98.32%) by the *ortho* substituted isoalloxazine (**7d**).

A strong electron donating substituent attached to the molecule most certainly was expected to effect the microbial growth particularly when illuminated with blue light. However, it was not surprising to observe the *meta* isomer (**8d**) showed no evidence of antimicrobial activity against either of the tested microorganisms as low yields of singlet oxygen and radical were generated.

The *para* substituted isomer, compound **9d** was the only molecule to present antimicrobial activity as complete biocidal cell death was observed against *S.aureus*, achieving an MIC value of 1.0 mM/mL. Observing antimicrobial activity with an electron donating substituent on the *para* position, whilst on the polymer support is a positive result to achieve, as this indicates that such compounds can potentially in future be used antimicrobial agents against these microbes.

#### 4.19 Antimicrobial studies for compounds 10d-12d

The antimicrobial results achieved for the synthesised compounds on polymer support (**10d-12d**) were tested for their antimicrobial activity against the gram negative and positive organisms using blue light illumination. The results achieved are shown in Table 66.

Table 66: MIC of compounds 10d-12d

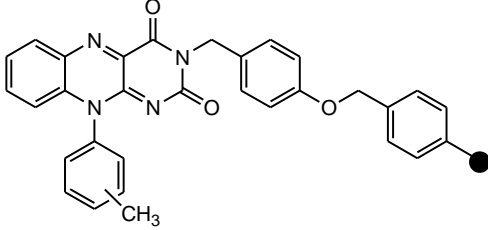
Antibacterial Agent/Biocide	Concentration: 1 mM/mL		
	Compound Code	<i>E.coli</i>	<i>S.aureus</i>
 10-Tolylphenyl isoalloxazine polymer bound	<b>10d</b>	MIC > 1.0	MIC > 1.0
	<b>11d</b>	MIC > 1.0	MIC > 1.0
	<b>12d</b>	MIC > 1.0	MIC 1.0

Table 66 presents no antimicrobial activity for majority of these compounds. Compounds **10d** and **11d** presented no evidence of total toxicity towards either of the investigated organisms.

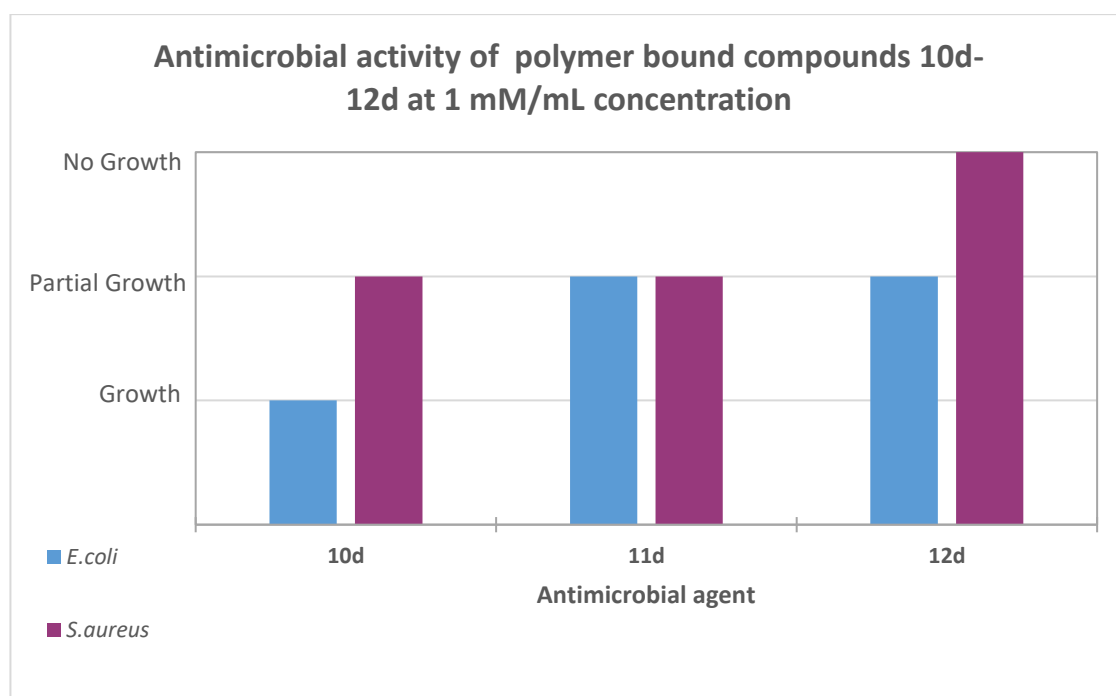


Figure 111: Antimicrobial activity for compounds 10d-12d

It was interesting to note that partial reduction in microorganism growth was observed against *S.aureus* for compound **10d**, whereas **11d** presented a partial reduction for both organisms. Interestingly compound **12d** presented no inhibition in growth towards *E.coli*, however, total inhibition was observed against the gram positive organism, *S.aureus*. The obtained results are indicative of having potential inhibitory potency towards the tested microorganisms. Having a tolyl moiety substituted to the molecule demonstrates that an electron donating substituent

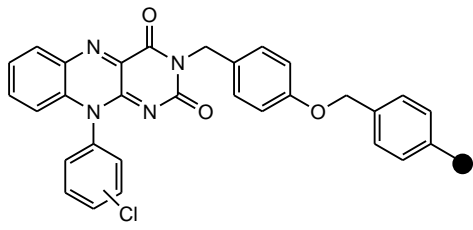


behaves as a biocide towards pathogenic microbes. This is evident as partial reduction in antimicrobial growth was recorded for both *E.coli* and *S.aureus*.

#### 4.20 Antimicrobial studies for compounds **15d** and **16d**

The microbial activity for compounds **15d** and **16d** was tested against the gram negative (*E.coli*) and gram positive organisms (*S.aureus*) that were illuminated with blue light. The results achieved are shown in Table 67.

Table 67 MIC of compounds 15d-16d

Antibacterial Agent/Biocide	Concentration: 1 mM/mL		
	Compound Code	<i>E.coli</i>	<i>S.aureus</i>
 10-Chlorophenyl isoalloxazine polymer bound	<b>15d</b>	MIC > 1.0	MIC > 1.0
	<b>16d</b>	MIC > 1.0	MIC 1.0

The antimicrobial activity for compounds **15d** recorded no toxic effects against *E.coli* but partial toxicity was observed against *S.aureus*. This suggests the MIC value is to be greater than the tested concentration (1.0 mM/mL). Compound **16d** recorded partial activity against *E.coli* and total growth inhibition was observed for *S.aureus* resulting in an achievable MIC at 1mM/mL. Although total inhibition was not observed for compound **15d**, partial antimicrobial activity is encouraging to observe as it is evidential that biocidal effect is being caused from the electron withdrawing moiety in combination with blue light.

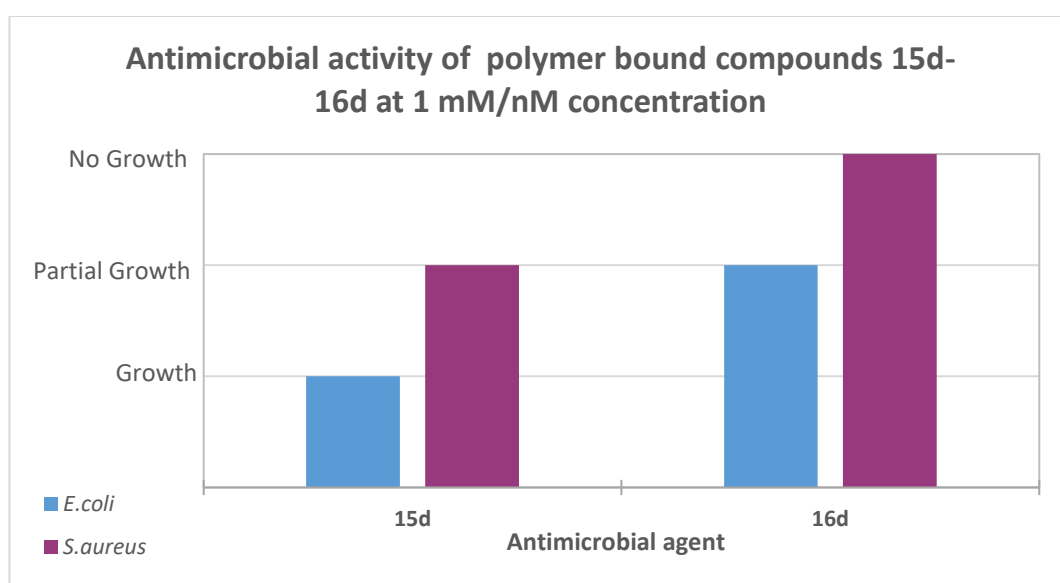


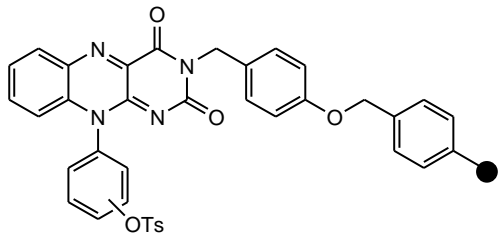
Figure 112: Antimicrobial activity for compounds 15d-16d

Figure 112 illustrates the results achieved for compound **15d** and **16d**. These results were interesting as compound **15c** (Appendix 2, Table 95) presented total antimicrobial activity against *S.aureus*. Yet, when this compound is substituted to a polymer support (**15d**) partial microbial inhibition was observed. This result is somewhat disappointing as the objective of this study is to achieve antimicrobial activity towards the pathogenic microbes when activated with blue light. With this in mind, positive result nonetheless was achieved as total inhibition was recorded against the microorganism *S.aureus* with compound **16d**.

#### 4.21 Antimicrobial studies for compounds **17d** and **19d**

The antimicrobial activity of compounds **17d-19d** was monitored against the gram negative and positive organism using blue light illumination. The results achieved are shown in Table 68.

Table 68: MIC of compounds **17d** and **19d**

Antibacterial Agent/Biocide	Concentration: 1 mM/mL		
	Compound Code	<i>E.coli</i>	<i>S.aureus</i>
 10-Tosyloxyphenyl isoalloxazine polymer bound	<b>17d</b>	MIC > 1.0	MIC > 1.0
	<b>18d</b>	MIC > 1.0	MIC > 1.0
	<b>19d</b>	MIC > 1.0	MIC > 1.0

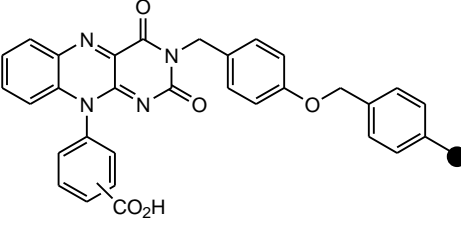
Compound **17d** recorded no biocidal effects against either of the organisms. This suggests the MIC value to be greater than the tested concentration. Compound **18d** and **19d** recorded no antimicrobial activity against *E.coli* however, partial activity was observed against *S.aureus* with both the tested compounds.

Although no MIC was achievable having a tosyloxy moiety substituted to the *N*-10 phenyl ring, observing partial antimicrobial activity is promising for the novel synthesised compounds **18d** and **19d**. Thus, fine-tuning of these compounds could potentially led to greater success in combating these pathogenic microbes having the tosyloxy, electron withdrawing substituents substituted to the molecule<sup>357</sup>.

## 4.22 Antimicrobial studies for compound 20d

Table 69 shows the results of the antimicrobial activity for the substituted carboxyphenyl isoalloxazine (**20d**) against the gram positive and negative organisms.

Table 69: MIC of compound 20d

Antibacterial Agent/Biocide	Concentration: 1 mM/mL		
 <p data-bbox="359 772 774 795">10-Carboxyphenyl isoalloxazine polymer bound</p>	Compound Code	<i>E.coli</i>	<i>S.aureus</i>
	<b>20d</b>	MIC > 1.0	MIC > 1.0

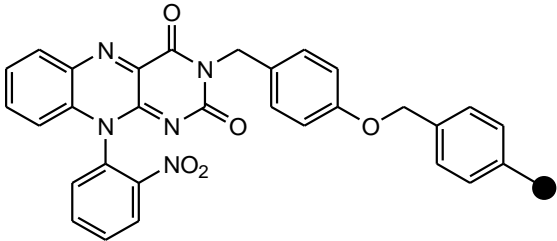
Total biocidal effects were not recorded for compound **20d** against either of the pathogens. This indicates the MIC value is greater than the tested concentration.

Although complete inhibition of microbial growth was not detected for the substituted carboxyphenyl isoalloxazine (**20d**), it is nonetheless encouraging to observe partial inhibition as this compound therefore shows potential of having antimicrobial activity. It was somewhat surprising to note no total biocidal effects occurred on the microbes especially as a strong electron withdrawing group (COOH) was attached to the *N*-10 phenyl ring and assumed that in combination with blue light microbial death would have incurred.

### 4.23 Antimicrobial studies for compound 23d

The antimicrobial activity of compound **23d** was monitored and recorded for both *E.coli* and *S.aureus*. The results achieved are shown in Table 70.

Table 70: MIC of compound **23d**

<b>Antibacterial Agent/Biocide</b>	<b>Concentration: 1 mM/mL</b>		
	<b>Compound Code</b>	<i>E.coli</i>	<i>S.aureus</i>
	<b>23d</b>	MIC > 1.0	MIC 1.0

For the gram negative organism, compound **23d** did not present total toxic effects. However, microbial results achieved against *S.aureus* presented total biocidal activity.

Partial growth inhibition was observed for the gram negative organism *E.coli*. This again was promising to observe as not many of the synthesised isoalloxazines presented antimicrobial activity against *E.coli*. Compound **23d** presented total antimicrobial activity against the gram positive organism. The result achieved was unexpected, as very low yields of cytotoxic species were generated by **23c** (section 215, Table 44). This clearly indicates that substituents attached to the phenyl ring affect the killing ability of the cells.

In order to test further microbial activity of this compound, a polymer support was substituted on to compound **23c** to form **23d**, as discussed in 4.23. It was interesting to note that having a low yield of cytotoxic species generated nonetheless resulted in partial antimicrobial activity that was detected under blue light illumination. Although 100% microbial inhibition was not observed, it is promising to see that the nitro substituent still has an inhibitory growth effect on the pathogenic *S.aureus* (Table 89).

# Chapter 5

## *Future work and conclusion*

### 5.1 Conclusion

#### 5.1.1 Conclusion on library of synthesised isoalloxazines

Scientists are searching for PDT agents that can penetrate deeply through biological tissue using long wavelengths of light.

Light penetration through biological tissue is complicated in the way light is either scattered or absorbed when entering the tissue. This process depends on both the wavelength of light used and type of tissue. The absorption characteristics of tissues decrease with increasing wavelength, hence longer wavelengths of light penetrate most efficiently through tissue<sup>202</sup>.

For the purpose of this research blue light was used for two key reasons:

- 1) It is attractive in PDT research similar to other wavelengths of light e.g. red light (620 – 780 nm)
- 2) It absorbs between 440 - 495 nm, this is the ideal range of absorption for the synthesised isoalloxazines.

Known photosensitisers for example phenothiazinium derivatives; e.g. toluidine blue are already being used in PDT with the combination of light. Several literature report interactions of light (blue or red)<sup>358</sup> with photosensitisers that absorb within these wavelengths and result in significant killing of microbes<sup>359,360</sup>. Hence, in this research the antimicrobial activity was monitored using blue light and varying photosensitisers with different electron withdrawing and donating substituents in order to evaluate the success of killing ability.

The primary goal of this research was to determine the antimicrobial effects using the synthesised isoalloxazines (photosensitisers) in combination with different light wavelengths for example blue light and darkness. It was noted that the photosensitisers irradiated under darkness produced a lower amount of singlet oxygen than the photosensitisers irradiated by a blue light source.

Upon evaluation of the results achieved for the synthesised library of isoalloxazines, the *meta* substituted isomers highlighted two key drawbacks:

- 1) Generally low yielding isomers
- 2) The synthesis proved to be problematic

As a result of these drawbacks some of the *meta* substituted isomers (e.g. OH, NO<sub>2</sub>, NH<sub>2</sub>) could not be synthesised successfully directly.

For each of the synthesised isoalloxazine, singlet oxygen was produced and monitored using a spectrophotometer. Even though some derivatives produced negligible amounts of singlet oxygen, it was nonetheless generated. Several isoalloxazines proved to be better producers than the compound that was used as the standard, **13c**. It was interesting to observe that an unsubstituted phenyl ring (hydrogens attached at the *N*-10th position), was generally the better generator of singlet oxygen with the exception of a couple of electron withdrawing and donating substituents. In addition to this, many of the compounds were also radical generators. This demonstrated that these molecules have the ability to undergo both type I and type II pathways to generate cytotoxic species. Thus, in turn induces antioxidative processes and causes damage to biological tissues and/or damage essential cellular components e.g cytoplasmic membrane resulting in cell death.

For each of the synthesised *N*-substituted nitrophenyl anilines and isoalloxazine derivatives the log P value was calculated using a cheminformatic software called: “*molinspiration*”. Molinspiration was used for the purpose of this study to get a better understanding and appreciation for the novel synthesised isoalloxazines. This software allows molecules to be manipulated and calculates a range of molecular properties required in QSAR and drug design for example log P values that are shown in Table 71 for these compounds.

Table 71: Log P values for all synthesised intermediates & final compounds, and <sup>1</sup>O<sub>2</sub> yields for *N*-substituted phenyl isoalloxazines

Photosensitiser	<i>o</i>	<i>m</i>	<i>p</i>	Log P	<sup>1</sup> O <sub>2</sub> % yield	Radical % yield
<b>1a*</b>	NH <sub>2</sub>	H	H	2.71.	N/A	N/A
<b>1c</b>	NH <sub>2</sub>	H	H	3.36	41.77	0.84
<b>4a*</b>	OH	H	H	3.57	N/A	N/A
<b>4c</b>	OH	H	H	2.00	26.79	2.11
<b>5a*</b>	H	H	OH	3.34	N/A	N/A
<b>6a*</b>	H	H	OH	3.36	N/A	N/A
<b>6c</b>	H	H	OH	1.58	8.11	0.08
<b>7a*</b>	OCH <sub>3</sub>	H	H	2.11	N/A	N/A
<b>7c</b>	OCH <sub>3</sub>	H	H	2.11	108.62	2.91
<b>8a*</b>	H	OCH <sub>3</sub>	H	3.87	N/A	N/A
<b>8c</b>	H	OCH <sub>3</sub>	H	2.84	19.05	1.71
<b>9a*</b>	H	H	OCH <sub>3</sub>	3.90	N/A	N/A
<b>9c</b>	H	H	OCH <sub>3</sub>	2.11	43.57	3.84
<b>10a*</b>	CH <sub>3</sub>	H	H	2.11	N/A	N/A
<b>10c</b>	CH <sub>3</sub>	H	H	2.67	92.9	0.007
<b>11a*</b>	H	CH <sub>3</sub>	H	4.26	N/A	N/A
<b>11c</b>	H	CH <sub>3</sub>	H	3.23	45.96	227.0
<b>12a*</b>	H	H	CH <sub>3</sub>	4.29	N/A	N/A
<b>12c</b>	H	H	CH <sub>3</sub>	2.51	190.22	3.53
<b>13a*</b>	H	H	H	3.84	N/A	N/A
<b>13c</b>	H	H	H	2.06	100.00	100.00
<b>14a*</b>	Cl	H	H	4.47	N/A	N/A
<b>14c</b>	Cl	H	H	2.90	6.65	8.64
<b>15a*</b>	H	Cl	H	4.49	N/A	N/A
<b>15c</b>	H	Cl	H	2.92	76.5	99.47
<b>16a*</b>	H	H	Cl	4.52	N/A	N/A
<b>16c</b>	H	H	Cl	2.74	20.83	27.09
<b>17c</b>	OTs	H	H	3.64	75.78	4.46
<b>18c</b>	H	OTs	H	3.66	68.08	0.12
<b>19c</b>	H	H	OTs	3.48	96.94	13.41
<b>20a*</b>	COOH	H	H	3.88	N/A	N/A
<b>20c</b>	COOH	H	H	1.80	14.12	0.29
<b>21a*</b>	H	COOH	H	3.73	N/A	N/A
<b>22a*</b>	H	H	COOH	3.75	N/A	N/A
<b>22c</b>	H	H	COOH	1.97	12.67	0.88
<b>23a*</b>	NO <sub>2</sub>	H	H	3.27	N/A	N/A
<b>23c</b>	NO <sub>2</sub>	H	H	2.19	7.39	7.39

All compounds denoted \* are intermediate compounds (*N*-substituted nitrophenyl anilines) and no <sup>1</sup>O<sub>2</sub> yields were measured for these.

Although each of the isoalloxazine derivatives produced singlet oxygen, no direct correlation is seen in Table 71 between the absorbance, log P and singlet oxygen yields.

In addition to these observations, it can be seen that the *N*-substituted isoalloxazine derivatives generally exhibit higher log P values compared to the standard isoalloxazine, **13c**. Compound **7c** and **12c** both have very low Log P values, yet these compounds demonstrated to be the best singlet oxygen generators as both compounds achieved enhanced yields of singlet oxygen than the standard phenyl isoalloxazine, **13c**. Substituents attached to the benzene ring influence reactivity in a profound manner. Thus, it is interesting to note that both these compounds have activating substituents attached.

When comparing the Log P value against the radical production, it can be seen that compound **11c** exhibits a slightly higher Log P value of 3.23 than compound 13c, yet 11c generated an excellent radical yield (**11c** = 227%). This compound has a tolyl substituent- electron donating moiety attached to the benzene. Unfortunately, no clear correlation can be made between the theoretically calculated Log P values, attached substituents in terms of electron donating/withdrawing and the antimicrobial activity.

### 5.1.2 Conclusion on antimicrobial studies for the synthesised library of isoalloxazines

From the obtained results it can be seen that antimicrobial studies performed on the gram negative organism (*E.coli*) have proven to be somewhat unclear as the synthesised isoalloxazines do not show positive antimicrobial action against the organism under the light regimes investigated. The lack of antimicrobial activity against *E.coli* suggests that this organism has a higher resistance towards the isoalloxazines tested as potential antimicrobial agent, possibly due to their complex double cellular membrane structure. However, this is not the case for the gram positive organism (*S.aureus*) as MIC was observed for a range of the isoalloxazines tested and full biocidal effect was noted. *S.aureus* would seem to be the most promising bacterium in terms of its response towards the cytotoxic species generated by the synthesised isoalloxazines i.e. greater antimicrobial action was observed against *S.aureus* than *E.coli*.

Evaluating the hypothesis predicted in section 2.6 confirms that antimicrobial activity for the compounds with a heavy atom (chlorine) (**14c-16c**) attached to the molecule demonstrate positive results against the gram positive organism, *S. aureus* but not towards *E.coli*. Compound **15c** generated a very good yield of singlet oxygen (77.49%) and an excellent yield for radical (99.47%), and these results show that biocidal effects were caused by the *meta* substituted chlorine atom at a concentration of 0.25 mM/mL under blue light illumination. The obtained results show that this observation of heavy atom effect is also demonstrated in similar research conducted by Mark Wainwright using a different system<sup>331</sup>.



Although limited antimicrobial activity is observed against the gram negative organism, the synthesised isalloxazines do not show to great potentiality towards ideal photosensitisers. The reason for this could possibly be related to the compounds being highly fluorescent molecules and thus have a long  $t_{1/2}$  life. A short half life ( $t_{1/2}$ ), which is less than ten minutes is often an indicator of a good photosensitiser.

Concluding remarks on this study shows that appropriate doses and intensity of light can kill *S. aureus* suggesting that similar effects can be produced in clinical cases of bacterial infection. The overall results presented throughout this study present concordant results to a similar study undertaken by Guffey *et al*<sup>361</sup>.

### 5.1.3 Conclusive comments for antimicrobial results of synthesised isalloxazines on polymer support

Evaluation of the overall results of antimicrobial activity against both the organisms, clearly indicates that having different substituents attached to the molecule affect the killing ability of the molecule. This is noticed particularly in the gram positive organism where an increased number of MIC values were obtained compared to the gram negative organism, *E.coli*. It is evident (Figure 107) that no MIC was achieved with the antimicrobial agents on the polymer support against *E.coli*, whereas *S.aureus* (Figure 108) gave MIC values for a number of compounds.

Although disappointing results were obtained for *E.coli*, it is encouraging to observe the presence of partial antimicrobial activity on a number of synthesised compounds (Figure 108). Using these isalloxazine's as potential antimicrobial agents enhanced antimicrobial activity is clearly evident in the results achieved for *S.aureus* compared to *E.coli*. It is noted that biocidal effects are seen for the gram positive organism *S. aureus*, as partial reduction in microbial growth was recorded for majority of the synthesised compounds against this organism (Figure 108) whilst attached to the polymer support.

*Concluding remark for this study*, it can be seen that that compound **12d** seems to be a promising candidate as it produced total antimicrobial activity for both the gram negative and positive organism whilst attached to the polymer support. This clearly indicates that the tolyl moiety containing electron donating properties effect the antimicrobial activity.

With some potential antimicrobial activity observed in the achieved results, it is nonetheless important to consider additional factors for the reduced antimicrobial activity. In addition to the low yields of cytotoxic species generated, an alternate reason for the lack of antimicrobial activity could also be a result of the efflux mechanism occurring within the cells<sup>362</sup>. As the nature of these efflux pumps is to expel toxic substances from within the cells, it is possible that the antimicrobial agent is either; being extruded from the cells, or not passing through the cell membrane and therefore unable to enter the cells. This mechanism is referred to as 'intrinsic bacterial resistance'<sup>363</sup>.

The promising result achieved by the standard phenyl isoalloxazine (**13d**) for *S. aureus* is extremely encouraging as this can be used as a proof of principle for their use in bandages to eradicate infection using blue light. However, it is vital to recognise that the polymer support will and cannot be detached from the antimicrobial agent as the polymer is covalently bound to it, thus no leaching of the agent can occur into the tissues.

## 5.2 Future Work

### 5.2.1 Future work on the library of synthesised isoalloxazines

Having developed the synthesis successfully for these photosensitisers, it would be interesting to investigate if additional changes were made to the tricyclic ring structure; would the production of either  $^1\text{O}_2$  and/or radical be affected. In respect to further work several other parameters need to be investigated further; e.g. 1. Alteration of the substituents, e.g. using other electron withdrawing/donating groups. 2. The substituents should be added onto both the phenyl rings and not only on the *N*-10 ring. 3. Addition of a chromophore group in order to alter the absorption into the Green region (490-570 nm) could hopefully result in better yields of singlet oxygen/radical.

With the urge to tackle antimicrobial resistance it is important to evaluate how effective the isoalloxazines are as potential antimicrobial agents having made the suggested changes. It would also be useful to monitor and compare if these photosensitisers can retain their microbial activity whilst attached to the polymer support.

Additional research would be to determine whether nylon strips of these compounds could be made in order to mimic real bandages.

The solid support utilised in this research was for the proof of concept. Therefore, using alternative polymer resins as the solid supports on which the photosensitiser is attached to should not alter the antimicrobial activity unless the support has antimicrobial activity itself. Hence, evaluation of how/if Wang brominated resin affects the singlet oxygen and radical generation on the synthesised isoalloxazines is of importance. This of-course would be a key finding as these infections are primarily HAI. This in turn would aid guidance in knowing which materials would be best suited fabrics for bandages.

### 5.2.2 Future work on the antimicrobial activity of the synthesised isoalloxazines

It is evident from the results achieved antimicrobial activity occurs using the synthesised isoalloxazines as novel potential antimicrobial agents. It would be interesting to compare results of the microbial activity for these isoalloxazines against other gram negative organisms for example *Enterobacteriaceae* in order to investigate whether these antimicrobial agents are able to cause cellular damage to the *E.coli* species. This finding would highlight if these agents are particularly resistant to the gram negative organisms as a whole or individually.

As it is apparent that *S.aureus* is demonstrating response to the synthesised antimicrobial agents in a desired way, it would be valuable to explore additional changes that can be made in order to increase the biocidal effects caused by the photosensitiser. To expand:

- Illumination time of blue light could be extended in order to investigate if illumination time affects the MIC.

- Extending the contact time of the microorganism and antimicrobial agent during the incubation period, resulting in enhanced microbial death.
- Slightly alter the isoalloxazine structure, or using alternate substituents on the molecule

The MIC of the newly synthesised dyes as potential antimicrobial agents was determined using a conventional method. It would be interesting to evaluate if alternative methods were used to monitor the antimicrobial activity such as use of fluorochromes to identify the viable cells (e.g. propidium iodide) in order to assess bacterial damage caused by the agents. In addition to this the comparison of other gram positive organisms e.g. *Enterococcus* should be tested against the synthesised antimicrobial agent particularly as the rise of *Enterococcus* is also causing great concern for their occurrence and impact on the clinical outcomes of HAI<sup>364</sup>. To progress further, antimicrobial testing should also be continued on other HA-microbes for example yeast and bacteria.

At present, the range of antibacterial agents effective against the Gram-negative bacteria is still significantly greater than for the Gram positive pathogens. In this investigation the Gram positive bacterium proved to be more responsive than the Gram negative. Researchers are faced with major challenges to develop drugs effective against problematic all resistant organisms. In light of this, it is promising to see that partial antimicrobial activity was present against both of these pathogens which are a constant problem on a global scale.

# Chapter 6

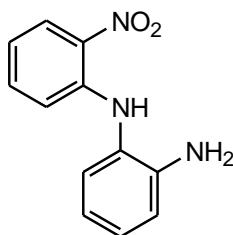
## *Synthesis and Experimental*

### 6.1 Chemical Synthesis

NMR spectra were recorded on a Bruker Fourier 300 (300 MHz) spectrometer. Chemical shifts are reported in ppm relative to residual protic solvent ( $^1\text{H}$  NMR  $\text{d}_6\text{-DMSO}$ , 2.500 ppm;  $^{13}\text{C}$  NMR  $\text{d}_5\text{-DMSO}$ , 39.520 ppm). Coupling constants are reported in Hertz (Hz) and are rounded to the nearest 0.5 Hz. Multiplicities are reported as singlets (s), doublets (d) triplets (t), multiplets (m) or a combination of these, peaks that appeared broad due to either H-bonding or restricted rotation are prefixed as broad (br). Due to the poor solubility of the formed compounds in appropriate deuterated solvents only a select few  $^{13}\text{C}$  NMR experiments are reported and the  $^1\text{H}$  NMR experiments were performed with 128 scans. Where purity by NMR is reported this is as an approximate molar ratio of impurities signals to one product signal (impurities that were unidentified may have been counted twice and as such these figures will generally be underestimates). All reactions were monitored by thin-layer chromatography (TLC) using 0.25 mm Al-backed silica-gel plates (Merck 60 F254). Melting points were measured on a Stuart SMP10 melting point apparatus in open capillary tubes and are uncorrected. The isoalloxazines did not melt at temperatures below 300 °C, although some darkening of colour was observed with heating this did not change the spectral properties of the samples to any measurable degree in several that were checked. Low resolution mass spectra were recorded on a Finnigan<sup>TM</sup> LCQ<sup>TM</sup> Advantage MAX in ESI mode. HRMS were performed by the EPSRC mass spectrometry service, Swansea. Infra-red spectra ( $1800\text{-}800\text{ cm}^{-1}$ ) were recorded on a Perkin Elmer Spectrum RX 1 with a Specac Golden Gate<sup>TM</sup> ATR accessory and values are quoted in wavenumbers.

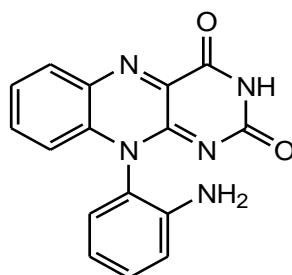
Microwave reactions were carried out using a CEM Discover<sup>®</sup> reactor in sealed CEM 10 mL reaction vials (scale-up into 50 mL vials) using 150 W power, fixed hold time and no cooling, all reactions were performed with stirring after ensuring the suspensions stirred on a magnetic stirrer hotplate. All chemicals were obtained commercially and used without further purification; with the exception that methanol was dried using an MBraun SPS-800 system to remove water.

## 6.2 Synthesis of 2-(2-nitrophenyl) aniline (**1a**)



A mixture of potassium carbonate (20.73 g, 150.0 mmol), 2-phenylenediamine (14.04 g, 130.0 mmol), and 1-fluoro-2-nitrobenzene (18.33 g, 130.0 mmol) was irradiated for 3 h at 150 °C in a CEM microwave at full power. The mixture was allowed to cool to room temperature, and with stirring poured onto ice water (300 mL). The reaction mixture was adjusted to pH 6 using c. HCl (aq), added to a separating funnel and extracted with CHCl<sub>3</sub> (5 x 50 mL). The organic layer was isolated, dried with anhydrous sodium sulphate, and evaporated under reduced pressure to yield the substituted 2-amino-(2-nitrophenyl) aniline as a black solid. The crude solid was purified by flash column chromatography over silica gel eluting with CHCl<sub>3</sub>: PE (1:1) to afford the pure product as a red solid. The solid was dried *in vacuo* to yield the solid **1a**, 17.94 g, 46% as dark red crystals. <sup>1</sup>H-NMR (CDCl<sub>3</sub>, 300 MHz) δppm; 9.03 (s, Ar-NH, 1H), 8.11 (d, *J* = 8.84 Hz, Ar-H, 1H), 7.42 (t, *J* = 7.86 Hz, Ar-H, 1H), 7.05 (m, Ar-H, 2H), 6.77 (m, Ar-H, 2H), 6.61 (m, Ar-H, 2H), 5.14 (s, Ar-NH<sub>2</sub>, 2H). <sup>13</sup>C NMR (CDCl<sub>3</sub>, 75 MHz) δppm; 145.36, 144.55, 136.48, 132.59, 128.51, 128.27, 126.43, 122.86, 116.85, 116.79, 116.36, 115.97. LRMS (ESI) *m/z* calcd for [C<sub>12</sub>H<sub>11</sub>N<sub>3</sub>O<sub>2</sub>]<sup>+</sup> 228.2346, found 229.0920 [M+H]<sup>+</sup>. Log P: 3.27.

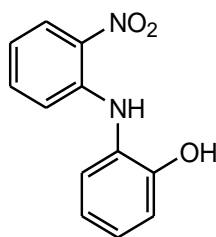
## 6.3 Synthesis of 10-(2-aminophenyl) isoalloxazine (**1c**)



To compound (**1a**) (2.43 g, 10.6 mmol) was dissolved in glacial acetic acid (50 mL) and with constant stirring the mixture was cooled in a slush bath for a few moments followed by the slow gradual addition of zinc dust (6.89 g, 106 mmol) ensuring the temperature did not rise uncontrollably. Upon the final addition of zinc, the reaction mixture was allowed to stir at room temperature for 2 h. The reaction mixture was filtered through celite to remove the zinc dust and the filter cake was washed with glacial acetic acid (80 mL) to yield the 2,2-diaminodiphenylamine (**1b**) as a dark brown solution. To the solution was added alloxan monohydrate (1.69 g, 10.6 mmol) and boric acid (0.64 g, 10.4 mmol) and the solution was stirred at room temperature for

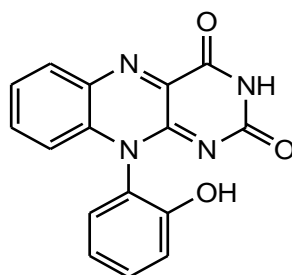
12 h, resulting in the formation of a yellow precipitate. The precipitate was isolated from the reaction mixture by filtration under reduced pressure and washed well with hexane (60 mL). The yellow solid was dried *in vacuo* to yield the 2-aminophenyl isoalloxazine (**1c**), 2.22 g, 69%, as a yellow powder, dec. mp 242-244°C. <sup>1</sup>H-NMR (d<sub>6</sub>-DMSO, 300MHz) δppm; 11.43 (s, Ar-NH, 1H), 8.17 (d, *J* = 7.9 Hz, Ar-H, 1H), 7.75 (t, *J* = 7.4 Hz, Ar-H, 1H), 7.60 (t, *J* = 7.4 Hz, Ar-H, 1H), 7.28 (t, *J* = 7.5 Hz, Ar-H, 1H), 7.03 (d, *J* = 7.9 Hz, Ar-H, 1H), 6.90 (d, *J* = 7.9 Hz, Ar-H, 1H), 6.81 (d, *J* = 8.0 Hz, Ar-H, 1H), 6.74 (t, *J* = 7.4 Hz, Ar-H, 1H), 5.30 (s, Ar-NH<sub>2</sub>, 2H). <sup>13</sup>C NMR (d<sub>6</sub>-DMSO, 75 MHz) δppm; 159.20, 155.21, 151.10, 145.08, 136.67, 135.37, 134.67, 133.04, 132.16, 131.65, 130.79, 129.52, 128.96, 126.67, 126.62, 116.67. FTIR (ATR): ν 3067, 1708, 1681, 1616, 1584, 1532, 1487, 1459, 1396, 1341, 1264, 1196, 1134, 1106, 932, 879, 835, 807, 787, 775, 764, 715, 695, 673 CM<sup>-1</sup>. HRMS (ESI) *m/z* calcd for [C<sub>16</sub>H<sub>11</sub>N<sub>5</sub>O<sub>2</sub>]<sup>+</sup> 305.2908, found 306.0987 [M+H]<sup>+</sup>. Log P: 2.71.

#### 6.4 Synthesis of 2-(2-nitrophenyl amino) phenol (**4a**)



A mixture of 2-aminophenol (1.10 g, 10.0 mmol), 1-fluoro-2-nitrobenzene (1.41 g, 10.0 mmol) and Et<sub>3</sub>N (2.0 mL, 0.15 mmol) in ethanol (20 mL) was irradiated for 3 h at 150 °C in a CEM microwave at full power. The mixture was allowed to cool to room temperature, and with stirring poured onto ice water (30 mL). The reaction mixture was adjusted to pH 6 using c. HCl (aq), added to a separating funnel and extracted with CHCl<sub>3</sub> (3 x 50 mL). The organic layer was isolated, dried with anhydrous sodium sulphate, and evaporated under reduced pressure to yield the substituted *N*-hydroxy-phenol as a burgundy solid. The burgundy solid was purified by flash column chromatography over silica gel eluting with EtOAc: PE (1:2) to afford the pure product as a red solid. The solid was recrystallized from toluene and dried *in vacuo* to yield 2-hydroxy amino phenol (**4a**), 0.90 g, 39% as dark red crystals. <sup>1</sup>H-NMR (CDCl<sub>3</sub>, 300 MHz) δppm; 9.03 (s, Ar-NH, 1H), 8.25 (dd, *J* = 8.6, 1.6 Hz, Ar-H, 1H), 7.40 (ddd, *J* = 8.5, 6.9, 1.6 Hz, Ar-H, 1H), 7.35 – 7.19 (m, Ar-H, 3H), 7.09 (dd, *J* = 8.6, 1.4 Hz, Ar-H, 1H), 7.01 (td, *J* = 7.6, 1.4 Hz, Ar-H, 1H), 6.84 (ddd, *J* = 8.5, 7.0, 1.5 Hz, Ar-H, 1H), 6.78 (dd, *J* = 8.6, 1.4 Hz, Ar-H, 1H), 5.56 (s, Ar-OH, 1H). <sup>13</sup>C NMR (CDCl<sub>3</sub>, 75 MHz) δppm; 152.21, 143.98, 136.18, 133.65, 128.94, 127.91, 126.60, 124.89, 121.49, 118.14, 116.34, 116.26. HRMS (ESI) *m/z* calcd for [C<sub>12</sub>H<sub>10</sub>N<sub>2</sub>O<sub>3</sub>]<sup>+</sup> 231.2194, found 230.0691 [M-H]<sup>+</sup>. Log P: 3.57.

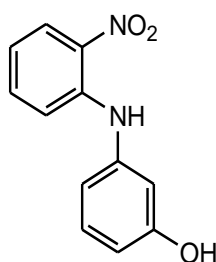
## 6.5 Synthesis of 10-(2-hydroxyphenyl) isoalloxazine (**4c**)



Compound **4a** (0.90 g, 3.91 mmol) was dissolved in glacial acetic acid (50 mL) and with constant stirring the mixture was cooled in a slush bath for a few moments followed by the slow gradual addition of zinc dust (2.54 g, 39.0 mmol) ensuring the temperature did not rise uncontrollably. Upon the final addition of zinc, the reaction mixture was allowed to stir at room temperature for 2 h. The reaction mixture was filtered through celite to remove the zinc dust and the filter cake was washed with glacial acetic acid (20 mL) to yield the substituted *N*-(amino phenyl amino) phenol (**4b**) as a dark brown solution. To the solution was added alloxan monohydrate (0.62 g, 3.9 mmol) and boric acid (0.24 g, 3.7 mmol) and the solution was stirred at room temperature for 12 h, resulting in the formation of a yellow precipitate. The precipitate was isolated from the reaction mixture by filtration under reduced pressure and washed well with hexane (40 mL). The yellow solid was dried *in vacuo* to yield the 2-hydroxyphenyl isoalloxazine (**4c**), 0.87 g, 63%, as a yellow powder, decomposed 223-225°C. <sup>1</sup>H-NMR (d<sub>6</sub>-DMSO, 300 MHz) δppm; 11.48 (s, NH, 1H), 9.95 (s, Ar-OH, 1H), 8.20 (d, *J* = 8.0 Hz, Ar-H, 1H), 7.78 ddd, *J* = 8.6, 7.2, 1.5 Hz, Ar-H, 1H), 7.68 – 7.58 (m, 1H), 7.53 – 7.42 (m, Ar-H, 1H), 7.26 (dd, *J* = 7.9, 1.6 Hz, Ar-H, 1H), 7.19 – 7.03 (m, Ar-H, 2H), 6.83 (dd, *J* = 8.6, 1.2 Hz, Ar-H, 1H). <sup>13</sup>C NMR (d<sub>6</sub>-DMSO, 75 MHz,) δppm; 160.00, 156.09, 152.82, 152.08, 139.90, 135.57, 135.30, 134.17, 131.90, 131.76, 129.28, 126.59, 122.94, 120.67, 118.09, 117.04. HRMS (ESI) *m/z* calcd for [C<sub>16</sub>H<sub>10</sub>N<sub>4</sub>O<sub>3</sub>]<sup>+</sup> 307.075, found 307.0827 [M+H]<sup>+</sup>. FTIR (ATR): ν 3069, 1726, 1637, 1607, 1580, 1533, 1481, 1455, 1417, 1353, 1267, 1112, 877, 840, 808, 768, 713 CM<sup>-1</sup>. Log P: 2.00.

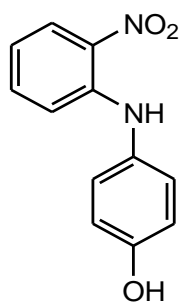


## 6.6 Synthesis of 2-(3-nitrophenyl amino) phenol (**5a**)



A mixture of 3-aminophenol (1.10 g, 10.0 mmol), 1-fluoro-2-nitrobenzene (1.41 g, 10.0 mmol) and Et<sub>3</sub>N (2.0 mL, 0.15 mmol) in ethanol (20 mL) was irradiated for 3 h at 150 °C in a CEM microwave at full power. The mixture was allowed to cool to room temperature, and with stirring poured onto ice water (30 mL). The reaction mixture was adjusted to pH 6 using c. HCl (aq), added to a separating funnel and extracted with CHCl<sub>3</sub> (3 x 50 mL). The organic layer was isolated, dried with anhydrous sodium sulphate, and evaporated under reduced pressure to yield the substituted *N*-hydroxy-phenol as a burgundy solid. The burgundy solid was purified by flash column chromatography over silica gel eluting with EtOAc: PE (1:2) to afford the pure product as a red solid. The solid was recrystallized from toluene and dried *in vacuo* to yield 3-hydroxy amino phenol (**5a**) 0.61 g, 28 % as dark red crystals. <sup>1</sup>H-NMR (CDCl<sub>3</sub>, 300 MHz) δppm; 9.43 (s, 1H), 8.19 (dd, *J* = 8.6, 1.6 Hz, 1H), 7.44 – 7.20 (m, 3H), 6.89 – 6.63 (m, 4H), 4.97 (s, 1H). <sup>13</sup>C NMR (75 MHz, CDCl<sub>3</sub>) δ 156.63, 142.61, 140.14, 135.70, 133.36, 130.68, 126.64, 117.77, 116.42, 116.36, 112.48, 110.90. HRMS (ESI) *m/z* calcd for [C<sub>12</sub>H<sub>10</sub>N<sub>2</sub>O<sub>3</sub>]<sup>+</sup> 231.2194, found 230.0622 [M-H]<sup>-</sup>. Log P: 3.34.

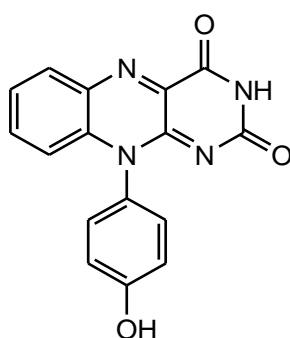
## 6.7 Synthesis of 4-(2-nitrophenyl amino) phenol (**6a**)



A mixture of 4-aminophenol (0.12 g, 1.1 mmol), 1-fluoro-2-nitrobenzene (0.14 g, 1.0 mmol) and Et<sub>3</sub>N (1.5 mL, 1.1 mmol) in ethanol (5 mL) was irradiated for 3 h at 150 °C in a CEM microwave at full power. The mixture was allowed to cool to room temperature, and with stirring poured onto ice water (30 mL). The reaction mixture was adjusted to pH 6 using c. HCl (aq), added to a separating funnel and extracted with CHCl<sub>3</sub> (3 x 20 mL). The organic layer was isolated, dried with anhydrous sodium sulphate, and evaporated under reduced pressure to yield the substituted 4-(2-nitrophenyl amino) phenol as a burgundy solid. The burgundy solid was purified by flash

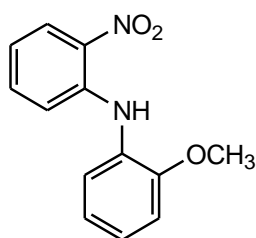
column chromatography over silica gel eluting with EtOAc: PE (1:2) to afford the pure product as a red solid. The solid was recrystallized from toluene and dried *in vacuo* to yield 4-hydroxy amino phenol (**6a**) 0.10 g, 43 % as dark red crystals. <sup>1</sup>H-NMR (CDCl<sub>3</sub>, 300 MHz) δppm; 9.41 (s, Ar-NH, 1H), 8.21 (dd, *J* = 8.7, 1.6 Hz, Ar-H, 1H), 7.35 (ddd, *J* = 8.6, 6.8, 1.6 Hz, Ar-H, 1H), 7.17 (d, *J* = 8.7 Hz, Ar-H, 2H), 7.01 (dd, *J* = 8.7, 1.3 Hz, Ar-H, 1H), 6.91 (d, *J* = 8.7 Hz, Ar-H, 2H), 6.73 (ddd, *J* = 8.6, 6.9, 1.3 Hz, Ar-H, 1H), 4.89 (s, Ar-OH, 1H). <sup>13</sup>C NMR (CDCl<sub>3</sub>, 75 MHz) δppm; 154.00, 144.53, 135.83, 132.39, 131.27, 127.39, 126.62, 116.83, 116.50, 115.76. HRMS (ESI) *m/z* calcd for [C<sub>12</sub>H<sub>10</sub>N<sub>2</sub>O<sub>3</sub>]<sup>+</sup> 231.2194, found 230.0622 [M-H]<sup>-</sup>. Log 3.36.

## 6.8 Synthesis of 10-(4-hydroxyphenyl) isoalloxazine (**6c**)



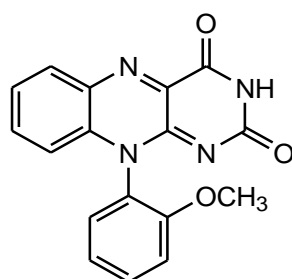
Compound **6a** (1.65 g, 7.17 mmol) was dissolved in glacial acetic acid (70 mL) and the mixture was cooled in an ice bath. Zinc dust (4.69 g, 71.7 mmol) was gradually added and the solution was allowed to stir at room temperature for 2 h and filtered through celite. The filter cake was washed with glacial acetic acid (40 mL) to yield the substituted *N*-(amino phenyl amino) phenol (**6b**) as a dark brown solution. To the solution of 4-(2-amino phenyl amino) phenol, was added alloxan monohydrate (1.15 g, 7.2 mmol) and boric acid (0.43 g, 7.0 mmol). The solution was stirred at room temperature for 12 h, resulting in a dark yellow solution. The yellow solid was filtered from the mixture and washed well with hexane (40 mL) to afford the pure product as a yellow solid. The yellow solid was dried *in vacuo* to yield the isoalloxazine (**6c**), as a yellow powder, 1.49 g, 59%. <sup>1</sup>H-NMR (d<sub>6</sub>-DMSO, 300 MHz) δppm; 11.41 (s, Ar-NH, 1H), 10.09 (s, Ar-OH 1H), 8.16 (dd, *J* = 8.1, 1.5 Hz, Ar-H, 1H), 7.75 (ddd, *J* = 8.7, 7.1, 1.5 Hz, Ar-H, 1H), 7.67 – 7.54 (m, Ar-H, 1H), 7.19 (d, *J* = 8.7 Hz, Ar-H, 2H), 7.03 (d, *J* = 8.7 Hz, Ar-H, 2H), 6.86 (dd, *J* = 8.3, 1.2 Hz, Ar-H, 1H). <sup>13</sup>C NMR (d<sub>6</sub>-DMSO, 75 MHz) δppm; 160.10, 158.78, 156.11, 152.52, 139.88, 135.22, 135.09, 131.75, 129.27, 127.43, 126.35, 117.50, 117.05, 99.99. FTIR (ATR): ν 3065, 1717, 1667, 1611, 1579, 1529, 1504, 1455, 1408, 1268, 1193, 1108, 927, 876, 802, 775, 752, 727 CM<sup>-1</sup>. HRMS (ESI) *m/z* calcd for [C<sub>16</sub>H<sub>10</sub>N<sub>4</sub>O<sub>3</sub>]<sup>+</sup> 307.075, found 307.0827 [M+H]<sup>+</sup>. Mp 202–204°C. Log P: 1.583.

## 6.9 Synthesis of 2-(2-nitrophenyl) 2-methoxy aniline (**7a**)



A mixture of potassium carbonate (4.14 g, 30.0 mmol), 2-anisidine (2.95 g, 20.0 mmol), and 1-bromo-2-nitrobenzene (4.04 g, 20.0 mmol) was irradiated for 3 h at 150 °C in a CEM microwave at full power. The mixture was allowed to cool to room temperature, and ice (100 mL) was added with stirring. The aqueous solution was adjusted to pH 6 using c. HCl<sub>(aq)</sub> added to a separating funnel and extracted with CHCl<sub>3</sub> (3x50 mL). The organic layer was isolated, dried with anhydrous sodium sulphate, and evaporated under reduced pressure to yield the substituted 2-methoxy-(2-nitrophenyl) aniline as a black solid. The crude solid was purified by flash column chromatography over silica gel eluting with EtOAc: PE (2:1) to afford the product as a red solid, (**7a**) 2.40 g, 38%. <sup>1</sup>H-NMR (CDCl<sub>3</sub>, 300 MHz) δppm; 9.45 (s, Ar-NH 1H), 8.19 (dd, *J* = 8.6, 1.4 Hz, Ar-H, 1H), 7.43 – 7.33 (m, Ar-H, 2H), 7.30 – 7.13 (m, Ar-H, 2H), 6.98 (t, *J* = 7.8 Hz, Ar-H, 2H), 6.76 (t, *J* = 8.1 Hz, Ar-H, 1H), 3.87 (s, Ar-OCH<sub>3</sub>, 3H). <sup>13</sup>C NMR (CDCl<sub>3</sub>, 75 MHz); 152.49, 142.48, 135.49, 133.71, 127.79, 126.67, 125.77, 123.25, 120.65, 117.44, 116.19, 111.57, 55.73. HRMS (ESI) *m/z* calcd for [C<sub>13</sub>H<sub>12</sub>N<sub>2</sub>O<sub>3</sub>]<sup>+</sup> 245.246, found 244.125 [M-H]<sup>-</sup>. Mp 263–265°C. Log P: 2.119.

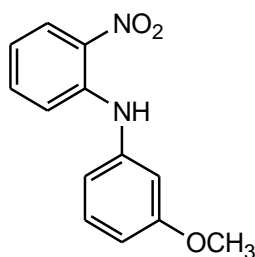
## 6.10 Synthesis of 10-(2-methoxyphenyl) isoalloxazine (**7c**)



Compound **7a** (2.00 g, 8.1 mmol) was dissolved in glacial acetic acid (60 mL) and the mixture was cooled in an ice bath. Zinc dust (5.33 g, 81.6 mmol) was gradually added and the solution was allowed to stir at room temperature for 2 h and filtered through celite. The filter cake was washed with glacial acetic acid (50 mL) to yield the substituted *N*-(methoxyphenyl amino) aniline, (**7b**), as a dark brown solution. To the solution of substituted *N*-(methoxyphenyl amino) aniline was added alloxan monohydrate (1.30 g, 8.1 mmol) and boric acid (0.51 g, 8.2 mmol). The solution was stirred at room temperature for 12 h, resulting in a dark yellow solution. The yellow solid was filtered from the mixture and washed well with hexane (20 mL) to afford the pure

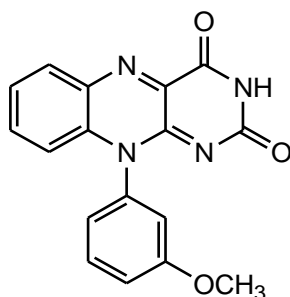
product as a yellow solid. The yellow solid was dried *in vacuo* to yield the isoalloxazine (**7c**), as a yellow powder, 1.37 g, 53%. FTIR (ATR):  $\nu$  2969, 1717, 1682, 1615, 1582, 1536, 1285, 1215, 1113, 1013, 874, 806, 768, 716, 695, 655, 727  $\text{cm}^{-1}$ .  $^1\text{H-NMR}$  ( $d_6$ -DMSO, 300 MHz)  $\delta$ ppm; 11.46 (s, Ar-NH, 1H), 8.19 (d,  $J = 8.1$  Hz, Ar-H, 1H), 7.77 (t,  $J = 7.8$  Hz, 1H), 7.70 – 7.58 (m, Ar-H, 2H), 7.44 – 7.34 (m, Ar-H, 2H), 7.25 (t,  $J = 7.7$  Hz, Ar-H, 1H), 6.79 (d,  $J = 8.0$  Hz, Ar-H, 1H), 3.71 (s, Ar-OCH<sub>3</sub>, 3H).  $^{13}\text{C-NMR}$  ( $d_6$ -DMSO, 75 MHz)  $\delta$ ppm; 159.90, 156.07, 154.27, 151.76, 139.87, 135.63, 135.08, 133.93, 132.14, 131.91, 129.41, 126.65, 124.22, 122.10, 116.92, 113.75, 56.42. HRMS (ESI)  $m/z$  calcd for  $[\text{C}_{17}\text{H}_{12}\text{N}_4\text{O}_3]^+$  320.091, found 321.0986  $[\text{M}+\text{H}]^+$ . Mp 263–265°C. Log P: 2.119.

### 6.11 Synthesis of 2-(2-nitrophenyl) 3-methoxy aniline (**8a**)



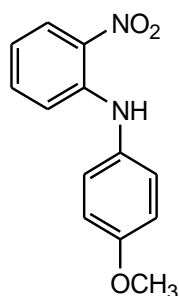
A mixture of potassium carbonate (24.8 g, 180.0 mmol), 3-anisidine (19.7 g, 160.0 mmol), and 1-fluoro-2-nitrobenzene (22.5 g, 160.0 mmol) was irradiated for 3 h at 150 °C in a CEM microwave at full power. The mixture was allowed to cool to room temperature, and ice (500 mL) was added with stirring. The aqueous solution was adjusted to pH 6 using c.  $\text{HCl}_{(\text{aq})}$  added to a separating funnel and extracted with  $\text{CHCl}_3$  (3x100 mL). The organic layer was isolated, dried with anhydrous sodium sulphate, and evaporated under reduced pressure to yield the substituted 3-methoxy-(2-nitrophenyl) aniline as a black solid. The crude solid was purified by flash column chromatography over silica gel eluting with EtOAc: PE (2:1) to afford the pure product as a red solid, (**8a**) 8.08 g, 20%.  $^1\text{H-NMR}$  ( $\text{CDCl}_3$ , 300 MHz)  $\delta$ ppm; 9.45 (s, N-H, 1H), 8.20 (d,  $J = 8.6$  Hz, Ar-H, 1H), 7.37 (t,  $J = 8.0$  Hz, Ar-H, 2H), 7.26 (m, Ar-H, 1H), 7.18 (t,  $J = 7.9$  Hz, Ar-H, 1H), 6.98 (m, Ar-H, 2H), 6.77 (t,  $J = 7.9$  Hz, Ar-H, 1H), 3.8 (s, OCH<sub>3</sub>, 3H).  $^{13}\text{C NMR}$  ( $\text{CDCl}_3$ , 75MHz); 152.61, 142.60, 135.59, 133.83, 127.91, 126.80, 125.88, 123.38, 120.77, 117.55, 116.30, 111.68, 55.85. HRMS (ESI)  $m/z$  calcd for  $[\text{C}_{13}\text{H}_{12}\text{N}_2\text{O}_3]^+$  245.246, found 244.128  $[\text{M}-\text{H}]^-$ . Mp 263–265°C. Log P: 2.119.

## 6.12 Synthesis of 10-(3-methoxyphenyl) isoalloxazine (**8c**)



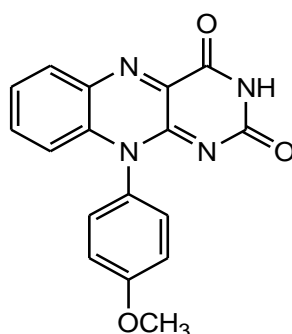
Compound **8a** (3.17 g, 13.0 mmol) was dissolved in glacial acetic acid (70 mL) and the mixture was cooled in an ice bath. Zinc dust (8.56 g, 131 mmol) was gradually added and the solution was allowed to stir at room temperature for 2 h and filtered through celite. The filter cake was washed with glacial acetic acid (20 mL) to yield the substituted *N*-(methoxyphenyl amino) aniline (**8b**) as a dark brown solution. To the solution of substituted *N*-phenylaniline was added alloxan monohydrate (2.08 g, 13.0 mmol) and boric acid (0.81 g, 13.1 mmol). The solution was stirred at room temperature for 12 h, resulting in a dark yellow solution. The yellow solid was filtered from the mixture and washed well with hexane (30 mL) to afford the pure product as a yellow solid. The yellow solid was dried *in vacuo* to yield the isoalloxazine (**8 h**), 4.30 g, 96%, as a yellow powder. FTIR (ATR):  $\nu$  3016, 1720, 1680, 1614, 1581, 1540, 1497, 1419, 1363, 1268, 1198, 1114, 1045, 1012, 877, 817, 806, 752, 709, 653  $\text{cm}^{-1}$ .  $^1\text{H-NMR}$  ( $\text{d}_6$ -DMSO, 300 MHz)  $\delta$ ppm; 11.46 (s, N-H, 1H), 8.19 (d,  $J = 8.2$  Hz, Ar-H, 1H), 7.75 (t,  $J = 7.9$  Hz, Ar-H, 1H), 7.64 (m, Ar-H, 2H), 7.39 (d,  $J = 7.9$  Hz, Ar-H, 2H), 7.26 (t,  $J = 7.8$  Hz, Ar-H, 1H), 6.79 (d,  $J = 8.3$  Hz, Ar-H, 1H), 3.71 (s,  $\text{OCH}_3$ , 3H).  $^{13}\text{C NMR}$  ( $\text{d}_6$ -DMSO, 75 MHz)  $\delta$ ppm; 173.78, 159.49, 155.67, 153.87, 151.35, 139.47, 135.22, 134.68, 133.53, 131.73, 131.51, 129.00, 126.24, 123.82, 121.70, 116.51, 113.34, 56.01. HRMS (ESI)  $m/z$  calcd for  $[\text{C}_{17}\text{H}_{12}\text{N}_4\text{O}_2]^+$  320.091, found 321.0985  $[\text{M}+\text{H}]^+$ . Mp 262–265°C. Log P: 2.307.

### 6.13 Synthesis of 2-(2-nitrophenyl) 4-methoxy aniline (**9a**)



A mixture of potassium carbonate (4.14 g, 30 mmol), 4-anisidine (1.23.0 g, 10 mmol), and 1-fluoro-2-nitrobenzene (1.4.1 g, 10 mmol) was irradiated for 3 h at 150 °C in a CEM microwave at full power. The mixture was allowed to cool to room temperature, and ice (100 mL) was added with stirring. The aqueous solution was adjusted to pH 6 using c. HCl<sub>(aq)</sub> added to a separating funnel and extracted with CHCl<sub>3</sub> (3x60 mL). The organic layer was isolated, dried with anhydrous sodium sulphate, and evaporated under reduced pressure to yield the substituted 4-methoxy-(2-nitrophenyl) aniline as a black solid. The crude solid was purified by flash column chromatography over silica gel eluting with EtOAc: PE (2:1) to afford the pure product as a red solid, (**9a**) 1.21 g, 50%. <sup>1</sup>H-NMR (CDCl<sub>3</sub>, 300 MHz) δppm; 9.41 (s, N-H, 1H), 8.17 (d, *J* = 8.6 Hz, Ar-H, 1H), 7.30 (t, *J* = 7.8 Hz, Ar-H, 1H), 7.18 (m, Ar-H, 2H), 6.97 (m, Ar-H, 3H), 6.70 (t, *J* = 7.8 Hz, Ar-H, 1H), 3.83 (s, OCH<sub>3</sub>, 3H). <sup>13</sup>C NMR (CDCl<sub>3</sub>, 75MHz); 157.91, 144.48, 135.78, 132.39, 131.13, 127.09, 126.58, 116.78, 115.76, 114.95. HRMS (ESI) *m/z* calcd for [C<sub>13</sub>H<sub>12</sub>N<sub>2</sub>O<sub>3</sub>]<sup>+</sup> 245.246, found 244.139 [M-H]<sup>-</sup>. Log P: 3.90.

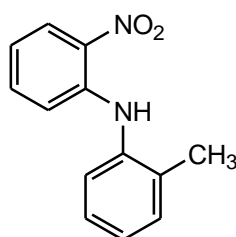
### 6.14 Synthesis of 10-(4-methoxyphenyl) isoalloxazine (**9c**)



Compound **9a** (3.00 g, 13.2 mmol) was dissolved in glacial acetic acid (20 mL) and the mixture was cooled in an ice bath. Zinc dust (8.55 g, 132 mmol) was gradually added and the solution was allowed to stir at room temperature for 2 h and filtered through celite. The filter cake was washed with glacial acetic acid (250 mL) to yield the substituted *N*-(methoxyphenyl amino) (**9b**) as a dark brown solution. To the solution of substituted *N*-(methoxyphenyl amino) aniline was added alloxan monohydrate (2.08 g, 13.0 mmol) and boric acid (0.81 g, 13.2 mmol). The solution

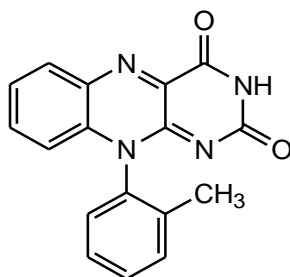
was stirred at room temperature for 12 h, resulting in a dark yellow solution. The yellow solid was filtered from the mixture and washed well with hexane (30 mL) to afford the pure product as a yellow solid. The yellow solid was dried *in vacuo* to yield the isoalloxazine (**9c**), 3.76 g, 82%, as a yellow powder. <sup>1</sup>H-NMR (d<sub>6</sub>-DMSO, 300 MHz) δppm; 11.43 (s, Ar-NH, 1H), 8.18 (d, *J* = 7.0 Hz, Ar-H, 1H), 7.75 (d, *J* = 7.0 Hz, Ar-H, 1H), 7.61 (t, *J* = 7.3 Hz, Ar-H, 1H), 7.35 (d, *J* = 8.7 Hz, Ar-H, 2H), 7.24 (d, *J* = 9.0 Hz, Ar-H, 2H), 6.84 (d, *J* = 8.3 Hz, Ar-H, 1H), 3.88 (s, Ar-OCH<sub>3</sub>, 3H). <sup>13</sup>C NMR (d<sub>6</sub>-DMSO, 75 MHz) δppm; 160.32, 160.08, 156.06, 152.51, 139.89, 135.20, 134.94, 131.81, 129.40, 129.40, 128.94, 126.39, 117.39, 115.87, 21.99. FTIR (ATR): ν 3073, 1746, 1706, 1638, 1613, 1583, 1539, 1501, 1459, 1404, 1329, 1276, 1249, 1197, 1175, 1114, 1032, 930, 883, 841, 809, 765, 755, 727, 706 CM<sup>-1</sup>. HRMS (ESI) *m/z* calcd for [C<sub>17</sub>H<sub>12</sub>N<sub>4</sub>O<sub>3</sub>]<sup>+</sup> 320.091, found 321.0987 [M+H]<sup>+</sup>. Mp 264–266°C. Log P: 2.119.

### 6.15 Synthesis of 2-(2-nitrophenyl) 2-tolyl aniline (**10a**)



A mixture of potassium carbonate (4.14 g, 30.0 mmol), 2-toluidine (1.07 g, 10.0 mmol), and 1-fluoro-2-nitrobenzene (1.41 g, 10.0 mmol) was irradiated for 3 h at 150 °C in a CEM microwave at full power. The mixture was allowed to cool to room temperature, and with stirring poured onto ice water (30 mL). The reaction mixture was adjusted to pH 6 using c. HCl (aq), added to a separating funnel and extracted with CHCl<sub>3</sub> (3 x 50 mL). The organic layer was isolated, dried with anhydrous sodium sulphate, and evaporated under reduced pressure to yield the substituted 2-tolyl-*N*-(2-nitrophenyl) aniline as a black solid. The crude solid was purified by flash column chromatography over silica gel eluting with EtOAc: PE (2:1) to afford the pure product as a red solid. The solid was dried *in vacuo* to yield **10a**, 1.37 g, 60% as dark red crystals. <sup>1</sup>H-NMR (CDCl<sub>3</sub>, 300 MHz) δppm; 9.39 (s, Ar-NH, 1H), 8.23 (d, *J* = 8.6 Hz, Ar-H, 1H), 7.42 – 7.17 (m, Ar-H, 5H), 6.87 (d, *J* = 8.6 Hz, Ar-H, 1H), 6.76 (t, *J* = 8.3 Hz, Ar-H, 1H), 2.29 (s, Ar-CH<sub>3</sub>, 3H). <sup>13</sup>C NMR (CDCl<sub>3</sub>, 75 MHz,) 143.85, 136.94, 135.89, 134.42, 132.60, 131.45, 127.15, 126.74, 126.65, 126.19, 116.97, 115.83, 17.97. HRMS (ESI) *m/z* calcd for [C<sub>13</sub>H<sub>12</sub>N<sub>2</sub>O<sub>2</sub>]<sup>+</sup> 228.224, found 228.99 [M+H]<sup>+</sup>. Mp 264-266°C. Log P: 2.119.

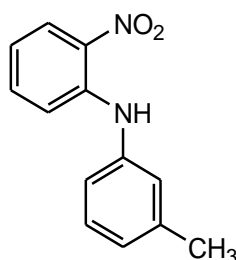
## 6.16 Synthesis of 10-(2-tolylphenyl) isoalloxazine (**10c**)



Compound **10a** (2.97 g, 13 mmol) was dissolved in glacial acetic acid (70 mL) and with constant stirring the mixture was cooled in a slush bath for a few moments followed by the slow gradual addition of zinc dust (8.56 g, 131 mmol) ensuring the temperature did not rise uncontrollably. Upon the final addition of zinc the reaction mixture was allowed to stir at room temperature for 2 h. The reaction mixture was filtered through celite to remove the zinc dust and the filter cake was washed with glacial acetic acid (20 mL) to yield the substituted *N*-(tolylphenyl amino) aniline (**10b**) as a dark brown solution. To the solution was added alloxan monohydrate (2.11 g, 13.2 mmol) and boric acid (0.80 g, 13.0 mmol) and the solution was stirred at room temperature for 12 h, resulting in the formation of a yellow precipitate. The precipitate was isolated from the reaction mixture by filtration under reduced pressure and washed well with hexane (40 mL). The yellow solid was dried *in vacuo* to yield the 10-(2-tolylphenyl) isoalloxazine (**10c**), 1.37 g, 53%, as a yellow powder, mp 240-242°C. <sup>1</sup>H-NMR (d<sub>6</sub>-DMSO, 300 MHz) δppm; 11.43 (s, Ar-NH, 1H), 8.21 (d, *J* = 8.0 Hz, Ar-H, 1H), 7.75 (t, *J* = 7.9 Hz, Ar-H, 1H), 7.56 (d, *J* = 7.9 Hz, Ar-H, 4H), 7.31 (d, *J* = 7.4 Hz, Ar-H, 1H), 6.67 (d, *J* = 8.3 Hz, Ar-H, 1H), 1.97 (s, Ar-CH<sub>3</sub>, 3H). <sup>13</sup>C NMR (d<sub>6</sub>-DMSO, 75 MHz,) δppm; 160.15, 156.19, 151.52, 140.41, 135.53, 135.47, 135.42, 135.17, 133.56, 132.00, 131.96, 130.49, 128.38, 128.17, 126.59, 116.62, 17.36. FTIR (ATR): ν 3019, 1709, 1649, 1610, 1579, 1545, 1508, 1460, 1428, 1369, 1283, 1223, 1187, 1160, 1118, 1012, 934, 878, 826, 808, 773, 724, 705, 655 CM<sup>-1</sup>. HRMS (ESI) *m/z* calcd for [C<sub>17</sub>H<sub>12</sub>N<sub>4</sub>O<sub>2</sub>]<sup>+</sup> 304.096, found 305.1035 [M+H]<sup>+</sup>. Mp dec.240-242°C. Log P: 2.67.

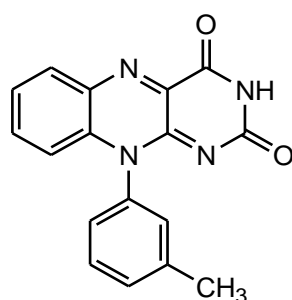


## 6.17 Synthesis of 2-(2-nitrophenyl) 3-tolyl aniline (**11a**)



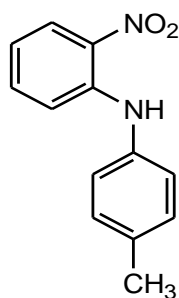
A mixture of potassium carbonate (6.91 g, 50.0 mmol), 3-toluidine (3.24 mL, 30 mmol), and 1-bromo-2-nitrobenzene (6.06 g, 30.0 mmol) was irradiated for 3 h at 150 °C in a CEM microwave at full power. The mixture was allowed to cool to room temperature, and with stirring poured onto ice water (100 mL). The reaction mixture was adjusted to pH 6 using c. HCl<sub>(aq)</sub>, added to a separating funnel and extracted with CHCl<sub>3</sub> (3 x 50 mL). The organic layer was isolated, dried with anhydrous sodium sulphate, and evaporated under reduced pressure to yield the substituted 2-(2-nitrophenyl) 3-tolyl-aniline as a black solid. The crude solid was purified by flash column chromatography over silica gel eluting with EtOAc: PE (2:1) to afford the pure product as a red solid. The solid was dried *in vacuo* to yield **11a**, 5.02 g, 73% as dark red crystals. <sup>1</sup>H-NMR (CDCl<sub>3</sub>, 300 MHz) δppm; 9.50 (s, Ar-NH, 1H), 8.21 (dd, *J* = 8.6, 1.4 Hz, Ar-H, 1H), 7.43 – 7.22 (m, Ar-H, 3H), 7.15 – 7.04 (m, Ar-H, 3H), 6.78 (t, *J* = 8.3 Hz, Ar-H, 1H), 2.40 (s, Ar-CH<sub>3</sub>, 3H). <sup>13</sup>C NMR (CDCl<sub>3</sub>, 75 MHz,) 143.21, 139.80, 138.56, 135.71, 133.03, 129.51, 126.64, 126.49, 125.04, 121.35, 117.36, 116.16, 21.43. HRMS. (ESI) *m/z* calcd for [C<sub>13</sub>H<sub>12</sub>N<sub>2</sub>O<sub>2</sub>]<sup>+</sup> 228.25, found 229.19 [M+H]<sup>+</sup>. Log P: 4.26.

## 6.18 Synthesis of 10-(3-tolylphenyl) isoalloxazine (**11c**)



Compound **11a** (5.01 g, 22.0 mmol) was dissolved in glacial acetic acid (105 mL) and with constant stirring the mixture was cooled in a slush bath for a few moments followed by the slow gradual addition of zinc dust (14.38 g, 220 mmol) ensuring the temperature did not rise uncontrollably. Upon the final addition of zinc the reaction mixture was allowed to stir at room temperature for 2 h. The reaction mixture was filtered through celite to remove the zinc dust and the filter cake was washed with glacial acetic acid (50 mL) to yield the substituted *N*-(tolylphenyl) amino) aniline, (**11b**) as a dark brown solution. To the solution was added alloxan monohydrate (3.52 g, 22.0 mmol) and boric acid (1.37 g, 22.2 mmol) and the solution was stirred at room temperature for 12 h, resulting in the formation of a yellow precipitate. The precipitate was isolated from the reaction mixture by filtration under reduced pressure and washed well with hexane (60 mL). The yellow solid was dried *in vacuo* to yield 10-(3-tolyl phenyl) isoalloxazine (**11c**), 2.45 g, 37 %, as a yellow powder, mp 242-244°C. <sup>1</sup>H-NMR (d<sub>6</sub>-DMSO, 300 MHz) δppm; 11.44 (s, 1H, Ar-NH), 8.18 (d, *J* = 6.0 Hz, Ar-H, 1H), 7.74 (t, *J* = 6.2 Hz, Ar-H, 1H), 7.63-7.57 (m, Ar-H, 2H), 7.47 (d, *J* = 6.5 Hz, Ar-H, 1H), 7.23-7.21 (m, Ar-H, 2H), 6.77 (d, *J* = 7.0 Hz, Ar-H, 1H), 2.43 (s, CH<sub>3</sub>, 3H). <sup>13</sup>C NMR (d<sub>6</sub>-DMSO, 75 MHz) δppm; 160.03, 156.05, 152.15, 140.48, 139.93, 136.49, 135.22, 135.16, 134.48, 131.79, 130.91, 130.60, 128.39, 126.45, 125.22, 117.33, 21.38. HRMS (ESI) *m/z* calcd for [C<sub>17</sub>H<sub>12</sub>N<sub>4</sub>O<sub>2</sub>]<sup>+</sup> 304.302 found 305.313 [M+H]<sup>+</sup>. Log P: 2.69.

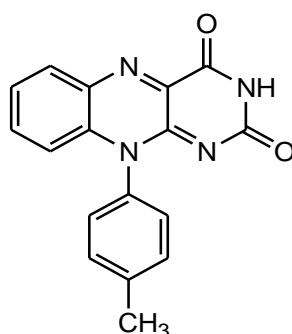
## 6.19 Synthesis of 2-(2-nitrophenyl) 4-tolyl aniline (**12a**)



A mixture of potassium carbonate (5.52 g, 40.0 mmol), 4-toluidine (2.89 g, 20.0 mmol), and 1-fluoro-2-nitrobenzene (2.82 g, 20.0 mmol) was irradiated for 3 h at 150 °C in a CEM microwave at full power. The mixture was allowed to cool to room temperature, and with stirring poured onto

ice water (80 mL). The reaction mixture was adjusted to pH 6 using c. HCl (aq), added to a separating funnel and extracted with CHCl<sub>3</sub> (3 x 50 mL). The organic layer was isolated, dried with anhydrous sodium sulphate, and evaporated under reduced pressure to yield the substituted 2-(2-nitrophenyl) 4-tolyl aniline as a black solid. The crude solid was purified by flash column chromatography over silica gel eluting with EtOAc: PE (2:1) to afford the pure product as a red solid. The solid was dried *in vacuo* to yield (**12a**), 3.52 g, 58% as dark red crystals. \* main signals showing with crude/impure material present; <sup>1</sup>H-NMR (CDCl<sub>3</sub>, 300 MHz) δppm; 10.02 (s, N-H, 1H), 9.36 (s, N-H, 1H), 8.08 (dd, *J* = 8.5 Hz, *J* = 8.0 Hz Ar-H, 1H), 7.78 (d, *J* = 8.1 Hz, Ar-H, 1H), 7.72 (t, *J* = 7.6 Hz, Ar-H, 1H), 7.61 (m, Ar-H, 1H), 7.46 (m, Ar-H, 1H), 7.22 (m, Ar-H, 6H), 7.09 (d, *J* = 8.7 Hz, Ar-H, 1H), 7.00 (t, *J* = 7.5 Hz, Ar-H, 1H), 6.81 (m, Ar-H, 1H), 6.52 (t, *J* = 7.5 Hz, Ar-H, 1H), 2.30 (s, CH<sub>3</sub>, 3H). \* Main signals showing with crude/impure material present; <sup>13</sup>C NMR (CDCl<sub>3</sub>, 75 MHz,) 148.30, 145.77, 142.12, 137.95, 136.91, 134.25, 133.63, 131.58, 128.17, 126.76, 126.68, 126.41, 115.99, 114.82, 116.03. HRMS. *m/z* (ESI) calcd for [C<sub>13</sub>H<sub>12</sub>N<sub>2</sub>O<sub>2</sub>]<sup>+</sup>: 228.25, found 229.03 [M+H]<sup>+</sup>. Log P: 4.29.

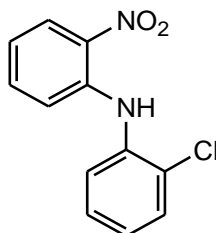
## 6.20 Synthesis of 10-(4-tolylphenyl) isoalloxazine (**12c**)



Compound **12a** (2.96 g, 13 mmol) was dissolved in glacial acetic acid (50 mL) and with constant stirring the mixture was cooled in a slush bath for a few moments followed by the slow gradual addition of zinc dust (8.58 g, 132 mmol) ensuring the temperature did not rise uncontrollably. Upon the final addition of zinc the reaction mixture was allowed to stir at room temperature for 2 h. The reaction mixture was filtered through celite to remove the zinc dust and the filter cake was washed with glacial acetic acid (30 mL) to yield the substituted *N*-(tolylphenyl amino) aniline, (**12b**) as a dark brown solution. To the solution was added alloxan monohydrate (2.11 g, 13.2 mmol) and boric acid (0.80 g, 13.0 mmol) and the solution was stirred at room temperature for 12 h, resulting in the formation of a yellow precipitate. The precipitate was isolated from the reaction mixture by filtration under reduced pressure and washed well with hexane (40 mL). The yellow solid was dried *in vacuo* to yield 10-(4-tolyl phenyl) isoalloxazine (**12c**), 3.76 g, 82 %, as a yellow powder, mp 242-244°C. <sup>1</sup>H-NMR (d<sub>6</sub>-DMSO, 300 MHz) δppm; 11.43 (s, Ar-NH, 1H), 8.18 (d, *J* = 7.9 Hz, Ar-H, 1H), 7.74 (t, *J* = 7.8 Hz, Ar-H, 1H), 7.61 (t, *J* = 7.8 Hz, Ar-H, 1H), 7.51 (d, *J* = 8.1 Hz, Ar-H, 2H), 7.30 (d, *J* = 8.1 Hz, Ar-H, 2H), 6.79 (d, *J* = 8.4 Hz, Ar-H, 1H), 2.46 (s,

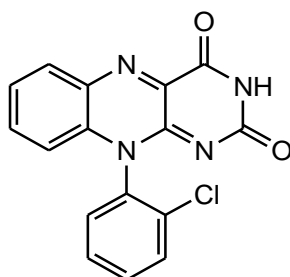
Ar-CH<sub>3</sub>H). <sup>13</sup>C NMR (d<sub>6</sub>-DMSO, 75.4 MHz) δppm; 160.04, 156.03, 152.28, 139.91, 139.89, 135.18, 134.63, 133.94, 131.80, 131.80, 131.21, 127.97, 126.42, 117.32, 21.99. FTIR (ATR): ν 3015, 2969, 1739, 1638, 1613, 1541, 1501, 1459, 1405, 1365, 1277, 1228, 1216, 1109, 1033, 883, 841, 766, 727 CM<sup>-1</sup>. HRMS (ESI) m/z calcd for [C<sub>17</sub>H<sub>12</sub>N<sub>4</sub>O<sub>2</sub>]<sup>+</sup> 304.1035, found 305.1035 [M+H]<sup>+</sup>. Log P:2.51.

## 6.21 Synthesis of 2-(2-chlorophenyl) aniline (**14a**)



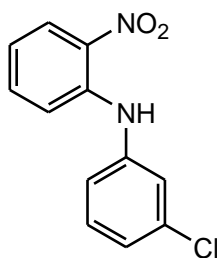
A mixture of potassium carbonate (5.52 g, 40.0 mmol), 2-chloroaniline (2.55 g, 20.0 mmol), and 1-fluoro-2-nitrobenzene (7.05 g, 50.0 mmol) was irradiated for 3 h at 150 °C in a CEM microwave at full power. The mixture was allowed to cool to room temperature, and ice (20 mL) was added with stirring. The aqueous solution was adjusted to pH 6 using c. HCl<sub>(aq)</sub> added to a separating funnel and extracted with CHCl<sub>3</sub> (3x50 mL). The organic layer was isolated, dried with anhydrous sodium sulphate, and evaporated under reduced pressure to yield the substituted 2-chloro-(2-nitrophenyl) aniline as a black solid. The crude solid was purified by flash column chromatography over silica gel eluting with EtOAc: PE (2:1) to afford the pure product as a red solid, (**14a**), 10.42 g, 98%. <sup>1</sup>H-NMR (CDCl<sub>3</sub>, 300 MHz) δppm; 9.50 (s, Ar-NH, 1H), 8.23 (dd, *J* = 8.6, 1.5 Hz, Ar-H, 1H), 7.57 – 7.38 (m, Ar-H, 2H), 7.36 – 7.26 (m, Ar-H, 1H), 7.24 – 7.12 (m, Ar-H, 3H), 6.87 (t, *J* = 7.8 Hz, Ar-H, 1H). <sup>13</sup>C NMR (CDCl<sub>3</sub>, 75 MHz) δppm; 141,51, 136.17, 135.63, 134.20, 130.59, 128.66, 127.59, 126.73, 126.08, 124.33, 118.46, 116.25. HRMS (ESI) m/z calcd for [C<sub>12</sub>H<sub>9</sub>ClN<sub>2</sub>O<sub>2</sub>]<sup>+</sup> 247.662, found 248.665 [M<sup>+</sup>]. Log P: 4.47.

## 6.22 Synthesis of 10-(2-chlorophenyl) isoalloxazine (**14c**)



Compound **14a** (0.30 g, 1.2 mmol) was dissolved in glacial acetic acid (10 mL) and the mixture was cooled in an ice bath. Zinc dust (0.78 g, 12 mmol) was gradually added and the solution was allowed to stir at room temperature for 2 h and filtered through celite. The filter cake was washed with glacial acetic acid (10 mL) to yield the substituted *N*-(chlorophenyl amino) aniline, (**14b**) as a dark brown solution. To the solution of substituted *N*-phenylaniline was added a further portion of glacial acetic acid (10 mL) along with alloxan monohydrate (0.2g, 1.30 mmol) and boric acid (0.1 g, 1.31 mmol). The solution was stirred at room temperature for 12 h, resulting in a dark yellow solution. The yellow solid was filtered from the mixture and washed well with hexane (10 mL) to afford the pure product as a yellow solid. The yellow solid was dried *in vacuo* to yield the isoalloxazine (**14c**) 0.10 g, 26%, as a yellow powder. FTIR (ATR):  $\nu$  3300, 1709, 1612, 1583, 1461, 1313, 1196, 1107, 833  $\text{CM}^{-1}$ .  $^1\text{H-NMR}$  ( $\text{d}_6$ -DMSO, 300 MHz)  $\delta$ ppm; 11.54 (s, Ar-NH, 1H), 8.23 (d,  $J = 8.1$  Hz, Ar-H, 1H), 7.94 – 7.54 (m, Ar-H, 6H), 6.74 (d,  $J = 8.5$  Hz, Ar-H, 1H).  $^{13}\text{C}$  NMR ( $\text{d}_6$ -DMSO, 75 MHz)  $\delta$ ppm; 159.78, 155.92, 151.40, 140.00, 139.81, 137.64, 135.84, 135.00, 133.60, 133.11, 132.14, 131.20, 130.46, 129.93, 126.94, 116.49. HRMS (ESI)  $m/z$  calcd for  $[\text{C}_{16}\text{H}_9\text{ClN}_4\text{O}_2]^+$  324.7213, found 325.0489  $[\text{M}+\text{H}]^+$ . Mp 236–238°C. Log P: 2.904.

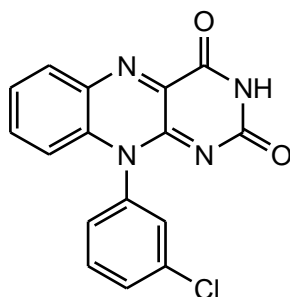
## 6.23 Synthesis of 2-(2-nitrophenyl) 3-chloro aniline (**15a**)



A mixture of potassium carbonate (9.67 g, 50.0 mmol), 2-chloroaniline (3.82 g 30.0 mmol), and 1-fluoro-2-nitrobenzene (30.0 mmol) was irradiated for 3 h at 150 °C in a CEM microwave at full power. The mixture was allowed to cool to room temperature, and ice (10 mL) was added with stirring. The aqueous solution was adjusted to pH 6 using c.  $\text{HCl}_{(\text{aq})}$  added to a separating funnel and extracted with  $\text{CHCl}_3$  (3x50 mL). The organic layer was isolated, dried with anhydrous sodium sulphate, and evaporated under reduced pressure to yield the substituted 3-chloro-*N*-(2-

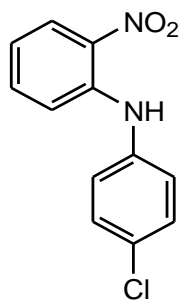
nitrophenyl) aniline as a black solid. The crude solid was purified by flash column chromatography over silica gel eluting with EtOAc: PE (2:1) to afford the pure product as a red solid, **15a**, 0.43 g, 5%. <sup>1</sup>H-NMR (CDCl<sub>3</sub>, 300 MHz) δppm; 9.28 (s, Ar-NH, 1H), 8.11 (d, *J* = 8.1 Hz, Ar-H, 1H), 7.55 (t, *J* = 7.3 Hz, Ar-H, 1H), 7.46 – 7.12 (m, Ar-H, 5H), 6.97 (t, *J* = 7.3 Hz, Ar-H, 1H). <sup>13</sup>C NMR (CDCl<sub>3</sub>, 75 MHz) δppm; 142.12, 140.84, 136.32, 135.54, 134.15, 131.41, 126.69, 124.18, 122.53, 121.27, 119.79, 118.43. HRMS (ESI) *m/z* calcd for [C<sub>12</sub>H<sub>9</sub>ClN<sub>2</sub>O<sub>2</sub>]<sup>+</sup> 248.665, found 249.0465 [M+H]<sup>+</sup>. Log P: 4.49.

## 6.24 Synthesis of 10-(3-chlorophenyl) isoalloxazine (**15c**)



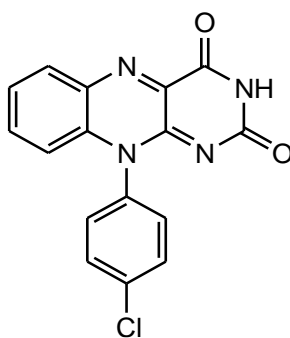
Compound **15a** (0.42 g, 1.7 mmol) was dissolved in glacial acetic acid (10 mL) and the mixture was cooled in an ice bath. Zinc dust (1.13g, 17.3 mmol) was gradually added and the solution was allowed to stir at room temperature for 2 h and filtered through celite. The filter cake was washed with glacial acetic acid (15 mL) to yield the substituted *N*-(chlorophenyl amino) aniline, (**15b**) as a dark brown solution. To the solution of substituted *N*-(chlorophenyl amino) aniline was added a further portion of glacial acetic acid (15 mL) along with alloxan monohydrate (0.27, 1.70 mmol) and boric acid (0.10 g, 1.71 mmol). The solution was stirred at room temperature for 12 h, resulting in a dark yellow solution. The yellow solid was filtered from the mixture and washed well with hexane (10 mL) to afford the pure product as a yellow solid. The yellow solid was dried *in vacuo* to yield the isoalloxazine (**15c**) 0.19 g, 34%, as a yellow powder. FTIR (ATR):  $\nu$  3300, 1704, 1680, 1537, 1459, 1410, 1317, 1268, 818  $\text{cm}^{-1}$ . <sup>1</sup>H-NMR (d<sub>6</sub>-DMSO, 300 MHz) δppm; 11.50 (s, Ar-NH, 1H), 8.20 (d, *J* = 8.0 Hz, Ar-H, 1H), 7.81 – 7.39 (m, Ar-H, 6H), 6.83 (d, *J* = 8.5 Hz, Ar-H, 1H). <sup>13</sup>C NMR (d<sub>6</sub>-DMSO, 75 MHz) δppm; 159.89, 155.91, 152.14, 139.81, 137.70, 135.48, 135.13, 134.79, 134.16, 132.55, 131.90, 130.52, 128.43, 127.33, 126.63, 117.19. HRMS (ESI) *m/z* calcd for [C<sub>16</sub>H<sub>9</sub>ClN<sub>4</sub>O<sub>2</sub>]<sup>+</sup> 324.0213, found 325.0487 [M+H]<sup>+</sup>. Mp 260–262°C. Log P: 2.928.

## 6.25 Synthesis of 2-(2-nitrophenyl) 4-chloro aniline (**16a**)



A mixture of potassium carbonate (6.91 g, 50.0 mmol), 2-chloroaniline (3.82g 30.0 mmol), and 1-fluoro-2-nitrobenzene (4.23 g, 30.0 mmol) was irradiated for 3 h at 150 °C in a CEM microwave at full power. The mixture was allowed to cool to room temperature, and ice (10 mL) was added with stirring. The aqueous solution was adjusted to pH 6 using c. HCl<sub>(aq)</sub> added to a separating funnel and extracted with CHCl<sub>3</sub> (4x50 mL). The organic layer was isolated, dried with anhydrous sodium sulphate, and evaporated under reduced pressure to yield the substituted (2-nitrophenyl) 4-chloro aniline, (**16a**) as a black solid, 1.55 g, 21%. <sup>1</sup>H-NMR (CDCl<sub>3</sub>, 300 MHz) δppm; 9.43 (s, Ar-NH, 1H), 8.23 (d, *J* = 9.9 Hz, Ar-H, 1H), 7.48 – 7.14 (m, Ar-H, 6H), 6.83 (t, *J* = 7.8 Hz, Ar-H, 1H). <sup>13</sup>C NMR (CDCl<sub>3</sub>, 75 MHz) δppm; 142.57, 137.37, 135.82, 133.47, 130.80, 129.86, 126.75, 125.51, 117.98, 115.92. HRMS (ESI) *m/z* calcd for [C<sub>12</sub>H<sub>9</sub>ClN<sub>2</sub>O<sub>2</sub>]<sup>+</sup> 248.665, found 249.0355 [M+H]<sup>+</sup>. Log P:4.52.

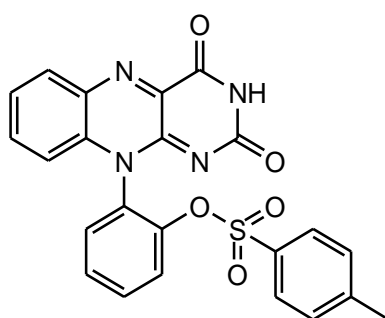
## 6.26 Synthesis of 10-(4-chlorophenyl) isoalloxazine (**16c**)



Compound **16a** (1.00 g, 4.0 mmol) was dissolved in glacial acetic acid (20 mL) and the mixture was cooled in an ice bath. Zinc dust (2.61 g, 40.3 mmol) was gradually added and the solution was allowed to stir at room temperature for 2 h and filtered through celite. The filter cake was washed with glacial acetic acid (30 mL) to yield the substituted *N*-(chlorophenyl amino) aniline as a dark brown solution. To the solution of substituted *N*-(chlorophenyl amino) aniline (**16b**) was added a further portion of glacial acetic acid (50 mL) along with alloxan monohydrate (0.64g, 4.0 mmol) and boric acid (0.23g, 3.8 mmol). The solution was stirred at room temperature for 12 h, resulting in a dark yellow solution. The yellow solid was filtered from the mixture and washed

well with hexane (10 mL) to afford the pure product as a yellow solid. The yellow solid was dried *in vacuo* to yield the isoalloxazine (**16c**) 0.93 g, 71%, as a yellow powder. FTIR (ATR):  $\nu$  3300, 1688, 1581, 1488, 1461, 1200, 1198, 881  $\text{cm}^{-1}$ .  $^1\text{H-NMR}$  ( $d_6$ -DMSO, 300 MHz)  $\delta$ ppm; 11.48 (s, Ar-NH, 1H), 8.19 (d,  $J = 8.1$  Hz, Ar-H, 1H), 7.85 – 7.71 (m, Ar-H, 3H), 7.62 (t,  $J = 7.9$  Hz, Ar-H, 1H), 7.52 – 7.45 (m, Ar-H, 2H), 6.83 (d,  $J = 8.5$  Hz, Ar-H, 1H).  $^{13}\text{C-NMR}$  ( $d_6$ -DMSO, 75 MHz)  $\delta$ ppm; 159.54, 155.50, 151.82, 139.46, 134.94, 134.91, 134.75, 134.54, 133.88, 131.47, 130.54, 129.93, 126.14, 116.81. HRMS (ESI)  $m/z$  calcd for  $[\text{C}_{16}\text{H}_9\text{ClN}_4\text{O}_2]^+$  324.053, found 325.0488  $[\text{M}+\text{H}]^+$ . Mp 258–260°C. Log P: 2.741.

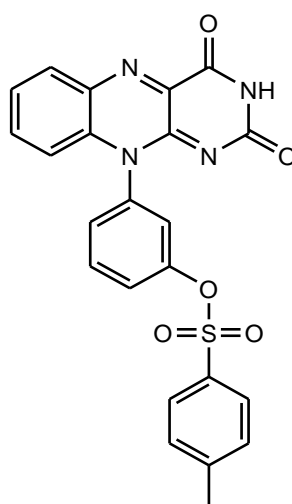
### 6.27 Synthesis of 10-(2-tosyloxyphenyl) isoalloxazine (**17c**)



Compound **4c** was dissolved (0.30 g, 1.0 mmol) in DCM (10 mL) and with continuous stirring the mixture was cooled to 0°C using an ice bath ensuring the temperature did not rise uncontrollably. To this was added *p*-toluene sulphonyl chloride (0.29 g, 1.5 mmol) and triethylamine (2.8 mL, 2.0 mmol). Upon the final addition of  $\text{Et}_3\text{N}$ , the reaction mixture was removed from the ice and allowed to stir at room temperature for 2 h. The solution was acidified to pH 7 with c.  $\text{HCl}_{(\text{aq})}$ , transferred to a separating funnel and extracted with water and ethyl acetate (3 x 15 mL), organics were collected and dried over anhydrous  $\text{Na}_2\text{SO}_4$  and concentrated under reduced pressure to afford the pure product as a yellow solid. The solid was dried *in vacuo* to yield the 10-(2-tosyloxyphenyl) isoalloxazine (**17c**) 0.28 g, 62% as a yellow powder, mp 248–250°C.  $^1\text{H-NMR}$  ( $d_6$ -DMSO, 300 MHz)  $\delta$ ppm; 11.52 (s, Ar-NH, 1H), 8.15 (d,  $J = 7.8$  Hz, Ar-H, 1H), 7.83 – 7.58 (m, Ar-H, 5H), 7.49 (d,  $J = 7.8$  Hz, Ar-H, 1H), 7.32 (d,  $J = 8.3$  Hz, Ar-H, 2H), 7.04 (d,  $J = 8.3$  Hz, Ar-H, 2H), 6.62 (d,  $J = 8.4$  Hz, Ar-H, 1H), 2.29 (s, Ar-CH, 3H).  $^{13}\text{C NMR}$  ( $d_6$ -DMSO 75 MHz,)  $\delta$  159.91, 155.88, 155.18, 152.19, 149.99, 146.59, 139.90, 139.01, 135.35, 135.21, 135.14, 134.30, 131.66, 130.85, 130.34, 128.84, 126.56, 124.68, 124.60, 116.94, 21.70. FTIR (ATR):  $\nu$  2969, 1725, 1662, 1609, 1662, 1579, 1536, 1509, 1457, 1366, 1275, 1197, 1158, 1109, 1090, 863, 799, 766, 721, 700, 664. HRMS (ESI)  $m/z$  calcd for  $[\text{C}_{23}\text{H}_{16}\text{N}_4\text{O}_5\text{S}]^+$  461.462, found 461.0913  $[\text{M}-\text{H}]^-$ . Log P: 3.64.

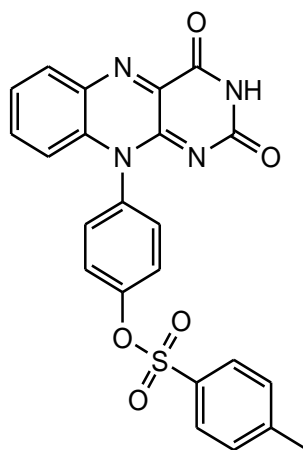


## 6.28 Synthesis of 10-(3-tosylphenyl) isoalloxazine (**18c**)



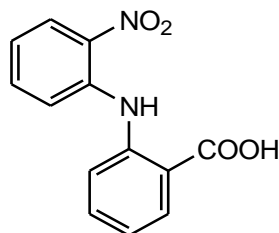
Compound **5c** was dissolved (0.30 g, 1.0 mmol) in DCM (10 mL) and with continuous stirring the mixture was cooled to 0° C using an ice bath ensuring the temperature did not rise uncontrollably. To this was added *p*-toluene sulphonyl chloride (0.29 g, 1.5 mmol) and triethylamine (2.8 mL, 2.0 mmol). Upon the final addition of Et<sub>3</sub>N, the reaction mixture was removed from the ice and allowed to stir at room temperature for 2 h. The solution was acidified to pH 7 with c. HCl<sub>(aq)</sub>, transferred to a separating funnel and extracted with water and ethyl acetate (3 x 10 mL), organics were collected and dried over anhydrous Na<sub>2</sub>SO<sub>4</sub> and concentrated under reduced pressure to afford the pure product as a yellow solid. The solid was dried in vacuo to yield the 10-(3-tosylphenyl) isoalloxazine (**18c**) 0.10 g, 22% as a yellow powder. <sup>1</sup>H-NMR (d<sub>6</sub>-DMSO, 300 MHz) δppm; 11.47 (s, Ar-NH, 1H), 8.21 – 8.13 (m, Ar-H, 1H), 7.86 – 7.57 (m, Ar-H, 5H), 7.46 - 7.40 (m, Ar-H, 4H), 7.11 (d, *J* = 2.0 Hz, Ar-H, 1H), 6.51 (d, *J* = 8.4 Hz, Ar-H, 1H), 2.33 (s, Ar-CH<sub>3</sub>, 3H). <sup>13</sup>C NMR (d<sub>6</sub>-DMSO 75 MHz,) δppm; 159.86, 155.87, 155.69, 152.13, 150.34, 146.43, 137.33, 135.44, 135.24, 135.06, 134.05, 132.37, 131.88, 131.00, 130.85, 128.92, 127.71, 126.49, 122.47, 116.83, 21.63. FTIR (ATR): ν 2923, 1661, 1585, 1539, 1482, 1360, 1269, 1178, 1082, 967, 861, 808, 764, 740, 664, 606, 564, 547, 513, 459, 436. HRMS (ESI) *m/z* calcd for [C<sub>23</sub>H<sub>16</sub>N<sub>4</sub>O<sub>5</sub>S]<sup>+</sup> 461.462, found 461.0913 [M-H]<sup>-</sup>. Mp 248-250 °C. Log P: 3.66.

## 6.29 Synthesis of 10-(4-tosyloxyphenyl) isoalloxazine (**19c**)



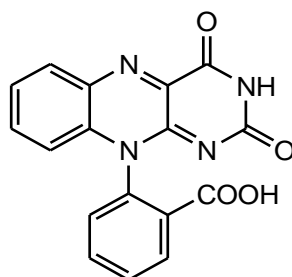
Compound **6c** was dissolved (0.30 g, 1.0 mmol) in DCM (10 mL) and with continuous stirring the mixture was cooled to 0° C using an ice bath ensuring the temperature did not rise uncontrollably. To this was added *p*-toluene sulphonyl chloride (0.29 g, 1.5 mmol) and triethylamine (0.15 mL, 2.0 mmol). Upon the final addition of Et<sub>3</sub>N, the reaction mixture was removed from the ice and allowed to stir at room temperature for 2 h. The solution was acidified to pH 7 with c. HCl<sub>(aq)</sub>, transferred to a separating funnel and extracted with water and ethyl acetate (3 x 15 mL), organics were collected and dried over anhydrous Na<sub>2</sub>SO<sub>4</sub> and concentrated under reduced pressure to afford the pure product as a yellow solid. The solid was dried in vacuo to yield the 10-(4-tosyloxyphenyl) isoalloxazine (**19c**), 0.13 g, 13% as a yellow powder. Mp 245-247 °C. <sup>1</sup>H-NMR (d<sub>6</sub>-DMSO, 300 MHz) δppm; 11.46 (s, Ar-NH, 1H), 8.19 (d, *J* = 8.0 Hz, Ar-H, 1H), 7.86 (d, *J* = 8.1 Hz, Ar-H, 2H), 7.78 (t, *J* = 8.0 Hz, Ar-H, 1H), 7.63 (t, *J* = 7.6 Hz, Ar-H, 1H), 7.58 – 7.32 (m, Ar-H, 7H), 2.44 (s, Ar-CH<sub>3</sub>, 3H). <sup>13</sup>C-NMR (d<sub>6</sub>-DMSO 75 MHz,) δppm; 159.91, 155.88, 152.19, 149.99, 146.59, 139.90, 139.01, 135.35, 135.21, 135.14, 134.30, 131.66, 130.85, 130.34, 128.84, 126.56, 124.60, 116.94, 21.70. FTIR (ATR): ν 2969, 1737, 1687, 1610, 1581, 1542, 1495, 1458, 1357, 1315, 1266, 1216, 1175, 1151, 1110, 1089, 1020, 966, 930, 857, 805, 769, 743, 725, 698, 669. HRMS (ESI) *m/z* calcd for [C<sub>23</sub>H<sub>16</sub>N<sub>4</sub>O<sub>5</sub>S]<sup>+</sup>460.462, found 461.0912 [M+H]<sup>+</sup>. Log P: 3.48.

### 6.30 Synthesis of 2-(2-nitrophenyl) 2-carboxy aniline (**20a**)



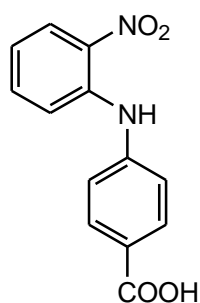
A mixture of potassium carbonate (4.14 g, 30.0 mmol), copper powder (0.20 g, 3.1mmol), 4-aminobenzoic acid (5.00 g, 36.5 mmol), and 1-bromo-2-nitrobenzene (6.44 g, 31.9 mmol) in 1-butanol was set to reflux for 12 h with stirring at 140 °C. The mixture was allowed to cool to room temperature resulting in an orange precipitate. The precipitate was crushed with diethyl ether (50 mL) collected by suction filtration. The orange solid was transferred into a conical flask and distilled water (100 mL) was added. The aqueous solution was adjusted to pH 9 using c.  $\text{NH}_4\text{OH}_{(\text{aq})}$  and heated to boil, and was cooled to room temperature and filtered through celite. The solution was adjusted to pH 5, using c.  $\text{HCl}_{(\text{aq})}$  forming a bright orange solid. The solid was filtered from the mixture and dried under *vacuo* to yield the substituted 2-carboxy-(2-nitrophenyl) aniline, (**20a**) as an orange powder, 5.68 g, 71%.  $^1\text{H-NMR}$  (DMSO, 300 MHz)  $\delta$ ppm; 12.70 (s, Ar-COOH, 1H), 9.33 (s, Ar-NH, 1H), 8.12 (d,  $J = 8.4$  Hz, Ar-H, 1H), 7.91 (d,  $J = 8.4$  Hz, Ar-H, 2H), 7.62 (t,  $J = 7.6$  Hz, Ar-H, 1H), 7.51 (d,  $J = 8.4$  Hz, Ar-H, 1H), 7.32 (d,  $J = 8.4$  Hz, Ar-H, 2H), 7.09 (t,  $J = 7.6$  Hz, Ar-H, 1H).  $^{13}\text{C-NMR}$  (DMSO, 75MHz);  $\delta$ ppm; 167.39, 145.49, 139.07, 137.44, 136.04, 131.43, 126.72, 124.93, 121.20, 120.31, 119.75. HRMS (ESI)  $m/z$  calcd for  $[\text{C}_{13}\text{H}_{10}\text{N}_2\text{O}_4]^+$  258.2229, found 259.0641  $[\text{M}+\text{H}]^+$ . Log P: 3.88.

### 6.31 Synthesis of 10-(2-carboxyphenyl) isoalloxazine (20c)



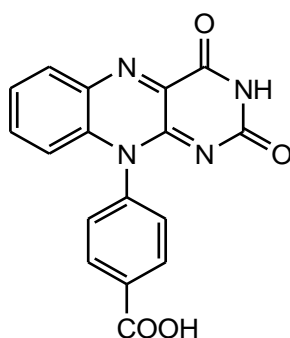
Compound **20a** (3.00 g, 11.6 mmol) was dissolved in glacial acetic acid (20 mL) and the mixture was cooled in an ice bath. Zinc dust (7.55 g, 116 mmol) was gradually added and the solution was allowed to stir at room temperature for 2 h and filtered through celite. The filter cake was washed with glacial acetic acid (250 mL) to yield the substituted *N*-(carboxyphenyl amino) aniline, (**20b**) as a dark brown solution. To the solution of substituted *N*-(carboxyphenyl amino) aniline, was added alloxan monohydrate (1.85 g, 11.6 mmol) and boric acid (0.70 g, 11.4 mmol). The solution was stirred at room temperature for 12 h, resulting in a dark yellow solution. The yellow solid was filtered from the mixture and washed well with hexane (30 mL) to afford the pure product as a yellow solid. The yellow solid was dried in *vacuo* to yield the isoalloxazine (**20c**), 1.53 g, 40%, as a yellow powder. <sup>1</sup>H-NMR (d<sub>6</sub>-DMSO, 300 MHz) δppm; 13.07 (s, Ar-COOH, 1H), 11.53 (s, Ar-NH, 1H), 8.25 (ddd, *J* = 15.6, 8.0, 1.5 Hz, Ar-H, 2H), 7.96 (t, *J* = 7.3 Hz, Ar-H, 1H), 7.87 – 7.71 (m, Ar-H, 2H), 7.63 (t, *J* = 7.3 Hz, Ar-H, 1H), 7.53 (d, *J* = 7.7 Hz, Ar-H, 1H), 6.74 (d, *J* = 8.5 Hz, Ar-H, 1H). <sup>13</sup>C-NMR (d<sub>6</sub>-DMSO, 75.4 MHz) δppm; 182.90, 159.81, 155.81, 151.94, 143.41, 139.16, 135.20, 136.12, 135.75, 135.25, 134.45, 132.92, 131.90, 131.03, 129.88, 126.66, 117.04. FTIR (ATR):  $\nu$  3073, 1746, 1706, 1638, 1613, 1583, 1539, 1501, 1459, 1404, 1329, 1276, 1249, 1197, 1175, 1114, 1032, 930, 883, 841, 809, 765, 755, 727, 706  $\text{cm}^{-1}$ . HRMS (ESI) *m/z* calcd for [C<sub>17</sub>H<sub>10</sub>N<sub>4</sub>O<sub>4</sub>]<sup>+</sup> 334.285, found 335.0702 [M+H]<sup>+</sup>. Mp 264–266°C. Log P: 2.33.

### 6.32 Synthesis of 2-(2-nitrophenyl) 4-carboxy aniline (**22a**)



A mixture of potassium carbonate (4.14 g, 30.0 mmol), copper powder (0.20 g, 3.1mmol), 4-aminobenzoic acid (5.00 g, 36.5 mmol) and 1-bromo-2-nitrobenzene (6.44 g, 31.9 mmol) in 1-butanol was set to reflux for 12 h with stirring at 140 °C. The mixture was allowed to cool to room temperature resulting in an orange precipitate. The precipitate was crushed with diethyl ether (50 mL) collected by suction filtration. The orange solid was transferred into a conical flask and distilled water (100 mL) was added. The aqueous solution was adjusted to pH 9 using c.  $\text{NH}_4\text{OH}_{(\text{aq})}$  and heated to boil, and was cooled to room temperature and filtered through celite. The solution was adjusted to pH 5, using c.  $\text{HCl}_{(\text{aq})}$  forming a bright orange solid. The solid was filtered from the mixture and dried under *vacuo* to yield the substituted 4-carboxy-(2-nitrophenyl) aniline, (**22a**) as an orange powder, 6.21 g, 77%.  $^1\text{H-NMR}$  (DMSO, 300 MHz)  $\delta$ ppm; 12.70 (s, Ar-COOH, 1H), 9.33 (s, Ar-NH, 1H), 8.12 (d,  $J = 8.4$  Hz, Ar-H, 1H), 7.91 (d,  $J = 8.4$  Hz, Ar-H, 2H), 7.62 (t,  $J = 7.6$  Hz, Ar-H, 1H), 7.51 (d,  $J = 8.4$  Hz, Ar-H, 1H), 7.32 (d,  $J = 8.4$  Hz, Ar-H, 2H), 7.09 (t,  $J = 7.6$  Hz, Ar-H, 1H).  $^{13}\text{C NMR}$  (DMSO, 75MHz);  $\delta$  167.39, 145.49, 139.07, 137.44, 136.04, 131.43, 126.72, 124.93, 121.20, 120.31, 119.75. HRMS (ESI)  $m/z$  calcd for  $[\text{C}_{13}\text{H}_{10}\text{N}_2\text{O}_4]^+$  258.2229, found 259.0641  $[\text{M}+\text{H}]^+$ . Log P: 3.75.

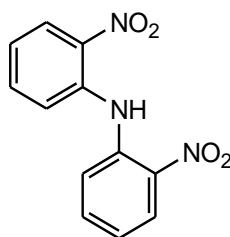
### 6.33 Synthesis of 10-(4-carboxyphenyl) isoalloxazine (**22c**)



Compound **22a** (3.00 g, 11.6 mmol) was dissolved in glacial acetic acid (20 mL) and the mixture was cooled in an ice bath. Zinc dust (7.55 g, 116 mmol) was gradually added and the solution was allowed to stir at room temperature for 2 h and filtered through celite. The filter cake was washed with glacial acetic acid (250 mL) to yield the substituted *N*-(carboxyphenyl amino)

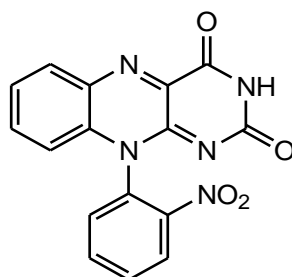
aniline, (**22b**) as a dark brown solution. To the solution of substituted *N*-(carboxyphenyl amino) aniline, was added alloxan monohydrate (1.85 g, 11.6 mmol) and boric acid (0.70 g, 11.4 mmol). The solution was stirred at room temperature for 12 h, resulting in a dark yellow solution. The yellow solid was filtered from the mixture and washed well with hexane (30 mL) to afford the pure product as a yellow solid. The yellow solid was dried *in vacuo* to yield the isoalloxazine **22c**, 2.57 g, 66%, as a yellow powder. <sup>1</sup>H-NMR (d<sub>6</sub>-DMSO, 300 MHz) δppm; 11.48 (s, Ar-NH, 1H), 8.27 – 8.19 (m, Ar-H, 3H), 7.83 – 7.45 (m, Ar-H, 4H), 6.79 (d, *J* = 8.6 Hz, Ar-H, 1H). <sup>13</sup>C NMR (d<sub>6</sub>-DMSO, 75.4 MHz) δppm; 167.36, 145.49, 139.02, 137.45, 136.04, 131.41, 126.71, 124.89, 121.24, 120.37, 119.68. FTIR (ATR): ν 3073, 1746, 1706, 1638, 1613, 1583, 1539, 1501, 1459, 1404, 1329, 1276, 1249, 1197, 1175, 1114, 1032, 930, 883, 841, 809, 765, 755, 727, 706 CM<sup>-1</sup>. HRMS (ESI) *m/z* calcd for [C<sub>17</sub>H<sub>10</sub>N<sub>4</sub>O<sub>4</sub>]<sup>+</sup> 334.285, found 335.0702 [M+H]<sup>+</sup>. Mp 264–266°C. Log P: 1.973.

### 6.34 Synthesis of 2-(2-nitrophenyl) benzene 1, 2-diamine (**23a**)



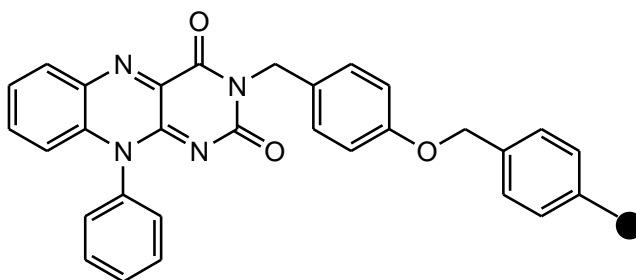
A mixture of potassium carbonate (20.7 g, 150.0 mmol), 2-phenylenediamine (14.0 g, 130.0 mmol), and 1-fluoro-2-nitrobenzene (18.3 g, 130.0 mmol) was irradiated for 3 h at 150 °C in a CEM microwave at full power. The mixture was allowed to cool to room temperature, and with stirring poured reduced pressure to yield the substituted 2-(2-nitrophenyl) benzene 1,2-diamine, (**23a**) as onto ice water (300 mL). The reaction mixture was adjusted to pH 6 using c. HCl<sub>(aq)</sub>, added to a separating funnel and extracted with CHCl<sub>3</sub> (5 x 50 mL). The organic layer was isolated, dried with anhydrous sodium sulphate, and evaporated under a black solid. The crude solid was purified by flash column chromatography over silica gel eluting with CHCl<sub>3</sub>: PE (1:1) to afford the pure product as a red solid. The solid was dried *in vacuo* to yield reaction number, 17.94 g, 46% as dark red crystals. <sup>1</sup>H-NMR (CDCl<sub>3</sub>, 300 MHz) δppm; 9.11 (s, Ar-NH, 1H), 8.23 (d, *J* = 7.7 Hz, Ar-H, 1H), 7.37 (t, *J* = 7.7 Hz, Ar-H, 1H), 7.26 – 7.09 (m, Ar-H, 2H), 6.94 – 6.69 (m, Ar-H, 4H). <sup>13</sup>C NMR (CDCl<sub>3</sub>, 75 MHz) δppm; 144.12, 142.96, 136.07, 132.77, 128.50, 128.39, 126.54, 123.87, 119.41, 117.17, 116.52, 116.14. HRMS (ESI) *m/z* calcd for [C<sub>12</sub>H<sub>9</sub>N<sub>3</sub>O<sub>4</sub>]<sup>+</sup> 259.217, found 260.059 [M+H]<sup>+</sup>. Log P: 3.27.

### 6.35 Synthesis of 10-(2-nitrophenyl) isoalloxazine (**23c**)



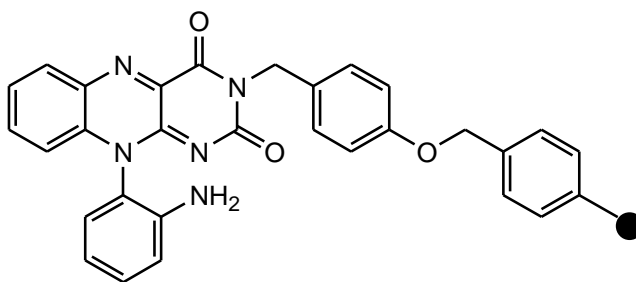
Compound **23a** (1.00 g, 4.4 mmol) was dissolved in glacial acetic acid (10 mL) and the mixture was cooled in an ice bath. to alloxan monohydrate (0.70 g, 4.4 mmol) and boric acid (0.25 g, 4.2 mmol), in acetic acid and the solution was stirred at room temperature for 12 h, resulting in the formation of a yellow precipitate. The precipitate was isolated from the reaction mixture by filtration under reduced pressure and washed well with hexane (30 mL). The yellow solid was by column chromatography over silica gel eluting with EtOAc to afford a bright yellow solid. The yellow solid was dried *in vacuo* to yield the 10-(2-nitrophenyl) isoalloxazine (**23c**), 2.59 g, 25%, as a yellow powder, dec.mp 242-244°C. <sup>1</sup>H-NMR (d<sub>6</sub>-DMSO, 300MHz) δppm; 11.55 (s, Ar-NH, 1H), 8.50 (d, *J* = 8.1 Hz, Ar-H, 1H), 8.25 (d, *J* = 8.1 Hz, Ar-H, 1H), 8.14 (t, *J* = 7.6 Hz, Ar-H, 1H), 8.00 (t, *J* = 7.6 Hz, Ar-H, 1H), 7.84 – 7.63 (m, Ar-H, 3H), 6.94 (d, *J* = 8.2 Hz, Ar-H, 1H). <sup>13</sup>C NMR (d<sub>6</sub>-DMSO, 75 MHz) δppm; 159.20, 155.21, 151.10, 145.08, 136.67, 135.37, 134.67, 133.04, 132.16, 131.65, 130.79, 129.52, 128.96, 126.67, 126.62, 116.67. FTIR (ATR): ν 3067, 1708, 1681, 1616, 1584, 1532, 1487, 1459, 1396, 1341, 1264, 1196, 1134, 1106, 932, 879, 835, 807, 787, 775, 764, 715, 695, 673 CM<sup>-1</sup>. HRMS (ESI) *m/z* calcd for [C<sub>16</sub>H<sub>9</sub>N<sub>5</sub>O<sub>4</sub>]<sup>+</sup> 335.2738, found 336.0728 [M+H]<sup>+</sup>. Log P: 2.71.

6.36 Synthesis of 10-phenyl isoalloxazine polymer bound (**13d**)



Compound (**13c**), (0.60 g, 1.9 mmol) was dissolved in anhydrous DMF (3 mL). To this was added  $K_2CO_3$  (0.28 g, 2.1 mmol), and 4-(benzyloxy)benzyl bromide (0.10 g). The reaction mixture was refluxed at 150 °C overnight to afford the polymer bound product. The reaction mixture was cooled to room temperature and filtered under suction. The polymer beads were washed well with the following solvents; cold DMF, distilled water, ethyl acetate, methanol, acetone and finally distilled water until the washings ran clear. The yellow solid was dried *in vacuo* to yield the 10-phenyl isoalloxazine polymer bound (**13d**), 0.23 g as yellow polymeric beads. FTIR (ATR):  $\nu$  3023, 2970, 2183, 2155, 2007, 1737, 1542, 1509, 1491, 1451, 1366, 1228, 1216, 1027, 895, 807, 756, 695  $CM^{-1}$ .

6.37 Synthesis of 10-(2-aminophenyl) isoalloxazine polymer bound (**1d**)

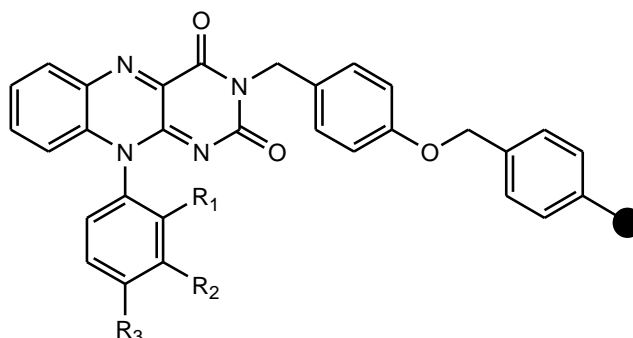


Compound (**1c**), (0.60 g, 1.9 mmol) was dissolved in anhydrous DMF (3 mL). To this was added  $K_2CO_3$  (0.28 g, 2.1 mmol), and 4-(benzyloxy)benzyl bromide (0.10 g). The reaction mixture was refluxed at 150 °C overnight to afford the polymer bound product. The reaction mixture was cooled to room temperature and filtered under suction. The polymer beads were washed well with the following solvents; cold DMF, distilled water, ethyl acetate, methanol, acetone and finally distilled water until the washings ran clear. The yellow solid was dried *in vacuo* to yield the 10-(*o*-amino phenyl) isoalloxazine polymer bound (**1d**), 0.21 g as yellow polymeric beads. FTIR



(ATR):  $\nu$  3381, 3142, 3025, 2926, 2331, 2222, 2178, 2148, 2063, 2051, 2015, 1985, 1948, 1491, 1451, 1379, 1221, 1172, 1025, 830, 753, 695, 471, 437  $\text{CM}^{-1}$ .

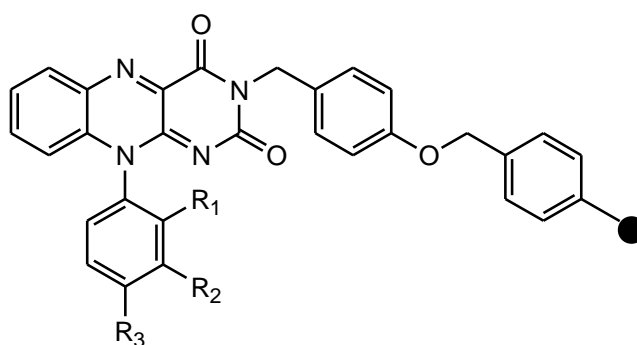
### 6.38 Synthesis of 10-(*N*-hydroxyphenyl) isoalloxazines polymer bound (**4d-6d**)



Compound code	R <sub>1</sub>	R <sub>2</sub>	R <sub>3</sub>	Starting material (g)	Yield (g)	
<b>4d</b>	OH	H	H	<b>4c</b>	0.15	0.06
<b>6d</b>	H	H	OH	<b>6c</b>	0.17	0.05

The starting material was dissolved in anhydrous DMF (3 mL). To this was added  $\text{K}_2\text{CO}_3$  (0.28 g, 2.1 mmol), and 4-(benzyloxy)benzyl bromide (0.10 g). The reaction mixture was refluxed at 150 °C overnight to afford the polymer bound product. The reaction mixture was cooled to room temperature and filtered under suction. The polymer beads were washed well with the following solvents; cold DMF, distilled water, ethyl acetate, methanol, acetone and finally distilled water until the washings ran clear. The yellow solid was dried *in vacuo* to yield the 10-(*N*-hydroxy phenyl) isoalloxazine polymer bound, as yellow polymeric beads. Compound **4d**: FTIR (ATR):  $\nu$  3025, 2922, 2039, 1975, 1673, 1601, 1554, 1511, 1492, 1451, 1385, 1223, 1175, 1090, 1027, 906, 822, 755, 697  $\text{CM}^{-1}$ . Compound **6d**: FTIR (ATR):  $\nu$  3024, 2925, 2365, 2255, 2206, 2160, 2137, 2060, 2010, 1980, 1738, 1600, 1555, 1511, 1492, 1451, 1221, 1174, 1026, 908, 818, 755, 696  $\text{CM}^{-1}$ .

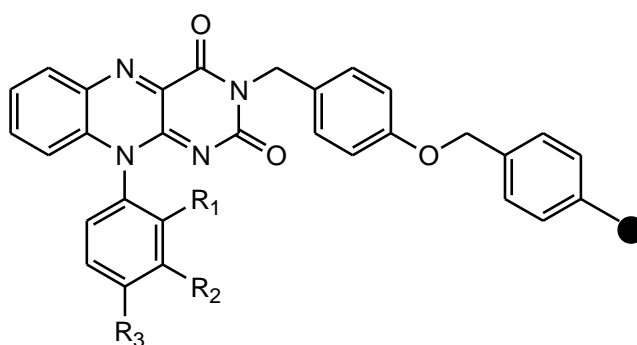
### 6.39 Synthesis of 10-(*N*-methoxyphenyl) isoalloxazines polymer bound (**7d-9d**)



Compound code	R <sub>1</sub>	R <sub>2</sub>	R <sub>3</sub>	Starting material (g)	Yield (g)	
<b>7d</b>	OCH <sub>3</sub>	H	H	<b>7c</b>	0.22	0.14
<b>8d</b>	H	OCH <sub>3</sub>	H	<b>8C</b>	0.20	0.10
<b>9d</b>	H	H	OCH <sub>3</sub>	<b>9c</b>	0.21	0.16

The starting material was dissolved in anhydrous DMF (3 mL). To this was added K<sub>2</sub>CO<sub>3</sub> (0.28 g, 2.1 mmol), and 4-(benzyloxy)benzyl bromide (0.10 g). The reaction mixture was refluxed at 150 °C overnight to afford the polymer bound product. The reaction mixture was cooled to room temperature and filtered under suction. The polymer beads were washed well with the following solvents; cold DMF, distilled water, ethyl acetate, methanol, acetone and finally distilled water until the washings ran clear. The yellow solid was dried *in vacuo* to yield the 10-(*N*-methoxy phenyl) isoalloxazine polymer bound, as yellow polymeric beads. Compound **7d**: FTIR (ATR):  $\nu$  3025, 2924, 2359, 2222, 2197, 2105, 2006, 1971, 1945, 1736, 1671, 1601, 1511, 1492, 1451, 1385, 1225, 1174, 1089, 1026, 908, 823, 758, 698, 658 CM<sup>-1</sup>. Compound **8d**: FTIR (ATR):  $\nu$  3418, 3024, 2926, 2360, 2192, 2167, 2151, 2135, 2033, 1986, 1738, 1666, 1492, 1451, 1386, 1253, 1175, 1093, 1026, 823, 757, 698, 659, 538 CM<sup>-1</sup>. Compound **9d**: FTIR (ATR):  $\nu$  3449, 3024, 2969, 2928, 2361, 2195, 2162, 2152, 2092, 1990, 1973, 1738, 1668, 1600, 1492, 1450, 1366, 1228, 1216, 1092, 1025, 905, 822, 755, 696, 539 CM<sup>-1</sup>.

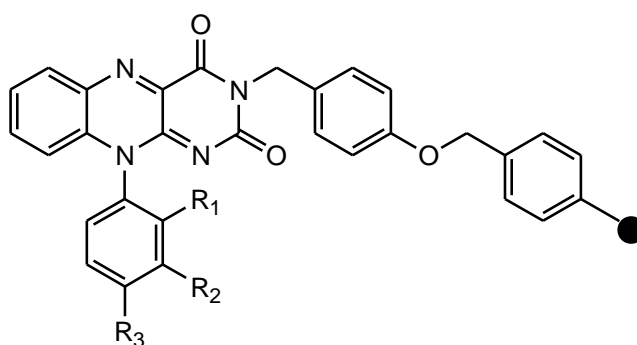
## 6.40 Synthesis of 10-(*N*-tolylphenyl) isoalloxazines polymer bound (**10d-12d**)



Compound code	R <sub>1</sub>	R <sub>2</sub>	R <sub>3</sub>	Starting material (g)	Yield (g)
<b>10d</b>	CH <sub>3</sub>	H	H	<b>10c</b>	0.22
<b>11d</b>	H	CH <sub>3</sub>	H	<b>11c</b>	0.20
<b>12d</b>	H	H	CH <sub>3</sub>	<b>12c</b>	0.21

The starting material was dissolved in anhydrous DMF (3 mL). To this was added K<sub>2</sub>CO<sub>3</sub> (0.28 g, 2.1 mmol), and 4-(benzyloxy)benzyl bromide (0.10 g). The reaction mixture was refluxed at 150 °C overnight to afford the polymer bound product. The reaction mixture was cooled to room temperature and filtered under suction. The polymer beads were washed well with the following solvents; cold DMF, distilled water, ethyl acetate, methanol, acetone and finally distilled water until the washings ran clear. The yellow solid was dried *in vacuo* to yield the 10-(*N*-tolyl phenyl) isoalloxazine polymer bound, as yellow polymeric beads. Compound **10d**: FTIR (ATR):  $\nu$  3025, 2917, 2358, 1669, 1584, 1555, 1509, 1492, 1451, 1220, 1173, 1111, 1028, 904, 820, 754, 697 CM<sup>-1</sup>. Compound **11d**: FTIR (ATR):  $\nu$  3029, 2969, 2937, 2359, 2060, 1738, 1491, 1450, 1365, 1228, 1216, 1018, 907, 816, 756, 697 CM<sup>-1</sup>. Compound **12d**: FTIR (ATR):  $\nu$  3026, 2955, 2918, 2847, 2435, 1682, 1625, 1535, 1460, 1242, 1220, 1183, 1032, 780, 727, 666 cm<sup>-1</sup>.

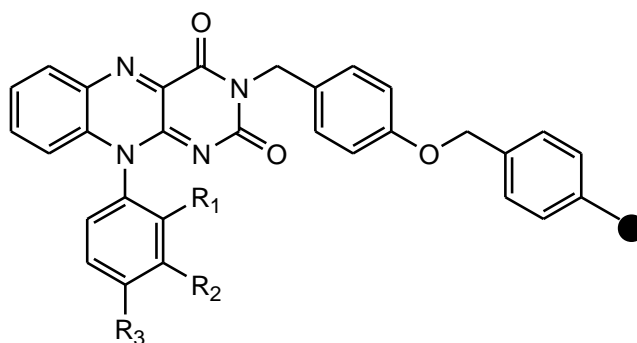
## 6.41 Synthesis of 10-(*N*-chlorophenyl) isoalloxazines polymer bound (**14d-16d**)



Compound code	R <sub>1</sub>	R <sub>2</sub>	R <sub>3</sub>	Starting material (g)	Yield (g)	
<b>14d</b>	CH <sub>3</sub>	H	H	<b>14c</b>	0.23	0.06
<b>15d</b>	H	CH <sub>3</sub>	H	<b>15c</b>	0.10	0.03
<b>16d</b>	H	H	CH <sub>3</sub>	<b>16c</b>	0.16	0.03

The starting material was dissolved in anhydrous DMF (3 mL). To this was added K<sub>2</sub>CO<sub>3</sub> (0.28 g, 2.1 mmol), and 4-(benzyloxy)benzyl bromide (0.10 g). The reaction mixture was refluxed at 150 °C overnight to afford the polymer bound product. The reaction mixture was cooled to room temperature and filtered under suction. The polymer beads were washed well with the following solvents; cold DMF, distilled water, ethyl acetate, methanol, acetone and finally distilled water until the washings ran clear. The yellow solid was dried *in vacuo* to yield the 10-(*N*-chloro phenyl) isoalloxazine polymer bound, as yellow polymeric beads. Compound **14d**: FTIR (ATR):  $\nu$  3025, 2920, 2358, 2251, 2149, 2052, 2030, 1990, 1979, 1957, 1927, 1678, 1601, 1510, 1492, 1451, 1382, 1224, 1155, 1088, 1027, 907, 822, 756, 697, 619, 539 CM<sup>-1</sup>. Compound **15d**: FTIR (ATR):  $\nu$  3024, 2917, 2361, 2190, 2149, 2032, 2017, 1957, 1927, 1750, 1601, 1510, 1492, 1450, 1376, 1223, 1173, 1026, 904, 821, 755, 540 CM<sup>-1</sup>. Compound **16d**: FTIR (ATR):  $\nu$  3024, 2924, 2361, 2350, 2230, 2165, 2140, 2032, 2015, 1735, 1601, 1510, 1492, 1450, 1375, 1222, 1173, 1025, 904, 822, 753, 697, 531 CM<sup>-1</sup>.

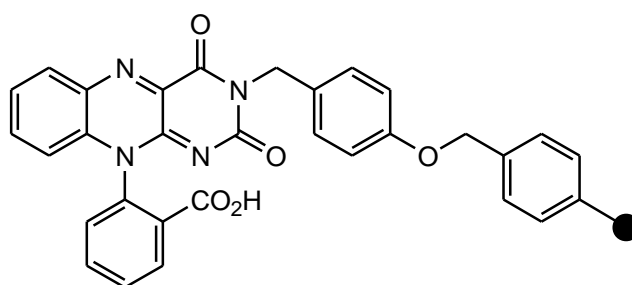
## 6.42 Synthesis of 10-(*N*-tosyloxyphenyl) isoalloxazines polymer bound (**17d**-**19d**)



Compound code	R <sub>1</sub>	R <sub>2</sub>	R <sub>3</sub>	Starting material (g)	Yield (g)
<b>17d</b>	OTs	H	H	<b>17c</b>	0.23
<b>18d</b>	H	OTs	H	<b>18c</b>	0.23
<b>19d</b>	H	H	OTs	<b>19c</b>	0.05

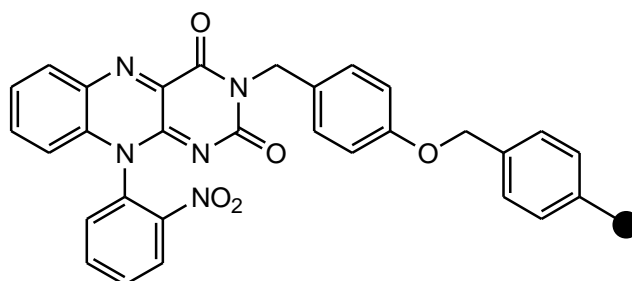
The starting material was dissolved in anhydrous DMF (3 mL). To this was added K<sub>2</sub>CO<sub>3</sub> (0.28 g, 2.1 mmol), and 4-(benzyloxy)benzyl bromide (0.10 g). The reaction mixture was refluxed at 150 °C overnight to afford the polymer bound product. The reaction mixture was cooled to room temperature and filtered under suction. The polymer beads were washed well with the following solvents; cold DMF, distilled water, ethyl acetate, methanol, acetone and finally distilled water until the washings ran clear. The yellow solid was dried *in vacuo* to yield the 10-(*N*-tosyloxy phenyl) isoalloxazine polymer bound, as yellow polymeric beads. Compound **17d**: FTIR (ATR):  $\nu$  2263, 2219, 2196, 2182, 2144, 2132, 2076, 2056, 2038, 2027, 2017, 2006, 986, 1972, 1953, 1151, 697 CM<sup>-1</sup>. Compound **18d**: FTIR (ATR):  $\nu$  3673, 2986, 2900, 2160, 2114, 2029, 1451, 1406, 1393, 1381, 1250, 1229, 1065, 1055, 892, 754, 695 CM<sup>-1</sup>. Compound **19d**: FTIR (ATR):  $\nu$  3733, 3647, 3472, 3026, 2924, 2185, 2162, 2044, 2030, 1668, 1558, 1493, 1451, 1383, 1256, 1173, 1153, 1091, 1016, 867, 758, 697 CM<sup>-1</sup>.

### 6.43 Synthesis of 10-(2-carboxyphenyl) isoalloxazine polymer bound (**20d**)



Compound (**20c**), (0.60 g, 1.9 mmol) was dissolved in anhydrous DMF (3 mL). To this was added  $K_2CO_3$  (0.28 g, 2.1 mmol), and 4-(benzyloxy)benzyl bromide (0.10 g). The reaction mixture was refluxed at 150 °C overnight to afford the polymer bound product. The reaction mixture was cooled to room temperature and filtered under suction. The polymer beads were washed well with the following solvents; cold DMF, distilled water, ethyl acetate, methanol, acetone and finally distilled water until the washings ran clear. The yellow solid was dried *in vacuo* to yield the 10-(*o*-carboxyphenyl) isoalloxazine polymer bound (**20d**), 0.06 g as yellow polymeric beads. FTIR (ATR):  $\nu$  3191, 3095, 2923, 2490, 2319, 2039, 1972, 1697, 1601, 1539, 1511, 1493, 1450, 1380, 1275, 1191, 1090, 1027, 906, 882, 755, 697, 541  $CM^{-1}$ .

### 6.44 Synthesis of 10-(2-nitrophenyl) isoalloxazine polymer bound (**23d**)



Compound (**23c**), (0.60 g, 1.9 mmol) was dissolved in anhydrous DMF (3 mL). To this was added  $K_2CO_3$  (0.28 g, 2.1 mmol), and 4-(benzyloxy)benzyl bromide (0.10 g). The reaction mixture was refluxed at 150 °C overnight to afford the polymer bound product. The reaction mixture was cooled to room temperature and filtered under suction. The polymer beads were washed well with the following solvents; cold DMF, distilled water, ethyl acetate, methanol, acetone and finally distilled water until the washings ran clear. The yellow solid was dried *in vacuo* to yield the 10-(*o*-nitro phenyl) isoalloxazine polymer bound (**23d**), 0.02 g as yellow polymeric beads. FTIR (ATR):  $\nu$  3667, 2987, 2901, 2360, 2339, 2174, 1710, 1682, 1600, 1584, 1536, 1511, 1491, 1451, 1393, 1342, 1225, 1066, 879, 753, 695, 543, 430.  $CM^{-1}$ .

#### 6.45 Antimicrobial testing using white light

#### 6.46 Criterion for cell preparation

Washing bacterial cells promotes dispersion of the bacteria and the removal of proteinaceous nutrients from the growth medium. This ensures maximum contact between the antimicrobial agent and bacteria is achieved and reduces the possibility of early bacterial adhesion. Biofilms are made up of cells which are embedded in Exo-Polymeric Substances (EPS). EPS behaves as a bacterial adhesive which also serves as a protective barrier for the embedded micro-organisms. This is considered to be a phenomenal survival mechanism for bacteria.

In order to carry out antimicrobial testing on gram negative and gram positive bacteria, a suitable method of preparing washed cells was developed at UCLan<sup>365</sup>.

The washing of cells with ¼ strength Ringer's solution ensures that the potential production of EPS is considerably reduced as the cells are thoroughly washed and cleared of any further nutrients, proteins, or other residual food material which aids EPS production. The formation of cell suspensions in ringer's solution is prepared to allow the suspension to be free from interfering proteins/nutrients. This is because numerous cations can bind to protein, consequently interfere with the biocide (e.g. antimicrobial agent) and thus not produce accurate results of the antimicrobial activities occurring.

As a result of preparing washed cells, the antimicrobial agents are more accessible to the bacteria in question<sup>366</sup>. Furthermore this enhances the cells to be exposed to the treatments to be applied (for example light and antimicrobial agents) to determine the antimicrobial activity under various conditions. Although this washing of cells method would not be possible to do on wounds, it is important to note this technique is utilised in order to test the principle on infected cells when there is an increased exposure to them.

### 6.47 Biological screening

### 6.48 Preparation of a washed cell suspensions in antimicrobial testing

Cultures of Gram negative (*E.coli*) and Gram positive (*S. aureus*) bacteria were used in this series of experiments. They were grown on plates of nutrient agar at 37 °C for 24 h. The bacteria were individually inoculated into universal bottles containing 10mL nutrient broth and incubated overnight at 37 °C.

The overnight cultures of cells were centrifuged at 6000 rpm for 10 minutes. The growth medium was decanted, leaving a pellet of cells. The pellets were re-suspended and washed in 10mL of ¼ strength ringer's solution These cells were washed and centrifuged an additional three times, and finally suspended in Ringer's to give a final cell suspension. The optical density of this cell suspension for *E.coli* and *S.aureus* respectively was measured at a wavelength of 595 nm.

### 6.49 MIC estimation

The initial 1 mM solution was made up in an eppendorf tube containing a mixture of 800µL ¼ strength Ringer's solution and 200 µL of methanol. To this solubilised solution the washed bacterial suspension cells (*E.coli* and *S.aureus*) were added.

A series of decreasing concentrations of the compounds to be tested were prepared in eppendorf tubes by the double dilution method from a concentration of 1 mM down to 0.063 mM. This method used ¼ strength Ringer's solution as the diluent, to give 1mL volumes of each concentration of the test compound in the eppendorf tubes.

Each of the eppendorf tubes containing 500 µL of decreasing concentrations in Ringer's solution as the diluent, 200 µL of the bacterial cell suspension (*E.coli* and *S.aureus*) was inoculated into each of the tubes. The contents of the tubes were mixed thoroughly and incubated for overnight at 37 °C. Controls were prepared by adding the bacterial suspension (*E.coli* and *S.aureus*) to Ringer's solution and methanol in an eppendorf tube. These were also incubated overnight at 37 °C. The cell suspensions were subsequently streaked out onto nutrient agar plates and incubated at 37 °C for upto 12 h.

### Results

The minimum inhibitory concentration (MIC) is that at which growth of the test organism is not detected. Thus, proving antimicrobial activity is/is not present against the tested organism.



## 6.50 Antimicrobial testing using blue LED light-conformational studies

### 6.50.1 Preliminary screening over time of antimicrobial activity after 1 h exposure to blue LED light with no biocide.

Freshly prepared washed bacterial cells of *E.coli* and *S. aureus* were each individually suspended in a mixture of methanol (200  $\mu$ L) and ringers (800  $\mu$ L) in eppendorf tubes. 200  $\mu$ L of each suspension was removed from both *E.coli* and *S. aureus* suspensions and streaked onto a plate of agar (labelled T = 0). This was done to determine whether antimicrobial activity was present immediately after exposure to blue light as shown in Figure 113.

A series of eppendorf tubes labelled T = 0 - T=60, containing the washed cell suspension were prepared and irradiated for twenty minutes using the blue LED light, emitting at 480 nm, at a height of 5 cm.



*Figure 113 Set-up of UV illumination on to bacterial cells and biocide*

Following irradiation, further 100  $\mu$ L aliquots were removed from both bacterial suspensions and spotted onto an agar plate (labelled T = 20). In addition to this, a control of  $\frac{1}{4}$  strength ringer's solution (900  $\mu$ L) was also added to the eppendorf tube and was inoculated on the same agar plate. This procedure was continued every ten minutes for 1h with continuous illumination. This agar plate was incubated at 37° C for up to overnight to determine the antimicrobial activity of blue light without the presence of an antimicrobial agent.

### 6.50.2 Preliminary screening of antimicrobial activity under dark conditions with no biocide

Freshly grown and prepared bacterial suspensions of *E.coli/S.aureus* (200  $\mu$ L) in 900  $\mu$ L ringers. Of this ringers 800  $\mu$ L was pipetted into eppendorf tubes. This suspension was mixed thoroughly, and was the bacterial suspension that was used. Ringer's solution (900  $\mu$ L) each was then pipetted into four separate universal bottles.

A series of serial dilutions from  $10^{-1}$  down  $10^{-5}$  were prepared. A concentration of  $10^{-1}$  of a bacterial suspension is achieved by adding 1 part suspension to 9 parts diluent, this process is repeated i.e. by serial dilution. From each of these suspensions 120  $\mu\text{L}$  was streaked individually onto an agar plate and incubated for 12 hours at  $37^\circ\text{C}$  to determine antimicrobial activity in the dark without the presence of an antimicrobial agent.

### 6.50.3 Antimicrobial activity for the synthesised antimicrobial agents using blue LED lights

Gram negative (*E.coli*) and Gram positive (*S. aureus*) bacterial cultures were grown in nutrient broth solution and incubated overnight at  $37^\circ\text{C}$ . The cell suspension was prepared using the washed cell method.

The desired antimicrobial agent (biocide) to be tested was dissolved in methanol (200  $\mu\text{L}$ ) and ringers (800  $\mu\text{L}$ ) to give a stock solution concentration of 1 mM solution in 1 mL. A series of decreasing concentrations of the compound were prepared by the double dilution method starting at 1 mM to 0.063 mM concentrations. Ringer's solution was used as the diluent to give 1 mL volumes of each concentration in eppendorf tubes. The 1 mM stock solution was double diluted down to 0.063 mM. Bacterial suspension (200  $\mu\text{L}$ ) (*E.coli* and *S.aureus*) was then inoculated into each of the eppendorf tubes. The contents of the tubes were mixed thoroughly and incubated for 12 h at  $37^\circ\text{C}$ . The controls were prepared by adding the bacterial suspension (200  $\mu\text{L}$ ) (*E.coli* and *S.aureus*) with 800  $\mu\text{L}$  ringers solution, and methanol (200  $\mu\text{L}$ ) in an eppendorf tube. These tubes were subsequently illuminated for twenty minutes using blue LED light at a height of 5 cm. During the illumination period, four agar plates were sectioned and labelled with the varying concentrations. Two of these plates were used to inoculate *E. coli* and *S. aureus* respectively Figure 114.

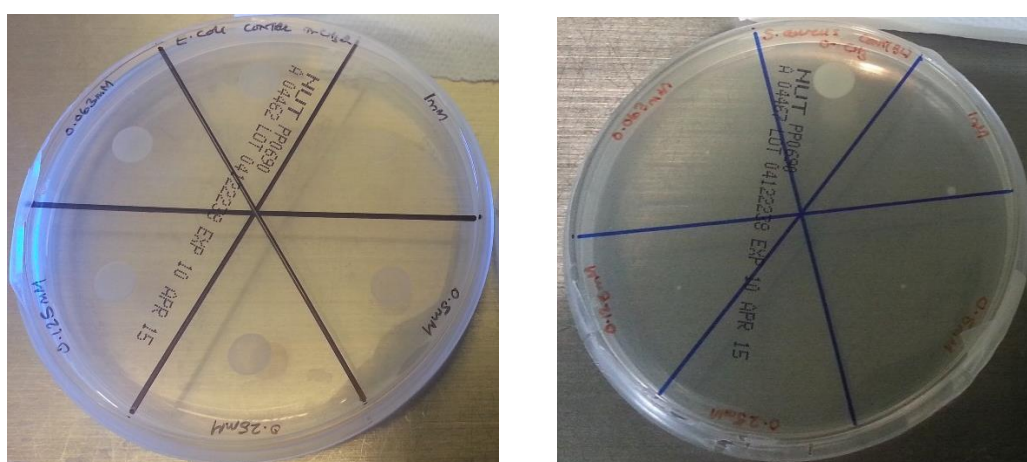


Figure 114: Labelled *E.coli* and *S. aureus* agar plates

After illumination, 120  $\mu\text{L}$  of each concentration of the cell suspensions were then used to inoculate a nutrient agar plate and incubated at  $37^\circ\text{C}$  for upto 12 h to determine the antimicrobial activity in the presence of both blue light and the antimicrobial agent in question.

## 6.51 Antimicrobial activity for polymer bound compounds

### 6.51.1 Antimicrobial activity for the synthesised antimicrobial agents on polymer support using blue LED lights

Fresh cell cultures were prepared using the washed cell method described in section 6.48. Each antimicrobial agent (biocide) to be tested was dissolved in methanol (200  $\mu$ L). To this was added 800  $\mu$ L  $\frac{1}{4}$  strength Ringer's solution in an eppendorf tube to prepare a 1 mM solution in 1 mL. To this solution, the washed bacterial suspension cells (200  $\mu$ L) (*E.coli* and *S.aureus*) were inoculated into (each of) the eppendorf tubes, mixed thoroughly and incubated for 12 h at 37 °C.

The controls were prepared by adding the bacterial suspension (200  $\mu$ L) (*E.coli* and *S.aureus*) with 800  $\mu$ L) ringers solution, and methanol (200  $\mu$ L) in an eppendorf tubes.

Both the tubes were then illuminated for one hour using blue LED light at a height of 5 cm. After illumination, 120  $\mu$ L of each cell suspensions was inoculated onto a nutrient agar plate and incubated at 37 °C for up-to 12 h to determine the antimicrobial activity of the antimicrobial agents attached to a polymer support.

## Appendix 1 of 4.1

Table 72: Antimicrobial activity of **13c**; *E.coli* (+ 100% growth detected, † partial growth, - MIC)

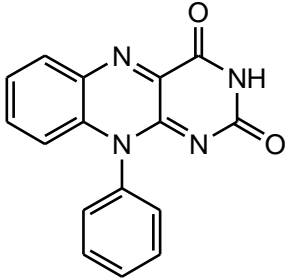
Antibacterial Agent/Bioicide	Compound Code	Gram negative organism: <i>E.coli</i>					
		Light	Concentration in mM/mL				
 10-Phenyl isoalloxazine			<b>1</b>	<b>0.5</b>	<b>0.25</b>	<b>0.125</b>	<b>0.063</b>
	<b>13c</b>	<b>Dark</b>	+	-	+	+	+
	<b>13c*</b>	<b>Blue Light</b>	†	-	+	+	+

Table 73: Antimicrobial activity of **13c**; *S.aureus* (+ 100% growth detected, † partial growth, - MIC)

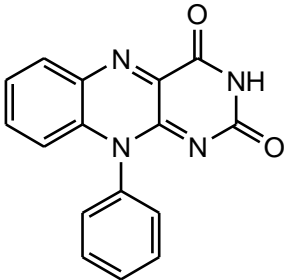
Antibacterial Agent/Bioicide	Compound Code	Gram positive organism: <i>S.aureus</i>					
		Light	Concentration in mM/mL				
 10-Phenyl isoalloxazine			<b>1</b>	<b>0.5</b>	<b>0.25</b>	<b>0.125</b>	<b>0.063</b>
	<b>13c</b>	<b>Dark</b>	+	-	+	+	+
	<b>13c*</b>	<b>Blue Light</b>	†	-	+	+	+

Table 74: Antimicrobial activity of **1c**: *E.coli* (+ 100% growth detected)

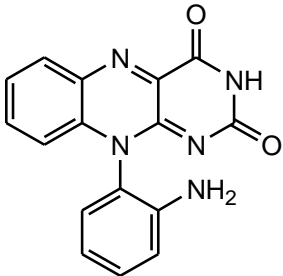
Antibacterial Agent/Biocide	Compound code	Gram negative organism: <i>E.coli</i>					
		Light	Concentration in mM/mL				
 10-Aminophenyl isoalloxazine			<b>1</b>	<b>0.5</b>	<b>0.25</b>	<b>0.125</b>	<b>0.063</b>
	<b>1c</b>	<b>Dark (ortho)</b>	+	+	+	+	+
	<b>1c</b>	<b>Blue Light (ortho)</b>	+	+	+	+	+

Table 75: Antimicrobial activity of **1c**: *S.aureus* (+ 100% growth detected)

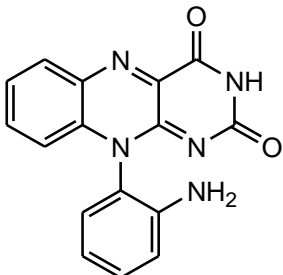
Antibacterial Agent/Biocide	Compound code	Gram positive organism: <i>S.aureus</i>					
		Light	Concentration in mM/mL				
 10-Aminophenyl isoalloxazine			<b>1</b>	<b>0.5</b>	<b>0.25</b>	<b>0.125</b>	<b>0.063</b>
	<b>1c</b>	<b>Dark (ortho)</b>	+	+	+	+	+
	<b>1c</b>	<b>Blue Light (ortho)</b>	+	+	+	+	+

Table 76: Antimicrobial activity of **4c** and **6c**: *E.coli* (+ 100% growth detected, † partial growth)

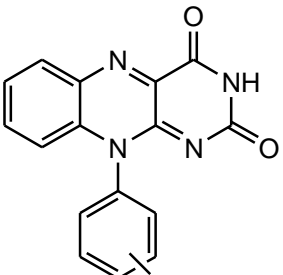
Antibacterial Agent/Biocide	Compound code	Gram negative organism: <i>E.coli</i>					
		Light	Concentration in mM/mL				
 10-Hydroxyphenyl isoalloxazine			<b>1</b>	<b>0.5</b>	<b>0.25</b>	<b>0.125</b>	<b>0.063</b>
	<b>4c*</b>	<b>Dark (ortho)</b>	+	-	+	+	+
	<b>4c</b>	<b>Blue Light (ortho)</b>	†	+	+	+	+
	<b>6c</b>	<b>Dark (para)</b>	+	+	+	+	+
	<b>6c</b>	<b>Blue Light (para)</b>	+	+	+	+	+

Table 77: Antimicrobial activity of **4c** and **6c**: *S.aureus* (+ 100% growth detected, † partial growth)

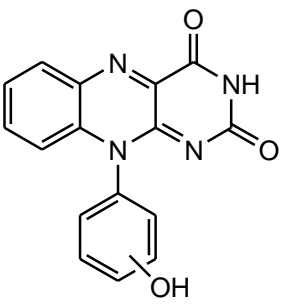
Antibacterial Agent/Bioicide	Compound code	Gram positive organism: <i>S. aureus</i>					
		Light	Concentration in mM/mL				
			1	0.5	0.25	0.125	0.063
 10-Hydroxyphenyl isoalloxazine	<b>4c*</b>	<b>Dark (ortho)</b>	+	-	+	+	+
	<b>4c</b>	<b>Blue Light (ortho)</b>	+	+	†	†	†
	<b>6c</b>	<b>Dark (para)</b>	+	†	+	+	+
	<b>6c</b>	<b>Blue Light (para)</b>	+	†	+	+	+

Table 78: Antimicrobial activity of **7c-9c**: *E.coli* (+ 100% growth detected, † partial growth, - MIC)

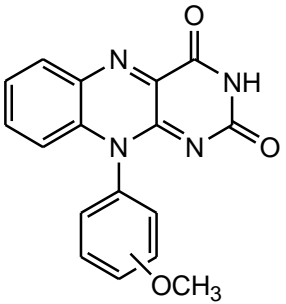
Antibacterial Agent/Bioicide	Compound code	Gram negative organism: <i>E. coli</i>					
		Light	Concentration in mM/mL				
			1	0.5	0.25	0.125	0.063
 10-Methoxyphenyl isoalloxazine	<b>7c</b>	<b>Dark (ortho)</b>	-	+	+	+	+
	<b>7c</b>	<b>Blue Light (ortho)</b>	†	+	+	+	+
	<b>8c</b>	<b>Dark (meta)</b>	+	+	+	+	+
	<b>8c</b>	<b>Blue Light (meta)</b>	†	+	+	+	+
	<b>9c</b>	<b>Dark (para)</b>	-	+	+	+	+
	<b>9c</b>	<b>Blue Light (para)</b>	-	+	+	+	+

Table 79: Antimicrobial activity of **7c-9c**: *S.aureus* (+ 100% growth detected, † partial growth, - MIC)

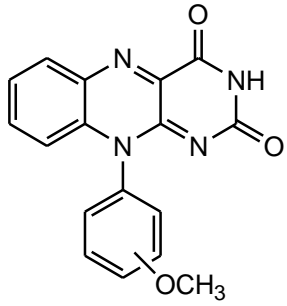
Antibacterial Agent/Biocide	Compound code	Gram positive organism: <i>S. aureus</i>					
		Light	Concentration in mM/mL				
			1	0.5	0.25	0.125	0.063
 <p>10-Methoxyphenyl isoalloxazine</p>	<b>7c*</b>	<b>Dark (ortho)</b>	+	-	+	+	+
	<b>7c</b>	<b>Blue Light (ortho)</b>	+	+	+	+	+
	<b>8c</b>	<b>Dark (meta)</b>	+	+	+	+	+
	<b>8c</b>	<b>Blue Light (meta)</b>	-	-	-	+	+
	<b>9c*</b>	<b>Dark (para)</b>	+	-	+	+	+
	<b>9c*</b>	<b>Blue Light (para)</b>	+	-	+	+	+

Table 80: Antimicrobial activity of **10c-12c**: *E.coli* (+100% growth detected, † partial growth,-MIC)

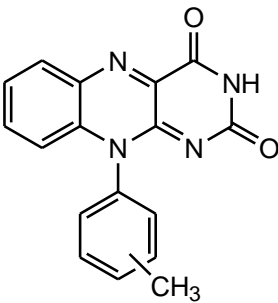
Antibacterial Agent/Biocide	Compound code	Gram negative organism: <i>E.coli</i>					
		Light	Concentration in mM/mL				
			<b>1</b>	<b>0.5</b>	<b>0.25</b>	<b>0.125</b>	<b>0.063</b>
 <p>10-Tolylphenyl isoalloxazine</p>	<b>10c*</b>	<b>Dark (ortho)</b>	+	+	-	+	+
	<b>10c</b>	<b>Blue Light (ortho)</b>	-	†	†	†	+
	<b>11c</b>	<b>Dark (meta)</b>	-	+	+	+	+
	<b>11c</b>	<b>Blue Light (meta)</b>	†	+	+	+	+
	<b>12c</b>	<b>Dark (para)</b>	+	+	†	+	+
	<b>12c</b>	<b>Blue Light (para)</b>	+	+	+	+	+



Table 81: Antimicrobial activity of **10c-12c**: *S.aureus* (+ 100% growth detected, -MIC)

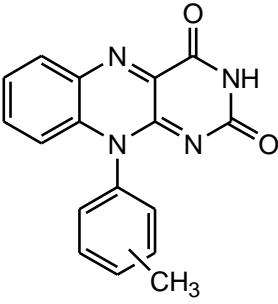
Antibacterial Agent/Biocide	Compound code	Gram negative organism: <i>S.aureus</i>					
		Light	Concentration in mM/mL				
			1	0.5	0.25	0.125	0.063
 <p>10-Tolylphenyl isoalloxazine</p>	<b>10c*</b>	Dark (ortho)	+	+	-	+	+
	<b>10c</b>	Blue Light (ortho)	+	+	+	+	+
	<b>11c*</b>	Dark (meta)	+	+	-	+	+
	<b>11c</b>	Blue Light (meta)	-	-	-	+	+
	<b>12c*</b>	Dark (para)	+	+	-	+	+
	<b>12c</b>	Blue Light (para)	+	+	+	+	+

Table 82: Antimicrobial activity of **14c-16c**: *E.coli* (+ 100% growth detected)

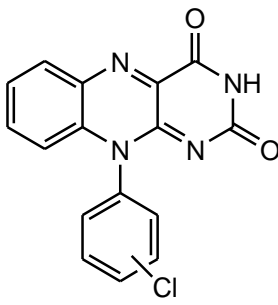
Antibacterial Agent/Biocide	Compound code	Gram negative organism: <i>E.coli</i>					
		Light	Concentration in mM/mL				
			1	0.5	0.25	0.125	0.063
 <p>10-Chlorophenyl isoalloxazine</p>	<b>14c</b>	Dark (ortho)	+	+	+	+	+
	<b>14c</b>	Blue Light (ortho)	+	+	+	+	+
	<b>15c</b>	Dark (meta)	+	+	+	+	+
	<b>15c</b>	Blue Light (meta)	+	+	+	+	+
	<b>16c</b>	Dark (para)	+	+	+	+	+
	<b>16c</b>	Blue Light (para)	+	+	+	+	+

Table 83: Antimicrobial activity of **14c-16c**-*S.aureus* (+ 100% growth detected, † partial growth, - MIC)

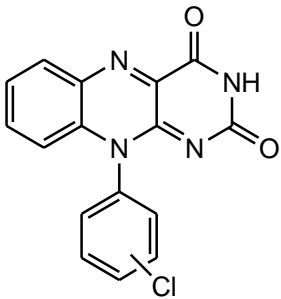
Antibacterial Agent/Biocide	Compound code	Gram negative organism: <i>S.aureus</i>					
		Light	Concentration in mM/mL				
			1	0.5	0.25	0.125	0.063
 10-Chlorophenyl isoalloxazine	<b>14c</b>	<b>Dark (ortho)</b>	+	+	+	+	+
	<b>14c</b>	<b>Blue Light (ortho)</b>	+	+	+	+	+
	<b>15c</b>	<b>Dark (meta)</b>	-	+	+	+	+
	<b>15c</b>	<b>Blue Light (meta)</b>	-	-	-	†	+
	<b>16c</b>	<b>Dark (para)</b>	-	+	+	+	+
	<b>16c*</b>	<b>Blue Light (para)</b>	†	†	-	+	+

Table 84: Antimicrobial activity of compounds **17c-19c**: *E.coli* (+ 100% growth detected)

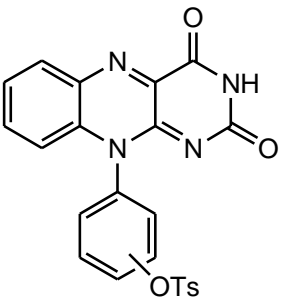
Antibacterial Agent/Biocide	Compound code	Gram negative organism: <i>E.coli</i>					
		Light	Concentration in mM/mL				
			1	0.5	0.25	0.125	0.063
 10-Tosyloxyphenyl isoalloxazine	<b>17c</b>	<b>Dark (ortho)</b>	+	+	+	+	+
	<b>17c</b>	<b>Blue Light (ortho)</b>	+	+	+	+	+
	<b>18c</b>	<b>White Light (meta)</b>	+	+	+	+	+
	<b>18c</b>	<b>Blue Light (meta)</b>	+	+	+	+	+
	<b>19c</b>	<b>White Light (para)</b>	+	+	+	+	+
	<b>19c</b>	<b>Blue Light (para)</b>	+	+	+	+	+

Table 85: Antimicrobial activity of **17c-19c**: *S.aureus* (+ 100% growth detected, † partial growth)

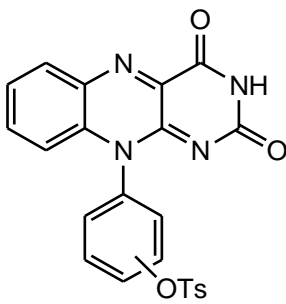
Antibacterial Agent/Biocide	Compound code	Gram positive organism: <i>S. aureus</i>					
		Light	Concentration in mM/mL				
			1	0.5	0.25	0.125	0.063
 10-Tosyloxyphenyl isoalloxazine	<b>17c</b>	<b>Dark (ortho)</b>	+	+	+	+	+
	<b>17c</b>	<b>Blue Light (ortho)</b>	†	†	†	†	+
	<b>18c</b>	<b>Dark (meta)</b>	+	+	+	+	+
	<b>18c</b>	<b>Blue Light (meta)</b>	†	†	†	+	+
	<b>19c</b>	<b>Dark (para)</b>	+	+	+	+	+
	<b>19c</b>	<b>Blue Light (para)</b>	†	†	†	†	+

Table 86: Antimicrobial activity of **20c** and **22c**: *E.coli* (+ 100% growth detected)

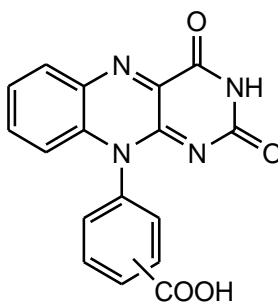
Antibacterial Agent/Biocide	Compound code	Gram negative organism: <i>E.coli</i>					
		Light	Concentration in mM/mL				
			1	0.5	0.25	0.125	0.063
 10-Carboxyphenyl isoalloxazine	<b>20c</b>	<b>Dark (ortho)</b>	+	+	+	+	+
	<b>20c</b>	<b>Blue Light (ortho)</b>	+	+	+	+	+
	<b>22c</b>	<b>Dark (meta)</b>	+	+	+	+	+
	<b>22c</b>	<b>Blue Light (meta)</b>	+	+	+	+	+

Table 87: Antimicrobial activity of **20c** and **22c**: *S.aureus* (+ 100% growth detected, † partial growth, - MIC)

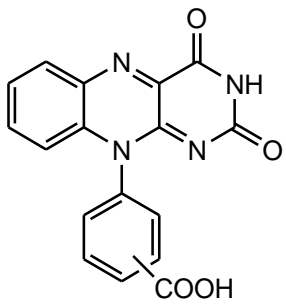
Antibacterial Agent/Biocide	Compound code	Gram positive organism: <i>S. aureus</i>					
		Light	Concentration in mM/mL				
 10-Carboxyphenyl isoalloxazine			<b>1</b>	<b>0.5</b>	<b>0.25</b>	<b>0.125</b>	<b>0.063</b>
	<b>20c</b>	<b>Dark (ortho)</b>	+	+	+	+	+
	<b>20c</b>	<b>Blue Light (ortho)</b>	†	†	+	+	+
	<b>22c</b>	<b>Dark (meta)</b>	-	+	+	+	+
	<b>22c</b>	<b>Blue Light (meta)</b>	-	†	†	†	+

Table 88: Antimicrobial activity of **23c**: *E.coli* (+ 100% growth detected)

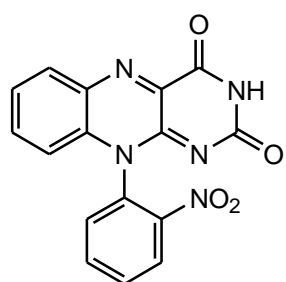
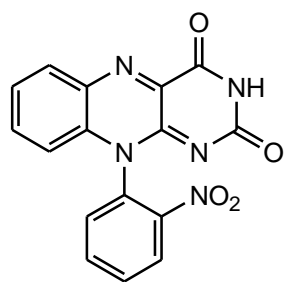
Antibacterial Agent/Biocide	Compound code	Gram negative organism: <i>E.coli</i>					
		Light	Concentration in mM/mL				
 10-Nitrophenyl isoalloxazine			<b>1</b>	<b>0.5</b>	<b>0.25</b>	<b>0.125</b>	<b>0.063</b>
	<b>23c</b>	<b>Dark (ortho)</b>	+	+	+	+	+
	<b>23c</b>	<b>Blue Light (ortho)</b>	+	+	+	+	+

Table 89: Antimicrobial activity of **23c**: *S.aureus* (+ 100% growth detected, † partial growth)

Antibacterial Agent/Biocide	Compound code	Gram positive organism: <i>S. aureus</i>					
		Light	Concentration in mM/mL				
 10-Nitrophenyl isoalloxazine			<b>1</b>	<b>0.5</b>	<b>0.25</b>	<b>0.125</b>	<b>0.063</b>
	<b>23c</b>	<b>Dark (ortho)</b>	+	+	+	+	+
	<b>23c</b>	<b>Blue Light (ortho)</b>	†	†	†	†	+

## Appendix 2 of 4.12

Table 90: Antimicrobial activity of compound 13d

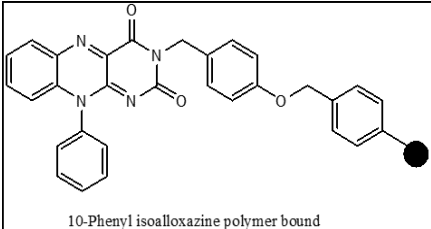
Antibacterial Agent/Biocide	Concentration: 1 mM/mL		
	Compound Code	<i>E.coli</i>	<i>S.aureus</i>
 <p>10-Phenyl isoalloxazine polymer bound</p>	13d	+	-

Table 91: Antimicrobial activity of compound 1d

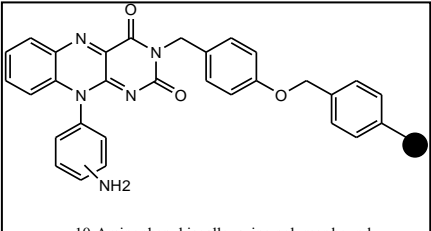
Antibacterial Agent/Biocide	Concentration: 1 mM/mL		
	Compound Code	<i>E.coli</i>	<i>S.aureus</i>
 <p>10-Aminophenyl isoalloxazine polymer bound</p>	1d	†	†

Table 92: Antimicrobial activity of compound 4d

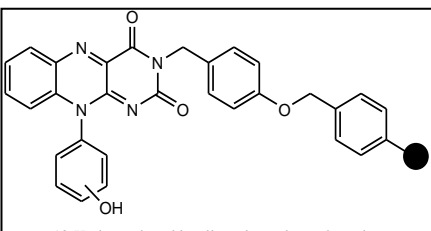
Antibacterial Agent/Biocide	Concentration: 1 mM/mL		
	Compound Code	<i>E.coli</i>	<i>S.aureus</i>
 <p>10-Hydroxyphenyl isoalloxazine polymer bound</p>	4d	+	†

Table 93: Antimicrobial activity of compounds 7d-9d

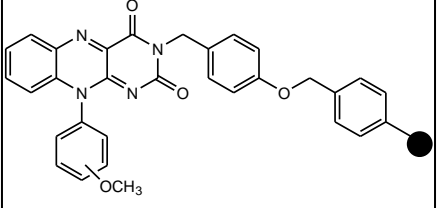
Antibacterial Agent/Biocide	Concentration: 1 mM/mL		
	Compound Code	<i>E.coli</i>	<i>S.aureus</i>
 <p>10-Methoxyphenyl isoalloxazine polymer bound</p>	7d	+	+
	8d	+	+
	9d	+	-

Table 94: Antimicrobial activity of compounds 10d-12d

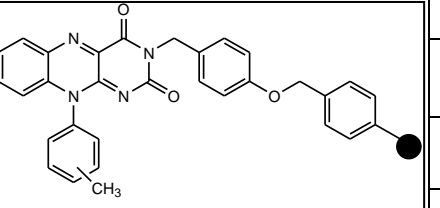
Antibacterial Agent/Biocide	Concentration: 1 mM/mL		
	Compound Code	<i>E.coli</i>	<i>S.aureus</i>
 <p>10-Tolylphenyl isoalloxazine polymer bound</p>	10d	+	†
	11d	†	†
	12d	†	-

Table 95: Antimicrobial activity of compounds 15d and 16d

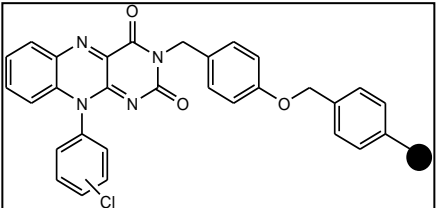
Antibacterial Agent/Biocide	Concentration: 1 mM/mL		
	Compound Code	<i>E.coli</i>	<i>S.aureus</i>
 <p>10-Chlorophenyl isoalloxazine polymer bound</p>	15d	+	†
	16d	†	-

Table 96: Antimicrobial activity of compounds 17d-19d

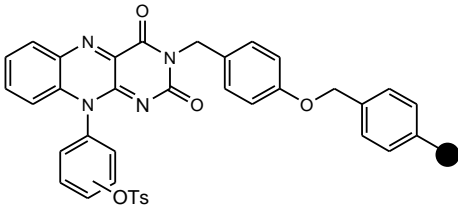
Antibacterial Agent/Biocide	Concentration: 1 mM/mL		
	Compound Code	<i>E.coli</i>	<i>S.aureus</i>
 <p>10-Tosyloxyphenyl isoalloxazine polymer bound</p>	<b>17d</b>	+	+
	<b>18d</b>	+	†
	<b>19d*</b>	+	†

Table 97: Antimicrobial activity of compound 20d

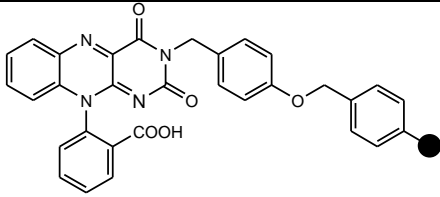
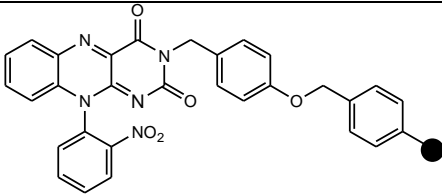
Antibacterial Agent/Biocide	Concentration: 1 mM/mL		
	Compound Code	<i>E.coli</i>	<i>S.aureus</i>
 <p>10-Carboxyphenyl isoalloxazine polymer bound</p>	<b>20d</b>	†	†

Table 98: Antimicrobial activity of compound 23d

Antibacterial Agent/Biocide	Concentration: 1 mM/mL		
	Compound Code	<i>E.coli</i>	<i>S.aureus</i>
 <p>10-Nitrophenyl isoalloxazine polymer bound</p>	<b>23d</b>	†	-

## References

- (1) Wainwright, M. *Photosensitisers in Biomedicine*; 1st ed.; Wiley-Blackwell: Liverpool, 2009
- (2) O'Neill, J. *Tackling drug resistant infections globally*, 2016.
- (3) Agerholm, H. In *Independent*; Harriet Agerholm: 2017.
- (4) Thomas, R. G. O.; Thrush, B. A. *Proc. R. Soc. London Ser. A* **1977**, *356*, 287.
- (5) ML., C. *Science* **1992**, *257*, 1050.
- (6) Laxminarayan, R., Bhutta, Z., Duse, A., Jenkins, P., O'Brien, T., Okeke, I. N., Pablo-Mendez, A., and Klugman, K. P. In *Disease Control Priorities in Developing Countries*.; 2nd edition ed.; AR., M., Ed. 2006, p 1031.
- (7) *The Resistance Phenomenon in Microbes and Infectious Disease Vectors: Implications for Human Health and Strategies for Containment: Workshop Summary*; National Academy of Sciences.: Washington DC, 2003.
- (8) Palumbi, S. R. *Science* **2001**, *293*, 1786.
- (9) Magiorakos, A. P.; Srinivasan, A.; Carey, R. B.; Carmeli, Y.; Falagas, M. E.; Giske, C. G.; Harbarth, S.; Hindler, J. F.; Kahlmeter, G.; Olsson-Liljequist, B.; Paterson, D. L.; Rice, L. B.; Stelling, J.; Struelens, M. J.; Vatopoulos, A.; Weber, J. T.; Monnet, D. L. *Clinical Microbiology and Infection* **2012**, *18*, 268.
- (10) Goossens, H.; Sprenger, M. J. W. *BMJ* **1998**, *317*, 654.
- (11) Komolafe, O. O. *malawi med journal* **2003**, *15*, 63.
- (12) Davies, J.; Davies, D. *Microbiology and Molecular Biology Reviews : MMBR* **2010**, *74*, 417.
- (13) H. W. Boucher, G. H. T., J. S. Bradley, J. E. Edwards, Jr, D. Gilbert, L. B. Rice, M. Scheld, B. Spellberg, and J. Bartlett *Clinical Infectious Diseases* **2009**, *48*, 1.
- (14) G.H.Talbot *Infect Control Hosp Epidemiol.* **2010**, *Suppl 1*, S55.
- (15) Nazir, A.; Kadri, S. M. *Int J Res Med Sci* **2014**, *2*, 21.
- (16) Ventola, C. L. *Pharmacy and Therapeutics* **2015**, *40*, 277.
- (17) Lee, N. A. S. a. M. A. *Real-Time PCR: Advanced Technologies and Applications*; Caister Academic Press, 2013.
- (18) Wang, X.; Quinn, P. In *Endotoxins: Structure, Function and Recognition*; Wang, X., Quinn, P. J., Eds.; Springer Netherlands: 2010; Vol. 53, p 3.
- (19) Helander, I. M.; von Wright, A.; Mattila-Sandholm, T. M. *Trends in Food Science & Technology* **1997**, *8*, 146.
- (20) Collins, A. S. In *Patient Safety and Quality. An Evidence-Based Handbook for Nurses* Hughes, R. G., Ed.; AHRQ--Agency for Healthcare Research and Quality: Advancing Excellence in Health Care: Agency for Healthcare Research and Quality, 2008, p 1.
- (21) Eileen R Choffnes, D. A. R., and Alison Mack *Implications for Global Health and Novel Intervention Strategies*; National Academy of Sciences.: Washington (DC), 2010.
- (22) Levy, S. B.; Marshall, B. *Nat Med* **2004**.
- (23) Wright, G. D. *Nat Rev Micro* **2007**, *5*, 175.
- (24) Wright, G. D. *Current Opinion in Microbiology* **2010**, *13*, 589.
- (25) Luning Prak, E. T.; Kazazian, H. H. *Nat Rev Genet* **2000**, *1*, 134.
- (26) Martinez, J. L. *Frontiers in Microbiology* **2012**, *2*.
- (27) Khachatourians, G. G. *Canadian Medical Association* **1998**, *159*, 1129.
- (28) *National Antimicrobial Resistance Monitoring System for Enteric Bacteria ( NARMS): Human Isolates Final report, 2010.*; Department of Health and Human Services, , 2010.
- (29) Angulo, F. J.; Baker, N. L.; Olsen, S. J.; Anderson, A.; Barrett, T. J. *Seminars in Pediatric Infectious Diseases* **2004**, *15*, 78.
- (30) CDC *Antibiotic Resistance Threats in the United States, 2013.* , 2013.
- (31) Mulvey, M. R.; Simor, A. E. *Canadian Medical Association Journal* **2009**, *180*, 408.
- (32) WHO 2016.



- (33) Frieden, T.; Centers for Disease Control and Prevention: 2013.
- (34) Dellit, T. H.; Owens, R. C.; McGowan, J. E.; Gerding, D. N.; Weinstein, R. A.; Burke, J. P.; Huskins, W. C.; Paterson, D. L.; Fishman, N. O.; Carpenter, C. F.; Brennan, P. J.; Billeter, M.; Hooton, T. M. *Clinical Infectious Diseases* **2007**, *44*, 159.
- (35) Robinson, D. A.; Kearns, A. M.; Holmes, A.; Morrison, D.; Grundmann, H.; Edwards, G.; O'Brien, F. G.; Tenover, F. C.; McDougal, L. K.; Monk, A. B.; Enright, M. C. *The Lancet* **2005**, *365*, 1256.
- (36) Livermore, D. M. *Journal of Antimicrobial Chemotherapy (JAC)* **2009**, *64*, i29.
- (37) McGowan, J. E. *Clinical Infectious Diseases* **2000**, *31*, S124.
- (38) F. Götz, T. B. a. K.-H. S. In *Prokaryotes* 2006; Vol. 4, p 5.
- (39) Kheder, S. I.; Ali, N. A.; Fathelrahman, A. I. *Pharmacology & Pharmacy* **2012**, *3*, 103.
- (40) Barber, M. *Journal of Clinical Pathology* **1961**, *14*, 385.
- (41) Hiramatsu, K.; Katayama, Y.; Matsuo, M.; Sasaki, T.; Morimoto, Y.; Sekiguchi, A.; Baba, T. *Journal of Infection and Chemotherapy* **2014**, *20*, 593.
- (42) Jorgensen, J. H. *Eur. J. Clin. Microbiol.* **1986**, *5*, 693.
- (43) Leski, T.; Oliveira, D.; Trzcinski, K.; Sanches, I. S.; Aires de Sousa, M.; Hryniewicz, W.; de Lencastre, H. *Journal of clinical microbiology* **1998**, *36*, 3532.
- (44) Carrillo-casas, E. M.; Suástegui-urquijo, Z.; Arroyo-escalante, S.; Morales-espinosa, R.; Moncada-barrón, D.; Hernández-delgado, L.; Méndez-sánchez, J. L.; Delgado-sapién, G.; Navarro-ocaña, A.; Manjarrez-hernández, Á.; Xicohtencatl-cortes, J.; Hernández-castro, R. *Folia Microbiologica* **2013**, *58*, 229.
- (45) von Baum, H.; Marre, R. *International Journal of Medical Microbiology* **2005**, *295*, 503.
- (46) Driscoll, J. A.; Brody, S. L.; Kollef, M. H. *Drugs* **2007**, *67*, 351.
- (47) Sunde, M.; Fossum, K.; Solberg, A.; Sorum, H. *Microbial drug resistance (Larchmont, N.Y.)* **1998**, *4*, 289.
- (48) Stoll, B. J.; Hansen, N.; Fanaroff, A. A.; Wright, L. L.; Carlo, W. A.; Ehrenkranz, R. A.; Lemons, J. A.; Donovan, E. F.; Stark, A. R.; Tyson, J. E.; Oh., W.; Bauer, C. R.; Korones, S. B.; Shankaran, S.; Lupton, A. R.; Stevenson, D. K.; Papile, L.-A.; Poole, W. K. *Pediatrics* **2002**, *110*, 285.
- (49) Gales, A. C.; Jones, R. N.; Gordon, K. A.; Sader, H. S.; Wilke, W. W.; Beach, M. L.; Pfaller, M. A.; Doern, G. V. *J Antimicrob Chemother* **2000**, *45*, 295.
- (50) Threlfall, E. J.; Cheasty, T.; Graham, A.; Rowe, B. *International journal of antimicrobial agents* **1997**, *9*, 201.
- (51) Larson, E. L.; Cimiotti, J. P.; Haas, J.; Nesin, M.; Allen, A.; Della-Latta, P.; Saiman, L. *Pediatric critical care medicine : a journal of the Society of Critical Care Medicine and the World Federation of Pediatric Intensive and Critical Care Societies* **2005**, *6*, 457.
- (52) R. Moniri, K. D. *Microbial Ecology in Health and Disease* **2005**, *17*, 69.
- (53) Teuber, M. *Cell Mol Life Sci* **1999**, *56*, 755.
- (54) Coleman, B. L.; Salvadori, M. I.; McGeer, A. J.; Sibley, K. A.; Neumann, N. F.; Bondy, S. J.; Gutmanis, I. A.; McEwen, S. A.; Lavoie, M.; Strong, D.; Johnson, I.; Jamieson, F. B.; Louie, M. *Epidemiol Infect* **2012**, *140*, 633.
- (55) Hamilton-Miller, J. M. T.; Shah, S. *Journal of Antimicrobial Chemotherapy* **2000**, *46*, 941.
- (56) G. A. Filice, J. A. N., C. Lexau, C. H. Lees, L. A. Bockstedt, K. Como-Sabetti, L. J. Leshner, R. Lynfield, *Infect Control Hosp Epidemiol* **2010**, *31*, 365.
- (57) Milch, H.; Paszti, J.; Erdosi, T.; Hetzmann, M. *Acta microbiologica et immunologica Hungarica* **2001**, *48*, 457.
- (58) Hinckley, J.; Allen, P. J. *Pediatric Nursing* **2008**, *34*, 64.
- (59) Furuya, E. Y.; Lowy, F. D. *Nature reviews. Microbiology* **2006**, *4*, 36.
- (60) Moran, G. J.; Krishnadasan, A.; Gorwitz, R. J.; Fosheim, G. E.; McDougal, L. K.; Carey, R. B.; Talan, D. A. *The New England journal of medicine* **2006**, *355*, 666.
- (61) Schraibman, I. G. *Ann R Coll Surg Engl* **1990**, *72*.
- (62) Greenfield, E.; McManus, A. T. *The Nursing clinics of North America* **1997**, *32*, 297.
- (63) Leaper, D. J. *American journal of surgery* **1994**, *167*, 15S.
- (64) Robson, M. C. *The Surgical clinics of North America* **1997**, *77*, 637.

- (65) Madsen, S. M.; Westh, H.; Danielsen, L.; Rosdahl, V. T. *APMIS : acta pathologica, microbiologica, et immunologica Scandinavica* **1996**, *104*, 895.
- (66) Esuvaranathan, K.; Kuan, Y. F.; Kumarasinghe, G.; Bassett, D. C.; Rauff, A. *The Journal of hospital infection* **1992**, *21*, 231.
- (67) R. K. WOODS, a. E. P. D. *Am Fam Physician* **1998** *57*, 2731.
- (68) Wenzel, R. P. *New England Journal of Medicine* **1992**, *326*, 337.
- (69) Levy, S. B. *Clinical Infectious Diseases* **2001**, *33*, S124.
- (70) Morrell, C. J.; Walters, S. J.; Dixon, S.; Collins, K. A.; Brereton, L. M. L.; Peters, J.; Brooker, C. G. D. *Cost effectiveness of community leg ulcer clinics: randomised controlled trial*, 1998; Vol. 316.
- (71) M J Callam; D R Harper; J J Dale; Ruckley, C. V. *Br Med J.* **1987**, *294*, 1389.
- (72) Campbell, W. B.; Thomson, H.; MacIntyre, J. B.; Coward, C.; Michaels, J. A. *European Journal of Vascular and Endovascular Surgery* **2005**, *30*, 437.
- (73) Morrison, W. B. *Journal of Veterinary Internal Medicine* **2010**, *24*, 1249.
- (74) Bosch, F.; Rosich, L. *Pharmacology* **2008**, *82*, 171.
- (75) Schirmer, R. H.; Adler, H.; Pickhardt, M.; Mandelkow, E. *Neurobiology of Aging* **2011**, *32*, 2325.e7.
- (76) Wainwright, M.; Amaral, L. *Tropical Medicine & International Health* **2005**, *10*, 501.
- (77) Bonazzo, J. In *Observer* 2016.
- (78) Clark, W. M.; Cohen, B.; Gibbs, H. D. *Public Health Reports (1896-1970)* **1925**, *40*, 1131.
- (79) Achan, J.; Talisuna, A. O.; Erhart, A.; Yeka, A.; Tibenderana, J. K.; Baliraine, F. N.; Rosenthal, P. J.; D'Alessandro, U. *Malaria Journal* **2011**, *10*, 144.
- (80) He, Z.; Chen, L.; You, J.; Qin, L.; Chen, X. *Experimental Parasitology* **2009**, *123*, 122.
- (81) Chain, E.; Florey, H. W.; Gardner, A. D.; Heatley, N. G.; Jennings, M. A.; Orr-Ewing, J.; Sanders, A. G. *The Lancet* **1940**, *236*, 226.
- (82) Markel, D. H.; DR. H. Markel: PBS Newshour, 2013.
- (83) Lee, M.; Heseck, D.; Suvorov, M.; Lee, W.; Vakulenko, S.; Mobashery, S. *J Am Chem Soc* **2003**, *125*, 16322.
- (84) Jovetic, S.; Zhu, Y.; Marcone, G. L.; Marinelli, F.; Tramper, J. *Trends in Biotechnology* **2010**, *28*, 596.
- (85) Kuriyama, T.; Nakagawa, K.; Karasawa, T.; Saiki, Y.; Yamamoto, E.; Nakamura, S. *Oral Surgery, Oral Medicine, Oral Pathology, Oral Radiology, and Endodontology* **2000**, *89*, 186.
- (86) Chambers, H. F. *Clin Microbiol Rev* **1997**, *10*, 781.
- (87) Kahsay, A.; Mihret, A.; Abebe, T.; Andualem, T. *Archives of Public Health* **2014**, *72*, 1.
- (88) Jack Benner, E.; Kayser, F. H. *The Lancet* **1968**, *292*, 741.
- (89) Bush, K. *Clinical Microbiology Reviews.* **1988**, *1*, 109.
- (90) Bush, K.; Jacoby, G. A.; Medeiros, A. A. *Antimicrobial Agents and Chemotherapy* **1995**, *39*, 1211.
- (91) Astrid Zervosen, E. S., Jean-Marie Frère, Paulette Charlier, André Luxen *Molecules* **2012**, *17*, 12478.
- (92) Krisztina M. Papp-Wallace, A. E., Magdalena A. Taracila, and Robert A. Bonomo *Antimicrob Agents Chemother* **2011**, *55*, 4943.
- (93) Papp-Wallace, K. M.; Endimiani, A.; Taracila, M. A.; Bonomo, R. A. *Antimicrobial Agents and Chemotherapy* **2011**, *55*, 4943.
- (94) Martinez-Martinez, L. *Clin Microbiol Infect* **2008**, *14 Suppl 1*, 82.
- (95) van Dam, V.; Olrichs, N.; Breukink, E. *ChemBiochem* **2009**, *10*, 617.
- (96) Wilke, M. S.; Lovering, A. L.; Strynadka, N. C. J. *Current Opinion in Microbiology* **2005**, *8*, 525.
- (97) Bonomo, S. M. D. a. R. A. *Clin. Microbiol. Rev* **2010**, *23*, 160.
- (98) Page, M. G. P.; Dantier, C.; Desarbres, E.; Gaucher, B.; Gebhardt, K.; Schmitt-Hoffmann, A. *Antimicrobial Agents and Chemotherapy* **2011**, *55*, 1510.
- (99) Finlay, J.; Miller, L.; Poupard, J. A. *Journal of Antimicrobial Chemotherapy* **2003**, *52*, 18.
- (100) Coleman, K. *Current Opinion in Microbiology* **2011**, *14*, 550.
- (101) Endimiani, A. C., Y.; Bonomo, R. A. *Antimicrob Agents Chemother.* **2009**, *53*, 3599.

- (102) Aminov, R. I. *Frontiers in Microbiology* **2010**, *1*, 134.
- (103) Genç, Y.; Özkanca, R.; Bekdemir, Y. *Ann Clin Microbiol Antimicrob* **2008**, *7*, 1.
- (104) Patrick, G. *An Introduction to Medicinal Chemistry*; 5th ed. Published in the United States by Oxford University Press Inc., New York, 1995.
- (105) Pelczar, M. J.; Chan, E. C. S.; Krieg, N. R. *Microbiology: Concepts and Applications*; McGraw-Hill, 1993.
- (106) Heyl, J. T. *Proc R Soc Med.* **1941**, *34* 782.
- (107) Huovinen, P. *Antimicrob Agents Chemother* **1987**, *31*, 1451.
- (108) S Giguère, J. P., JD Baggot, RD Walker and PM Dowling *Antimicrobial Drug Action and Interaction: An Introduction. Antimicrobial therapy in Veterinary Medicine*; 4th ed.; Blackwell Publishing,: Ames Iowa, USA., 2006.
- (109) Bermingham, A.; Derrick, J. P. *BioEssays : news and reviews in molecular, cellular and developmental biology* **2002**, *24*, 637.
- (110) Wolk, J. L.; Frimer, A. A. *Molecules* **2010**, *15*, 5473.
- (111) Friedländer, P. *Berichte der deutschen chemischen Gesellschaft* **1909**, *42*, 765.
- (112) Murray, O. *The Classical Review (New Series)* **1972**, *22*, 293.
- (113) Stubbs, H. W. *The Journal of Roman Studies* **1973**, *63*, 267.
- (114) Cooksey, C. *Molecules* **2001**, *6*, 736.
- (115) Lauth, C. *On the new aniline dye, 'Violet de Paris, 1867*; Vol. 1.
- (116) Titford, M. *J Histotechnol* **1993**, *16*, 155.
- (117) Maley, A. M.; Arbiser, J. L. *Exp Dermatol* **2013**, *22*, 775.
- (118) Austrian, R. *Bacteriological Reviews* **1960**, *24*, 261.
- (119) Steven K. Alexander Ph.D., D. S. *Microbiology: A Photographic Atlas for the Laboratory*; Benjamin Cummings, 2000.
- (120) Docampo, R.; Moreno, S. N. J. *Drug Metabolism Reviews* **1990**, *22*, 161.
- (121) Stilling, J. *The Lancet*, *136*, 965.
- (122) Churchman, J. W. *The Journal of Experimental Medicine* **1912**, *16*, 221.
- (123) Hinton, D. *Annals of Surgery* **1925**, *81*, 687.
- (124) Yang, Y.-I.; Jung, D.-W.; Bai, D.-G.; Yoo, G.-S.; Choi, J.-K. *Electrophoresis* **2001**, *22*, 855.
- (125) Biochemicals, N.; National Biochemicals, LLC: 2013.
- (126) Kaufman, T. S.; Rúveda, E. A. *Angewandte Chemie International Edition* **2005**, *44*, 854.
- (127) Schweitzer, H. *Science* **1906**, *24*, 481.
- (128) Nagendrappa, G. Sir William Henry Perkin: The Man and his 'Mauve. *GENERAL ARTICLE* [Online Early Access]. Published Online: 2010. <http://www.ias.ac.in/resonance/Volumes/15/09/0779-0793.pdf>.
- (129) Manchester, T. M. o. S. a. I. i. Sir William Henry Perkin (1838-1907): the Discovery of Aniline Purple. [Online Early Access]. Published Online: 2006. <http://www.mosi.org.uk/media/33871452/sirwilliamhenryperkin.pdf>.
- (130) BASF BASF, 2015.
- (131) Anderson, L.; Wittkopp, S. M.; Painter, C. J.; Liegel, J. J.; Schreiner, R.; Bell, J. A.; Shkhashiri, B. Z. *Journal of Chemical Education* **2012**, *89*, 1425.
- (132) Tuite, E. M.; Kelly, J. M. *J Photochem Photobiol B* **1993**, *21*, 103.
- (133) De Crozals, G.; Farre, C.; Sigaud, M.; Fortgang, P.; Sanglar, C.; Chaix, C. *Chemical Communications* **2015**, *51*, 4458.
- (134) Wainwright, M. *Dyes and Pigments* **2007**, *73*, 7.
- (135) Vadivelan, V.; Kumar, K. V. *J Colloid Interface Sci* **2005**, *286*, 90.
- (136) Lee, S.; Kim, J.-A.; Yu, K.-E.; Choi, Y.-J.; Kim, J.-H.; Nam, S.-J.; Yang, J.-H. *J Breast Cancer* **2007**, *10*, 153.
- (137) Simmons, R. M.; Smith, S. M.; Osborne, M. P. *Breast J* **2001**, *7*, 181.
- (138) Wainwright, M. *Chem Soc Rev* **2002**, *31*, 128.
- (139) Ginimuge, P. R.; Jyothi, S. D. *Journal of Anaesthesiology, Clinical Pharmacology* **2010**, *26*, 517.
- (140) Pinheiro, S. L.; Schenka, A. A.; Neto, A. A.; de Souza, C. P.; Rodriguez, H. M.; Hiar; Ribeiro, M. C. *Lasers Med Sci* **2009**, *24*, 521.
- (141) Simões, A.; Benites, B. M.; Benassi, C.; Torres-Schroter, G.; de Castro, J. R.; Campos, L. *Photodiagnosis and Photodynamic Therapy* **2017**, *20*, 18.

- (142) Tavares, L. J.; Pavarina, A. C.; Vergani, C. E.; de Avila, E. D. *Photodiagnosis and Photodynamic Therapy* **2017**, *17*, 236.
- (143) Ibbotson, S. H. *Photodiagnosis and Photodynamic Therapy* **2010**, *7*, 16.
- (144) Brown, S. B.; Brown, E. A.; Walker, I. *The Lancet Oncology* **2004**, *5*, 497.
- (145) Daniell, M. D.; Hill, J. S. *Australian and New Zealand Journal of Surgery* **1991**, *61*, 340.
- (146) Celli, J. P.; Spring, B. Q.; Rizvi, I.; Evans, C. L.; Samkoe, K. S.; Verma, S.; Pogue, B. W.; Hasan, T. *Chemical reviews* **2010**, *110*, 2795.
- (147) Castano, A. P.; Demidova, T. N.; Hamblin, M. R. *Photodiagnosis and Photodynamic Therapy* **2004**, *1*, 279.
- (148) Schafer, M.; Schmitz, C.; Facius, R.; Horneck, G.; Milow, B.; Funken, K. H.; Ortner, J. *Photochem Photobiol* **2000**, *71*, 514.
- (149) Maisch, T.; Szeimies, R.-M.; Jori, G.; Abels, C. *Photochemical & Photobiological Sciences* **2004**, *3*, 907.
- (150) Embleton, M. L.; Nair, S. P.; Cookson, B. D.; Wilson, M. *Journal of Antimicrobial Chemotherapy* **2002**, *50*, 857.
- (151) Mitchell, G. S.; Gill, R. K.; Boucher, D. L.; Li, C.; Cherry, S. R. *Philosophical transactions. Series A, Mathematical, physical, and engineering sciences* **2011**, 369, 4605.
- (152) Massoud, T. F.; Gambhir, S. S. *Genes & Development* **2003**, *17*, 545.
- (153) Lenka Ryskova, V. B., Radovan Slezak *Cent. Eur. J. Biol.* **2010**, *5*, 400.
- (154) Plaetzer, K.; Kiesslich, T.; Verwanger, T.; Krammer, B. *Medical Laser Application* **2003**, *18*, 7.
- (155) Malagi\*\*\*\*\*, S.; B\*\*\*\*\*, R.; Kamath\*\*\*\*\*, V. *NJIRM* **2014**, *5*, 72.
- (156) Paul, P.; Suresh Kumar, G. *The Journal of Chemical Thermodynamics* **2013**, *64*, 50.
- (157) O'Riordan, K.; Akilov, O. E.; Chang, S. K.; Foley, J. W.; Hasan, T. *Photochem Photobiol Sci* **2007**, *6*, 1117.
- (158) Wainwright, M.; Giddens, R. M. *Dyes and Pigments* **2003**, *57*, 245.
- (159) Castano, A. P.; Demidova, T. N.; Hamblin, M. R. *Photodiagnosis and photodynamic therapy* **2005**, *2*, 91.
- (160) Moreira, L. M.; Lyon, J. P.; Tursi, S. M. S.; Trajano, I.; Felipe, M. P.; Costa, M. S.; Rodrigues, M. R.; Codognoto, L.; de Oliveira, H. P. M. *Spectroscopy* **2010**, *24*.
- (161) Wainwright, M.; Phoenix, D. A.; Laycock, S. L.; Wareing, D. R. A.; Wright, P. A. *FEMS Microbiology Letters* **1998**, *160*, 177.
- (162) M.C. DeRosa, R. J. C. *Coordination Chemistry Reviews* **2002**, 351.
- (163) Wainwright, M. *Journal of Antimicrobial Chemotherapy* **2001**, *47*, 1.
- (164) C. H. Browning, R. G., and L. H. D. Thornton. *Br.med. J* **1917**, *2*, 71.
- (165) Prieto, S. P.; Powless, A. J.; Boice, J. W.; Sharma, S. G.; Muldoon, T. J. *PLoS ONE* **2015**, *10*, e0125598.
- (166) Lu, L. C., Qiyin; Zhu, Xiaozhang; Chen, Chuanfeng; *Synthesis* **2003**, 2464.
- (167) Vera, D. M. A.; Haynes, M. H.; Ball, A. R.; Dai, D. T.; Astrakas, C.; Kelso, M. J.; Hamblin, M. R.; Tegos, G. P. *Photochemistry and Photobiology* **2012**, *88*, 499.
- (168) Cook, M. P.; Ando, S.; Koide, K. *Tetrahedron Letters* **2012**, *53*, 5284.
- (169) M., W. *Photosensitisers in Biomedicine*; Wiley-Blackwel, 2009.
- (170) Wainwright, M. *Journal compilation Society of Dyers and Colourists, Color. Technol.* **2010**, *126*, 115.
- (171) Taichman, G. C.; Hendry, P. J.; Keon, W. J. *Texas Heart Institute Journal* **1987**, *14*, 133.
- (172) Khati, M. *Journal of Clinical Pathology* **2010**, *63*, 480.
- (173) Benson, J.; Loh, S.-W.; Jones, L.; Wishart, G. *Cancer Research* **2012**, *72*, P1.
- (174) Y. Chen, G. C., Y.. Zhao and W. Wang *J Nanomed Nanotechol* **2012**, *3*, 1.
- (175) Narayanan, N.; Patonay, G. *The Journal of Organic Chemistry* **1995**, *60*, 2391.
- (176) Flanagan, J. H.; Khan, S. H.; Menchen, S.; Soper, S. A.; Hammer, R. P. *Bioconjugate Chemistry* **1997**, *8*, 751.
- (177) Pardal, A.; Ramos, S.; Santos, P.; Reis, L.; Almeida, P. *Molecules* **2002**, *7*, 320.
- (178) Kim, S. H.; Han, S. K. *Coloration Technology* **2001**, *117*, 61.
- (179) Fabian, J.; Nakazumi, H.; Matsuoka, M. *Chemical Reviews* **1992**, *92*, 1197.
- (180) Santos, P. F.; Reis, L. V.; Almeida, P.; Oliveira, A. S.; Vieira Ferreira, L. F. *Journal of Photochemistry and Photobiology A: Chemistry* **2003**, *160*, 159.

- (181) Reis, L. V.; Serrano, J. P.; Almeida, P.; Santos, P. F. *Dyes and Pigments* **2009**, *81*, 197.
- (182) Reis, L. V.; Serrano, J. P. C.; Almeida, P.; Santos, P. F. *Synlett* **2003**, *2003*, 142.
- (183) Encinas, C.; Otazo, E.; Rivera, L.; Miltsov, S.; Alonso, J. *Tetrahedron Letters* **2002**, *43*, 8391.
- (184) Song, X.; Foley, J. W. *Dyes and Pigments* **2008**, *78*, 60.
- (185) Keil, D., Hartmann, H., Reichardt, C. *European Journal of Organic Chemistry* **1993**, *9*, 935.
- (186) Keil, D.; Hartmann, H.; Reichardt, C. *Liebigs Annalen der Chemie* **1993**, *1993*, 935.
- (187) Christopher R. Shea, N. C., Joanne Wimberly, et al. *CANCER RESEARCH* **1989**, *49*, 3961.
- (188) Menzel, R.; Thiel, E. *Chemical Physics Letters* **1998**, *291*, 237.
- (189) Attia, A. B. E.; Balasundaram, G.; Driessen, W.; Ntziachristos, V.; Olivo, M. *Biomedical Optics Express* **2015**, *6*, 591.
- (190) Wagner, J. R.; Ali, H.; Langlois, R.; Brasseur, N.; Van Ller, J. E. *Photochemistry and Photobiology* **1987**, *45*, 587.
- (191) Cakr, D.; Goksel, M.; Cakr, V.; Durmus, M.; Biyiklioglu, Z.; Kantekin, H. *Dalton Transactions* **2015**, *44*, 9646.
- (192) Mondal, S. B.; Gao, S.; Zhu, N.; Liang, R.; Gruev, V.; Achilefu, S. *Advances in cancer research* **2014**, *124*, 171.
- (193) Gibbs, S. L. *Quantitative Imaging in Medicine and Surgery* **2012**, *2*, 177.
- (194) H.A. Shindy, A. I. M. K. *proceedings of the Indian Academy of Sciences* **2002**, 125.
- (195) Vahrmeijer, A. L.; Hutteman, M.; van der Vorst, J. R.; van de Velde, C. J. H.; Frangioni, J. V. *Nat Rev Clin Oncol* **2013**, *10*, 507.
- (196) Frangioni, J. V. *Curr Opin Chem Biol* **2003**, *7*, 626.
- (197) Oleinick, N. L. In *Department of Radiation Oncology Case Western Reserve University School of Medicine*, 2010; Vol. 2011.
- (198) Mroz, P., Y. A., Kharkwal, G., Hamblin, M. *Cancers* **2011**, 2516.
- (199) Nyman, E. S.; Hynninen, P. H. *J Photochem Photobiol B* **2004**, *73*, 1.
- (200) Redmond, R. W.; Gamlin, J. N. *Photochem. Photobiol.* **1999**, *70*, 391.
- (201) Merkel, P. B.; Kearns, D. R. *Journal of the American Chemical Society* **1972**, *94*, 7244.
- (202) Yoon, I.; Li, J. Z.; Shim, Y. K. *Clinical Endoscopy* **2013**, *46*, 7.
- (203) Issa, M. C. A.; Manela-Azulay, M. *Anais Brasileiros de Dermatologia* **2010**, *85*, 501.
- (204) Kharkwal, G. B.; Sharma, S. K.; Huang, Y. Y.; Dai, T.; Hamblin, M. R. *Lasers Surg Med* **2011**, *43*, 755.
- (205) Baptista, M. S.; Wainwright, M. *Brazilian Journal of Medical and Biological Research* **2011**, *44*, 1.
- (206) Wainwright, M. *Journal of Antimicrobial Chemotherapy* **1998**, 13.
- (207) Wainwright, M. *J. Antimicrob. Chemotherapy* **2012**, 67
- (208) Andersen, R.; Loebel, N.; Hammond, D.; Wilson, M. *J Clin Dent* **2007**, *18*, 34.
- (209) Huang, Z. *Technology in cancer research & treatment* **2005**, *4*, 283.
- (210) Agostinis, P.; Berg, K.; Cengel, K. A.; Foster, T. H.; Girotti, A. W.; Gollnick, S. O.; Hahn, S. M.; Hamblin, M. R.; Juzeniene, A.; Kessel, D.; Korbelik, M.; Moan, J.; Mroz, P.; Nowis, D.; Piette, J.; Wilson, B. C.; Golab, J. *CA: a cancer journal for clinicians* **2011**, *61*, 250.
- (211) Dolmans, D. E.; Fukumura, D.; Jain, R. K. *Nature reviews. Cancer* **2003**, *3*, 380.
- (212) Huang, Z.; Xu, H.; Meyers, A. D.; Musani, A. I.; Wang, L.; Tagg, R.; Barqawi, A. B.; Chen, Y. K. *Technology in cancer research & treatment* **2008**, *7*, 309.
- (213) Muller, P. J.; Wilson, B. C. *Lasers Surg Med* **2006**, *38*, 384.
- (214) Cancer research UK: 2014.
- (215) Society, C. C.; Society, C. C., Ed. 2015.
- (216) Rud, E.; Gederaas, O.; Hogset, A.; Berg, K. *Photochem Photobiol* **2000**, *71*, 640.
- (217) Raspagliesi, F.; Fontanelli, R.; Rossi, G.; Ditto, A.; Solima, E.; Hanozet, F.; Kusamura, S. *Gynecologic Oncology* **2006**, *103*, 581.
- (218) Taylor, E. L.; Brown, S. B. *Journal of Dermatological Treatment* **2002**, *13*, s3.
- (219) Ericson, M. B.; Wennberg, A.-M.; Larkö, O. *Therapeutics and Clinical Risk Management* **2008**, *4*, 1.

- (220) Warren, C. B.; Karai, L. J.; Vidimos, A.; Maytin, E. V. *Journal of the American Academy of Dermatology* **2009**, *61*, 1033.
- (221) Zane, C.; Venturini, M.; Sala, R.; Calzavara-Pinton, P. *Photodermatol Photoimmunol Photomed* **2006**, *22*, 254.
- (222) Ferrario, A.; Gomer, C. J. *J Environ Pathol Toxicol Oncol* **2006**, *25*, 251.
- (223) Ho, S. A.; Aw, D. C. *Dermatol Ther* **2010**, *23*, 423.
- (224) Suarez, A. L.; Pulitzer, M.; Horwitz, S.; Moskowitz, A.; Querfeld, C.; Myskowski, P. L. *J Am Acad Dermatol* **2013**, *69*, 329 e1.
- (225) Chen, J. K.; Ghasri, P.; Aguilar, G.; van Drooge, A. M.; Wolkerstorfer, A.; Kelly, K. M.; Heger, M. *Journal of the American Academy of Dermatology* **2012**, *67*, 289.
- (226) Yuan, K. H.; Li, Q.; Yu, W. L.; Huang, Z. *Photodiagnosis Photodyn Ther* **2009**, *6*, 189.
- (227) Morelli, J. G.; Tan, O. T.; Margolis, R.; Seki, Y.; Boll, J.; Carney, J. M.; Anderson, R. R.; Parrish, J. A.; Furumoto, H.; Garden, J. *Lasers in Surgery and Medicine* **1986**, *6*, 94.
- (228) Tanzi, E. L.; Lupton, J. R.; Alster, T. S. *Journal of the American Academy of Dermatology*, *49*, 1.
- (229) Phung, T. L.; Oble, D. A.; Jia, W.; Benjamin, L. E.; Mihm, M. C.; Nelson, J. S. *Lasers in surgery and medicine* **2008**, *40*, 1.
- (230) Gao, K.; Huang, Z.; Yuan, K. H.; Zhang, B.; Hu, Z. Q. *Br J Dermatol* **2013**, *168*, 1040.
- (231) Yuan, K. H.; Li, Q.; Yu, W. L.; Zeng, D.; Zhang, C.; Huang, Z. *Photodiagnosis Photodyn Ther* **2008**, *5*, 50.
- (232) Dai, T.; Huang, Y.-Y.; Hamblin, M. R. *Photodiagnosis and photodynamic therapy* **2009**, *6*, 170.
- (233) Bockstahler, L. E.; Coohill, T. P.; Hellman, K. B.; David Lytle, C.; Roberts, J. E. *Pharmacology & Therapeutics* **1979**, *4*, 473.
- (234) Myers, M. G.; Oxman, M. N.; Clark, J. E.; Arndt, K. A. *New England Journal of Medicine* **1975**, *293*, 945.
- (235) Kharkwal, G. B.; Sharma, S. K.; Huang, Y.-Y.; Dai, T.; Hamblin, M. R. *Lasers in Surgery and Medicine* **2011**, *43*, 755.
- (236) Kim, M.; Jung, H.; Park, H. *International Journal of Molecular Sciences* **2015**, *16*, 23259.
- (237) Kim, J. E.; Kim, S. J.; Hwang, J. I.; Lee, K. J.; Park, H. J.; Cho, B. K. *J Dermatolog Treat* **2012**, *23*, 192.
- (238) Moore, C.; Wallis, C.; Melnick, J. L.; Kuns, M. D. *Infection and Immunity* **1972**, *5*, 169.
- (239) Chang, T.-W.; Fiumara, N.; Weinstein, L. *International Journal of Dermatology* **1975**, *14*, 69.
- (240) Hillemanns, P.; Einstein, M. H.; Iversen, O. E. *Expert Opin Investig Drugs* **2015**, *24*, 273.
- (241) Abramson, A. L.; Shikowitz, M. J.; Mullooly, V. M.; Steinberg, B. M.; Amella, C.; Rothstein, H. R. *Archives of Otolaryngology–Head & Neck Surgery* **1992**, *118*, 25.
- (242) Shikowitz, M. J.; Abramson, A. L.; Freeman, K.; Steinberg, B. M.; Nouri, M. *The Laryngoscope* **1998**, *108*, 962.
- (243) Detty, M. R.; Gibson, S. L.; Wagner, S. J. *Journal of Medicinal Chemistry* **2004**, *47*, 3897.
- (244) Rebeiz, C. A.; Reddy, K. N.; Nandihalli, U. B.; Velu, J. *Photochemistry and Photobiology* **1990**, *52*, 1099.
- (245) Brovko, L. *Adv Food Nutr Res* **2010**, *61*, 119.
- (246) Brovko, L. Y.; Meyer, A.; Tiwana, A. S.; Chen, W.; Liu, H.; Filipe, C. D.; Griffiths, M. W. *J Food Prot* **2009**, *72*, 1020.
- (247) Gupta, A.; Avci, P.; Dai, T.; Huang, Y.-Y.; Hamblin, M. R. *Advances in Wound Care* **2013**, *2*, 422.
- (248) Sperandio, F. F.; Huang, Y. Y.; Hamblin, M. R. *Recent Pat Antiinfect Drug Discov* **2013**, *8*, 108.
- (249) Zeina, B.; Greenman, J.; Purcell, W. M.; Das, B. *Br J Dermatol* **2001**, *144*, 274.
- (250) Zolfaghari, P.; Packer, S.; Singer, M.; Nair, S.; Bennett, J.; Street, C.; Wilson, M. *BMC Microbiology* **2009**, *9*, 27.
- (251) Dobson, J.; Wilson, M. *Archives of Oral Biology* **1992**, *37*, 883.
- (252) Usacheva, M. N.; Teichert, M. C.; Biel, M. A. *Lasers Surg Med* **2001**, *29*, 165.
- (253) Hay, R. J.; Adriaans, B. M. In *Rook's Textbook of Dermatology*; Wiley-Blackwell: 2010, p 1.

- (254) Lyon, J. P.; Moreira, L. M.; de Moraes, P. C.; dos Santos, F. V.; de Resende, M. A. *Mycoses* **2011**, *54*, e265.
- (255) Donnelly, R. F.; McCarron, P. A.; Tunney, M. M. *Microbiol Res* **2008**, *163*, 1.
- (256) Lyon, J. P.; Moreira, L. M.; Cardoso, M. A. G.; Saade, J.; Resende, M. A. *Brazilian Journal of Microbiology* **2008**, *39*, 668.
- (257) Deris, J. B.; Kim, M.; Zhang, Z.; Okano, H.; Hermsen, R.; Groisman, A.; Hwa, T. *Science (New York, N.Y.)* **2013**, *342*, 1237435.
- (258) Baird, R. M.; Crowden, C. A.; O'Farrell, S. M.; Shooter, R. A. *The Journal of Hygiene* **1979**, *83*, 277.
- (259) Ratajczak, M.; Kubicka, M. M.; Kamińska, D.; Sawicka, P.; Długaszewska, J. *Saudi Pharmaceutical Journal* **2015**, *23*, 303.
- (260) K., T. In *Control of Microbial Growth* 2012, p 6.
- (261) Hussain, M. In *Microbiology online* 2009.
- (262) Block, S. S. *Disinfection, sterilization, and preservation*; Lippincott Williams & Wilkins, 2001.
- (263) Chen, P.; Shakhnovich, E. I. *Biophysical Journal* **2010**, *98*, 1109.
- (264) M.T. Madigan, J. M. M., D. A. Stahl, D. P. Clark; 13 ed. 2012.
- (265) Aparecida, K. A. S. In *Sterilization by Gamma Irradiation*; Adrovic, F., Ed. 2012.
- (266) Levy, S. B. *Journal of Antimicrobial Chemotherapy* **2002**, *49*, 25.
- (267) Rodriguez, J. C.; Pastor, E.; Ruiz, M.; Flores, E.; Royo, G. *Infect Disord Drug Targets* **2007**, *7*, 43.
- (268) Lee, C.-R.; Cho, I. H.; Jeong, B. C.; Lee, S. H. *International Journal of Environmental Research and Public Health* **2013**, *10*, 4274.
- (269) Ghannoum, M. A.; Rice, L. B. *Clinical Microbiology Reviews* **1999**, *12*, 501.
- (270) Peterson, L. R.; Shanholtzer, C. J. *Clinical Microbiology Reviews* **1992**, *5*, 420.
- (271) M. A. Pfaller, D. J. S., and J. H. Rex *Clinical Microbiology Reviews* **2004**, *17*, 268.
- (272) Scott, E. M.; Gorman, S. P.; McGrath, S. J. *J Clin Hosp Pharm* **1986**, *11*, 199.
- (273) Butaye, P.; Devriese, L. A.; Haesebrouck, F. *Clinical Microbiology Reviews* **2003**, *16*, 175.
- (274) Droumev, D. *Vet Res Commun* **1983**, *7*, 85.
- (275) Michigan State University: Michigan State University, 2011.
- (276) Pankey, G. A.; Sabath, L. D. *Clinical Infectious Diseases* **2004**, *38*, 864.
- (277) Ocampo, P. S.; Lazar, V.; Papp, B.; Arnoldini, M.; Abel zur Wiesch, P.; Busa-Fekete, R.; Fekete, G.; Pal, C.; Ackermann, M.; Bonhoeffer, S. *Antimicrob Agents Chemother* **2014**, *58*, 4573.
- (278) McDonnell, G.; Russell, A. D. *Clinical Microbiology Reviews* **1999**, *12*, 147.
- (279) Hani A. Masaadeh, A. S. J. *American Journal of Applied Sciences* **2009**, *6*, 811.
- (280) Sandle, T. In *Institute of Validation Technology (IVT)* 2014.
- (281) Piddock, L. J. V. *Journal of Applied Bacteriology* **1990**, *68*, 307.
- (282) Curtin, J.; Cormican, M. *Re/Views in Environmental Science and Bio/Technology* **2003**, *2*, 285.
- (283) Morton, L. H. G., Minimal inhibitory concentration-antimicrobial agents.
- (284) European Committee for Antimicrobial Susceptibility Testing of the European Society of Clinical, M.; Infectious, D. *Clinical Microbiology and Infection* **2003**, *9*, ix.
- (285) Reller, L. B.; Weinstein, M.; Jorgensen, J. H.; Ferraro, M. J. *Clinical Infectious Diseases* **2009**, *49*, 1749.
- (286) Khaki, P.; Sharma, A.; Bhalla, P. *Annals of Medical and Health Sciences Research* **2014**, *4*, 453.
- (287) Spellberg, B.; Powers, J. H.; Brass, E. P.; Miller, L. G.; Edwards, J. E. *Clinical Infectious Diseases* **2004**, *38*, 1279.
- (288) Powers, J. H. *Clin Microbiol Infect* **2004**, *10 Suppl 4*, 23.
- (289) Vecki, V. G.; Ottinger, M. R. *California State Journal of Medicine* **1921**, *19*, 438.
- (290) Garishah, M. F. *Canadian Medical Association* **2009**, 408.
- (291) Medeiros, A. A. *Clinical Infectious Diseases* **1997**, *24*, S19.
- (292) Levy, S. B. *Scientific American* **1998**, 46.
- (293) Sardiello, M.; Tripoli, G.; Oliva, M.; Santolamazza, F.; Moschetti, R.; Barsanti, P.; Lanave, C.; Caizzi, R.; Caggese, C. *Gene* **2003**, *317*, 111.

- (294) Galdiero, S.; Falanga, A.; Cantisani, M.; Tarallo, R.; Pepa, M. E. D.; D’Orlando, V.; Galdiero, M. *Current Protein & Peptide Science* **2012**, *13*, 843.
- (295) organization, W. h.; organization, W. h., Ed. 2015.
- (296) Morton, G., Biocides.
- (297) Finch, R. *Clin Microbiol Infect* **2002**, *8*, 317
- (298) prevention, C. f. d. c. a. *Antibiotic/Antimicrobial Resistance*, 2015.
- (299) Baquero, F.; Blázquez, J. *Trends in Ecology & Evolution* **1997**, *12*, 482.
- (300) Tenover, F. C. *American Journal of Infection Control* **2006**, *34*, S3.
- (301) Alekshun, M. N.; Levy, S. B. *Cell* **2007**, *128*, 1037.
- (302) commissions, E., Ed.; European commissions -public health: 2009.
- (303) Askew, P. *Journal of Chemical Technology & Biotechnology* **1996**, *66*, 213.
- (304) Rossmore, H. W. *Handbook of Biocide and Preservative Use*; Springer Netherlands : Imprint : Springer: Dordrecht, 1995.
- (305) Executive, H. a. S.; Executive, H. a. S., Ed. 2014.
- (306) Giedraitiene, A.; Vitkauskienė, A.; Naginiene, R.; Pavilonis, A. *Medicina (Kaunas)* **2011**, *47*, 137.
- (307) Golbraikh, A.; Wang, X. S.; Zhu, H.; Tropsha, A. In *Handbook of Computational Chemistry*; Leszczynski, J., Ed.; Springer Netherlands: Dordrecht, 2012, p 1309.
- (308) Fischer, M.; Bacher, A. In *Comprehensive Natural Products II*; Liu, H.-W., Mander, L., Eds.; Elsevier: Oxford, 2010, p 3.
- (309) Geetanjali, R. S. a. *J. Serb. Chem. Soc.* **2006**, *71*, 575.
- (310) Chauhan, S. M. S.; Geetanjali, R. S. *Synthetic Communications* **2003**, *33*, 1179.
- (311) Chauhan, S. M. S. G. S., R. J. *Heterocycl. Chem.* **2000**, *10*, 157.
- (312) Daďová, J.; Kümmel, S.; Feldmeier, C.; Cibulková, J.; Pažout, R.; Maixner, J.; Gschwind, R. M.; König, B.; Cibulka, R. *Chemistry – A European Journal* **2013**, *19*, 1066.
- (313) Wenner, A. V. H. a. W. **1963** *Coll 4*, 23.
- (314) Kanhed, A. M.; Sinha, A.; Machhi, J.; Tripathi, A.; Parikh, Z. S.; Pillai, P. P.; Giridhar, R.; Yadav, M. R. *Bioorganic Chemistry* **2015**, *61*, 7.
- (315) Baumann, M.; Baxendale, I.; Hornung, C.; Ley, S.; Rojo, M.; Roper, K. *Molecules* **2014**, *19*, 9736.
- (316) Kumar, V.; Woode, K. A.; Bryan, R. F.; Averill, B. A. *Journal of the American Chemical Society* **1986**, *108*, 490.
- (317) Miiller, f., Dudley, K *Helvetica Chimica Acta* **1971**, *54*, 1487.
- (318) Weinstock, L. T.; Wiegand, C. J. W.; Cheng, C. C. *Journal of Heterocyclic Chemistry* **1977**, *14*, 1261.
- (319) Yoneda, F.; Sakuma, Y. *Journal of the Chemical Society, Chemical Communications* **1976**, 203.
- (320) Nagamatsu, T.; Yamato, H.; Ono, M.; Takarada, S.; Yoneda, F. *Journal of the Chemical Society, Perkin Transactions 1* **1992**, 2101.
- (321) Youssif, S. *Monatshefte für Chemie / Chemical Monthly* **1999**, *130*, 819.
- (322) Nijvipakul, S.; Ballou, D. P.; Chaiyen, P. *Biochemistry* **2010**, *49*, 9241.
- (323) Yamazaki, I.; Tamura, M.; Nakajima, R.; Nakamura, M. *Environmental Health Perspectives* **1985**, *64*, 331.
- (324) Higdon, J.; Linus Pauling Institute, Oregon State University: Linus Pauling Institute. Micronutrient Information Center, 2000.
- (325) Liu, Z.; Wang, L.; Zhong, D. *Physical chemistry chemical physics : PCCP* **2015**, *17*, 11933.
- (326) Massey, V. *Journal of Biological Chemistry* **1994**, *269*, 22459.
- (327) Walsey, A., Parsons, V., Wright, O. In *Indendent* 2016.
- (328) Piddock, L. J. V. *The Lancet Infectious Diseases*, *16*, 767.
- (329) Hammett, L. P. *Journal of the American Chemical Society* **1937**, *59*, 96.
- (330) Keenan, S. L.; Peterson, K. P.; Peterson, K.; Jacobson, K. *Journal of Chemical Education* **2008**, *85*, 558.
- (331) Wainwright, M. *Coloration Technology* **2017**, *133*, 3.
- (332) Caldwell, R. A.; Jacobs, L. D.; Furlani, T. R.; Nalley, E. A.; Laboy, J. *Journal of the American Chemical Society* **1992**, *114*, 1623.



- (333) Ravichandran, S.; Karthikeyan, E. *Microwave Synthesis-A Potential Tool for Green Chemistry*, 0002; Vol. 3.
- (334) Lidström, P.; Tierney, J.; Wathey, B.; Westman, J. *Tetrahedron* **2001**, 57, 9225.
- (335) Caddick, S.; Fitzmaurice, R. *Tetrahedron* **2009**, 65, 3325.
- (336) Bejugam, M.; Sewitz, S.; Shirude, P. S.; Rodriguez, R.; Shahid, R.; Balasubramanian, S. *Journal of the American Chemical Society* **2007**, 129, 12926.
- (337) Caldwell, S. T.; Farrugia, L. J.; Hewage, S. G.; Kryvokhyzha, N.; Rotello, V. M.; Cooke, G. *Chemical Communications* **2009**, 1350.
- (338) Chattopadhyay, P.; Rai, R.; Pandey, P. S. *Synthetic Communications* **2006**, 36, 1857.
- (339) Hu, W.; Zhang, X.-F.; Lu, X.; Lan, S.; Tian, D.; Li, T.; Wang, L.; Zhao, S.; Feng, M.; Zhang, J. *Dyes and Pigments* **2018**, 149, 306.
- (340) Jonathan Clayden, N. G., Stuart Warren *Organic Chemistry*; 2nd ed.; Oxford University Press, 2012.
- (341) Chen, X.; Choo, H.; Huang, X.-P.; Yang, X.; Stone, O.; Roth, B. L.; Jin, J. *ACS Chemical Neuroscience* **2015**, 6, 476.
- (342) Yu, Y.; Wu, J.; Lei, F.; Chen, L.; Wan, W.; Hai, L.; Guan, M.; Wu, Y. *Design, Synthesis and Anticancer Activity Evaluation of Diazepinomicin Derivatives*, 2013; Vol. 10.
- (343) Abrahamse, H.; Hamblin, M. R. *Biochem J* **2016**, 473, 347.
- (344) Bäumlner, W.; Abels, C.; Karrer, S.; Weiß, T.; Messmann, H.; Landthaler, M.; Szeimies, R. M. *British Journal of Cancer* **1999**, 80, 360.
- (345) Urbanska, K.; Romanowska-Dixon, B.; Matuszak, Z.; Oszejca, J.; Nowak-Sliwinska, P.; Stochel, G. *Acta Biochim Pol* **2002**, 49, 387.
- (346) F. Wilkinson, W. P. H. a. A. B. R. *J. Phys. Chem.* **1995**, 24, 663.
- (347) Sikorski, M.; Sikorska, E.; Gonzalez Moreno, R.; Bourdelande, J. L.; Worrall, D. R. *Journal of Photochemistry and Photobiology A: Chemistry* **2002**, 149, 39.
- (348) Wöhrle, D.; Hirth, A.; Bogdahn-Rai, T.; Schnurpfeil, G.; Shopova, M. *Russian Chemical Bulletin* **1998**, 47, 807.
- (349) Wainwright, M.; Meegan, K.; Loughran, C.; Giddens, R. M. *Dyes and Pigments* **2009**, 82, 387.
- (350) Okawa, M.; Kinjo, J.; Nohara, T.; Ono, M. *Biological & pharmaceutical bulletin* **2001**, 24, 1202.
- (351) Lü, J.-M.; Lin, P. H.; Yao, Q.; Chen, C. *Journal of Cellular and Molecular Medicine* **2010**, 14, 840.
- (352) Bosca, F.; Fernandez, L.; Heelis, P. F.; Yano, Y. *Journal of Photochemistry and Photobiology B: Biology* **2000**, 55, 183.
- (353) Ritter, J.; Borst, H. U.; Lindner, T.; Hauser, M.; Brosig, S.; Bredereck, K.; Steiner, U. E.; Kühn, D.; Kelemen, J.; Kramer, H. E. A. *Journal of Photochemistry and Photobiology A: Chemistry* **1988**, 41, 227.
- (354) Silhavy, T. J.; Kahne, D.; Walker, S. *Cold Spring Harbor Perspectives in Biology* **2010**, 2, a000414.
- (355) Yu, K. G.; Li, D. H.; Zhou, C. H.; Diao, J. L. *Chinese Chemical Letters* **2009**, 20, 411.
- (356) Tiwari, S.; Seijas, J.; Vazquez-Tato, M.; Sarkate, A.; Karnik, K.; Nikalje, A. *Molecules* **2017**, 22, 1172.
- (357) Kendre, B. V.; Landge, M. G.; Bhusare, S. R. *Arabian Journal of Chemistry* **2015**.
- (358) Maclean, M.; MacGregor, S. J.; Anderson, J. G.; Woolsey, G. *FEMS Microbiology Letters* **2008**, 285, 227.
- (359) Melo, M. A. S.; de-Paula, D. M.; Lima, J. P. M.; Borges, F. M. C.; Steiner-Oliveira, C.; Nobre-dos-Santos, M.; Zanin, I. C. J.; Barros, E. B.; Rodrigues, L. K. A. *Laser Physics* **2010**, 20, 1504.
- (360) Lubart, R.; Lipovski, A.; Nitzan, Y.; Friedmann, H. *Laser Therapy* **2011**, 20, 17.
- (361) Guffey, J. S.; Wilborn, J. *Photomedicine and laser surgery* **2006**, 24, 680.
- (362) Webber, M. A.; Piddock, L. J. V. *Journal of Antimicrobial Chemotherapy* **2003**, 51, 9.
- (363) Piddock, L. J. *Clin Microbiol Rev* **2006**, 19, 382.
- (364) Chen, D. K.; McGeer, A.; de Azavedo, J. C.; Low, D. E. *New England Journal of Medicine* **1999**, 341, 233.
- (365) Dennison, S. R.; Morton, L. H. G.; Harris, F.; Phoenix, D. A. *Biophysical Chemistry* **2007**, 129, 279.

- (366) Sarah R. Dennison, J. H., Leslie. H. G. Morton, Klaus Brandenburg, Frederick Harris and David A. Phoenix *Biochemical and Biophysical Research Communications* **2006**, 347, 1006.

## Abbreviations & Acronyms

AcOH	Acetic acid
ALA	5-Aminolevulinic acid
AMR	Antimicrobial Resistance
$\beta$	Beta
CA-MRSA	Community Associated Methicillin-Resistant <i>Staphylococcus aureus</i>
CAI	Community Associated Infections
<i>C.albicans</i>	<i>Candida albicans</i>
CDCl <sub>3</sub>	Chloroform-deutarated
CHCl <sub>3</sub>	Chloroform
c. HCl	Concentrated hydrochloric acid
COSY	Correlation Spectroscopy
<sup>13</sup> C NMR	Carbon Nuclear Magnetic Resonance Spectroscopy
DAD	Diethyl azodicarboxylate
DCM	Dichloromethane
Der	Derivatives
DMF	Dimethylformamide
DMSO	Dimethylsulphoxide
DNA	Deoxyribonucleic acid
DPPH	2,2-Diphenyl-1-(2,4,6-trinitrophenyl) hydrazyl
<i>E.coli</i>	<i>Escherichia coli</i>
EtOAc	Ethyl acetate
EtOH	Ethanol
Et <sub>3</sub> N	Triethylamine
FDA	Food and drug administration
g	Grams
HA-MRSA	Hospital Associated Methicillin-Resistant <i>Staphylococcus aureus</i>
H <sub>3</sub> BO <sub>3</sub>	Boric acid
HCl	Hydrochloric acid
<sup>1</sup> H NMR	Proton Nuclear Magnetic Resonance Spectroscopy

HpD	Hematoporphyrin
HPV	Human Papilloma Virus
HRMS	High Resolution Mass Spectra
ICG	Indocyanine Green
IR	InfraRed
<i>K. pneumoniae</i>	<i>Klebsiella pneumoniae</i>
KtBuO	Potassium <i>tert</i> -butoxide
$\lambda_{\max}$	Absorption maxima
LCMS – EI	Liquid Chromatography Mass Spectrometry – Electron Ionisation
<i>m</i>	Meta
MAL	Methyl-aminolevulinic acid
MC540	Merocyanine 540
MeCN	Acetonitrile
MES	Microwave Enhanced Synthesis
MeOH	Methanol
mg	Milligrams
MHRA	The Medicines and Healthcare Products Regulatory Agency
MIC	Minimum Inhibitory Concentration
mL	Millilitres
mM/mL	Millimolar per millilitre
MRSA	Methicillin-Resistant <i>Staphylococcus aureus</i>
MW	Microwave
<i>M. tuberculosis</i>	<i>Mycobacterium tuberculosis</i>
<i>N.gonorrhoeae</i>	<i>Neisseria gonorrhoeae</i>
NIR	Near-Infrared
<i>o</i>	<i>Ortho</i>
$^1\text{O}_2$	Singlet oxygen
<i>p</i>	<i>Para</i>
<i>P.acnes</i>	<i>Propionibacterium acnes</i>
PBP	Penicillin Binding Protein

PD	Pulse dyes
PDT	Photodynamic therapy
PACT	Photodynamic antimicrobial chemotherapy
Pcs	Phthalocyanines
<i>P. aeruginosa</i>	<i>Pseudomonas aeruginosa</i>
<i>P. notatum</i>	<i>Penicillium notatum</i>
PLD	Pulse laser dye
PPA	Polyphosphoric acid
<i>p</i> -TsCl	4-Toluenesulphonyl chloride
PWS	Port wine stains
ROS	Reactive Oxygen Species
rtp	Room temperature
S <sub>0</sub>	Singlet state
<i>S. aureus</i>	<i>Staphylococcus aureus</i>
<i>S. albus</i>	<i>Staphylococcus albus</i>
T <sub>1</sub>	Triplet excited state
Sn(II)Cl	Tin (II) chloride
<i>S. pneumonia</i>	<i>Streptococcus pneumonia</i>
TPCPD	2,3,4,5-tetraphenylcyclopentadienone
TMS	Tetramethylsilane
TLC	Thin layer chromatography
UV/Vis	Ultra-violet/visible
†	Partial antimicrobial activity
+	Antimicrobial activity
-	No antimicrobial activity
Π	Pi electrons